

**A Knowledge Based System to Predict the Lateral Failure Pressure  
of Masonry Panels under Bi-axial Bending**

**Anu Mathew**

**A thesis submitted for the  
Degree of Doctor of Philosophy**

**Department of Civil and Environmental Engineering  
The University of Edinburgh**

**April 1999**



## ABSTRACT

Cladding panels in framed construction and brick walls of the upper floors of multi-storied building are subjected to out-of-plane bi-axial bending due to wind loading. These panels carry hardly any axial load and resist the bi-axial moments purely due to their flexural strength. The failure mechanism of a ductile material like steel under bi-axial bending is well defined by the theories of failure. A failure criterion for orthotropic brittle material has been formulated as a result of some recent developments in masonry. However, when an isotropic brittle material like mortar or glass is subjected to bi-axial bending, these theories of failures cannot represent the behaviour of this material. Hence, an experimental investigation has been carried out on mortar material, the results of which are used to develop a failure criterion for a brittle isotropic material.

The behaviour of mortar panels under bi-axial bending was studied by carrying out tests on cross beams. The tests were identical to brickwork cross beam tests that had already been done and hence it was possible to compare the behaviour of isotropic and orthotropic materials. Three mortar cross beams each of 5 different aspect ratios were tested in the laboratory to study the behaviour in bi-axial bending. A failure criterion was established for isotropic material based on mortar cross beam test results. These results, along with brickwork cross beam test results were used to compare the behaviour of isotropic and orthotropic materials under bi-axial bending. The comparative studies helped to identify the importance of considering the orthotropic properties in the failure pressure of a panel. A conventional finite element program was modified to incorporate the failure criterion to obtain the failure pressure of a panel subjected to bi-axial bending. A few tests were carried out on mortar panels in order to apply the theoretical model. A total of 4 panels of two different boundary conditions were tested for this purpose and a high degree of correlation between the theoretical and experimental results was observed.

A considerable amount of experimental research has been done on masonry panels under bi-axial bending. Finite element analysis can be very time consuming and in many cases requires a careful study of the output files to determine the failure load. Therefore, a novel approach for predicting the failure pressure of a masonry panel subjected to bi-axial bending has been developed in this thesis. This includes a hybrid system that combines the capabilities of artificial neural networks and case-based reasoning. A large number of experimental results contributed towards the successful implementation of this hybrid system.

Artificial neural networks have been found successful in solving many complex non-linear problems with little theoretical back up and have proved successful in several civil and structural engineering problems to establish an un-identified relationship between the variables. The strength and the behaviour of masonry panels under lateral loading is in a similar category and hence the same is applied for calculating the failure loads of isotropic or orthotropic of panels having various support conditions. In this project, a neural network was trained using panels of 8 different types of boundary conditions. A trained network is found to be able to predict the failure pressure of a panel under bi-axial bending with similar accuracy to the finite element method, but in considerably less processing time. To develop this application, a neural network program was developed in C++ incorporating a back propagation algorithm and sigmoid activation function. An excellent user interface for this program was developed using the Microsoft Foundation Class (MFC) libraries.

Case-based reasoning is an Artificial Intelligence technique that is used to solve new problems by adapting solutions to problems solved in the past. In the case of masonry panels under bi-axial bending, case-based reasoning is used to make best use of the experimental results that are available in the literature. This is done by storing the panels that are tested at a variety of research centres as cases. Panels can be identified through various properties and experimental failure pressure. In addition to the experimental failure pressure, the theoretical values of the failure pressure

from several existing methods of analysis of masonry panels are also stored in the case-base. This helps to determine, under given laboratory conditions which of the theoretical methods will be able to predict the experimental results closely. Thus, a new case will be analysed using the most appropriate method from the case-base.

## **DECLARATION**

This thesis is the result of research work undertaken in the Department of Civil & Environmental Engineering at the University of Edinburgh for the degree of Doctor of Philosophy.

I declare that all the work in this thesis has been carried out by myself unless or otherwise clearly stated, and that the thesis has been composed by myself under the supervision of Dr. B P Sinha, Dr. B Kumar and Dr. R F Pedreschi.

Edinburgh, April 1999

Anu Mathew

## ACKNOWLEDGEMENTS

First of all, I would like to thank Dr. B P Sinha for his patience and guidance in seeing me through this dissertation. Under his tuition I had the opportunity to formulate my ideas carefully and implement them as part of my work. The close student-advisor relationship we had made this arduous task of completing the dissertation all the more easier. I would also like to thank my other two supervisors who are Dr. B Kumar and Dr. R F Pedreschi. Dr. Kumar's help was most valuable in one of the main components of my dissertation. His useful comments and timely suggestions are highly appreciated. Dr. Pedreschi was kind enough to read my completed thesis and offer appropriate help where necessary.

The Faculty of Science and Engineering and the ORS committee were instrumental in co-ordinating the funding for this research up to and including its completion. Thanks is also extended to the department head, Prof. Mike Forde, for providing the exceptional facilities within this department.

While on the subject of departmental facilities, I must thank Mr. Chris Burnside our computing officer, for all the computer related problems that have occurred during the course of this project. Thanks is also extended to the lab technicians of this department. This includes Mr. Norman Erskine for building my specimens, Mr. Kevin Broughton for all the electrical work, Mr. Peter Lehany and Mr. Jim Hutcheson for co-ordinating my laboratory work as well as additional help in certain areas. Thanks also go to other members of the technical staff who helped me.

How can I forget my friends and colleagues here in Edinburgh? Particular thanks are due to Anup, Isilda, Dimitris, Reena, Gerard and several others who extended their kind and generous help to me throughout my stay here. I have to admit their friendship has made my stay in Edinburgh all the more happier.

This acknowledgement section would not be complete without mentioning my family. The invaluable support and comfort provided by my uncle, auntie and cousins in London are highly appreciated. Special thanks to my auntie Lissy who made me a member of their family and provided me with a home away from home. I am greatly indebted to them. My parents, sister and brothers are specially remembered for their love and affection that gave me a great deal of mental strength and encouragement to complete this work, especially at times when I had to question my decision for doing a Ph.D. Thanks for always being there for me. Special thanks to Shibuchayan for his unfailing support during the correction stages of this thesis.

I would also like to pay tribute to three of my uncles Mr. M O Kuruvilla, Mr. V A Johnykutty and Mr. A K Mathew who departed this world during my stay here. Their loss is unrecoverable. May their souls rest in peace.

Finally, what would I have achieved if it was not for the blessings of Almighty God. I am proud to say that the abundant mercy and the everlasting love of Jesus Christ was with me throughout and protected my family, especially my parents in his safe hands.

As always, responsibility for any shortcomings, which remain is mine alone.

*Dedicated to*  
*My Parents for their boundless affection*



## PUBLICATIONS

The following papers were published by the author in collaboration with the supervisors during the course of this thesis:

1. "A Neural Network Approach for Predicting the Failure Load of Masonry Cladding Panel in Bending", Proceedings of the 4th Australasian Masonry Conference, November 1995, Sydney, Australia, pp.240-248.
2. "Application of Neural Network to Masonry Panels", proceedings of the International Conference on Computing and Information Technology for Architecture, Engineering and Construction, May 1996, Singapore.
3. "Strength and Behaviour of Orthotropic and Isotropic Panels Under Bi-axial Bending", Proceedings of the 11th International Brick/Block Masonry Conference, October 1997, Shanghai, Peoples Republic of China, pp.141-150.
4. "Analysis of Masonry Panel Under Bi-axial Bending Using ANNs and CBR" (Accepted for publication in the Journal of Computing in Civil Engineering, ASCE)

# NOTATIONS

The following symbols are used in this thesis:

- $a, b$  - Projected lengths of yield lines in  $x$  and  $y$  directions
- $d_j$  - The desired output of a node
- $e_j$  - The error at a node
- $E$  - Modulus of elasticity of the material
- $E_x, E_y$  - Modulus of elasticity in  $x$  and  $y$  directions
- $F$  - Flexural Strength
- $F_x, F_y$  - Flexural strength in  $x$  and  $y$  directions
- $G$  - Shear modulus of a material
- $G_{xy}, G_{yx}$  - Shear Modulus in  $x$  and  $y$  directions
- $H$  - Height of the panel
- $I$  - Second moment of area
- $I_x, I_y$  - Second moment of area in  $x$  and  $y$  directions
- $K$  - Load Coefficient
- $L$  - Length of the panel
- $L_x, L_y$  - Span in  $x$  and  $y$  directions
- $m$  - Moment of resistance
- $M$  - Bending moment
- $M_x, M_y$  - Applied moment in  $x$  and  $y$  directions
- $M_{ux}, M_{uy}$  - Uni-axial flexural strength in  $x$  and  $y$  directions
- $R_x, R_y$  - Reactions in  $x$  and  $y$  directions
- $T$  - Torque
- $t$  - Thickness of the Specimen
- $w_{ij}$  - Connection weight from an  $i^{th}$  node to the  $j^{th}$  node in the preceding layer
- $w$  - Failure Pressure
- $W$  - Point Load
- $W_x, W_y$  - Load in  $x$  and  $y$  directions

- $S$  - The net input to a node
- $w_{ij}$  - Connection weights in a multi-layered net
- $x_i$  - Inputs to a node in the net
- $y_i$  - Net output
- $Z$  - Section modulus
- $\nu$  - Poisson's ratio
- $\delta$  - Displacement due to applied load
- $\theta$  - The threshold of a node in the net
- $\theta_x, \theta_y$  - Rotation along the yield lines in the  $x$  and  $y$  directions
- $\mu$  - Orthotropic strength ratio ( $F_x/F_y$ )
- $\beta, \phi$  - Reduction factors
- $\xi$  - Sum of the squared errors at a node
- $v$  - The internal activity at the input of a net
- $\eta$  - Learning rate parameter of back propagation algorithm
- $\alpha$  - The momentum term of back propagation algorithm
- $\varepsilon$  - Measured strain

# TABLE OF CONTENTS

	<b>PAGES</b>
<b>ABSTRACT</b> .....	<b>i</b>
<b>DECLARATIONS</b> .....	<b>iv</b>
<b>ACKNOWLEDGEMENTS</b> .....	<b>v</b>
<b>DEDICATION</b> .....	<b>vii</b>
<b>PUBLICATIONS</b> .....	<b>viii</b>
<b>NOTATIONS</b> .....	<b>ix</b>
<b>CONTENTS</b> .....	<b>xi</b>

## **CHAPTER 1. INTRODUCTION**

1.1 INTRODUCTION .....	1
1.2 OUTLINE OF THE THESIS .....	4

## **CHAPER 2. LITERATURE REVIEW**

2.1 INTRODUCTION .....	6
2.2 REVIEW OF PAST RESEARCH ON BI-AXIAL BENDING OF MASONRY .....	7
2.3 A DISCUSSION OF ISSUES CONCERNING MASONRY UNDER BI- AXIAL BENDING.....	21
2.4 APPLICATION OF ARTIFICIAL NEURAL NETWORKS IN CIVIL & STRUCTURAL ENGINEERING.....	23
2.5 APPLICATION OF CASE-BASED REASONING TO CIVIL ENGINEERING .....	29
2.6 SCOPE OF CURRENT RESEARCH .....	32

## CHAPTER 3. THEORY AND DEVELOPMENT OF ARTIFICIAL NEURAL NETWORKS

3.1 INTRODUCTION .....	34
3.2 HISTORY OF ARTIFICIAL NEURAL NETWORKS .....	35
3.3 BIOLOGICAL NEURAL NETWORKS .....	36
3.4 NEURONS .....	37
3.5 ARTIFICIAL NEURAL NETWORKS (ANNS) .....	39
3.6 MULTI-LAYERED NEURAL NETWORKS .....	40
3.7 DERIVATION OF BACK-PROPAGATION ALGORITHM .....	41
3.8 DEVELOPMENT OF AN ANN APPLICATION .....	46
3.8.1 <i>Initial Studies</i> .....	46
3.8.1.1 Identifying the Learning Algorithm .....	48
3.8.1.2 Feasibility Study .....	48
3.8.2 <i>Data Preparation</i> .....	49
3.8.2.1 Problem Definition .....	50
3.8.2.2 Define Input and Output Variables .....	50
3.8.2.3 Data Collection .....	51
3.8.2.4 Preparing the Training and Test Set .....	53
3.8.2.5 Pre-processing the Data .....	54
3.8.3 <i>Network Architecture</i> .....	55
3.8.3.1 Number of Input and Output Nodes .....	56
3.8.3.2 Size of Hidden Layers .....	56
3.8.3.3 Activation Function .....	58
3.8.3.4 Learning Parameters .....	59
3.8.3.5 Stopping Criteria .....	59
3.8.4 <i>Implementation</i> .....	60
3.8.4.1 Weight Initialisation .....	60
3.8.4.2 Mode of Training .....	61
3.8.4.3 Training the Net .....	62
3.8.4.4 Validation of the Performance .....	63
3.8.4.5 Store the Net .....	64
3.9 DRAWBACKS OF BACK-PROPAGATION ALGORITHM .....	64
3.9.1 <i>Slow Training</i> .....	65
3.9.2 <i>Stabilising at Local Minima</i> .....	70
3.9.3 <i>Generalisation</i> .....	71
3.9.4 <i>Interpretation of Connection Weights</i> .....	72
3.10 DEVELOPMENT OF NEURAL NETWORK .....	74
3.10.1 <i>User Interface for Neural Network</i> .....	74
3.10.2 <i>Neural Network Program</i> .....	75

3.11 SUMMARY.....	78
-------------------	----

## CHAPTER 4. EXPERIMENTAL INVESTIGATION OF ISOTROPIC MATERIAL UNDER BI-AXIAL BENDING

4.1 INTRODUCTION.....	79
4.2 PROPERTIES OF MATERIALS.....	80
4.2.1 Compressive Strength of Mortar.....	80
4.2.2 Modulus of Elasticity and Flexural Strength.....	81
4.2.3 Poisson's ratio.....	85
4.2.4 Shear Modulus.....	86
4.3 CROSS BEAMS TESTS.....	88
4.3.1 Construction of Cross Beams.....	88
4.3.2 Test Arrangement.....	90
4.3.3 Tests on Cross Beams.....	91
4.3.4 Experimental Results.....	92
4.3.4.1 Support Reactions.....	93
4.3.4.2 Crack Pattern.....	93
4.3.5 Theoretical Methods.....	96
4.3.5.1 Grashoff-Rankine Method.....	96
4.3.5.2 Rankine's Maximum Stress Theory.....	98
4.3.5.3 Yield Line Analysis.....	99
4.3.5.4 Elastic Finite Element Analysis.....	101
4.3.6 Discussion of Test Results.....	102
4.3.6.1 Load Distribution and Support Reactions.....	102
4.3.6.2 Cracking and Failure.....	105
4.3.6.3 Failure Criterion.....	106
4.3.7 Comparison of the Experimental and Theoretical Results.....	107
4.3.8 Comparison of the Behaviour of Isotropic and Orthotropic Materials under Bi-axial Bending.....	111
4.3.8.1 Load Distribution.....	111
4.3.8.2 Type of Failures.....	112
4.3.8.3 Failure Criteria.....	114
4.4 THE PANEL TESTS.....	115
4.4.1 Panel Construction.....	115
4.4.2 Test Arrangement.....	116
4.4.3 Instrumentation.....	118
4.4.4 Test Procedure.....	120
4.4.5 Experimental Results.....	121
4.4.5.1 Crack Pattern.....	121
4.4.5.2 Strain Measurements.....	122
4.4.6 Effect of Shear Modulus on the Failure Pressure of a Panel.....	125

4.4.7 <i>The Effect of Shear Modulus on the Failure Pressure of Panels</i> .....	127
4.4.8 <i>Comparison of the Experimental and Theoretical Results</i> .....	128
4.5 CONCLUSION .....	131

## **CHAPTER 5. A MODEL FOR HYBRID SYSTEM INCORPORATING ARTIFICIAL NEURAL NETWORKS AND CASE-BASED REASONING**

5.1 INTRODUCTION.....	132
5.2 THEORETICAL METHODS FOR THE ANALYSIS OF A MASONRY PANEL .....	133
5.3 THE MODEL FOR THE DEVELOPMENT OF THE HYBRID SYSTEM FOR THE ANALYSIS OF MASONRY PANELS UNDER BI-AXIAL BENDING .....	134
5.3.1 <i>ANN Applied to Masonry Panel Subjected to Bi-axial Bending</i> .....	134
5.3.2 <i>CBR Applied to Masonry Panel Subjected to Bi-axial Bending</i> .....	137
5.4 SCHEMATIC REPRESENTATION OF THE MODEL .....	139
5.5 CLUSTERING APPROACH.....	140
5.6 CONCLUSION .....	141

## **CHAPTER 6. IMPLEMENTATION OF THE HYBRID SYSTEM FOR PREDICTING THE FAILURE PRESSURE OF MASONRY PANELS UNDER BI-AXIAL BENDING**

6.1 INTRODUCTION .....	143
6.2 APPLICATION OF ANNS TO PREDICT THE FAILURE PRESSURE OF MASONRY PANELS UNDER BI-AXIAL BENDING.....	143
6.2.1 <i>Initial Studies</i> .....	144
6.2.2 <i>Data Preparation</i> .....	146
6.2.3 <i>Network Architecture</i> .....	150
6.3 THEORETICAL METHODS OF ANALYSIS FOR DATA GENERATION	154
6.3.1 <i>BS 8110</i> .....	155
6.3.2 <i>Australian Code of Practice</i> .....	155
6.3.3 <i>Finite Element Method</i> .....	155
6.3.4 <i>Comparison of the Various Theoretical Methods</i> .....	158

6.4 CASE BASED REASONING TO PREDICT THE FAILURE PRESSURE OF MASONRY PANELS UNDER BI-AXIAL BENDING.....	161
6.4.1 <i>Building a Case Base</i> .....	162
6.4.2 <i>Representation of a Case in CBR Express</i> .....	162
6.4.2.1 Case Title and Description.....	163
6.4.2.2 Questions.....	164
6.4.2.3 Actions .....	167
6.4.3 <i>Indexing and Retrieval of a Case in CBR Express</i> .....	170
6.5 WEIGHT ADAPTATION IN CBR.....	171
6.5.1 <i>Weight Analysis - A Sample Calculation</i> .....	172
6.6 EVALUATION OF TRAINED NET TO PREDICT THE FAILURE PRESSURE OF MASONRY PANELS UNDER BI-AXIAL BENDING.....	175
6.7 PERFORMANCE OF THE NET ON EXPERIMENTAL RESULTS .....	194
6.7.1 <i>'Set1' (Four Sides Simply Supported) Panels</i> .....	194
6.7.2 <i>'Set2' Panels (Three Side Simply Supported, Top Free)</i> .....	196
6.7.3 <i>'Set3' Panels (Three Sides Simply Supported and One Vertical Edge Free)</i> .....	197
6.7.4 <i>'Set4' Panels (Two Vertical Edges Restrained and Top and Bottom Simply Supported)</i> .....	198
6.7.5 <i>'Set6' Panels (Top and Bottom Simply Supported, One Vertical Edge Restrained and the Other Free)</i> .....	200
6.7.6 <i>'Set8' Panels (Vertical Edges Restrained, Bottom Simply Supported and Top Free)</i> .....	201
6.8 THE ADVANTAGES OF TRAINED NEURAL NETWORK OVER THE FINITE ELEMENT METHOD.....	202
6.9 THE HYBRID SYSTEM (ANNS AND CBR) .....	205
6.10 CONCLUSION .....	210

## CHAPTER 7. CONCLUSIONS

7.1 SUMMARY AND CONCLUSIONS.....	212
7.2 SUGGESTIONS FOR FURTHER RESEARCH.....	214

<b>REFERENCES</b>	215
-------------------	-----

## APPENDIX I

SECTION 36.4 OF BS 5628 CODE OF PRACTICE FOR USE OF MASONRY	228
---	-----



<b>APPENDIX II</b>	
SECTION 6.3.4 OF AUSTRALIAN MASONRY MANUAL	233
<b>APPENDIX III</b>	
THE INTERACTIVE QUESTIONNAIRE TO PREPARE THE INPUT DATA FOR THE IN-HOUSE FINITE ELEMENT PROGRAM	236
<b>APPENDIX IV</b>	
USER INTERFACE FOR THE NEURAL NETWORK PROGRAM	243
<b>APPENDIX V</b>	
MOMENT COEFFICIENTS FOR DESIGN OF LATERALLY LOADED ORTHOTROPIC PANELS BASED ON THE FINITE ELEMENT ANALYSIS INCORPORATING THE BI-AXIAL FAILURE CRITERION	249
<b>APPENDIX VI</b>	
FINITE ELEMENT MESH USED IN THE CROSS BEAM ANALYSIS	256
<b>APPENDIX VII</b>	
TYPICAL FINITE ELEMENT MESH USED IN THE PANEL ANALYSIS	257
<b>APPENDIX VIII</b>	
THE TRAINING SET USED IN TRAINING THE NET WITH THE NET OUTPUTS	258
<b>APPENDIX IX</b>	
LISTING OF THE SOURCE CODE FOR THE NEURAL NETWORK PROGRAM	299

# CHAPTER 1

## INTRODUCTION

### 1.1 Introduction

Isotropic and orthotropic panels are widely used in the building industry as load bearing and non-load bearing structural elements. Cladding panels of framed buildings and walls of the upper floors of multi-storey buildings carry very little axial load and consequently little axial pre-compression. These panels may be subjected to out-of-plane bending due to wind loading or gas explosions and therefore the design becomes critical as these members have low tensile strength. When such panels are supported on two opposite sides, the design is rather simple. However, when these panels are supported on three or more sides, they are subjected to bi-axial bending and an extensive knowledge of their structural behaviour is needed to determine the failure pressure. This thesis deals mainly with predicting the lateral failure pressure of isotropic and orthotropic panels with little axial pre-compression.

Masonry, being an orthotropic material, shows distinct properties in the two orthogonal directions, parallel and perpendicular to the bed joints. The complexity of analysing an orthotropic and non-linear material like masonry encouraged the use of simple methods such as the yield line (JOHANSEN 1972) and the strip method (REGAN & YU 1973), which form the basis for the BS and the Australian code of practice respectively. The experimental research carried out by various researchers (BAKER 1972; KHEIR 1975; LAWRENCE 1983; WEST *et al.* 1977; HASELTINE *et al.* 1977; DUARTE 1993) showed that, even though there is no rational basis, the failure pressures predicted by these methods are close to the experimental values in some cases. Such a close prediction by these methods could be due to the fact that the boundary conditions in these tests were not well defined and dead weight stresses and rotational restraints were neglected.

An elastic analysis of masonry can be carried out either by considering a constitutive model, where the brick and mortar are modelled as individual elements, or by assuming homogenous material properties. This requires a failure criterion which is representative of the material behaviour under bi-axial bending. Even though several approaches can be found in the literature, the failure criterion in bi-axial bending proposed by SINHA *et al.* (1996) for an orthotropic material predicts the failure pressures closer to the experimental results. However, no failure criterion exists for an isotropic material in bi-axial bending. Hence, to fill this gap in our knowledge, an experimental investigation on mortar cross beams was carried out as first phase of the work described in this thesis.

Mortar exhibits similar strength and stiffness properties in the two orthogonal directions and was considered ideal to represent an isotropic material. Tests were carried out on mortar cross beams, the results of which were used to study the behaviour of the material under bi-axial bending. As similar tests were already done for the orthotropic material, both these results were used to compare the behaviour of orthotropic and isotropic materials subjected to lateral loading. A failure criterion was established for an isotropic material from these results and was incorporated into a finite element plate bending program. A few mortar panels were also tested to prove the validity of this criterion.

A finite element method of analysis requires considerable amounts of computer time and memory. Hence, a hybrid system combining artificial neural networks and case-based reasoning was developed as the second phase of this project. This system serves as an appropriate design method that could be used to obtain results quickly with similar accuracy as the finite element method. A brief description of the system is outlined below.

Artificial neural networks are computer models that simulate the functioning of the human brain on a small scale. They can be considered as a significant step in machine learning and their contribution to different areas can be enormous. They

have been used successfully in many civil and structural engineering problems to solve complex, non-linear relationships. In their application to masonry panels, neural networks are trained using a set of patterns representing a panel under bi-axial bending, to produce the failure pressure as the desired output. The finite element technique incorporating the failure criteria for both the orthotropic and isotropic materials under bi-axial bending will be used to generate the majority of the training data. A trained net will be able to learn the relationship between the input and output patterns with which the net is presented and predict the failure pressures of similar panels that are not used for training. Neural networks will be trained to predict the failure pressure for panels of eight different types of boundary conditions when subjected to bi-axial bending.

Case-Based Reasoning (CBR) is an Artificial Intelligence technique that can be used to obtain solutions to new problems by studying similar problems that have been resolved in the past. A new problem can be solved by recognising its similarities to a specific known (past) problem. The solution of the known problem can either be adopted as such or be modified for the new problem depending on the degree of similarity between the two and the nature of the problem. As pointed out earlier, researchers have put forward methods such as the BS, the Australian code of practice and the elastic methods to analyse a panel under bi-axial bending as these methods are found to predict the experimental failure pressure closely in some cases. Nevertheless, a closer prediction of the experimental results by some of these methods can be seen as a mere coincidence as there is no rational basis for the application of these methods. Case-based reasoning is used to further evaluate this situation. In this application, the panels that were tested at the various research centres were analysed using the various theoretical methods to decide the most reliable theoretical method for a particular type of panel. The experimental and theoretical failure pressures, along with the properties, of each panel are stored as cases in a case-base. The failure pressure of a new panel can now be calculated by selecting a case from the case base, which most resembles the new problem and by adopting the method that provided the closest result for the selected problem.

The hybrid system developed for this thesis is able to aid the designer in finding out the failure load of laterally loaded isotropic or orthotropic panels. Panels of 8 different boundary conditions are analysed by the hybrid system. For an isotropic panel, the failure criterion established in this work can be used in a finite element analysis to obtain the failure pressure. As an alternative to the finite element method, the trained net can be used to obtain the failure pressure. In the case of an orthotropic panel, CBR is used to suggest a method that could be used to obtain the failure pressure of the panel. This is accomplished by CBR on the basis of past experience from the cases that are stored in the case base. If CBR suggests the use of the finite element method to find out the failure pressure of the new problem, the trained neural network is used to obtain the result with the same degree of accuracy. The other methods that could possibly be suggested by CBR for an orthotropic material include the BS and the Australian code of practice.

## **1.2 Outline of the Thesis**

The work carried out as part of this research project can be seen in the thesis as outlined here. A survey of literature carried out is given in Chapter 2. This reviews the theoretical and experimental research that has been carried out on the behaviour of masonry panels under bi-axial bending. The application of artificial neural networks and case-based reasoning on various civil and structural engineering problems that has already been done by others can also be seen in this chapter.

Chapter 3 provides a detailed description of the theory of artificial neural networks. A development methodology adopted for the application of neural networks can also be seen here. The neural network program was developed in C++ and a user interface was developed using Microsoft Foundation Class (MFC) libraries. The programming codes that are used for this purpose can be summarised from the flow charts presented in this chapter.

Chapter 4 describes the experimental work that was carried out on isotropic material. This includes the work on the cross beams, the panels and the associated control specimens made of cement:sand mortar. Along with the experimental work, the theoretical analysis was done using the methods outlined in this chapter. A comparison of the behaviour of the orthotropic and isotropic panels can also be seen in this chapter.

The model for the development of the hybrid system for cladding panels under bi-axial bending using artificial neural networks and case-based reasoning is presented in Chapter 5, whereas Chapter 6 focuses on the implementation of the hybrid system. Details on the training of neural networks for panels of different boundary conditions and the evaluation of the performance of the trained net are demonstrated here. This chapter also outlines the development of the CBR application for masonry panels along with its integration into neural networks. The relative importance of the various input parameters on the failure pressure of a panel can be determined by analysing the connection weights of a trained neural network. The values obtained as a result of this study are incorporated in CBR as match weights, which aid in determining the similarity between two cases. This helps to achieve a better integration between neural networks and case-based reasoning. The chapter concludes with an example problem illustrating the working of the hybrid system. A summary of the work is given in Chapter 7 along with the conclusions that are drawn on the basis of this research work.

Tables, Figures and Photographs are included in relevant chapters and can be seen immediately after they are referenced, wherever possible. Moment coefficients are developed on the basis of the finite element analysis of panels of different boundary conditions and are given in the Appendix. Other Appendices provide information on the programming code for neural network program, the description of the interface developed for its application, the finite element mesh used in the analysis of cross beams and panels and the relevant parts of the BS and the Australian Code of practice that were used in this research.

# CHAPTER 2

## LITERATURE REVIEW

### 2.1 Introduction

The use of masonry as a building material dates back centuries. But, the design was based on 'rules of thumb' and practices, without the need for special structural consideration. However, this kind of approach cannot be applied beyond the scale of two-storey houses of conventional construction without having to use very thick walls as in the case of 'Monadnock' building (GROSS 1965), where the thickness of the wall at the base is 1.82m. This results in the waste of materials. Use of masonry as a structural material for taller buildings gradually declined and the use of steel and concrete flourished since the 1950s. The application of structural engineering principles to the design has resulted in the use of masonry for high-rise buildings. In high-rise buildings, the panels have to resist wind loading which causes tension. The tensile strength of masonry was never taken into account in the design previously and the walls were designed to resist the tension only by the pre-compression caused by the imposed load. Later on, with the amendment to the BS, the wind load was increased and the research was focused on exploiting the load carrying capacity of the material. The panels subjected to uni-axial bending were designed mainly by considering the flexural strength in the direction of spanning. The design becomes complicated when the panels are supported on three or four sides, which induces bi-axial bending stresses in the member. Extensive investigation has been carried out at the various research centres to study the behaviour of the masonry panels under bi-axial bending (BAKER 1972; KHEIR 1975; LAWRENCE 1983; SINHA *et al.* 1997; WEST *et al.* 1977; HASELTINE *et al.* 1977). These include tests on clay and concrete panels of various aspect ratios under different support conditions. Tests were carried out on single and cavity walls with and without openings. Although test

results are available, many of these tests were not carried out under ideal conditions where proper consideration was given to factors such as rotational restraints and dead weight effects.

A review of the existing literature on the research in masonry panels under bi-axial bending is presented in this chapter. In Section 2.2, an attempt is made to investigate the experimental and the theoretical research that has been carried out on masonry panels subjected to bi-axial bending. Section 2.3 highlights some of the problems that are currently being recognised for the masonry panels. The use of Artificial Neural Networks (ANNs) and Case-Based Reasoning (CBR) is proposed in this section to calculate the failure pressures of panels of various boundary conditions, when subjected to lateral loading. Some of the applications of ANNs and CBR in civil and structural engineering are described in Sections 2.4 & 2.5.

## **2.2 Review of Past Research on Bi-axial Bending of Masonry**

In 1972, SATTI (1972) reported an experimental investigation on laterally loaded masonry panels as part of his PhD work. He carried out tests on solid panels supported on three and four sides, with and without pre-compression. He observed that the cracking of these panels followed a yield line pattern. However, the prediction of the failure pressure using the yield line theory over-estimated the experimental results in many cases, whilst reasonable accuracy was obtained in some cases. From his studies it is difficult to generalise the properties of the panels where the yield line theory can be successfully applied. The failure load, the deflections and the failure patterns were reasonably well predicted by an elastic analysis using the finite element method.

In 1973, BAKER (1973a; 1973b) published the results of the tests on third scale brick panels with different support conditions. The results were analysed using the then available methods namely, the yield line method and the elastic plate method. A



comparison of the moment coefficients using the strength in the vertical direction showed that the elastic plate theory under-estimated and the yield line theory over-estimated the results. A proposed empirical strip method gave good agreement with the observed results, when isotropic elastic stiffness was used. He suggested the use of the strip method as a better approach than the yield line method and the elastic method.

In the same year, the BCRA (WEST *et al.* 1973) published a part of an extensive investigation, which comprised tests on single leaf and cavity type panels with different levels of pre-compression. They described a three-pinned arch mode of failure for panels without any returns and the same theory was applied for the analysis of these cases. The provision of returns changed the pattern of failure to that of a yield line. The paper (HASELTINE & HODGKINSON 1973) presented at the Third International Conference on Brick Masonry gave details of the test program. It was concluded on the basis of the preliminary set of investigations that the yield line method may be used as a satisfactory means of designing the walls even though its application is irrational. This contradicted Baker's (BAKER 1973b) opinion at the same conference, where he questioned the use of yield line theory on the grounds of its applicability to a brittle material like masonry. HASELTINE & HODGKINSON (1973) showed that the elastic plate theory gave a safe estimate of the ultimate load.

HENDRY (1973) gave an excellent review of the work on the lateral loading of the masonry panels. He analysed the work done by SATTI (1972) and found that the yield line theory gave fairly good agreement when the strength ratio was taken as one. He admitted that the above value of strength ratio was different from the test result. He pointed out the limitation of the application of elastic theory as the non-linearity of the brickwork, leading to the underestimation of the results. He developed a chart of moment coefficients for panels simply supported on three and four sides based on a simple calculation of the experimental results and recommended the same as a better way of generalisation of the results.

KHEIR (1975) published his results on the lateral loading tests on sixth scale model brick wallettes and panels. From his wallette tests, he noticed little difference between the stiffness of brickwork in the two orthogonal directions and, hence, used isotropic stiffness properties in his calculations. He observed that the failure of the panels simply supported on three and four sides followed an yield line pattern and the yield line theory gave satisfactory results. An elastic analysis using a simple finite element method under-estimated the failure load in most of the cases. The strip method, though under-estimated, gave better predictions than the elastic analysis.

In 1975, at the International Symposium of Bearing Walls, SINHA & HENDRY (1975) opposed the general view of summing up the failure loads of individual leaves of a cavity wall. They showed that the yield line theory predicted the strength of the cavity wall when treated as an equivalent solid wall, where the thickness was calculated from an empirical relationship. An increase in strength was noticed by reducing the spacing of the ties. ANDERSON (1976) carried out tests on full scale brick panels, where a distributed series of point loads was applied on the panels to simulate wind loading and compared his results with the design loads based on the draft BS specification for the structural use of masonry.

At the Sixth International Symposium on Bearing Walls in 1977, Baker presented a paper (BAKER 1977) which analysed the experimental work done at various research centres and pointed out the importance of the secondary effects of various aspects during testing. The major part of the research done at BCRA was consolidated in two papers (WEST *et al.* 1977; HASELTINE *et al.* 1977). This consisted of wallette tests and full-scale tests on panels of different aspect ratios and boundary conditions on single leaf and cavity walls. They observed that the lateral load resistance of a panel is inversely proportional to some power of its length. Upon analysis, the elastic plate method under-estimated the failure load for longer walls, but worked well for shorter walls. The yield line method gave good predictions for longer panels even though it over-estimated the results for shorter panels. The load carrying capacity of the cavity wall was obtained by summing the individual leaf

capacities, where sufficiently stiff ties were used. They proposed a design method and derived the moment coefficients for panels of different support conditions and orthotropic strength ratios.

In 1978, SINHA (1978) introduced the fracture line method of analysis, where he modified the yield line method to incorporate the stiffness orthotropy of the material. Comparison of the experimental and theoretical moments (SINHA 1978; SINHA *et al.* 1979) showed that the elastic plate theory under-estimated the failure loads and the yield line theory over-estimated results. A very good agreement was noted between the experimental and the analytical results using the fracture line method for panels supported on four sides.

Several papers were presented at the Fifth International Brick Masonry Conference in 1979 on lateral loading. BAKER (1979) developed a failure criterion for the panels subjected to bi-axial bending based on a series of tests on single joint specimens subjected to moment in both directions. He argued that there is an elliptical interaction between the horizontal and the vertical moments on a panel. However, it has to be pointed out that, as these tests were done on a single-joint specimen, they represented the behaviour of a joint under bi-axial bending rather than that of the material. As brickwork is orthotropic in strength and stiffness, any test carried out to study the behaviour of the panel under bi-axial bending should take into account the orthotropic properties as well. In addition to this, Baker carried out his analysis using the flexural strengths obtained from a relationship he derived. It would be more appropriate to use the values obtained from the wallette tests, as masonry exhibits varying properties.

WEST *et al.* (1979a) tested storey height walls made of calcium silicate bricks and found that the walls resisted more load than that obtained by using the coefficients in the BS. They attributed the reason for the above to the use of the characteristic strengths given in the code and the partial restraints provided at the sides. They also tested walls supported on three sides (WEST *et al.* 1979b) and showed that sufficient

factor of safety for loads is obtained with the use of the code coefficients. In another paper, WEST *et al.* (1979c) analysed the results of 20 cavity walls and noticed that the strength of the cavity wall was almost equal to the sum of the individual leaf strengths. The use of truss type reinforcement and quadrupling the number of twisted ties enhanced the result. A theoretical analysis of the cavity walls was carried out by BROWN & ELLING (1979) and they concluded that the distribution of load in both the leafs is in accordance with their flexural rigidity. No improvement in strength was achieved theoretically by reducing the spacing from the standard. This paper also gave some useful suggestions to improve the design of cavity walls. In the same year, LAWRENCE (1979) published some early observations of the tests on full-scale brick walls.

SINHA (1980) applied the fracture line method to panels of different shapes and with openings. The good agreement observed in these cases supported the use of this theory in spite of its origin from the yield line theory. It was during this time that PAGE (1980) developed a failure criterion for brick masonry under bi-axial tension. The criterion was obtained from an iterative finite element program to simulate bi-axial stresses on brickwork panels.

Baker carried out tests on half scale model brick panels as part of his PhD (BAKER 1981). These results, along with his MSc work (BAKER 1972), were used for the verification of the elastic theory proposed by him. Baker presented two papers (BAKER 1982a; 1982b) on lateral loading at the Sixth International Brick Masonry Conference. He modified (BAKER 1982a) the failure criterion earlier developed (BAKER 1979) to a general case, where the principal moments are considered in the elliptical interaction instead of the horizontal and vertical moments. The above criterion was incorporated in a finite element model and tested against full and third scale panels supported on three and four sides. The finite element program was found to predict the failure pressure of these panels close to the experimental values. Random joint strength was assigned from a normally distributed population and was averaged over two adjacent joints. However, the validity of this criterion still remains

questionable due to the lack of an idealised experimental set up to take into account the orthotropic nature of masonry.

ANDERSON & HELD (1982) tried to assess the load carrying capacity of a vertically spanning wall by assuming a crack being formed at 0.7 of the span above the base and hinges formed at the crack and the base. WEST *et al.* (1982) analysed 58 cavity walls using the yield line method and also the coefficients in the BS. By assuming partial fixity at the base, the yield line method gave safe prediction of the failure loads in these cases, when the individual leaf capacities are summed up. An adequate factor of safety was obtained by using the code coefficients, where the cavity wall strength was taken as the sum of the individual wall strengths.

In the same year, SEWARD (1982) proposed an elastic analysis for the design of panels under lateral loading. A simple elastic theory based on the ultimate collapse failure criterion was assumed in this analysis. The moment calculations were primarily carried out in two stages. In the first stage, the moment coefficients were developed in the horizontal and the vertical directions using the elastic analysis for unit load and by assuming an orthotropic stiffness value of 1.4. The moment coefficients in the vertical direction were multiplied by the orthotropic strength ratio, which was taken as 3 to find out the critical bending moment. He noticed that in the case of panels with top edge free, the horizontal moments always initiated cracking. In the second stage, Mohr's circle of moments was constructed to obtain the major principal moment and its inclination. The moment of resistance along the principal axis was calculated using an elliptical transition between the orthogonal values. The moment coefficients from the above two steps were compared to obtain the critical moment. He studied the test results published by HASELTINE *et al.* (1977) and found that the failure pressure lies in between that of a panel of fixed and simply supported boundary conditions when the above method is used. They claimed that partial fixity was provided in these tests. However, the method failed to predict the results by SINHA (1978) and also showed significant variation from the BS predictions. He also studied the effect of considering the orthotropic stiffness ratio

and stated that it was insignificant.

LAWRENCE (1983) carried out an experimental study on panels under bi-axial bending as part of his PhD research. Panels of various aspect ratios were tested under different support conditions. The analysis of his results showed that both the yield line and the strip method were un-conservative. He argued that the random variation in the material properties played an important role in the failure pressure and had to be considered in the analysis. But, in spite of this consideration, the analysis proposed by Baker using the 'principal moment interaction' failure criterion did not give a good agreement with the test results. The elastic plate method gave reasonably good agreement for three and four sides simply supported panels

In 1984, ANDERSON (1984) studied the effect of arching on the laterally loaded one-way spanning walls and found that such panels are capable of resisting loads in excess of their flexural strengths when satisfactory support conditions are provided. CHANDRAKEERTHY (1984) developed charts based on the BS for the design of panels that are in common use in the design offices. He showed that this saves considerable amount of time in design.

GAIRNS & SCRIVENER (1984; 1985) published two papers in which they detailed the studies on the flexural behaviour of concrete brick walls. From the wallette and the pier tests, they found that the concrete brickwork behave very similar to the reported clay brickwork in flexure. Tests were done on panels of different aspect ratios supported on three or four sides and the results were compared with various methods such as the elastic plate theory, the principal stress method, the yield line method and the strip method. It was surprising to note that even the yield line method, which generally over-estimated the load, under-estimated the failure pressure in these cases. BRINCKER (1985) carried out compression tests on brick piers at various eccentricities to study the behaviour of the horizontal and the oblique yield lines in panels. From his studies he concluded that the yield line method could be adopted for the design of panels with confidence. But his tests did not truly

represent the bi-axial forces in a panel and the above conclusion is disputable.

LOVERGROVE (1985) prepared a dimensional analysis for single leaf panels to study the effect of the thickness on the ultimate strength. A set of experimental results was used for this purpose and it was shown that the wall strength is proportional to the power of 1.36 of the thickness as against a value of 2 commonly used in the analysis. It can be seen from literature that the strength and the stiffness values of masonry vary within a wide range. It is important to mention that the material properties of masonry were completely ignored in Lovergrove's analysis. ESSAWY *et al.* (1985) developed a macroscopic finite element model incorporating both the transverse shear effects and the non-linearity due to cracking. The performance of this model has been verified by known solutions of elastic and non-linear behaviour of single and layered plates. An initial analysis showed that the model was capable of predicting the initial crack and the crack pattern for block walls under out-of-plane bending.

BAKER *et al.* (1985) presented an excellent review of the work on lateral loading at the Seventh International Brick Masonry Conference. The experimental results of LAWRENCE (1983) were analysed by various methods and it was shown that the yield line method over-estimated the results consistently. The strip method, though gave better results than the yield line method, under-estimated the failure load. The elastic plate theory also over-estimated the results for shorter panels. When all these methods failed to incorporate the random variation in strength, the same was taken into account in the finite element analysis using the failure criterion (BAKER 1982a) and gave good agreement with the experimental results.

MAY & TELLETT (1986) developed a non-linear finite element model incorporating a square failure criterion. Isotropic strength and stiffness properties were chosen and the deflections were compared with the analysis using assumed material properties and found to be in good agreement. MAY & MA (1986) replaced the square failure criterion with the elliptical criterion developed by BAKER

(1982a). Some of the test results reported by HASELTINE *et al.* (1977) were used to verify the model. Even though the deflections agreed with the theoretical predictions, some difference was seen in the failure pressure. MA & MAY (1986) modified the bi-axial failure criterion developed by BAKER (1982a) to incorporate the varying bed joint orientations using a linear relationship. 'Load-Displacement' studies were done using the above model and the one suggested by MAY & TELLETT (1986). Both were found to match well with the experimental results. HASELTINE & TUTT (1986) examined the BCRA results on different types of panels using the yield line method and the BS. The yield line method over-estimated the failure load at higher load carrying capacities. However, it was shown that the BS coefficients could be used for a wide range of panels with an adequate factor of safety. SINHA & MALLIK (1986) carried out lateral loading tests on panels using a 16-point distributed loading and reasonably close predictions were obtained using the fracture line method (SINHA 1978).

In 1987, ESSAWY & DRYSDALE (1987) presented a paper at the Forth North American Masonry Conference in which they analysed the various existing methods of design for laterally loaded masonry panels. The finite element model developed by the author (ESSAWY *et al.* 1985) is claimed to give good results for three and four sides supported panels and the same is used as a basis of comparison with the other methods. It is said that the elastic plate solutions using isotropic properties gave better results than that with orthotropic properties. Even though the yield line and the fracture line analysis were criticised for lacking a rational basis, both the methods gave good results up to an aspect ratio of 2.0, which is the practical range for panels, and over-estimated above that. The strip method under-estimated the results up to an aspect ratio of 2.0. It has to be noticed that as the above comparison is based on another finite element model, the percentage of difference given for these methods need not represent a practical comparison with the experimental cases.

ANDERSON (1987) carried out tests on more than 80 single leaf and cavity walls of various configurations by applying distributed point loading. He analysed these



panels using the elastic plate method and the yield line method with wallette strengths obtained either by tests or taken from the code. They found that the yield line method gave the most satisfactory result when compared to the elastic plate solution for panels with simple edge support and with return. They derived an empirical formula for calculating the failure load for panels with short returns.

Five papers were presented at the Eighth International Brick Masonry Conference in 1988 on lateral loading. THURLIMANN & GUGGISBERG (1988) tested eight masonry panels under transverse bending by applying normal force and moments at the supported ends. They used their results to develop an elliptical interaction failure criterion which coincided with that suggested by BAKER (1982a). It has to be pointed out that the actual wind loading and thereby the actual load distribution in a panel cannot be simulated by applying moments at the supported ends.

CANDY (1988) carried out a statistical analysis on the theoretical predictions of the available experimental results. Using a value of 3 as the orthotropic strength ratio, he found the yield line theory to be un-conservative. The predictions required substantial safety factor for the design. The strip method of analysis was done using the orthotropic ratios recommended by BAKER (1981) and found to be still on the un-conservative side. He proposed an energy line method which takes up the internal energy of the system and was shown to have improved the statistical fit greatly to the same reported set. He showed theoretically that the torsional moment plays a significant part on the strength of the panel.

FRIED *et al.* (1988) proposed the normal moment method to calculate the cracking load and the crack pattern in masonry panels. They analysed a three side supported panel with top edge free and showed that the crack originated at a corner element, which contradicted the general observation. They also compared the BS and the Australian code of practice and suggested that the difference between the predicted and actual results could be reduced when the respective methods are used to determine the wallette strengths.

LAWRENCE & CAO (1988) focused their work on the cracking load of a laterally loaded panel. Monte Carlo analysis was used to take into account the random variation in strength with a Coefficient of Variation (CV) of 0.4 to 0.05. They examined four failure criteria. An isotropic elastic analysis was carried out and the results were compared with the experimental results (LAWRENCE 1983). They found that the 'straight line interaction' and the 'principal moment/elliptical' interaction recommended by BAKER (1982b) significantly under-estimated the cracking load, whereas the 'no interaction' and the 'elliptical interaction' produced better comparison. They also noticed a drop in strength of nearly 50% by increasing the CV from 0.05 to 0.4. MANN & TONN (1988) attempted to modify the yield line theory to take into account the brittleness of masonry by giving separate consideration for the failure of the block and the bed joints. This technique was applied to some of the laboratory-tested cases and found to give satisfactory results.

BAKER (1989) addressed the various theoretical aspects of the design of a panel under uni-axial and bi-axial conditions. He also discussed the importance of tensile strength, mechanism strength, reinforced strength and pre-stressed strength in the design. PANDE *et al.* (1989) proposed an equivalent material approach to determine the elastic stress-strain relationship for masonry and was suggested to calculate the distribution of stresses in a masonry panel. The distribution of stresses in the equivalent material can be converted into stress values in the unit and the joints and can be used to assess the failure of the material.

GOLDING & MORTON (1991) attempted to simplify the design of panels by presenting the various design recommendations in a chart form which could be used for reinforced, un-reinforced and pre-stressed panels under distributed loading. They also presented some examples of the design of panels in this way. LAWRENCE & LU (1991a) studied the cracking behaviour of a panel using the finite element method by assigning random strength properties. This time, the 'principal moment/elliptical' interaction criterion was compared with the 'straight line' interaction and the former gave better results for shorter panels. The reason for this

was attributed to the torsional resistance developed in these panels which is taken into account in a 'principal moment/elliptical' interaction. They studied the effect of self-weight and hardly any influence was observed. The grid size used in the analysis was shown to affect the cracking load.

Lawrence presented two papers (LAWRENCE 1991; LAWRENCE & LU 1991b) at the First International Symposium on Computer Methods in Structural Masonry. He analysed (LAWRENCE 1991) panels with and without openings and studied the first cracking load using a finite element model combined with the Monte Carlo simulation to take into account the random variation in the flexural strength. He studied the 'principal moment/ elliptical interaction' and 'no interaction' and found that the cracking load is best predicted by the latter. This contradicted the finding of BAKER (1982b) and SEWARD (1982). But it has to be noticed that BAKER and SEWARD used the principal moment interaction mainly to calculate the failure load of laterally loaded panels, where the panel becomes inelastic after the first cracking. Also, the design based on cracking load might be highly un-economical as it was noticed by some researchers that the cracking load was as low as only 26% of the failure load in some cases. In his second paper (LAWRENCE & LU 1991b) , Lawrence showed that the bending strength of a beam and a wall could be predicted by a stochastic analysis. His analysis showed that the prism strength is only 60% of the joint strength when the CV is taken as 0.35. CHONG *et al.* (1991) further extended their work on laterally loaded panels using their finite element model with the modified failure criterion (MA & MAY 1986). They have analysed the tests of HASELTINE *et al.* (1977) and some tests carried out by one of the authors. A good correlation between the predicted and the experimental results was obtained in most of the cases for both solid panels and panels with openings. The over-estimation noticed in smaller panels were attributed to the possibility of shear failure at d.p.c.

MIDDLETON *et al.* (1991) presented a constitutive law for masonry to overcome the difficulties faced in modelling masonry as discrete elements of brick and mortar. An elastic, non-linear model was developed based on a homogenisation technique and

was used to find out the stresses in the constituent material. Comparing the results from this model with that from the discrete model showed the accuracy of the model, which can be used to save considerable amount of computer space and time.

PAPA & NAPPI (1993) developed a finite element model where they adopted a homogenisation technique to arrive at the mechanical properties of masonry from that of the components. This numerical model was evaluated by a limited number of experimental results on miniaturised panels and appeared to be satisfactory. However, it has to be mentioned that this model did not take into consideration any interaction between the horizontal and the vertical moments as suggested by other researchers.

DUARTE (1993) carried out an experimental study on the lateral strength of panels with openings. He proposed the idea of testing cross beams to study the bi-axial material behaviour and carried out tests on masonry cross beams at different aspect ratios. From his test results he arrived at a criterion for the cracking of masonry under bi-axial bending and for the failure along with the cracking. He carried out tests on panels with openings where the load on the openings was transferred as point loads at the corners. His results were analysed using the yield line method, the strip method and the elastic methods. The strip method did not correlate well with the experimental results whereas the yield line method gave very good predictions of the failure pressures. Even though the cracking load was under-estimated by the finite element method using isotropic material properties, reasonable agreement was obtained when orthotropic material properties were included in the above criterion.

At the Tenth International Brick/Block Masonry Conference, PANDE *et al.* (1994) presented a three-dimensional finite element model based on the homogenisation technique (PAPA & NAPPI 1993). Equivalent orthotropic material properties were obtained by the homogenisation. Cracks, if any, developed in the constituent material were homogenised into the neighbouring equivalent material to model their propagation. They adopted separate failure criterion for the brick and the mortar

(PAPA & NAPPI 1993). The forces in the equivalent material were converted into the constituent material and the panel was checked for cracking against the failure criterion. There was no mention of any criterion to check the ultimate failure. It was stated that the model was checked against the test results on panels of various boundary conditions and was found to be in very good agreement. Though the authors cast some doubt on assuming continuous head joints, its effect was stated to be insignificant later on. SINHA & NG (1994) presented the results on a limited number of experimental results at the same conference. They carried out tests on half scale brick wall panels and panels supported on three and four sides and showed that brickwork possesses definite strength and stiffness orthotropies. They noticed that the load was transferred from the weaker to the stronger direction after the panel is cracked and the yield line method invariably over-estimated the failure load.

NG (1996) conducted an experimental investigation on brickwork cross beams of different aspect ratios. These tests on cross beams were used to study the bi-axial behaviour of the material as this takes into account the material properties in both directions. From the results on cross beams, he developed a failure criterion and incorporated the same in a finite element program, which also considered a smeared cracking technique to model the post cracking behaviour of the material. He showed that Baker's failure criterion does not represent the actual behaviour of a material like masonry that possesses both strength and stiffness orthotropies. The panels supported on three and four sides were tested at different aspect ratios. The modified finite element with the failure criterion was able to predict these results within  $\pm 6\%$  variation. He analysed the tests done on panels with and without openings by various other researchers and showed that the finite element analysis with the failure criterion predicted the results with reasonable accuracy. This clearly showed that both the strength and the stiffness orthotropies of brickwork have significant effect on its behaviour and, hence, it is important to take these properties into account while analysing the panel for failure or cracking.

Various theoretical and experimental research that has been done in the area of

masonry panels subjected to bi-axial bending is explained in this section. The following section highlights some of the problems that can be observed in this area and suggests a possible solution to overcome the same.

### **2.3 A Discussion of Issues Concerning Masonry Under Bi-axial Bending**

It can be seen from Section 2.2 that a considerable amount of research has been done on masonry panels under bi-axial bending without any axial compression. The methods that are being widely used include the BS and the Australian code of practice and are shown to predict the results close to the experimental values. Nevertheless, the rational basis for these methods can be found questionable for applying to a brittle material like masonry. The yield line theory adopted in deriving the moment coefficients in the BS assumes rotation along certain pre-defined yield lines at constant bending moment. The plastic behaviour assumed in the yield line theory cannot develop in brickwork which is brittle in nature. The Australian code of practice is based on the strip method, where a constant bending moment is achieved along strips of the panel. The strip method is used generally for an under-reinforced concrete. The percentage reinforcement can be varied in a reinforced concrete slab according to the moment field. In un-reinforced masonry, it is difficult to achieve this behaviour. A third method that is commonly used in masonry is the elastic analysis. As explained in Section 2.2, brickwork shows distinct properties in the two orthogonal directions. A wide variation in the material properties can be seen from the results published by the various researchers. The inherent non-linearity and the complex material properties add to the complexity of the analysis. The finite element analysis incorporating the failure criterion for the orthotropic material developed by SINHA *et al.* (1997) can be seen to predict the failure pressures close to the experimental results than any other methods. However, the finite element method requires an iterative analysis and can be extremely time consuming.

Under such circumstances, it is very desirable to develop a method based on the test results that could be universally accepted for the design of masonry panel. The emergence of Artificial Neural Networks (ANNs) and their successful application in various fields including civil engineering has opened up a promising approach to solve many of the engineering problems, especially in areas where an un-identified relationship exists between the inputs and the outputs of a problem. The strength and the behaviour of masonry panels under lateral loading falls under a similar category and, hence, the same is applied for finding out the failure loads of panels with various support conditions. Of the various machine learning methods, ANNs turns out to be outstanding due to its ability to draw a hidden relationship from a complex set of data such as the case of masonry panels subjected to lateral loading. Section 2.4 details some of the successful applications of ANNs to civil and structural engineering problems.

It can also be seen from Section 2.2 that there are several cases where the BS or the Australian code of practice is able to predict the failure pressure of a panel under bi-axial bending. This can lead to a possible conclusion that these codes can be used for panels of certain material properties. As the code provides rather direct and quick solutions to problems, it is of interest to study the cases where these can be used with reasonable accuracy. Case-Based Reasoning (CBR) is another area of Artificial Intelligence (AI) that involves solving problems based on similar past solutions. CBR, by virtue of its very nature, lends itself as an extremely credible approach for domains which are not properly understood and are, thus, ill-structured and not well formalised. The ability of CBR in deriving solutions from the past experience has opened up a broad area of research in AI and is used in several applications as can be seen in Section 2.5. The application of CBR and ANNs in the current research is explained in Chapters 5 and 6.

## **2.4 Application of Artificial Neural Networks in Civil & Structural Engineering**

The potential of artificial neural networks to mimic the functioning of the brain has been utilised by researchers in mapping un-identified non-linear relationships between the given set of inputs and outputs. In civil engineering, there are several problems which are difficult to solve by the procedural computer languages. Empirical relationships have been drawn for many problems based on statistical analysis. Rule Based Expert Systems (RBMS) were developed as solutions to many existing problems. They help engineers to incorporate knowledge from the past experience. Laborious knowledge elicitation has been considered as a major drawback to RBMS. In structural design problems, the optimal design of an object requires repetition of the extensive finite element programs several times. These computational difficulties in problem solving can be overcome by the use of artificial neural networks. The following review of the literature shows how ANNs have been effectively used in solving many of the above mentioned problems in engineering.

An early application of neural networks was attempted by VANLUCHENE & ROUFEI (1990). Three civil engineering problems, which included a load location problem, a concrete beam design problem and a rectangular plate analysis problem, were chosen in this study and represented a broad range of engineering problems. Multi-layered networks with one or two hidden layers were able to predict the results for unseen problems. They observed that the net was taking a considerable amount of time in training, but obtained instantaneous results while testing. He suggested that the application of this method may be focused on problems that are difficult or time-consuming to solve. The spatial application of neural networks in computer aided design was addressed by COYNE & POSTMUS (1990) by studying a simple PDP (Parallel Distributed Processing) model. This model was used to facilitate associative reasoning and pattern mapping, where partial data was used to obtain the complete data. Though this application was simple in nature, it illustrated the potential application of ANNs in this area.



GUNARATNAM & GERO (1991) tried to improve the results of VANLUNCHENE & ROUFEI (1990) by introducing high level representation of the input variables. Reworking the above examples, they showed that the representation played an important role in the performance of networks and that domain knowledge provided a suitable representational framework within which effective learning can take place. They applied dimensional analysis to provide the required domain knowledge and dimensionless parameters were used to construct the knowledge dependent representational framework within which learning is to take place. A significant improvement in the performance of the net was observed by this modification.

HAJELA & BERKE (1991a) adopted neural networks for an optimal design of truss structures by implementing them in an automated optimal design environment. Given the displacement constraints, the problem was to obtain the cross sectional areas of the members with minimum weight. The net was used to obtain the displacement for the given members and the design was changed if the constraints were violated. A considerable amount of time was saved in such problems, where optimisation required re-analysis of the structure several times before the satisfactory design conditions were met. They also noticed an improved rate of learning over multi-layered networks in functional networks by presenting proper input enhancement to the net. Another paper was published by HAJELA & BERKE (1991b), which described the use of artificial neural networks in multi-level decomposition based strategy for the optimal design of structural systems. A multi-layered, feed-forward network was used effectively to map the co-ordination problem design variables into sub-problem optimal solutions.

A material behaviour modelling using neural networks was done by GHABOUSSI *et al.* (1991) using the available experimental results. They modelled the bi-axial behaviour of plain concrete to predict the strain increments, given the current state of stress, strain, stress increment and uni-axial cyclic behaviour of plain concrete. They suggested that such a model, when fully trained, can be incorporated into finite element programs as an alternative to the procedural representations of complex

material behaviour that are currently used.

A broad overview of the neural computing application in civil & structural design as well as analysis problems was done by HAJELA & BERKE (1992). They discussed the various types of networks and their application in several civil engineering problems. The models that were successfully adopted include back-propagation, counter-propagation, Hopfield and ART (Adaptive Reasoning Theory) networks.

GUNARATNAM AND GERO (1993) addressed some of the techniques that can be used to improve the performance of multi-layered, feed-forward networks. These included changes which can be made at different levels during the development and the application of neural networks. The inter-dependency of these different techniques is yet to be explored before their application. Another feasibility study of using neural networks in civil engineering problems was carried out by GOH (1994). The first example was to find out the ultimate bearing capacity of a square footing resting on sand and the training data was developed using an available formulae. The second example used the field data as the training set to find out the ultimate shear strength of a deep reinforced concrete beam and the results were compared with that of the conventional methods. The comparison of the results on test data using neural networks and the conventional methods indicate that neural networks can be used successfully in learning the relationship between the input and the output data. However, the percentage difference in the net prediction has to be brought down by suitable modification in the application methods. In civil engineering, there are number of problems which lack a rational solution. The second example, thus, supports the application of neural networks as a powerful tool to overcome such difficulties in the analysis and the design.

HUNG & ADELI (1994) developed an artificial neural network development environment using an object oriented programming paradigm. Some of the previously reported examples (VANLUNCHENE & ROUFEI 1990) were used to evaluate the performance of the program and their study concluded that the back-

propagation learning strategy could be applied to both simple and complex domains. Integrating such a system with a knowledge-based system for structural design can provide the capacity of creating an intelligent integrated structural design system with automated learning.

Yet another paper was published by GUNARATNAM & GERO (1994) on the improved performance of neural networks. They addressed both the domain dependent and the domain independent issues that affect the performance. The importance of high level representation of the inputs using dimensionless parameters was emphatically presented with the examples in VANLUNCHENE & ROUFEI (1990). The dimensionless representation results in a simpler mapping function and makes it possible to train the network on a smaller data set and still have the capability of reasonably accurate predictions.

Another application of neural networks in engineering is shown by JADID & FAIRBAIRN (1994) in adaptive re-meshing of idealised square shaped structures and individual triangles by using triangular elements. The training and the test set were generated using the finite element method and the model proved that this powerful tool can be used as an alternative to the finite element method, which required intensive computational effort and longer CPU time.

Several papers were published on the application of neural networks to various civil engineering problems in a special edition of the journal of computing in civil engineering. These include the use of ANNs for computing truck attributes by GAGARIN *et al.* (1994), river flow prediction by KARUNANITHI *et al.* (1994), estimating construction productivity by CHAO & SKIBNIEWSKI (1994), damage detection in structures by SZEWEZY & HAJELA (1994) and modular construction decision making by MURTAZA & FISHER (1994). Some guidelines for designing and training neural networks to simulate a structural analysis program was detailed by ROGERS (1994). In an attempt to show that neural networks can considerably reduce time in structural optimisation problems, he studied different methods of data

generation and showed that a hypercube method gave better approximation. Based on the results of this study, it appeared that an under-determined network could provide an adequate approximation of the results for a structural analysis problem.

While addressing the various misconceptions about neural networks, CARPENTER & BERTHELEMY (1994) pointed out the importance of having an over-determined training set, where the number of training pairs are more than the associated undetermined parameters in the net. A recommended value of 20-50% tends to be computationally efficient. They also emphasised the danger of having deficient design-points in the approximation.

In the first of the two-part paper, FLOOD & KARTAM (1994a) focused on the general principles and an understanding of the functioning of neural networks in the real world applications. They discussed issues such as the number of hidden layers, the nodes in each hidden layers and the number, the distribution and the format of the training patterns. They suggested some useful guidelines for arriving at optimum values for these parameters. "Problems, where the time required to generate solutions is critical, such as real-time applications that require many solutions in quick succession, mark another important area that can benefit from neural network approach". "A neural network may be used as a quick check on the solution developed by a more time consuming in-depth analysis". The second paper by FLOOD & KARTAM (1994b) focused on various areas in civil engineering which could benefit from the capabilities of neural networks. These included mapping non-linear function from a given set of input and output, modelling dynamic approach where a series of output results are required over time, transitory problems and optimisation problems. The modular approach suggested for mapping a relationship can bring down the complexity of a problem considerably. Neural network applications were found to support the optimisation problem to arrive at the initial design parameters as the lack of precision were very minor for the results and, hence, can compromise with the high computational expenses.

MUKHERJEE & DESHPANDE (1995a) presented the idea of a hybrid approach, combining ANNs and a rule base for the design of an RC single span beam. Neural networks were used to arrive at an initial design model and were proposed for the analysis during the design phase. The idea of using neural networks to obtain the initial design could be used as a means of deriving knowledge from the past experience, which is difficult to store/incorporate in any knowledge-based systems. Using the net during the analysis phase saves a considerable amount of computer time. Thus, such an approach will be a promising method to overcome the present day shortcomings of expert systems. The modelling of the initial design process using ANNs was published in more detail later on by MUKHERJEE & DESHPANDE (1995b). Though the net gave an error on the test set as high as 19.8%, it can be overlooked by the fact that the application aimed at an initial design which was modified during further analysis. They also studied the effect of damaged nodes on the performance of the net. It was shown that the net performed without any significant difference in its prediction when a maximum of two nodes were damaged in the hidden layers. But this needs to be further investigated, as all the connections in a net are not equally important.

GOH published three papers on his work on the application of neural networks to several geo-technical problems. These problems were solved mainly by empirical methods and, hence, the available field data was used for training and testing neural networks. These include the evaluation of seismic liquefaction of soil (GOH 1995a), the maximum wall displacement for braced excavations in soft to medium clays (GOH *et al.* 1995) and the prediction of ultimate load capacity of driven piles and the analysis of cone penetration tests on sand (GOH 1995b). He noticed that the reliability of the model increased with the number of input parameters. This contradicted the early observation made by GUNARATNAM & GERO (1991; 1994), where they achieved better generalisation with a reduced dimensionality. After training the net on these problems, he calculated the coefficient of correlation of the net results with the field results and found that the net gave results with better coefficient of correlation than the existing empirical methods. He used the trained net

for a parametric study on many of the problems. These papers emphasised the practical application of neural networks in civil engineering problems. It is a powerful tool to solve many of the complex non-linear problems.

LOU & PEREZ (1995) attempted to solve the linear elastic structural stiffness matrix equations used in structural analysis using a Hopfield network and BAM (Bi-directional Associative Memory) network. The similarity that existed between the energy function of the Hopfield network or the continuous BAM system and the structural energy function was exploited in this approach. A faster convergence was observed in the BAM system than the Hopfield networks or the steepest descent method. JENKINS (1995) used neural networks for the analysis of a six storey structural frame with rigid joints. The problem was simplified greatly by considering many of the variables as fixed. Though the test set gave error as high as 40%, it might be possible to reduce the same by adopting different configurations. While selecting the number of hidden layers and the training pairs, it was noticed that an over-determined net was more easily trained and gave more reasonably acceptable results. He also suggested a method to arrive at the distribution of patterns in the training set. In his opinion, a data set consisting of the corners, the mid faces and the centre of a hypercube formed by the inputs, along with some random set of data, represent a better training set.

## **2.5 Application of Case-Based Reasoning to Civil Engineering**

Case-Based Reasoning (CBR) can be seen as a process model that reuses the previous knowledge as a source of design knowledge which can be used to synthesise domain knowledge to analyse designs. It involves retrieving relevant cases and adapting the solution from a previous case. In many domains, where the design knowledge is difficult to acquire and may not be objectively available, the case-based paradigm provides a model for acquisition, organisation and reuse of specific design knowledge. Hence, there is a growing interest in using CBR approach to aid in the

design process. Some of the applications of CBR are described in this section.

WANG & HOWARD (1991) attempted to integrate CBR with a knowledge-based structural design system that combined the design-dependant and the design-independent knowledge. The cases store information about a particular previous design, including the problem specification, the final solution, the intermediate proposition, the design history, the design plan and the redesign plan. Rule-based and Frame-based methods were used to represent the abstract knowledge about problem domain and the problem solving strategies of the design-independent components. The aim of this system is to produce an integrated system that interacts with designers during the design tasks, functioning both as intelligent design assistants and as knowledge acquisition systems that record the designers' step and rationale. A past design can be applied to a similar new design problem by replaying its previous design plans and can be modified by the knowledge base module.

An example of using CBR in structural optimisation was demonstrated by ARCISZEWSKI & ZIARKO (1991). In this example, CBR was used to make predictions regarding the optimal cross sections of individual members and the total weight of a rigid steel frame based on a number of examples of optimal design. From their studies, they concluded that a knowledge-based decision tool may improve the present practice of decision making in all civil engineering domains, where decision making is of significant importance.

HUA & FALTINGS (1993) implemented CAse-based building design system through Dimensionality REduction (CADRE) to adapt building designs into new environment. They addressed some of the problems that were associated with a case-based design system and the ways to overcome these difficulties. These were mainly related to the retrieval and the adaptation of cases.

MAHER & ZHANG (1991) developed CADSYN as a structural design model, where cases were previous design situations represented by attribute-value pairs

comprising the design specifications and the resulting design description. In addition to this, the domain knowledge was represented separately as generalised decomposition and constraint knowledge. CADSYN, thus, served as a hybrid system that combined CBR with a decomposition approach, where both approaches complemented each other to provide a flexible and comprehensive model of design. In this model, a previous solution was used as a starting point for a new design situation, which was modified to resolve the conflicts caused by the differences between the original and the new contexts.

MAHER & ZHANG (1993) illustrated the working of the above model by describing how cases are organised and retrieved from the memory and how the design solutions are transformed to fit into the present situation. This was demonstrated with an example of the design of a 12-storey hotel building. The cases were decomposed into several sub-problems and each of them could be solved by further decomposition. It can be seen that the relevant case was modified at different sub-levels by checking the constraints associated with each sub-problem. Several issues in CBR, including case representation, indexing design cases and transformation of cases were also discussed.

KUMAR & RAPHAEL (1997) developed a CAase based Design from REconstructive Memory (CADREM) to generate conceptual structural design for a given layout by identifying known patterns in the layout. They addressed the issues of indexing and retrieval of cases in a case-base. The processing knowledge used in individual retrieval examples was used to create generalised retrieval methods. Thus, storing a method to reconstruct a past event enabled more effective use of the past information. They also suggested that retrieval, using retrieval methods, addresses many of the problems with the existing approaches for retrieval.



## 2.6 Scope of Current Research

In spite of the research in masonry under lateral loading for the past more than two decades, it is still considered as an area which lacks a rational design method for panels subjected to bi-axial bending. Owing to its low tensile strength and variable mechanical properties, a better understanding of its behaviour under bi-axial bending would definitely be able to ensure a highly efficient method of design. The widely used existing methods include the BS, which is based on the yield line method, the Australian code of practice which is based on the strip method and the elastic analysis. From the above review it is quite clear that even though the yield line method gives agreeable results in many cases, its application lacks a rational basis. This is due to the brittle nature of masonry which is incapable of resisting further moment at a section which has already reached its moment carrying capacity. The strip method, being an empirical method, is mainly applied to reinforced concrete slabs and casts doubt on the reliability of the Australian code of practice. The use of an elastic analysis is hindered by the disparity over the mechanical properties of the material and the use of a proper failure criterion. Apart from that, a finite element analysis takes up a considerable amount of computer space and time. The failure criterion proposed by SINHA *et al.* (1997) takes into account the strength and the stiffness orthotropies of the material and is found to give reasonably good predictions with the test results. The use of the stiffness orthotropy has been a subject of dispute by many researchers. It is felt necessary to support the proposed failure criterion by carrying out similar cross beam tests on isotropic material. The emergence of neural networks and their successful application in many civil engineering problems offers a novel method that can be adopted for the design of masonry panels. Therefore, the scope of the current research can be summarised in the following points.

1. To establish a failure criterion for an isotropic brittle material in bi-axial bending and to compare the behaviour of the isotropic and orthotropic material subjected to bi-axial bending.

2. To develop a neural network program in C++ incorporating the back-propagation paradigm.
3. To train artificial neural networks to predict the failure pressure of a masonry panel subjected to lateral loading and, thus, to obtain quick results for the design.
4. To develop a CBR (Case-Based Reasoning) model using the set of available experimental results to arrive at a rational method to find out the failure pressure of the masonry panel under bi-axial bending.
5. To develop a knowledge-based system combining neural networks and CBR model and, thus, increase the capacity of the system so that laterally loaded panel of any boundary conditions can be designed efficiently.
6. To develop moment coefficients for panels under bi-axial bending by carrying out the finite element analysis with the orthotropic failure criterion. These values will be compared with the moment coefficients recommended by the BS.

## CHAPTER 3

# THEORY AND DEVELOPMENT OF ARTIFICIAL NEURAL NETWORKS

### 3.1 Introduction

Between the 1970s and the 1980s, the Rule-Based Expert Systems (RBES) were invented based on the idea of coding knowledge into computers so that it could be consulted in much the same way as one consults a human expert (COYNE *et al.* 1990). Based on the incorporation of 'if-then' rules and logical reasoning, expert systems are able to consolidate judgement, intuition, experience and creative abilities, in addition to mere number crunching techniques. However, the difficulty in knowledge elicitation from human experts and the inability of RBES to learn from examples are viewed as serious drawbacks of the system and the research in Artificial Intelligence (AI) has now advanced beyond these. Artificial neural networks (ANNs) were developed to simulate the functioning of the human brain on a smaller scale. ANN models have been studied for many years in the fields of speech and image recognition. A multi-layered, feed-forward net with back-propagation algorithm (RUMELHART *et al.* 1986) is found to be widely used and has been successfully applied in several areas. Neural networks solve problems by learning the internal representation implicit in a set of input and output examples presented to it during training. ANNs have been successfully applied in many civil and structural engineering problems, specifically in areas of optimisation (HAJELA & BERKE 1992), material modelling (GHABOUSSI 1991), damage assessment (ELKORDLY *et al.* 1993; YEH *et al.* 1993) and in several other problems, where a particular relationship between the given input and output is un-identified. Despite its capabilities, the back-propagation suffers from several drawbacks such as slow

training and poor generalisation. A considerable amount of research has been done to resolve these problems and several modifications are proposed to the basic algorithm. After briefly discussing ANNs, this chapter deals thoroughly with a developmental methodology used in the current work. The various proposals to overcome the drawbacks of back-propagation algorithm are also outlined.

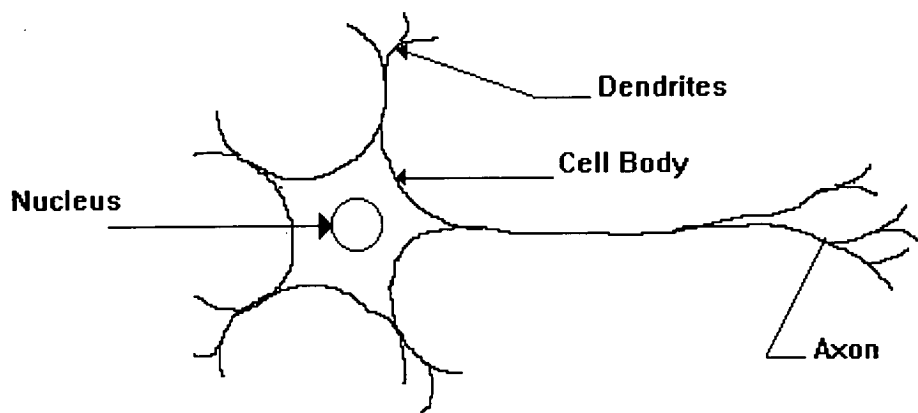
### 3.2 History of Artificial Neural Networks

The early stages of the development of ANNs date back to 1940s, where the idea of modelling the brain came into discussion. McCULLOCH and PITTS (1943) introduced the first abstract model of a neuron, the M\_P neuron, based on their understanding of neurology. The results of this model were simple logic functions and were considered to be binary devices with fixed thresholds. The limitations of this model were identified by ROSENBLATT (1958), when he designed and developed 'perceptrone' by combining the M-P neurons with the idea of adjustable synopsis proposed by HEBB (1949). The 'perceptrone' had three layers and its contribution was considered as a milestone at the time, establishing the nature of the relationship between the given set of inputs and outputs, thereby, making distinct and separate classifications. However, this development was challenged by MINSKY & PAPERT (1969). They argued that the model failed to classify non-linear functions, showing the example of the 'Exclusive Or' (XOR) problem. The research in this area came to almost a standstill until RUMELHART *et al.* (1986) developed the back-propagation algorithm to train non-linear problems using the network. Thereafter, the area of artificial neural networks has captured the imagination of several researchers and this branch of artificial intelligence has diversified into its present form.

The basic architecture and functioning of artificial neural networks can be seen in HECHT NIELSEN (1988). Neural networks used by engineers are modelled on biology, the gross structure of the brain, which is a collection of interconnected neurons.

### 3.3 Biological Neural Networks

Neural networks are computing systems that simulate the structure and the functions of the biological neural networks of the human brain. A neuron is a living cell and is characterised by many of the common features of a biological cell as shown in Figure 3.1. The cell body has several short dendrites, which receive signals, and a single axon, which transmits signals. The end of the axon is extensively branched and terminates in the dendrites of other adjacent neurons through a synaptic junction.



**FIG. 3.1 A Biological Neuron**

When a biological neuron is excited by electrical impulses, it sends out pulses through its axon and the signal is transmitted through the synopsis to the dendrites of the connected neurons. The soma (cell body) of the receiving neuron sums its electrical potential between its dendrites and is utilised to output a voltage spike along its axon. This output voltage is biologically transmitted to the part of the body associated with the particular neuron. The brain accepts and generates responses to the stimuli, partly in accordance with the genetically programmed structure, but mainly through learning, organising itself in reaction to inputs rather than by doing only what it is told (HECHT NIELSEN 1988). It is understood that human brain has approximately 100 billion neurons that are interconnected in a complex manner

constituting a large-scale network. While single neurons are interesting, it is the interaction of several neurons that make learning, recognition, discrimination and decision making possible.

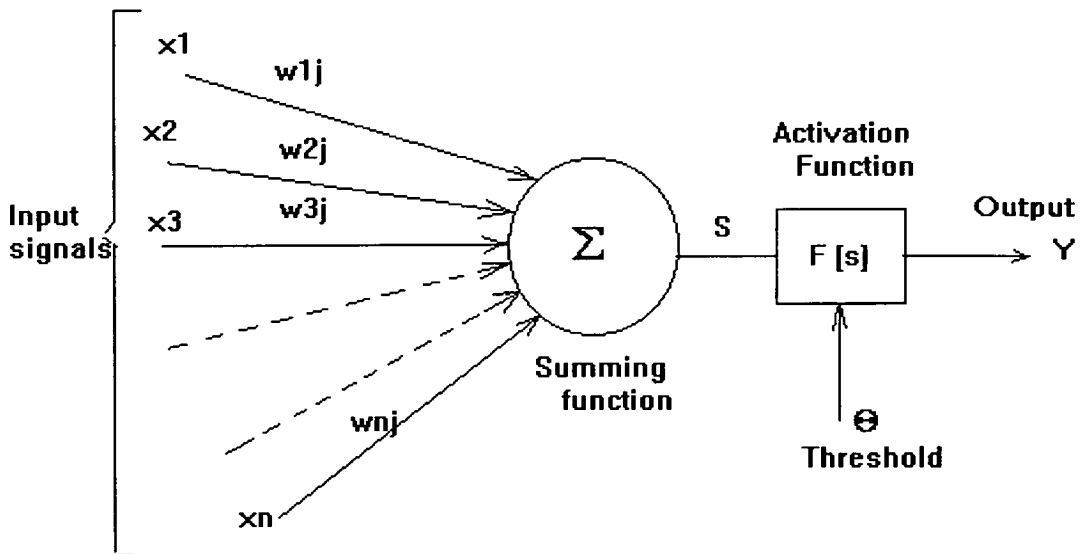
### 3.4 Neurons

Artificial neural networks (ANNs) are models based on our present understanding of the biological nervous systems and are highly simplified version of the human neural systems. Neurons (nodes) are the basic computational units of ANNs. The working of a net can be best explained with a simple processing element as shown in Figure 3.2 (HAYKIN 1994). Each element receives a set of input values  $x_1, x_2, x_3, \dots, x_n$ . These inputs are similar to the electrochemical signals received by the neuron in a biological model. In the simplest model, the input signals to an element are multiplied by connection weights. The weighted inputs are summed up (Eqn. 3.1) to form the net input to the neuron (LIPPMANN 1987).

$$S = \sum_{i=1}^n w_{ij}x_i \quad 3.1$$

In a neurobiological system, the neuron fires or produces an output signal only if the strength of the incoming signal builds up to a certain level. This is simulated in ANNs by assigning a threshold level for each processing element. The nodes are, thus, characterised by the internal threshold,  $\theta$ , and the type of non-linearity that is used to obtain the output of the node. At each processing element, the threshold is added to the net input and the sum is passed through an activation function to obtain the output signal (Eqn. 3.2).

$$Y = F[s] \quad 3.2$$



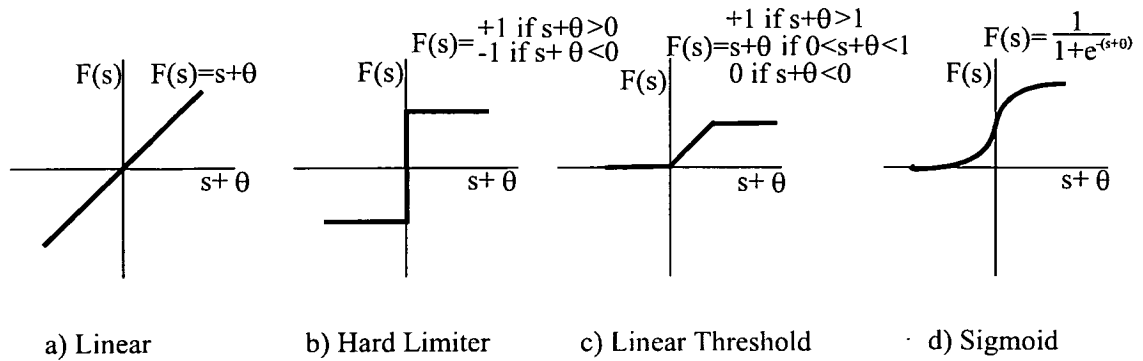
**FIG. 3.2 Model of a Single Neuron**

The most commonly used activation functions are *simple linear*, *linear threshold*, *hard limiter*, and *non-linear logistic (sigmoid)* (HAYKIN 1994; LIPPMANN 1987; KEMPKA 1994) and are shown in Figure 3.3. The *linear function* merely passes the ‘weighted’ sum of the value straight through. No squashing<sup>1</sup> occurs in this function and, hence, the range of output lies from  $-\alpha$  to  $+\alpha$ . This is generally used in the output nodes of networks due to its mathematical properties. The *hard limiter* takes a value of either -1 or +1. It offers the basic non-linear aspect required to obtain the complex behaviour expected in neural networks. The *linear threshold* is a hybrid between the linear and the *hard limiter* and is similar to the *logistic function*. The *sigmoid function* is the commonly used logistic activation function and is given by Eqn. 3.3. It is continuously differentiable at all points and provides the non-linear characteristic essential to neural networks.

$$F(s) = \frac{1}{1 + e^{-(s+\theta)}} \quad 3.3$$

where,  $\theta$  is the threshold value that is used to adjust the bias of the activation function. Artificial neural networks are group of several such interconnected neurons.

<sup>1</sup> Output of the node will be the same as the input to the node



**FIG. 3.3 Commonly Used Activation Functions**

### 3.5 Artificial Neural Networks (ANNs)

ANNs are collection of artificial neurons, which are interconnected to produce a massively parallel computational facility. There is an ‘input layer of neurons’ that receives the data from the external source and an ‘output layer of neurons’ that provides the required responses of the network. These computational elements (neurons) interact with each other through ‘weighted’ connections, which are adapted during training to improve the performance.

There are different types of neural network models that have been evolved as a result of the research in AI. They can be classified based on the type of data used for training. The input to a net can be presented either in a binary form or as continuous valued numbers. The learning takes place in a net either in a supervised or unsupervised manner, depending on whether or not the target output values for the given set of inputs are specified in the training pattern. In the supervised learning method, the user specifies the desired output the net has to learn during training along with the inputs. In unsupervised learning, the net learns to form classifications based on the patterns presented to it. Further classifications are model specific and are as shown in Figure 3.4.

A detailed description of each of the different types of models shown in Figure 3.4 can be found in LIPPMANN (1987). As multi-layered perceptrones are used in the



present study, the same will be discussed in more detail. The reason for choosing a multi-layered net is discussed in Section 3.8.

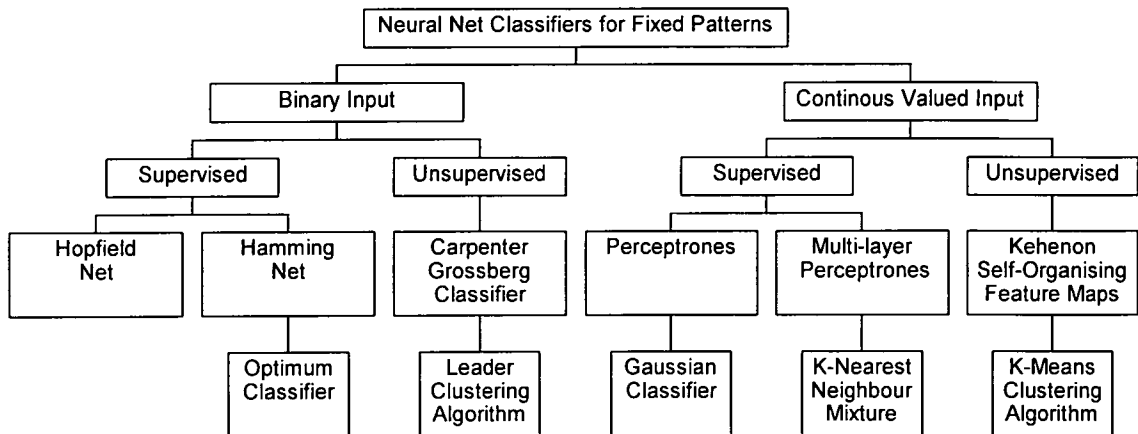


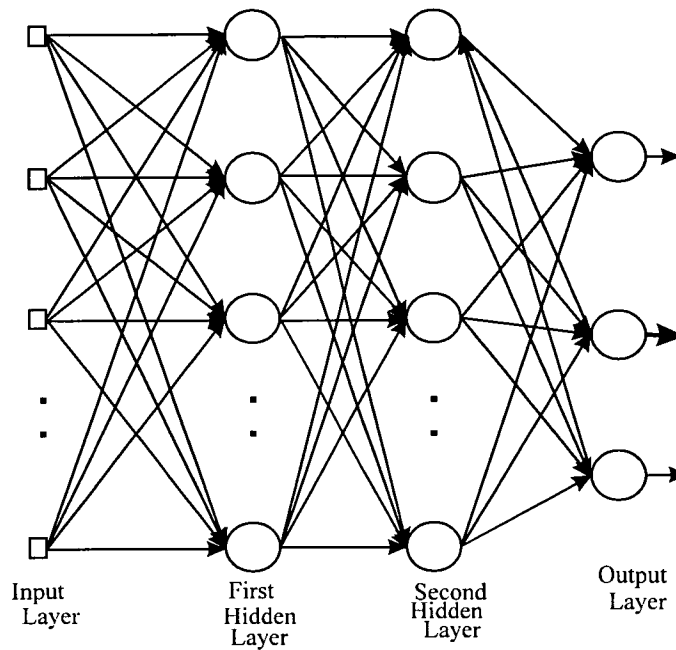
FIG. 3.4 A Taxonomy of Neural Nets (LIPPMANN 1987)

### 3.6 Multi-layered Neural Networks

Multi-layered perceptrones have been applied successfully to solve difficult and diverse problems by training them in a supervised manner, using a highly popular algorithm known as the *error back-propagation algorithm*. In multi-layered networks, in addition to the input and output layers, there are one or more intermediate layers, also known as ‘hidden layers’, which enable the network to handle complicated mapping more effectively. During training, the input data is presented to the nodes at the input layer and the output of the net is obtained from the nodes at the output layer. The hidden layers enable the functional mapping of the complex relationship between the input and the output pairs presented to the net. Basically, the error back-propagation algorithm consists of two distinct passes through the various layers of the network: the forward pass and the backward pass. In the forward pass, the data flows in the forward direction from the input layer to the output layer. In supervised learning, the net output at the end of forward pass is compared with the specified target (desired) output. An error term is calculated at the output layer on the basis of the difference between the net output and the desired

output. During the backward pass, a fraction of the computed error at each layer is propagated backward from the output layer to the input layer for modifying the connection weights. The errors at the hidden layers are calculated on the basis of the error that is transmitted from the preceding layer. These two passes are repeated several times until the Root Means Square (RMS) error at the output layer reaches a pre-defined value and this completes the training of the net.

The architectural graph of a multi-layered perceptrone with two hidden layers is shown in Figure 3.5 (HAYKIN 1994).



**FIG. 3.5 Multi-layered Neural Net with Two Hidden Layers and One Input and Output Layer**

### 3.7 Derivation of Back-Propagation Algorithm

As explained in the previous section, the back-propagation algorithm consists of two passes: The forward pass and the backward pass. At the end of the forward pass, the net output is compared with the target output and the error signals at the output

neurons are calculated. The sum of the instantaneous values of the squared errors for all the neurons at the output layer, at iteration  $n$  can be written as:

$$\xi(n) = \frac{1}{2} \sum_j (d_j(n) - y_j(n))^2 \quad 3.4$$

where,  $d_j(n)$  is the desired output and  $y_j(n)$  is the net output for the neuron  $j$ .

The average squared error,  $\xi_{av}$  over all the patterns represents the cost function and is a measure of the learning performance of the net. The objective of the learning process is to adjust the synaptic weights and thresholds so as to minimise the  $\xi_{av}$  and is done as follows. A pattern mode of training, where the weights and the thresholds are updated after presenting each pair of training pattern is considered in the derivation here. The net input,  $v_j(n)$  to the neuron  $j$  is given by:

$$v_j(n) = \sum_{i=0}^p w_{ji}(n) y_i(n), \quad 3.5$$

where,  $p$  is the total number of inputs to the neuron  $j$  and  $w_{ij}$  is the weighted connection to the node  $j$  from the  $i^{th}$  node in the previous layer, including the threshold. If  $\psi(\ )$  represents the sigmoid activation function, the output  $y_j(n)$  of neuron  $j$  at iteration  $n$  can be written as:

$$y_j(n) = \psi_j(v_j(n)) \quad 3.6$$

In the back-propagation algorithm, the correction  $\Delta w_{ji}(n)$  to the synaptic weight  $w_{ji}$

is calculated as proportional to the gradient  $\frac{\partial \xi(n)}{\partial w_{ji}(n)}$ , which can be expressed as:

$$\frac{\partial \xi(n)}{\partial w_{ji}(n)} = \frac{\partial \xi(n) \partial y_j(n) \partial v_j(n)}{\partial y_j(n) \partial v_j(n) \partial w_{ji}(n)} \quad 3.7$$

The gradient,  $\frac{\partial \xi(n)}{\partial w_{ji}(n)}$ , represents the sensitivity factor, determining the direction of search in the weight space for the synaptic weight  $w_{ji}$ .

Differentiating both sides of Eqn. 3.6 with respect to  $v_j(n)$ , we get

$$\frac{\partial y_j(n)}{\partial v_j(n)} = \psi'_j(v_j(n)) \quad 3.8$$

Similarly, differentiating Eqn. 3.5 with respect to  $w_{ji}(n)$  yields:

$$\frac{\partial v_j(n)}{\partial w_{ji}(n)} = y_i(n) \quad 3.9$$

For an output node  $j$ ,

$$\frac{\partial \xi(n)}{\partial y_j(n)} = -(d_j(n) - y_j(n)) \quad 3.10$$

Combining Eqns. 3.7 to 3.10, we get:

$$\frac{\partial \xi(n)}{\partial w_{ji}(n)} = -e_j(n) \psi'_j(v_j(n)) y_i(n) \quad 3.11$$

The correction applied to  $w_{ji}(n)$  is defined by delta rule and is

$$\Delta w_{ji}(n) = -\eta \frac{\partial \xi(n)}{\partial w_{ji}(n)} \quad 3.12$$

where,  $\eta$  is a constant called the learning parameter of the back-propagation algorithm. Substituting Eqn. 3.11 in Eqn. 3.12,

$$\Delta w_{ji}(n) = \eta \delta_j(n) y_i(n) \quad 3.13$$

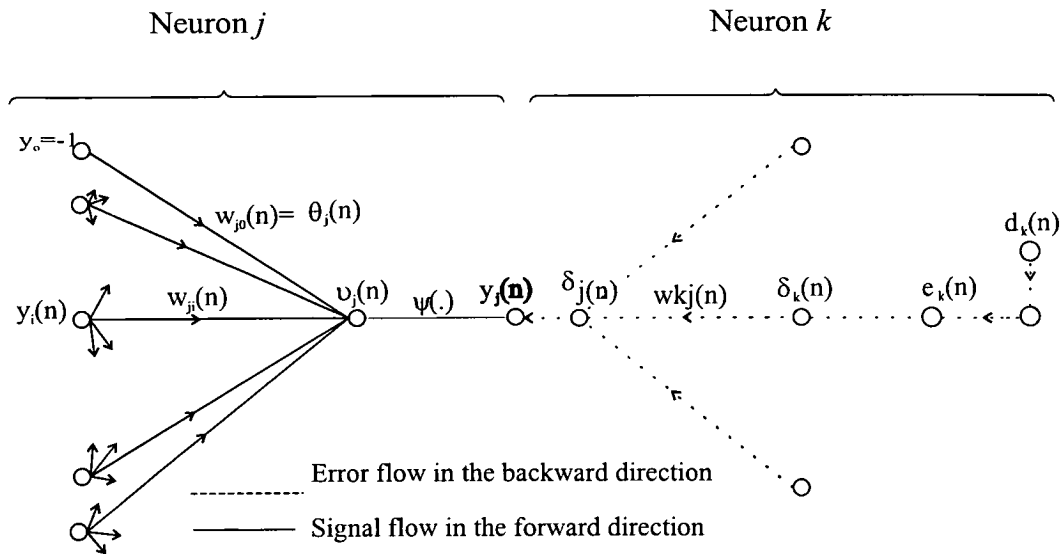
where,  $\delta_j(n)$  is the local gradient and can be written as:

$$\begin{aligned} \delta_j(n) &= \frac{\partial \xi(n) \partial y_j(n)}{\partial y_j(n) \partial v_j(n)} \\ &= e_j(n) \psi'_j(v_j(n)) \end{aligned} \quad 3.14$$

Thus, the local gradient  $\delta_j(n)$  of an output neuron can be calculated as the product of the corresponding error signal,  $e_j(n)$ , and the derivative,  $\psi'_j(v_j(n))$  of the associated activation function.

The calculation of the error signal,  $e_j(n)$ , in Eqn. 3.11 for an output neuron is relatively simple and direct as the net is supplied with the desired output for each of the training patterns in supervised training. However, when neuron  $j$  is located at one of the hidden layers, there is no desired response for that neuron and the error signal

for a hidden neuron would have to be determined recursively in terms of the error signals of all the neurons in the succeeding layer to which the hidden neuron is connected.



**FIG. 3.6 Signal-Flow Graph Highlighting the Details of the Net (HAYKIN 1994)<sup>2</sup>**

Figure 3.6 shows neuron  $j$  being fed by a set of signals and transmitting signals to another neuron  $k$ . Neuron  $k$  can be ignored and  $j$  can be considered as the output node when the error term for an output node is being calculated. The incoming signals at this neuron are used in the calculation of the error term at this node. While calculating the error term for a hidden layer node, neuron  $j$  is taken as a hidden layer node with neuron  $k$  acting as the output node. As can be seen in this figure, neuron  $j$  receives error signals from the neurons in the succeeding layer.

Hence, for a hidden node,

$$\frac{\partial \xi(n)}{\partial y_{ji}(n)} = \sum_k \frac{\partial \xi_k(n)}{\partial v_k(n)} \frac{\partial v_k(n)}{\partial y_j(n)} \quad 3.15$$

<sup>2</sup> Neuron  $j$  is considered as the output node for calculating the weight modification factor for an output node and is taken as a hidden node while calculating that for a hidden node.

$$= -\sum_k \frac{\partial \mathcal{E}_k(n)}{\partial v_k(n)} w_{kj}(n) \quad 3.16$$

$$= -\sum_k \delta_k(n) w_{kj}(n) \quad 3.17$$

From Eqns. 3.8, 3.14 & 3.17, we get the local gradient  $\delta_j(n)$  for a hidden neuron  $j$  as

$$\delta_j(n) = \psi'_j(v_j(n)) \sum_k \delta_k(n) w_{kj}(n) \quad 3.18$$

Therefore, the correction  $\Delta w_{ji}(n)$  applied to the connection weight from neuron  $i$  to neuron  $j$  in the back-propagation algorithm can be summarised as:

$$\begin{pmatrix} \text{Weight} \\ \text{Correction} \\ \Delta w_{ji}(n) \end{pmatrix} = \begin{pmatrix} \text{learning -} \\ \text{rate parameter} \\ \eta \end{pmatrix} \cdot \begin{pmatrix} \text{local} \\ \text{Gradient} \\ \delta_j(n) \end{pmatrix} \cdot \begin{pmatrix} \text{input signal} \\ \text{of neuron } j \\ y_j(n) \end{pmatrix} \quad 3.19$$

The local gradient,  $\delta_j(n)$ , depends on whether the neuron  $j$  is an output node or a hidden node and can be calculated as:

1. If neuron  $j$  is an output node,  $\delta_j(n)$  equals the product of the derivative,  $\psi'_j(v_j(n))$ , and the error signal,  $e_j(n)$ , both of which are associated with neuron  $j$ .
2. If neuron  $j$  is a hidden node,  $\delta_j(n)$  equals the product of the associated derivative,  $\psi'_j(v_j(n))$ , and the weighted sum of the  $\delta$ 's computed for the neurons in the next hidden layer or output layer that neuron  $j$  is connected to.

In the above equation, if the learning rate  $\eta$  is very small, the corresponding movement of the weight vector down the line of steepest descent will be very slow and to speed it up, a larger value of  $\eta$  is recommended. At the same time, a large value of  $\eta$  may cause oscillations across both sides of the ravines. To dampen these oscillations down, a momentum term with coefficient  $\alpha$  is introduced as:

$$\Delta w_{ji}(n) = \eta \delta_j(n) y_j(n) + \alpha \Delta w_{ji}(n-1) \quad 3.20$$

This ensures that if the weight changes were causing motion downhill last time, there will be a force on the weight changes to keep the next one moving more or less in the same direction (CAUDILL 1991a). Here,  $\eta$  acts as a “gain” coefficient and  $\alpha$  as a “damping” coefficient. When  $\eta$  and  $\alpha$  are small, the training behaviour can be speeded up by increasing  $\eta$  and counteracting oscillations by increasing  $\alpha$ . However, beyond a critical value of  $\eta$ , large momentum would have a negative effect (CHAN & FALLSIDE 1987). Larger values of  $\eta$  can lead to the build-up of large weight values, which tend to over-shoot or even lock-up units fully on or off resulting in a very slow movement along the trajectory. Too large value of momentum coefficient will dominate the weight updates and the resulting updating direction can deviate far away from the steepest descent, especially when a gentle slope is followed by a steep slope.

### **3.8 Development of an ANN Application**

While developing any neural network application, it is essential to identify the various tasks involved and assign suitable values to them. Several guidelines for developing a successful application have been suggested by researchers (BAILEY & THOMSON 1990a; 1990b; ANDERSON 1990; CAUDILL 1991a; 1991b; HEGAZY *et al.* 1994). The methodology adopted for the development in the current work is explained in this section. This involves the initial studies, the data preparation, the network architecture and the implementation as shown in Table 3.1.

#### **3.8.1 Initial Studies**

The initial Studies involve identifying the appropriate learning algorithm and its feasibility for the current problem.

**Table 3.1 Various Stages of Development of ANN Application for the Current Work.**

Initial Studies	{	<ul style="list-style-type: none"> <li>Identifying the learning algorithm</li> <li>Feasibility of the current problem</li> </ul>
Data Preparation	{	<ul style="list-style-type: none"> <li>Problem definition</li> <li>Define input and output variables</li> <li>Data collection {                             <ul style="list-style-type: none"> <li>Quality of data</li> <li>Quantity of data</li> </ul> </li> <li>Prepare the training and test set</li> <li>Preprocessing the data</li> </ul>
Network Architecture	{	<ul style="list-style-type: none"> <li>Number of inputs and outputs</li> <li>Number of hidden layers and hidden layer nodes</li> <li>Activation function</li> <li>Learning parameters</li> <li>Stopping criteria</li> </ul>
Implementation	{	<ul style="list-style-type: none"> <li>Weight initialization</li> <li>Mode of training</li> <li>Presenting the training set</li> <li>Validation of the performance</li> <li>Store the net and the weight coefficients</li> </ul>



### **3.8.1.1 Identifying the Learning Algorithm**

A thorough investigation into the various applications of neural networks in engineering sheds light on the best paradigm suitable for the current application. BAILEY & THOMSON (1990a) presented a chart specifying the relationship between the application requirements and the capabilities of a selected paradigm. Back-propagation (BP) algorithm is found to be widely used in many neural network applications (BAILEY & THOMSON 1990a; CAUDILL 1991a). Nearly 80% of the neural net applications use the back-propagation algorithm (CAUDILL 1992). The BP algorithm works well at function estimation and time series tasks, especially when the result can easily be expressed as a set of continuous variables. The BP is also good at representing complex non-linear relationships in the form of compact efficient networks (HAMMERSTROM, 1993). It is simple to conceive, easy to code in simulation and can relatively easily be trained. The approximation capabilities of a multi-layered feed-forward network was examined by HORNIK (1991) and showed that they can be used as universal approximators, provided sufficiently many hidden units are available. The supervised learning technique is recommended for pattern mapping problems, where it is required to map the unknown functional relationship between the given set of input and output patterns.

### **3.8.1.2 Feasibility Study**

The validity of an application can be determined by examining the common characteristics within the various successful applications. BAILEY & THOMSON (1990a) identified the following features of the problem that assist in inspecting the feasibility of an application.

- The application is data intensive and dependent upon multiple interacting parameters.
- Problem area is rich in historic data or examples.

- Data set is incomplete, contains errors and describes specific examples.
- Discriminator or function to determine the solution is unknown or expensive to discover.

From a survey of the successful neural network application developers, some of the preliminary heuristics for selecting an applications are found as (BAILEY & THOMSON, 1990a):

- conventional computer technology is inadequate;
- problem requires qualitative or quantitative reasoning;
- solution is derived from highly interdependent parameters that have no precise quantification;
- data is readily available, but multi-variate and intrinsically noisy or error-prone &
- project development time is short, but sufficient neural network time is available.

Apart from the above, an application can be developed for a sub-set of the actual problem. The generalisation capability of a net trained on the sub-set helps to analyse the feature extraction capability of the net in a specific situation. The success of such an application can be considered as a reliable basis for its feasibility on the current problem.

### ***3.8.2 Data Preparation***

A successful application of artificial neural networks involves preparing the most suitable data set. The development of the correct data set is generally most critical to the eventual success of the application. The task here starts with the correct definition of the problem, identifying the various input variables contributing to the output, collecting the proper data and the pre-processing of the data.

GUNARATNAM AND GERO (1991; 1993) studied the effect of representation on the performance of neural networks. They argued that dimensional analysis could be

used to reduce the dimensionality of the space in which the domain relationship is defined. They showed that an improved performance could be achieved by such dimensionless representation of the data.

### 3.8.2.1 Problem Definition

Problem definition is intended to decide upon the type of relationship the net is expected to learn and the type of data used in representing the input and the output. The four common interpretations of neural network outputs are *pattern classification*, *pattern mapping*, *functional mapping* and *optimisation*. *Pattern classification* and *pattern mapping* type application deals with binary data. In *functional mapping* and *optimisation* problems, continuous valued input and output values are dealt with. It is also possible to create binary valued inputs in *functional mapping* .

### 3.8.2.2 Define Input and Output Variables

The supervised learning requires training patterns consisting of a set of input data and the desired outputs. The training data, therefore, contains the solution of the problem that the net is expected to produce as its output. Identifying the inputs is very important as it should be able to represent the problem the net has to learn. All the possible parameters that can influence the output of the problem have to be taken into account while creating the data set. In many cases, it is advised to combine the various input parameters affecting the outputs rather than presenting them separately. The net is found to perform extremely well in situations where binary type of input is used instead of normalised continuous-valued inputs (MUKHERJEE & DESHPANDE 1995). However, it would be impractical to use binary valued data in many practical situations, where a wide range of continuous valued inputs is to be dealt with. According to CROOKS (1992) '*one goal of data preparation is to reduce the non-linearity when we know its character and leave the hidden non-linearities we do not understand for the net to solve*'. Thus, any known relationship between the

input and the output can be incorporated in the training pattern to achieve an enhanced performance. The importance of introducing hints is pointed out by several other researchers (ABU-MOSTAFA 1990; AL-MASHOUQ & REED 1991). Hints are pieces of information that we wish the network to learn. In many practical cases we do have some knowledge about the nature of the relationship. AL-MASHOUQ & REED (1991) used the 'minimum hamming distance' between the patterns as a hint and showed an improvement in training. Statistical methods can be employed to examine the importance of the variables in a problem. The relevance of a data can be judged by inspecting the raw data on the basis of the strength of correlation between the input and the output. Similarly, a strong correlation between two inputs might suggest that only one of them is required to represent the problem (HAMMERSTORM 1993).

In most of the applications, the output of the problem can easily be defined as it is the solution the researcher is aiming at and, hence, is the simplest task in the development of an application. Having defined the problem, it is the easiest part to arrive at the outputs. However, sometimes it is a practice to provide extra nodes at the output layer to facilitate easy mapping of the functional relationship between the input and output parameters (HAMMERSTORM 1993). The redundant node at the output layer may be neglected after training.

### **3.8.2.3 Data Collection**

The functional relationship the net has to learn is implicit in the training examples presented to it. Hence, the quality and the quantity of the training set contribute greatly to the success of an application.



### **a) Quality of the data**

A good training set should be well distributed within the maximum possible practical range of inputs and outputs and allow the net to learn the internal representation of the problem. It is recommended that a good training set contains routine, unusual and boundary condition cases (BAILEY & THOMSON 1990b). One measure of the data's representativeness is the breadth of the problem that the training cases cover and the salient features in the case of a continuous function. The more complete the set, the better the performance of the net. Various methods are suggested to develop an ideal training set which can improve the generalisation capacity of the net (BAILEY & THOMSON 1990a; 1990b; ANDERSON 1990; CAUDILL 1992; STEIN 1993). When the data is selected from a set of available experimental results, statistical methods help to select the best patterns out of it. Calculating the coefficient of variation between the various input and output variables or the error term gives a measure of their relative importance. Also, it is a common practice to add a small amount of noise (incorrect data) to the training set to overcome some of the problems associated with training (SIETSMA & DOW 1991). The network becomes more robust to noisy data by including noisy or erroneous data in the training set. Another important factor is the distribution of the input patterns and the target results. A clustered distribution tends to decrease the amount of data required, whereas, the subtle and overlapping features tend to increase it (HAMMERSTROM 1993).

### **b) Quantity of the data**

How much data is required is a complex issue and is often determined by practical concerns such as the cost and time of gathering data. The network can learn to ignore inputs that have little or nothing to do with the problem, provided, enough examples are supplied with. The training set should be large enough to represent the internal features and the relationships in the problem. A rule of thumb is to have five to ten training patterns for each connection weight (HAMMERSTROM 1993). JENKINS (1995) and ROGERS (1994) supported the idea of considering a 'hypercube' of all

the possible input variables. The points lying at the corners and the midpoints of each face will be able to represent the boundary values. In addition to this, a random combination of several points all over the volume of the hypercube will be sufficient to represent the internal values. ROGERS (1994) also proposed a simple formula to find out the number of training data required as  $[1+h(n+m+1)/m]$ , where  $h$  is the number of hidden layer nodes and  $n$  and  $m$  are the number of inputs and outputs respectively. The net is generally trained using two thirds of the total data set and the remaining one third is set aside as a test set. The performance of the trained net is evaluated using the test set, which essentially consists of a completely new and unseen set of problems.

#### **3.8.2.4 Preparing the Training and Test Set**

Various existing sources of information and methods can be used to generate the data set. In many cases, it is possible to use the available data, in the form of historical data or experimental results. The data set can also be created by conducting experiments or by theoretical methods. BAILEY & THOMSON (1990a) proposed the following four steps to determine the proper data sources:

- identify all the data that in any way relates to the application area;
- remove data sources that are regarded as peripheral or unreliable;
- filter out data sources that are impractical for technical or economic reasons &
- explore the methods of combining or pre-processing the data to make it more meaningful.

While preparing the data, it is helpful to examine its distribution. Like many other modelling techniques, neural networks also tend to perform much better when the input data is normally distributed (STEIN 1993). He recommended the values of the skewness coefficient and the kurtosis coefficient as a means of determining the symmetry and the dispersion of a distribution. Normally distributed samples have a

skewness coefficient in the range -0.5 to 0.5 and kurtosis coefficient in the range -1.0 to 1.0, which are calculated using Eqns. 3.21 and 3.22.

$$\text{skewness coefficient} = \frac{\sum \left( \frac{x_i - \text{Avg}(\text{all } x)}{SD(\text{all } x)} \right)^3}{\text{total number of observations}} \quad 3.21$$

$$\text{Kurtosis coefficient} = \frac{\sum \left( \frac{x_i - \text{Avg}(\text{all } x)}{SD(\text{all } x)} \right)^4}{\text{total number of observations}} - 3 \quad 3.22$$

Anomalous outliers, which are the extreme data points that may have an undue influence on the data, are another aspect to be discarded after careful examination. Outliers can be identified by methods such as the frequency histograms of individual data (STEIN 1993).

VERSAGGI (1995) proposed a method to identify and remove the conflicting data from the training set and claimed to have achieved an increase in the accuracy as nearly as 25% for binary valued data. He used the concept of an ‘epsilon ball’ to remove data which are either ‘exact match’ or ‘lose enough’ to any other data in the set. However, this contradicts the opinion of other researchers to introduce noise to improve the generalisation capacity of the net.

### 3.8.2.5 Pre-processing the Data

When using a sigmoid activation function, it is important to consider the absolute values of the data. If one of the inputs varies within a larger range and the second one within a smaller range, the fluctuation in the first input will tend to swamp any importance given to the second, even if the second has more influence on the output. All inputs should, therefore, be scaled so that they lie roughly within the same range of values to minimise this influence. Commonly chosen ranges are 0 to 1 or -1 to +1 and can be carried out by:

$$\bar{x}_i = \frac{X_i - X_{\min}}{X_{\max} - X_{\min}} \quad 3.23$$

where,  $\bar{x}_i$  is the normalised value of the input  $X_i$  and  $X_{\min}$  and  $X_{\max}$  are the minimum and the maximum values in the range of the input  $X$  respectively. At the output node, the values can be de-normalised by carrying out a reverse operation. However, it has to be pointed out that the net behaves poorly in cases where it is expected to extrapolate results from the example patterns used for the training. This is due to the fact that the net is trained to have an upper bound for the values it could predict. MUKHERJEE & DESHPANDE (1995) noticed an enhancement in the performance of the net when the input and output values are normalised within the range 0.2 to 0.8, the reason being attributed to the nature of the sigmoidal nodal function. This can be done by modifying Eqn 3.23 as:

$$\bar{x}_i = 0.2 + \frac{(X_i - X_{\min}) * 0.6}{X_{\max} - X_{\min}} \quad 3.24$$

In some cases, even though an input lies within a larger range, its variability within that range may be less. The network not only pays attention to the magnitude of the input, but also to their variability as well. CROOKS (1992) suggested the use of Z-score scaling for the inputs to overcome this problem. In Z-score scaling, the mean and the standard variation of each of the inputs in the data set is calculated. While scaling the variable, the mean is subtracted from each value and is divided by the standard variation. This method helps to partly compensate for both the different magnitude and the variability.

### 3.8.3 Network Architecture

The design of the network architecture is a very important phase in the development of any neural network application. The correct choice of the various parameters can considerably affect the learning and hence, the generalisation capacity of the net. The various parameters that are to be decided during this stage include the number of input and output nodes, size of the hidden layers and the type of activation function



to be used. It is also important to decide upon the learning parameters and the criteria used for stopping the training.

### **3.8.3.1 Number of Input and Output Nodes**

The number of nodes in the input and output layers can easily be decided based on the input and the output variables and is discussed in detail in Section 3.8.2.2. In binary inputs and outputs, the number of nodes in the input and output layers are equal to the sum of the possible values for all the input and output attributes respectively. In continuous valued inputs and outputs, the number of nodes will be equal to the number of input and output attributes. HAMMERSTROM (1993) recommended adding extra nodes at the output layer to enhance the performance of the net.

### **3.8.3.2 Size of Hidden Layers**

The hidden layers play a critical role in the operation of the multi-layer perceptrones by extracting higher orders of abstraction from the input data and, thus, enhancing the network's ability to model complex functions. The size of the hidden layers includes the number of hidden layers and the number of nodes in each of the hidden layers. It must be emphasised that the training time increases as the size of the training set and the number of layers increases and, for a very large middle layer, as the size of the middle layer increases (CAUDILL 1991a).

#### **a) Number of Hidden Layers**

A three layered net is generally preferred for most of the pattern mapping problems. Increasing the number of hidden layers augments the processing power of neural networks, but significantly complicates the learning and increases the 'black box

effect<sup>3</sup> (BAILEY & THOMSON 1990a). CAUDILL (1991a) pointed out that the error that is passed on to the hidden layers becomes less and less sensible as the number of hidden layers increases. Hence, it is a general practice to start with one hidden layer and increase it only if unavoidable (BAILEY & THOMSON 1990a; CAUDILL 1990; CAUDILL 1991a; CAUDILL 1992). CAUDILL (1991a) suggested to use the number of nodes in the hidden layers as equal to  $(2n + 1)$ , where  $n$  is the number of nodes in the input layer. The sufficiency of a single hidden layer in the multi-layered perceptrone to compute a uniform approximation to any mapping given by the input-output pairs is demonstrated by the universal approximation theorem (HAYKIN 1994). Adding multiple parallel slabs within a single hidden layer has been considered as another method to increase the processing power of the network. However, CHESTER (1990) argued that more than one hidden layer is required to achieve any arbitrary mapping when continuous valued data are dealt with. This contradicts the observation made by other researchers on restricting the number of hidden layers to only one.

#### **b) Number of Nodes in the Hidden Layers**

Determining the number of hidden nodes in the hidden layers is the most difficult part of the development of the network architecture and is determined through trial and error. Too few hidden nodes impair the network and prevent it from correctly mapping the input-output relationship. On the other hand, too many hidden nodes promote a 'table look-up'<sup>4</sup> and impede generalisation (BAILEY & THOMSON 1990a; HAMMERSTROM 1993). Hence, a critical job during training is to find a net that is large enough to learn the application, but small enough to generalise well. It is recommended to start with a suitable initial size of 75% of the number of nodes in the input layer and add more as required. If the middle layer size is too small, it can be increased by 10% each time until the desirable training is achieved. JENKINS

---

<sup>3</sup> 'Black Box' is used to represent the inability to give a logical explanation to the behaviour of the model

<sup>4</sup> 'Table look-up' is a case of simply referring to a set of data that are stored in a table

(1994) observed that an over-determined net, where the number of training patterns is greater than the number of connection weights, was able to provide an adequate representation of the problem he studied. He recommended to start with the number of nodes in the hidden layer equal to the sum of the nodes in the input and output layers. However, the middle layer size in a three-layered net is never set equal to the number of patterns, as a measure to prevent memorisation (CAUDILL 1991a).

### 3.8.3.3 Activation Function

The type of activation function to be used is another important decision to be made at the node level and is generally problem specific. BAILEY & THOMSON (1990a) presented a chart that helps to select an ideal learning paradigm. Nodes that manipulate continuous values use the linear or the sigmoid transfer function. According to HORNIK (1991), it is not the specific choice of the activation function, but rather the multi-layered, feed-forward architecture that gives neural networks the potential of being universal learning machines. But, different activation functions result in networks that train and function differently. KEMPKA (1994a) studied different types of activation functions. The various types include the *logistic activation function*, the *linear activation*, the *hard limiter* and the *linear threshold* as discussed in Section 3.4. The back-propagation requires the function to be differentiable at all points and, thus, utilises the *linear threshold* or the *logistic activation function*.

An example of a continuously differentiable non-linear activation function commonly used in the back-propagation is sigmoid non-linearity, which can be defined for a node  $j$  as :

$$y_j(n) = \psi_j(v_j(n)) = \frac{1}{1 + e^{(-v_j(n))}} \quad 3.25$$

where,  $v_j(n)$  is the internal activity of the node  $j$ . The variation of the output for the above sigmoid non-linearity is within the range 0 to 1. A hyperbolic tangent is an

example of an asymmetric non-linearity and its amplitude lies within the range -1 to +1. It is given by:

$$y_j(n) = \psi_j(v_j(n)) = \tanh(v_j(n)) = \frac{e^{(v_j(n))} - e^{(-v_j(n))}}{e^{(v_j(n))} + e^{(-v_j(n))}} \quad 3.26$$

The above two logistic functions are differentiable as:

$$\frac{\partial y_j(n)}{\partial v_j(n)} = \frac{e^{(-v_j(n))}}{[1 + e^{(-v_j(n))}]^2} = y_j(n)[1 - y_j(n)] \text{ for Eqn. 3.25} \quad 3.27$$

$$\text{And, } \frac{\partial y_j(n)}{\partial v_j(n)} = 1 - \tanh^2(v_j(n)) = 1 - (y_j(n))^2 \text{ for Eqn. 3.26} \quad 3.28$$

Several modifications to the simple sigmoid function have been recommended to improve the capacity of the network (VOGL *et al.* 1988; SCALERO *et al.* 1990; SAMAD 1990). KEMPKA (1994b) claims that combining the different activation functions helps in developing a neural net system that will train quickly.

### 3.8.3.4 Learning Parameters

The learning parameters include the learning rate and the momentum term. It is possible to modify the values of these parameters at any time during the training. The learning rate and the momentum term can be set as 0.7 and 0.9 respectively (PAO 1989). VOGL *et al.* (1988) suggested to adopt varying values for the learning parameters. The values of these parameters are modified based on the success or failure of a particular step of weight modification. MURRAY (1994) has put forward genetic algorithm techniques to select the optimal values of the various parameters associated with a neural network model.

### 3.8.3.5 Stopping Criteria

Training is carried out in the back-propagation algorithm until a well-defined stopping criterion is satisfied. It is a usual practice to train the network until a

predefined value of the target RMS error is achieved. The RMS error is calculated as the root mean squared (RMS) error of all the outputs, for all the patterns used in the training. The net can be considered to have learned the training set reasonably well when the RMS error falls in the order of  $10^{-3}$  to  $10^{-4}$  (HEGAZY *et al.* 1994). HAYKIN (1994) has looked at the work of other researchers and suggested that the convergence of the algorithm is achieved when the Euclidean norm of the gradient vector of the error surface with respect to the error surface reaches a sufficiently small value. He also suggested checking the absolute rate of change in the average squared error per epoch<sup>5</sup> to be in the range of 0.1 to 1 percent. However, a better way of assessing the training is by the method of cross validation, where the performance of the net on a test set is evaluated at regular intervals. The training of the net is stopped once the RMS error of the test set ceases to improve.

### **3.8.4 Implementation**

#### **3.8.4.1 Weight Initialisation**

The synaptic connection weights and the threshold levels are initialised within a small range of values in a uniformly distributed pattern. The incorrect choice of the initial weights can cause 'premature saturation', which is characterised by a situation where the RMS error remains almost as a constant for some period during the training (LEE *et al.* 1991). If the output value is close to -1 and the desired value is close to +1, the slope of the sigmoid activation function for the node will be very small and the net will take a lot of time to escape from it. LEE & KIM (1991) noticed that the net is less likely to enter in this situation if the number of hidden nodes is maintained low, consistent with a satisfactory operating of the net. Starting from a smaller value of the connection weights helps to avoid being trapped in any local minima. The range of the initial weights for an asymmetric hyperbolic

---

<sup>5</sup> An Epoch is a complete set of presentation of the input-output pairs to the net during learning.

activation function (as proposed by GUYON) is given as  $-\frac{2.4}{F_i}, +\frac{2.4}{F_i}$  where;  $F_i$  is the fan-in (the total number of inputs).

### 3.8.4.2 Mode of Training

The training patterns can be presented to the net either in a batch mode or a pattern mode. In the pattern mode, the weight updates are carried out after presenting each of the input-output pairs, whereas in the batch mode, the weights are updated after the complete set of data is passed forward through the network.

VOGL *et al.* (1988) claim that a step that reduces the error with respect to one pattern will not, in general, produce a network with reduced errors with respect to all the other patterns which the system is going to learn. Such a system may misdirect the optimisation path and, thus, may increase considerably the number of iterations required for convergence. Hence, the batch mode of training, where a cumulative sum of the errors are used for the weight modifications is recommended as it helps to avoid misdirecting the optimisation path that can occur in the pattern mode. The changes for each weight are summed over all of the input patterns and is applied to modify the weights only after one complete cycle. Hence, Eqn. 3.20 can be written as:

$$\Delta w_{ji}(m) = \eta \sum_p \delta_{pj} y_{pj}(n) + \alpha \Delta w_{ji}(m-1) \quad 3.29$$

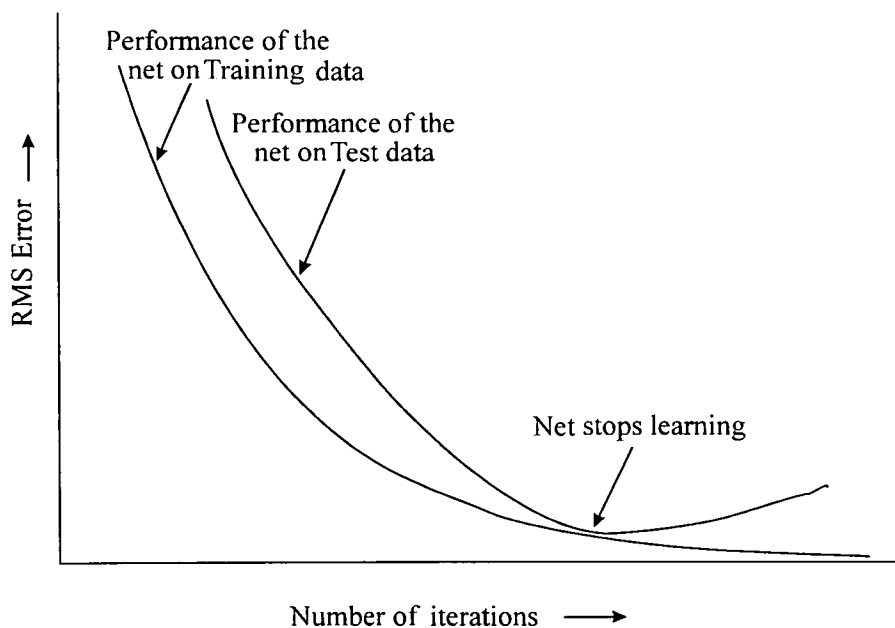
where,  $m$  represents the iteration number as opposed to presentation number  $n$  in Eqn. (3.20).

HAYKIN (1994) argues that the pattern mode of training takes less storage space for each synaptic weight and the fact that the patterns are presented to the net in a random manner makes the search in the weight space more stochastic, which reduces the likelihood of being trapped in a local minima. However, the effectiveness of the

two training modes depends on the nature of the problem at hand (HERTZ *et al.* 1991).

### 3.8.4.3 Training the Net

The training is carried out until the RMS error falls within a specified value of target error. A network can easily learn something totally different from what the developer had in mind. It can memorise the patterns instead of learning the hidden features in the training samples and mapping the functional relationship. This will result in a net, which acts as a look-up table, that can produce correct results for the cases that are used for training, but fail to produce correct results on unseen problems. Hence, an alternate way to check the training is by examining the RMS error in the test set. As can be seen in Figure 3.7, the RMS errors of the training and the test sets reduce with the number of iterations.



**FIG. 3.7 Evaluating the Performance of the Net on Training and Test Data**

After a certain period, the RMS error of the test set stops showing any improvement, while that of the training set still continues to be reducing. The net is supposed to be memorising the training set if the training is carried out beyond this stage. The

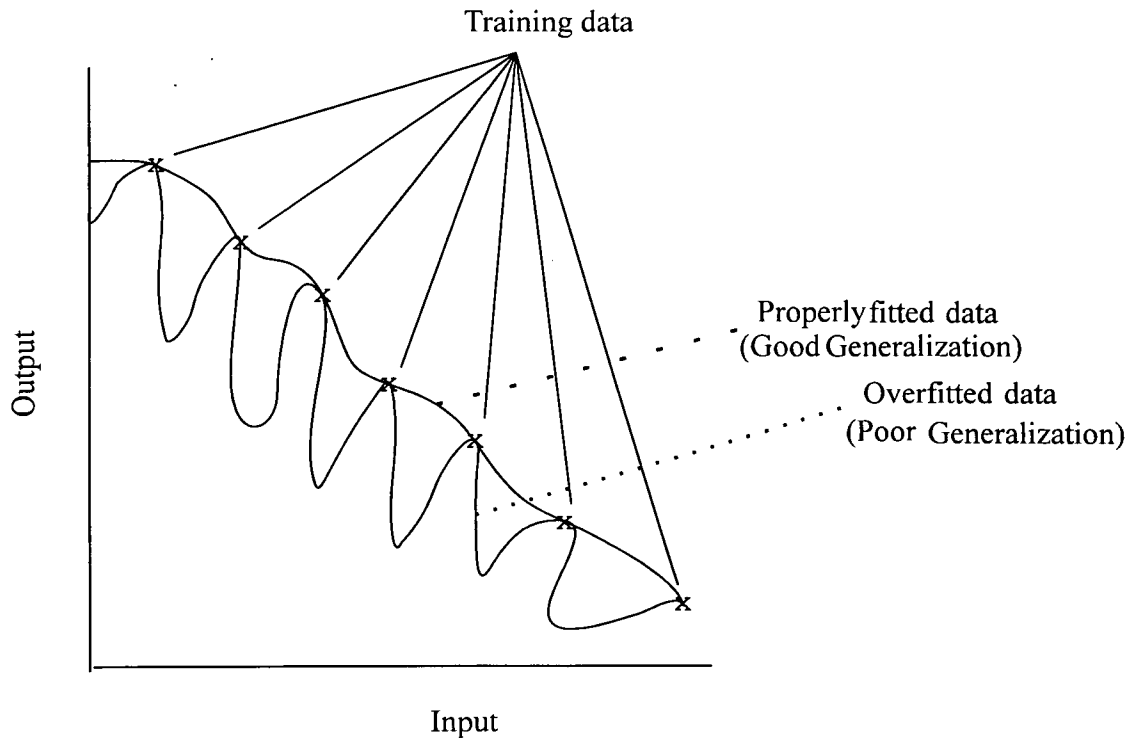
training of the net is stopped at this stage, when the RMS error of the test set ceases to improve. During the training, the net can be examined for the weights entering and leaving each node and any node without significant connections can be removed.

#### **3.8.4.4 Validation of the Performance**

The essence of the back-propagation learning is to extract the knowledge implicit in the input-output patterns presented to the net using a multi-layer perceptron to such an extent that the net learns enough about the past to generalise about the future. The training is stopped at certain intervals and the performance of the net on the test set is evaluated. The training is continued until the RMS error ceases to improve. After the training, the net must have generated a mapping between the input and the output patterns. The generalisation capacity of the net is evaluated mainly by its performance on an unseen set of data, the test set. The correctness of the neural network's problem-solving approach can be roughly determined by strongly activating any one of the input nodes and examining the output. The net output should vary proportionately according to its relationship with the modified input.

Figure 3.8 illustrates how a trained network can poorly generalise the data due to memorisation, which if properly trained, can achieve good generalisation. The figure shows that if the net is not properly trained using the patterns, it can mislead the user by producing correct results to the patterns that are used for the training. Such a net would not be able to give correct results to completely new problems, whereas a properly trained net would be able to learn the relationship between the input-output pairs presented to it and can produce correct results to any problem.





**FIG. 3.8 Generalisation in a Trained Network (HAYKIN 1994)**

#### 3.8.4.5 Store the Net

After the successful training and the validation of the performance of the net, the matrix of the weight coefficients is stored as a separate file. This matrix file can be accessed by the net any time subsequently to calculate the result for any new problem. The trained net will be able to produce the results within a fraction of a second for a new problem.

### 3.9 Drawbacks of Back-Propagation Algorithm

The back-propagation is a gradient descent algorithm that tries to minimise the mean squared error by moving down the gradient of the error curve. The error curve is generally highly complex, multi-dimensional and more or less bowl-shaped curve that has all kinds of bumps, valleys and hills, which the net must negotiate before

finding its lowest point. As a result, training the net to reach the lowest point becomes more of a challenge (CAUDILL 1991a). The commonly faced problems during training a network are:

- stabilising at local minima;
- over-training;
- network paralysis;
- dependency on initial weights &
- the 'black-box' effect.

Several methods have been recommended to improve the performance of the back-propagation algorithm. Injecting a small amount of noise<sup>6</sup> into the system helps to overcome the above drawbacks to some extent. The other methods include resetting the learning parameters and reinitialising the training process. Some heuristics used to improve the performance of the back-propagation applications as highlighted by HEGAZY *et al.* (1994) are given in Table 3.2.

### 3.9.1 Slow Training

Slow training has been recognised as one of the main disadvantages of the back-propagation algorithm. The reason for the slow training can be explained on the basis of the characteristics of the error surface being traversed. In the case of a single perceptrone with linear activation function, the error surface is in the shape of a quadratic bowl with a single minimum, which is global. For a multi-layered neural network with sigmoidal activation function, the error surface is quite harsh with large amount of flatness and extreme steepness. It is possible to come across several local minima which could be mistaken for the global and the gradient search moves very slowly along the surface.

---

<sup>6</sup> 'Noise' is a term that represents a small amount of incorrect data inserted into a data set.

**TABLE 3.2 Heuristics to improve the performance of back-propagation.**

	Back-propagation problem	Heuristic Rule
1	Local minima	Restarting: reinitialise the network weights to some new set of random values.
2	Local minima	Shaking the network weights: vary the network weights by adding to each a random number as much as 10% of the original weight range.
3	Local minima and slow training	Starting with a learning rate coefficient, $\mu$ of 0.7. This coefficient may be reduced during training or adapted dynamically.
4	Slow training	Adding a momentum term to the weight adjustment formulas. The momentum coefficient $\alpha$ is kept as high as 0.7.
5	Inadequate training and/or generalisation	Using alternative data representation and problem-structuring techniques.
6	Inadequate training and/or generalisation	Increasing the number of training patterns.
7	Inadequate training and/or generalisation	Using simulation, test results and field observations to generate examples.
8	Inadequate training and/or generalisation	Adding noise to the training examples.
9	Inadequate training and/or generalisation	Using modular neural network structure and data compression technique.
10	Inadequate training and/or generalisation	Using a network that is slightly larger than the minimum necessary to perform the job.
11	Inadequate training and/or generalisation	Use automated network optimisation techniques: genetic algorithms, pruning.

Several suggestions and modifications to the original BP algorithm have been put forth to achieve a faster training time. The main focus was on the values of the

learning parameter,  $\mu$  and the momentum term,  $\alpha$ . RUMELHART *et al.* (1986) suggested ranges of  $0.05 \leq \eta \leq 0.75$  and  $0 \leq \alpha \leq 0.9$ . Though switching between the values of these coefficients is reported to improve the speed of learning, it is problem dependent and needs numerical tuning for each problem (CHAN & FALLSIDE 1987). They also studied the different methods of optimising the choice of the coefficients by studying a vowel recognition problem and an image recognition problem. An adaptive algorithm for the learning parameter and the momentum term has been introduced for training the back-propagation algorithm and found to improve the training speed and the behaviour. They claimed that, the additional computational load required for this was insignificant and no extra storage was required over the fixed coefficient.

VOGL *et al.* (1988) suggested the following three ways of improving the speed of the back-propagation algorithm.

- Updating the network weights only after the entire patterns to be learned is presented to the network instead of updating it after the presentation of each pattern.
- The learning rate  $\mu$  is varied dynamically so that the algorithm utilises a near-optimum  $\mu$ .
- Setting the momentum term to zero at a step failed to reduce the total error and resetting it to the original value at the succeeding step of success.

The value of  $\mu$ , which modulates the step size, is sensitive to the local shape of the multi-dimensional terrain which is being traversed during the optimisation. Thus, the optimum value of  $\mu$  depends on the topography of the terrain being traversed. VOGL *et al.* (1988) proposed to vary the learning rate  $\mu$ , according to whether or not an iteration decreases the performance index (The RMS error of all the patterns). If an update results in a reduced total error,  $\mu$  is multiplied by a factor  $\phi > 1$  for the next iteration. If a step produces a network with total error more than a few percent

above the previous value, then all the changes to the weights are rejected,  $\mu$  is multiplied by a factor  $\beta < 1$ ,  $\alpha$  is set to zero, and the step is repeated and  $\alpha$  is reset to its original value when a successful step takes place. They have also explained the rationale behind the above modification as that, as long as the topography of the terrain is relatively uniform and the descent is in a relatively smooth line, the memory implicit in  $\alpha$  will aid in the convergence. When a step results in the degradation of the performance of the system,  $\alpha$  is set to zero until a step reduces the total error, so that the memory from the previous step is lost. They recommended the values of  $\phi = 1.05, \beta = 0.7$  for this modified method. The above changes were attempted on a simple 'character learning' problem and showed that it can significantly improve the convergence of problems of moderate complexity.

The back-propagation algorithm was modified by SCALERO (1990), where the non-linear functions in the network are reduced to a linear problem and solved by using Kalman filter at each layer (HAYKIN 1986). In spite of its additional mathematical complexity, this method is shown to reduce the training time by several orders of magnitude.

REZGUI & TEPEDELENLIOGLU (1990) studied the effect of the shape of the activation function used in the back-propagation algorithm. The slope of a linear soft limiter activation function was made adaptive during the training and faster convergence was observed. However, this needs further study for its application to the sigmoid activation function, which is non-linear in nature. SAMAD (1990) attempted to modify the algorithm so that similar results can be achieved with less computational effort. The derivative term in the original algorithm was replaced by a term which is constant in its central region and linearly varying elsewhere, thus reducing the computation. The results of a number of problems demonstrate that neither the derivative computation nor the continuously differentiable activation functions are necessary for the back-propagation learning. Nevertheless, further research is required on problems of continuous valued outputs, as the above study was carried out on binary outputs.

TVETER (1990) argues that by using the periodic updates of weights, a considerable amount of time and arithmetic can be saved which can reduce the training time. A substantial saving in time was achieved by replacing the sigmoid function of the back-propagation algorithm using a piece-wise linear approximation on a machine with no floating-point processor. An evolutionary network applying genetic algorithm (GA) technique is proposed by CAUDILL (1991b). The GA operations such as, reproduction, mutation and cross over are carried out on a population of nets repeatedly until a net with acceptable performance is found. Even though this technique consumes considerable memory, it is shown to be faster in training.

GUYON (1991) observed that the net with the BP algorithm learns faster when the sigmoid activation function is asymmetric instead of symmetric. He recommended the use of a hyperbolic tangent function which is biased and re-scaled as:

$$\phi(v) = a \tanh(bv) = a \frac{e^{(bv)} - e^{(-bv)}}{e^{(bv)} + e^{(-bv)}} \quad 3.30$$

The values of the constants a and b are recommended as 1.716 and 0.667 respectively. It is also advised that the desired responses should be offset by some amount away from the limiting value of the sigmoid activation function so that the algorithm does not drive the free parameters of the network to infinity and thereby slow down the learning process.

MUKHERJEE & DESHPANDE (1995) pointed out the advantage of flattening the middle portion of the sigmoid function. It is clear from Figure 3.3 that the output of the sigmoid function changes abruptly over the middle portion for a small change in the input. They suggested flattening the curve slightly as shown below:

$$F(s) = \frac{1}{1 + e^{-\alpha(s-\theta)}} \quad 3.31$$

where,  $\alpha$  is a scalar quantity slightly higher than 1.0 and is taken as 1.2.

FAHLMAN (1989) suggested to increase the derivative term in the BP algorithm by 0.1 at the output layer neurons to improve the training time. CHEN & MARS (1990) proposed to drop the derivative term altogether from the output layer and to use a different learning rate for the output layer, which is one-tenth of the value for other layers. The above two methods were studied by TVETER (1991) and observed that fudging the derivative term in improving the training time is so useful that there probably is no occasion where the original derivative term is called for. He also studied the Delta-Bar-Delta rule proposed by JACOBS (1988) and found to be working quite well. In this method, each weight will have its own learning rate and will be changed according to how well the network converges.

RIGLER *et al.* (1991) proposed re-scaling the backward error propagation to accelerate the gradient search procedure. The re-scaling applied to a layered network is the reciprocals of 6,36,216,....., applied as multipliers for each partial derivative in layers counted backward from the output nodes. When the re-scaling was applied with a modified back-propagation algorithm suggested by RIGLER *et al.* (1991), a significant reduction in the average number of iterations was obtained.

Some of the researchers suggested a modular approach to overcome the difficulties associated with training complex problems (FLOOD & KARTAM 1994). This can be done by breaking the problem down into a number of well defined and simpler sub-problems and solve each of them with a separate network.

### ***3.9.2 Stabilising at Local Minima***

Since the gradient descent always follows the locally steepest path, the BP algorithm can train the network into a local minimum that it cannot escape. This effect depends on the initial position of the weights and the path it has been following. The periodic update of weights is suggested as one of the ways to overcome being trapped in local

minima (TVETER 1990). It also allows the use of larger learning rates without getting into local minima.

By reinitialising, the net is restarted to train with a totally new set of weights. Thus, if the starting position of the network is changed far enough from the original set of weights, as the network moves down the error surface, it will skirt whatever local problems it could not scale at the first time. Sometimes, simply starting with a new set of random weights is enough for minor problems. Another way is to modify the weights in the network by randomly moving them to a new position on the error surface, one not too far from the current position, but far enough from the trap that it can side-step down the surface. As a rule of thumb, the weights can be varied by adding a random amount, which is 10% of the original weight range (CAUDILL 1991a).

### ***3.9.3 Generalisation***

SIETSMA & DOW (1991) investigated the relationship between the network structure and the ability of the net to generalise from the training set and the effect of noise on the generalisation. From their study, they concluded that the net, when started with a size larger than the minimum required to perform the task, could be pruned to produce a net with better generalisation capacity. They applied pruning at stages and this, along with the noise distorted inputs, created a more stable and robust network, which uses more of the available units and produced surprising improvements on the ability of the net. Their study was mainly on binary data. Hence, the impact of the above suggestions on continuous valued data has to be investigated further. Also, it would be of interest to study the amount of noise to be applied to this type of data.

HAJELA & BERKE (1991a) proposed the clustering of the training patterns to achieve a faster training and more accurate outputs. They presented the training pairs



as a N-dimensional feature space, where similarities existed amongst the selected members. They grouped the training patterns into several clusters and each group was trained separately by a different network, which consumed less time due to the reduced number of input - output pairs and the strong similarity in the patterns.

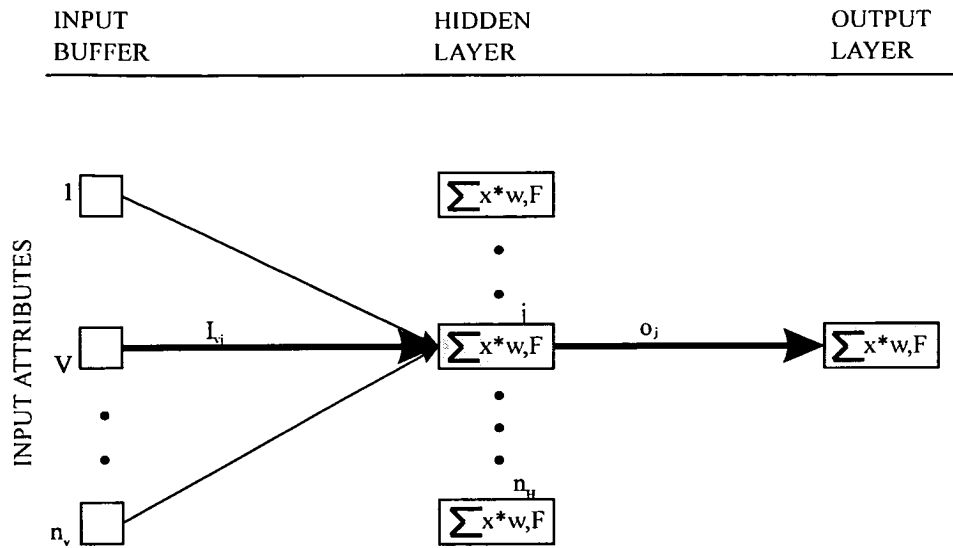
### 3.9.4 Interpretation of Connection Weights

One other drawback of neural networks can be attributed to its black box effect. It is difficult to explain the function it learns from the examples during the training. GARSON *et al.* (1991) developed a simple, but innovative technique to overcome this drawback by looking at the connection weights.

The connection weights from the input layer to the hidden layers and from the hidden layers to the output nodes are used to explain the relative importance of each of the input-attribute to the output used in the training. GARSON *et al.* (1991) used Eqn. 3.32 to evaluate the relative importance of attribute V, through a process of partitioning the output layer connection weights, for a three layered network with one hidden layer, into components associated with each input attribute.

$$\frac{\sum_j^{N_H} \left( \frac{I_{Vj}}{\sum_k^{N_V} I_{Vj}} O_j \right)}{\sum_i^{N_V} \left( \sum_j^{N_H} \left( \frac{I_{Vj}}{\sum_k^{N_V} I_{Vj}} O_j \right) \right)} \quad 3.32$$

where the variables are as shown in Figure 3.9.



**FIG. 3.9 Partitioning Output Layer Weights into Components Associated with Input Attributes.**

The above process can be well illustrated for a three-layered network by the following simple steps (Figure 3.9). The connection weights of a three-layered network shown in Figure 3.9 can be written in a matrix form as:

$$\begin{bmatrix}
 & \text{input1} & \text{input2} & \text{input3} & \text{output1} \\
 \text{Hidden1} & w_{11i} & w_{21i} & w_{31i} & w_{11o} \\
 \text{Hidden2} & w_{12i} & w_{22i} & w_{32i} & w_{21o} \\
 \text{Hidden3} & w_{13i} & w_{23i} & w_{33i} & w_{31o} \\
 \text{Hidden4} & w_{14i} & w_{24i} & w_{34i} & w_{41o}
 \end{bmatrix}$$

1. For each hidden neuron, divide the input-hidden connection weight by the sum of the input-hidden layer connection weights for all the input nodes and multiply this ratio by the hidden-output node connection weight. i.e.

$$R_{11} = \frac{w_{11i}}{w_{11i} + w_{21i} + w_{31i} + w_{41i}} \times w_{11o} \quad 3.33$$

2. For each neuron, sum the values of  $R_{ij}$  obtained in the above step. Thus we have,

	<i>input1</i>	<i>input2</i>	<i>input3</i>
<i>Hidden1</i>	$R_{11}$	$R_{12}$	$R_{13}$
<i>Hidden2</i>	$R_{21}$	$R_{22}$	$R_{23}$
<i>Hidden3</i>	$R_{31}$	$R_{32}$	$R_{33}$
<i>Hidden4</i>	$R_{41}$	$R_{42}$	$R_{43}$
<i>Sum</i>	$S_1 = R_{11} + R_{21} + R_{31} + R_{41}$	$S_2 = R_{12} + R_{22} + R_{32} + R_{42}$	$S_3 = R_{13} + R_{23} + R_{33} + R_{43}$

3. Now, divide the value  $S_i$  by the sum of the values for all the inputs to express it as a percentage and this value give the relative importance of the input node to the concerned output.

$$\text{i.e. relative importance} = \frac{S_1}{S_1 + S_2 + S_3} \times 100 \quad 3.34$$

### 3.10 Development of Neural Network

An artificial neural network software has been developed in C++ incorporating many of the features described in this chapter. A user interface is also developed to interact with the program more efficiently. A brief description of these is given in this section. The flow chart given in Figure 3.10 shows the steps involved in training the net for the given set of input and output. Separate programs are developed for each of the functions shown in the flow chart. The programming code developed for the various functions are given in Appendix VII.

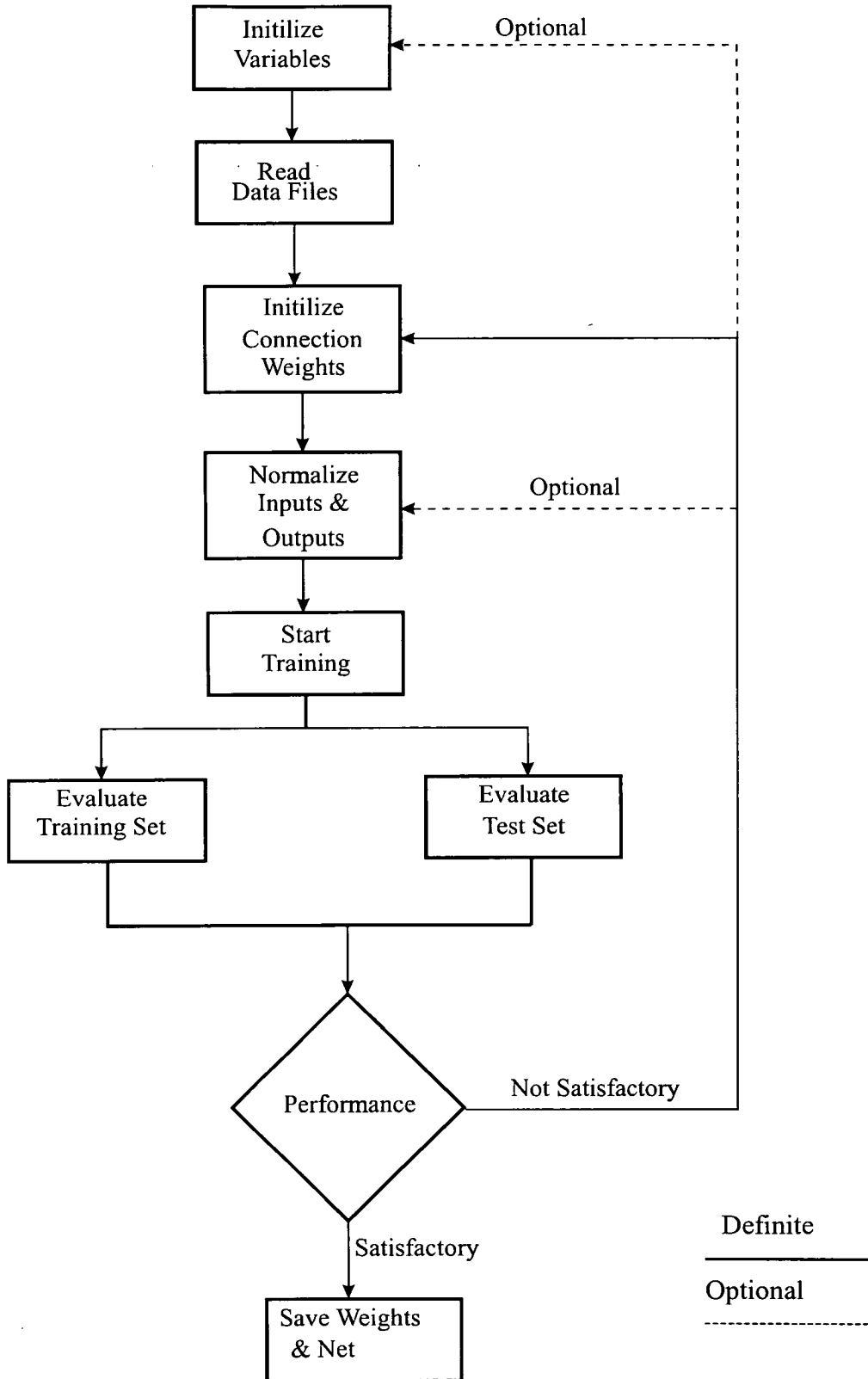
#### 3.10.1 User Interface for Neural Network

A satisfactory user interface is an essential part in developing an application using neural networks. This allows easy and friendly communication between the user and the program. While developing the neural network application, the user should have easy access to make modifications to the variables and transfer these modifications to the various functions. Also it should be possible to halt training temporarily and view the performance of the net on the training as well as the test data. The interface

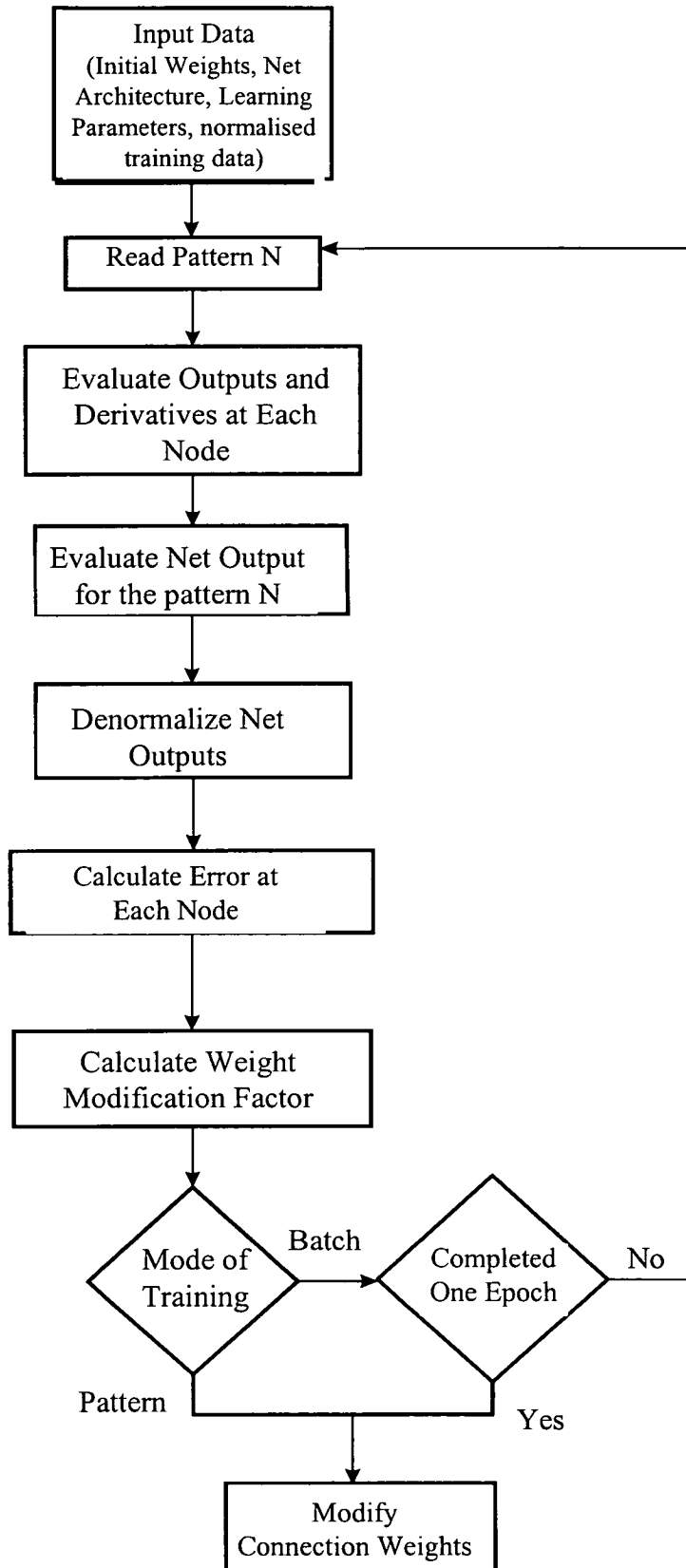
developed as part of this project is given in Appendix IV. The various features that can be exploited in this are also explained in this appendix. The various inherited classes in Microsoft foundation class (MFC) libraries are used to develop the interface and are integrated with the main program.

### ***3.10.2 Neural Network Program***

The main neural network program is accessed from the 'Control Panel' menu using the 'Start Training', 'Test Training Set' or 'Test Test Set'. The program is split into several functions and these are executed from within the main program. The object-oriented approach of programming using the classes and the inherited classes is adopted to develop the program. Figure 3.11 shows the flow chart of the main program. This shows the functions that are executed up to a single weight modification. After each weight modification, the performance of the net is evaluated against the criterion defined by the user and several cycles of these functions are carried out until satisfactory performance is obtained.



**FIG. 3.10 Flow Chart Showing the Steps Involved in Training the Neural Network for a given set of Data**



**FIG. 3.11 Flow Chart of the Neural Network Program (Direction of Flow Up to Single Weight Modification)**

### **3.11 Summary**

After giving an introduction to the theory and the development of artificial neural networks, this chapter explains the development methodology adapted in the current work for training neural networks for a specific problem. The steps that are followed for a successful training are explained in detail. Some of the drawbacks are also highlighted along with some heuristics to improve the performance of a net during training. The connection weights of a trained network are used to establish the relative importance of the input variables to the output variables. A neural network program is developed in C++ with a friendly user interface using the Microsoft foundation class (MFC) libraries.

## CHAPTER 4

# INVESTIGATION OF THE BEHAVIOUR OF AN ISOTROPIC MATERIAL UNDER BI-AXIAL BENDING

### 4.1 Introduction

Cladding panels are constructed out of isotropic or orthotropic material such as concrete or masonry. Under lateral loading, such panels are subjected to uni-axial or bi-axial bending depending on their support conditions and rely mainly on their flexural strength to resist these forces. When the panel is supported on the two opposite sides, it is under uni-axial bending and the failure load can be calculated using simple theory of bending based on static equilibrium. However, when the panel is supported on three or four sides, it is subjected to bi-axial bending and the calculation of the failure load requires a detailed understanding of the strength and the stiffness properties of the material. It is essential to consider the behaviour of the material under bi-axial bending while analysing such panels. Hence, the proper evolution of a failure criterion under bi-axial bending is imperative before any mathematical solution can be proposed.

A novel idea of testing cross beams (SINHA *et al.* 1997) has been proposed to study the fundamental behaviour of a material under bi-axial bending. In this research, a total of 15 cross beam tests were carried out on an isotropic material to study the behaviour of the material when subjected to bi-axial bending. Cement : sand mortar, which is isotropic in strength and stiffness, was chosen for this study. The test results on the isotropic cross beams are compared with that of the orthotropic cross beams to study the behaviour of the two types of materials under bi-axial bending. A total of four mortar panels, simply supported on three or four sides, were also tested in order to validate the behaviour of the panels subjected to lateral loading due to wind.



After discussing the properties of the material used in the research, this chapter is divided into two major sections. In the first section, the cross beam tests are described and are used to develop a failure criterion for an isotropic material under bi-axial bending. In the second section, the panel tests are discussed.

## **4.2 Properties of Materials**

Tests were carried out on cement : sand mortar cross beams and panels to study the behaviour of the isotropic material under bi-axial bending. All the specimens were built using rapid hardening cement at the same mix proportion of 1:3 (Cement : Sand by weight), with a water cement ratio of 0.6. Control specimens were built along with all the test specimens to determine the material properties. A minimum of 3 samples of beams (21 in total) and cubes were tested wherever possible for each set to find out the properties. The exact number of these tests can be seen in Tables 4.1 to 4.3.

### ***4.2.1 Compressive Strength of Mortar***

100 mm x 100 mm x 100 mm cubes were tested to obtain the compressive strength (Table 4.1). The average compressive strength was found to be 19.56 N/mm<sup>2</sup> for the first batch of cement. For the second batch, the compressive strength varied from 25.27 N/mm<sup>2</sup> to 29.45N/mm<sup>2</sup> with an average of 26.5 N/mm<sup>2</sup>.

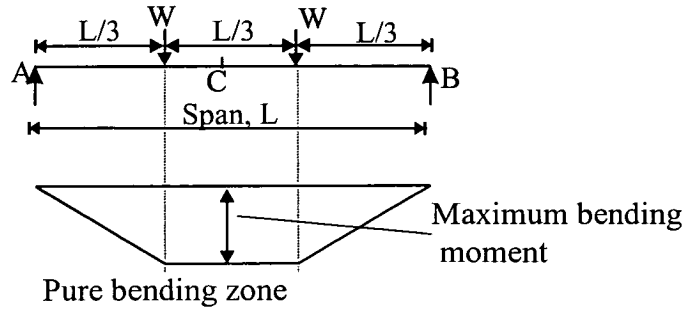
**Table 4.1 Compressive Strength of Mortar Cubes**

Cross Beam/ Panel	Mortar Cube	Compressive Strength N/mm <sup>2</sup>	Average Strength N/mm <sup>2</sup>
CB(1-3)	1	19.2	19.56
	2	17.8	
	3	21.6	
	4	18.6	
	5	20.6	
CB 4	1	29.3	29.45
	2	29.5	
	3	29.0	
	4	28.7	
	5	30.2	
	6	30.0	
CB 5	1	28.1	25.87
	2	25.8	
	3	24.5	
	4	25.9	
	5	25.9	
	6	25.0	
P-1 & P-2	1	25.4	25.27
	2	25.6	
	3	24.8	
P-3	1	22.2*	25.95
	2	25.6	
	3	26.3	
P-4	1	26.7	25.97
	2	25.4	
	3	25.8	

\*This value was not considered as it falls below 10% of the average.

#### ***4.2.2 Modulus of Elasticity and Flexural Strength***

Beams (30 mm x 30 mm x 300 mm) were tested under two-point loading as shown in Figure 4.1 to obtain the flexural strength and the initial tangent modulus of elasticity. The above test results are given in Tables 4.2 & 4.3 respectively. Electrical strain gauges were used to measure the tensile and the compressive strains at the centre of the beam (at point C) as shown in Figure 4.1 at various incremental loading.



**FIG. 4.1 A Beam Subjected to Two-Point Loading**

Under such loading condition, the maximum bending moment in the beam can be given by:

$$M = \frac{WL}{3} \quad 4.1$$

and the stress is,

$$\sigma = \frac{M}{Z} = \frac{WL}{3Z} \quad 4.2$$

By Hooke's law,  $E = \frac{\text{Stress}}{\text{Strain}}$

$$\text{Hence, } E = \frac{WL}{3Z\varepsilon} \quad 4.3$$

The initial tangent modulus of elasticity was also obtained from the deflection measurements. The deflection of the beam at the centre and the supports were measured by dial gauges. The maximum deflection at the centre is given by:

$$\delta_{\max} = \frac{23WL^3}{648EI} \quad 4.4$$

By re-arranging the above equation, E can be obtained as:

$$E = \frac{23WL^3}{648I\delta_{\max}} \quad 4.5$$

where, M is the bending moment,

W is the applied load,

L is the span of the beam,

Z is the section modulus,

$I$  is the second moment of area,

$\varepsilon$  is the measured strain,

$\sigma$  is the bending stress in the beam and

$\delta_{\max}$  is the maximum deflection at the centre.

**Table 4.2 Flexural Strength of Mortar as Obtained from the Beam Test**

Cross Beams/ Panel	Beam No.	Flexural Strength N/mm <sup>2</sup>	Average Flexural Strength N/mm <sup>2</sup>
CB (1-3)	1	4.29	4.11
	2	3.99	
	3	3.73	
	4	4.29	
	5	4.203	
	6	4.203	
CB 4	1	4.22	4.25
	2	4.48	
	3	4.31	
	4	4.0	
	5	4.12	
	6	4.35	
CB 5	1	4.49	4.14
	2	4.1	
	3	4.01	
	4	3.94	
P-1 & P-2	1	3.90	4.12
	2	4.3	
	3	4.16	
P-3 & P-4	1	4.62	4.64
	2	4.66	

The stress-strain relationship used to obtain the initial tangent modulus is given in Figure 4.2. The load-deflection relationship is given in Figure 4.3. The slope of these curves was used to calculate the initial tangent modulus of elasticity and are given in Table 4.3. It can be seen from the table that the moduli of elasticity calculated from the above two methods are almost the same. It can also be seen from Figures 4.2 and 4.3 that the stress-strain and the load-deflection relationships are linear and the material behaved elastically up to the failure.

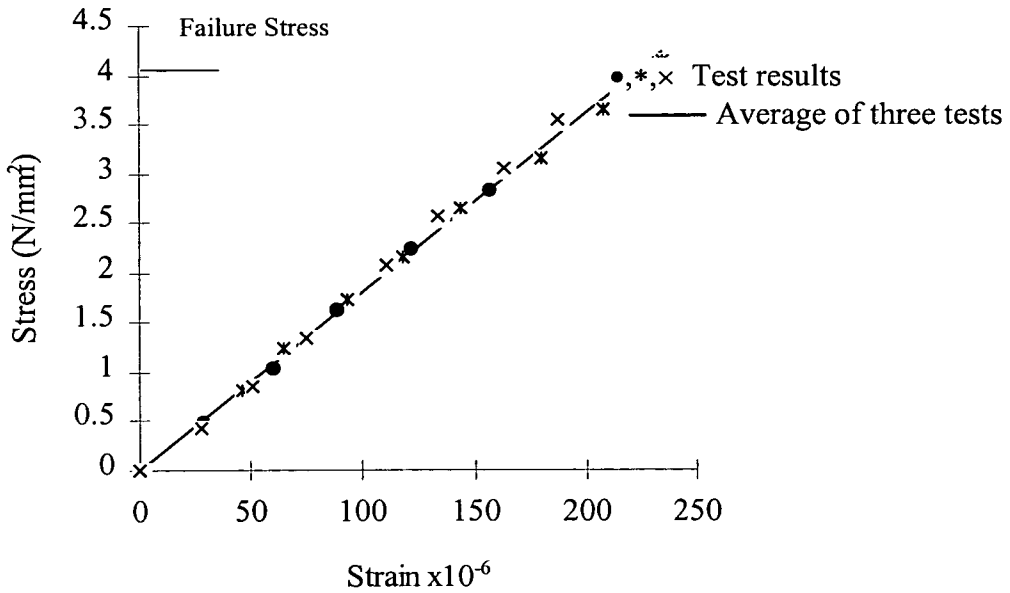


FIG. 4.2 Stress-Strain Relationship for the Mortar Specimens

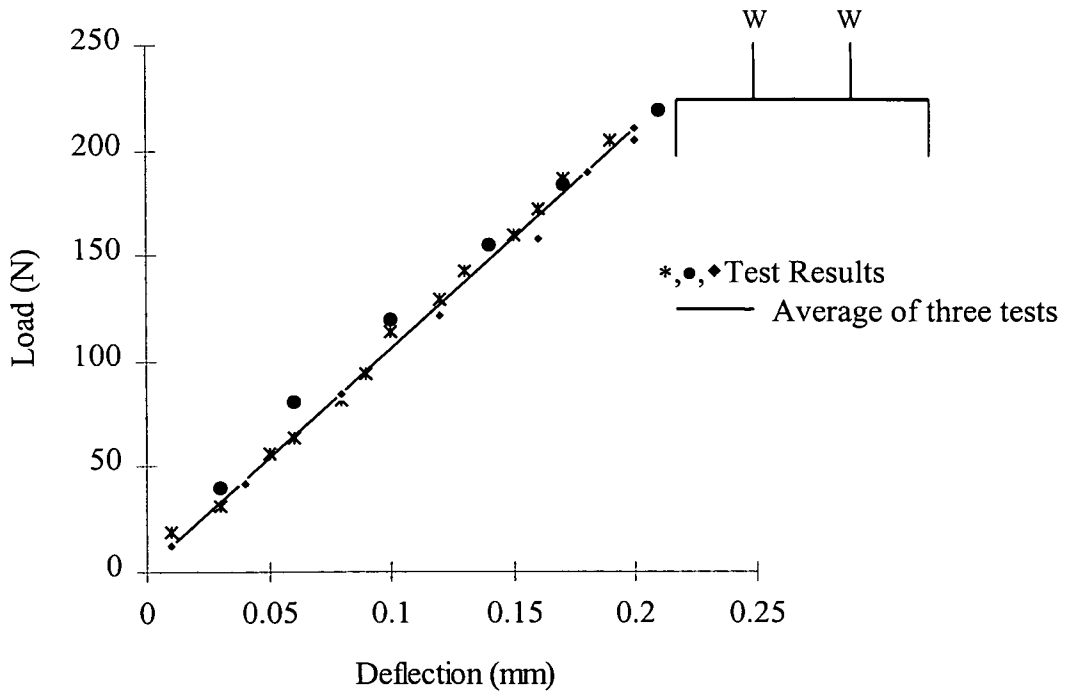


FIG. 4.3 Load-Deflection Relationship for the Mortar Specimens

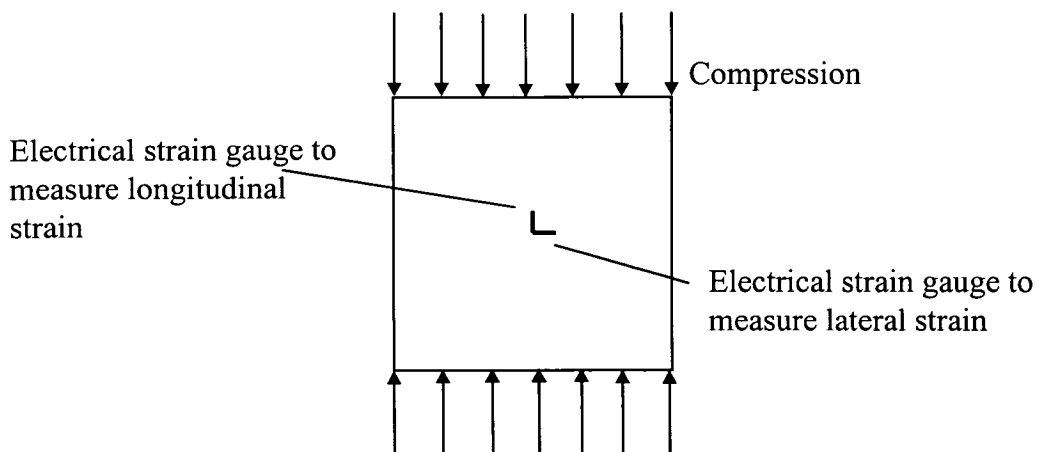
**Table 4.3 Modulus of Elasticity and Poisson's Ratio of Mortar**

		Beam		Average
Initial Tangent Modulus N/mm <sup>2</sup>	From Strain Measurements	1	17563	18328
		2	18773	
		3	18647	
	From Deflection Measurements	1	18136	18444
		2	17333	
		3	19570	
		4	18735	
Poisson's Ratio		1	0.13	0.137
		2	0.15	
		3	0.13	

**4.2.3 Poisson's ratio**

The Poisson's ratio was obtained from the compression test as shown in Figure 4.4. The strain was measured using electrical strain gauges parallel and perpendicular to the direction of applied load. The stress-strain relationships were linear for both the longitudinal and the lateral strains as given in Figure 4.5. The Poisson's ratio was obtained as a ratio of the lateral strain to the longitudinal strain as:

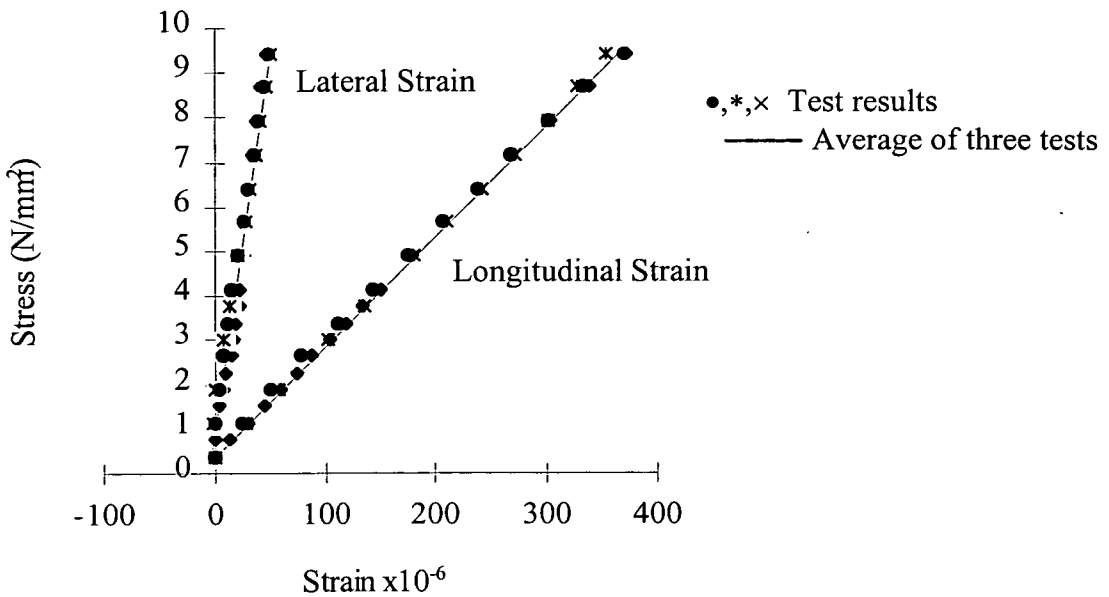
$$\nu = \frac{\text{Lateral Strain}}{\text{Longitudinal Strain}}$$



**FIG. 4.4 The Experimental Set-Up to Obtain the Poisson's ratio**

The modulus of elasticity was also calculated from the compression test and the

average value was found to be 25000N/mm<sup>2</sup>. However, the value obtained from the flexural test was considered in analysing the beams and the panels.



**FIG. 4.5 Stress-Strain Relationship for a Mortar Specimen**

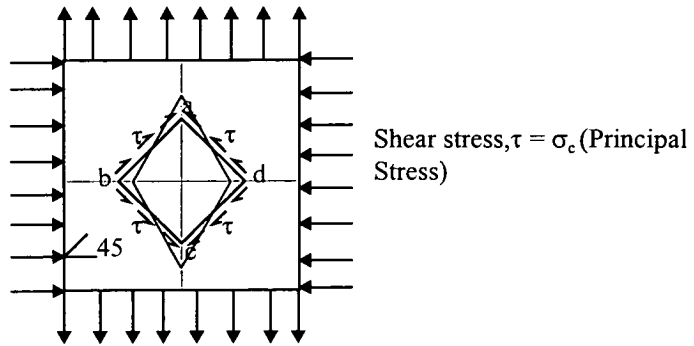
#### 4.2.4 Shear Modulus

The shear modulus of the material was also obtained by carrying out a simple test on a mortar specimen as shown in Figure 4.6. An equal amount of compressive and tensile stresses was applied simultaneously on the opposite edges of a rectangular mortar specimen of dimensions 170 mm x 170 mm x 31 mm (Figure 4.6).

Under such loading, the element ‘abcd’ which is at 45<sup>0</sup> inclined to the principal axes will be under pure shear. It can be shown that the shear stress along the plain would be equal to the principal stress and the shear strain would be equal to 2 times the principal strain. Thus, in order to obtain the shear modulus, the strain in the direction ‘ac’ and ‘bd’ were measured at various stages of loading. The shear strain can be obtained as:

$$G = \frac{\sigma}{2\varepsilon} = \frac{\tau}{2\varepsilon} \tag{4.6}$$

Shear stress,  $\tau = \sigma_t$  (Principal Stress)



**FIG.4.6 Application of Equal Compressive and Tensile Stresses on a Rectangular Plate to Obtain the Shear Modulus**

where  $\sigma$  is the principal stress,  $\epsilon$  is the measured principal strain and  $\tau$  is the shear stress. The shear modulus obtained from the above experiment was  $7800\text{N/mm}^2$ . It was observed that the experimental value of the shear modulus was only 70% of that obtained theoretically from the relationship:

$$G = \frac{E}{2(1 + \nu)} \quad 4.7$$

where  $E$  and  $\nu$  were obtained from the experiment used to calculate the Poisson's ratio (Figure 4.4). This clearly shows that plain mortar is weak in torsional resistance and the shear modulus is less than that obtained from the elastic theory. However, the measured strains were comparatively low: The values were only 2-3 times the least possible measurement of the instrument used to read the strain. Hence, a second type of experiment was carried out by applying torsion on both the ends of a rectangular specimen. The angle of twist was measured at different values of applied torque. The shear modulus can be obtained from the equation:

$$G = \frac{Tl}{K_2 b^2 d \theta} \quad 4.8$$

where  $T$  is the applied torque,  $l$  is the length of the specimen,  $b$  and  $d$  are the cross sectional dimensions of the specimen and  $K_2$  is a constant obtained from a given table (TIMOSHENKO 1962). The experimental value of the shear modulus was compared with that obtained from the theoretical relationship (Eqn. 4.7), where the



modulus of elasticity obtained from the flexural test was used. The shear modulus obtained from the torsion test was  $2353\text{N/mm}^2$ , which was only 30% of the theoretical value obtained from Eqn. 4.7.

### **4.3 Cross Beams Tests**

An experimental investigation has been carried out on cross beams to study the behaviour and to establish a failure criterion for an isotropic material under bi-axial bending.

#### ***4.3.1 Construction of Cross Beams***

The mortar cross beam tested and studied in this research is shown in Figure 4.7. A similar brickwork cross beam as shown in the figure was used to compare the behaviour of the orthotropic and the isotropic materials. Each cross beam consisted of a central portion for which the material property was to be studied and four arms connected to it as shown in Figure 4.7. The arms of the isotropic cross beams were made of high strength mortar (epoxy resin : sand mortar ) to prevent the premature failure of the arms, either in bending or in shear. Each arm was made up of four finger-like beams of the same thickness as the central part and was connected to the central portion leaving a gap in between as shown in the figure, thus, allowing the propagation of cracks.

In mortar beams, the arms were completely made of epoxy sand mortar. Such cross beams were cast in two stages. The arms and central portions were cast separately and were cured under water. The central portion was glued to the arms using epoxy resin at least 7 days before testing to allow proper bond between the two parts. As the arms were made of epoxy resin, they were repeatedly used for specimens of all aspect ratios by reducing the size each time. This allowed the reuse of the arms, thus, saving the material and the cost of construction. Figure 4.8 shows a mortar cross

beam ready for testing, with the arms glued to the central portion.

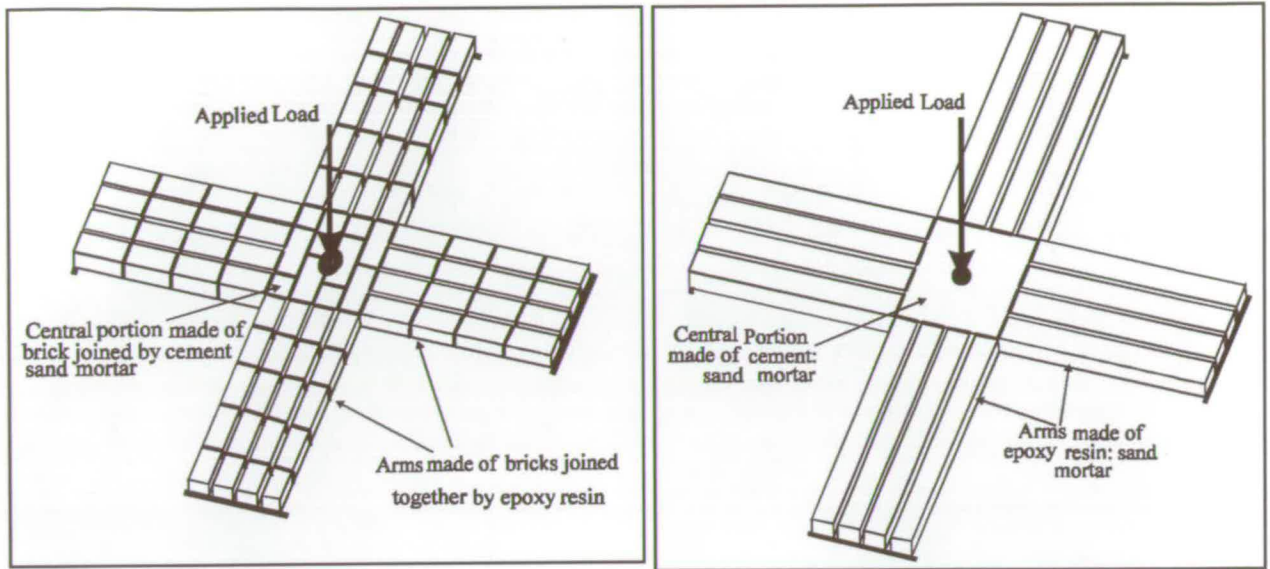


FIG. 4.7 a) Masonry Cross Beams, b) Mortar Cross Beams.

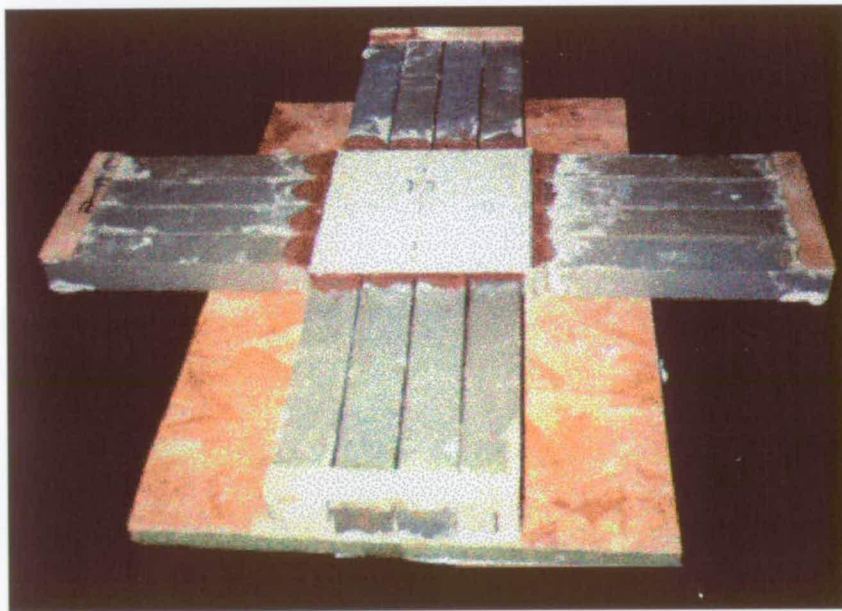


FIG. 4.8 Mortar Cross Beam: Arms are Glued to the Central Portion and Ready for Testing

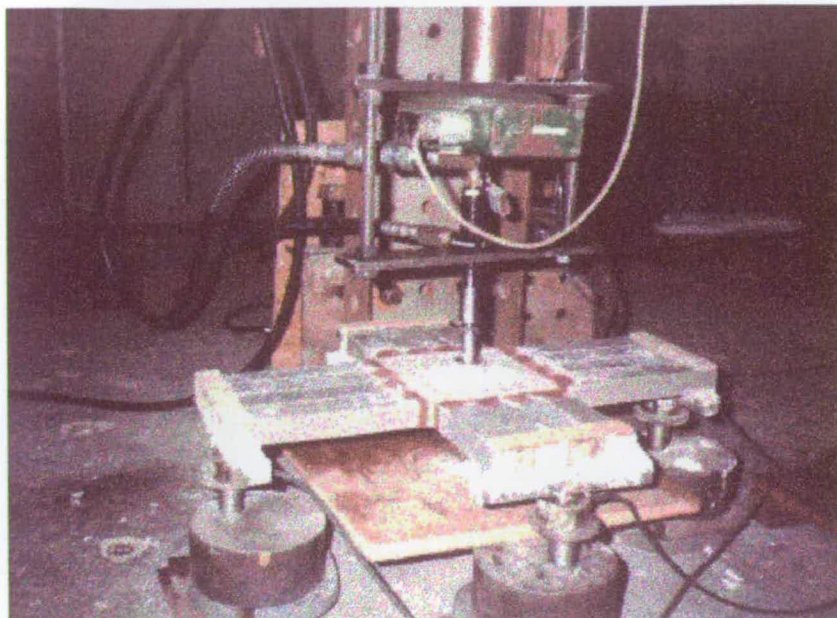
Three mortar cross beams, each of aspect ratio 1:2, 1:1.8, 1:1.2, 1:1 & 1: 0.75, were tested. Thus, a total of 15 cross beams were tested. The central portion was of

approximate dimensions 170 mm x 170 mm x 31 mm. Arms of varying lengths were used to obtain the required aspect ratios for the cross beams. The dimensions of the cross beams used in this study are given in Table 4.4. The load was applied at the centre using a hydraulic jack.

#### ***4.3.2 Test Arrangement***

The cross beams were supported at four sides along the free end of the arms. The supports consisted of solid blocks of steel with a circular disk bolted on the top of the steel blocks so that the height of the supports could be adjusted to the same level. The support reactions were measured with the help of load cells that were kept under the arms on top of these circular-supporting disks.

The cross beams were tested by applying a concentrated load at the centre. This was done with the help of a hydraulic jack that was supported on a separate frame. As it was difficult and inconvenient to lift the frame each time, the jack was connected to the frame using a threaded bolt. The load was applied on the specimen using a circular disk of diameter 40 mm, screwed to the bottom of the jack. The jack was lifted up and the circular disk was removed to provide sufficient space while placing the specimens on the supports without causing any damage to it. A thin layer of 'dental plaster' was applied beneath the arms to account for any minor irregularities on the supports and to provide an adequate surface of contact between the specimen and the supports. The loading arrangement can be seen in Figure 4.9.



**FIG. 4.9 Mortar Cross Beam: Testing Arrangement**

### **4.3.3 Tests on Cross Beams**

The support reactions and the applied load were measured by the load cells connected to a data logger. A 3-ton load cell was used to measure the applied load. Two 500-Kg load cells and two 1-tonne load cells were used under the longer and the shorter arms respectively to measure the support reactions. These were used to verify that there was no discrepancy between the applied load and the resultant reactions. The total applied load gets distributed in both the directions and can be measured as the sum of all the support reactions. Some minor differences (up to 3-5 %) between the applied load and the support reactions were observed, which could be attributed to the lack of sensitivity of the 3-ton load cells at the lower range of loading.

A spirit level was used to ensure that the beam was supported at the same level at all the four supports before loading. Any difference in level was adjusted by bringing up the circular disks on which the arms were resting. The data logger readings were taken before and after placing the specimens and were compared with the self-weight of the specimen. A small amount of load was applied and the reactions at the four supports were checked against the distribution obtained according to the Grashoff-

Rankine method. This also helped to check whether the specimens were supported at the same height on the four sides. The applied load was increased at small steps in a controlled manner and was monitored by the data logger through out the experiment. Print outs of the applied load and the support reactions were taken at regular intervals.

The beams and the cubes cast along with the cross beams were tested on the same day to find out the flexural and the compressive strengths of the mortar.

#### 4.3.4 Experimental Results

The observations made while testing the mortar cross beams are given in this section. The failure loads of all the tested specimens are given in Table 4.4. A detailed discussion on these observations can be seen in Section 4.3.6.

**Table 4.4 Cracking and Failure Loads of Mortar Cross Beams**

Cross Beams	Lx (mm)	Ly (mm)	t (mm)	Aspect Ratio $L_x/L_y$ or $L_y/L_x$	Flexural Strength (N/mm <sup>2</sup> )	Failure Load (N)	
							Average
CB1	1200	600	31.25	2.0 or 0.5	4.11	1035	1016
						1010	
						1003	
CB2	1080	600	31.25	1.8 or 0.56	4.11	1067	1036
						958	
						1083	
CB3	720	600	31.25	1.2 or 0.83	4.11	1344	1376
						1310	
						1476	
CB4	600	600	30.5	1.0	4.25	1401	1429
						1458	
						1428	
CB5	450	600	30.32	0.75 or 1.33	4.14	1440	1447
						1399	
						1502	

#### 4.3.4.1 Support Reactions

The distribution of the applied load in the two orthogonal directions can be obtained from the total support reactions. The theoretical values of the load distribution are calculated using the Grashoff-Rankine method (FENNER 1989) and are compared with the experimental results in Section 4.3.6.1.

#### 4.3.4.2 Crack Pattern

All the mortar cross beams were characterised by a sudden brittle failure of the central portion. Two types of crack patterns were noticed in these cross beams. In the first type, the specimens were broken into two pieces perpendicular to the direction of maximum bending moment as can be seen in Figures 4.10 and 4.11. As can be noticed in Figures 4.12 to 4.15, in the second type, the crack started in a direction perpendicular to that of the maximum bending moment and then moved towards the corner of the central portion, giving it a yield line appearance. However, the development of a yield line is unlikely to happen in mortar, which is brittle in nature.

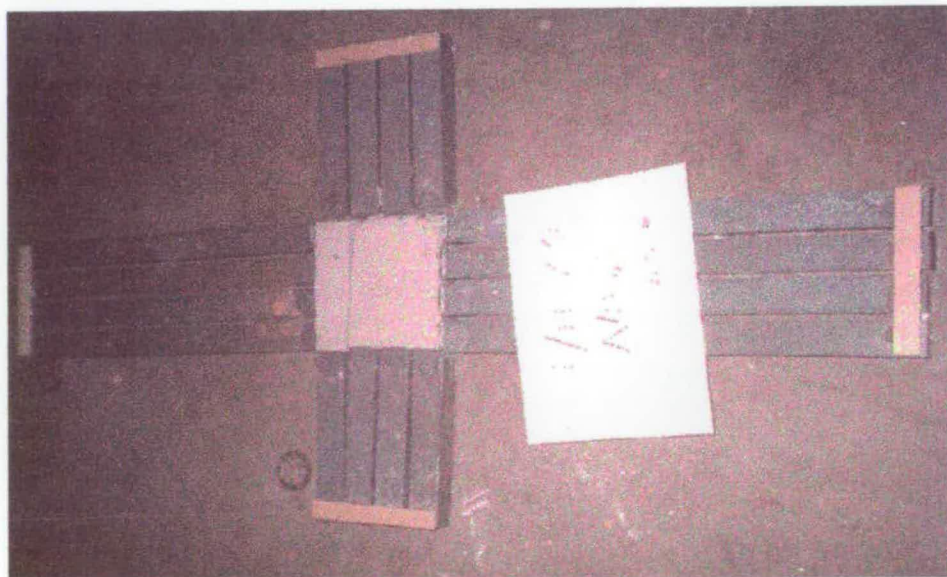
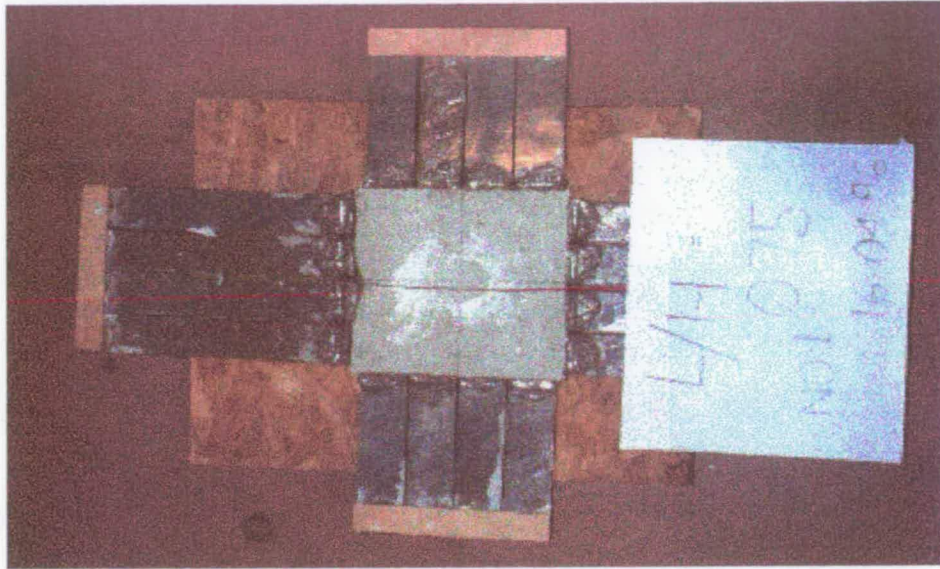
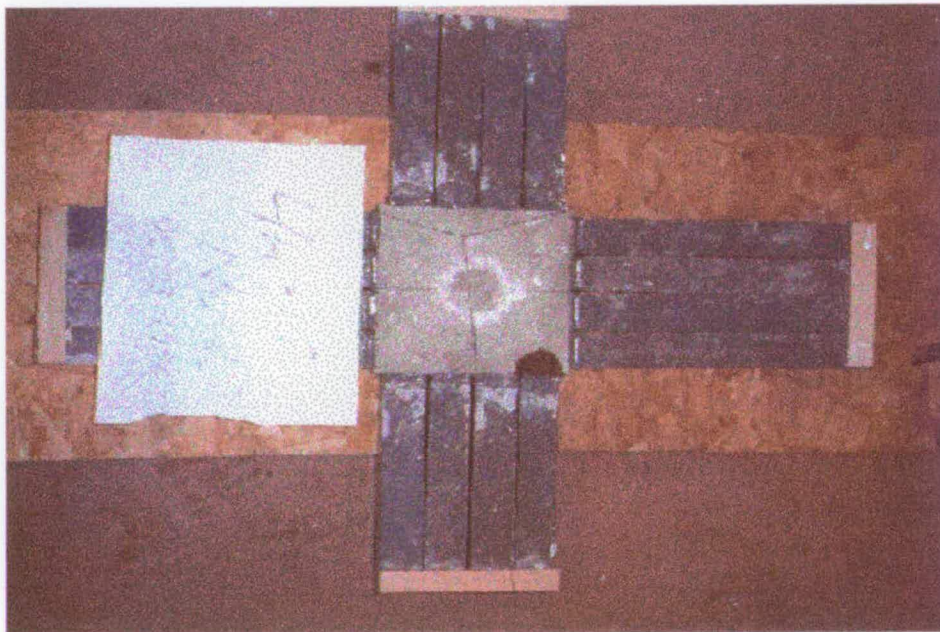


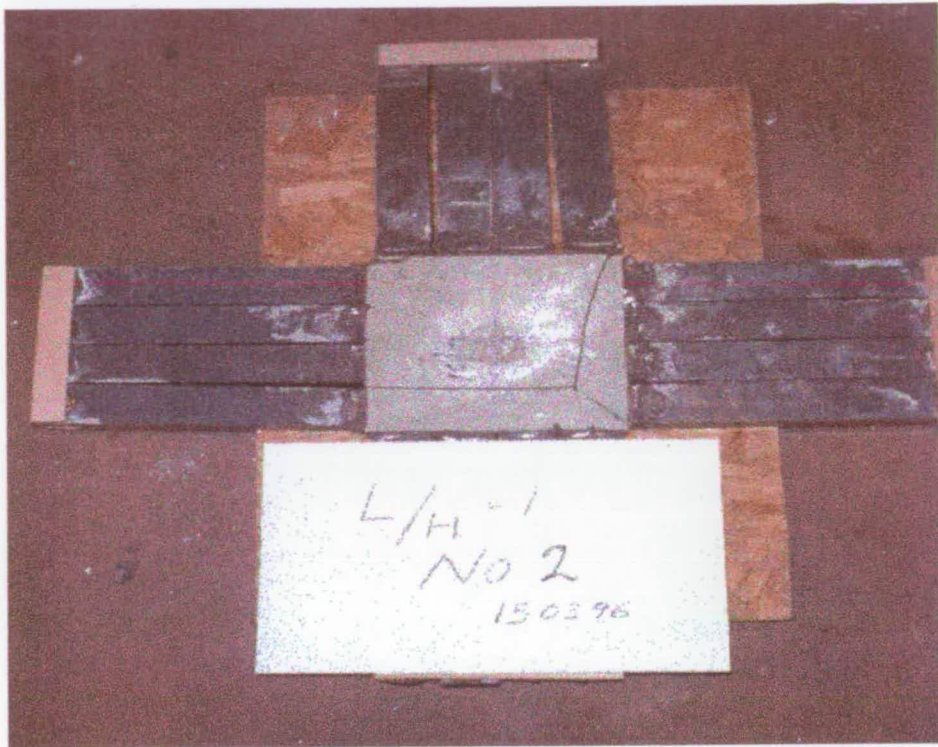
FIG. 4.10 Failure of Cross Beam (Aspect Ratio 1:1.8)



**FIG. 4.11 Failure of Cross Beam (Aspect Ratio 1:0.75)**



**FIG. 4.12 Failure Pattern in Cross Beams (Aspect Ratio 1:1)**

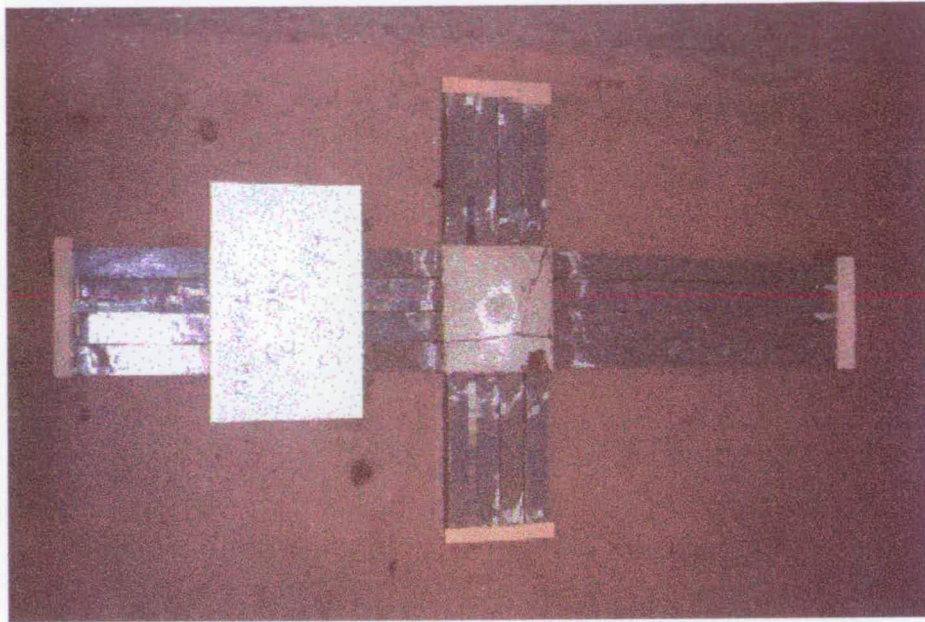


**FIG. 4.13 Failure Pattern for Cross Beams (Aspect Ratio 1:1.2)**



**FIG. 4.14 Failure Pattern in Cross Beams (Aspect Ratio 1:0.75)**





**FIG. 4.15 Failure Pattern of Cross Beams (Aspect Ratio 1:2)**

#### ***4.3.5 Theoretical Methods***

The theoretical methods used for the analysis of the cross beams and the panels are described in this section. The various methods explained below are used to evaluate the behaviour of the material in terms of the measured quantities such as the load distribution, the strain and the failure load.

##### **4.3.5.1 Grashoff-Rankine Method**

The Grashoff-Rankine method (FENNER 1989) is based on the principle of achieving the deflection compatibility at the centre in both the directions and is used to study the distribution of loading in the cross beams. Here, the applied load is shared in both the directions so that the deflection at the centre of the specimen in both the directions is the same. Consider a beam as shown in Figure 4.16.

Neglecting the effect of Poisson's ratio, the applied load  $W$  can be divided into  $W_x$  and  $W_y$  in the  $x$  and  $y$  directions so that:

$$W = W_x + W_y$$

4.9

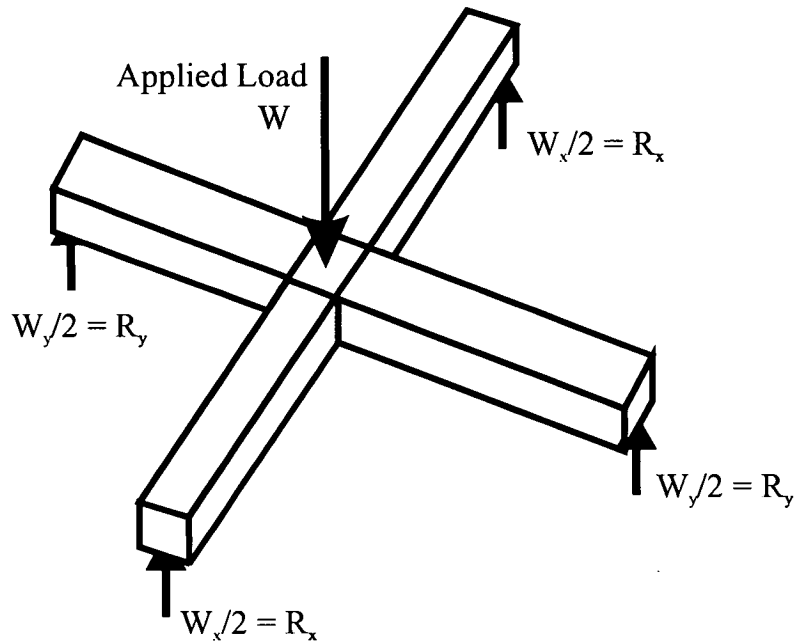


FIG. 4.16 The Distribution of Load in a Cross Beam

The deflection at the centre due to the load  $W_x$  is given by:

$$\delta_x = \frac{W_x L_x^3}{48EI} \quad 4.10$$

Similarly, the deflection at the centre due to the load  $W_y$  is given by:

$$\delta_y = \frac{W_y L_y^3}{48EI} \quad 4.11$$

For Compatibility,

$$\delta_x = \delta_y$$

Hence,  $\frac{W_x L_x^3}{48EI} = \frac{W_y L_y^3}{48EI}$  or,  $W_x L_x^3 = W_y L_y^3$

$$W_x = W_y \frac{L_y^3}{L_x^3} \quad 4.12$$

Substituting Eqn. 4.12 in Eqn. 4.9,

$$W_y = \frac{W}{1 + \left(\frac{L_y}{L_x}\right)^3} \quad 4.13a$$

$$\text{or } W_x = \frac{W}{1 + \left(\frac{L_x}{L_y}\right)^3} \quad 4.13b$$

Thus, knowing the applied load at the centre, the load distributed to the two orthogonal directions can be calculated from Eqns. 4.13a & 4.13b.

#### 4.3.5.2 Rankine's Maximum Stress Theory

The Rankine's maximum stress theory (FENNER 1989) can be used to find out the failure load in a specimen. Let  $F_x$  and  $F_y$  represents the moduli of rupture of the material in the  $x$  and  $y$  directions respectively. Mortar, being an isotropic material, has the same modulus of rupture in both the directions and, hence, we have:

$$F_x = F_y = F \quad 4.14$$

The moduli of elasticity of mortar in the central portion and the arms of the cross beams have been taken as a constant for simplification. The experimental value of modulus of elasticity of the arms made of epoxy and sand was marginally different, affecting the results up to a maximum of 2.5% only, and, hence, was neglected. For the cross beams which are simply supported on all sides and centrally loaded, the maximum moment in the  $x$  and  $y$  directions are,

$$M_x = \frac{W_x L_x}{4} \quad \text{and} \quad M_y = \frac{W_y L_y}{4} \quad 4.15$$

If  $Z$  is the section modulus, the bending stresses in  $x$  and  $y$  directions will be equal to the flexural strength and can be given by:

$$F = \frac{W_x L_x}{4Z} \quad 4.16a$$

and

$$F = \frac{W_y L_y}{4Z} \quad 4.16b$$

Substituting Eqn. 4.13b in Eqn. 4.16a and Eqn. 4.13a in 4.16b,

$$W = \frac{4FZ}{L_x} \left[ 1 + \left( \frac{L_x}{L_y} \right)^3 \right] \quad 4.17a$$

$$\text{or } W = \frac{4FZ}{L_y} \left[ 1 + \left( \frac{L_y}{L_x} \right)^3 \right] \quad 4.17b$$

The failure of the specimen occurs when the moment capacity is reached first either in the  $x$  or the  $y$  direction. The failure load can be obtained from Eqn. 4.17a or Eqn. 4.17b, whichever is smaller.

#### 4.3.5.3 Yield Line Analysis

Although strictly not applicable, the yield line analysis as applied to reinforced concrete slabs (JOHANSON 1972) may be applied to mortar beams and panels to find out the failure load. Once the moment capacity is reached at any point within the specimen, the specimen rotates along certain pre-defined yield lines. The shape of these yield lines depends on the geometry of the specimen and its support conditions. The failure of the specimen is characterised by its moment capacity reaching the ultimate strength all along the yield lines. The yield lines are as shown in Figure 4.17.

Once the slab has been converted as a mechanism, assuming a virtual deflection of unity at the centre,

$$\text{The external work done} = W_x l \quad 4.18$$

The internal work is done due to the rotation along the yield lines and is equal to  $2(m_x \theta_x b + m_y \theta_y a)$ , where  $a$  and  $b$  are the projections of the yield lines along the horizontal and the vertical supporting axes and  $\theta_x$  and  $\theta_y$  are the rotations along these

axes. The rotations,  $\theta_x$  and  $\theta_y$ , are  $\frac{1}{L_x/2}$  and  $\frac{1}{L_y/2}$  respectively.

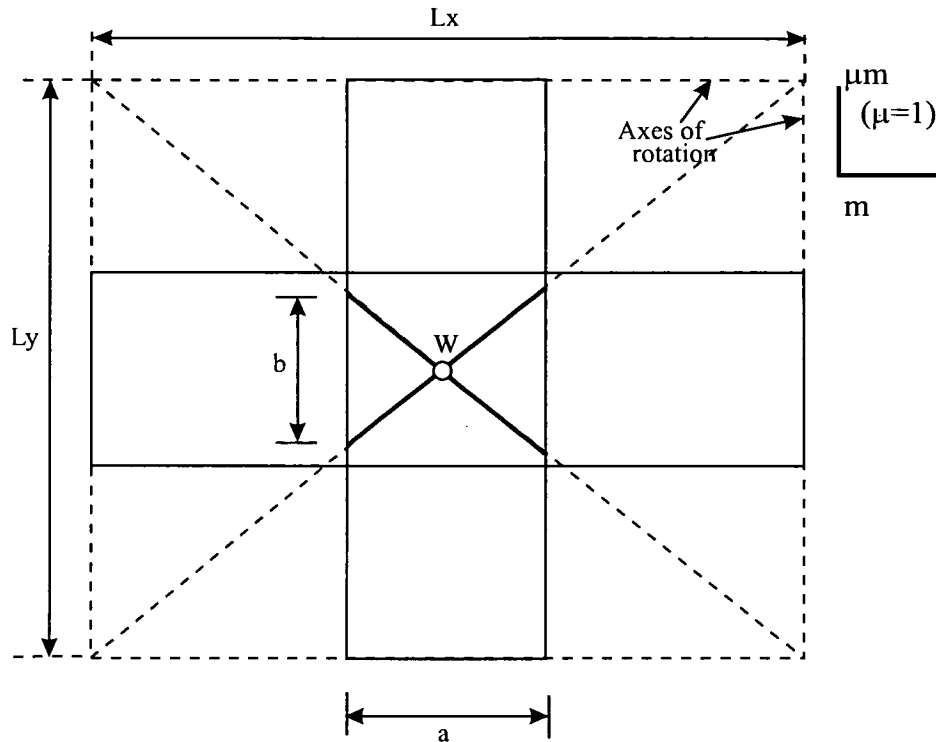


FIG. 4.17 Yield Line Failure Pattern

Hence,

$$\begin{aligned} \text{The internal work done} &= 2 \left( m \frac{2}{L_x} b + m \frac{2}{L_y} a \right) \\ &= 4 \left( \frac{mb}{L_x} + \frac{ma}{L_y} \right) \end{aligned} \quad 4.19$$

Equating the external work to the internal work done,

$$W = 4 \left( \frac{mb}{L_x} + \frac{ma}{L_y} \right) \quad 4.20$$

$$\text{From the geometry, } \frac{L_x}{a} = \frac{L_y}{b} \quad 4.21$$

Hence,  $b = \frac{L_y}{L_x} a = \frac{a}{\alpha}$ , where  $\alpha$  is the aspect ratio  $\frac{L_x}{L_y}$

$$\text{Therefore, } W = 4m \left( \frac{a}{L_x \alpha} + \frac{a}{L_y} \right) \quad 4.22$$

$$\begin{aligned} W &= 4ma \left( \frac{1}{\alpha L_x} + \frac{\alpha}{L_x} \right) = \frac{4F_x Z}{L_x} \left( \frac{1}{\alpha} + \alpha \right) \\ &= K \frac{4F_x Z}{L_x}, \text{ where } K = \frac{1}{\alpha} + \alpha \end{aligned} \quad 4.23$$

#### 4.3.5.4 Elastic Finite Element Analysis

The elastic analysis of the cross beams and the panels was carried out using the finite element method. An in-house finite element program developed at the University of Edinburgh (ROTTER 1988) has been adopted to carry out the analysis. The program has been modified by NG (1996) to incorporate a 'smeared cracking' modelling for the post cracking behaviour of the material. The effect of the number and the distribution of elements on the results of the finite element analysis has been studied by NG (1996). He showed that there was only marginal variation (up to 1%) in the results by increasing the number of elements in the cross from 11x11 to 13x13. He recommended the use of the smaller mesh for the analysis of the cross beams and panels. The number of elements at the arms did not have any significant effect on the analysis. The number of elements at the central portion of the cross was taken as 11x11 in the analysis. A linear elastic analysis was carried out for the cross beams and the panels using 8 noded quadratic elements. The mesh plots for the cross beams and the panels are given in Appendices VI and VII.

In the modified finite element program, the load was increased at smaller intervals and the mesh was checked at regular intervals to see if any of the elements had cracked. Once a cracked element was detected, the rigidity matrix of that particular element was reduced to a very small value (SINHA *et al.* 1997) in the direction

perpendicular to the crack. The rigidity matrix was not reduced to zero values to avoid a singular matrix. Modifying the rigidity matrix caused a redistribution of the loads, which might lead to the cracking of more elements. Hence, the analysis was repeated several times at the same load until no further cracked element was detected. The loading can be increased at higher steps in the linear range before the onset of cracking. However, after cracking the load was increased at smaller steps (0.0002 N/mm<sup>2</sup>) until the specimen failed in the stronger direction. A smaller value of the load increment was selected to achieve better accuracy in the failure load. However, there were cases when the panel cracked at a pressure of 0.14 N/mm<sup>2</sup> and failed only at 0.18 N/mm<sup>2</sup>. In such cases, where there is a large difference between the cracking load and the failure load, more number of load increments was required.

The cross beam tests were carried out with the purpose of arriving at a failure criterion for the isotropic material under bi-axial bending. The failure criterion for the isotropic material was incorporated in the above finite element plate bending program (ROTTER 1998).

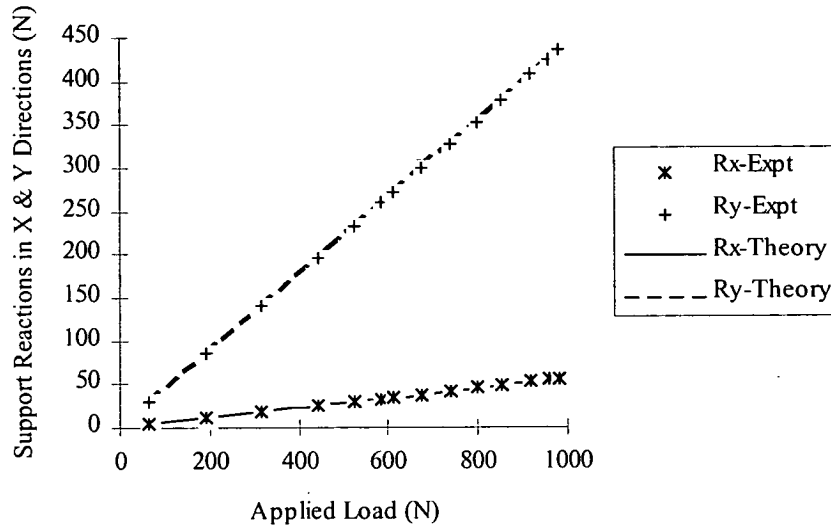
#### ***4.3.6 Discussion of Test Results***

A theoretical analysis has been carried out for the cross beams to find out the distribution of the applied load. The theoretical values are compared with the experimental results and are given in this section.

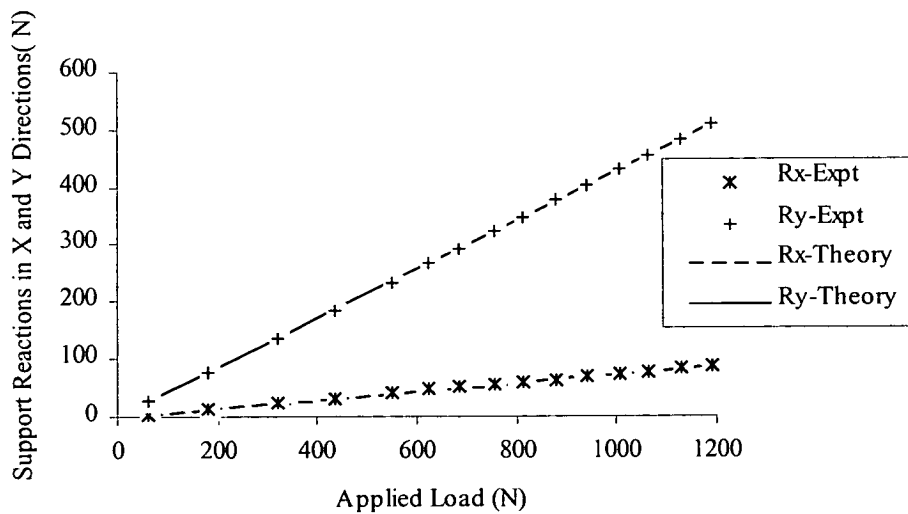
##### **4.3.6.1 Load Distribution and Support Reactions**

The Grashoff-Rankine method (FENNER 1989), where the load is distributed according to the relative stiffness, was used to calculate the load distribution in the two directions. The measured support reactions are compared with the theoretical values and are given in Figures 4.18 to 4.22. It can be seen from these figures that

the specimens behaved well in accordance with the theory. The specimens were found to fail in both directions simultaneously for all aspect ratios. The material showed a linear elastic behaviour up to the failure.

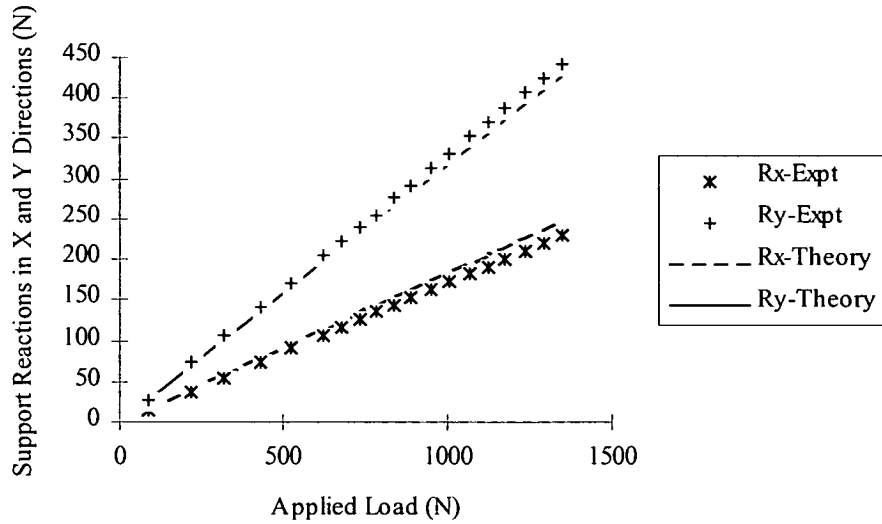


**FIG. 4.18** Distribution of the Central Applied Load vs. Support Reactions in X and Y Directions ( $L_x = 1200$  mm,  $L_y = 600$  mm)

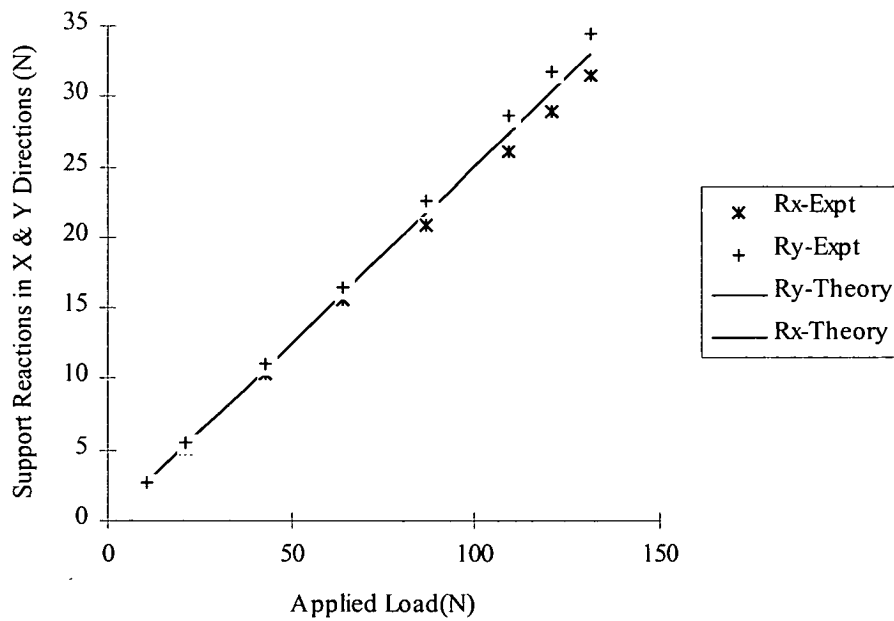


**FIG. 4.19** Distribution of the Central Applied Load vs. Support Reactions in X and Y Directions ( $L_x = 1080$  mm,  $L_y = 600$  mm)

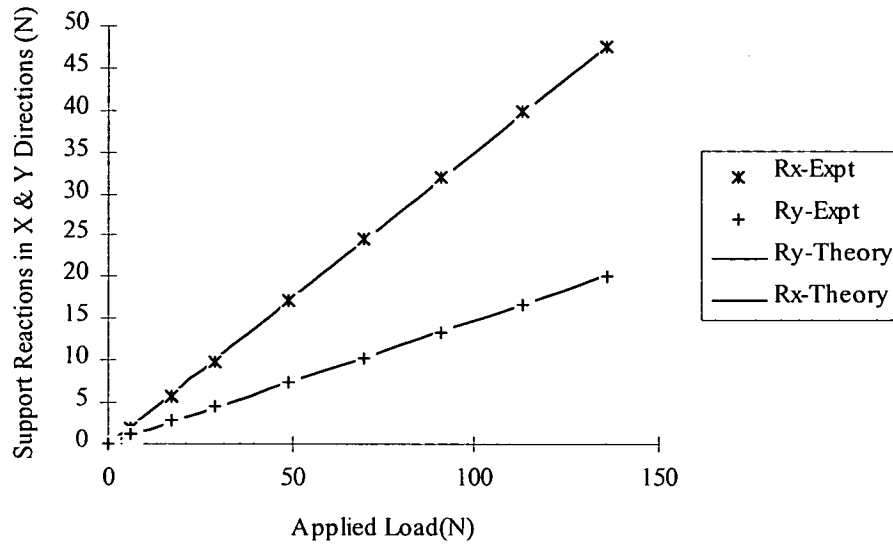




**FIG. 4.20** Distribution of the Central Applied Load vs. Support Reactions in X and Y Directions ( $L_x = 720$  mm,  $L_y = 600$  mm)



**FIG. 4.21** Distribution of the Central Applied Load vs. Support Reactions in X and Y Directions ( $L_x = 600$  mm,  $L_y = 600$  mm)



**FIG. 4.22 Distribution of the Central Applied Load vs. Support Reactions in X and Y Directions ( $L_x = 450$  mm,  $L_y = 600$  mm)**

#### 4.3.6.2 Cracking and Failure

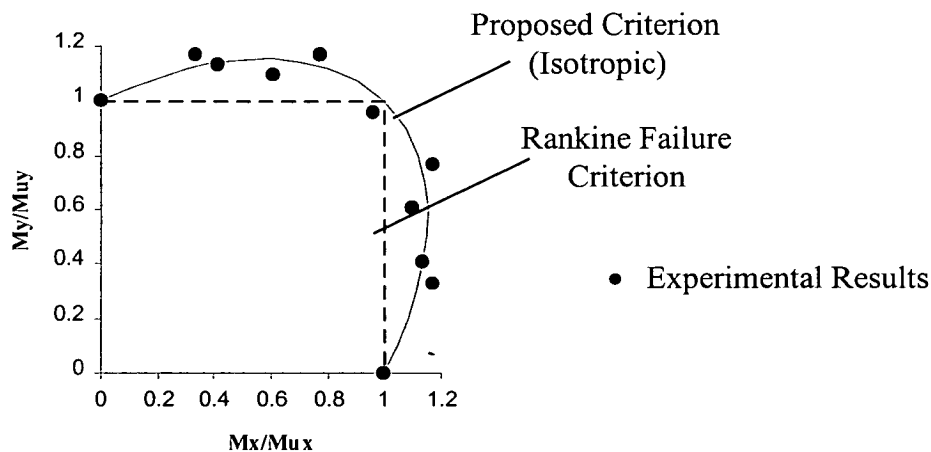
Cracking and failure happened simultaneously in the case of mortar cross beams for all aspect ratios. Once the specimen reached its failure strength in any one of the directions, it was no longer capable of supporting any further loading. The data logger used to measure the applied load and the support reactions was consistently monitored for any variation in the reading at the time of cracking. When the specimen cracked, none of the load cells picked up any extra load and the load carried by all the load cells dropped immediately. However, in the case of orthotropic material, upon cracking in the weaker direction, the load that was carried by the specimen in that direction was shed to the stronger direction. It is clear that the phenomenon of 'load shedding' that was observed in the orthotropic material was absent in the isotropic material.

### 4.3.6.3 Failure Criterion

The results of the cross beam tests have been plotted in a non-dimensional form as shown in Figure 4.23. This is done by considering the ratio of the bending stress at the time of failure to the average uni-axial flexural strength in the two orthogonal directions. A failure criterion was developed for the isotropic material from the test results of mortar cross beams. The best-fit curve through the experimental points gives the following relationship.

$$\left(\frac{M_y}{M_{uy}}\right)^2 - \frac{M_x}{M_{ux}} \frac{M_y}{M_{uy}} + \left(\frac{M_x}{M_{ux}}\right)^2 = 1.0 \quad 4.24$$

The above equation is similar to the Von Mises failure criterion for a ductile material subjected to a two dimensional stress system (FENNER 1989). The failure envelope based on the above equation is shown in Figure 4.23 and is compared with the Rankine's failure criterion for a brittle material, in which it is assumed that the material fails when the ultimate strength in tension is reached in any one of the directions. It is clear from the figure that the experimental results for the mortar cross beams cannot be explained by the Rankine's failure theory. It can be seen that the strength of an isotropic material in bi-axial bending is higher than that in uni-axial bending.



**FIG. 4.23 The Proposed Failure Envelope for Isotropic Material in Bi-axial Bending**

According to this failure criterion, the specimen fails when the ratio of the moments in any one of the directions meets the curve defined by the above equation (Eqn. 4.24). An increase in strength can be noticed in bi-axial bending when compared to uni-axial bending. The maximum increase in strength that can be achieved under bi-axial bending is 15.47% of that under uni-axial strength. As can be seen in the figure, for each value of  $\frac{M_x}{M_{ux}}$ , there is a corresponding value of  $\frac{M_y}{M_{uy}}$  when the specimens reach the failure criterion. The maximum increase in strength is achieved when either  $\frac{M_x}{M_{ux}}$  or  $\frac{M_y}{M_{uy}}$  reaches a value of 0.59. This is developed in a panel when its aspect ratio is 0.75. Nevertheless, no such increase in strength was noticed when there were equal stresses in the two orthogonal directions.

Similar observation was made by KUPFER *et al.* (1969) on concrete specimens subjected to bi-axial direct compression. According to his observation, the strength of concrete under bi-axial compression is larger than that under uni-axial compression. The test results showed that the strength of concrete in bi-axial compression may be up to 27% higher than the uni-axial strength of concrete. For equal compressive stresses in two principal directions, the strength increase was approximately 16%. However, the strength of concrete under bi-axial tension was found to be approximately equal to its uni-axial tensile strength.

#### **4.3.7 Comparison of the Experimental and Theoretical Results**

Having established the failure criterion for the isotropic material, the same was incorporated in a finite element plate-bending program to evaluate the cracking and the failure load. The results were obtained using the finite element method with and without any criterion, the Rankine's maximum stress theory and the Yield line method. The results of the analysis are given in Tables 4.5 and 4.6 for cross beams. It can be noticed from Table 4.5 that the even though the yield line method gave a

closer prediction for the failure pressure, the Rankine's method and the finite element method without any failure criterion under-estimated the experimental failure pressure by up to 19% and 14% respectively.

**Table 4.5 Experimental and Theoretical failure load of Mortar Cross Beams**

L <sub>x</sub> (mm)	L <sub>y</sub> (mm)	Expt. Failure load (N)	$\frac{L_x}{L_y}$	Theoretical Failure load (N)					
				Yield Line Analysis	$\frac{\text{Expt}}{\text{YL}}$	Rankine's Method of (RM) Analysis	$\frac{\text{Expt}}{\text{RM}}$	FEM without any failure criterion	$\frac{\text{Expt}}{\text{FEM}}$
1200	600	1016	2.0	947.7	1.07	853	1.19	894	1.14
1080	600	1036	1.8	992.1	1.04	888.3	1.17	929	1.12
720	600	1376	1.2	1284.6	1.07	1197.1	1.15	1182	1.16
600	600	1429	1.0	1493.6	0.96	1493.6	0.96	1413	1.01
450	600	1447	0.75	1497.7	0.97	1363	1.06	1419	1.02

The results of the finite element analysis with the failure criterion are given in Table 4.6. As can be seen in the table, the theoretical results are much closer to the experimental values and the variation lies within 8%. The importance of considering the failure criterion for the isotropic material under bi-axial bending is very clear from this comparison.

It can also be seen from Table 4.5 that the Rankine's method consistently under-estimated the failure load in the case of cross beams. This is mainly due to the fact that no increase in strength has been considered in this analysis. However, it can be seen from the failure criterion (Eqn. 4.24 and Figure 4.23) that the material showed an increase in strength under bi-axial bending over the uni-axial strength. This effect has been neglected in the Rankine's method and can be incorporated by considering a factor from the failure criterion (Eqn. 4.24) by which the strength has been increased. The bending moments in both the directions are obtained from the Rankine's distribution of forces. It can also be seen that the failure in the cross beams were initiated due to the bending moment in the shorter direction (y).

$$\text{At the time of failure, from Eqn 4.16b, } W_y = \frac{4FZ}{L_y} \quad 4.25$$

$$\text{We have, } M_x = \frac{W_x L_x}{4} \quad 4.26$$

Substituting Eqns. 4.12 and 4.25 in Eqn. 4.26,

$$M_x = \frac{W_y \left(\frac{L_y}{L_x}\right)^3 L_x}{4} = \frac{W_y \frac{1}{\alpha^3} L_x}{4} = \frac{4FZ \frac{1}{\alpha^3} L_x}{4L_y} = FZ \frac{L_x}{L_y} \frac{1}{\alpha^3} \quad 4.27$$

$$\frac{M_x}{M_{ux}} = \frac{FZ \alpha \frac{1}{\alpha^3}}{FZ} = \frac{1}{\alpha^2} \quad 4.28$$

Hence, for each aspect ratio, the above ratio can be calculated in the longer (x) direction. Similar ratio in the shorter (y) direction can be obtained from the failure criterion graph (Figure 4.23) and represents the increase in strength in that direction as the failure is due to the maximum moment reaching the ultimate strength in this direction. The failure load has been recalculated by increasing the load by the factor obtained from the graph and the results are given in Table 4.6.

**Table 4.6 Failure Load Calculated by Various Methods Incorporating the Proposed Failure Criterion under Bi-axial Bending.**

L <sub>x</sub> (mm)	L <sub>y</sub> (mm)	α	Multipl ication Factor	Failure Load in N				
				Expt.	FEM'	$\frac{\text{Expt}}{\text{FEM}'}$	RM'	$\frac{\text{Expt}}{\text{RM}'}$
1200	600	2.0	1.101	1016	975	1.04	939.2	1.08
1080	600	1.8	1.118	1036	1056	0.98	993.1	1.04
720	600	1.2	1.146	1376	1296	1.06	1372.1	1.00
600	600	1.0	1.0	1429	1413	1.01	1493.6	0.96
450	600	0.75	1.1546	1447	1592	0.91	1573.7	0.92

It can be noticed from Table 4.6 that the increase in strength under bi-axial bending can be incorporated in the Rankine's method to obtain faster solutions to the failure pressure for an isotropic material subjected to bi-axial bending.

A closer comparison can be seen between the experimental results and the theoretical values obtained by the yield line method in these results (Table 4.5). This can be attributed to the over-estimating nature of the yield line method, where the material is assumed to yield at constant bending moment along the pre-defined yield lines. This can be further explained by comparing the load distribution that would have occurred in both the yield line analysis and the Rankine's method. According to Rankine's maximum stress theory, the cracking will be initiated in the shorter direction in the case of an isotropic material. The coefficient  $K$  to obtain the failure load in the yield line (Eqn. 4.23) method is compared with that of the Rankine's method (Eqn. 4.17b). Table 4.7 shows the coefficient  $K$  obtained by both the methods for all the aspect ratios considered in this research.

**Table 4.7 Comparison of the Load Coefficients by Yield Line and Rankine's Methods**

Aspect Ratio L/H	Coefficient $K = \left( \frac{WL_x}{4FZ} \right)$		
	Yield Line method	Rankine's method	Rankine's method with increased strength
2.0	2.5	2.25	2.48
1.8	2.36	2.11	2.36
1.2	2.03	1.90	2.18
1.0	2.00	2.00	2.00
0.75	2.08	1.90	2.19

Table 4.7 also shows the coefficients obtained by incorporating the modification factor in the Rankine's method to take into account the increase in strength under bi-axial bending. It can be seen from the table that the coefficients obtained in all these cases are almost equal, which supports that a distribution of loading as given by the Rankine's method might have developed in these cases. The reason for obtaining the closer prediction of experimental failure load by the yield line method can be explained by this.

### ***4.3.8 Comparison of the Behaviour of Isotropic and Orthotropic Materials under Bi-axial Bending***

The behaviour of the isotropic material under bi-axial bending is compared with that of the orthotropic material and some of the important points are highlighted in this section. To compare the behaviour of the orthotropic and isotropic materials, brickwork and cement mortar cross beams have been used. Brickwork beams have different strength and stiffness properties in the two orthogonal directions due to the orientation of the bricks and the presence of bed joints and head joints. The flexural tests on brick wallettes, where the tension develops in parallel or perpendicular to the bed joints, show that they exhibit definite strength and stiffness properties in these directions. Hence, brickwork cross beams were considered ideal for the study of the orthotropic material under bi-axial bending. The cross beam tests that have already been done on the brickwork specimens (NG 1996) are considered for this purpose. The following major issues were discussed in this comparative study.

#### **4.3.8.1 Load Distribution**

The applied load is distributed according to the relative stiffness in both types of materials. In brickwork, most of the specimens cracked when the ultimate strength was reached in the weaker direction. It can be seen that after cracking, the load carried by the weaker direction was shed to the stronger direction, as the specimen was no longer capable of supporting any further load in the weak direction. The specimens continued to support additional load in the stronger direction until they failed. No such 'load shedding' was observed in mortar cross beams (Figure 4.18 to 4.22). The specimens cracked and failed together in both directions simultaneously for all aspect ratios. Thus, the presence of 'load shedding' was exclusively found in material having both the strength and stiffness orthotropies, which shows the importance of considering the orthotropic properties in any analysis to obtain the failure pressure of such material.



#### 4.3.8.2 Type of Failures

Three types of failures were noticed in brickwork cross beams as opposed to the single type of brittle sudden collapse in the case of mortar beams. These three types of failures derived their characteristics from the different flexural strengths in the two orthogonal directions. The types of failures include:

- Simultaneous failure in both directions without any prior cracking (Figure 4.24).
- Cross beams cracked in the weaker direction and the load was shed to the stronger direction. However, these specimens failed immediately because the shed load was sufficient to cause the failure of the beam in the stronger direction (Figure 4.25).
- The specimens continued taking load in the stronger direction after cracking as the shed load was not large enough to cause the failure (Figure 4.26). Hence, the cracking and the failure in this case was quite distinguishable.

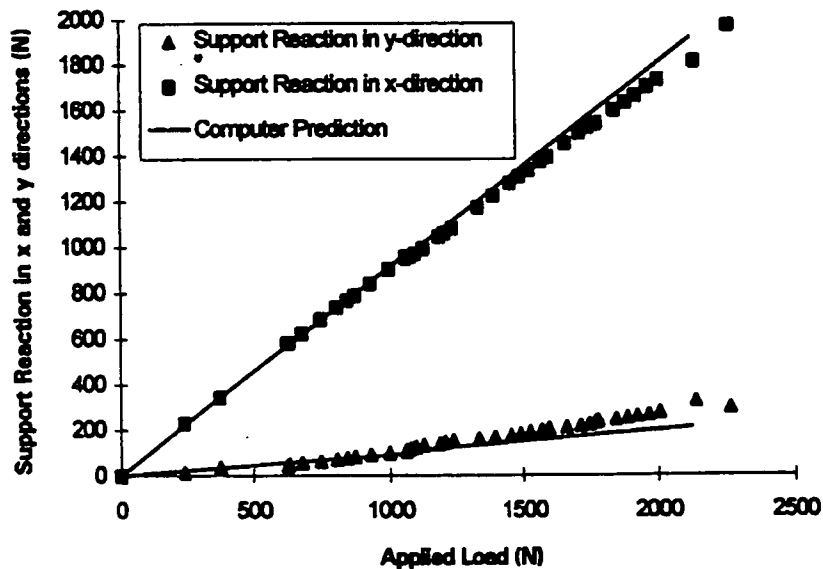


FIG. 4.24 Typical Load Distribution in Masonry Cross Beams (Failure Type 1) (NG 1996)

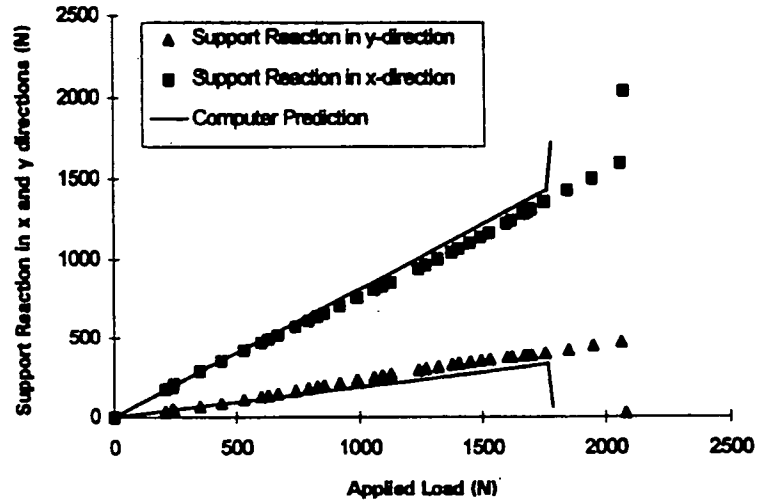


FIG. 4.25 Typical Load Distribution in Masonry Cross Beams (Failure Type 2) (NG 1996)

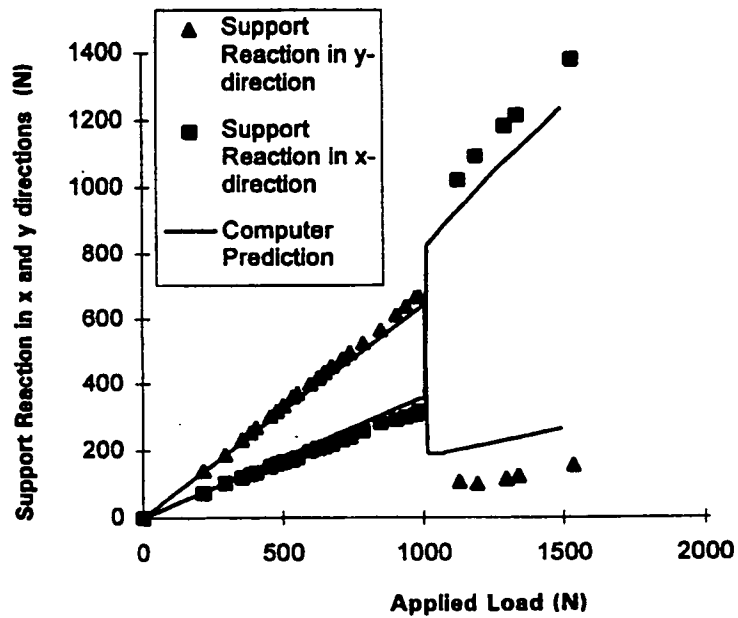


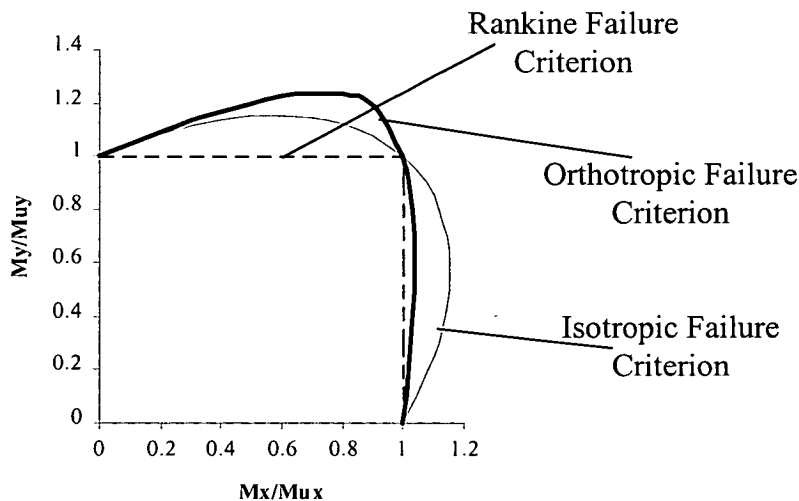
FIG. 4.26 Typical Load Distribution in Masonry Cross Beams (Failure Type 3) (NG 1996)

It can be seen in Figure 4.26 that the load gets distributed according to the relative stiffness of the specimen. The shorter direction takes more load than the longer direction for the same applied load. As a result, the specimen cracks first in the direction of the shorter arm and a major portion of the load carried by this arm will be shed to the longer arm. This causes an increase in the load carried by the longer arm.

#### 4.3.8.3 Failure Criteria

A comparison of the failure criteria developed for the isotropic and the orthotropic materials can be seen in Figure 4.27. The failure criterion that was developed for the orthotropic material and used in the comparison is given by Eqn. 4.29 (SINHA *et al.* 1997).

$$\left(\frac{M_y}{M_{uy}}\right)^2 - 0.75\frac{M_x}{M_{ux}}\left(\frac{M_y}{M_{uy}}\right)^2 - 0.25\frac{M_x}{M_{ux}}\frac{M_y}{M_{uy}} + \left(\frac{M_x}{M_{ux}}\right)^2 = 1 \quad 4.29$$



**FIG. 4.27 Failure Envelop for Isotropic and Orthotropic Materials**

The flexural strength is increased greater in the bi-axial bending than in the uni-axial bending for both the isotropic and the orthotropic materials. However, in the

orthotropic material the increase in strength occurs only in the weaker direction. The stronger direction did not show any significant improvement in strength over the uni-axial strength.

It is evident from the experimental results that the behaviour of the isotropic and orthotropic materials are dissimilar and a separate failure criterion needs to be used in the analysis.

## **4.4 The Panel Tests**

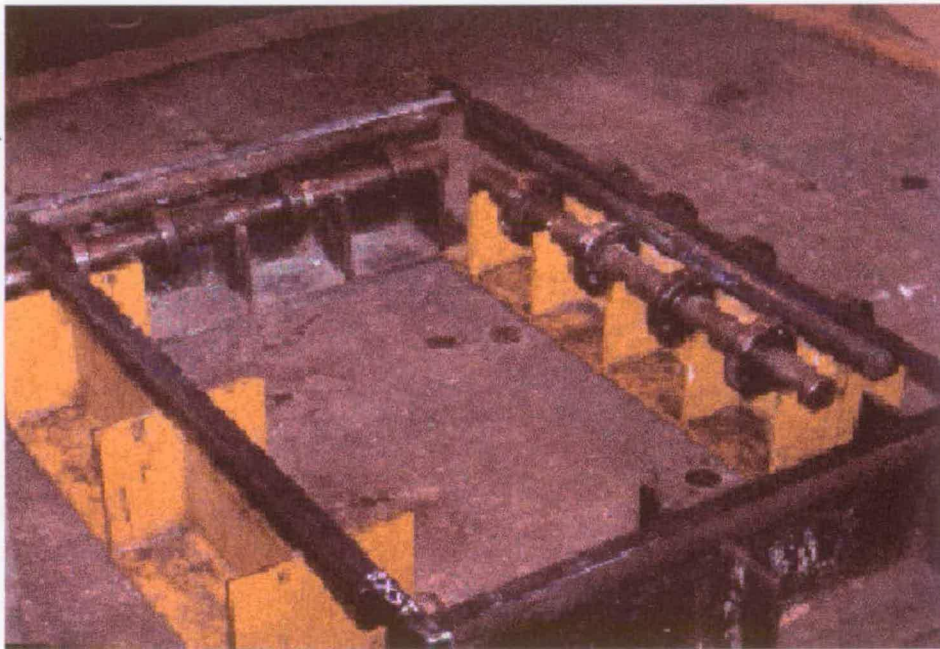
### ***4.4.1 Panel Construction***

Mortar panels of the same mix were tested to ascertain the behaviour of the material under bi-axial bending. Panels of aspect ratio 1:0.9, supported at three and four sides were tested in a horizontal position. It is very clear that there has been no increase in strength for equal flexural stresses in the two orthogonal directions (Figure 4.23 and Eqn. 4.24). It can also be seen from Tables 4.5 and 4.6 that the failure pressure predicted by the various methods for a square panel is almost same. Hence, a panel of aspect ratio 0.9 was taken in this study to prove the validity of the failure criterion. A total of four panels were tested with two different types of boundary conditions.

The panels and the associated control specimens were constructed at the same time. The panels were cast horizontally on a polythene sheet so that they could be lifted easily and were taken to the test rig carefully without inducing any handling stresses. The panels and the control specimens were not covered and were cured at the ambient temperature of the laboratory. Water was sprinkled on top of these specimens while curing to prevent the shrinkage of mortar. The dimensions and the boundary conditions of the panels tested in this study are given in Table 4.8.

#### 4.4.2 Test Arrangement

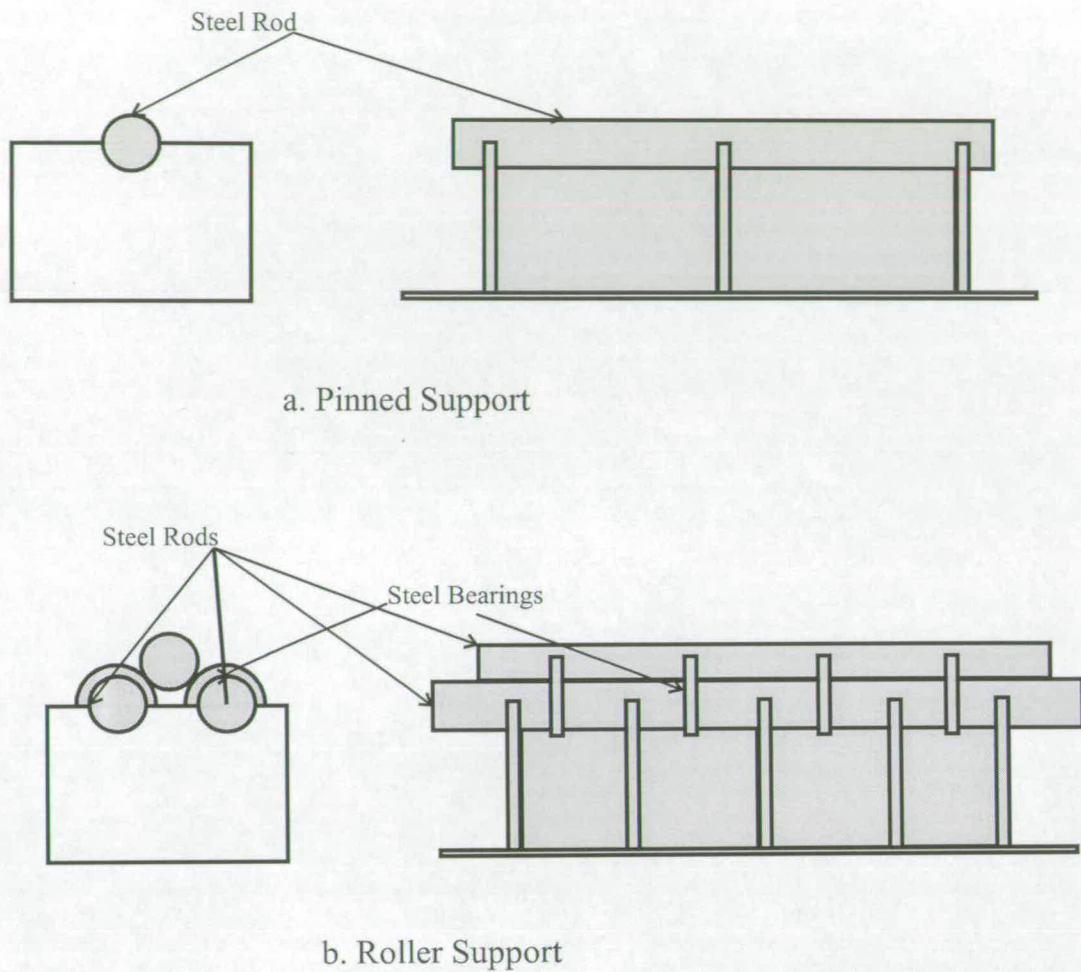
The panels were resting on roller and pinned supports during testing. These supports were laid on the strong floor of the laboratory. The four sides supported panels were resting on two roller supports and two pinned supports, whereas the three sides supported panels were resting on two pinned supports and a roller support. Figure 4.28 shows both types of supports used in the experiment. The details of the pinned and roller supports can be seen in Figure 4.29.



**FIG. 4.28 Supporting Arrangements Used for Testing the Panels**

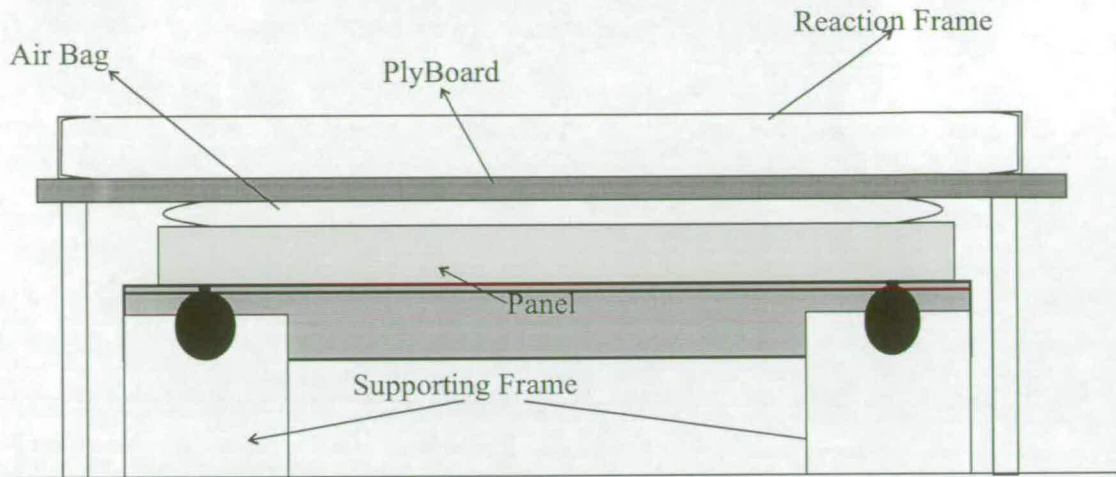
The load was applied by inflating an airbag using an air compressor. A reaction frame was required to hold the air bag firmly against the specimen. A simple steel frame was used for this purpose. The specimens were cast at a separate place and were moved to the test rig at the time of testing. A plyboard was kept on top of the airbag, which acted against the steel frame while applying the load through the air bag. Suitable packing material was kept in between the panel and the air bag to ensure that the bag was not damaged by any broken pieces of mortar at the time of its failure. A steel bar was kept on top of the supports to ensure that the panels were resting properly along its edges on the supports. The testing arrangement described above can be seen in

Figure 4.30.



**FIG. 4.29 Details of a Pinned and Roller Support Used for Panel Testing**

Lime-gypsum mortar was applied on top of these steel plates to take care of any irregularities on the surface. The reaction frame was completely lifted up and removed each time before the specimens were placed on the supports and was brought back carefully without damaging the specimen. A small gap of 2-3cm was left between the reaction frame and the specimen to allow the inflation of the airbag.



**FIG. 4.30 The Testing Arrangement for Mortar Panels**

#### **4.4.3 Instrumentation**

Even though the compressor gave some indication of the applied pressure, it was not sensitive enough for the experiments. Hence, a water manometer was used to obtain more accurate measurements of the applied pressure.

In addition to measuring the applied load on the panels, the strain measurements were taken at each load increment. This was to study the load distribution in the panel. The strain was measured in both the orthogonal directions at various points on the surface of the panel using electrical resistance gauges. The location of these gauges for strain measurements for the three and four sides supported panels are shown in Figure 4.31. The strains were measured at the centre and also at an offset from the centre in both directions.

The panels were moved to a table after seven days to prepare the specimens for the strain gauges. The points were marked on the panel and the electrical strain gauges were fixed very carefully after cleaning the surface with acetone as per the given instructions. The electrical resistance gauges were connected to a data logger (Sangamo), which gave the strain measurements directly. A panel, with the strain

gauges connected to it and ready for testing is shown in Figure 4.32.

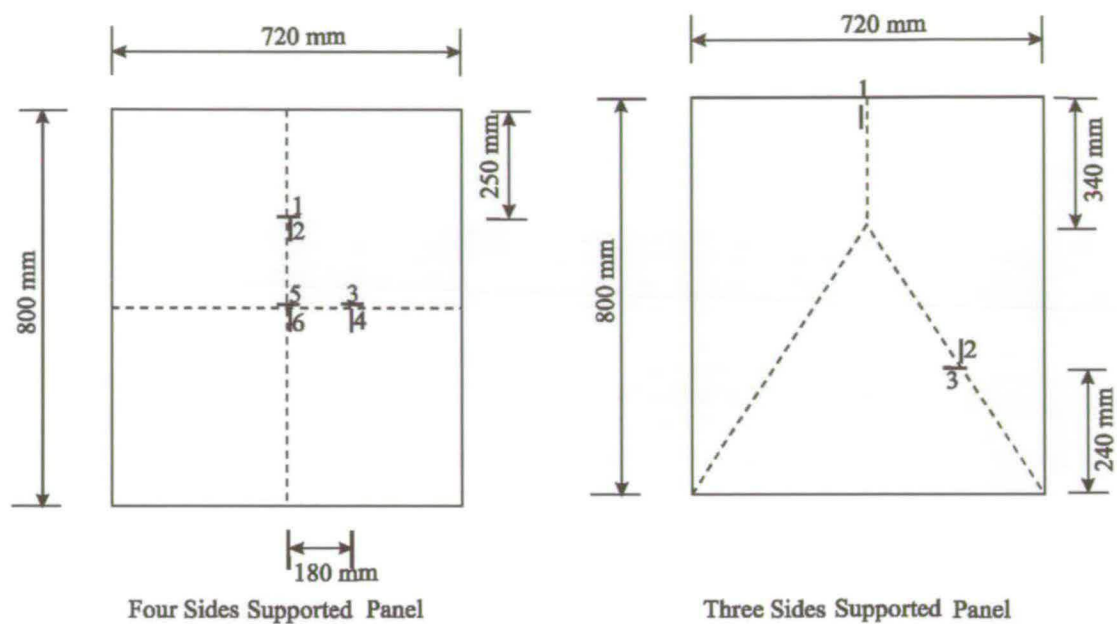


FIG. 4.31 Location of Strain Gauges on Four and Three Sides Supported Panel

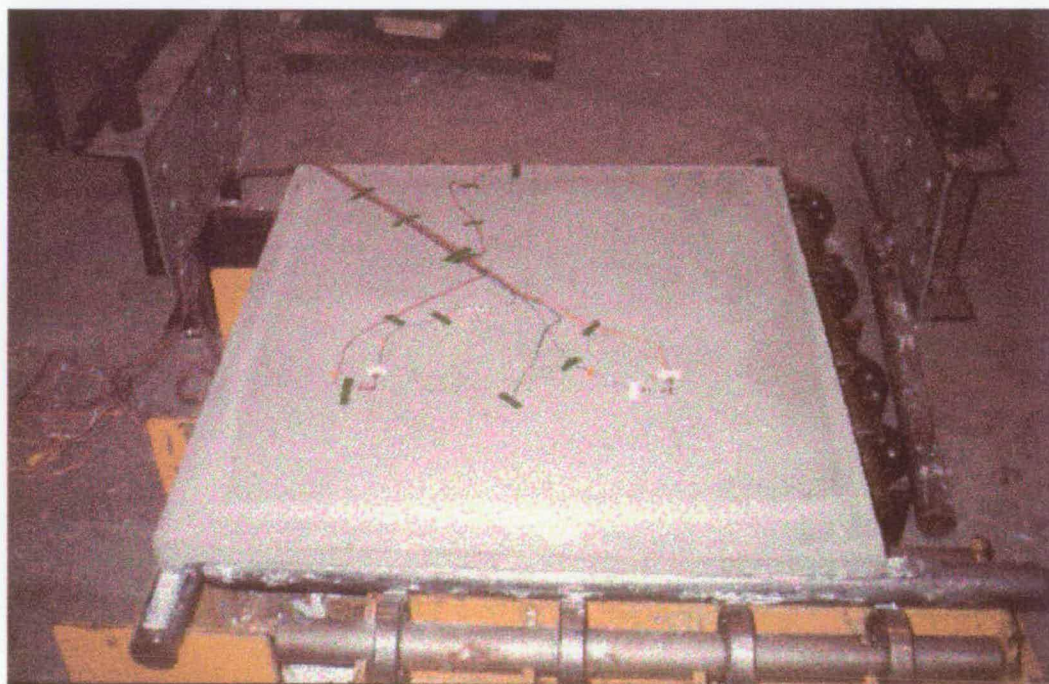


FIG. 4.32 A Three Sides Supported Panel, Arrangement of Strain Gauges



#### **4.4.4 Test Procedure**

A simple test procedure as explained in this section was followed. Two panels each were tested for both the support conditions and the average of the results was taken. All the panels were tested at 14 days. The control specimens were also tested on the same day to find out the compressive and the flexural strengths. The panels were tested by increasing the pressure in the airbag at smaller steps. A small amount of load was applied and then released to see if the strain measurements were consistent. The strain readings were taken at each step of the load increment. The loading was continued until the failure of the specimen. The specimens failed in a brittle manner by a sudden collapse. After the completion of the test, the reaction frame was completely removed and the specimen was inspected for the crack pattern and any other visual indication of the panel behaviour. It can be seen in Figure 4.33 how the panels were tested at the laboratory. The reaction frame, the air compressor, the water manometer and the data logger can be clearly seen in this figure.

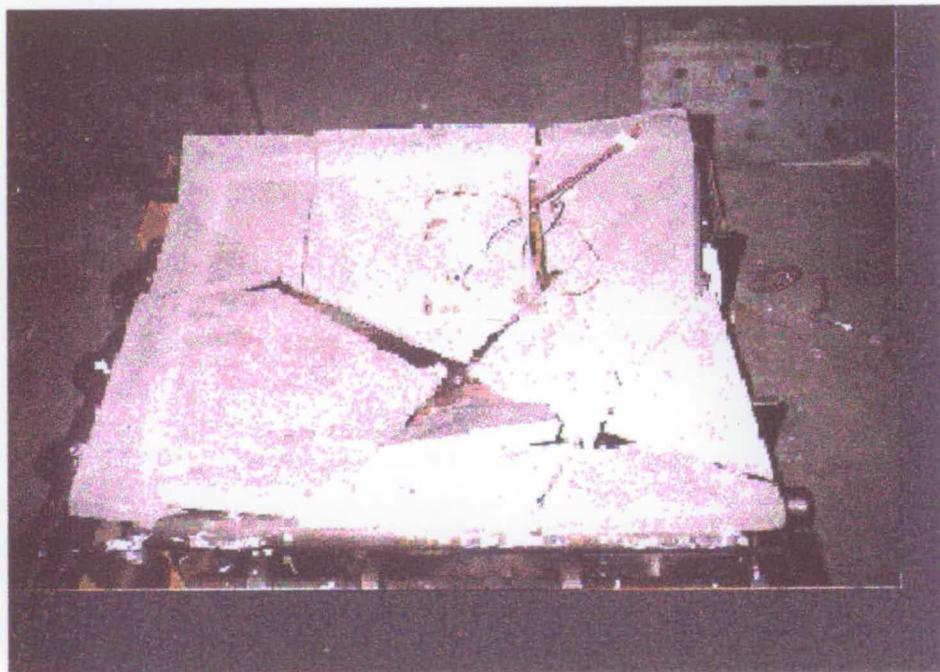


**FIG. 4.33 A Panel Ready for Testing**

#### 4.4.5 Experimental Results

##### 4.4.5.1 Crack Pattern

Most of the panels supported on three and four sides failed in a brittle manner. The crack patterns depended on the boundary conditions. The typical failure/crack pattern of the panels can be seen in Figures 4.34 and 4.35. The failure pressure of the panels is given in Table 4.8.



**FIG. 4.34 Crack Pattern of a Four Sides Supported Panel**

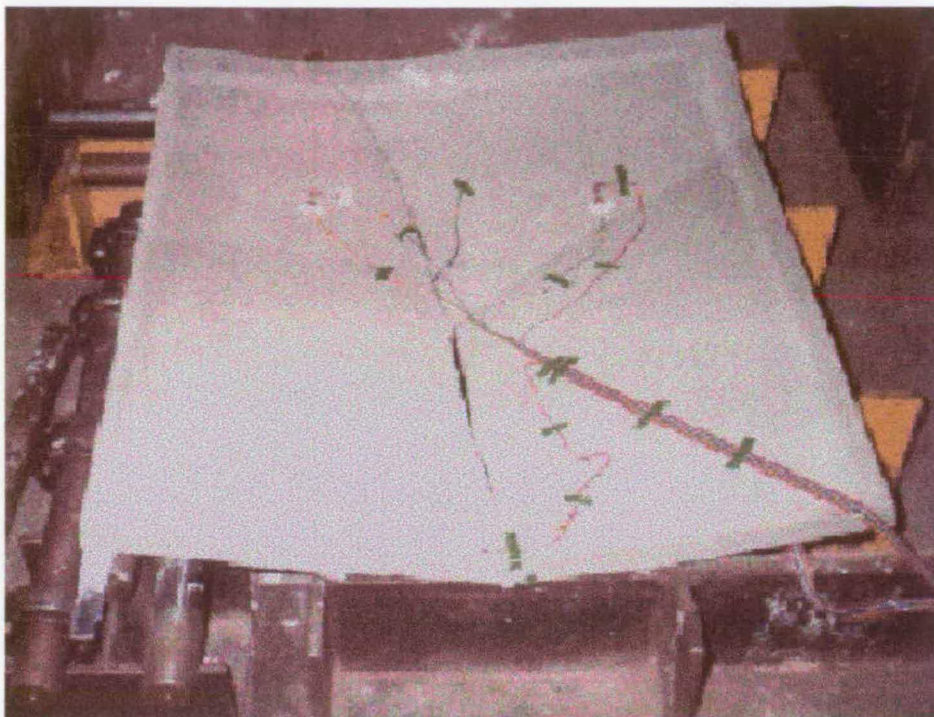


FIG. 4.35 Crack Pattern of a Three Sides Supported Panel

Table 4.8 Failure Pressure of Mortar Panels

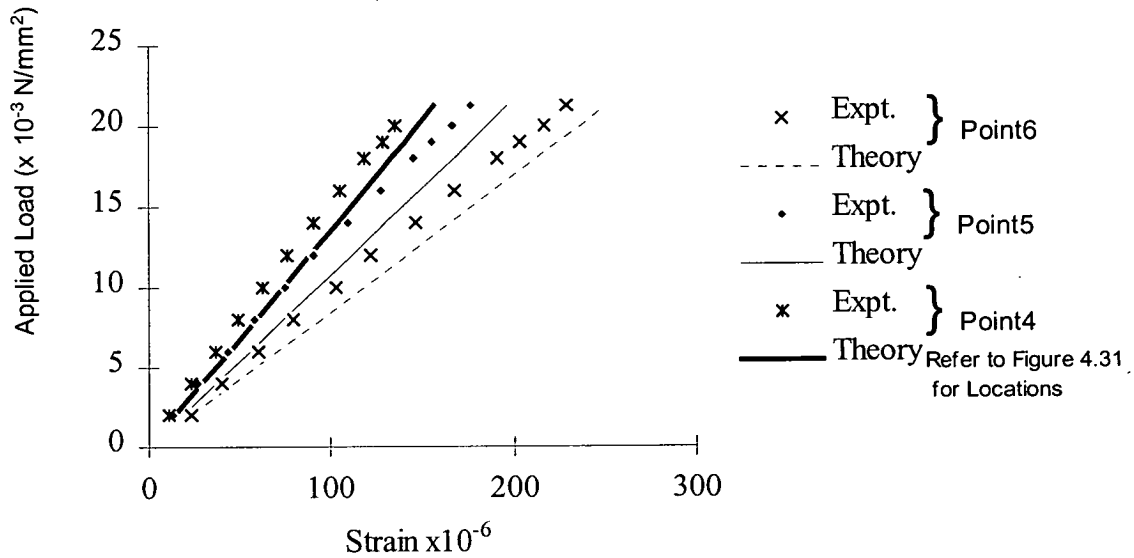
Panels	$L_x$ (mm)	$L_y$ (mm)	$t$ (mm)	$F$ (N/mm <sup>2</sup> )	Boundary Conditions	Failure Pressure (x 10 <sup>-3</sup> N/mm <sup>2</sup> )
P -1	800	720	31.34	4.12	4 Sides Simply Supported	21.86
P -2	800	720	30.74	4.12		19.8
P -3	800	720	31.32	4.62	3 Sides Simply Supported	13.84
P -4	800	720	30.0	4.66		12.8

F:Flexural Strength

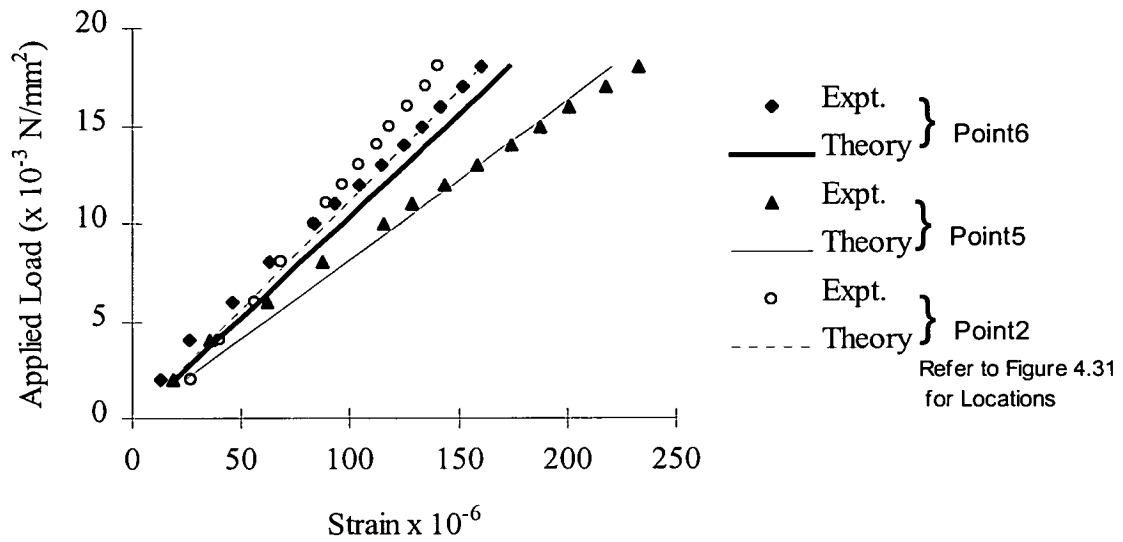
#### 4.4.5.2 Strain Measurements

The strain was measured on the compression and the tension faces of the specimens at the various points shown in Figure 4.31 at each load increment up to the failure of the specimens. Figures 4.36 to 4.37 show some of the typical relationships between the theoretical and the experimental stress-strain values. As can be observed in these figures, the strain increases linearly with the stress up to the failure. The data logger was observed very carefully towards the failure of the specimen for any sudden increase in the values of the strain readings. None of the strain gauges showed any

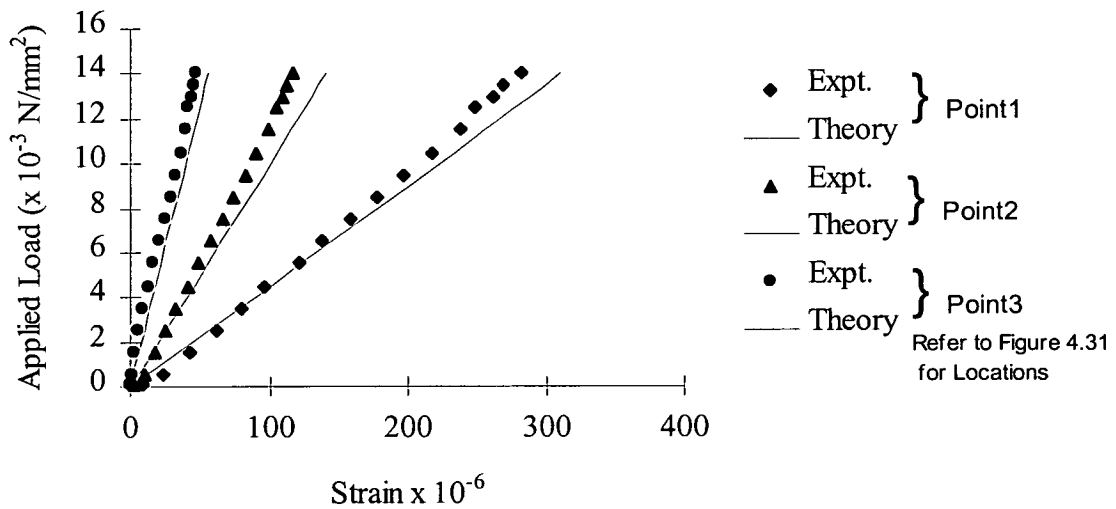
such increase at the time of failure. This again shows that the shedding of load from the weaker to the stronger direction after cracking as shown by the orthotropic material was absent in the case of mortar panels. The theoretical values of strain were calculated from a finite element analysis by considering the shear modulus obtained from the experiment which was only 30% of the theoretical value (Eqn. 4.7). A good agreement between the theoretical values and the experimental values of the strain was noticed in all the tests, the maximum variation being only up to 10%. This again supports that the value of shear modulus of mortar is lower than that obtained from the theoretical relationship.



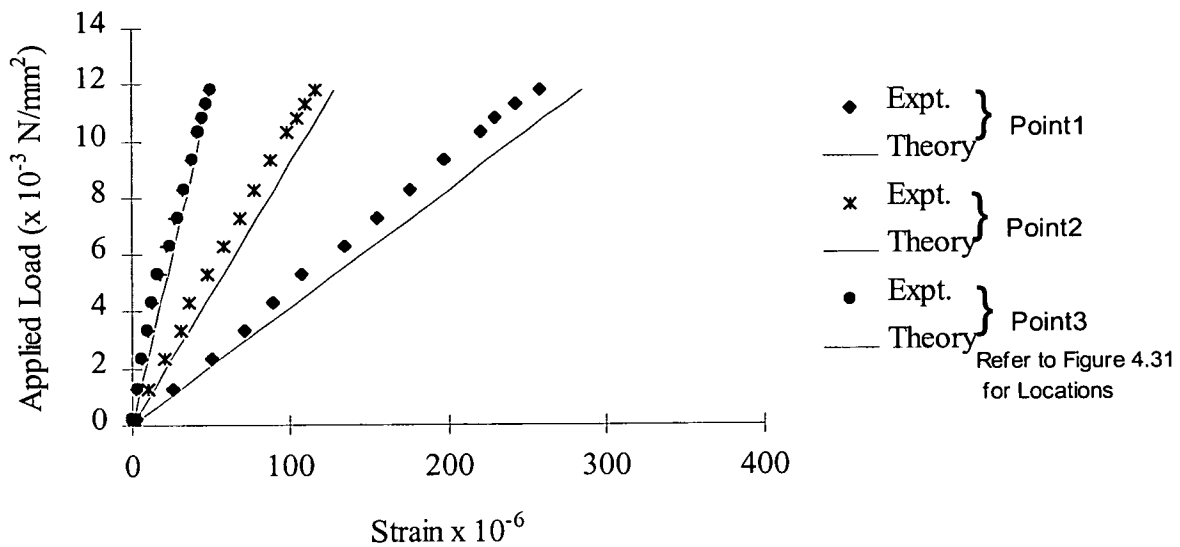
**FIG. 4.36a Strain: Theoretical and Experimental Values for 4 Sides Supported Panel, P-1**



**FIG. 4.36b Strain: Theoretical and Experimental Values for 4 Sides Supported Panel, P-2**



**FIG. 4.37a Strain: Theoretical and Experimental Values for 3 Sides Supported Panel, P-3**



**FIG. 4.37b Strain: Theoretical and Experimental Values for 3 Sides Supported Panel, P-4**

#### 4.4.6 Effect of Shear Modulus on the Failure Pressure of a Panel

In order to demonstrate the effect of the shear modulus on the failure pressure of the mortar panel under bi-axial bending, the moment coefficients given in the BS for a simply supported panel subjected to lateral loading is studied. According to the BS 8110 Part 1(1985)-Section 3.5.3.3, “when simply supported slabs do not have adequate provision to resist torsion at the corners, and to prevent the corners from lifting”, the maximum bending moment coefficients in both the directions as given in the code are reproduced in Table 4.9. The calculation of these coefficients is based on the Grashoff-Rankine method, ignoring the effect of the Poisson’s ratio. However, in a plate bending finite element solution, the effect of the Poisson’s ratio and the shear modulus (Eqn. 4.7, page 87) are taken into account. Hence, the moment coefficients are much lower than that given in the BS8110 (Table 4.9). The values of the Poisson’s ratio and the shear modulus were reduced in the finite element analysis to

obtain the same coefficients as in the BS 8110 by modifying the rigidity matrix (Eqn. 4.27).

$$D = \begin{bmatrix} D & \nu D & 0 & 0 & 0 \\ \nu D & D & 0 & 0 & 0 \\ 0 & 0 & \frac{(1-\nu)}{2} D & 0 & 0 \\ 0 & 0 & 0 & S & 0 \\ 0 & 0 & 0 & 0 & S \end{bmatrix} \quad 4.27$$

where for a plate thickness of  $t$ ,  $D = \frac{Et^3}{12(1-\nu^2)}$  and  $S = \frac{Gt}{1.2}$

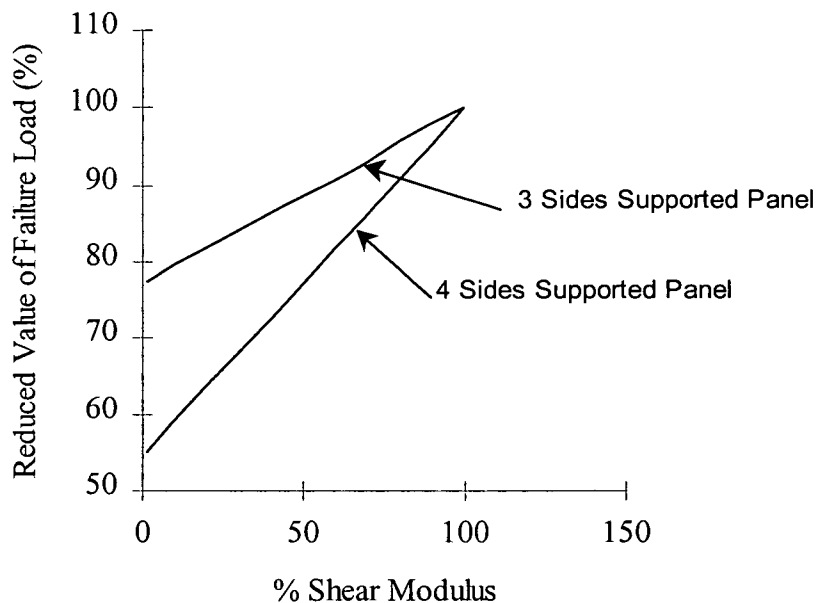
**Table 4.9 Comparison of the Moment Coefficients for a Four Sides Simply Supported Panel.**

Aspect Ratio H/L	BS 8110 Table 3.14		FE Analysis ( $G_{\text{theo}}$ and $\nu=0.137$ )		FE Analysis ( $0.285G_{\text{theo}}$ and $\nu=0.0001$ )	
	$\alpha_x$	$\alpha_y$	$\alpha_x$	$\alpha_y$	$\alpha_x$	$\alpha_y$
1.0	0.062	0.062	0.042	0.042	0.0573	0.0573
1.1	0.074	0.061	0.05	0.042	0.071	0.0573
1.2	0.084	0.059	0.057	0.041	0.0818	0.054
1.3	0.093	0.055	0.064	0.040	0.0913	0.05
1.4	0.099	0.051	0.071	0.039	0.0995	0.0455
1.5	0.104	0.046	0.077	0.038	0.106	0.0418
1.75	0.113	0.037	0.090	0.034	0.118	0.0363
2.0	0.118	0.029	0.098	0.030	0.125	0.034

The effect of the shear modulus and the Poisson's ratio can be reduced by modifying the elements  $D(3,3)$ ,  $D(4,4)$  and  $D(5,5)$  of the rigidity matrix given in Eqn. 4.27 and by considering very low values for the Poisson's ratio. The analysis has been carried out for panels of various aspect ratios to obtain the moment coefficients and are compared with those given in the BS (Table 4.9). It was observed that by considering 28.5% of the theoretical value of the shear modulus, the moment coefficients for different aspect ratios are similar to that given in the BS. This clearly indicates that the shear modulus of mortar is less than that given by the elastic theory and the experimental value of 30% of the theoretical value can be considered for the analysis of the panels.

#### 4.4.7 The Effect of Shear Modulus on the Failure Pressure of Panels

A parametric study was done on the effect of varying the shear modulus on the failure pressure of a panel. The finite element analysis of the cross beams and the panels was carried out by varying the values of the shear modulus. The Effect of varying the shear modulus on the failure pressure of panels can be seen in Figure 4.38. This figure shows a plot of the change in shear modulus against the change in the value of the failure pressure, which is expressed as the % of the failure pressure when the shear modulus is the same as that obtained from the theory (100% shear modulus). It can be seen from the figure that the failure pressure predicted by the plate bending theory drops with the reduction of shear modulus. In the case of the four sides supported panels, the theoretical value of the failure pressure was reduced by 55% by reducing  $G$  to a very small value (0.01%) of the theoretical value obtained from Eqn. 4.7. However, this reduction was only 77% in the case of three sides supported panel. This shows that assuming  $G$  obtained from the elastic relationship (Eqn. 4.7 in page 87) may lead to an over-estimation of the failure load for plain mortar under lateral loading. Hence, it is advisable to consider a lower value as obtained from the experiment in the analysis for safe designs.



**FIG. 4.38 Effect of Shear Modulus on the Failure Pressure of Mortar Panels**



#### ***4.4.8 Comparison of the Experimental and Theoretical Results***

It has been shown that the finite element method incorporating the failure criterion for the isotropic material is able to predict the failure load of cross beams very close to the experimental results.

Further validity of the criterion was checked against the results of the panel tests. The failure pressures of panels were calculated by the Rankine's method, the Yield line method, the Finite element method incorporating the failure criterion for the isotropic material and the Rankine's method incorporating the increase in strength under bi-axial bending as explained in Section 4.3.7. The theoretical results are compared with the experimental failure load and are given in Table 4.10.

While analysing the panels supported on three sides by the Rankine's method, an equivalent panel supported on four sides was considered. This was done by doubling the length of the panel so that the deflection at the centre of the free edge of the panel supported on three sides was equal to the central deflection of the 4 sides supported panel. A finite element analysis was carried out on a panel supported on four sides and a three sides supported panel of half the length. The deflection at the centre of the panel supported on four sides was found to be the same as that at the centre of the free edge of the panel supported on three sides.

It is clear from Table 4.10 that even though the yield line method gave good results in the case of cross beams, it over-estimated the failure load for panels by a very high factor. It can be seen from the table that the yield line method consistently over-estimated the failure load for panels of both types of support conditions. The over-estimation of the failure load by the yield line method is as high as 29%. The Rankine's method under-estimated the failure load for both types of panels when the uni-axial flexural strength of mortar was used. However, closer predictions are achieved by incorporating the increase in strength under bi-axial bending. It is also evident from Table 4.10 that the finite element analysis with the failure criterion is

able to predict the failure pressure very close to the experimental values. While analysing the panels by the finite element method, the shear modulus was taken as 30% of the theoretical value as pointed in 4.4.6. It can be noticed that better results are obtained by both the Rankine's method and the finite element analysis, where the increase in strength under bi-axial bending is considered in the analysis.

**Table 4.10 Experimental and Theoretical failure load of Mortar Panels ( $\times 10^{-3}$  N/mm<sup>2</sup>)**

Panel	$\frac{L}{H}$	Expt.	YL	RM	FEM	FEM*	RM*	$\frac{\text{Expt}}{\text{YL}}$	$\frac{\text{Expt}}{\text{FEM}}$	$\frac{\text{Expt}}{\text{FEM}^*}$	$\frac{\text{Expt}}{\text{RM}}$	$\frac{\text{Expt}}{\text{RM}^*}$
P-1	0.9	21.86	28.22	17.24	17.66	19.1	19.27	0.78	1.24	1.14	1.27	1.13
P-2	0.9	19.8	27.15	16.58	17.01	18.4	18.54	0.73	1.16	1.08	1.19	1.07
P-3	0.9	13.84	19.49	12.08	11.48	12.7	13.07	0.71	1.21	1.09	1.15	1.06
P-4	0.9	12.8	18.03	11.18	9.93	11.8	12.09	0.71	1.29	1.09	1.15	1.06

\*The proposed failure criterion has been incorporated in these methods.

## **4.5 Conclusion**

The tests on mortar specimens represented the behaviour of the isotropic material. The following conclusions can be drawn on the behaviour of an isotropic material subjected to bi-axial bending.

- The applied load is distributed in the two orthogonal directions according to the relative stiffness of the material.
- Isotropic material cracks and fails simultaneously in a brittle manner and does not exhibit any 'load shedding', whereas in the case of material with strength and stiffness orthotropies, upon cracking, the load carried by the weaker direction was shed to the stronger direction.
- An increase in strength over the uni-axial flexural strength was noticed in the case of isotropic material under bi-axial bending when unequal moments act in the orthogonal directions.
- The behaviour of an isotropic material under bi-axial bending can clearly be distinguished from that of an orthotropic material and a separate failure criteria needs to be considered for the analysis of both.
- The yield line method predicted the failure load of the cross beams very close to the experiment results. However, failure pressure of mortar panels were highly over-estimated by the yield line method and, hence, cannot be used safely in design.
- The failure load of an isotropic panels subjected to bi-axial bending can be predicted by the finite element method or the Grashoff-Rankine method, incorporating the failure criterion for the isotropic material.

## **CHAPTER 5**

# **A MODEL FOR A HYBRID SYSTEM INCORPORATING ARTIFICIAL NEURAL NETWORKS AND CASE-BASED REASONING**

### **5.1 Introduction**

The emergence of Artificial Neural Networks (ANNs) and their successful application in various fields have opened up a promising approach to solve many engineering problems, especially in specific areas where a complex un-identified relationship exists between a given set of inputs and outputs. Their application has been adopted widely in civil and structural engineering problems and has been shown to perform reasonably well in drawing non-linear relationships. Hybridisation of artificial neural networks with other information processing technologies helps to exploit the strengths of each, in combination, so as to produce a more effective system than using them in isolation. A hybrid system that utilises the capabilities of both Artificial Neural Networks (ANNs) and Case-Based Reasoning (CBR) has been adopted in the current research for the analysis of masonry panels under bi-axial bending. The potential of ANNs in solving complex non-linear problems is utilised to find out the failure pressure of a laterally loaded panel. A network, trained using a set of data which is representative of the problem domain, is shown to be successful in solving new problems of similar nature with reasonable accuracy. CBR has been used to solve new problems by adapting solutions to similar problems solved in the past, which are stored in the case library. Cases provide memories of the past solutions that have been used successfully. The experimental results obtained from the tests on panels are analysed using the existing theories and the method that gives the most accurate correlation between the theoretical prediction and the experimental

result is recommended for other panels of similar properties and boundary conditions. In this hybrid approach, CBR is used to identify a theoretical method which is most suitable for a specific panel with given properties, while ANNs is used to arrive at a solution with great saving in computational time.

## **5.2 Theoretical Methods for the Analysis of a Masonry Panel**

At present, no proper mathematical solution is available to predict the ultimate failure pressure of brickwork cladding panels supported on three or four sides. A considerable amount of test data is available on panels subjected to lateral pressure as a result of the experimental research since the early '70s. Nevertheless, lack of information regarding the stiffness orthotropy, the Poisson's ratio, and the failure criterion and the uncertainty of the tests' boundary conditions make it very difficult to use these results in the development of a rational method of design. The BS, which is based on the yield line analysis and the Australian code of practice, which is based on the strip method of analysis have been shown to give reasonably good results in some of the test cases although there is limited theoretical justification for using these methods. The good agreement observed in these cases could be due to the fact that the boundary conditions in the tests were not well defined and the dead weight stresses and the rotational restraints were neglected. The finite element method incorporating the failure criterion (SINHA *et al.* 1997) has closely predicted the failure pressure of many of the panels that are tested and reported in the literature. However, the finite element analysis is extremely expensive in terms of CPU time and memory. Apart from that, the analysis has to be carried out several times, varying the number of elements in the mesh to obtain a fairly accurate solution. Artificial neural network technique should provide an efficient tool to obtain approximate finite element solutions of the failure pressure of a panel under bi-axial bending, if trained using the appropriate data set. A trained net can produce these results in a fraction of the time required for the computational analysis.

Even though the justification for using the various existing theories for the design of masonry under bi-axial bending is disputable, these methods are shown to give accurate predictions of the failure load in some of the experimental cases. By applying case-based reasoning technique, it is possible to infer some knowledge about the relationship that could possibly exist between these various methods and the properties of the panel. The application of CBR, thus, helps to make best use of the available experimental data.

### **5.3 The Model for the Development of the Hybrid System for the Analysis of Masonry Panels under Bi-axial Bending**

A schematic diagram for the development of a hybrid system for the analysis of masonry panels under bi-axial bending is shown in Figure 5.2. The hybrid system combines the application of ANNs for the analysis of a panel and CBR for advising on a suitable method for the analysis. ANNs can be trained using a set of data and can be used to obtain solutions quickly. The idea of using past experience in solving new problems and, thus, exploiting its memories instead of relying entirely on a set of rules is employed in case-based problem solving technique. Even though the application of ANNs and CBR seems to be relatively simple and straight forward, it is their combined effect and the unique approach in this application that makes the hybrid system an efficient tool for analysing masonry panels under bi-axial bending. The application of ANNs and CBR as adopted in this hybrid system is explained below.

#### ***5.3.1 ANN Applied to Masonry Panel Subjected to Bi-axial Bending***

ANN application to a particular problem consists of training the net using a set of data which is representative of the problem domain. Hence, the first step is to generate a suitable training set that can well represent the problem at hand. The

essential characteristics required for a training set to develop a successful application have been described in Section 3.8. In the present application, a considerable amount of data is available as a result of the experimental research that could be used as a training set. However, as the net is shown to be poor in extrapolating the results, it is essential that the training set consist of all the practical range of data. Hence, in order to cover the whole range of data, the training set has to be expanded using the existing theoretical methods of analysis.

The theoretical methods that are currently being applied to the panel analysis include the BS, the Australian code of practice and the finite element analysis. Of the three, the finite element method with the modified failure criterion proposed by SINHA *et al.* (1997) has been shown to predict the failure pressure closer to the experimental results than the other two. Hence, the finite element method was used to generate majority of the training set. However, in order to improve the performance of the net on improperly defined problems, the BS and the Australian code were used to add noisy data into the training set. This is done by finding out the failure pressure of all the panels by the finite element method, the BS and the Australian code of practice. If the values of the failure pressures obtained by the BS and the Australian code varies within 10% of the value obtained by the finite element method, an average of the three values are taken as the failure pressure of the panel in the training set. This incorporates a slightly incorrect data in the training set. If the above variation exceeds 10%, then the BS and the Australian code values are neglected and only the finite element results are considered. Panels of various physical and mechanical properties are analysed using these three methods to generate the training set.

The neural net is, thus, trained to produce the failure pressure of a panel subjected to bi-axial bending. The properties of the panel that are used in generating the training set include the length, the height and the thickness of the panel, the strength and the stiffness orthotropies and the flexural strength of brickwork in the direction parallel to the bed joint.



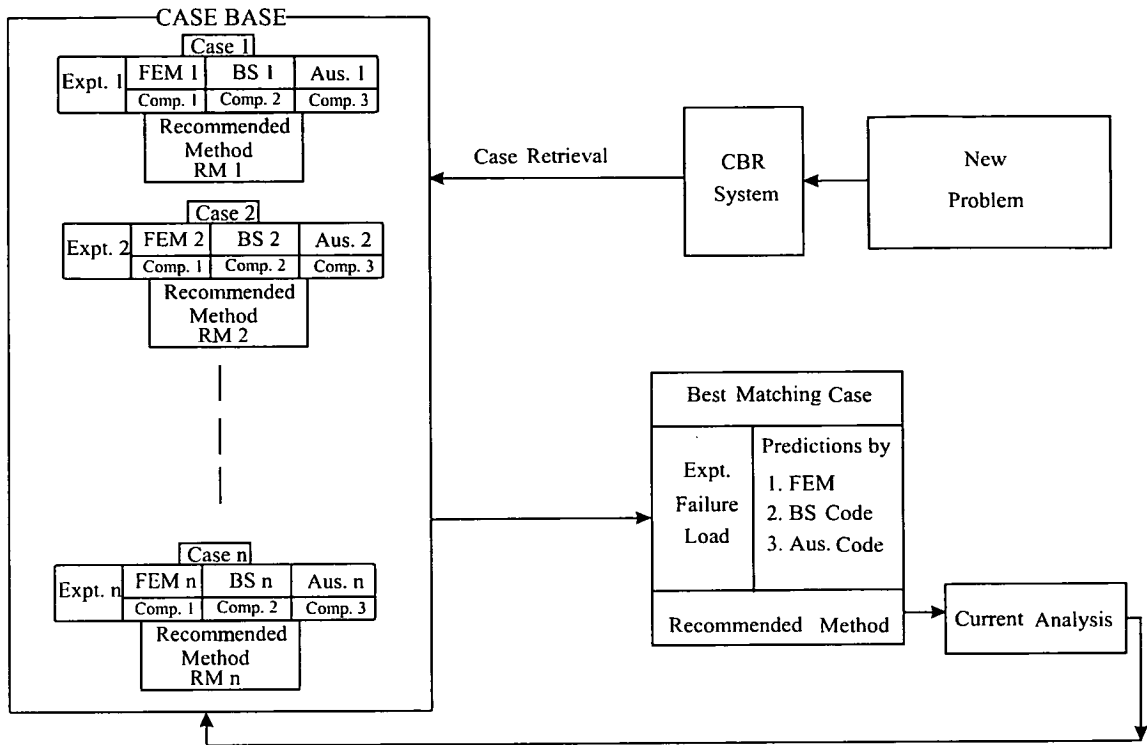
After training, the net should have learned the unknown relationship between the inputs and the outputs specified in the training set. However, it is important to evaluate the performance of the net on unseen problems. This is to ensure that the net has not memorised the data instead of learning the relationship. In order to assess the net performance, a test set is generated in exactly the same way as the training set. The test set, thus, consists of problems that are not used for training and are completely new to the trained net. As majority of the data used in training the net consisted of the results of the finite element analysis, a trained net, which has proven successful on the test set, could be used to obtain solutions to new problems with reasonable accuracy instead of the time consuming finite element analysis. This would result in considerable savings in the computational time.

The trained network could now be evaluated to measure its performance on a practical situation. This is done by generating a second test set, consisting of the experimental results that are available in the literature. The data consists mainly of the results of the laboratory-based experimental research carried out at different parts of the world. These include research at University of Edinburgh (UK), University of Melbourne (Australia) and BCRA (UK). As the tests were carried out at various research centres, it is possible that these tests were done under different experimental set up and can be erroneous. It was also difficult to obtain the correct value of the orthotropic stiffness ratio of the tested brickwork. In many cases, the mechanical properties were taken as an average of all the test results. However, maximum control over the experimental set up was achieved for the tests done at the University of Edinburgh and it was possible to obtain the properties of the brickwork used in individual tests. Hence, even though it was difficult to control the quality of the experimental data, due consideration was given to this aspect while the results were analysed. For example, a higher degree of closeness between the experimental failure load and that predicted by the trained net is expected for cases that are tested at University of Edinburgh. The same level of accuracy may not be achieved for other panels tested elsewhere.

### **5.3.2 CBR Applied to Masonry Panel Subjected to Bi-axial Bending**

Case-based reasoning involves retrieving solutions of similar past problems and adapting them for the current problem. The hybrid system developed in this research incorporates CBR as a system that simply assists the user by replaying similar past cases. Computing the similarity between the new case and those in the case base is an important step in CBR technique. The overall evaluation of the similarity between two cases is based on the computation of local similarities between each attribute used to describe the case. The local similarity may vary, depending on the attributes' type or the size of the sets on which the similarity is computed. For instance, 10 is more similar to 20 if the size of the possible interval varies from 0 to 1000, than if it varies from 0 to 20. After computing the local similarities with each case, the global similarities can be calculated by combining them using a similarity measure. Based on the similarities in problem specification, a number of similar past solutions can be retrieved from the case base. The user can choose to pick either a solution from the set and adapt according to his/her requirements or pick different parts of the solutions and synthesise them to form the final solution. The application of CBR in this hybrid approach can be represented schematically with the help of a sketch as shown below in Figure 5.1.

The case base is generated from the experimental results, where the failure load is compared with the theoretical predictions. Panels, for which the experimental failure load is available, are analysed using the various existing methods of analysis. The method which gives the closest prediction can be obtained by comparing the theoretical results with the experimental values. It is possible that the method that gives the closest prediction varies from panel to panel. This could be mainly due to its physical properties such as the aspect ratio and the thickness or the mechanical properties like the strength and stiffness orthotropies and the support conditions. Each case is identified in the case base by the above properties. The output essentially consists of the comparison of the experimental failure load with the various theoretical values.



**FIG. 5.1 Case Based Reasoning applied to masonry panels**

When a new problem is to be solved, the case-based reasoning system module retrieves matching cases from its case base. The criteria for choosing a matching case is based on the input values of the new problem and that of the cases stored in the case base and will be explained in detail in Chapter 6. More than one matching case will be retrieved by the CBR system with varying degrees of similarities between the cases in the case base and the new problem. Out of all the matching cases, one with the highest degree of similarity is generally adopted for the current application. The method that is used for the best matching case is recommended to be used for the current analysis. However, the user is given an option to browse through the matching cases and their results and decide by himself/herself the method to be used based on his/her own judgements.

## **5.4 Schematic Representation of the Model**

The hybrid system adopted in this research and explained in the previous section can be best explained with the help of a schematic diagram (Figure 5.2). As pointed out in the above section, a considerable amount of data is required for the development of this system to train and test ANNs and to create a case base in CBR. The modules I and II in Figure 5.2 represent the source of data required for this purpose. The training set is prepared from the existing methods of analysis (Module I) and is supplied to (Line A) the Neural Network software (Module III). One set of test data is prepared from the existing methods of analysis (Line B1) and another set is prepared from the experimental results (Module II, Line B2) and are presented to the Neural Network software (Module III) for the evaluation of its performance (Line B). The network, trained and tested for its performance with the data, can now be used to analyse panels and produces results very quickly (Module V, Line C).

The experimental results (Module II) are now used to develop the case base in the CBR system (Module IV). This involves the analysis of the experimental results using the existing methods of analysis (Line D) and by the trained neural network (Line E). The experimental results, along with the theoretical analysis, are used to create the case base (Line F). The Hybrid system is, thus, ready with the trained neural network and the case bases in CBR.

When a new problem is to be solved, the CBR module (Module IV) is invoked to find out the matching cases (Line G). The matching cases will be presented to the user and he/she picks up the best matching case (Line H) and decides the method to be applied in the current analysis. If the system recommends the finite element method, the analysis can be carried out by using the trained network, thus, saving a considerable amount of time as the majority of the data set is generated using the same method. The user is given the option to carry out the finite element analysis by allowing the access to the finite element program (Module V). On the other hand, if

the system recommends the BS or the Australian Code of Practice, the results can be obtained by referring to the respective code. The code coefficients are incorporated in a computer program.

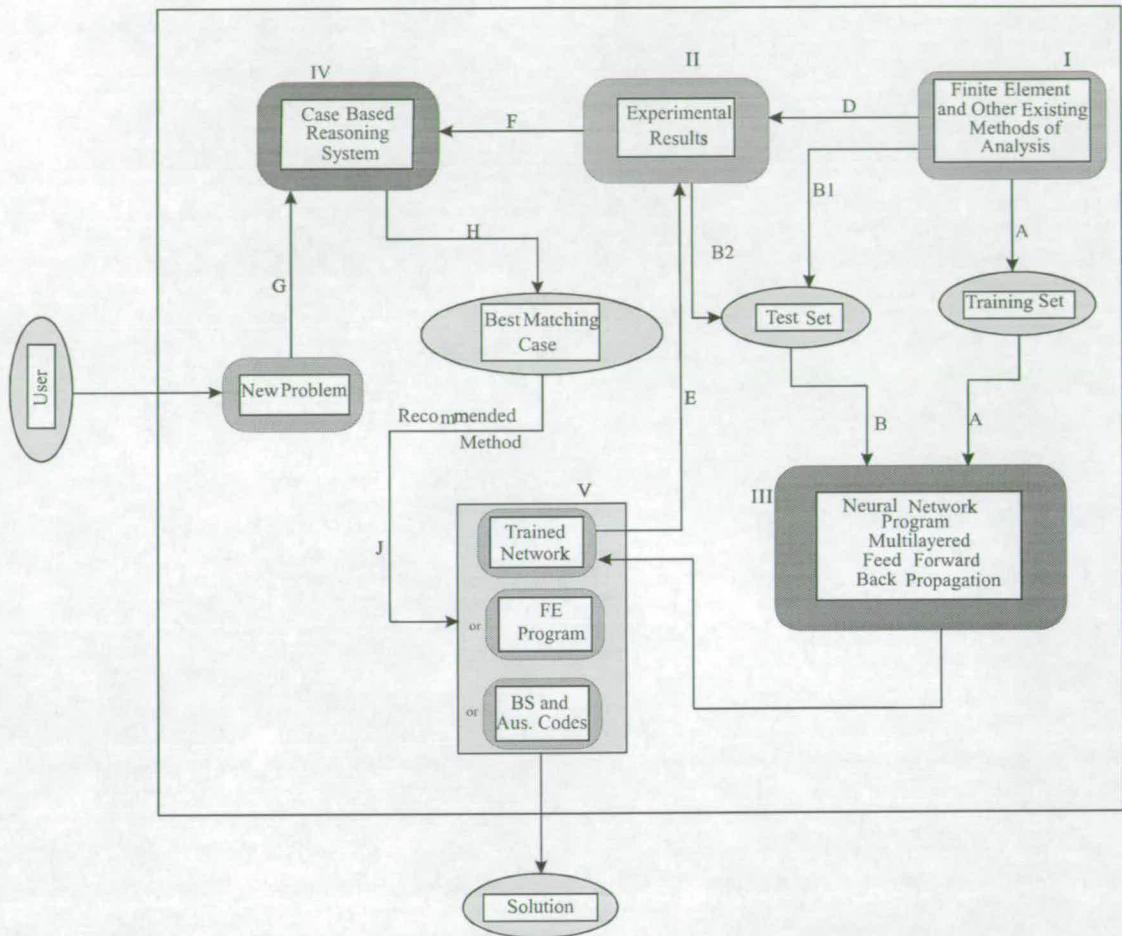


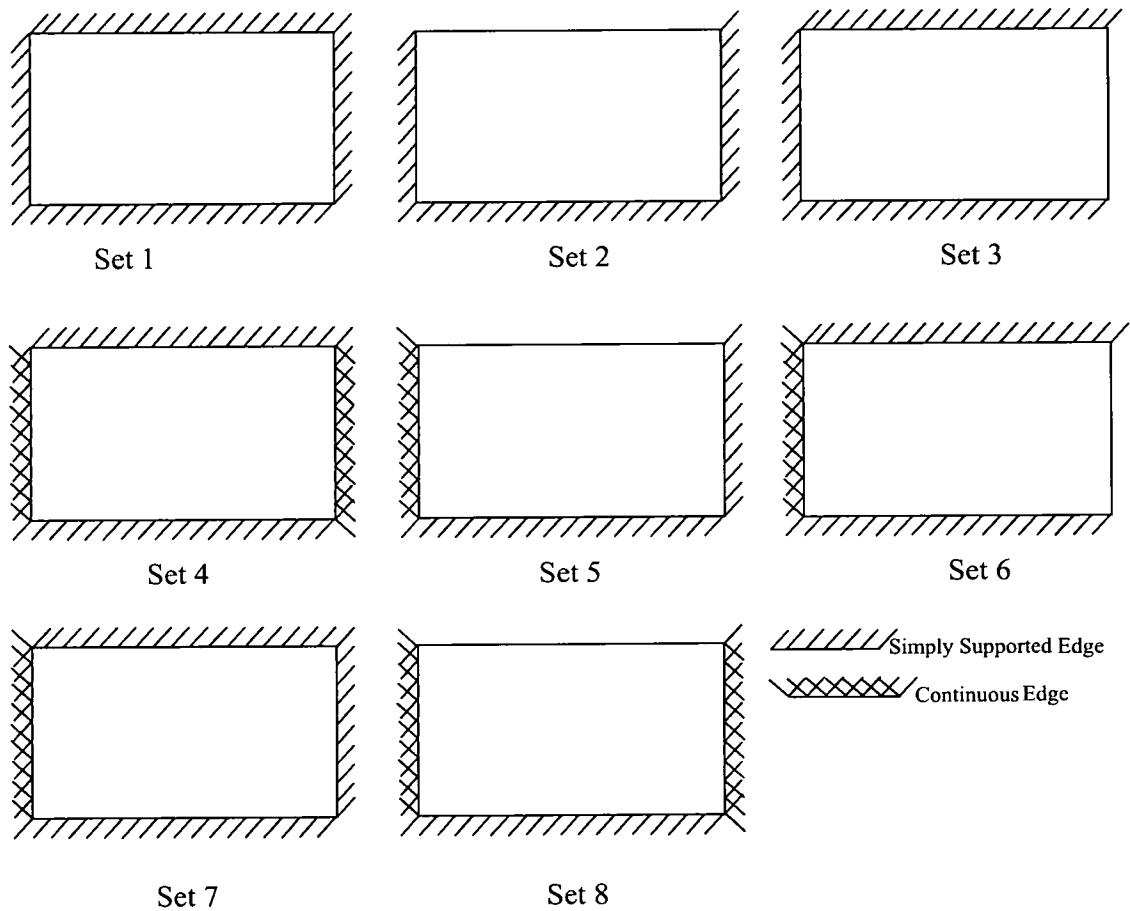
FIG. 5.2 The Model of the Hybrid System Combining ANN and CBR used for the Analysis of Masonry Panels

### 5.5 Clustering Approach

It has been pointed out by researchers that a complex problem can be easily trained in ANNs by adopting a clustering approach (HAJELA & BERKE 1991). In this approach, the main problem is split into several smaller and simpler sub-problems. In the present problem, the support conditions of the panel have been taken as the basis

for clustering the panels. Panels that are to be designed can be clustered into various groups based on the number of sides supported and the degree of fixity at each support. Each group can be trained separately in ANNs using a separate training and test set. However, a single case base is sufficient to generate the CBR application.

The various support conditions that are generally found in buildings for masonry walls and are considered in the current research are shown in Figure 5.3.



**FIG. 5.3 Panels of Different Support Conditions**

## 5.6 Conclusion

A considerable amount of data is available in this area as a result of the experimental research in masonry over the past two decades. Given that the various methods lack a

rational justification and that considerable amount of experimental results are available, the problem lends itself well to the application of ANNs and CBR.

The hybrid system combines the application of artificial neural networks (ANNs) and case based reasoning technologies to analyse a panel. A trained neural network can find out the failure pressure of a panel, given the geometry and the mechanical properties of the panel. As the majority of the data used in training the net was generated from the finite element analysis, the net can be used to obtain quicker results and can, thus, save a substantial amount of computational time and CPU space. The case based reasoning module makes use of the available experimental data and forms a case base which can be used to suggest the best method for the analysis of a panel of specific mechanical and geometrical properties.

The hybrid system, thus, makes best use of the potential of both Artificial Neural Networks and Case Based Reasoning and forms an efficient tool for the analysis of masonry panels under bi-axial bending.

## CHAPTER 6

# IMPLEMENTATION OF THE HYBRID SYSTEM FOR PREDICTING THE FAILURE PRESSURE OF MASONRY PANELS SUBJECTED TO BI-AXIAL BENDING

### 6.1 Introduction

The hybrid system described in this chapter utilises the capabilities of both Artificial Neural Networks (ANNs) and Case Based Reasoning (CBR). The potential of ANNs in solving complex non-linear problems is utilised to find out the failure pressure of masonry panels under bi-axial bending. A network, trained using a set of data, which is representative of the problem domain, is shown to be successful in solving new problems with reasonable accuracy. The experimental results obtained from the testing of the panels are analysed using the existing theories and the method that gives good correlation between the theoretical prediction and the experimental result is recommended for other panels of similar properties and boundary conditions. Case based reasoning (CBR) has been used to solve new problems by adapting solutions to similar problems solved in the past, which are stored in the case base. In this hybrid approach, CBR is used to identify a method which is most suitable for the present problem, while ANNs are used to arrive at a solution with considerable amount of saving in computational time.

### 6.2 Application of ANNs to Predict the Failure Pressure of Masonry Panels under Bi-axial Bending

The development methodology adopted in this chapter for the analysis of masonry panel is described in detail in Chapter 3 (Section 3.8). This included the various steps for the development of an ANNs application, describing the possible values to be adopted to develop a network which could generalise well using a non-linear



mapping. The values of the various parameters that are considered during the current application are further described here.

### **6.2.1 Initial Studies**

After a thorough analysis of the recommendations and suggestions by various researchers, a multi-layered feed-forward network with back-propagation algorithm and sigmoid activation function was adopted in the current application for the analysis of masonry panels to obtain the failure pressure. The feasibility study of the selected paradigm was carried out on a four sides simply supported panel subjected to lateral loading. The training and the test sets for the initial studies were taken from the data that was available in the literature as a result of the experimental research (BAKER 1972; KHEIR 1975; LAWRENCE 1983; NG 1996). Two thirds of the available experimental results were used for training the net and the remaining one third was used subsequently for checking the performance of the trained net.

A trial and error approach was used to finalise the number of hidden layers and the number of nodes in each layer. A three layered net with 9 input layer nodes, 5 hidden layer nodes and a single output node was finally accepted. The length, the height and the thickness of the panel, along with the flexural strength in the two orthogonal directions were used to represent the input variables. As the experimental results consisted of tests carried out on different scale models of brick, the same was also used as a variable to check any possible influence. Thus, the input variables included the Length of the panel (L), the Height of the panel (H), the Scale model of the brick used (M), the Aspect ratio (L/H),  $1/L^2$ ,  $1/H^2$ ,  $F_x Z$ , and the Orthotropic strength ratio (R). The net was trained to predict the failure pressure of the panel under bi-axial bending.

After training, the net was evaluated for its performance using the test set. The neural net results for the training and the test sets are given in Tables 6.1 & 6.2 respectively.

As can be seen from Table 6.2, the trained net was able to predict the failure pressure of the panel within 8.75%, except in two cases only. The maximum error in these cases was 12% and 17%. Thus, it is evident from the performance of the trained net that the ability of neural networks can be quite fruitfully adopted in problems of a similar nature.

**Table 6.1 Training Set and the Neural Net Results Used for Feasibility Study**

L m	H m	M <sup>1</sup>	1/M <sup>2</sup>	L/ H	1/L <sup>2</sup> m <sup>-2</sup>	1/H <sup>2</sup> m <sup>-2</sup>	F <sub>x</sub> Z Nm	R	Target Output	NN result	% error
2.4	1.2	6	0.028	2	0.174	0.695	0.00374	2.88	18200	18241	0.22
2.4	2.4	6	0.028	1	0.174	0.174	0.003234	2.34	10500	10522	0.21
1.51	2.26	2	0.25	0.5	0.44	0.196	0.00686	4	20580	20497	0.4
2.4	4.8	6	0.028	0.5	0.174	0.043	0.003366	3.25	7000	6915	1.21
3.75	2.5	1	1	1.5	0.071	0.16	0.00412	2.5	4900	4869	0.63
2.06	2.06	3	0.111	1	0.235	0.235	0.005542	4.21	10980	10989	0.08
4.12	2.06	3	0.111	2	0.059	0.235	0.005525	5.31	5220	5195	0.48
2.06	2.06	3	0.111	1	0.235	0.235	0.004304	3.65	9420	9430	0.11
2.3	2.3	2	0.25	1	0.189	0.189	0.00533	4.11	12200	12280	0.65
2.3	2.3	2	0.25	1	0.189	0.189	0.00533	4.11	12360	12280	0.66
2.4	1.2	6	0.028	2	0.174	0.695	0.003828	3.5	19000	18989	0.06
2.4	2.4	6	0.028	1	0.174	0.174	0.00297	2.9	8400	8410	0.12
2.4	4.8	6	0.028	0.5	0.174	0.043	0.003212	3.07	5600	5607	0.13
4.12	2.06	3	0.111	2	0.059	0.236	0.00595	2.46	6150	6139	0.18
2.5	2.5	1	1	1	0.16	0.16	0.004053	2.38	8600	8587	0.15
6	3	1	1	2	0.028	0.111	0.00392	1.57	3200	3302	3.19

**Table 6.2 Test Set and Neural Net Results Used for Feasibility Study**

L m	H m	M <sup>1</sup>	1/M <sup>2</sup>	L/H	1/L <sup>2</sup> m <sup>-2</sup>	1/H <sup>2</sup> m <sup>-2</sup>	F <sub>x</sub> Z Nm	R	Target Output	NN result	% error
2.4	1.2	6	0.028	2	0.174	0.695	0.0032	3.25	18000	15835	12.03
2.4	2.4	6	0.028	1	0.174	0.174	0.0037	3.47	10000	9888	1.12
3.1	2.1	3	0.111	1.5	0.104	0.236	0.0068	4.29	8300	9024	8.73
3.1	2.1	3	0.111	1.5	0.104	0.236	0.0049	3.55	6000	7020	17
6	3	1	1	2	0.028	0.111	0.0047	1.32	3500	3363	3.91
2.3	2.3	2	0.25	1	0.193	0.193	0.0031	2.56	7590	7926	4.43
2.1	2.1	3	0.111	1	0.235	0.235	0.0069	3.47	16350	17291	5.76

<sup>1</sup> The values in this column represents the scale model of bricks used. e.g. 6 for 1/6<sup>th</sup> scale brick, 2 for 1/2 scale bricks, 3 for 1/3<sup>rd</sup> scale bricks and 1 for full scale bricks.

### 6.2.2 Data Preparation

As pointed out in Chapter 5 (Section 5.5), masonry panels are categorised into 8 sets depending upon the boundary conditions of the panel. While applying ANNs for the analysis, the clustering approach described in Section 5.5 is adopted to simplify the problem. Hence, the net is trained for each of the categories of the panel using a separate set of training data.

The preparation of an appropriate training set is the prime factor towards the development of a successful application and has to be done with great care. The important aspects to be considered while preparing the training set is set out in Chapter 3 (Section 3.8).

In the current application, the problem was thoroughly studied to develop the best possible training set. Bi-axial bending is induced in masonry panel due to the uniform lateral pressure on the surface when the panel is supported on three or more sides. As the analysis aims at finding out the pressure at the time of failure, the mechanism of failure in the bending of a structure was looked at to see the possible parameters that affect the failure pressure. The failure moment of a masonry panel can be calculated as  $KwL^2$  when the plane of the failure is perpendicular to the bed joint or  $\mu KwL^2$  when the plane of bending is parallel to the bed joint (BS8110),

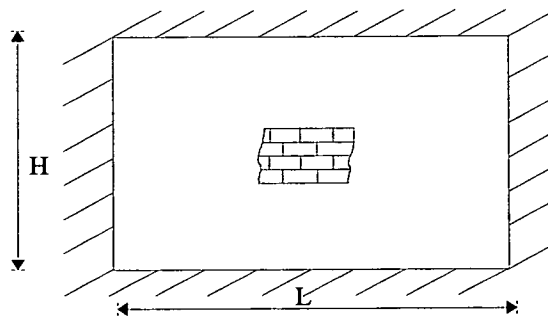


FIG. 6.1 The Panel Dimensions

where,  $w$  is the uniform lateral pressure  $L$  is the length (Figure 6.1) and  $K$  is a constant depending on the boundary conditions, the aspect ratio and the stiffness orthotropy and  $\mu$  is the orthotropic strength ratio.

At the time of failure, the bending stress is equal to the flexural strength ( $F_x$ ).

Hence,

$$F_x = \frac{KwL^2}{Z} \quad 6.1$$

where,  $Z$  is the section modulus.

Eqn. 6.1 can now be rewritten as:

$$w = \frac{F_x Z}{KL^2} \quad 6.2$$

It is obvious from Eqn. 6.2 that the parameters that affect the failure pressure of a panel are its physical properties such as the length, the aspect ratio and the section modulus of the panel and its mechanical properties such as the flexural strength in the stronger direction and the orthotropic strength and stiffness ratios. However, various researchers do not agree on the issue of whether or not to consider the stiffness orthotropy of brickwork while analysing a panel. SEWARD (1982) argued that the effect of including the stiffness orthotropy of brickwork in the analysis of the panels is quite insignificant. On the other hand, the distinct effect of stiffness orthotropy on the resistance of a panel under bi-axial bending has been demonstrated by NG (1996). A finite element program incorporating the failure criterion proposed by SINHA *et al.* (1997) was used in this research to analyse panels of different stiffness orthotropies. This study supported the findings of NG (1996) and it was decided to consider the stiffness orthotropy in the present investigation.

As explained in Chapter 3 (Section 3.8.2.2), it is recommended to reduce the dimensionality of the problem to obtain faster training and better generalisations in ANNs. Eqn. 6.2 shows that the failure pressure  $w$  is directly proportional to  $\frac{F_x Z}{L^2}$ .

Hence, the dimensionality of the problem can be reduced considerably by using  $\frac{F_x Z}{L^2}$  as single term while representing the data to the net for training, rather than using them separately. This also helped to reduce the non-linearity of the problem by incorporating the known relationships between some of the inputs and the output. Thus, the net would be left with only the hidden non-linearity to solve. The inputs to the network can now be reduced to the term  $\frac{F_x Z}{L^2}$ , the aspect ratio ( $L/H$ ) and the strength and stiffness orthotropies ( $F_x/F_y$  and  $E_x/E_y$ ).

Even though the available experimental data was used to run the feasibility study, it was observed that the data set did not cover all the possible practical range of panel dimensions and properties. Hence, it was essential to generate more data by theoretical methods of design. The methods used in the current analysis include the BS, the Australian Code of Practice and the Finite element analysis. The finite element program developed at the University of Edinburgh (ROTTER 1988) was modified by NG (1996) incorporating the failure criterion for the orthotropic material (SINHA *et al.*, 1997). The modified FEA was evaluated against the experimental results that were carried out at various research laboratories and was found to predict the failure pressure closer to the experimental values than any other existing methods. Hence, the major part of the data was generated using the modified FE analysis. Additional data was also created using other methods such as the BS and the Australian Codes of Practice. This helped to add a certain amount of noise to the training data so as to enhance the performance of the net. The methods of analysis used in the data generation and the discussion of the results are given in Section 6.3.

The range of data used for developing the training set is given in Table 6.3. The panels subjected to lateral pressure within this range are analysed using the various theoretical methods such as the BS, the Australian Code of Practice and the Finite element analysis in order to generate the data set. For each boundary condition, two hundred and eighty panels of different properties are analysed to obtain the failure

pressure using the three methods. As pointed out earlier, the BS over-estimated the results, the Australian Code of Practice under-estimated the results and the modified finite element with the failure criterion gave reasonable predictions of the failure load in majority of the cases. Hence, the data set consisting of the failure load predicted by the above methods included over-estimated and under-estimated results. However, a large variation in the failure pressures by the three methods results in a training set containing widely varying values of outputs for the same set of inputs, resulting in increased training time for the net. Therefore, the results by the BS and the Australian code of practice were compared with that of the finite element method and an average of the values was taken if the variation lied within 10%. Thus, it was possible to generate a training set for neural networks with slightly incorrect value for the output which could take into account any possible noisy data, such as the ill-defined support conditions or the incorrect mechanical properties. A part of the data set was set aside as the validation set to check the performance of the trained network. Nearly two-thirds of the data (230 panel results) was used to create the training set and the rest was used as a test/evaluation set. The available experimental results were used to create an additional test set which was used for further validation of the performance of the net. The amount of data collected in the current application was roughly within the range of five to ten training patterns for each connection weight (HAMMERSTROM 1993).

**TABLE 6.3 The Range of Input Data Used to Create the Training Set**

$L$	$H$	$\frac{L}{H}$	$\frac{F_x Z}{L^2}$ (N/mm)	$\frac{F_x}{F_y}$	$\frac{E_x}{E_y}$
(1)	(2)	(3)	(4)	(5)	(6)
800mm - 6000mm	1300mm - 3300mm	0.5 - 2.0	70 - 8100	1.3 - 4.0	0.8 - 1.8

While training the net for the different categories of panels, a relatively poor performance of the net was noticed in the case of ‘Set1’<sup>2</sup> and ‘Set3’<sup>3</sup>. Hence, the

<sup>2</sup> Set1: Four Sides Simply Supported Panel

<sup>3</sup> Set3: Three Sides Simply Supported Panel with Vertical Edge Free

training set was increased in these cases by adding more data on panels with different orthotropic stiffness ratios. Hence, the range of orthotropic stiffness ratio for these panels was 0.5 to 1.8.

While training the net, the input values were normalised within the range 0 to 1.0 and the output values were normalised within the range 0.2 to 0.8. The normalisation was done using the equations given in Chapter 3 (Section 3.8.2.5).

### **6.2.3 Network Architecture**

The design of the network architecture is a very important phase of the development of any neural network application. The various parameters that need to be decided during this stage are given in Table 3.1. The correct choice of the various parameters can considerably affect the learning and, hence, the performance of the net.

The number of nodes in the input layer can easily be decided based on the parameters used to define the problem. A three layered net was selected for the current application and was used for all the 8 sets of panels described in Chapter 5. The architecture of the selected net is shown in Figure 6.2.

As described in Section 6.2.2, the number of nodes in the input layer was equal to the number of inputs used to represent the problem ( $\frac{F_x Z}{L^2}$ ,  $\frac{L}{H}$ ,  $\frac{F_x}{F_y}$  and  $\frac{E_x}{E_y}$ ). As the aim of the application was to analyse the panel, the output of the net was the failure pressure of the panel. No extra nodes were added at the output layer in this application. The number of nodes in the hidden layers was decided by a trial and error method and was finally adopted as 6. Thus, there were a total of 37 connection weights ((4+1)x6+(6+1)x1= 37). HAMMERSTROM (1993) recommended the number of training patterns to be equal to 5 to 10 times the weight connections. Thus, an ideal training set should contain 185 (37x5) to 370 (37x10) number of patterns in

the training set. The training set used in this application had 224 patterns and was within the above range.

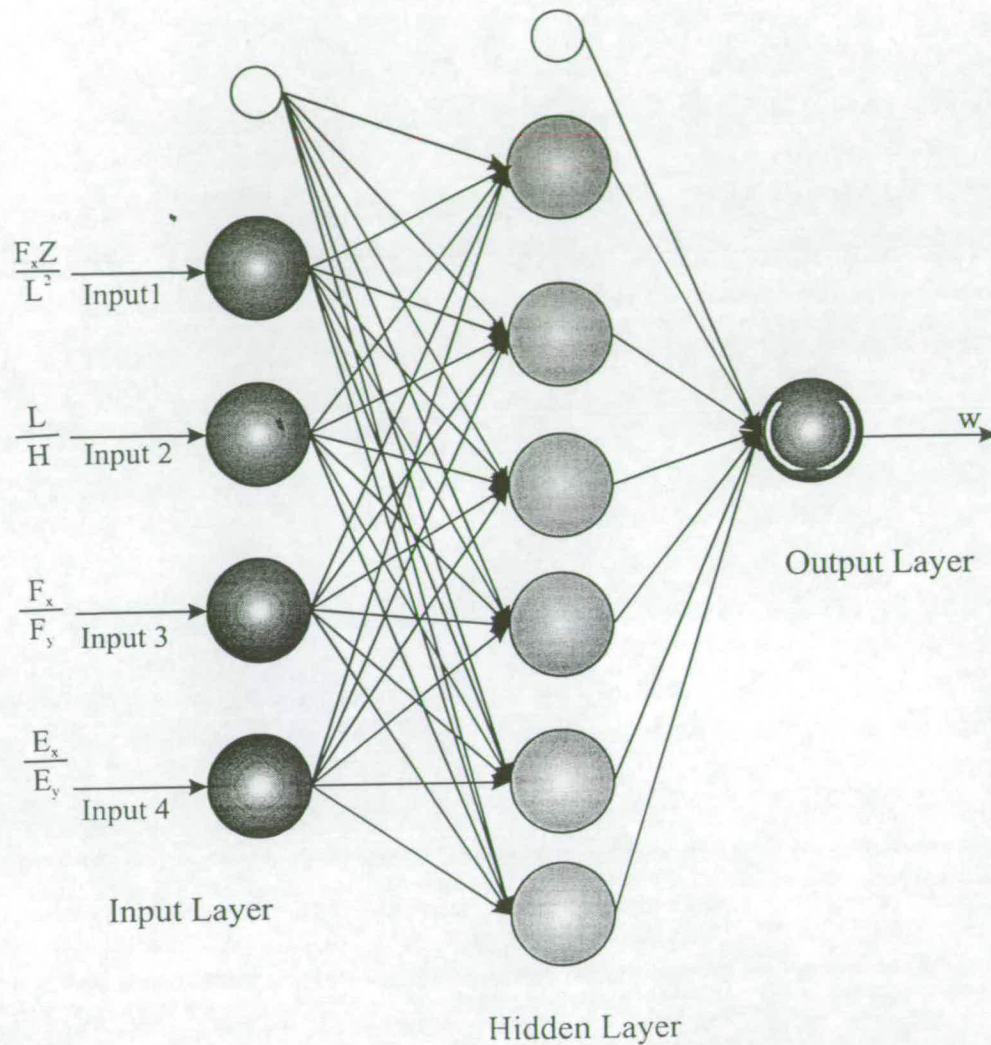


FIG. 6.2 The Architecture of the Net Used in the Implementation

A multi-layered feed-forward net with the back-propagation algorithm was selected as it is the most widely used and the seemingly recommended one for the current application (Chapter 3, Section 3.8.3.3). As the problem of analysing a panel for its failure pressure requires mapping an unknown non-linear relationship between the given inputs and output, a sigmoid activation function was chosen with the back-propagation algorithm.



The learning parameters include the learning rate and the momentum term. The training was started with the initial values of learning rate and momentum term as 0.2 and 0.5 respectively. The momentum term was kept as a constant during training, while the learning rate was dynamically adopted after each cycle<sup>4</sup>. This means that, at each step, the value of the learning rate was modified depending on whether or not the weight changes during that step caused an increase or decrease in the total RMS error. The learning rate was increased by 1.02 at a successful step and was decreased by 0.96 at a failure step.

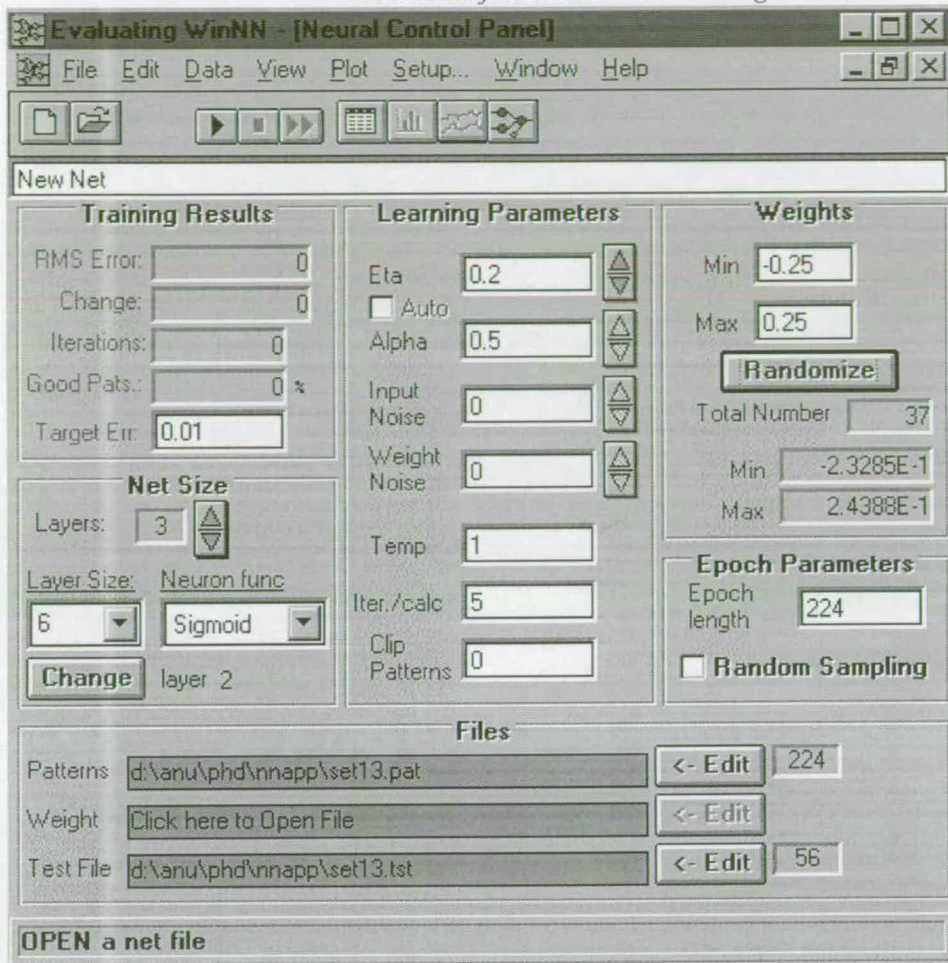
Before presenting the data for training, the connection weights were initialised within a certain range. Starting from a smaller value of connection weights helps to avoid being trapped in any local minima. Training was carried out using different ranges of initial values and the final value adopted was within the range of -0.25 to +0.25.

The training was done in a batch mode, where the weight updates were carried out after presenting all the patterns in the training set once to the net. The neural net control panel with the variables initialised to values as described above can be seen in Figure 6.3.

The training was started with a pre-defined target RMS error of 0.01. This forced the program to stop training when the RMS error of all the patterns used in the training set fell below the pre-defined value. However, the training was halted at regular intervals to check its performance on the test sets. This was to prevent any possibility of the net memorising the training patterns presented to it rather than learning the hidden relationship. The RMS error of the test set was, thus, monitored continuously and the training was continued until the RMS error of the test set ceased to improve. The generalisation capacity of the net was evaluated mainly by its performance on an unseen set of data, which is the test set.

---

<sup>4</sup> One 'Cycle' represents the presentation of the entire training patterns and the subsequent weight modification either in a pattern or batch mode.



**FIG. 6.3** The Neural Control Panel: the variables can be adjusted on this panel at any time during the training.

The net was stuck at local minima several times during training and no improvement in the RMS error was noticed at this time. It was necessary to restart the net by changing the number of hidden layers or with a different set of initial weights, whenever it was stuck at local minima. The complete training and test sets used in this application for all the 8 types of panels along with the net results are given in Appendix VIII.

The performance of the net on the various types of panels is explained in Section 6.6. The performance of the net on the experimental results is discussed in Section 6.7. Figure 6.4 shows how the performance of the net can be monitored at various stages during the training of the net.

As can be seen in Figure 6.4, the 'Plot Output' window gives a graphical display of the performance of the net on the various sets. The set to be displayed can be selected from the pop-up menu that can be seen within the 'Plot Output' window. A numerical display and a comparison of the net on the various sets can also be seen on the small window at the bottom left corner in Figure 6.4. The control for the selection of the set is within the control panel as an icon and a command in the 'File' menu.

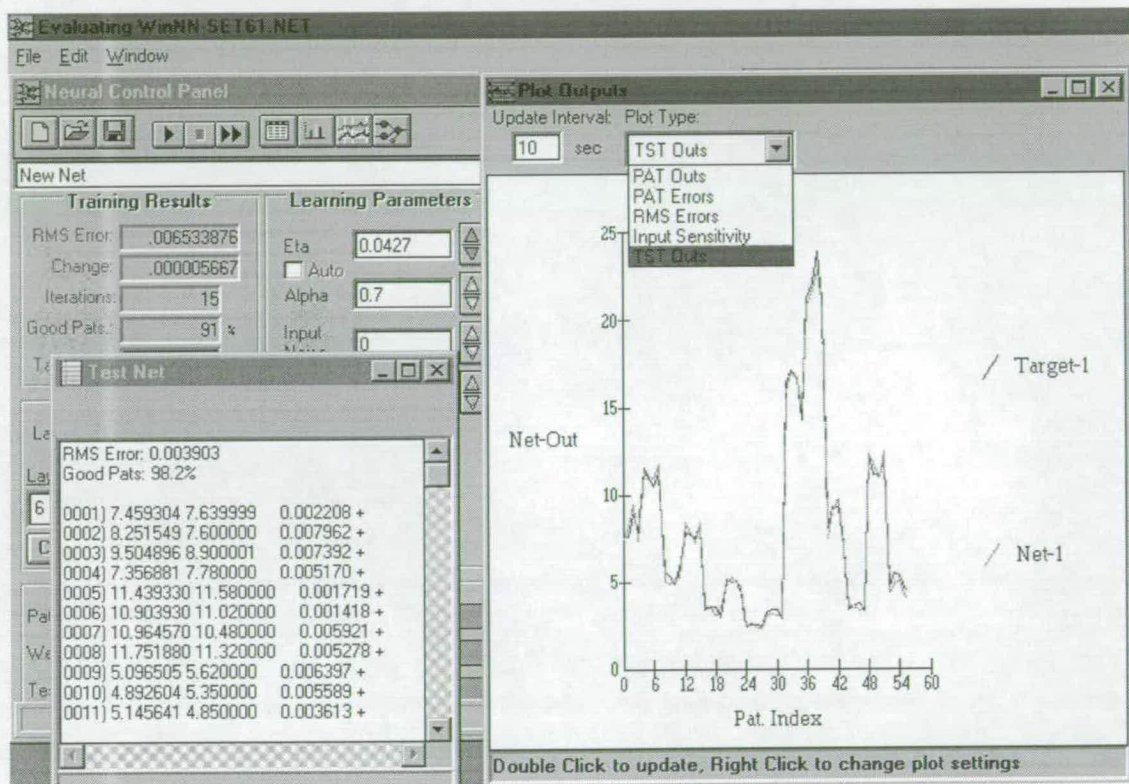


FIG. 6.4 The Neural Net Performance Panel

### 6.3 Theoretical Methods of Analysis for Data Generation

Following are the three methods that were used for the generation of the training and test set for the neural network application. In addition to generating the training set, the theoretical methods were also used to calculate the failure pressure of the panels that were tested at the laboratories and compare it with the experimental results.

### **6.3.1 BS 8110**

The BS is mainly based on the yield line analysis. The material is assumed to rotate along certain pre-defined yield-lines according to their geometry and boundary conditions. After yielding, the material rotates along these yield-lines at constant bending moment. Brickwork is a brittle material and cannot behave as a fully rigid plastic material on which the yield line theory is based. Nevertheless, the crack pattern observed in the test results is similar to the yield-line pattern and, thus, the method is successful in predicting the failure pressure in several cases. As the yield-line analysis is an upper-bound solution, an over-estimation in the predicted results has been pointed out by several researchers. The relevant pages from the BS, showing the coefficient of bi-axial bending for masonry panels are given in Appendix I.

### **6.3.2 Australian Code of Practice**

The Australian code of practice adopts a strip method of analysis. The strip method is generally applied to reinforced concrete slabs, where the reinforcements are varied in the strips according to the moment fields. As it is practically impossible to have this arrangement in the case of an un-reinforced masonry panel, the applicability of this method remains questionable. However, being a lower-bound solution for panel analysis, the method is being recommended by some researchers. The relevant parts of the Australian Code showing the bending moment coefficients are given in Appendix II.

### **6.3.3 Finite Element Method**

An in-house finite element method was used to generate a major chunk of the training and test data. This was originally developed by ROTTER (1988) for plate bending and later modified by NG (1996) for brickwork incorporating the failure

criterion for the orthotropic material (SINHA *et al.* 1997). The convergence of the finite element program while analysing the panels has been demonstrated by NG (1996) and is also explained in Section 4.3.5.4. Typical plots of the mesh used in the analysis of cross beams and panels are given in Appendices VI and VII. The panels tested at the various research centres were analysed using the modified finite element method. It was found that the finite element method predicted the experimental failure pressure very closely. More details on the program and the finite element analysis can be seen in Chapter 4 (Section 4.6.4). The input data for the analysis is prepared by answering a series of questions and a sample input data along with the questions is given in Appendix III. While preparing the data, the shear modulus of the material has to be given as an input data. Brickwork, being an orthotropic material, the above value was calculated using the formula:

$$\frac{1}{G_{xy}} = \frac{1}{E_x} + \frac{1}{E_y} + \frac{2\nu_{xy}}{E_x} \quad 6.4$$

The finite element analysis has been carried out for panels of different support conditions and of various properties listed under the range of variables given in Table 6.3. Nearly 280 panels were analysed for each of the support conditions. The results of the analysis were examined to study the effect of orthotropic stiffness ratio on the failure pressure of these panels. For some of the panels, the cracking and the failure happened simultaneously, while in others there were considerable variation between the initial cracking load and the final failure pressure. The various boundary conditions of the panels studied in this research are shown in Chapter 5 (Figure 5.3).

Table 6.4 shows the effect of varying the orthotropic stiffness ratio on the failure pressure of the panel. For each set of panels, the orthotropic strength ratio was varied from 1.3, 2.0, 3.0 and 4.0, while the orthotropic stiffness ratio was varied from 1.0, 1.4, 1.8 and 0.8. The aspect ratio of the panels analysed include 0.5, 0.75, 1.0, 1.5 and 2.0. The maximum variation in failure pressure was noticed while changing the orthotropic stiffness ratio from 1 to 1.8. The first row in the above table shows the number of panels in percentage that showed less than 10% variation in the failure pressure by changing the orthotropic stiffness ratio from 1 to 1.8. The second row

shows the maximum variation in the failure pressure by changing the orthotropic stiffness ratio from 1 to 1.8. It can be seen from Table 6.4 that even though the effect of stiffness orthotropy makes insignificant variation in 66-94% of the cases, its effect can be as high as 88% as in Set3 or 52% as in Set7. As these are significantly high variations, it is highly recommended that the stiffness orthotropy may be considered while analysing the panels for their failure pressure.

**Table 6.4 Effect of Orthotropic Stiffness Ratio (Varied from 0.8 to 1.8) on the Failure Pressure of Panels of Different Boundary Conditions.**


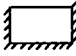
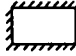
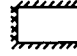
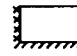

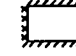
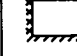
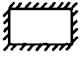
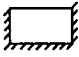
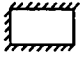
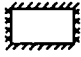
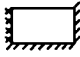
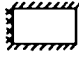
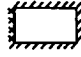

	Set1	Set2	Set3	Set4	Set5	Set6	Set7	Set8
								
<10%	71.4%	89.5%	66.2%	81.4%	88%	74.3%	73%	94%
Max. Variation	26.5%	23%	88%	22%	18%	30%	52%	15%

Table 6.5 shows the number of panels that cracked and failed together and the difference between the cracking load and the failure load. In cases where the panel did not fail along with cracking, the panel had to be analysed several times by varying the number of mesh elements. While carrying out the analysis, it was noticed that the failure pressure can vary by changing the number of mesh elements, whereas the cracking pressure remained more or less the same. The variation in the failure pressure can be attributed to the redistribution of loading from the cracked elements to the non-cracked elements within the mesh. The number of elements that are cracked at a particular load step can vary depending on the size of the element. The panel was analysed 6 times in these cases by changing the number of elements to ensure convergence.

From Table 6.4, it can be seen that the effect of the stiffness orthotropy falls within 10% for almost 90% of the cases analysed in Set2, Set5 and Set8. The failure and cracking of this set of panels occurred simultaneously as can be seen in Table 6.5. Only fewer panels failed after cracking. A common feature that can be pointed out here is that all the three panels have their top edge free. It can, hence, be

recommended that a top free panel can be analysed using finite element method with less computational time.

**Table 6.5 Cracking and Failure of Panels of Different Boundary Conditions**

	Set1 	Set2 	Set3 	Set4 	Set5 	Set6 	Set7 	Set8 
Simultaneous	47.5%	79%	46.5%	53%	80%	41%	57%	70%
<10%	9%	5.5%	6.5%	7%	4.3%	3%	5%	9%
10-20%	5.5%	4%	5.5%	7%	5%	5.7%	2%	6%
20-50%	20%	9%	28%	18%	9.3%	32%	20%	14%
>50%	18%	2.5%	13%	15%	1.5%	18.2%	16%	1%
Max.	71.4%	67.4%	67.5%	72.5%	56.3%	69.4%	71%	56.5%

Moment coefficients were derived from the results of the finite element analysis of the panels that were used to generate the training and test data for the neural network application and are given in Appendix V. It has to be pointed out that a linear interpolation of these coefficients for any intermediate values might be difficult here as the panels exhibit a non-linear post cracking behaviour.

### 6.3.4 Comparison of the Various Theoretical Methods

The results of the panels analysed by the finite element method, the BS and the Australian code of practice are studied further to find out the possible cases where any of these three methods give similar results. It has been shown by NG (1996) that the finite element analysis produced closer predictions of the failure pressure to the experimental results when compared to the other two methods. The experimental results used in his study were carried out at different parts of the world and were of wide variation. Hence, the BS and the Australian code predictions are compared with the finite element results in this research. As the codes give coefficients only for panels of isotropic stiffness, panels of orthotropic stiffness are not considered in this study. Table 6.6 gives a comparison of the failure pressures calculated from the codes with that of the finite element method.

As can be seen in Table 6.6, there are many cases where the Australian Code and the BS are producing results similar to that of the finite element analysis. The table presented here is on the basis of an average of three results for each aspect ratio by varying the length and the height of the panel. It is worth mentioning that the three results for each of these cases produced very close values and can, hence, be generalised.

The BS is found to be over-estimating the results when compared to the FE analysis except in Set8. It can be noticed that the BS gives results similar to the FEM for majority of the panels with Set4, Set5 and Set7 boundary conditions. The variation in these cases lies within 10%. There are several cases in Set1, Set2 and Set8 where the BS and the FEM results are within 10% variation. However, in Set3 and Set6, where one of the vertical edges is free ('C' Type), a considerable variation in the results can be noticed.

The Australian Code gives results lower than that of the finite element analysis in majority of the cases, the variation being quite high in many cases. Set3 and Set6 could not be analysed by the Australian code of practice due to non-availability of the coefficients. It has to be pointed out that the Australian Code of Practice gives unreliable results in Set4 and Set8 type panels. However, in Set1, Set2, Set5 and Set7, this method produced results close to the finite element analysis.

It was mentioned earlier that even though the analysis based on the code coefficients has no rational justification, these methods are being recommended by several researchers as they are found to predict the experimental results closely. It is possible that the physical properties of the panels for which the experimental analysis was carried out comes under those categories where there is a close match between the finite element and the BS/Australian Code results and, hence, these methods are found to give matching results.



Table 6.6 Comparison of BS and Australian Code Predictions of Failure Pressure with that of Finite Element Method (Set1 - Set8)

$\frac{F_x}{F_y}$	$\frac{L}{H}$	Set1		Set2		Set3*		Set4		Set5		Set6*		Set7		Set8	
		$\frac{BS}{FEM}$	$\frac{Aus}{FEM}$	$\frac{BS}{FEM}$	$\frac{Aus}{FEM}$	$\frac{BS}{FEM}$		$\frac{BS}{FEM}$	$\frac{Aus}{FEM}$	$\frac{BS}{FEM}$	$\frac{Aus}{FEM}$	$\frac{BS}{FEM}$		$\frac{BS}{FEM}$	$\frac{Aus}{FEM}$	$\frac{BS}{FEM}$	$\frac{Aus}{FEM}$
1.3	0.5	134	114.5	128	126	103		97	70	103	90	99		118	92	80	64
	0.75	109	82	129	122	119		99	71.5	108	92	91		109	85	85	65
	1.0	95.6	82.5	115	114	134		96	69	112	92	140		101	77	94	69
	1.5	121	102	94	92.5	135		115	82	110	85	151		121	93	100	71
	2.0	110	104	82	82	128		130	100	100	77	143		113	112	96	68
2.0	0.5	120	108	120	122	116		89	66	97	89	91		108	88	77	63
	0.75	103.8	91.4	120	118	111		89.5	65	100	89	111		98.6	79	80	64
	1.0	121	103.5	115	107	113		96	69	104	87	117		111	86	86	66
	1.5	118	97	121	109	153		120	85	100	79	139		122	94	91	65
	2.0	103	85	122	102	140		109	81	110	85	166		107	84	97	68
3.0	0.5	113	107	114	120	98		84	65	94	87	88		101	85	75	62
	0.75	127	116	113	115	87		92	69	97	87	92		108	89	78	63
	1.0	114	100	109	106	100		102	74	97.5	85	98		113	91	82	64
	1.5	92	80	121	109	175		108	75	109	89	107		105	80	89	66
	2.0	80	60	114	95	140		92	67	111	89	140		90	69	96	69
4.0	0.5	122	116	114	120	92		91	69	96	89	90		106	92	82	68
	0.75	122	110	115	115	80		99	68	100	86	91		110	89	77	63
	1.0	111	95	124	119	104		101	74	97	84	95		113	89	83	63
	1.5	95	70	120	103	205		105	70	100	100	117		101	83	88	64
	2.0	75	60	112	92	130		97	63	105	82	160		95	66	99	69

\* The Australian code coefficients were not available in these types of boundary conditions

## **6.4 Case Based Reasoning to Predict the Failure Pressure of Masonry Panels Under Bi-axial Bending**

Even though the rationality of the various existing theories for the design of masonry panels under bi-axial bending is disputable, these methods are shown to give accurate predictions of the failure load for many of the experimental cases. As explained in the previous section, this can be noticed for panels with specific properties. By applying case based reasoning technique, it is possible to infer some knowledge about the relationship that could possibly exist between these various methods and the properties of the panel.

The experimental results reported in the literature are used to develop the case base. The information consists mainly of the experimental failure load for the different types of panels along with the properties used to define these panels. The problem is defined by the aspect ratio ( $L/H$ ), the ratio of the flexural strength to the second power of the length ( $FZ/L^2$ ), the strength orthotropy ( $F_x/F_y$ ) and the stiffness orthotropy ( $E_x/E_y$ ). The failure pressure is theoretically calculated using the finite element method, the BS and the Australian code of practice and are also included in the case base. Thus, each problem is characterised by four outputs, which consists of the experimental failure load and the theoretical results calculated using the above three methods, alongwith the percentage variation of the theoretical results from the experimental result. By comparing the experimental and the theoretical values for each problem, it is possible to recommend a method which produces the most reliable results for the particular problem. Thus, the case base essentially consists of the experimental results and the theoretical predictions for the various cases and an appraisal of the recommended method of analysis

When a new panel has to be analysed, the matching cases will be retrieved from the case base. Along with the experimental results, the theoretical predictions of the failure load and the most potentially reliable method of analysis for the matching cases are also retrieved. The current panel can be analysed by the method

recommended by the best matching case. A schematic representation of the working of the prototype case based reasoning system is shown in Figure 5.3.

#### **6.4.1 Building a Case Base**

CBR Express was used to implement the prototype CBR system (CBR Express/windows 1.3 1990). CBR Express appeared to be a tool that provided a number of standard CBR features with a friendly user interface and fast retrieval mechanism.

A case base can be viewed as a data object that has certain associated features. In a case base, a 'case' is an example of an episode in a particular domain with associated attribute-value pairs to describe various aspects. A case might correspond to a law, a medical diagnosis, a faulty machinery or a numerical analysis. CBR Express allows the user to toggle between a 'search mode' and a 'maintenance mode'. The user has to switch over to the 'maintenance mode' to develop a case base. The menu 'panels' allows one to select the 'case panel' to start developing the application. The various cases are represented by the distinct properties of the panel and the experimental and the theoretical failure pressures.

#### **6.4.2 Representation of a Case in CBR Express**

The correct representation of the features of a case contributes a great deal to the identification of the similar case. Each case is associated with three important features. They include:

- Case Title and Description;
- Questions &
- Actions.

#### **6.4.2.1 Case Title and Description**

Each case is uniquely identified by a case title. The title should accurately identify the case by emphasising the unique features that makes the case important and forms the basis for the first search. A short description of the case can be given along with the case title. This can be either a single sentence or a short paragraph of text that can briefly describe the problem. In the present application, the textual description of the case is of importance and is explained below.

The aim of the current application is to identify the most suitable method of analysis to find out the failure pressure of a masonry panel of given properties. This involves comparing the theoretical predictions of the failure load with the experimental results for panels of different support conditions. Hence, the title of the cases mainly distinguishes between the different categories of the panel. The panels are basically divided into three categories:

- Four Sides Supported Panel;
- Three Sides Supported Panel with Top Free (Type U) &
- Three Sides Supported Panel with One Vertical Edge Free (Type C).

There are further divisions in the above categories depending on the degree of freedom along the supported edges. This is incorporated as a description of the panel and is detailed below:

- Four Sides Supported Panel: The four sides are simply supported;
- Three Sides Supported Panel with Top Edge Free: The sides are simply supported;
- Three Sides Supported Panel with One Vertical Edge Free: The sides are simply supported;
- Four Sides Supported Panel: Vertical Edges are restrained and top and bottom are simply supported;

- Three Sides Supported Panel with One Vertical Edge Free: Top and Bottom are simply supported and the other vertical edge is restrained &
- Three Sides Supported Panel with Top Edge Free: Vertical Edges are restrained and the bottom edge is simply supported.

The above classification of the panels based on the boundary conditions can also be seen in Figure 6.5. In the present situation, the case title helps only to distinguish between different types of panels. Hence, the cases are to be described by various properties and are incorporated in the case base as the answers to a set of questions.

#### **6.4.2.2 Questions**

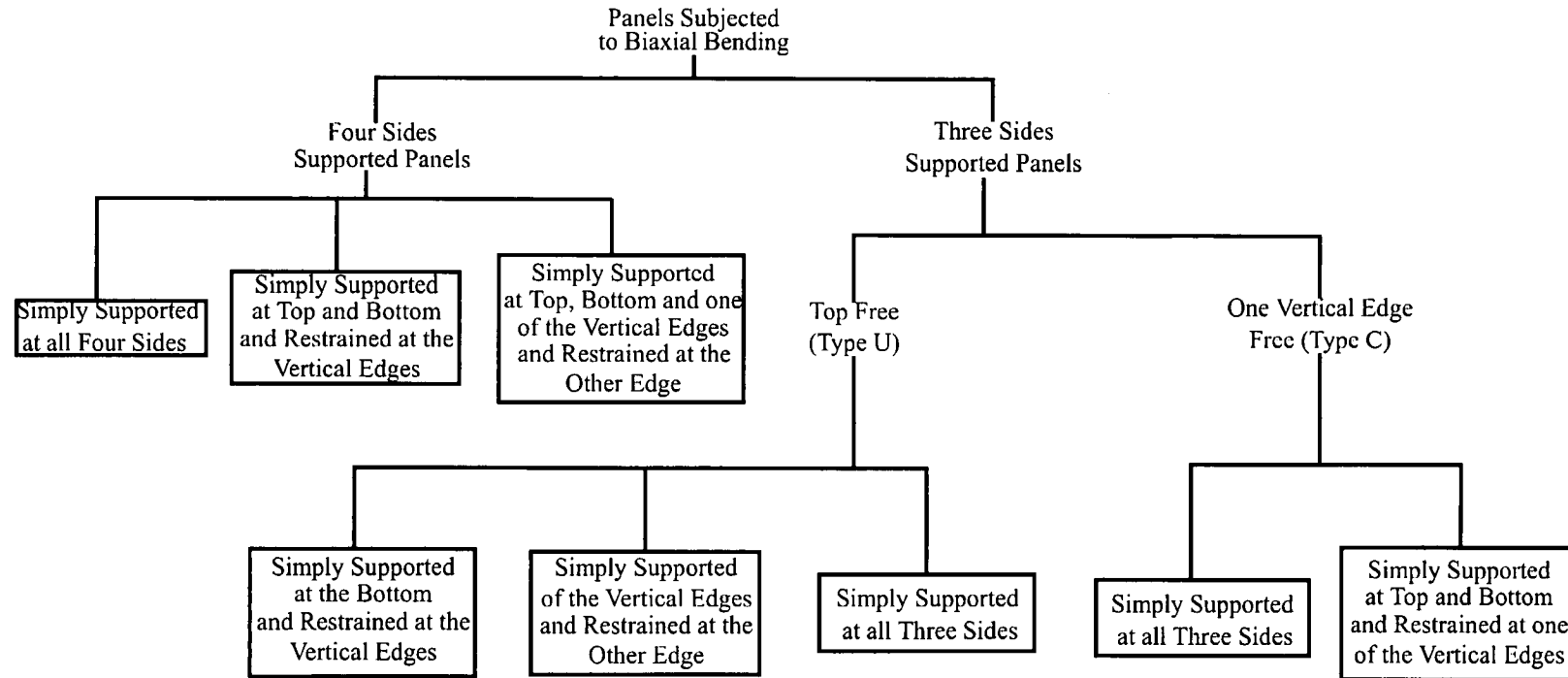
The questions form part of the case description and help to confirm the various aspects of a case. The questions may also be used to rule out cases or to confirm them absolutely during case retrieval. Figure 6.6 shows a typical sketch of the question panel in CBR Express. It is possible to incorporate additional information about the questions that are used to describe the case. CBR Express supports four types of answers to questions: 'Yes/No', 'Numeric', 'Text' and 'List'. The scores of retrieved cases are evaluated on the basis of the type of answer as can be seen in Figure 6.6.

**'Yes/No':** The question may be answered 'Yes', 'No' or 'Not Answered' by highlighting the radio button.

**'Text':** The answer can be a text of unrestricted length.

**'Numeric':** These questions may have positive or negative integers and floating point numbers as their answers. The minimum and the maximum legal values of the expected answers can be pre-defined while developing the questions.

**'List':** This type of questions allows you to List out the various options for the questions and the user is free to make a selection from the given list. The answer can be selected by scrolling the list of legal answers.



**FIG. 6.5 Classification of Cladding Panels Based on Boundary Conditions**

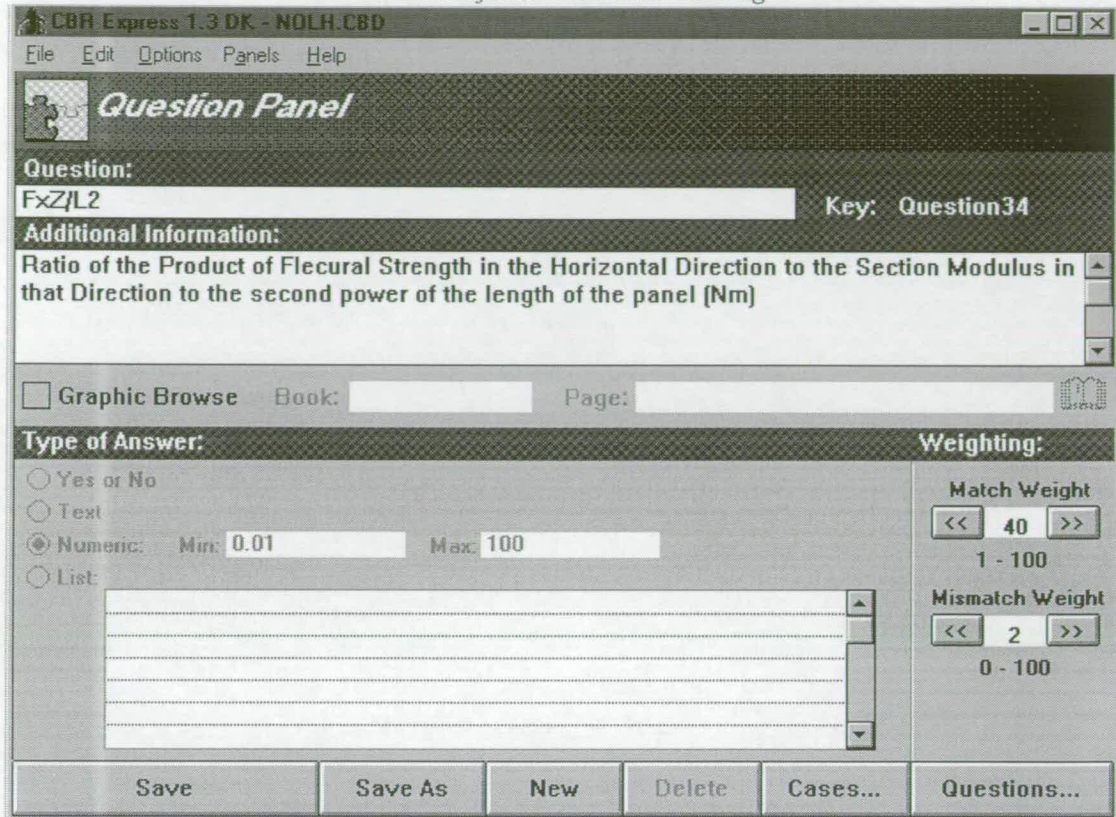


FIG. 6.6 The Question Panel in CBR Express

CBR Express also provides the facility to allow special scoring behaviour to individual cases. These are in the form of absence weight, mismatch weight and absolute scoring.

**Absence weight:** This reduces the score of all the cases that do not use a particular question by a certain amount and are applied to the case base as a whole. This helps to break ties between cases that are very similar.

**Mismatch weight:** This enables to penalise the scores of cases that have contradicting answers in the search description. This special feature is also applied to the case base a whole.

**Absolute Scoring:** This is applied to cases within particular cases. A correct answer to this question in a case absolutely confirms that the particular case should be selected. At the same time, a wrong answer to this question completely disqualifies the case.

CBR Express also allows one to alter the question weights field on the question panel (Figure 6.6). A match weight of a question influences the relative importance of the question in determining the case's score. If all the questions have the same weight, they will all contribute equally to the score of that case. If a question has much higher match weight than the others, then it will tend to dominate the scoring process. The mismatch weight influences the score of cases where the question does not match and is kept as a small fraction of the match weight. The default values are 10 and 2 for match weight and mismatch weight respectively. These values are modified in the current application and are explained in Section 6.5.

### **6.4.2.3 Actions**

Each case is associated with an action, which is the solution to the problem. The action incorporates additional information with the case and is the output of CBR Express system. These actions are not used in case matching. Any special knowledge associated with an action can be included in the system by adding the information in the space provided.

In this application, the action is mainly the method of analysis that is found to be more reliable and is recommended for other problems of similar nature. This is done by comparing the theoretical and the experimental failure pressures. Hence, the experimental failure load and the theoretical predictions by the various methods can be incorporated in the case base as additional information as shown in Figure 6.7 A comparative figure is also included alongside as a percentage within brackets (Figure 6.7). It has to be pointed out that CBR will recommend a method out of the three existing methods that are discussed in this thesis namely the FE analysis, the BS or the Australian code of practice. If the results of CBR analysis brings up the FEM as the recommended method, the user is given an option to choose either to take up the time consuming finite element method or the trained neural network. As the training of the net has used the data obtained from the FE analysis, the net would be able to



provide the value of the failure pressure close to that obtained from the FE analysis and can, thereby, obtain substantial savings in computational time. In cases where CBR recommends the BS or the Australian code of practice, the results can be obtained quickly by referring to the respective codes.

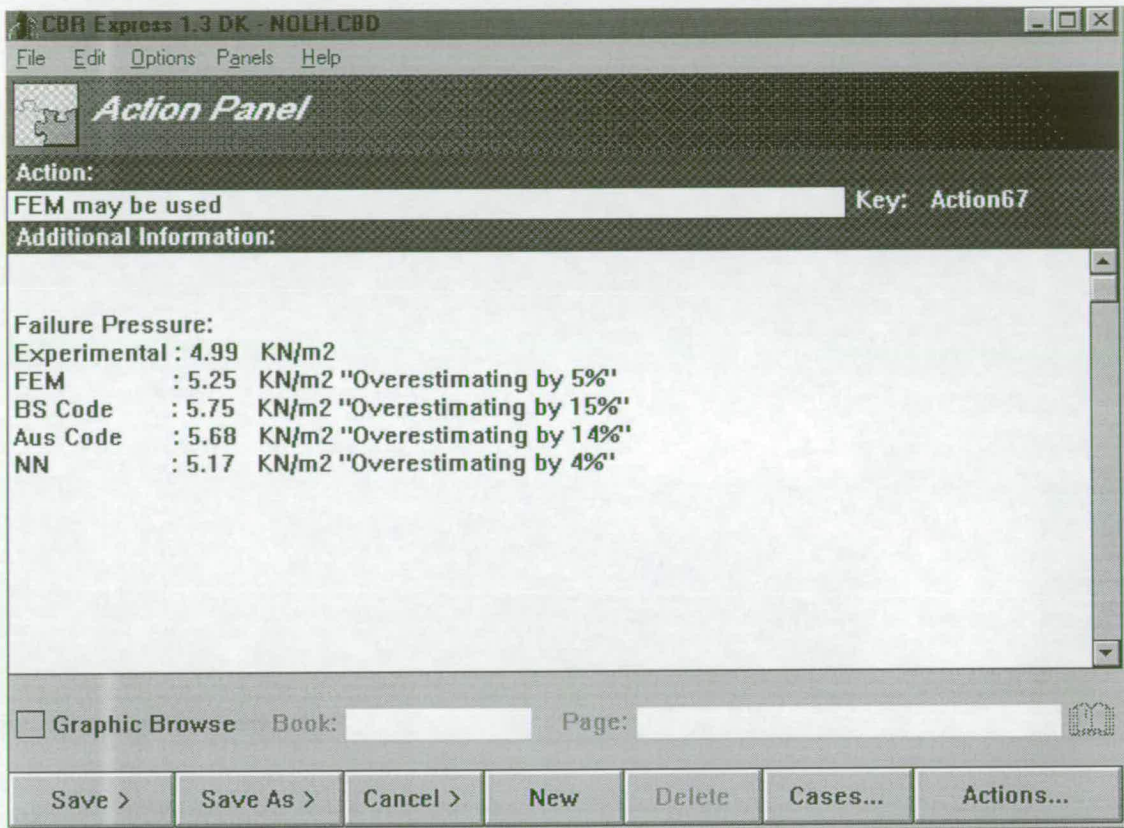


FIG. 6.7 An Action Panel in CBR Express

Each of the experimental results reported in the literature forms a case and is included in the case base. Each case is associated with a title, title description, possible associated questions and their answers and the action. As mentioned above, the action is the method recommended and can also include any additional information associated with the case (Figure 6.7). A typical case panel for a three sides simply supported panel can be seen in Figure 6.8.

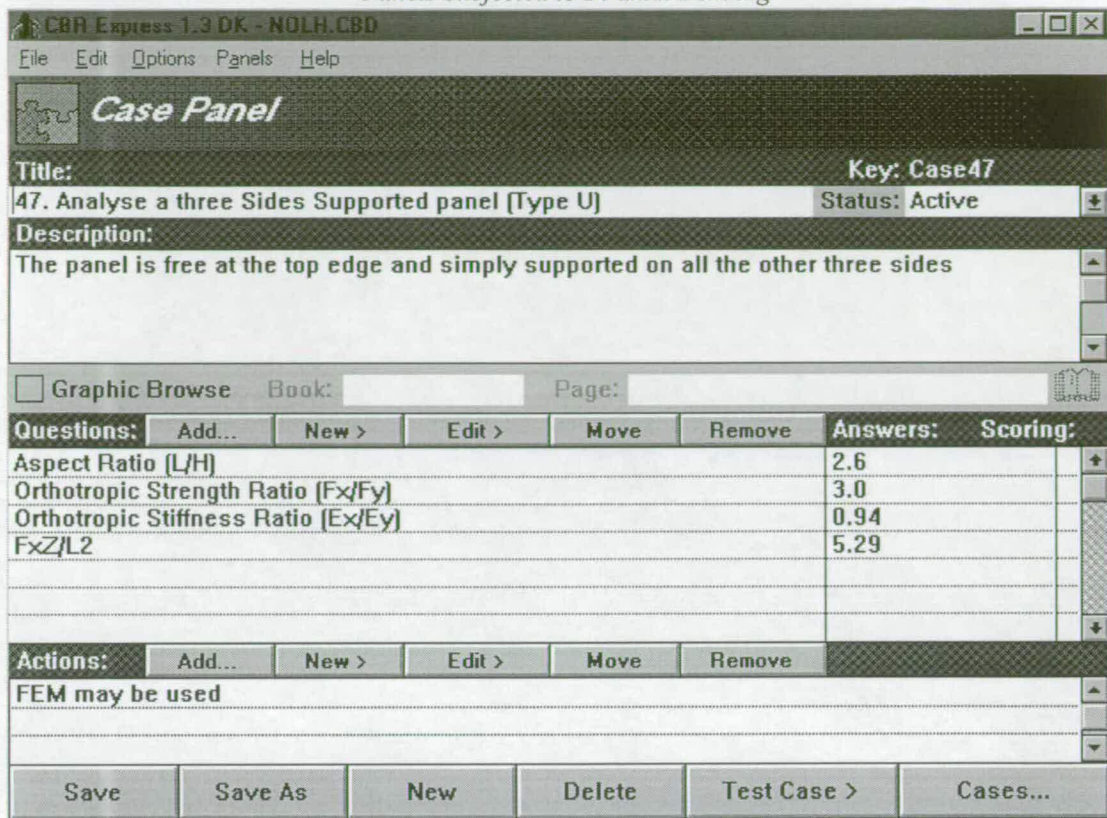


FIG. 6.8 A Case Panel in CBR Express.

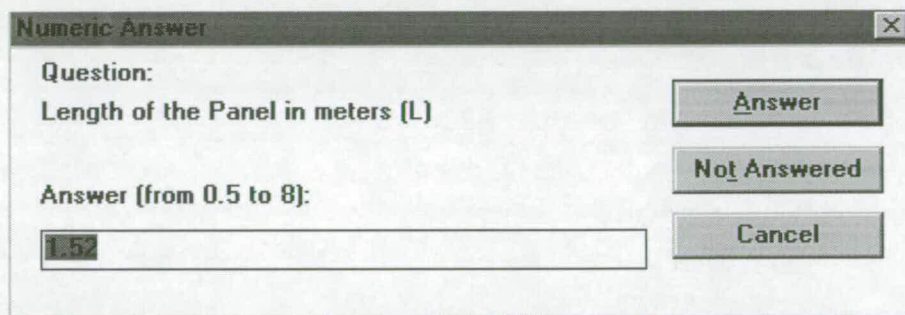


FIG. 6.9 A 'Numeric Answer' Dialog Box

As can be seen in Figure 6.8, the title of the case is supported by the description provided. The problem is characterised by the additional information supplied in the form of answers to the set of questions. A small dialog box as shown in Figure 6.9 appears when the user tries to answer a particular question. As all the questions used in this application are of 'Numeric' types, the minimum and the maximum values also appear in the dialog box (Figure 6.9). Answers that lie outside these limiting values are rejected. CBR Express provides the facility to use one case as a template

for creating other cases. The cases can be modified by selecting the various options given for the 'questions' and the 'actions' boxes. These include creating a completely new item or modifying the item by Editing or by Adding or Removing the items from the given list.

### **6.4.3 Indexing and Retrieval of a Case in CBR Express**

The object of a case base search is to locate a case or a set of cases that closely resembles the new problem described by the user. An initial search is carried out by CBR Express based on the description of the current problem. CBR Express uses a sophisticated text-matching algorithm to compare the description of the current problem with the descriptions of the cases stored in the case library. Five closest cases are generally returned by the search engine, which will be displayed in the order of their closeness. Along with this, CBR Express returns a set of questions for each of the five retrieved cases and a combined set of questions are presented to the user. These questions help to sharpen the focus of the search and to differentiate among the competing cases. The degree of closeness of each case will be further assessed based on the answers to these questions. Each time a question is answered, CBR Express updates the search and lists the matching cases in the order of their closeness. The user can also leave some of the questions unanswered depending on the availability of a possible answer.

The following methodology is adopted to evaluate the answers to the questions. A question having an answer 'Yes/No' or a List answer is directly compared with the cases in the case base and the score can be raised or reduced depending on the match. For a 'Text' type answer, each of the words in the answer are compared with that in the case base and the score is modified according to the number of matching words. Matching on 'Numeric' answers is rather complex. CBR Express treats the legal range (the spread from the maximum to the minimum legal value) as 100% of the possible spread. If the search falls within 10% of the case value, some credit, which

is proportional to the distance between the two numbers, is awarded to the matching score. An exact match gets full credit and a complete miss lowers the score of the case.

Further search is carried out based on the answers to these questions and the existing list of questions is augmented with additional queries drawn from the current list of matching cases. The matching scores of the cases are modified and the field of possibilities is narrowed down. Subsequent searches are carried out until one of the cases shows an acceptably high score, or until all pertinent questions have been answered.

When CBR Express finishes searching for cases, a list of cases will appear in the panel in the order of their closeness to the problem to be analysed. A match score of 100 is unlikely and the threshold of acceptance can be decided by the user. The user can browse the matching cases and their recommended actions from the search panel to ascertain their applicability to the current problem. It is also possible to get the additional information associated with an action. In the present application, this includes the experimental failure pressure and the theoretical predictions. The user is, thus, able to judge by himself the reason for adopting a particular method in the current analysis.

## **6.5 Weight Adaptation in CBR**

As pointed out in Section 6.4.3, the match and the mismatch weights for each of the questions can be modified in CBR Express for the cases, where special matching behaviour is available. The match weight associated with each of the questions is related to the relative importance of a particular question to the final output of the case.

As we are interested in the failure pressure of the panel, the input variables  $\frac{F_x Z}{L^2}$ ,  $L/H$ ,  $F_x/F_y$  and  $E_x/E_y$  have varying influence on this value. The relative importance

of each of the variables on the output can be obtained by analysing the connection weights of a trained neural network. This allows a better integration between neural networks and case based reasoning used in the hybrid approach. GARSON *et al.* (1991) have given mathematical formulae to interpret the connection weights and establish a relationship to find out the relative importance of the inputs on the outputs of the training patterns used in neural network. The connection weight matrix for each set of trained neural networks is used for this purpose.

### 6.5.1 Weight Analysis - A Sample Calculation

A sample calculation to analyse the weight matrix of the trained neural network to obtain the relative importance of the inputs on the failure pressure of the panel is given in this section. The relative importance has been calculated by the method proposed by GARSON *et al.* (1991). The calculation based on the above method is shown in the following section. A network with 4 input nodes, 6 hidden nodes and one output node had the connection weight as given below for 'Set4' type panels of (Simply supported at top and bottom and restrained at the vertical edges).

	<i>Input1</i> $\frac{F_x Z}{L^2}$	<i>Input2</i> $\frac{L}{H}$	<i>Input3</i> $\frac{F_x}{F_y}$	<i>Input4</i> $\frac{E_x}{E_y}$	<i>Output</i>
<i>Hidden1</i>	1.0013	0.6495	1.0822	-0.2589	2.3168
<i>Hidden2</i>	2.3356	0.5782	-0.1244	0.7574	3.4399
<i>Hidden3</i>	-1.582	-2.1196	0.7593	0.4327	-2.373
<i>Hidden4</i>	-3.6148	0.7326	-0.0629	0.6871	-2.7527
<i>Hidden5</i>	-1.8986	1.6177	1.5356	-0.5775	-1.3728
<i>Hidden6</i>	-3.7616	1.5299	-0.3075	-0.6718	-2.9125

The absolute values are taken for the weight analysis and is carried out as follows:

Step 1: The sum of all the interconnection weights between the input layer neurons and the  $j^{th}$  neuron in the hidden layer is computed as:

	Sum of the Inputs
Hidden1	$1.0013 + 0.6495 + 1.0822 + 0.2589 = 2.9919$
Hidden2	$2.3356 + 0.5782 + 0.1244 + 0.7574 = 3.7956$
Hidden3	$1.582 + 2.1196 + 0.7593 + 0.4327 = 4.8936$
Hidden4	$3.6148 + 0.7326 + 0.0629 + 0.6871 = 5.0974$
Hidden5	$1.8986 + 1.6177 + 1.5356 + 0.5775 = 5.6294$
Hidden6	$3.7616 + 1.5299 + 0.3075 + 0.6718 = 6.2708$

Step 2: A fraction of the signal received by the  $j^{th}$  hidden neuron from the  $i^{th}$  input neuron can be roughly computed as the ratio of the connection weight to the hidden node to the sum of the connection weights from all the input nodes to the same node. This fraction is now multiplied by the connection weight from the hidden node to the output node. Thus, a matrix is formed as:

	Input1	Input2	Input3	Input4
	$\frac{F_x Z}{L^2}$	$\frac{L}{H}$	$\frac{F_x}{F_y}$	$\frac{E_x}{E_y}$
Hidden1	0.775	0.503	0.838	0.2
Hidden2	2.117	0.524	0.113	0.686
Hidden3	0.767	1.028	0.368	0.21
Hidden4	1.952	0.396	0.034	0.371
Hidden5	0.463	0.394	0.374	0.141
Hidden6	1.747	0.711	0.143	0.312
Sum	7.821	3.556	1.87	1.92

The sum of all such signals through various hidden neurons is also calculated and is given in the above matrix. The sum of the contributions from all the input neurons to the output neuron is obtained as :  $(7.821+3.556+1.87+1.92) = 15.167$ .

Step 3 A fraction of an output weight that can be attributed to each of the input neurons can now be expressed as the elements of a transition matrix T, which is obtained as a ratio of the signal from each input neuron to the sum of the signals from all the input neurons and is given below:

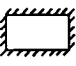
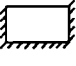

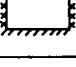

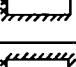

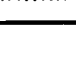
	Input1	Input2	Input3	Input4
	$\frac{F_x Z}{L^2}$	$\frac{L}{H}$	$\frac{F_x}{F_y}$	$\frac{E_x}{E_y}$
Relative Importance (%)	51.57	23.45	12.33	12.66

The above values show that for a panel with 'Set4' boundary conditions, the ratio

$\frac{F_x Z}{L^2}$  is the most governing parameter compared to the other three, with the aspect

ratio of the panel coming next. It can be seen that the strength and the stiffness orthotropies contribute equally in this particular case. However, this is not the case with other types of panels. The relative importance of the inputs on the failure pressure of the panels are calculated for all the 8 different types of boundary conditions and is given in Table 6.7.

**Table 6.7 Relative Importance of the Inputs on the Failure Pressure of the Panel (Expressed as Percentage).**

	$\frac{F_x Z}{L^2}$ (Input 1)	$\frac{L}{H}$ (Input 2)	$\frac{F_x}{F_y}$ (Input 3)	$\frac{E_x}{E_y}$ (Input 4)
Set1 	35.17	28.06	28.2	8.57
Set2 	50.2	18.2	20.26	11.34
Set3 	39.89	31.45	23.46	5.2
Set4 	51.57	23.45	12.33	12.66
Set5 	55.71	9.28	27.21	7.8
Set6 	42.99	30.14	19.98	6.88
Set7 	37.46	31.87	19.61	11.07
Set8 	39.3	20.94	5.79	33.97

The relative importance of the above variables as obtained from the weight analysis of the trained neural network is incorporated in the case base. This helps to attribute a match weight to the variables and, thus, helps to improve the search within the case base.

## 6.6 Evaluation of Trained Net to Predict the Failure Pressure of Masonry Panels Under Bi-axial Bending

An individual set of data was used while training the net for each of the categories of the panels. After training, the performance of the net was checked using the two test sets as explained below. Upon successful training, the weight coefficients were stored as separate matrices.

The performance of the trained net was evaluated by testing it on problems that were completely new to the net. As explained earlier, the test set consisted of patterns that were not used for training. No weight modifications were made while testing the net. The performance of the net on the test sets is given in Tables 6.8 to 6.15 & 6.17 to 6.22. A graphical display of the net outputs and the target outputs can be seen in Figures 6.10 to 6.17.

As the first test set was created in the same way as the training set, the performance of the net on this set shows that it has learned the unknown mapping between the inputs and the output used for training (Tables 6.8 - 6.15, Figures 6.10 to 6.17). The second test set comprised of the data available in the literature as a result of the experimental studies (Table 6.17 - 6.22). This consists of data which have ill-defined support conditions and certain un-known properties. As the data contained experimental results carried out at different research centres, the method used to obtain the mechanical properties was inconsistent. Hence, the tolerance of the net for noisy data could be assessed by its performance on this set of data. The net results on the second test set are compared with that of the modified finite element method (SINHA *et al.* 1997), which is shown to predict the results more accurately. The net results and the comparisons are given in Tables 6.17-6.22. As can be seen from these tables, it is clear that the percentage variation of the neural net results from the finite element results lie within 10% in 98% of the tested panels. In a few cases, (less than 1-2%) the above variation goes up to 15-18% in some of the sets. This can be viewed as insignificant compared to the computational savings achieved by this method. In



order to put forward the high level of performance achieved by the trained neural network, a statistical analysis was done on the data. The failure pressure predicted by the trained net is compared with that by the finite element method with the failure criterion in Figures 6.18 to 6.25. The predictions by the finite element method can be well compared against the equal prediction line drawn at  $45^{\circ}$ . It can also be seen from these figures that the data falls well within a variation of one standard deviation (SD). The performance of the net on the experimental results is discussed in the following section.

NN Performance - Set1

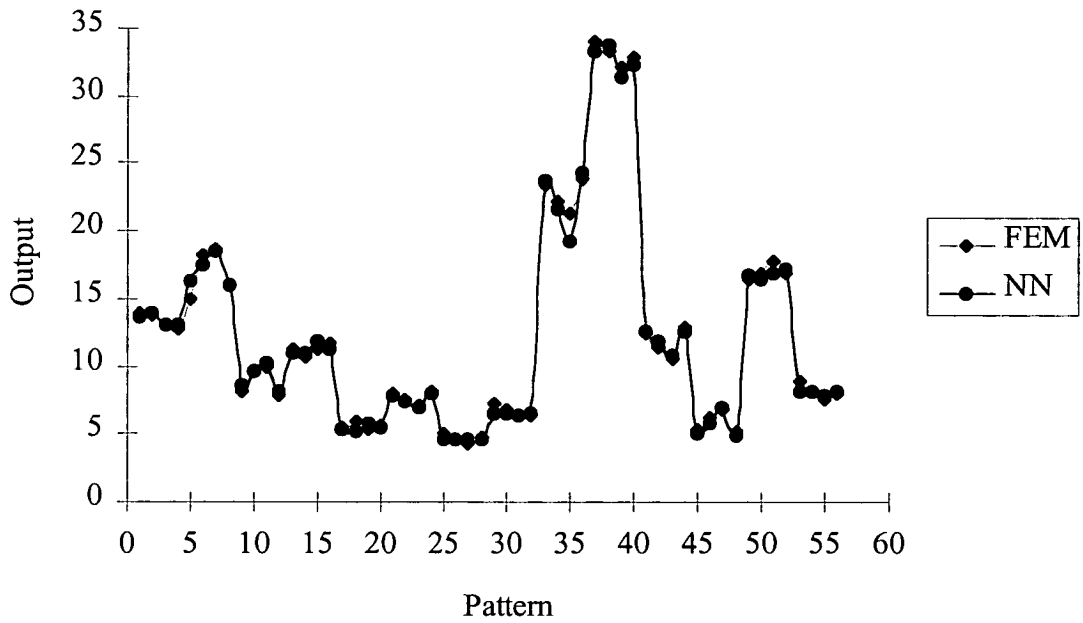


FIG 6.10 Performance of the Net on Test Set - Set1

NN Performance - Set2

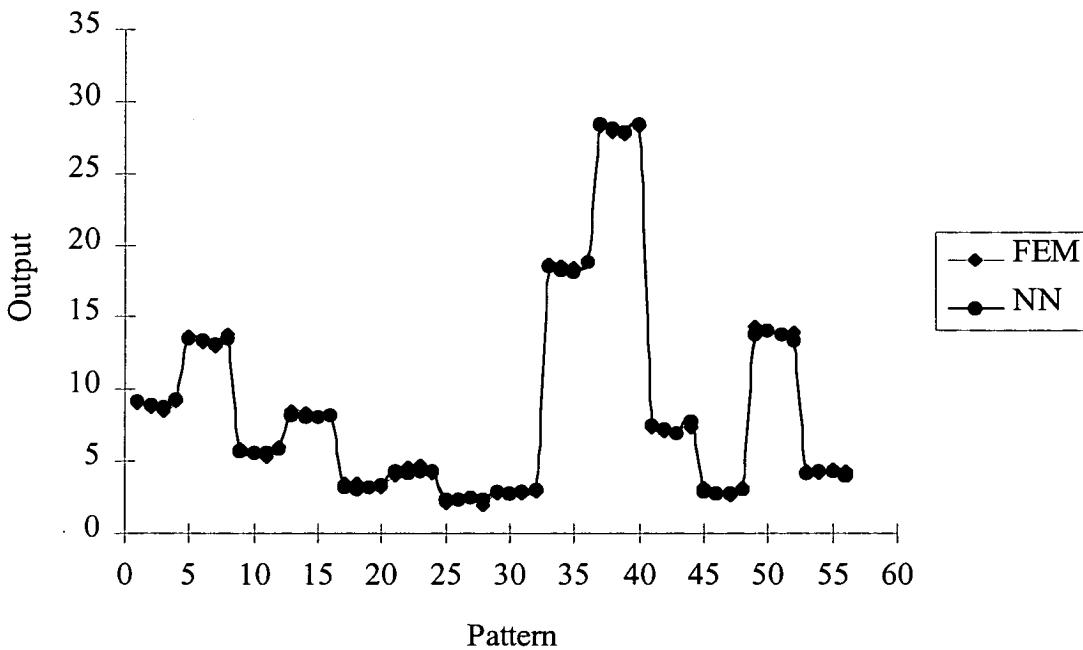


FIG 6.11 Performance of the Net on the Test Set - Set2

NN Performance - Set3

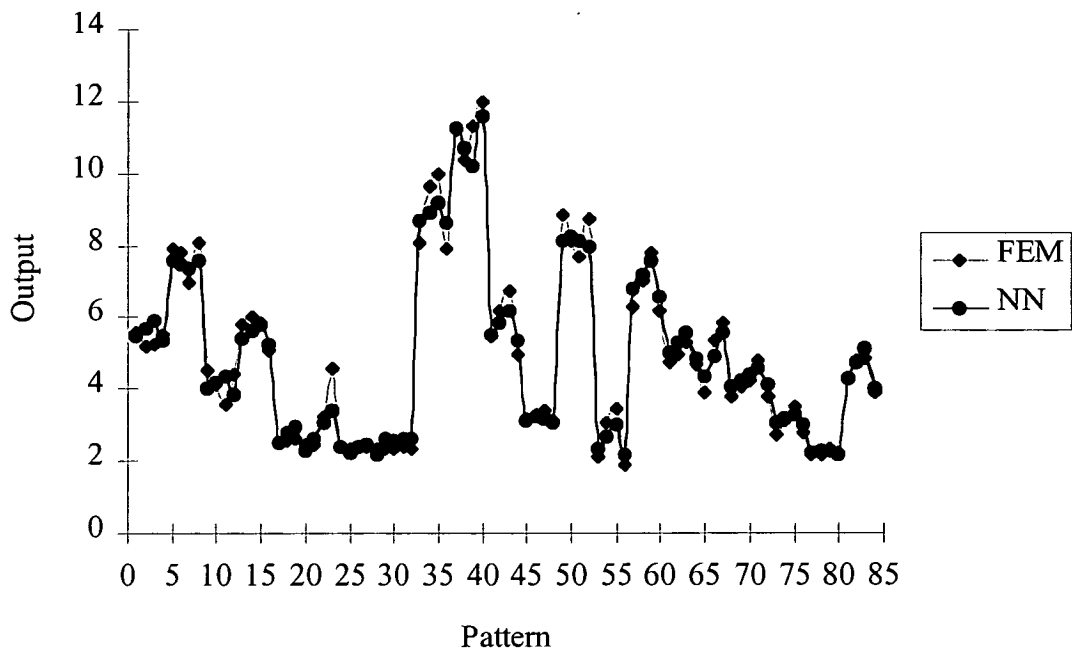


FIG. 6.12 Performance of the Net on Test Set - Set3

NN Performance - Set4

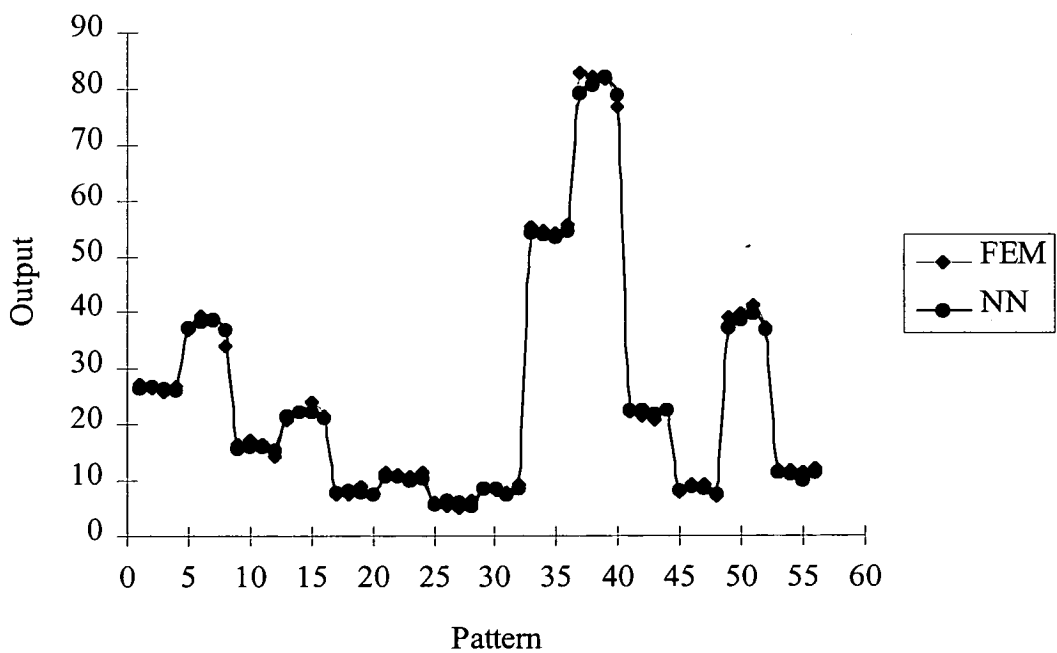


FIG 6.13 Performance of the Net on Test Set - Set4

NN Performance - Set5

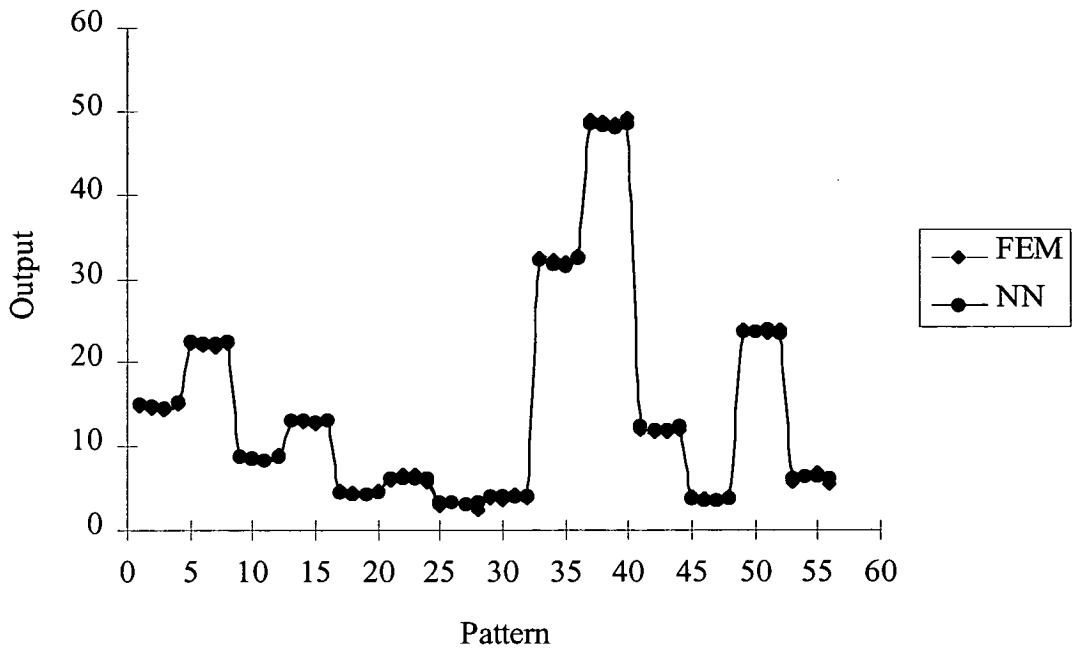


FIG. 6.14. Performance of the Net on Test Set - Set5

NN Performance - Set6

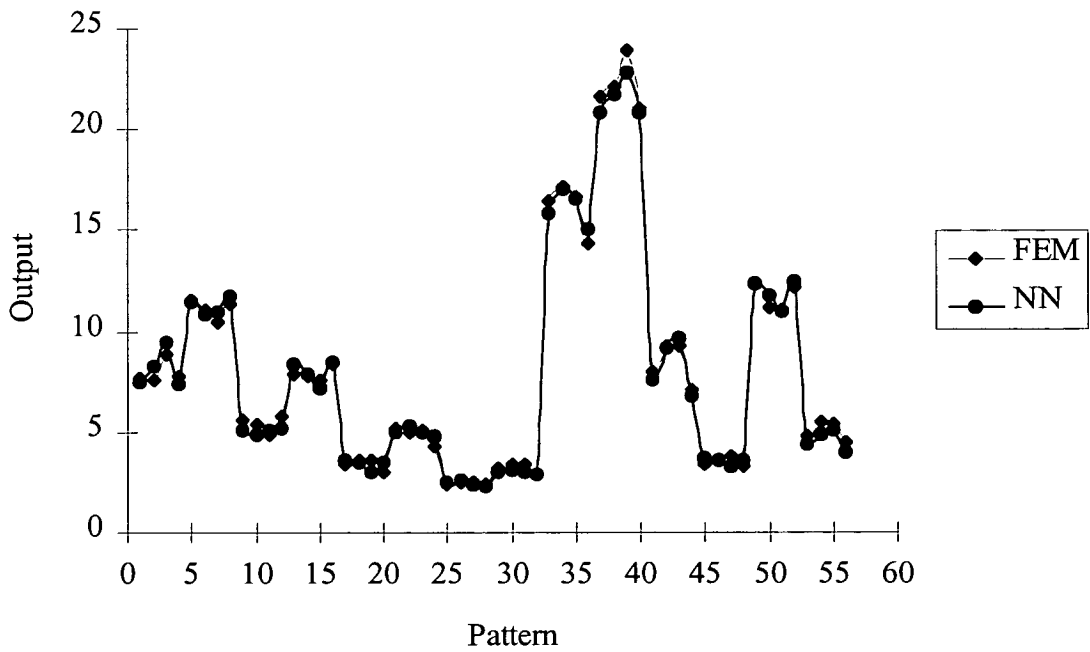


FIG. 6.15 Performance of the Net on Test Set - Set6

NN Performance - Set7

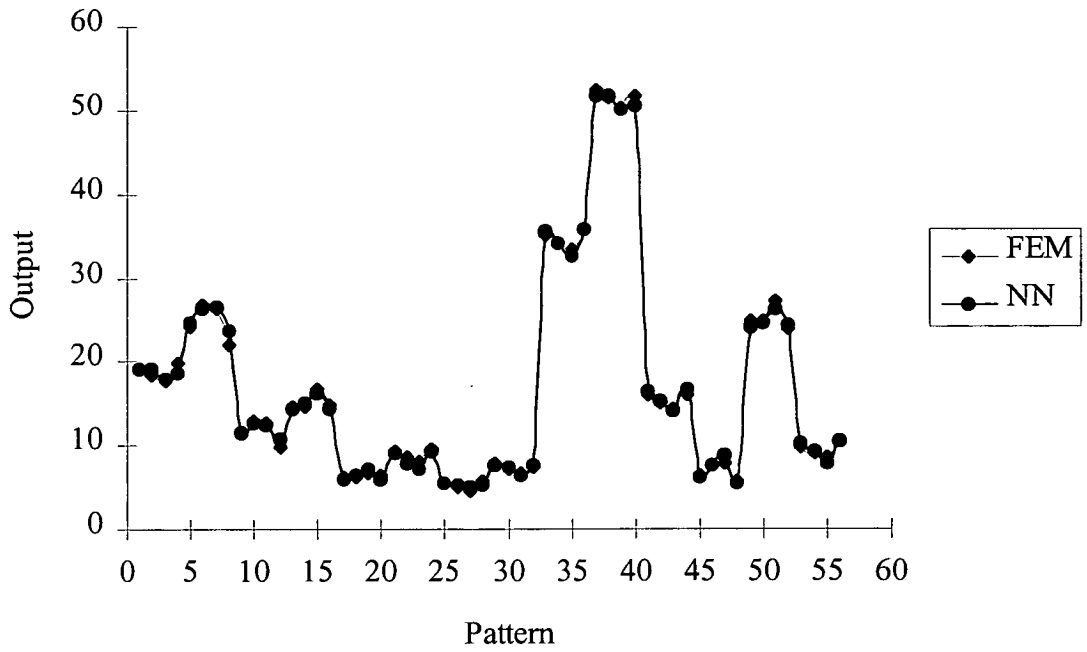


FIG. 6.16 Performance of the Net on Test Set - Set7

NN Performance - Set8

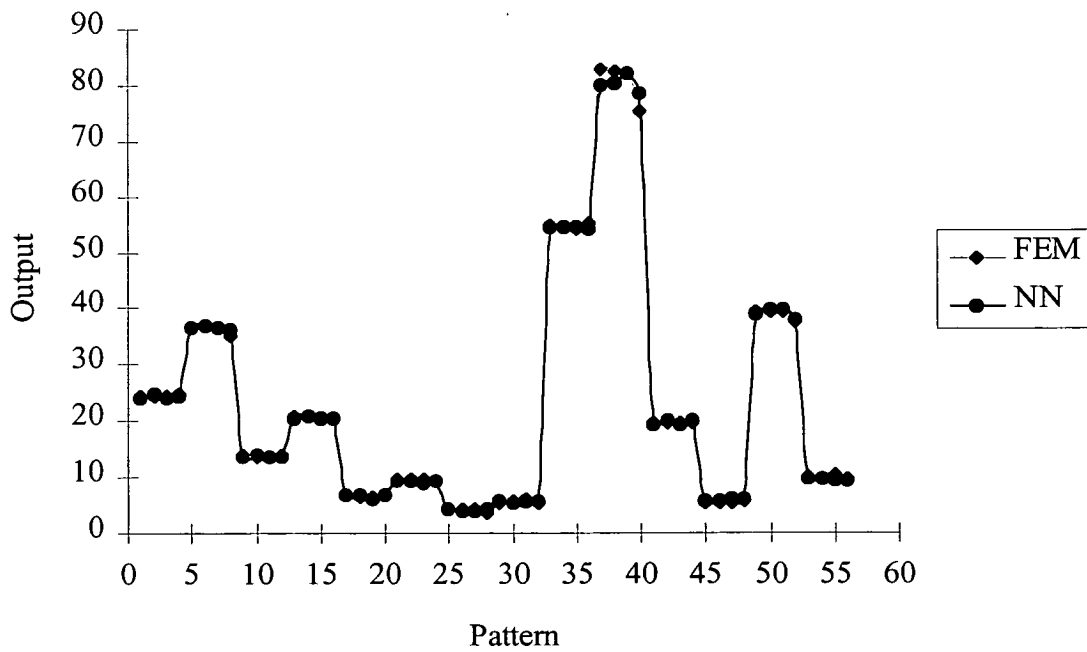


FIG. 6.17 Performance of the Net on Test Set - Set8

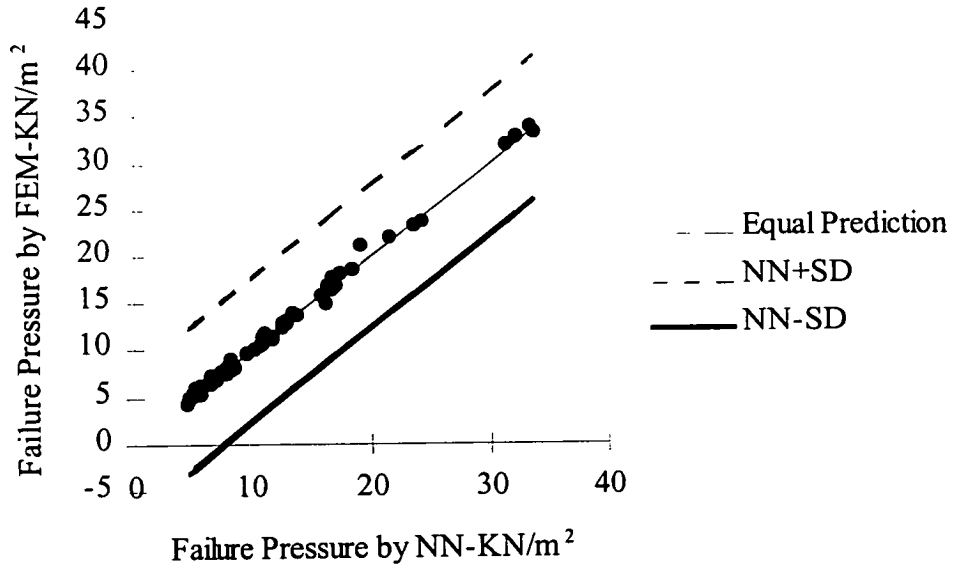


FIG. 6.18 Failure Pressure Predictions NN Vs. FEM (Set1)

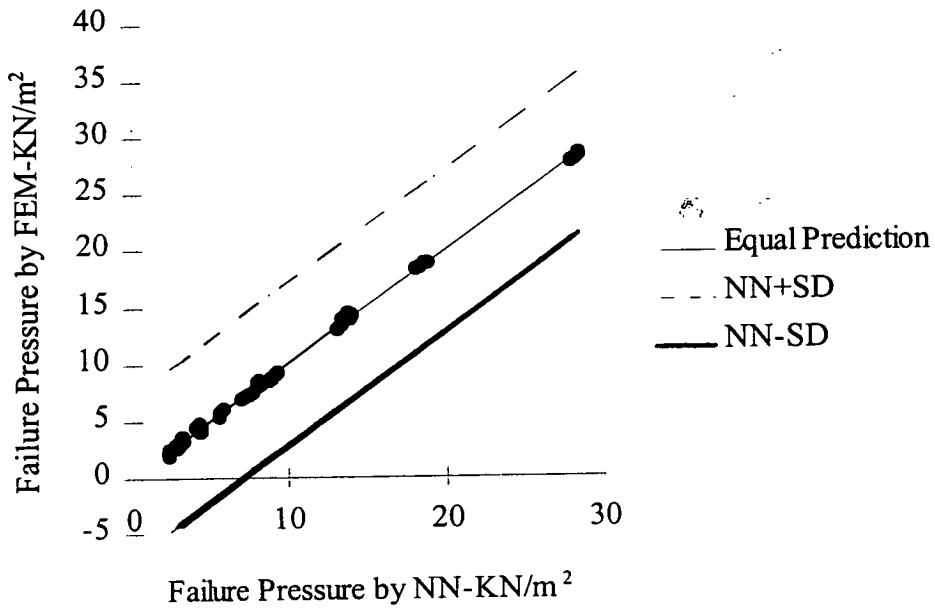


FIG. 6.19 Failure Pressure Predictions NN vs. FEM (Set2)

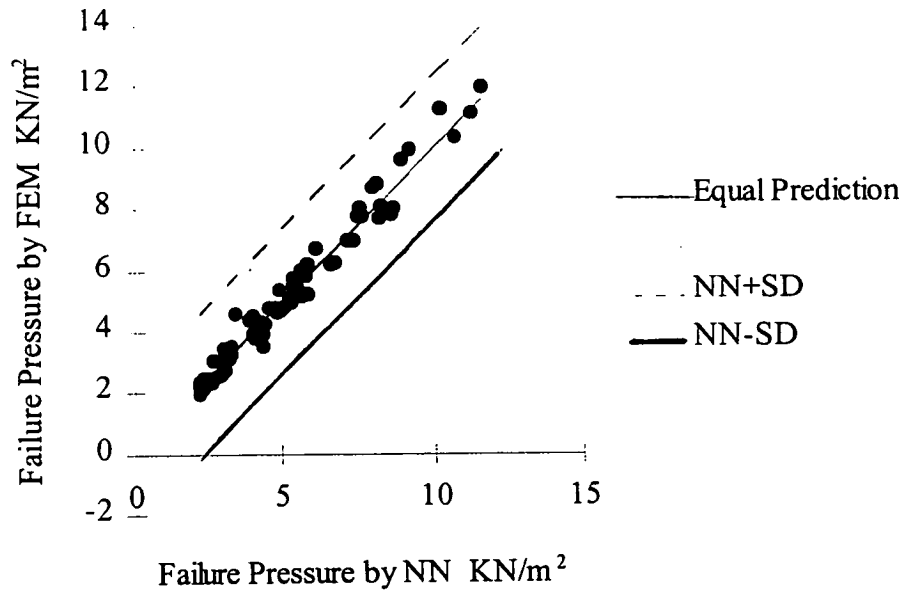


FIG. 6.20 Failure Pressure Predictions NN vs. FEM (Set3)

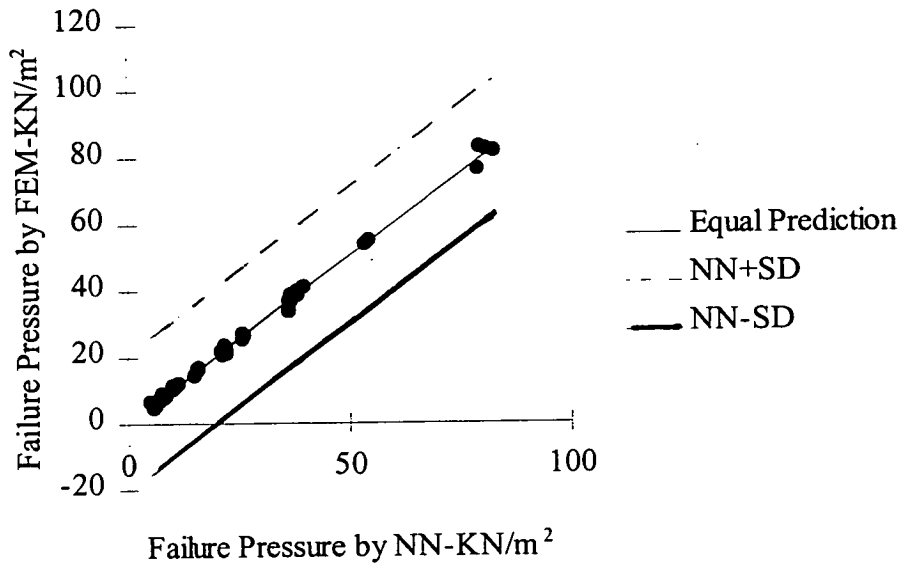


FIG. 6.21 Failure Pressure Predictions NN vs. FEM (Set4)

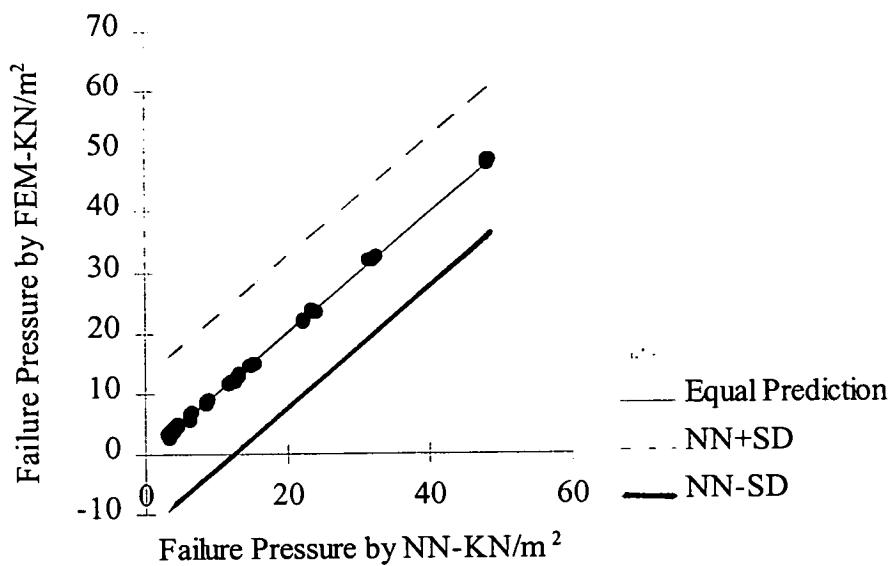


FIG. 6.22 Failure Pressure Predictions NN vs. FEM (Set5)

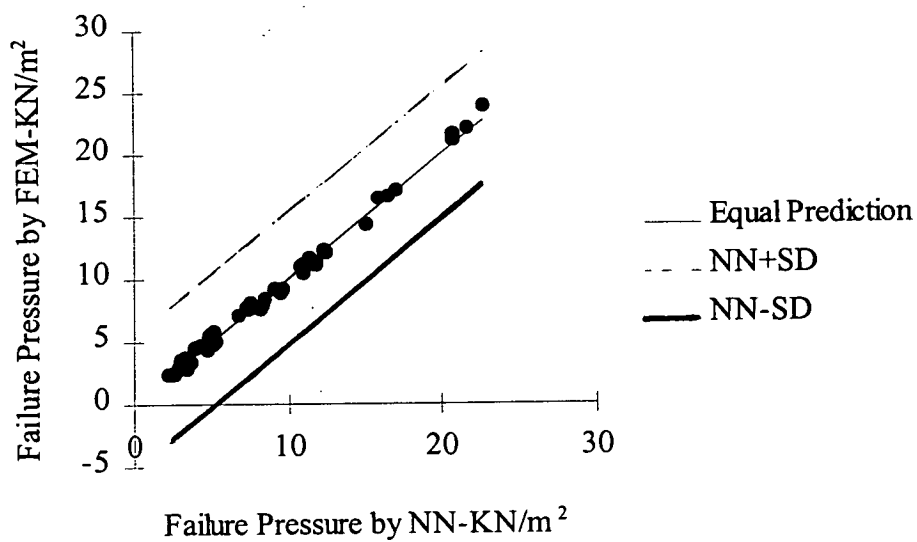


FIG. 6.23 Failure Pressure Predictions NN vs. FEM (Set6)



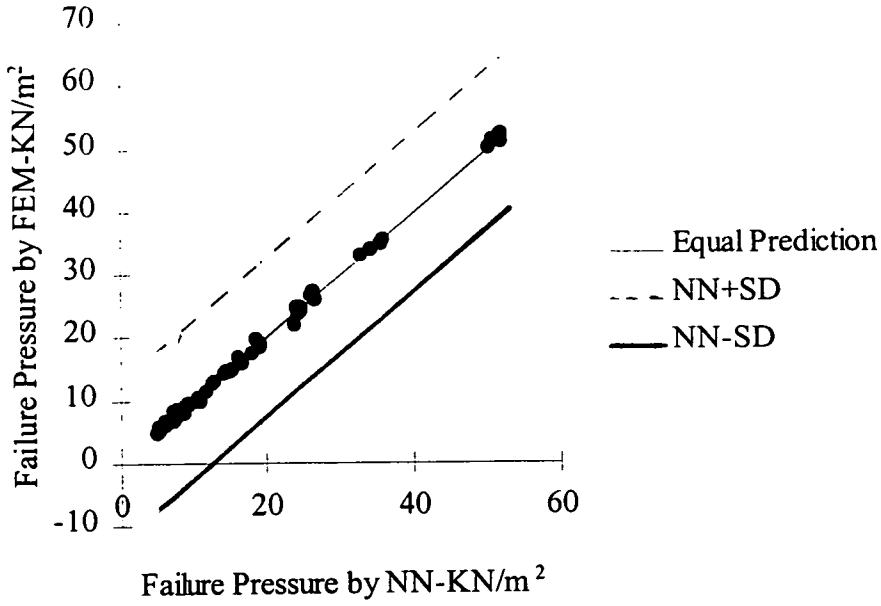


FIG. 6.24 Failure Pressure Predictions NN vs. FEM (Set7)

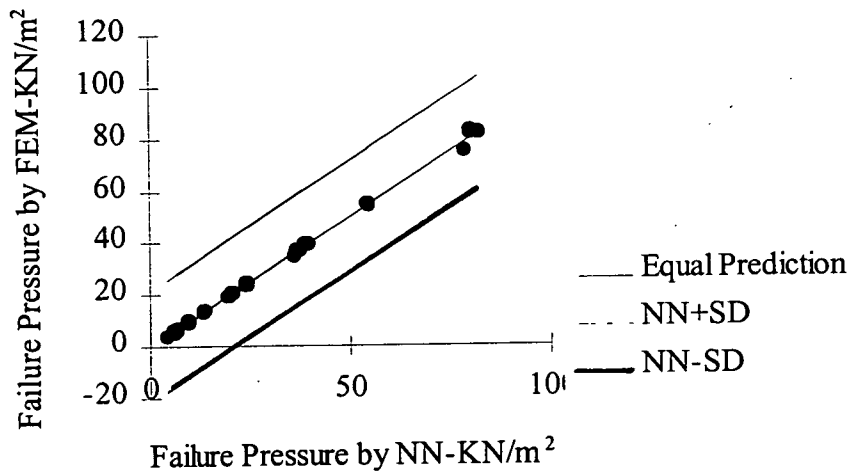


FIG. 6.25 Failure Pressure Predictions NN vs. FEM (Set8)

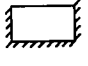
**Table 6.8. Test Set: Comparing The Neural Net And The Finite Element Results**

**of the Failure Pressure for Laterally Loaded Masonry Panels (Set1 -  )**

No	Net inputs				Failure Pressure		
	$\frac{F_x Z}{L^2}$	L/H	Fx/Fy	Ex/Ey	NN x10 <sup>-3</sup> (N/mm <sup>2</sup> )	FEM x10 <sup>-3</sup> (N/mm <sup>2</sup> )	Ratio $\frac{FEM}{NN}$
1	996	0.75	2.0	1.0	13.63	13.95	1.02
2	996	0.75	2.0	1.4	13.94	13.8	0.99
3	996	0.75	2.0	1.8	13.04	13.0	1.00
4	996	0.75	2.0	0.8	13.09	12.8	0.98
5	1494	0.75	3.0	1.0	16.3	15.0	0.92
6	1494	0.75	3.0	1.4	17.56	18.25	1.04
7	1494	0.75	3.0	1.8	18.55	18.75	1.01
8	1494	0.75	3.0	0.8	15.97	15.95	1.00
9	560	1.0	2.0	1.0	8.58	8.1	0.94
10	560	1.0	2.0	1.4	9.64	9.65	1.00
11	560	1.0	2.0	1.8	10.22	10.0	0.98
12	560	1.0	2.0	0.8	8.23	7.9	0.96
13	840	1.0	3.0	1.0	10.97	11.32	1.03
14	840	1.0	3.0	1.4	11.0	10.63	0.97
15	840	1.0	3.0	1.8	11.89	11.25	0.95
16	840	1.0	3.0	0.8	11.22	11.75	1.05
17	249	1.5	2.0	1.0	5.35	5.48	1.02
18	249	1.5	2.0	1.4	5.19	5.95	1.15
19	249	1.5	2.0	1.8	5.75	5.3	0.92
20	249	1.5	2.0	0.8	5.56	5.7	1.03
21	374	1.5	3.0	1.0	7.84	8.05	1.03
22	374	1.5	3.0	1.4	7.43	7.62	1.03
23	374	1.5	3.0	1.8	7.01	7.05	1.01
24	374	1.5	3.0	0.8	7.96	8.23	1.03
25	140	2.0	2.0	1.0	4.65	5.02	1.08
26	140	2.0	2.0	1.4	4.62	4.65	1.00
27	140	2.0	2.0	1.8	4.53	4.25	0.94
28	140	2.0	2.0	0.8	4.61	4.78	1.04
29	210	2.0	3.0	1.0	6.56	7.22	1.10
30	210	2.0	3.0	1.4	6.58	6.88	1.05
31	210	2.0	3.0	1.8	6.45	6.32	0.98
32	210	2.0	3.0	0.8	6.49	6.4	0.99
33	2241	0.5	2.0	1.0	23.74	23.4	0.99
34	2241	0.5	2.0	1.4	21.58	22.2	1.03
35	2241	0.5	2.0	1.8	19.27	21.3	1.11
36	2241	0.5	2.0	0.8	24.3	23.95	0.99
37	3361	0.5	3.0	1.0	33.44	34.1	1.02

Contd.....

No	$\frac{F_x Z}{L^2}$	L/H	Fx/Fy	Ex/Ey	NN output	FEM	$\frac{FEM}{NN}$
38	3361	0.5	3.0	1.4	33.87	33.3	0.98
39	3361	0.5	3.0	1.8	31.42	32.15	1.02
40	3361	0.5	3.0	0.8	32.34	32.85	1.02
41	809	0.75	1.3	1.0	12.63	12.5	0.99
42	809	0.75	1.3	1.4	11.85	11.4	0.96
43	809	0.75	1.3	1.8	10.82	10.55	0.98
44	809	0.75	1.3	0.8	12.66	12.45	0.98
45	202	1.5	1.3	1.0	4.98	5.4	1.08
46	202	1.5	1.3	1.4	5.74	6.2	1.08
47	202	1.5	1.3	1.8	7.03	6.75	0.96
48	202	1.5	1.3	0.8	4.9	5.15	1.05
49	1594	0.75	4.0	1.0	16.83	16.52	0.98
50	1594	0.75	4.0	1.4	16.4	16.92	1.03
51	1594	0.75	4.0	1.8	16.9	17.8	1.05
52	1594	0.75	4.0	0.8	17.25	16.92	0.98
53	398	1.5	4.0	1.0	8.23	8.95	1.09
54	398	1.5	4.0	1.4	8.22	8.15	0.99
55	398	1.5	4.0	1.8	7.9	7.58	0.96
56	398	1.5	4.0	0.8	8.12	7.98	0.98

Table 6.10. Test Set: Comparing the Neural Net and Finite Element Results of the Failure Pressure for Laterally Loaded Masonry Panels (Set2 - )

No	Net inputs				Failure Pressure		
	$\frac{F_x Z}{L^2}$	L/H	Fx/Fy	Ex/Ey	NN output $\times 10^{-3}$ (N/mm <sup>2</sup> )	FEM $\times 10^{-3}$ (N/mm <sup>2</sup> )	Ratio $\frac{FEM}{NN}$
1	996	0.75	2.0	1.0	9.1	9.16	1.01
2	996	0.75	2.0	1.4	8.75	8.9	1.02
3	996	0.75	2.0	1.8	8.55	8.77	1.03
4	996	0.75	2.0	0.8	9.25	9.36	1.01
5	1494	0.75	3.0	1.0	13.6	13.51	0.99
6	1494	0.75	3.0	1.4	13.25	13.35	1.01
7	1494	0.75	3.0	1.8	12.95	13.15	1.02
8	1494	0.75	3.0	0.8	13.8	13.56	0.98
9	560	1.0	2.0	1.0	5.9	5.74	0.97
10	560	1.0	2.0	1.4	5.6	5.56	0.99
11	560	1.0	2.0	1.8	5.35	5.54	1.04
12	560	1.0	2.0	0.8	6.0	5.9	0.98
13	840	1.0	3.0	1.0	8.55	8.23	0.96

Contd.....

*Chapter Six - Implementation of the Hybrid System for Predicting the Failure Pressure of Masonry Panels Subjected to Bi-axial Bending*

No	$\frac{F_x Z}{L^2}$	L/H	F <sub>x</sub> /F <sub>y</sub>	E <sub>x</sub> /E <sub>y</sub>	$\times 10^{-3}$ (N/mm <sup>2</sup> )	$\times 10^{-3}$ (N/mm <sup>2</sup> )	$\frac{FEM}{NN}$
14	840	1.0	3.0	1.4	8.35	8.11	0.97
15	840	1.0	3.0	1.8	8.05	8.05	1.00
16	840	1.0	3.0	0.8	8.25	8.29	1.01
17	249	1.5	2.0	1.0	3.5	3.19	0.91
18	249	1.5	2.0	1.4	3.45	3.13	0.91
19	249	1.5	2.0	1.8	3.25	3.25	1.00
20	249	1.5	2.0	0.8	3.2	3.31	1.03
21	374	1.5	3.0	1.0	4.05	4.29	1.06
22	374	1.5	3.0	1.4	4.6	4.22	0.92
23	374	1.5	3.0	1.8	4.7	4.34	0.92
24	374	1.5	3.0	0.8	4.15	4.37	1.05
25	140	2.0	2.0	1.0	2.15	2.31	1.07
26	140	2.0	2.0	1.4	2.4	2.31	0.96
27	140	2.0	2.0	1.8	2.5	2.49	1.00
28	140	2.0	2.0	0.8	2.02	2.39	1.18
29	210	2.0	3.0	1.0	2.85	2.88	1.01
30	210	2.0	3.0	1.4	2.75	2.79	1.02
31	210	2.0	3.0	1.8	2.8	2.97	1.06
32	210	2.0	3.0	0.8	2.98	3.0	1.01
33	2241	0.5	2.0	1.0	18.75	18.61	0.99
34	2241	0.5	2.0	1.4	18.5	18.3	0.99
35	2241	0.5	2.0	1.8	18.35	18.08	0.96
36	2241	0.5	2.0	0.8	18.85	18.83	1.00
37	3361	0.5	3.0	1.0	28.3	28.39	1.00
38	3361	0.5	3.0	1.4	27.9	28.21	1.01
39	3361	0.5	3.0	1.8	27.7	27.87	1.01
40	3361	0.5	3.0	0.8	28.35	28.4	1.02
41	809	0.75	1.3	1.0	7.35	7.59	1.03
42	809	0.75	1.3	1.4	7.1	7.23	1.02
43	809	0.75	1.3	1.8	6.95	6.97	1.03
44	809	0.75	1.3	0.8	7.45	7.84	1.05
45	202	1.5	1.3	1.0	3.15	2.97	0.94
46	202	1.5	1.3	1.4	2.85	2.81	0.99
47	202	1.5	1.3	1.8	2.65	2.81	1.06
48	202	1.5	1.3	0.8	3.25	3.1	0.95
49	1594	0.75	4.0	1.0	14.3	13.79	0.96
50	1594	0.75	4.0	1.4	14.15	14.09	1.00
51	1594	0.75	4.0	1.8	13.85	13.87	1.00
52	1594	0.75	4.0	0.8	13.94	13.43	0.96
53	398	1.5	4.0	1.0	4.32	4.2	0.97
54	398	1.5	4.0	1.4	4.2	4.35	1.04
55	398	1.5	4.0	1.8	4.45	4.38	0.98
56	398	1.5	4.0	0.8	4.38	4.06	0.93

**Table 6.11. Test Set: Comparing the Neural Net and Finite Element Results of**

**the Failure Pressure for Laterally Loaded Masonry Panels (Set3 -  )**

No	Net inputs				Failure Pressure		
	$\frac{F_x Z}{L^2}$	L/H	Fx/Fy	Ex/Ey	NN output $\times 10^{-3}$ (N/mm <sup>2</sup> )	FEM $\times 10^{-3}$ (N/mm <sup>2</sup> )	Ratio $\frac{FEM}{NN}$
1	996	0.75	2.0	1.0	5.54	5.6	1.01
2	996	0.75	2.0	1.4	5.71	5.18	0.91
3	996	0.75	2.0	1.8	5.84	5.25	0.9
4	996	0.75	2.0	0.8	5.41	5.5	1.02
5	1494	0.75	3.0	1.0	7.73	7.9	1.02
6	1494	0.75	3.0	1.4	7.36	7.8	1.06
7	1494	0.75	3.0	1.8	7.09	7	0.99
8	1494	0.75	3.0	0.8	7.84	8.1	1.03
9	560	1.0	2.0	1.0	4	4.5	1.13
10	560	1.0	2.0	1.4	4.16	4.1	0.99
11	560	1.0	2.0	1.8	4.14	3.55	0.86
12	560	1.0	2.0	0.8	3.83	4.4	1.15
13	840	1.0	3.0	1.0	5.67	5.78	1.02
14	840	1.0	3.0	1.4	5.97	6.04	1.01
15	840	1.0	3.0	1.8	5.89	5.83	0.99
16	840	1.0	3.0	0.8	5.33	5.1	0.96
17	249	1.5	2.0	1.0	2.61	2.49	0.95
18	249	1.5	2.0	1.4	3.02	2.56	0.85
19	249	1.5	2.0	1.8	2.93	2.63	0.9
20	249	1.5	2.0	0.8	2.31	2.45	1.06
21	374	1.5	3.0	1.0	2.82	2.45	0.87
22	374	1.5	3.0	1.4	3.43	3.25	0.95
23	374	1.5	3.0	1.8	3.62	4.25	1.17
24	374	1.5	3.0	0.8	2.41	2.42	1
25	140	2.0	2.0	1.0	2.28	2.37	1.04
26	140	2.0	2.0	1.4	2.49	2.4	0.96
27	140	2.0	2.0	1.8	2.23	2.42	1.09
28	140	2.0	2.0	0.8	2.12	2.36	1.11
29	210	2.0	3.0	1.0	2.16	2.34	1.08
30	210	2.0	3.0	1.4	2.52	2.36	0.94
31	210	2.0	3.0	1.8	2.37	2.38	1
32	2241	0.5	2.0	1.0	8.67	8.1	0.93
33	2241	0.5	2.0	1.4	8.79	9.65	1.1
34	2241	0.5	2.0	1.8	8.89	10	1.12

**Table 6.12. Test Set: Comparing the Neural Net and Finite Element Results of**

**the Failure Pressure for Laterally Loaded Masonry Panels (Set4 -  )**

No	Net inputs				Failure Pressure		
	$\frac{F_x Z}{L^2}$	L/H	Fx/Fy	Ex/Ey	NN output $\times 10^{-3}$ (N/mm <sup>2</sup> )	FEM $\times 10^{-3}$ (N/mm <sup>2</sup> )	Ratio $\frac{FEM}{NN}$
1	996	0.75	2.0	1.0	26.49	27.15	1.02
2	996	0.75	2.0	1.4	26.75	26.45	0.99
3	1494	0.75	3.0	1.0	37.34	36.9	0.99
4	1494	0.75	3.0	0.8	36.85	34.15	0.93
5	560	1.0	2.0	1.8	15.98	16.65	1.04
6	560	1.0	2.0	0.8	15.24	14.3	0.94
7	840	1.0	3.0	1.0	21.6	20.95	0.97
8	840	1.0	3.0	0.8	21.19	21.65	1.02
9	249	1.5	2.0	1.0	7.91	7.7	0.97
10	249	1.5	2.0	1.4	8.35	7.6	0.91
11	374	1.5	3.0	1.8	9.98	10.6	1.06
12	374	1.5	3.0	0.8	10.47	11.6	1.11
13	140	2.0	2.0	1.0	5.84	6.12	1.05
14	140	2.0	2.0	0.8	5.27	6.4	1.21
15	210	2.0	3.0	1.0	8.74	8.45	0.97
16	210	2.0	3.0	1.4	8.5	8.25	0.97
17	2241	0.5	2.0	1.0	54.29	55.05	1.01
18	2241	0.5	2.0	1.4	53.91	54.4	1.01
19	2241	0.5	2.0	0.8	54.45	55.4	1.02
20	3361	0.5	3.0	1.0	79.35	82.9	1.04
21	3361	0.5	3.0	1.8	82.26	81.6	0.99
22	3361	0.5	3.0	0.8	78.91	76.65	0.97
23	809	0.75	1.3	1.0	22.75	22.2	0.98
24	809	0.75	1.3	1.4	22.58	21.35	0.95
25	809	0.75	1.3	0.8	22.57	22.65	1
26	202	1.5	1.3	1.4	8.95	9.25	1.03
27	202	1.5	1.3	1.8	8.78	9.25	1.05
28	202	1.5	1.3	0.8	7.49	7.1	0.95
29	1594	0.75	4.0	1.0	37.35	38.92	1.04
30	1594	0.75	4.0	1.8	39.87	41.1	1.03
31	1594	0.75	4.0	0.8	36.78	37.25	1.01
32	398	1.5	4.0	1.0	11.59	11.94	1.03
33	398	1.5	4.0	1.4	11.12	11.66	1.05
34	398	1.5	4.0	0.8	11.59	12.35	1.07

**Table 6.13. Test Set: Comparing the Neural Net and Finite Element Results of**

**the Failure Pressure for Laterally Loaded Masonry Panels (Set5 - )**

No	Net inputs				Failure Pressure		
	$\frac{F_x Z}{L^2}$	L/H	F <sub>x</sub> /F <sub>y</sub>	E <sub>x</sub> /E <sub>y</sub>	NN	FEM	Ratio
					output		
					$\times 10^{-3}$ (N/mm <sup>2</sup> )	$\times 10^{-3}$ (N/mm <sup>2</sup> )	$\frac{\text{FEM}}{\text{NN}}$
1	996	0.75	2.0	1.4	14.9	14.6	0.98
2	996	0.75	2.0	1.8	14.67	14.45	0.99
3	996	0.75	2.0	0.8	15.29	14.95	0.98
4	1494	0.75	3.0	1.0	22.39	22.3	1
5	1494	0.75	3.0	1.4	22.31	22	0.99
6	1494	0.75	3.0	1.8	22.19	21.8	0.98
7	560	1.0	2.0	1.0	8.83	8.85	1
8	560	1.0	2.0	1.4	8.64	8.6	1
9	560	1.0	2.0	1.8	8.48	8.4	0.99
10	840	1.0	3.0	1.8	12.99	12.7	0.98
11	840	1.0	3.0	0.8	13.1	13.1	1
12	249	1.5	2.0	1.0	4.44	4.8	1.08
13	249	1.5	2.0	1.8	4.21	4.41	1.05
14	249	1.5	2.0	0.8	4.51	4.7	1.04
15	374	1.5	3.0	1.0	6.26	6.05	0.97
16	374	1.5	3.0	0.8	6.24	5.7	0.91
17	140	2.0	2.0	1.4	3.27	3.25	0.99
18	140	2.0	2.0	1.8	3.19	3.15	0.99
19	210	2.0	3.0	1.4	4.1	3.65	0.89
20	210	2.0	3.0	1.8	4.1	4.2	1.02
21	2241	0.5	2.0	1.4	31.86	32.3	1.01
22	2241	0.5	2.0	1.8	31.45	32.15	1.02
23	2241	0.5	2.0	0.8	32.49	32.7	1.01
24	3361	0.5	3.0	1.0	48.43	49.1	1.01
25	3361	0.5	3.0	1.4	48.34	48.8	1.01
26	3361	0.5	3.0	0.8	48.42	49.25	1.02
27	809	0.75	1.3	1.0	12.34	11.95	0.97
28	809	0.75	1.3	1.8	11.84	11.65	0.98
29	202	1.5	1.3	1.0	3.8	4	1.05
30	202	1.5	1.3	1.4	3.65	3.75	1.03
31	202	1.5	1.3	0.8	3.89	4.15	1.07
32	1594	0.75	4.0	1.4	23.78	23.65	0.99
33	1594	0.75	4.0	1.8	23.95	23.45	0.98
34	398	1.5	4.0	1.8	6.55	6.85	1.05

**Table 6.14. Test Set: Comparing the Neural Net and Finite Element Results of**

**the Failure Pressure for Laterally Loaded Masonry Panels (Set6 -  )**

No	Net inputs				Failure Pressure		
	$\frac{F_x Z}{L^2}$	L/H	Fx/Fy	Ex/Ey	NN output x10 <sup>-3</sup> (N/mm <sup>2</sup> )	FEM x10 <sup>-3</sup> (N/mm <sup>2</sup> )	Ratio $\frac{FEM}{NN}$
1	996	0.75	2.0	1.0	7.44	7.64	1.03
2	996	0.75	2.0	1.8	9.47	8.9	0.94
3	1494	0.75	3.0	1.0	11.41	11.58	1.01
4	1494	0.75	3.0	1.4	10.87	11.02	1.01
5	1494	0.75	3.0	1.8	10.93	10.48	0.96
6	560	1.0	2.0	1.4	4.87	5.35	1.1
7	560	1.0	2.0	1.8	5.12	4.85	0.95
8	560	1.0	2.0	0.8	5.21	5.78	1.11
9	840	1.0	3.0	1.4	7.89	7.72	0.98
10	840	1.0	3.0	1.8	7.22	7.52	1.04
11	840	1.0	3.0	0.8	8.44	8.35	0.99
12	249	1.5	2.0	1.4	3.52	3.55	1.01
13	249	1.5	2.0	0.8	3.48	2.98	0.86
14	374	1.5	3.0	1.8	4.99	5.08	1.02
15	374	1.5	3.0	0.8	4.76	4.32	0.91
16	140	2.0	2.0	1.0	2.46	2.4	0.98
17	140	2.0	2.0	0.8	2.31	2.4	1.04
18	210	2.0	3.0	1.0	3.01	3.2	1.06
19	210	2.0	3.0	1.8	3.01	3.38	1.12
20	210	2.0	3.0	0.8	2.91	2.85	0.98
21	2241	0.5	2.0	1.0	15.84	16.4	1.04
22	2241	0.5	2.0	1.4	17.04	17.15	1.01
23	2241	0.5	2.0	1.8	16.58	16.65	1
24	3361	0.5	3.0	1.0	20.8	21.58	1.04
25	3361	0.5	3.0	1.4	21.7	22.1	1.02
26	809	0.75	1.3	1.4	9.12	9.25	1.01
27	809	0.75	1.3	1.8	9.71	9.25	0.95
28	809	0.75	1.3	0.8	6.8	7.05	1.04
29	202	1.5	1.3	1.4	3.58	3.6	1.01
30	202	1.5	1.3	0.8	3.55	3.3	0.93
31	1594	0.75	4.0	1.0	12.33	12.32	1
32	1594	0.75	4.0	1.4	11.74	11.12	0.95
33	398	1.5	4.0	1.0	4.35	4.75	1.09
34	398	1.5	4.0	0.8	4.02	4.48	1.11



**Table 6.15. Test Set: Comparing the Neural Net and Finite Element Results of**

**the Failure Pressure for Laterally Loaded Masonry Panels (Set7 -  )**

No	Net inputs				Failure Pressure		
	$\frac{F_x Z}{L^2}$	L/H	Fx/Fy	Ex/Ey	NN output x10 <sup>-3</sup> (N/mm <sup>2</sup> )	FEM x10 <sup>-3</sup> (N/mm <sup>2</sup> )	Ratio $\frac{FEM}{NN}$
1	996	0.75	2.0	1.0	19.21	19.2	1
2	996	0.75	2.0	1.8	17.94	17.6	0.98
3	996	0.75	2.0	0.8	18.59	19.8	1.07
4	1494	0.75	3.0	1.4	26.24	26.75	1.02
5	1494	0.75	3.0	1.8	26.63	26.3	0.99
6	560	1.0	2.0	1.0	11.53	11.5	1
7	560	1.0	2.0	1.4	12.66	12.9	1.02
8	840	1.0	3.0	1.8	16.2	16.75	1.03
9	840	1.0	3.0	0.8	14.4	14.72	1.02
10	249	1.5	2.0	1.0	6.04	6.15	1.02
11	249	1.5	2.0	1.4	6.37	6.25	0.98
12	374	1.5	3.0	1.0	8.97	9.33	1.04
13	374	1.5	3.0	1.4	7.99	8.62	1.08
14	140	2.0	2.0	1.0	9.3	9.62	1.03
15	140	2.0	2.0	1.4	5.3	4.92	0.93
16	210	2.0	3.0	1.0	7.67	7.95	1.04
17	210	2.0	3.0	1.4	7.35	7.22	0.98
18	210	2.0	3.0	1.8	6.52	6.68	1.02
19	2241	0.5	2.0	1.0	35.55	35.25	0.99
20	2241	0.5	2.0	1.4	34.1	34.2	1
21	2241	0.5	2.0	0.8	35.91	35.9	1
22	3361	0.5	3.0	1.4	51.94	51.6	0.99
23	3361	0.5	3.0	1.8	50.28	50.5	1
24	3361	0.5	3.0	0.8	50.76	51.8	1.02
25	809	0.75	1.3	1.4	15.38	15	0.98
26	809	0.75	1.3	1.8	14.04	14.25	1.01
27	202	1.5	1.3	1.0	6.21	6.5	1.05
28	202	1.5	1.3	1.8	8.74	7.95	0.91
29	202	1.5	1.3	0.8	5.57	5.8	1.04
30	1594	0.75	4.0	1.4	24.64	24.75	1
31	1594	0.75	4.0	1.8	26.36	27.3	1.04
32	398	1.5	4.0	1.4	9.22	9.18	1
33	398	1.5	4.0	1.8	7.91	8.6	1.09
34	398	1.5	4.0	0.8	10.46	10.48	1

**Table 6.16. Test Set: Comparing the Neural Net and Finite Element Results of**

**the Failure Pressure for Laterally Loaded Masonry Panels (Set8 - )**

No	Net inputs				Failure Pressure		
	$\frac{F_x Z}{L^2}$	L/H	Fx/Fy	Ex/Ey	NN output x10 <sup>-3</sup> (N/mm <sup>2</sup> )	FEM x10 <sup>-3</sup> (N/mm <sup>2</sup> )	Ratio $\frac{FEM}{NN}$
1	996	0.75	2.0	1.0	24.07	24.55	1.02
2	996	0.75	2.0	0.8	24.3	24.6	1.01
3	1494	0.75	3.0	1.0	36.64	36.65	1
4	1494	0.75	3.0	1.4	36.97	36.9	1
5	1494	0.75	3.0	0.8	36.27	35.05	0.97
6	560	1.0	2.0	1.0	13.48	13.85	1.03
7	560	1.0	2.0	0.8	13.79	13.95	1.01
8	840	1.0	3.0	1.0	20.4	20.85	1.02
9	840	1.0	3.0	0.8	20.31	20.52	1.01
10	249	1.5	2.0	1.0	6.64	6.8	1.02
11	249	1.5	2.0	1.4	6.72	6.6	0.98
12	374	1.5	3.0	1.0	9.37	9.55	1.02
13	374	1.5	3.0	1.4	9.46	9.85	1.04
14	374	1.5	3.0	0.8	9.28	9.2	0.99
15	140	2.0	2.0	1.0	4.24	4.15	0.98
16	140	2.0	2.0	1.4	4.03	4.3	1.07
17	140	2.0	2.0	1.8	4.06	4.2	1.03
18	210	2.0	3.0	1.4	5.55	5.65	1.02
19	210	2.0	3.0	1.8	5.67	6	1.06
20	2241	0.5	2.0	1.0	54.53	54.9	1.01
21	2241	0.5	2.0	1.4	54.66	54.55	1
22	2241	0.5	2.0	1.8	54.44	54.3	1
23	3361	0.5	3.0	1.4	80.22	82.4	1.03
24	3361	0.5	3.0	1.8	82.03	81.95	1
25	809	0.75	1.3	1.0	19.45	19.8	1.02
26	809	0.75	1.3	1.4	20.03	19.7	0.98
27	202	1.5	1.3	1.0	5.78	5.55	0.96
28	202	1.5	1.3	1.4	5.82	5.35	0.92
29	202	1.5	1.3	0.8	6.2	5.65	0.91
30	1594	0.75	4.0	1.0	38.91	39.28	1.01
31	1594	0.75	4.0	1.8	39.92	39.4	0.99
32	398	1.5	4.0	1.0	9.69	10.08	1.04
33	398	1.5	4.0	1.8	9.46	10.25	1.08
34	398	1.5	4.0	0.8	9.41	9.78	1.04

## 6.7 Performance of the Net on Experimental Results

This section deals with the net performance on panels that were tested at the different research centres. It is important to bear in mind that the experimental set up at various places were not the same and, hence, variations in the experimental results from the theoretical predictions are unavoidable. The data available covered only 6 different types of boundary conditions and are discussed in detail here. No data was available on Set5 and Set7 type panels.

The Root Mean Square (RMS) of the difference between the experimental failure pressure and the theoretical predictions are carried out to find out the method that gives the better results (Table 6.16). It can be seen that there is a considerable improvement in the results while the trained neural network is used.

**Table 6.16 Root Mean Square of the Difference between the Experimental and Theoretical Failure Pressure of Panels**

Type	RMS(BS-Expt)	RMS(Aus-Expt)	RMS(FEM-Expt)	RMS(NN-Expt)
Set1	2.663	2.194	2.587	1.789
Set2	1.331	1.598	0.594	0.533
Set3	0.8		1.041	0.738
Set4	3.402	1.928	3.125	2.863
Set6	1.442		0.822	0.779
Set8	0.626	1.288	0.993	1.373

### 6.7.1 'Set1' (Four Sides Simply Supported) Panels

The results published by BAKER (1972), KHEIR (1975), LAWRENCE (1983) and NG (1996) are used in this case. The comparison of the predicted failure pressures with the experimental values is given in Table 6.17. The experimental results of BAKER (1972) are over-estimated by all the theories. The flexural strengths given were modified by factors recommended in his work. It can be seen that the finite element, the Australian code of practice and the trained net predicted results close to each other in this case, even though the predicted values over-estimated the

experimental results. The reason for the discrepancy could be due to the different approach adopted in finding out the flexural strengths of the material.

**Table 6.17 Comparison of Experimental Results with Theoretical Predictions - Set1**

No.		Failure Pressure ( $\times 10^{-3}$ N/mm <sup>2</sup> )					Ratio			
		Expt	FEM	BS	Aus	NN	$\frac{\text{Expt}}{\text{FEM}}$	$\frac{\text{Expt}}{\text{BS}}$	$\frac{\text{Expt}}{\text{Aus}}$	$\frac{\text{Expt}}{\text{NN}}$
1	Baker (1972)	10.98	13	15.27	13.47	13.47	0.84	0.72	0.82	0.82
2		9.42	10.4	13.27	11.51	11.23	0.91	0.71	0.82	0.84
3		16.35	16	20.44	17.68	17.14	1.02	0.8	0.92	0.95
4		5.22	5.02	6.81	5.02	7.54	1.04	0.77	1.04	0.69
5		6.15	8	10.01	8.43	8.96	0.77	0.61	0.73	0.69
6		6	8.1	9.01	7.46	8.66	0.74	0.67	0.8	0.69
7		8.3	11.4	11.48	9.38	11.64	0.73	0.72	0.88	0.71
8	Kheir (1975)	8.4	7.3	7.87	6.83	6.7	1.15	1.07	1.23	1.25
9		10.5	7.6	9.12	7.9	7.73	1.38	1.15	1.33	1.36
10		10	9	9.4	8.24	8.52	1.11	1.06	1.21	1.17
11		18.2	13.1	18.16	15.27	20.3	1.39	1	1.19	0.9
12		19	12.2	17.22	13.99	20.74	1.56	1.1	1.36	0.92
13		18	10.9	14.64	12.26	17.26	1.65	1.23	1.47	1.04
14		7	5.95	4.6	6.2	4.81	1.18	1.52	1.13	1.46
15	5.6	5.7	4.39	5.94	4.84	0.98	1.28	0.94	1.16	
16	Ng (1996)	7.46	8.3	9.57	8.31	8.61	0.9	0.78	0.9	0.87
17		12.38	12.3	14.8	12.52	12.76	1.01	0.84	0.99	0.97
18		20.6	22.7	23.16	18.08	20.83	0.91	0.89	1.14	0.99
19		18.9	21.4	22.37	17.6	19.96	0.88	0.84	1.07	0.95
20		25	27.55	29.2	27.44	26.34	0.91	0.86	0.91	0.95
21	31.8	31.25	34.07	31.76	29.82	1.02	0.93	1	1.07	
22	Lawrence (1983)	8.6	8.8	10.21	8.84	8.64	0.98	0.84	0.97	1
23		3.2	4	4.53	3.9	4.03	0.8	0.71	0.82	0.79
24		3.5	4.2	5.98	5.27	4.89	0.83	0.59	0.66	0.72
25		4.7	5.1	5.58	4.69	5.21	0.92	0.84	1	0.9
26	4.9	5.2	6.75	5.57	5.89	0.94	0.73	0.88	0.83	

Significant improvement in the results can be observed in the case of KHEIR (1973) and NG (1996). While a closer prediction by the Australian code can be noticed in case of NG (1996) results, the BS over-estimated the results. However, in the case of LAWRENCE (1983), most of the results are again over-estimated by the theories. An

overall assessment of the performance of the net can be seen by the RMS of the differences shown in Table 6.16. It can be seen that for Set1 type panels, the NN results have got lowest difference with the experimental failure load.

### **6.7.2 ‘Set2’ Panels (Three Side Simply Supported, Top Free)**

The experimental results considered in this type of panels include that of BAKER (1972), LAWRENCE (1983), NG (1996) and BCRA results by WEST *et al.* (1977). The theoretical comparisons are given in Table 6.18. A very high correlation between the NN and the FEM results with the experimental results can be observed in the first three cases. The BS is over-estimating the results in all these cases. Nevertheless, the BS can be seen to give closer results to the experimental results in the BCRA work, whereas the other methods are under-estimating. It can be seen from Table 6.6 that the BS over-estimates the failure load when compared to the finite element analysis. A similar observation can be seen in the results of the first three researchers. It has to be pointed out that WEST *et al.* (1977) considered an average value for the flexural strength. As the values of moduli of elasticity of the specimens were not given anywhere in their publication, an isotropic material property was assumed to carry out the finite element and the neural network analysis. It is also worth mentioning that the support conditions for the panels were not simply supported. Partial fixity was provided at the vertical edges as the panels were built within a rectangular steel frame. This could have induced slight restraints at the vertical edges and, in turn, would have increased the load carrying capacity. As can be seen in Table 6.16, the finite element analysis and the trained neural network gives lower values of RMS difference, which gives an indication of its performance in a group of data.

**Table 6.18 Comparison of Experimental Results of Failure Pressure with Theoretical Predictions - Set2**

No.		Failure Pressure ( $\times 10^{-3}$ N/mm <sup>2</sup> )					Ratio			
		Expt	FEM	BS	Aus	NN	$\frac{\text{Expt}}{\text{FEM}}$	$\frac{\text{Expt}}{\text{BS}}$	$\frac{\text{Expt}}{\text{Aus}}$	$\frac{\text{Expt}}{\text{NN}}$
1	Baker (1972)	7.81	8.9	9.73	9.4	8.54	0.88	0.8	0.83	0.91
2		3.27	3.38	4.03	3.57	3.3	0.97	0.81	0.92	0.99
3		2.78	2.52	3.01	2.51	2.63	1.1	0.92	1.11	1.06
4	Lawrence (1983)	7.8	7	8.39	7.85	7.41	1.11	0.93	0.99	1.05
5		3.4	3.05	3.91	3.41	3.51	1.11	0.87	1	0.97
6		2.7	2.38	2.92	2.46	2.82	1.13	0.92	1.1	0.96
7		2.3	2.3	2.58	2.32	2.95	1	0.89	0.99	0.78
8		1.7	1.75	2	1.71	1.78	0.97	0.85	0.99	0.96
9		1.9	1.7	1.6	1.42	1.76	1.12	1.19	1.34	1.08
10	Ng (1996)	8.54	9.5	10.63	10.3	9.16	0.9	0.8	0.83	0.93
11		23.5	24.25	27.64	28.79	24.41	0.97	0.85	0.82	0.96
12		27.8	26.65	30.41	31.69	26.89	1.04	0.91	0.88	1.03
13	BCRA West. <i>et al.</i> (1977)	2.37	1.95	2.12	1.82	1.78	1.22	1.12	1.3	1.33
14		3.15	2.45	3.01	2.74	2.53	1.29	1.05	1.15	1.25
15		4.01	3.1	3.82	3.49	3.26	1.29	1.05	1.15	1.23
16		2.08	1.65	1.99	1.81	1.63	1.26	1.05	1.15	1.28
17		3.19	2.5	3.05	2.77	2.57	1.28	1.05	1.15	1.24
18		6.6	7.1	7.8	7.7	6.95	0.93	0.85	0.86	0.95
19		4.99	5.25	5.75	5.68	5.17	0.95	0.87	0.88	0.97
20		5.45	6.65	7.32	7.23	6.54	0.82	0.74	0.75	0.83
21		4.76	5.3	5.82	5.75	5.22	0.9	0.82	0.83	0.91
22		8.18	8.5	9.3	9.19	8.25	0.96	0.88	0.89	0.99
23		15.51	16	17.97	19.02	16.06	0.97	0.86	0.82	0.97
24		12.06	11.75	13.26	14.03	11.97	1.03	0.91	0.86	1.01
25		6	6.05	6.63	6.39	5.85	0.99	0.9	0.94	1.03
26		2.2	1.85	2.22	1.95	1.77	1.19	0.99	1.13	1.24
27		4.3	3.95	4.44	4.53	4.12	1.09	0.97	0.95	1.04
28		4	4.5	4.89	4.71	4.34	0.89	0.82	0.85	0.92
29	5.8	6.15	6.83	5.88	6.75	0.94	0.85	0.99	0.86	

### 6.7.3 'Set3' Panels (Three Sides Simply Supported and One Vertical Edge Free)

The experimental work by KHEIR (1975) and NG (1996) was studied for this type of panels. Table 6.19 shows the comparison of the experimental and the theoretical

values of the failure pressure. The Australian code was not used in this case as the coefficients for the same was not given in the Code of practice. As can be seen in Table 6.19, the finite element and the neural network predict the failure pressure close to the experimental values.

**Table 6.19 Comparison of Experimental Results of the Failure Pressure with Theoretical Predictions - Set3**

No.		Failure Pressure ( $\times 10^{-3}$ N/mm <sup>2</sup> )				Ratio		
		Expt	FEM	BS	NN	$\frac{\text{Expt}}{\text{FEM}}$	$\frac{\text{Expt}}{\text{BS}}$	$\frac{\text{Expt}}{\text{NN}}$
1	Kheir (1975)	4.7	3.42	4.24	3.88	1.37	1.11	1.21
2		4.6	3.48	3.95	4.03	1.32	1.16	1.14
3		3.1	2.64	3.13	3.09	1.17	0.99	1
4		2.9	1.75	2.75	2	1.66	1.05	1.45
5		2.8	1.32	2.35	1.93	2.12	1.19	1.45
6		2.35	1.82	2.2	1.72	1.29	1.07	1.37
7		8.4	7.3	6.67	7.32	1.15	1.26	1.15
8		5.8	6.75	6.15	6.75	0.86	0.94	0.86
9		6.3	6.95	6.46	6.28	0.91	0.98	1
10		9.3	8.85	8.91	8.75	1.05	1.04	1.06
11		10	9.18	9.84	9.37	1.09	1.02	1.07
12	Ng (1996)	5.2	5.78	5.64	5.83	0.9	0.92	0.89
13		4.51	5.58	5.55	5.63	0.81	0.81	0.8
14		12.2	11.02	10.85	12.75	1.11	1.12	0.96
15		11.9	10.15	10.38	12.6	1.17	1.15	0.94

#### 6.7.4 'Set4' Panels (Two Vertical Edges Restrained and Top and Bottom Simply Supported)

The experimental results of SINHA *et al.* (1975), LAWRENCE (1983) and BAKER (1972) are considered in this type of panels. 'Set4' panels can be seen as carrying the highest load than panels of any other boundary conditions as both the vertical edges in this case are fully restrained. It can be seen from Table 6.20 that the finite element analysis, the BS and the trained net over-estimated the experimental results in most of the cases. It is very difficult to achieve complete fixity for panels at their vertical edges. It can be seen that SINHA *et al.* (1975) used return walls to achieve fixity of

the edges, whereas BAKER (1972) used steel bolts to hold the edges against any rotational movements and LAWRENCE (1983) built the panels within steel frames with additional ties.

**Table 6.20 Comparison of Experimental Results of the Failure Pressure with Theoretical Predictions - Set4**

No.		Failure Pressure ( $\times 10^{-3}$ N/mm <sup>2</sup> )					Ratio			
		Expt	FEM	BS	Aus	NN	$\frac{\text{Expt}}{\text{FEM}}$	$\frac{\text{Expt}}{\text{BS}}$	$\frac{\text{Expt}}{\text{Aus}}$	$\frac{\text{Expt}}{\text{NN}}$
1	Sinha (1973)	10.7	15	14.68	10.77	15.25	0.71	0.73	0.99	0.7
2		11.6	14.9	15.88	11.34	15.56	0.78	0.73	1.02	0.75
3		4.7	5.35	6.2	4.32	4.87	0.88	0.76	1.09	0.97
4		6	6.28	7.86	5.55	6.91	0.96	0.76	1.08	0.87
5		5.2	6.68	6.67	4.63	7.25	0.78	0.78	1.12	0.72
6		6.7	7.38	8.28	5.95	7.91	0.91	0.81	1.13	0.85
7	Lawre nce (1983)	20	18.05	19.35	13.92	19.26	1.11	1.03	1.44	1.04
8		6.7	7.85	8.74	6.13	6.78	0.85	0.77	1.09	0.99
9		6.4	10.02	10.12	7.46	7.95	0.64	0.63	0.86	0.81
10		4.7	8.85	9.4	7.12	3.05	0.53	0.5	0.66	1.54
11		5.5	5.85	6.16	4.48	4.99	0.94	0.89	1.23	1.1
12		3.9	5.12	6.92	5.33	3.43	0.76	0.56	0.73	1.14
13	Baker (1972)	21.57	28.08	27.5	19.99	28.15	0.77	0.78	1.08	0.77
14		9.81	14.78	15.49	10.74	14.54	0.66	0.63	0.91	0.67

It can be seen from Table 6.6 that the results based on the BS for Set4 panels are very close to that of the finite element analysis. The Australian code consistently underestimated the results by 70% (average). It is clear from Table 6.20 that the Australian code results were close to the experimental results, whereas the other methods overestimated the result. The reason for this can be the practical difficulty in achieving complete fixity at the vertical edges. It can be noticed from these results that the Australian code can be used in this type of panels, where similar difficulties are faced.



### 6.7.5 'Set6' Panels (Top and Bottom Simply Supported, One Vertical Edge Restrained and the Other Free)

The results that are studied for this type of panel are the work by SINHA *et al.* (1979) and BCRA (1979) and are given in Table 6.21. The fixity at one of the vertical edges was achieved by return walls in the former and by building the panels within steel channel section in the latter case. In this case also, the lack of achieving complete fixity can be a reason for any possible over-estimation of the results by the theoretical methods.

**Table 6.21 Comparison of Experimental Results of the Failure Pressure with Theoretical Predictions - Set6**

No.		Failure Pressure ( $\times 10^{-3}$ N/mm <sup>2</sup> )				Ratio		
		Expt	FEM	BS	NN	$\frac{\text{Expt}}{\text{FEM}}$	$\frac{\text{Expt}}{\text{BS}}$	$\frac{\text{Expt}}{\text{NN}}$
1	Sinha (1973)	7.45	9	4.67	9.09	0.83	1.6	0.82
2		10.2	12.3	6.08	11.68	0.83	1.68	0.87
3		5.89	5.55	5.49	5.46	1.06	1.07	1.08
4		1.37	1.32	1.79	1.14	1.04	0.77	1.2
5		2.55	1.62	2.35	1.4	1.57	1.09	1.82
6	Kheir (1975)	0.7	0.91	1.32	1.33	0.77	0.53	0.53
7		1	1.05	1.71	1.31	0.95	0.58	0.76
8		1.7	1.67	2.34	1.29	1.02	0.73	1.32
9		1.5	1.02	1.47	1.24	1.47	1.02	1.21
10		2.4	1.92	2.03	2.3	1.25	1.18	1.04
11		3.6	3.08	2.96	3.95	1.17	1.22	0.91
12		2.7	2.28	3.52	2.1	1.18	0.77	1.29
13		3.8	4.18	4.76	4.39	0.91	0.8	0.87
14		6	6.75	6.78	6.69	0.89	0.88	0.9

As can be seen from Table 6.21, even though the finite element method over-estimates the failure load, the variation is considerably less than that of 'Set4'. The above two cases (Set4 and Set6) can be compared in terms of the load shared in the two orthogonal directions. For a panel of aspect ratio 2.0, 75% of the total load is acting in the vertical direction for 'Set6' type panels, whereas only 50% is acting in

the vertical direction for a Set4 type panel. This forces the vertical moments and the vertical flexural strengths influencing the failure of the panels in the former more than in the later type.

A scatter in the theoretical predictions can be noticed in BCRA results. This could be due to assuming isotropic properties for the brickwork and the use of an average value for the flexural strengths in the two directions. The effect of the orthotropic stiffness ratio can be as high as 30% variation in the failure pressure as given in Table 6.4.

### 6.7.6 'Set8' Panels (Vertical Edges Restrained, Bottom Simply Supported and Top Free)

The work of LAWRENCE (1983) and WEST *et al.* (1978) are considered in this type of panel and the comparison of the theoretical and the experimental results are given in Table 6.22.

**Table 6.22 Comparison of Experimental Results of Failure Pressure with Theoretical Predictions - Set8**

No.		Failure Pressure ( $\times 10^{-3}$ N/mm <sup>2</sup> )					Ratio			
		Expt	FEM	BS	Aus	NN	$\frac{\text{Expt}}{\text{FEM}}$	$\frac{\text{Expt}}{\text{BS}}$	$\frac{\text{Expt}}{\text{Aus}}$	$\frac{\text{Expt}}{\text{NN}}$
1	Lawrence (1972)	14	16.6	13.93	10.34	16.79	0.84	1.01	1.35	0.83
2		3.9	4.6	4.98	2.63	5.68	0.85	0.78	1.48	0.69
3		3.5	3.55	4.16	1.82	4.72	0.99	0.84	1.92	0.74
4		2.5	2.75	3.14	1.52	4.36	0.91	0.8	1.64	0.57
5	BCRA West <i>et al.</i> 1978	1.78	2.35	2.33	1.36	2.38	0.76	0.76	1.31	0.75
6		2.35	3.18	3.13	1.97	3.33	0.74	0.75	1.19	0.71
7		3.42	4.88	4.51	3.06	5.35	0.7	0.76	1.12	0.64
8		1.81	2.1	2.1	1.23	2.44	0.86	0.86	1.47	0.74
9		2.26	2.95	2.82	1.77	3.13	0.77	0.8	1.28	0.72
10		3.35	4.58	4.06	2.75	4.59	0.73	0.83	1.22	0.73
11		1.54	1.68	1.62	0.95	1.84	0.92	0.95	1.62	0.84
12		1.94	2.2	2.17	1.37	2.42	0.88	0.89	1.42	0.8
13		2.97	3.42	3.13	2.13	3.7	0.87	0.95	1.39	0.8

As pointed out earlier, the degree of fixity provided for the vertical edges is important in this type of panels also as they are assumed to be fully restrained at both the vertical edges in the theoretical analysis. It can again be noticed that the finite element method, the BS and the trained net over-estimated the results and the Australian code under-estimated the results. None of the methods seem to give any close predictions. Even though the trained neural network is performing extremely well in the first test set, the same level of performance is not reached in the experimental results.

## **6.8 The Advantages of Trained Neural Network over the Finite Element Method**

It can be seen from the performance of the net that the trained neural networks give results very close to the finite element analysis. This section aims at explaining the reasons why the networks are trained to produce results close to the finite element analysis and the advantages of using the trained network. A computer analysis based on the finite element method consumes considerable amount of CPU memory and time for a single analysis. While doing the analysis, it was necessary to start the analysis with an assumed pressure close to the initial cracking load to avoid considerable increase in computer time and space. This can be done with a preliminary analysis or manual calculation of the cracking load. Apart from this, it is explained in Section 6.3 that the cracking and the failure does not occur together in a lot of panels. In such cases, the panels are to be analysed several times in order to obtain an average failure load. This can also cause confusion as a change in the number of mesh elements can cause variation in the failure pressure. This is mainly due to the convergence of the elements and the redistribution of the loading after the initial cracking. This can be best explained with an example as given below.

This section explains some of the difficulties experienced while the finite element analysis was undertaken to generate the training set. Consider a 'Set4' type of panel

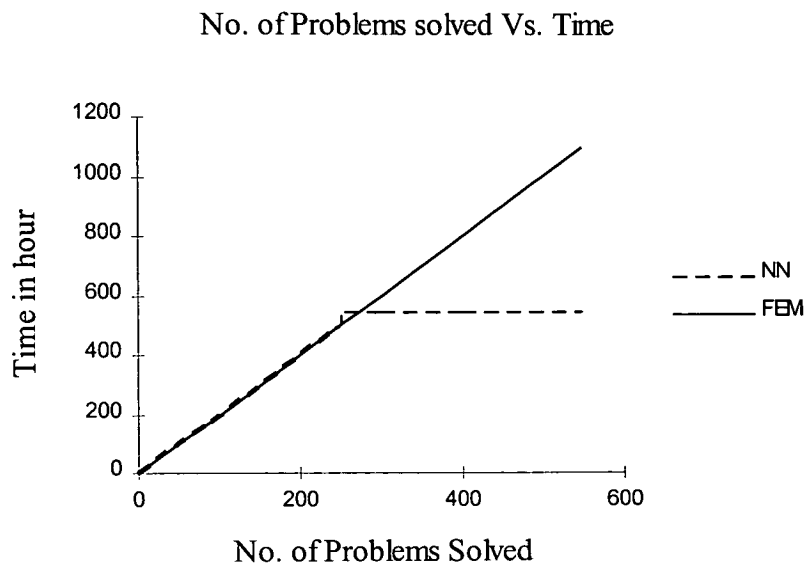
where the vertical edges are restrained and the top and bottom are simply supported. The panel had dimensions  $L \times H \times T$  as 3000x2000x110mm. The flexural strength of the panel was taken as 4.0 N/mm<sup>2</sup> in the horizontal direction and 1.0 N/mm<sup>2</sup> in the vertical direction with an orthotropic stiffness ratio of 1.4. ZIENKIEWICZ & TAYLOR (1991) have shown that the convergence of a finite element solution is obtained with a mesh size of 8x8 by the use of rectangular elements for a plate with simply supported or restrained boundary conditions. In the current analysis, a linear elastic analysis was carried out until the specimen cracked in one direction. A smeared cracking model was adopted for the material after cracking up to the failure, where the stiffness of the cracked element was reduced to zero and the load carried by these elements was distributed to the neighbouring uncracked elements. Hence, the failure and the crack pattern followed a different pattern depending on the number of elements assumed in the mesh. The panel was analysed 6 times by varying the initial load and the number of elements. The analysis was done on a personal computer, Pentium machine 166Mhz, RAM 16 Megabytes. Each analysis took nearly an average of 45 minutes and the output file was as big as 20Megs. Table 6.23 shows the failure load obtained for each analysis.

The variation in the finite element results by changing the mesh size and the initial load can be seen from the above table. At this stage, it is difficult to take any of the above values in spite of spending 5 hours of computational time. However, a closer examination of the results shows that in the first two attempts, where a coarse mesh is used in the analysis the results are far away from the rest. When a finer mesh is used, the variation is less than 4%. The average of these 4 values was only slightly (2-3%) varying from the lowest/highest value and was taken as the failure pressure in this particular case. It has to be pointed out that in the case of masonry panels, where a large variation in the properties of the panels can be expected, the above kind of variation may be accepted. The results were further modified by comparing the bending moment coefficients of panels of similar boundary conditions, aspect ratio and strength and stiffness orthotropies. Hence, the finite element analysis can be very time consuming in analysing panels that exhibit distinct cracking and failure.

**Table 6.23. Variation in Finite Element Results by Changing the Initial Load and the Mesh Elements**

	Failure Load ( $\times 10^{-3}$ N/mm <sup>2</sup> )
Number of Mesh Elements: 96 Initial Load : 12.0	22.6
Number of Mesh Elements: 96 Initial Load : 12.1	22.5
Number of Mesh Elements: 126 Initial Load : 12.0	26.7
Number of Mesh Elements: 126 Initial Load : 12.1	26.6
Number of Mesh Elements: 140 Initial Load : 12.0	25.6
Number of Mesh Elements: 140 Initial Load : 12.1	25.5

A trained neural network can produce the results for several such panels over a fraction of the time. A simple data file can be generated in 'Notepad' to present the patterns to the trained net, which gives the output immediately. The use of trained neural networks, thus, helps to achieve tremendous amount of computational efficiency. This can be demonstrated with the help of Figure 6.26 given below. It can be seen that even though there may be no apparent saving in computational time until the net is trained, there will be a considerable saving in time to obtain the failure pressure of a panel for the design.



**FIG. 6.26 Comparison of the Time Required for a Finite Element Analysis and To Develop a Neural Net Application**

### 6.9 The Hybrid System (ANNs and CBR)

The working of the hybrid system has been explained in detail in Chapter 5. However, a brief description along with a demonstration using an example problem is given in this section.

When a panel has to be analysed, CBR Express is approached as an initial step. CBR Express makes a search in the case base using the information provided by the user and comes up with 5 matching cases to the user. The matching cases can be of varying degrees of closeness and the best matching case is generally adopted for the present case. However, there are situations where the best matching case suggests the use of the next matching case. This happens in situations where it is difficult to arrive at a reliable method based on the results of that case. The present panel can be analysed by the method obtained after studying the matching cases from the case base. When the Australian code of practice or the BS is recommended, the analysis can be done by taking the coefficients given in the respective codes. Whenever the

finite element analysis is to be used, the analysis can be carried out using the trained neural networks. This can be explained with an example problem as below:

Support Conditions - Three Sides Simply Supported Panel (Type U), simply supported at three sides and free at the top

Length,  $L$  = 1.59 m

Height,  $H$  = 2.38 m

Thickness,  $t$  = 110 mm

$F_x$  = 3.85 N/mm<sup>2</sup>;  $F_y$  = 1.1 N/mm<sup>2</sup>

$E_x$  = 15500 N/mm<sup>2</sup>;  $E_y$  = 10698 N/mm<sup>2</sup>

Experimental Failure Pressure,  $w$  = 27.8 x 10<sup>-3</sup> N/mm<sup>2</sup>

The above information were fed to CBR Express as shown in Figure 6.27.

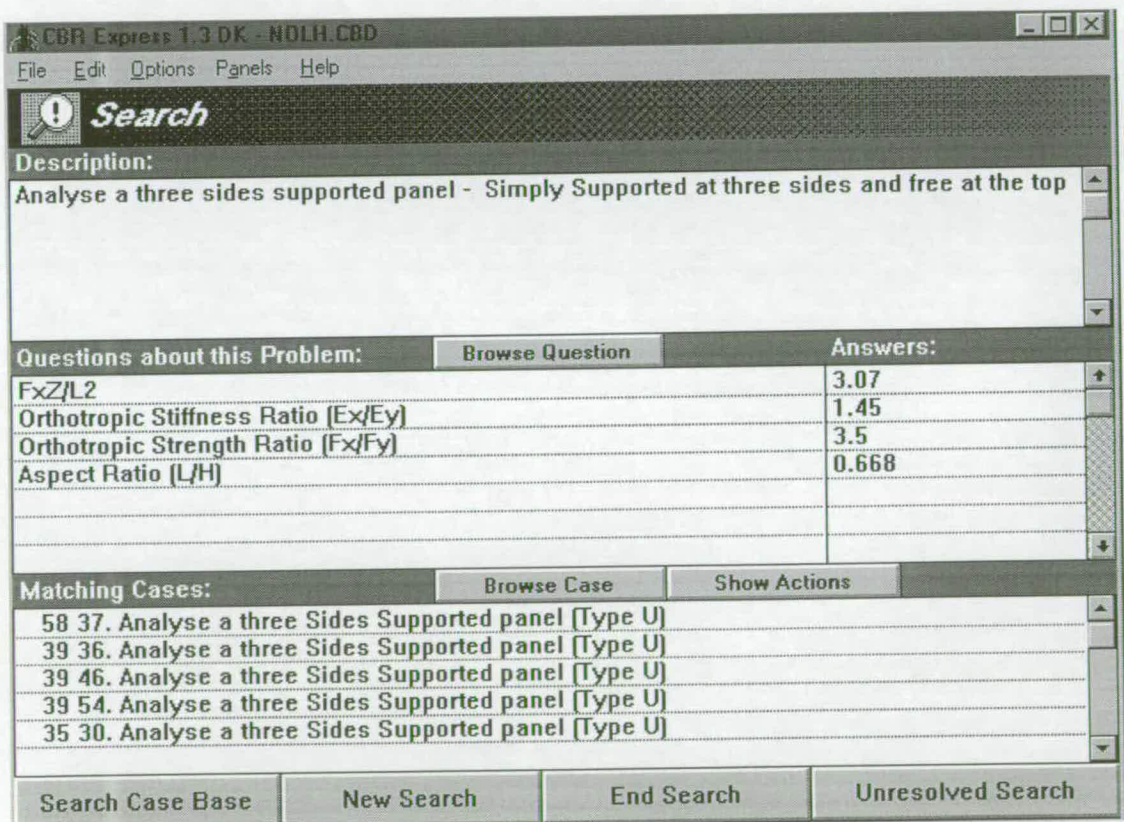


FIG. 6.27 The CBR Express Output Panel with the Search Results <sup>5</sup>

<sup>5</sup> The first number seen within the "Matching Cases" window indicates the degree of closeness of the present case with the selected case. The second number is merely an identification number of the case that is stored within the case base.

As a result of the in-built search technique, CBR Express comes up with several matching cases from the case library with varying degrees of closeness to the present input. Each case is associated with a match score, a number between 0 and 100, that shows how closely that case matched the description. As can be seen in Figure 6.27, the best matching case with the matching score is listed at the top and is recommended for the present analysis.

Each of the matching cases listed in the box can be looked in detail. The recommended actions for each of the matching case can be studied by highlighting the specific case and then clicking on the icon 'Show Actions' (Figure 6.27) that can be seen against the 'matching cases'. This will open another window which displays the recommended action for the case with any description given in the case base (Figure 6.28).

Recommended Actions:		Browse Action	Show Cases
58 FEM may be used			▲
39 FEM may be used			
39 FEM may be used			
39 BS, Australian Code of Practice or FEM may be used			
35 FEM or BS Code or Australian Code can be used			▼
Search Case Base	New Search	End Search	Unresolved Search

**FIG. 6.28 The Output Panel - Recommended Actions for the Matching Cases**

The user can browse the matching cases and examine the comparison of the experimental results with the theoretical predictions. This is done by highlighting the case and then clicking the icon 'Browse case' seen next to the 'matching cases' (Figure 6.27). Generally, the closest case is recommended and the solution can be adopted for the current problem. However, the user is given an option to make his/her own judgement and see how each case contribute to the present situation. Figure 6.29 shows this comparison for the best matching case.



Browsing Action:		Dismiss Browse	Show Cases
<b>Failure Pressure:</b>			
Experimental : 23.5 KN/m <sup>2</sup>			
FEM	: 24.25 KN/m <sup>2</sup>	"Overestimating by 3%"	
BS Code	: 27.64 KN/m <sup>2</sup>	"Overestimating by 18%"	
Aus Code	: 28.79 KN/m <sup>2</sup>	"Overestimating by 23%"	
NN	: 24.41 KN/m <sup>2</sup>	"Overestimating by 4%"	
Search Case Base	New Search	End Search	Unresolved Search

**FIG. 6.29 Comparison of the Experimental Results with the Theoretical Predictions for the Best Matching Case.**

For the present problem, the recommended method for the best matching case can be adopted for further analysis. The theoretical predictions can also be done using the other methods and the results can be compared to ascertain the reliability of this approach.

As can be seen from the Figures 6.28 & 6.29, the finite element method is highly recommended for the current analysis. However, the finite element analysis is rather complex and time consuming. As explained in the previous section, the trained neural networks can be used instead of the time consuming finite element analysis. The failure load obtained by various theoretical methods for the above panel is given in Table 6.24. It is evident from the table that the method recommended by CBR produced results that are closer to the experimental values.

**TABLE 6.24 Comparison of the Experimental Results with Theoretical Predictions**

Method of Analysis	Predicted Failure Pressure $\times 10^{-3}$ (N/mm <sup>2</sup> )	Expt. Failure load $\times 10^{-3}$ (N/mm <sup>2</sup> )	$\frac{\text{Expt. Load}}{\text{Theo. Prediction}}$
Finite Element Analysis	26.65		1.04
Trained Neural Network	26.85	27.8	1.04
BS	30.41		0.91
Australian Code of Practice	31.69		0.88

The case that is considered in this example problem has its boundary conditions as “Three Sides Simply Supported and Top Free”. It can be seen from Table 6.7 that the relative importance of the four variables used to define the problem is different. For example,  $\frac{F_x Z}{L^2}$  contributes 50% towards the failure pressure, whereas,  $\frac{L}{H}$ ,  $\frac{F_x}{F_y}$  and  $\frac{E_x}{E_y}$  are only 18%, 20% and 11% important in arriving at the failure pressure. As  $\frac{E_x}{E_y}$  is least important in this case, any variation in its value should not affect the method recommended by the case base. As described in Section 6.7, there are several cases where the value of  $\frac{E_x}{E_y}$  is not mentioned by the researchers. In order to demonstrate the importance of incorporating the relative importance of the variables in the CBR system, another case base was generated with the same cases, but without any connection weights. The same problem was re-analysed by both the case bases by reducing the  $\frac{E_x}{E_y}$  to a value of 1.0 instead of the actual value of 1.45. The results of the recommended methods by both the case bases can be seen in Figures 6.30 & 6.31.

Questions about this Problem:		Browse Question	Answers:
$F_x Z / L^2$			3.07
Orthotropic Stiffness Ratio ( $E_x / E_y$ )			1.0
Orthotropic Strength Ratio ( $F_x / F_y$ )			3.5
Aspect Ratio ( $L / H$ )			0.668
Recommended Actions:		Browse Action	Show Cases
50 FEM may be used			
49 BS, Australian Code of Practice or FEM may be used			
47 FEM may be used			
44 BS Code of Practice may be used			
42 FEM may be used			
Search Case Base	New Search	End Search	Unresolved Search

FIG. 6.30 The Output Panel of a Case Base Search with Relative Importance of Variables



*Chapter Six - Implementation of the Hybrid System for Predicting the Failure Pressure of Masonry Panels Subjected to Bi-axial Bending*  
of laterally loaded masonry panels as an alternative to the time consuming finite element analysis.

# CHAPTER 7

## CONCLUSIONS

### 7.1 Summary and Conclusions

The experimental investigation carried out on mortar cross beams enabled the study of the behaviour of the isotropic material under bi-axial, out-of-plane bending. The failure criterion developed from these test results was incorporated in a finite element plate-bending program and was verified by the tests done on panels subjected to bi-axial bending. The tests on cross beams also helped to compare the behaviour of the isotropic and the orthotropic materials under bi-axial bending.

A hybrid system that combined the capabilities of both Artificial Neural Networks (ANNs) and Case-Based Reasoning (CBR) was developed to aid the designer in quickly arriving at the failure pressure of a laterally loaded masonry panel.

The following conclusions can be drawn on the basis of the present work.

1. Cross beam and panel tests showed that mortar specimens failed in a sudden brittle manner. The load distribution in the two orthogonal directions was according to the relative stiffness.
2. When brickwork was subjected to bi-axial bending, upon cracking the specimen in the weaker direction, the load that was carried by that direction was shed to the stronger un-cracked direction. No such 'load shedding' was observed in mortar specimens at the time of cracking.

3. The finite element plate bending program, incorporating the failure criterion for the isotropic material was able to predict the failure pressure of panels close to the experimental results.
4. Neural networks were successfully trained to predict the failure pressure of panels subjected to bi-axial bending by generating the data from the finite element method incorporating the failure criterion for the orthotropic material. The trained net is able to predict the failure pressure in a fraction of the time required by the finite element program.
5. The connection weights of the trained network were used to find out the relative importance of the input variables in the failure pressure of the panel. The input variables included the ratio  $\frac{F_x Z}{L^2}$ , the aspect ratio  $\frac{L}{H}$ , the orthotropic strength ratio  $\frac{F_x}{F_y}$  and the orthotropic stiffness ratio  $\frac{E_x}{E_y}$  and can be seen that  $\frac{F_x Z}{L^2}$  is the most important of all in finding out the failure pressure.
6. A case base of the existing experimental results and the theoretical predictions of the failure pressure was generated and was used in the hybrid system to obtain the most reliable method to find out the failure pressure of a panel of given properties.
7. The hybrid system developed in this thesis combined case-based reasoning and artificial neural networks. The system acts as a relatively fast design tool to predict the failure pressure of cladding panels (isotropic or orthotropic) subjected to bi-axial bending. This system can be used in the design of panels of 8 different boundary conditions, which are commonly used in practice.
8. The relative importance of the variables that affect the failure pressure of the panel were used as match weights to improve the case retrieval mechanism within CBR. This also provided a better integration between CBR and ANNs as the connection

weights in the trained net were used in calculating the relative importance of these variables.

9. The moment coefficients were developed on the basis of the finite element analysis with the failure criterion for masonry panels of the 8 different types of commonly found boundary conditions.

## **7.2 Suggestions for Further Research**

The hybrid system described and implemented in this research is a very useful technique providing reliable and accurate values of the failure pressure of a masonry panel under bi-axial bending. However, the present study was focused only on laterally loaded panels with little or no axial loading. The implementation of this system illustrates that it could be extended to other similar types of problems as well. It can also be noticed that neural networks can be combined with other artificial intelligence techniques to improve the efficiency of the system and provide a practical aid to designers. The following areas of research could be explored in light of the success of this hybrid system.

- Symbolic learning systems could be employed for problems of similar nature so as to infer some knowledge about the input and output variables from practical results.
- The retrieval mechanism of case-based reasoning can be improved by incorporating an expected value of the failure pressure of the panel. This can be done by carrying out a preliminary analysis using the trained neural network and approaching CBR with an initial value.

## REFERENCES

ABU-MOSTAFA Y S, (1990), "Learning from Hints in Neural Networks", *Journal of Complexity*, 6: 192-198.

AL-MASHOUQ K A & REED I S, (1991), "Including Hints in Training Neural Nets", *Neural Computing*, 3: 418-427.

ANDERSON C, (1976), "Lateral Loading Tests on Concrete Block Walls", *The Structural Engineer*, 54(7): 239-246.

ANDERSON C, (1984), "Arching Action in Transverse Loaded Masonry Wall Panels", *The Structural Engineer*, 62B(1): 12-23.

ANDERSON C, (1987), "Lateral Strength from Full Sized Tests Related to the Flexural Properties of Masonry", *Masonry International*, 1(2): 51-55.

ANDERSON J A, (1990), "Data Representation in Neural Networks", *AI Expert*, June: 30-37.

ANDERSON C & HELD L, (1982), "The Stability of Cracked Walls to Lateral Loading", *Proceedings of the 6<sup>th</sup> International Brick Masonry Conference, Rome*, May: 402-411.

ARCISZEWSKI T & ZIARKO W, (1991), "Structural Optimization: Case-Based Approach", *Journal of Computing in civil Engineering, ASCE*, 5(2): 159-173.

BAILEY D & THOMSON D, (1990a), "How to Develop Neural Network Applications", *AI Expert*, June: 38-47.

BAILEY D & THOMSON D, (1990b), "Developing Neural Network Applications", *AI Expert*, September: 34-41.

BAKER L R, (1972), "Brickwork Panels Subjected to Face Wind Loads", *M. Sc. Thesis, University of Melbourne*, June.

BAKER L R, (1973a), "Structural Action of Brickwork Panels Subjected to Wind Loads", *Journal of Australian Ceramic Society*, 9(1): 8-13

BAKER L R, (1973b), "Flexural Strength of Brickwork Panels", *Proceedings of the III International Brick Masonry Conference*, 378-383.

BAKER L R, (1977), "The Lateral Strength of Brickwork - An Overview", *Proceedings of the 6<sup>th</sup> International Symposium on Load Bearing Brickwork*, 169-187.



BAKER L R, (1979), "A Failure Criterion for Brickwork in Biaxial Bending", Proceedings of the V<sup>th</sup> International Brick Masonry Conference, Washington, October: 71-78.

BAKER L R, (1981), "Flexural Action of Masonry Structures Under Lateral Load", Ph.D. Thesis, Deakin University, July.

BAKER L R, (1982a), "A Principal Stress Failure Criterion for Brickwork Panels in Biaxial Bending", Proc. of the 6<sup>th</sup> Int. Brick Masonry Conference, Rome, May: 121-130.

BAKER L R, (1982b), "An Elastic Principal Stress Theory for Brickwork Panels in Flexure", Proc. of the 6<sup>th</sup> Int. Brick Masonry Conference, Rome, May: 522-537

BAKER L R, GAIRNS D A, LAWRENCE S J & SCRIVENER J C, (1985), "Flexural Behaviour of Masonry Panels- A State of The Art", Proceedings of the 7<sup>th</sup> International Brick Masonry Conference, Melbourne, February: 27-55.

Brickwork in Buildings, (1969), "CSAA Brickwork Code AS CA47-1969", Standards Association of Australia, Sydney.

BRINCKER R, (1985), "Yield line Theory and Material Properties of Laterally Loaded Masonry Walls", Masonry International, No.1: 8-17.

British Standards Institution, (1986), "Code of Practice for Structural Use of Masonry - Part 1: Un-reinforced Masonry", BS 5628: Part 1, London, 39 pages.

BROWN R S & ELLING R E, (1979), "Lateral Load Distribution in Cavity Walls", Proc. of the V<sup>th</sup> Int. Brick Masonry Conference, Washington, October: 351-359.

CANDY C C E, (1988), "The Energy Line Method for Masonry Panels under Lateral Loading", Proceedings of the 8<sup>th</sup> International Brick and Block Masonry Conference, Dublin, September: 1159-1170.

CARPENTER W C, & BARTHELEMY J F, (1994), "Common Misconceptions about Neural Networks As Approximators", Journal of Computing in Civil Engineering, 8(2): 345-358.

CAUDILL M, (1991a), "Neural Network Training Tips and Techniques", AI Expert, January: 56-61.

CAUDILL M, (1991b), "Evolutionary Neural Networks", AI Expert, March: 28-33.

CAUDILL M, (1992), "The View from Now", AI Expert, June: 24-31.

CBR Express/ Windows 1.3. (1990). Inference Corporation, California.

CHAN L W & FALLSIDE F, (1987), "An adaptive training algorithm for back propagation networks", *Computer, Speech and Language*, 2: 205-218.

CHANDRAKEERTHY S R De S, (1984), "A Design Chart for Non-load bearing Masonry Wall Panels under Wind Loads", *Masonry International*, No.3: 17-22.

CHAO L & SKIBNIEWSKI M J, (1994), "Estimating Construction Productivity: Neural-Network-Based Approach", *Journal of Computing in Civil Engineering*, 8(2): 234-251.

CHEN W F & SALEEB A F, (1982), "Constitutive Equations for Engineering Materials", John Wiley & Sons, New York, Vol.1.

CHEN H M, TSAI K H, QI G N, YANG J C S & AMINI F, (1995), "Neural Network for Structural Control", *Journal of Computing in Civil Engineering*, 9(2): 168-175.

CHEN R & MARS P, (1990), "Step-size Variation Methods for Accelerating the Back-propagation Algorithm", *IJCNN-90-WASH-DC*.

CHESTER D L, (1990), "Why Two Hidden Layers are Better than One", *Proceedings of the International Joint Conference on Neural Networks*, Neural Network Society, Washington DC, I265-I268.

CHONG V L, MAY I M, SOUTHCOMBE C & MA S Y A, (1991), "An Investigation of Laterally Loaded Masonry Panels Using Non-Linear Finite Element analysis", *Proceedings of the International Symposium on Computer Methods in Structural Masonry*, Swansea, April: 49-63.

COYNE R D & POSTMUS A G, (1990), "Spatial Application of Neural Networks in Computer Aided Design", *Journal of AI in Engineering*, 5(1): 9-22.

COYNE R D, ROSEMAN M A, RADFORD A D, BALACHANDRAN M & GERO J S, (1990), "Knowledge-Based Design Systems", Addison-Wesley Publishing Company, Wokingham, England.

CROOKS T, (1992), "Care and Feeding of Neural Networks", *AI Expert*, July: 36-41.

DUARTE R B, (1993), "A Study of the Lateral Strength of Brickwork Panels with openings", Ph.D. Thesis, University of Edinburgh, February.

ELKORDY M F *et al.*, (1993), "Neural Networks Trained by Analytically Simulated Damage States", *Journal of Computing in Civil Engineering*, ASCE, 7(2): 130-145.

ESSAWY A S, DRYSDALE R G & MIRZA F A, (1985), "Non-linear Macroscopic Finite Element Model for Masonry Walls", Proceedings of the New Analysis Techniques for Structural Masonry, ASCE Structures Congress, 19-45.

ESSAWY A S & DRYSDALE R G, (1987), "Evaluation of Available Design Methods for Masonry Walls Subjected to Out-of-Plane bending", Proceedings of the 4<sup>th</sup> North American Masonry Conference, Los Angeles, August: 32-1-32-13.

FALHMANN S E, (1989), "Faster Learning Variations on Back Propagation: An Empirical Study", Proceedings of the 1988 Connectionist Models Summer School.

FENNER R T, (1989), "Mechanics of Solids", Blackwell Scientific, London.

FLOOD I & KARTAM N, (1994a), "Neural Network in Civil Engg.: I : Principles and Understanding", Journal of Computing in Civil Engineering, 8(2): 131-148.

FLOOD I & KARTAM N, (1994b), "Neural Networks in Civil Engineering. II : Systems and application", Journal of Computing in Civil Engineering, 8(2): 149-162.

FRIED A, ANDERSON C & SMITH D, (1988), "Predicting the Transverse Lateral Strength of Masonry Walls", Proceedings of the 8<sup>th</sup> International Brick and Block Masonry Conference, Dublin, September: 1171-1183.

GAGARIN N, FLOOD I & ALBRECHT P, (1994), "Computing Truck Attributes with Artificial Neural Networks", Journal of Computing in Civil Engineering, 8(2): 179-200.

GAIRNS D A & SCRIVENER J S, (1984), "Lateral Load Behaviour of Concrete Masonry Panels Part 1- Flexural Properties of Concrete Masonry", Masonry International, No.3: 23-32.

GAIRNS D A & SCRIVENER J S, (1985), "Lateral Load Behaviour of Concrete Masonry Panels Part 2- Panel Performance", Masonry International, No.4: 6-14.

GARSON G D, (1991), "Interpreting Neural Network Connection Weights", AI Expert, April: 47-51.

GHABOUSSI J, GARRETT J H & WU X, (1991), "Knowledge Based Modeling of Material Behavior with Neural Networks", Journal of Engineering Mechanics, ASCE, 117(1): 132-153.

GOH A T C, (1994), "Some Civil Engineering Applications of Neural Networks", Proceedings of the Institution of Civil Engineers, Structures & Buildings, 104: 463-469.

GOH A T C, (1995a), "Evaluation of Seismic Liquefaction Using Neural Networks", Developments in Neural Network and Evolutionary Computing for Civil and Structural Engineering By B H V Topping, Civil-Comp Press, Edinburgh, 121-125.

GOH A T C, (1995b), "Back-Propagation Neural Networks for Modeling Complex Systems", Journal of Artificial Intelligence in Design, 9: 143-151.

GOH A T C , WONG K S & BROMS B B, (1995), "Multivariate Modelling of FEM Data Using Neural Networks", Developments in Neural Network and Evolutionary Computing for Civil and Structural Engineering By B H V Topping, Civil-Comp Press, Edinburgh, 59-64.

GOLDING J & MORTON J, (1991), "Practical Design of Laterally Loaded Masonry Panels", The Structural Engineer, 69(4): 55-65.

GROSS J G, (1965), "Introduction to the Contemporary Bearing Walls", Proceedings of National Brick & Tile Bearing Conference, Sponsored by Structural Clay Products Institute, N W, Washington.

GUNARATNAM D J & GERO J S, (1991), "High Level Relationships for Structural design: The effect of representation in Learning", ANZAScA Conference Proceedings

GUNARATNAM D J & GERO J S, (1993), "Neural Network Learning in Structural Engineering Applications", Journal of Computing in Civil & Building Engineering, 1448-1455.

GUNARATNAM D J & J S GERO, (1994), "Effect of Representation on the Performance of Neural Networks in Structural Engineering Applications", Microcomputers in Civil Engineering, 9: 97-108.

GUYON I, (1991), "Application of Neural Networks to Character Recognition", International Journal of Pattern Recognition and Artificial Recognition, 5: 353-382.

HAJELA P & BERKE L, (1991a), "Neurobiological Computational Models in Structural Analysis and Design", Computers & Structures, 41(4): 657-667.

HAJELA P & BERKE L, (1991b), "Neural Network Based Decomposition in Optimal Structural Synthesis", Computing Systems in Engineering, 0 (0): 1-9.

HAJELA P & BERKE L, (1992), "Neural Networks in Structural Analysis and Design: An Overview", Computing Systems in Engineering, 3(1): 525-538.

HAMMERSTROM D, (1993), "Working with Neural Networks", IEEE Spectrum, 46-53.

HASELTINE B A & HODGKINSON H R, (1973), " Wind Effects Upon Brick Panel Walls - Design Information", Proceedings of the III International Brick Masonry Conference, 399-406.

HASELTINE B A, WEST H W H & TUTT J N, (1977), " Design of Walls to Resist Lateral Loads Part II", The Structural Engineer, 55(10): 422-430.

HASELTINE B A & TUTT J N, (1986), "Implications of Research on Design Recommendations", The Structural Engineer, 64A(11): 341-350.

HAYKIN S, (1994), "Neural Networks - A Comprehensive Foundation", Macmillan College Publishing Company.

HEBB D O, (1949), "The Organization of Behavior", John Wiley & Sons, New York.

HECHT-NIELSEN R, (1988), "Neurocomputing: picking the human brain", IEEE Spectrum, 25(3): 36-41.

HEGAZY T, FAZIO P & MOSELHI O, (1994), "Developing Practical Neural Network Application Using Back-Propagation", Microcomputers in Civil Engineering, 9: 145-159.

HENDRY A W, (1973), "The Lateral Strength of Un-reinforced Brickwork", The Structural Engineer, 51(2): 43-51.

HERTZ J, KROGH A & PALMER R G, (1991), "Introduction to the Theory of Neural Computation", Addison-Wesley.

HORNIK K, (1991), "Approximation Capabilities of Multilayer Feedforward Networks", Neural Networks, 4: 251-257.

HUA K & FALTINGS B, (1993), "Exploring Case-Based Building Design - CADRE", AIEDAM, 7(2): 135-143.

HUNG S L & ADELI H, (1994), "Object Oriented Back-Propagation and Its Application to Structural Design", Neurocomputing, 6: 45-55.

HUSH D F & HORNE B G, (1993), "Progress in Supervised Neural Networks", IEEE Signal Processing Magazine, 8-39.

JACOBS R A, (1988), "Increased Rates of Convergence through Learning Rate Adaptation", Neural Networks, 1(4).

JADID M N & FAIRBAIRN D R, (1994), "The Application of Neural Network Techniques to Structural Analysis by Implementing an Adaptive Finite Element

- Mesh Generation”, *Artificial Intelligence for Design, Analysis and Manufacturing*, 8, 177-191.
- JENKINS W M, (1995), “Neural Network Based Approximations for Structural Analysis”, *Developments in Neural Network and Evolutionary Computing for Civil and Structural Engineering* By B H V Topping, Civil-Comp Press, Edinburgh, 25-35
- JOHANSEN K, (1972), “Yield-line Formulae for Slabs”, *Cement & Concrete Association*, London.
- KARUNANITHI N, GRENNEY W J, WHITLEY D & BOVEE K, (1994), “Neural Networks for River Flow Prediction”, *Journal of Computing in Civil Engineering*, 8(2): 201-220.
- KEMPKA A A, (1994a), “Activating Neural Networks Part I”, *AI Expert* June: 33-37.
- KEMPKA A A, (1994b), “Activating Neural Networks Part II”, *AI Expert*, August: 42-49.
- KHEIR A M A, (1975), “Brickwork Panels under Lateral Loading”, M. Phill. Thesis, University of Edinburgh.
- KNAUS R, (1991), “Putting Knowledge into Nets”, *AI Expert*, September: 19-25.
- KUMAR B & RAPHAEL B, (1997), “Reconstructive Memory in Case-Based Design”, *Journal of Artificial Intelligence in Engineering*, 11, 245-258.
- KUPFER H, HILSDORF H K & RUSCH H (1969), “Behaviour of Concrete Under Biaxial Stresses”, *ACI Journal*, 656-666.
- LAWRENCE J, (1991), “Data Preparation for a Neural Network”, *AI Expert*, November: 34-41.
- LAWRENCE S J, (1979), “Full Scale Tests of Brickwork Panels Under Simulated Wind Loading”, *Proc. of V<sup>th</sup> Int. Brick Masonry Conference*, Washington, October, 419-423.
- LAWRENCE S J, (1983), “Behaviour of Brick Masonry Walls Under Lateral Loading”, Ph.D. Thesis, University of South Wales, November.
- LAWRENCE S J, (1991), “Stochastic Analysis of Masonry Structures”, *Proceedings of the International Symposium on Computer Methods in Structural Masonry*, Swansea, April: 104-113.

LAWRENCE S J & CAO H T, (1988), "Cracking of Non Load Bearing Walls Under Lateral Forces", Proceedings of the 8<sup>th</sup> International Brick and Block Masonry Conference, Dublin, September, 1184-1194.

LAWRENCE S J & Lu J P, (1991a), "Cracking of Brickwork Walls with Lateral Loading", Proc. of the Asia Pacific Conference on Masonry, Singapore March: 109-113.

LAWRENCE S J & LU J P, (1991b), "An Elastic Analysis of Laterally Loaded Masonry Walls with Openings", Proceedings of the International Symposium on Computer Methods in Structural Masonry, Swansea, April: 39-48.

LIPPMANN R P, (1987), "An Introduction to Computing with Neural Nets". IEEE Acoustics Speech and Signal Processing, 4(2): 4-22.

LEE Y S Oh & KIM M, (1991), "The Effect of Initial Weights on Premature Saturation in Back Propagation Learning", Proceedings of the International Joint Conference on Neural Networks, Vol.1, 765-771, Seattle, WA.

LOU K & PEREZ R A, (1996), "A New System Identification Technique Using Kalman Filtering and Multilayer Neural Networks", Journal of AI in Engineering, 10: 1-8.

LOVERGROVE R, (1985), "The Effect of Wall Dimensions upon the Ultimate Lateral Load of Single Leaf Walls", Masonry International, No.4: 15-21.

MANN W & TONN V, (1988), "The Load Bearing Behaviour of Biaxially Spanned Masonry Walls Subjected Simultaneously to Horizontal and Vertical Loading", Proceedings of the 8<sup>th</sup> International Brick and Block Masonry Conference, Dublin, September: 1195-1204.

MA S Y A & MAY I M, (1986), "A Complete Biaxial Stress Failure Criterion for Brick Masonry", Proceedings of the 1st International Masonry Conference, 115-117.

MAHER M L & ZHANG D M, (1991), "CADSYN: Using Case and Decomposition Knowledge for Design Synthesis", Proceedings of Artificial Intelligence in Design '91, Butterworth-Heinemann: Oxford, 137-150.

MAHER M L & ZHANG D M, (1993), "CADSYN: A Case-Based Design Process Model", AIEDAM, 7(2):97-110.

MAY I M & TELLETT J, (1986), "Non-linear Finite Element Analysis of Reinforced and Unreinforced Brickwork", Proceedings of British Masonry Society 1, 96-99.

- MAY I M & MA S Y A, (1986), "Design of Masonry Panels Under Lateral Loading", Proceedings of the 1st International Masonry Conference, 118-120.
- McCULLOCH W S & PITTS W, (1943), "A Logical Calculus of the Ideas Imminent in Nervous Activity", Bulletin of Mathematical Biophysics, 5: 115-133.
- MIDDLETON J, PANDE G N, LIANG J X & KRALJ B, (1991), "Some Recent Advances in Computer Methods in Structural Masonry", Proceedings of Computer Methods in Structural Masonry, Swansea, April: 1-21.
- MINSKY M & PAPERT S, (1969), "Perceptrons: An Introduction to Computational Geometry", MIT Press.
- MUKHERJEE A & DESHPANDE J M, (1995), "Application of Artificial Neural Networks in Structural Design Expert Systems", Computers & Structures, 54(3): 367-375.
- MUKHERJEE A & DESHPANDE J M, (1995), "Modelling Initial Design Process Using Artificial Neural Networks", Journal of Computing in Civil Engineering, 9(3): 194-200.
- MURRAY D Y, (1994), "Tuning Neural Networks with Genetic Algorithm", AI Expert, June: 27-31.
- MURTAZA M B & FISHER D J, (1994), "Neuromodex - Neural Network System for Modular Construction Decision Making", Journal of Computing in Civil Engineering, 8(2): 221 - 233.
- NG C L, (1996), "Experimental and Theoretical Investigation of the Behaviour of Brickwork Cladding Panel Subjected to Lateral Loading", Ph. D. Thesis, University of Edinburgh, August.
- PAGE A W, (1980), "A Biaxial Failure Criterion for Brick Masonry in the Tension - Tension Range", International Journal of Masonry Construction, 1(1): 26-29.
- PANDE G N, LIANG J X & MIDDLETON J, (1989), "Equivalent Elastic Moduli for Brick Masonry", Computers and Structures, 8: 243-265.
- PANDE G N, MIDDLETON J, LEE J S & KRALJ B, (1994), "Numeric Simulation of Cracking and Collapse of Masonry Panels Subject to Lateral Loading", Proceedings of the 10<sup>th</sup> International Brick/Block Masonry Conference, Canada, July: 107-116.
- PAO Y H, (1989), "Adaptive Pattern Recognition and Neural Networks", Addison - Wesley Reading, Mass.



- PAPA E & NAPPI A, (1993), "A Numerical Approach for the Analysis of Masonry Structures", *Masonry International*, 7(1): 18-24.
- PRESELY R K & HAGGARD R L, (1994), "A Fixed Point Implementation of the BackPropagation Learning Algorithm", *IEEE SouthEast Con.*, Miami, 136-138.
- REGAN P E & YU C W, (1973), "Limit State Design of Structural Concrete", Chatto & Windus, London.
- REZGUI A & TEPEDELENLIOGLU N, (1990), "The Effect of the slope of the Activation Function on the BackPropagation Algorithm", *Proceedings of the International Joint Conference on Neural Networks*, Neural Network Society, Washington DC, I707-I710.
- RIGLER A K, IRVINEJ M & VOGL T P, (1991), "Rescaling of Variables in BackPropagation Learning", *Neural Networks*, 4: 225-229.
- ROGERS J L, (1994), "Simulating structural Analysis with Neural Network", *Journal of Computing in Civil Engineering*, 8(2): 252 -265.
- ROSENBLATT R, (1959), "Principles of Neurodynamics", Spartan Books, New York.
- ROTTER J M, (1988), "Finite Element Program", Civil Engineering Dept., University of Edinburgh.
- ROY S & SHYNK J J, (1990), "Analysis of the Momentum LMS Algorithm", *IEEE Transactions on Acoustics, Speech and Signal Processing*, 38(12): 2088-2098.
- RUMELHART D E, McCLELLAND J L & The PDP RESEARCH GROUP (1986), "Parallel Distributed Processing - Explorations in the Cognition, Vol. 1: Foundations", MIT Press, London.
- SAMAD T, (1990), "BackPropagation Improvements Based on Heuristic Arguments", *Proceedings of the International Joint Conference on Neural Networks*, Neural Network Society, Washington DC, I565-I568.
- SATTI K M H, (1972), "Model Brickwork Wall Panels Under Lateral Loading", Ph.D. Thesis, University of Edinburgh, July.
- SCALERO R S & TEPEDELENLIOGLU N, (1990), "A Fast Training Algorithm for Neural Networks", *Proceedings of the International Joint Conference on Neural Networks*, Neural Network Society, Washington DC, I715-I718.

SEWARD D W, (1982), "A Developed Elastic Analysis of Lightly Loaded Brickwork Walls with Lateral Loading", *International Journal of Masonry Construction*, 2(3): 129-134.

SIETSMA J & DOW R J F, (1991), "Creating Artificial Neural Networks That Generalize", *Neural Networks*, 4: 67-79.

SINHA B P & HENDRY A W, (1975), "Test on Full Scale Cavity Wall Under Lateral Loading", *Proceedings of II Int. Symp. on Bearing Walls, Warsaw, Sept. 11-17*.

SINHA B P, (1978), "A Simplified Ultimate Load Analysis of Laterally Loaded Model Orthotropic Brickwork Panels of Low Tensile Strength", *The Structural Engineer*, 56B(4): 81-84.

SINHA B P, LOFTUS M D & TEMPLE R, (1979), "Lateral Strength of Model Brickwork Panels", *Proceedings of Institution of Structural Engineers*, 67(2): 191-197.

SINHA B P, (1980), "An Ultimate Load Analysis of Laterally Loaded Brickwork Panels", *International Journal of Masonry Construction*, 1(2): 57-61.

SINHA B P & NG C L, (1994), "Behaviour of Brickwork Panels under Lateral Pressure", *Proceedings of the 10<sup>th</sup> International Brick/ Block Masonry Conference, Canada, July: 649-658*.

SINHA B P, NG C L & PEDRESCHI R F, (1997), "Failure Criterion and Behaviour of Brickwork in Biaxial Bending", *Journal of Materials in Civil Engineering, ASCE*, 9(2): 70-75.

SINHA P & MALLICK S K, (1986), "Behaviour of Model Brickwork Facade Wall under Lateral Loading", *Masonry International*, No.8: 8-16

STEIN R, (1993), "Selecting Data for Neural Networks", *AI Expert*, February: 42-47.

SZEWEZYK P & HAJELA P, (1994), "Damage Detection in Structures Based on Feature-Sensitive Neural Networks", *Journal of Computing in Civil Engineering*, 8(2): 163-178.

THURLIMANN B & GUGGISBERG R, (1988), "Failure Criterion for Laterally Loaded Masonry Walls: Experimental Investigations, *Proceedings of the 8<sup>th</sup> International Brick and Block Masonry Conference, Dublin, September: 699-706*.

TIMOSHENKO S, (1940), "Theory of Plates and Shells", McGraw-Hill Book, London.

- TIMOSHENKO S & YOUNG D H, (1962), "Elements of Strength of Materials", D Van Nostrand Company Inc., New Jersey.
- TVETER D R, (1990), "Better Speed Through Integers", AI Expert, November: 40-46.
- TVETER D R, (1991), "Getting a Fast Break with Brackprop", AI Expert, July: 36-43.
- VANLUCHENE & SUN R., (1990), "Neural Network in Structural Engineering". Micro Computers in Civil Engineering, 5: 207-215.
- VERSAGGI M R, (1995), "Understanding Conflicting Data", AI Expert, April: 21-25.
- VOGL T P, MANGIS J K, RIGLER A K, ZINK W T & ALKON D L, (1988), "Accelerating the Convergence of Back-Propagation Algorithm", Biological Cybernetics, 59: 257-263.
- WANG J & HOWARD H C, (1991), "A Design Dependent Approach to Integrated Structural Design", Proceedings of Artificial Intelligence in Design '91, Butterworth-Heinemann: Oxford, 151-170.
- WEIR M K, (1991), "A Method for Self Determination of Adaptive Learning Rates in BackPropagation", Neural Networks, 4: 371-379.
- WEST H W H, HODGKINSON H R & WEBB W F, (1973), "The Resistance of Brick Walls to Lateral Loading", Proceedings of British Masonry Society, 21: 141-163.
- WEST H M H, HODGKINSON H R & HASELTINE B A, (1977), "The Resistance of Brickwork to Lateral Loading Part 1, Experimental Methods and Results of Tests on Small Specimens and Full Sized walls", The Structural Engineer, 55(10): 411-421.
- WEST H W H, HODGKINSON H R & GOODWIN J F, (1979a), "The Resistance to Lateral Loads of Walls Built of Calcium Silicate Bricks", Proceedings of the V<sup>th</sup> International Brick Masonry Conference, Washington, October: 302-313.
- WEST H W H, HODGKINSON H R & HASELTINE B A, (1979b), "The Lateral Resistance of Walls with One Free Vertical Edge", Proc. of the V<sup>th</sup> Int. Brick Masonry Conference, Washington, October: 382-386.
- WEST H W H, HODGKINSON H R & DE VEKEY R C, (1979c), "The Lateral Resistance of Cavity Walls with Different Types of Wall Ties", Proceedings of the V<sup>th</sup> International Brick Masonry Conference, Washington, October: 387-390.

WEST H W H, HASELTINE B A, HODGEKINSON H R & TUTT J N, (1982), "The Lateral Resistance of Cavity Walls with Dissimilar Walls", Proceedings of the 6<sup>th</sup> International Brick Masonry Conference, Rome, May: 781-793.

WILLIAMS T P & GUCUNSKI N, (1995), "Neural Networks for Back calculation of Moduli from SASW Test", Journal of Computing in Civil Engineering, 9(1): 1-9.

YEH Y C *et al.*, (1993), "Building KBES with Diagnosing PC Piles with Artificial Neural Networks", Journal of Computing in Civil Engineering, ASCE, 7(1): 71-93.

ZENG P, (1995), "Artificial Neural Network Computing in Structural Engineering", Developments in Neural Network and Evolutionary Computing for Civil and Structural Engineering By B H V Topping, Civil-Comp Press, Edinburgh, 37-50.

ZIENKIEWICZ O C, (1977), "The Finite Element Method", McGraw-Hill Book, London.

## APPENDIX I

### Section 36.4 of BS 5628 Code of Practice for use of masonry: Part 1. Unreinforced masonry 1978

#### 36.4 Methods of design for laterally loaded panels

**36.4.1 General.** Masonry walls subjected to mainly lateral loads are not capable of precise design. There are, however, two approximate methods which at present may be used for assessing the strength of such walls:

- (a) as a panel supported on a number of sides
- (b) as an arch spanning between suitable supports

When a wall has opening in it or is of an irregular shape such that this clause cannot be used directly, some guidance is given in Appendix D.

**36.4.2 Calculation of design moments in panels.** Masonry walls are not isotropic and there is an orthogonal strength ratio,  $\mu$  (see 3.16), depending on the brick or block and mortar used, as may be found from the characteristic flexural strength given in clause 24.

The calculation of the design moment per unit height of a panel has to take into account the masonry properties referred to above and may be taken as either

$\alpha W_k \gamma_f L^2$ , when the plane of failure is perpendicular to the bed joints; or

$\mu \alpha W_k \gamma_f L^2$ , when the plane of failure is parallel to the bed joints

where

- $\alpha$  is the bending moment coefficients taken from table 9;
- $\gamma_f$  is the partial safety factor for loads (clause 22);
- $\mu$  is the orthogonal strength ratio;
- $L$  is the length of the panel between supports;
- $W_k$  is the characteristic wind load per unit area.

When a vertical load acts so as to increase the flexural strength in the parallel direction, the orthogonal strength ratio,  $\mu$  may be modified by using a flexural strength in the parallel direction of:

$$f_{kx} + \gamma_m g_d$$

where

- $f_{kx}$  is the flexural strength in the parallel direction, taken from table 3;
- $\gamma_m$  is the appropriate partial safety factor for materials (clause 27);
- $g_d$  is the design vertical dead load per unit area.

The bending moment coefficient,  $\mu\alpha$ , at a damp proof course may be taken as for an edge over which full continuity exists when there is sufficient vertical load on the damp proof course to ensure that its flexural strength (see 24.1) is not exceeded.

Table 9 gives values of bending moment coefficients,  $\alpha$ , for various values of  $\mu$ , the orthogonal ratio derived from table 3, modified as necessary for vertical load.

For walls spanning vertically, the design moment per unit length of wall at mid-height of the panel may be taken as:

$$W_k \gamma_f h^2 / 8$$

unless the end conditions justify treating the panel as partially fixed. Piers should be treated in the same way, and the proportion of load being carried by the pier should be assessed from normal structural principles.

**36.4.3 Calculation of design moment of resistance of panels.** The design moment of resistance of a masonry wall is given by:

$$\frac{f_{kx}}{\gamma_m} Z$$

where

$f_{kx}$  is the characteristic flexural strength appropriate to the plane of bending (clause 24);

$\gamma_m$  is the partial safety factor for materials (clause 27);

$Z$  is the section modulus.

In assessing the section modulus of a wall including piers, the outstanding length of flange from the face of the pier should be taken as:

(a) 4x thickness of wall forming the flange when the flange is unrestrained, or

(b) 6 x thickness of wall forming the flange when the flange is continuous,

but in no case more than half the clear distance between piers.

**Table 9. Bending moment coefficients in laterally loaded wall panels**

NOTE 1. Linear interpolation of  $\mu$  and  $h/L$  is permitted.

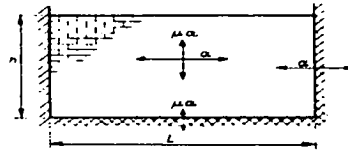
NOTE 2. When the dimensions of a wall are outside the range of  $h/L$  given in this table, it will usually be sufficient to calculate the moments on the basis of a simple span. For example, a panel of type A having  $h/L$  less than 0.3 will tend to act as a freestanding wall, whilst the same panel having  $h/L$  greater than 1.75 will tend to span horizontally.

Key to support conditions

— denotes free edge

— simply supported edge

— an edge over which full continuity exists



	$\mu$	Values of $\alpha$						
		$h/L$						
		0.30	0.50	0.75	1.00	1.25	1.50	1.75
	1.00	0.031	0.045	0.059	0.071	0.079	0.085	0.090
	0.90	0.032	0.047	0.061	0.073	0.081	0.087	0.092
	0.80	0.034	0.049	0.064	0.075	0.083	0.089	0.093
	0.70	0.035	0.051	0.066	0.077	0.085	0.091	0.095
	0.60	0.038	0.053	0.069	0.080	0.088	0.093	0.097
	0.50	0.040	0.056	0.073	0.083	0.090	0.095	0.099
	0.40	0.043	0.061	0.077	0.087	0.093	0.098	0.101
	0.35	0.045	0.064	0.080	0.089	0.095	0.100	0.103
	0.30	0.048	0.067	0.082	0.091	0.097	0.101	0.104
	1.00	0.024	0.035	0.046	0.053	0.059	0.062	0.065
	0.90	0.025	0.036	0.047	0.055	0.060	0.063	0.066
	0.80	0.027	0.037	0.049	0.056	0.061	0.065	0.067
	0.70	0.028	0.039	0.051	0.058	0.062	0.066	0.068
	0.60	0.030	0.042	0.053	0.059	0.064	0.067	0.069
	0.50	0.031	0.044	0.055	0.061	0.066	0.069	0.071
	0.40	0.034	0.047	0.057	0.063	0.067	0.070	0.072
	0.35	0.035	0.049	0.059	0.065	0.068	0.071	0.073
	0.30	0.037	0.051	0.061	0.066	0.070	0.072	0.074
	1.00	0.020	0.028	0.037	0.042	0.045	0.048	0.050
	0.90	0.021	0.029	0.038	0.043	0.046	0.048	0.050
	0.80	0.022	0.031	0.039	0.043	0.047	0.049	0.051
	0.70	0.023	0.032	0.040	0.044	0.048	0.050	0.051
	0.60	0.024	0.034	0.041	0.046	0.049	0.051	0.052
	0.50	0.025	0.035	0.043	0.047	0.050	0.052	0.053
	0.40	0.027	0.038	0.044	0.048	0.051	0.053	0.054
	0.35	0.029	0.039	0.045	0.049	0.052	0.053	0.054
	0.30	0.030	0.040	0.046	0.050	0.052	0.054	0.055
	1.00	0.013	0.021	0.029	0.035	0.040	0.043	0.045
	0.90	0.014	0.022	0.031	0.036	0.040	0.043	0.045
	0.80	0.015	0.023	0.032	0.038	0.041	0.044	0.047
	0.70	0.016	0.025	0.033	0.039	0.043	0.045	0.047
	0.60	0.017	0.026	0.035	0.040	0.044	0.046	0.048
	0.50	0.018	0.028	0.037	0.042	0.045	0.048	0.050
	0.40	0.020	0.031	0.039	0.043	0.047	0.049	0.051
	0.35	0.022	0.032	0.040	0.044	0.048	0.050	0.051
	0.30	0.023	0.034	0.041	0.046	0.049	0.051	0.052

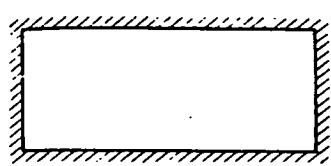

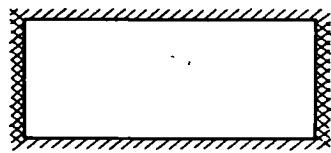
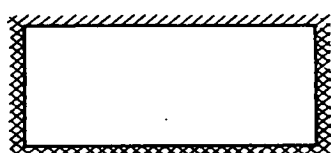
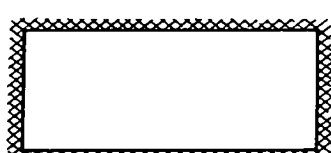



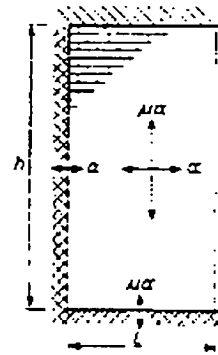
		Values of $\alpha$								
		$\mu$	$h/L$							
			0.30	0.50	0.75	1.00	1.25	1.50	1.75	
	E	1.00	0.008	0.018	0.030	0.042	0.061	0.069	0.086	
		0.90	0.009	0.019	0.032	0.044	0.064	0.062	0.068	
		0.80	0.010	0.021	0.035	0.046	0.058	0.064	0.071	
		0.70	0.011	0.023	0.037	0.049	0.069	0.067	0.073	
		0.60	0.012	0.025	0.040	0.053	0.062	0.070	0.076	
		0.50	0.014	0.028	0.044	0.057	0.066	0.074	0.080	
		0.40	0.017	0.032	0.049	0.062	0.071	0.078	0.084	
		0.35	0.018	0.035	0.052	0.064	0.074	0.081	0.086	
		0.30	0.020	0.038	0.055	0.068	0.077	0.083	0.089	
	F	1.00	0.008	0.016	0.026	0.034	0.041	0.046	0.061	
		0.90	0.008	0.017	0.027	0.036	0.042	0.048	0.052	
		0.80	0.009	0.018	0.029	0.037	0.044	0.049	0.054	
		0.70	0.010	0.020	0.031	0.039	0.046	0.051	0.055	
		0.60	0.011	0.022	0.033	0.042	0.048	0.053	0.057	
		0.50	0.013	0.024	0.036	0.044	0.051	0.056	0.059	
		0.40	0.015	0.027	0.039	0.048	0.054	0.058	0.062	
		0.35	0.016	0.029	0.041	0.050	0.055	0.060	0.063	
		0.30	0.018	0.031	0.044	0.052	0.057	0.062	0.065	
	G	1.00	0.007	0.014	0.022	0.028	0.033	0.037	0.040	
		0.90	0.008	0.015	0.023	0.029	0.034	0.038	0.041	
		0.80	0.008	0.016	0.024	0.031	0.035	0.039	0.042	
		0.70	0.009	0.017	0.026	0.032	0.037	0.040	0.043	
		0.60	0.010	0.019	0.028	0.034	0.038	0.042	0.044	
		0.50	0.011	0.021	0.030	0.036	0.040	0.043	0.046	
		0.40	0.013	0.023	0.032	0.038	0.042	0.045	0.047	
		0.35	0.014	0.025	0.033	0.039	0.043	0.046	0.048	
		0.30	0.016	0.026	0.035	0.041	0.044	0.047	0.049	
	H	1.00	0.005	0.011	0.018	0.024	0.029	0.033	0.036	
		0.90	0.006	0.012	0.019	0.025	0.030	0.034	0.037	
		0.80	0.006	0.013	0.020	0.027	0.032	0.035	0.038	
		0.70	0.007	0.014	0.022	0.028	0.033	0.037	0.040	
		0.60	0.008	0.015	0.024	0.030	0.035	0.038	0.041	
		0.50	0.009	0.017	0.025	0.032	0.036	0.040	0.043	
		0.40	0.010	0.019	0.028	0.034	0.039	0.042	0.045	
		0.35	0.011	0.021	0.029	0.036	0.040	0.043	0.046	
		0.30	0.013	0.022	0.031	0.037	0.041	0.044	0.047	
	I	1.00	0.004	0.009	0.016	0.021	0.026	0.030	0.033	
		0.90	0.004	0.010	0.016	0.022	0.027	0.031	0.034	
		0.80	0.005	0.010	0.017	0.023	0.028	0.032	0.035	
		0.70	0.006	0.011	0.019	0.025	0.030	0.033	0.037	
		0.60	0.006	0.013	0.020	0.026	0.031	0.035	0.038	
		0.50	0.007	0.014	0.022	0.028	0.033	0.037	0.040	
		0.40	0.008	0.016	0.024	0.031	0.035	0.039	0.042	
		0.35	0.009	0.017	0.026	0.032	0.037	0.040	0.043	
		0.30	0.010	0.019	0.028	0.034	0.038	0.042	0.044	

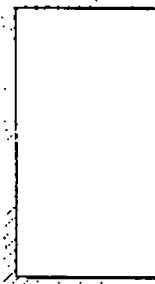
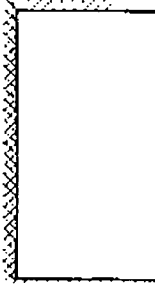



Table 9 (concluded).

Key to support conditions

-  denotes free edge
-  simply supported edge
-  an edge over which full continuity exists



		Values of $\alpha$							
		$h/L$	0.30	0.50	0.75	1.00	1.25	1.50	1.75
	J	1.00	0.009	0.020	0.046	0.071	0.096	0.122	0.151
		0.90	0.010	0.026	0.050	0.078	0.102	0.121	0.152
		0.80	0.012	0.029	0.054	0.080	0.111	0.142	0.173
		0.70	0.013	0.032	0.060	0.081	0.101	0.136	0.167
		0.60	0.015	0.036	0.067	0.100	0.125	0.173	0.211
		0.50	0.018	0.042	0.077	0.113	0.163	0.186	0.237
		0.40	0.021	0.050	0.090	0.121	0.177	0.225	0.270
		0.35	0.024	0.055	0.098	0.144	0.194	0.244	0.296
		0.30	0.027	0.062	0.108	0.160	0.214	0.269	0.325
	K	1.00	0.009	0.021	0.038	0.056	0.074	0.091	0.108
		0.90	0.010	0.023	0.041	0.060	0.078	0.097	0.113
		0.80	0.011	0.025	0.045	0.065	0.084	0.103	0.120
		0.70	0.012	0.028	0.048	0.070	0.091	0.110	0.128
		0.60	0.014	0.031	0.054	0.077	0.099	0.119	0.138
		0.50	0.016	0.035	0.061	0.085	0.109	0.130	0.149
		0.40	0.019	0.041	0.069	0.097	0.121	0.144	0.164
		0.35	0.021	0.045	0.075	0.104	0.129	0.152	0.173
		0.30	0.024	0.050	0.082	0.112	0.139	0.162	0.183
	L	1.00	0.006	0.016	0.029	0.044	0.059	0.073	0.088
		0.90	0.007	0.017	0.032	0.047	0.063	0.078	0.093
		0.80	0.008	0.018	0.034	0.051	0.067	0.084	0.099
		0.70	0.009	0.021	0.038	0.056	0.073	0.090	0.105
		0.60	0.010	0.023	0.042	0.061	0.080	0.098	0.115
		0.50	0.012	0.027	0.048	0.068	0.089	0.108	0.126
		0.40	0.014	0.032	0.055	0.078	0.100	0.121	0.139
		0.35	0.016	0.035	0.060	0.084	0.108	0.129	0.148
		0.30	0.018	0.039	0.066	0.092	0.116	0.138	0.168

## APPENDIX II

### Section 6.3.4 of Australian Masonry Manual (Formerly “Masonry Code of Practice”)

#### 6.3.4 Design Capacity of a Single Leaf Panel

The design uniform lateral pressure on a single leaf unreinforced wall panel may be calculated by an empirical expression:

$$w_d = 10(b_v \frac{M_{cv}}{H^2} + b_h \frac{M_{ch}}{L^2}) \quad \dots(6.11)$$

where:

$w_d$  = design pressure(kPa)

$M_{cv}$  = design bending strength in vertical flexure (kNm/m)

$M_{ch}$  = design bending strength in horizontal flexure (kNm/m)

$H$  = height of panel (m)

$L$  = length of panel (m)

$b_v$  = a coefficient depending on the top and bottom supports,

$b_h$  = a coefficient depending on the side supports,

This expression simply adds the lateral load capacity of an independent vertically spanning strip to the load capacity of a horizontally spanning strip.

Values of  $b_v$  &  $b_h$  for various panels are shown in Figures 6.12 and 6.13.

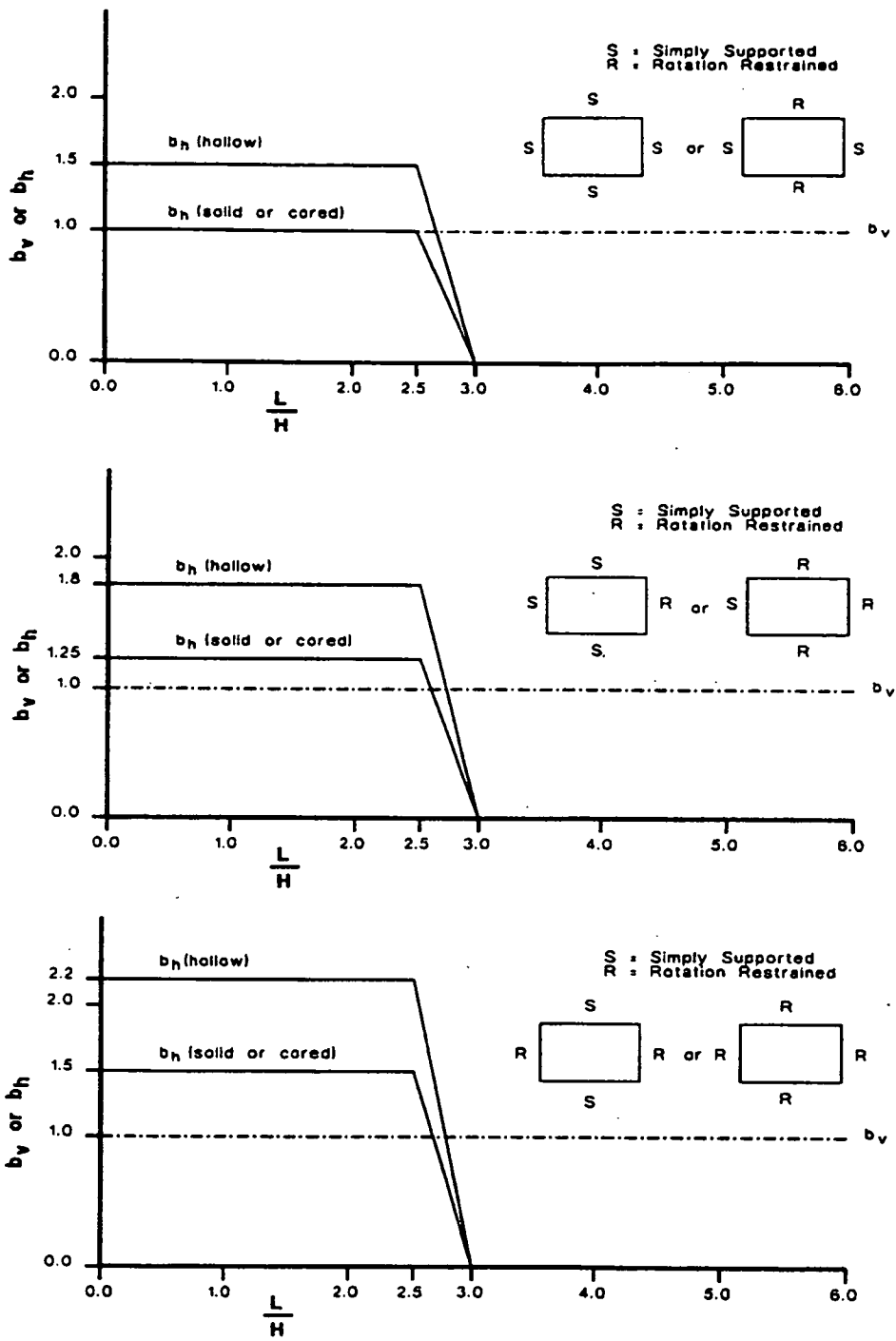


Figure 6.12 - Moment Coefficients for Panels Supported on Four Edges

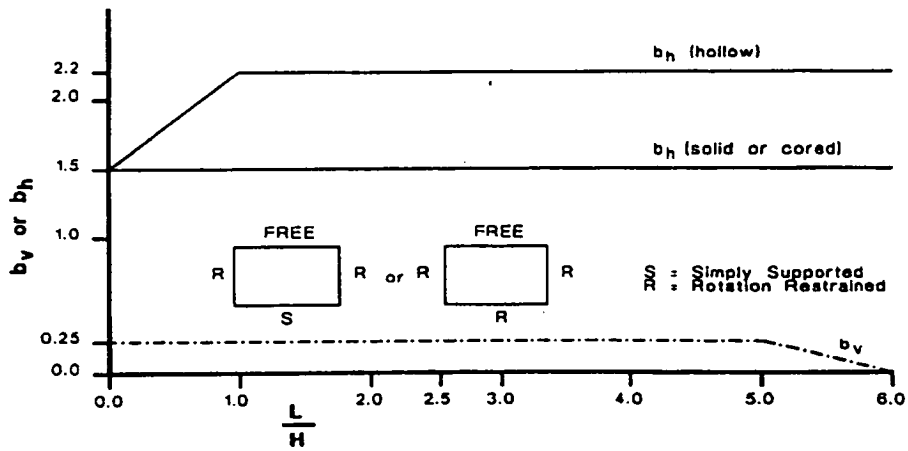
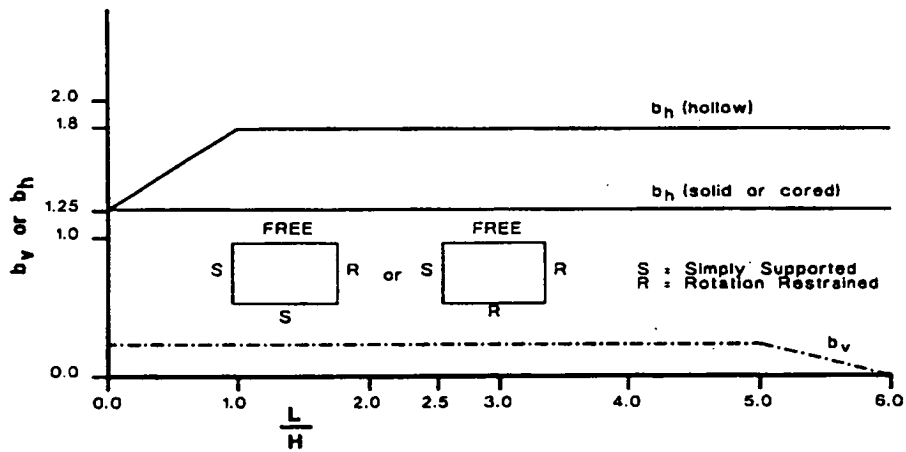
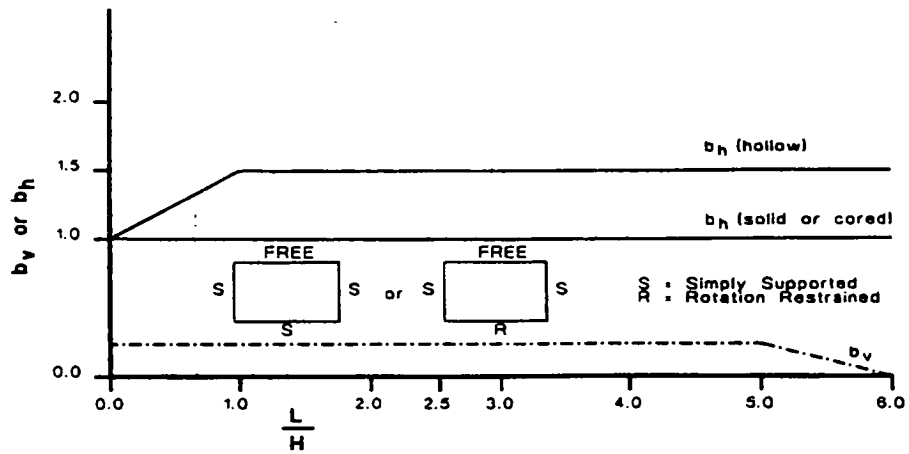


Figure 6.13 - Moment Coefficients for Panels Supported on Three Edges

## APPENDIX III

### The Interactive Questionnaire to Prepare the Input Data for the In-house Finite Element Program

The files for this program will have the same root name, but with different extensions to indicate their roles. Nodal data and element data are stored separately as well as in the input data file.

GIVE THE ROOT NAME FOR YOUR SET OF FILES

X

WOULD LIKE THIS PROGRAM TO RUN FROM A FILE OF INTERACTIVE QUESTIONS PREPARED? (If so, it should be names x.sor)

N

DO THE FILES CONTAINING NODAL AND ELEMENT DATA ALREADY EXIST?

N

GIVE A TITLE FOR YOUR PROBLEM

ANALYSIS

Please make sure that you use consistent units throughout your work: eg. Newton, mm, Mpa etc.,

WOULD YOU LIKE THIS PROGRAM TO GENERATE THE MESH?

Before you begin, please note the limits on the number of nodes, elements and blocks in the program at present:

Maximum number of blocks	= 70
Maximum number of master points	= 170
Maximum number of elements on a block side	= 16
Maximum number of nodes total	= 2661
Maximum number of elements total	= 523
Maximum number of restrained nodes total	= 297
Maximum number of different material types	= 21
Maximum assumed frontwidth in total	= 180

STATE THE ELEMENT YOU WISH TO USE

TYPE 4 FOR 4 NODED LINEAR ELEMENT  
TYPE 8 FOR 8 NODED QUADRATIC ELEMENT  
TYPE 12 FOR 12 NODED CUBIC ELEMENT

8

GIVE THE NUMBER OF QUADRILATERAL BLOCKS OF ELEMENTS  
REQUIRED FOR THIS MESH

2

INPUT THE NUMBER OF MASTER POINTS USED TO DEFINE THE BLOCK  
CORNERS

6

GIVE THE MASTER POINT NUMBER, AND THE TWO COORDINATES OF  
EACH MASTER POINT

1 0 0  
2 10 0  
3 20 0  
4 20 10  
5 10 10  
6 0 10

Arrange the blocks into vertical or horizontal sequences (piles), numbering  
sequentially up each pile in turn.

The base of the blocks is defined as parallel to the base of the pile  
FOR EACH BLOCK, GIVE THE BLOCK NUMBER, AND THE FOUR MASTER  
POINT NUMBERS DEFINING THE BLOCK CORNERS (ANTICLOCKWISE,  
STARTING AT THE LEFT HAND BOTTOM CORNER)

1 1 2 5 6  
2 2 3 4 5

Block common side features. Block 2 has LHS attached to block 1.

Recall your block arrangement. Base of the block is defined as parallel to the base of  
the pile. The base, termed side 1 should extend from the 1st to the second master  
point. The L.H. side, termed side 4 should extend from 1st to the final masterpoint

FOR THE FOLLOWING BLOCKS, GIVE THE NUMBER OF ELEMENTS  
ALONG THE BLOCK BASE, OR L.H. SIDE AS REQUESTED

FOR BLOCK NUMBER 1 AT START OF PILE 1, GIVE THE NUMBER OF ELEMENTS FIRST ON THE BASE (in the 1-2 direction), THEN ON THE VERTICAL SIDE (in the 1-4 direction)

3 3

GIVE THE RELATIVE SIZES OF THE 3 ELEMENT SIZE LENGTHS ON THE BASE (1-2 direction) FOR BLOCK NUMBER 1

1 1 2

GIVE THE RELATIVE SIZES OF THE 3 ELEMENT SIZE LENGTHS ON THE VERTICAL SIDE (1-4 direction) FOR BLOCK NUMBER 1

1 2 1

FOR BLOCK NUMBER 2 AT START OF PILE 2, GIVE THE NUMBER OF ELEMENTS ON THE BASE (1-2 direction)

3

GIVE THE RELATIVE SIZES OF THE 3 ELEMENT SIZE LENGTHS ON THE BASE (1-2 direction) FOR BLOCK NUMBER 2

2 1 1

copying side 2 of block1 into side 4 of block2, there are 6 master points which have the following node numbers

Master Point	Node Number
1	1
2	34
3	67
4	73
5	40
6	7

PRESS ENTER TO CONTINUE

Total no. Of nodes           = 73  
Total no. Of elements       = 18

WOULD YOU LIKE TO PLOT THE MESH?

Y

PRESS C AND RETURN TO CONTINUE

C

WOULD YOU LIKE TO CONTINUE TO DEVELOP THE TOTAL DATA FILE?

Y

TYPE 1 FOR PLAIN STRESS  
2 FOR PLAIN STRAIN  
3 FOR AXISYMMETRY  
4 FOR PLATE BENDING

4

Max. Required frontwidth = 36

GIVE THE ORDER OF GAUSSIAN INTEGRATION TO BE USED

TYPE 1 FOR SINGLE POINT  
TYPE 2 FOR 2X2 = FOUR POINT  
TYPE 3 FOR 3X3 = NINE POINT  
TYPE 4 FOR 4X4 = SIXTEEN POINT

To avoid singularity in the global stiffness matrix, you must restrain at least the following number of degrees of freedom

Gauss Order	Minimum restrained DOFs
1	129
2	3
3	3
4	3

Elements are generated numbering most rapidly in the vertical direction (Up the pile of blocks) and starting at the L.H. bottom corner, node numbering follows the same pattern. Make sure your sketch of the mesh follows this system.

Now, consider the element properties. It is assumed that all elements in a block have the same properties. It is also assumed that all blocks have the same properties (Material type 1) unless you specify otherwise.

HOW MANY ELEMENT BLOCKS ARE NOT MADE OF MATERIAL TYPE 1?

1

GIVE THE NUMBER OF EACH OF THESE BLOCKS AND ITS MATERIAL NUMBER : ONE BLOCK TO A LINE



2 2

GIVE THE NO. OF LOAD CASES TO BE SOLVED

1

Now consider restraints. For your restrained sides or nodes, prepare the restraint code 1 for a restrained degree of freedom and 0 for a free degree of freedom.

Restraints are defined by block sides or nodes.

HOW MANY BLOCK SIDES ARE RESTRAINED IN ONE OR MORE DEGREES OF FREEDOM

6

The sequence of variables for the plate bending is :  $W$ ,  $DW/DX$ ,  $DW/DY$   
e.g. for plate bending with restraints against rotation about the X-axis only, (i.e. against sloping in the Y direction) the restraint code is 001.

FOR THE 1ST OF THESE BLOCK SIDES, GIVE THE BLOCK NUMBER, THE BLOCK SIDE (e.g. EITHER 1,2,3 OR 4) AND THE RESTRAINT CODE (eg. 101)

1 1 110

FOR THE 2ND OF THESE BLOCK SIDES, GIVE THE BLOCK NUMBER, THE BLOCK SIDE (e.g. EITHER 1,2,3 OR 4) AND THE RESTRAINT CODE (eg. 101)

2 1 110

FOR THE 3RD OF THESE BLOCK SIDES, GIVE THE BLOCK NUMBER, THE BLOCK SIDE (e.g. EITHER 1,2,3 OR 4) AND THE RESTRAINT CODE (eg. 101)

2 2 101

FOR THE 4TH OF THESE BLOCK SIDES, GIVE THE BLOCK NUMBER, THE BLOCK SIDE (e.g. EITHER 1,2,3 OR 4) AND THE RESTRAINT CODE (eg. 101)

2 3 110

FOR THE 5TH OF THESE BLOCK SIDES, GIVE THE BLOCK NUMBER, THE BLOCK SIDE (e.g. EITHER 1,2,3 OR 4) AND THE RESTRAINT CODE (eg. 101)

1 3 110

FOR THE 6TH OF THESE BLOCK SIDES, GIVE THE BLOCK NUMBER, THE BLOCK SIDE (e.g. EITHER 1,2,3 OR 4) AND THE RESTRAINT CODE (eg. 101)

1 4 101

NOW CONSIDER THE SINGLE RESTRAINED NODES

AT HOW MANY NODES WOULD YOU LIKE TO ADD EXTRA RESTRAINTS?

0

NOW DESCRIBE THE MATERIALS

You may use either isotropic or orthotropic materials

WOULD YOU LIKE ISOTROPIC PROPERTIES?

N

FOR YOUR 2 DIFFERENT MATERIALS

GIVE THE MATERIAL NUMBER, THICKNESS, YOUNG'S MODULUS IN THE X-DIRECTION, YOUNG'S MODULUS IN THE Y-DIRECTION, POISSONS RATIO XY ( $SIGY = -NUXY * EPSX * EX$ ), AND SHEAR MODULUS GXY

1 10 17500 10000 0.15 5000

1 10 15000 8000 0.15 4000

NOW GIVE THE LOAD INFORMATION FOR LOAD CASE NO.1

FIRST GIVE THE TITLE FOR THIS LOAD CASE

UDL

HOW MANY NODES CARRYING NODAL LOADS ARE THERE?

0

HOW MANY ELEMENT EDGES CARRY DISTRIBUTED LOADS?

Note that each loaded counts as another edge whether its on the same element or on a different one

0

For uniformly distributed loading on plates, each material may be given a single U/D loading. Alternatively, you may define the pressure at the chosen nodes, with the

undefined values assumed to be zero. The later feature allows non-uniform pressure loading.

FOR EACH OF YOUR 2 MATERIALS, GIVE THE MATERIAL NO., AND THE UNIFORMLY DISTRIBUTED PRESSURE.

1 0.0005

1 0.0002

AT HOW MANY NODES DO YOU WISH TO DEFINE THE PRESSURE?

0

YOUR DATA PREPARATION IS NOW COMPLETE. YOUR DATA FILE FOR FINITE ELEMENT ANALYSIS IS CALLED X.DAT

## APPENDIX IV

The user interface developed as part of this research for the neural network application is given in this appendix. The variables that can be initialised/modified during an application can be seen in Figure 1. These include the setting network architecture, selecting a suitable neural network paradigm, initialising the connection weights, etc. The various parameters can be grouped as can be seen in Figure 1 and are explained below.

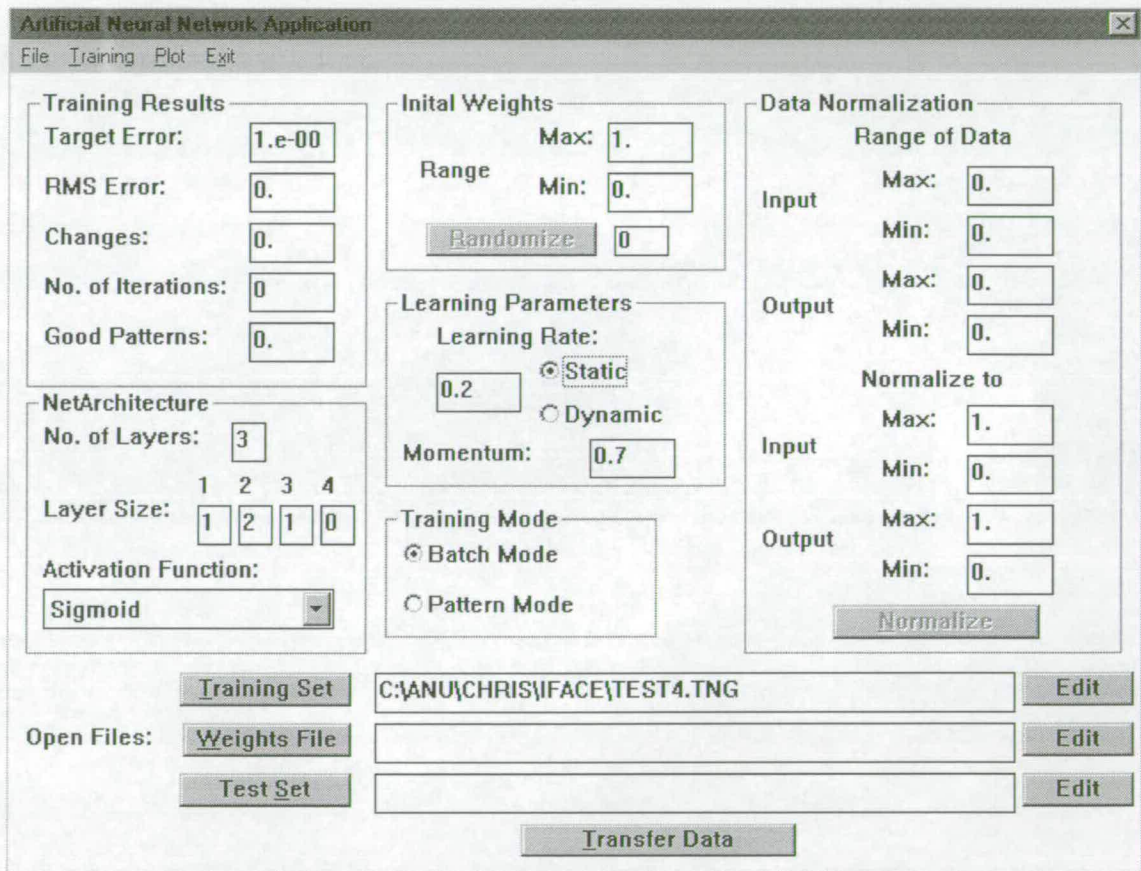


FIG. 1 The User Interface Developed for the Neural Network Program

## 1.1 Training Results

**Target Error:** Allows the user to predefine the target RMS error that the user would like to achieve during training (default 0.01).

**RMS Error:** Displays the RMS error of the training patterns during training.

**Changes:** Displays the change in RMS error at each successive step during training.

**No. of Iterations:** Displays the number of iterations that has passed since the training started.

**Good Patterns:** Displays the percentage of the number of patterns in the training set that are falling within the pre-defined target error.

## 1.2 Network Architecture

This allows the user to define the architecture of the net to be used for training.

**No. of Layers:** Specifies the total number of layers in the net including the input and output layers (default 3). However, the layer size is restricted to 4 in this application as the disadvantage of using more than 4 has been pointed out by several researchers.

**Layer Size:** The number of nodes in each of the layers can be specified here. The default values can be seen in the figure.

**Activation Function:** The type of activation function that can be selected by the user is given here. The default is 'sigmoid activation' function. However, the other options given under this 'Combo Box' include 'Tanh' and 'Linear' functions.

## 1.3 Initial Weights

The connection weights can be initialised here within the range specified by the user.

**Max.:** The upper limit of the initial connection weight.

**Min.:** The lower limit of the initial connection weight.

**Randomize:** This is a 'Push Button' that can access the function which create a set of random numbers within the upper and lower limits specified by the user and is used as the initial weights for training. This button can be seen 'Disabled' at the beginning as it requires transfer of the data to the main program before executing the function. The button will be 'Enabled' once the data is transferred using the 'Transfer Data' button. After executing the function, the total number of weights that are initialised will be displayed in the box next to it.

#### 1.4 Learning Parameters

The learning parameters are used for updating the connection weights while training and is explained in Section 3.8.3.4.

**Learning Rate:** Specifies the initial learning rate to be used for training (default 0.2). The 'radio buttons' given next to the learning rate allows the user to select the static or dynamic mode for training.

**Static:** The learning rate is kept as a constant if this option is chosen. (by default)

**Dynamic:** The learning rate is modified at each step and is increased by 1.05 at a successful step and is reduced by 0.7 when it fails.

**Momentum:** Specifies the momentum to be used for training. (default 0.7)

#### 1.5 Training Mode

The 'radio buttons' allows the user to specify the type of training to be adopted.

**Batch Mode:** A batch mode of training will be performed, where the connection weights are modified after presenting all the patterns in the training set to the net. (by default)

**Pattern Mode:** A pattern mode of training will be performed, where the weight modifications are made after presenting each pattern to the net.

## 1.6 Data Normalization

The Normalization of the data is carried out here. The default values are as given in the figure.

**Range of Data:** Displays the maximum and minimum value of input and output values present in the data set. The values are displayed only after the data is transferred to the program.

**Normalize to:** The user can specify the upper and lower limit of the input and output values to which the training and test set has to be normalised. The default values are as shown in the figure.

**Normalize:** The 'push Button' allows the user to access the function that Normalizes the data. The Normalization is done as per Section 3.8.2.5. This button is 'Enabled' only after transferring the data to the main program.

## 1.7 Other Essential Features

**Open Files:** This allows the user to select the files that contain the various files that are to be used for training.

**Training Set:** The 'push button' allows the user to select the file containing the training set. The default extension for this file is '.tng'. The dialog box that can usually be seen in any windows application to open a file will appear when this 'push button' is activated. The selected filename will be displayed in the 'edit' box that can be seen next to it.

**Weights File:** This allows the use of the file containing the connection weights, if it exists. If there is no such file, the training can be carried out by initialising the weights.

**Test Set:** The 'push button' allows the user to select the file containing the test set. The default extension for this data file is '.tst' and file name will be displayed when the user selects a file.

**Edit:** These controls allows the user to view the various files that are selected by the user and appears in the boxes against each of them. A 'notepad' will be activated and the file will be opened in the notepad. The user can make any modifications and save the file.

**Transfer Data:** This is a very important 'push button' that transfers the variables specified by the user to the program. Any modifications that are made in the panel will be transferred to the main program only if this button is activated. This also points out any error in the input data. e.g. If the number of input/output layers doesn't match with the data given in the training, a dialog box will appear and inform the user the need to change the number of layers or to select the correct input file.

## 1.8 File Menu

Various operations can be performed by the commands given under this menu item. Some of them are already given as 'controls' in the panel and is explained above and include 'Open Training Set', 'Open Weights File' and 'Open Test Set'. The other commands are explained below.

**'New Net':** Opens a new net with the default variables

**'Open Net':** Opens an existing net file. The file contains information about a net that is already trained.

**'Save Net As':** A trained net can be saved as a file using this command. This is similar to 'Save As' command found in windows application. A dialog box will be appear with a default file name extension '.net'.

**'Save Net':** Save an open net. If there is no file name specified for this, the dialog box will appear asking the user to specify the file name.

**'Save Weights As':** This saves the connection weights data as a file with '.wgt' extension.

**'Save Weights':** This saves a weight file that is being used for the training.



## 1.9 Training Menu

**‘Start Training’:** This activates the main neural network program and the training will be initiated with this command using the data that has already been transferred to the program. The results of the training such as ‘RMS Error’, ‘Changes’, ‘Good Patterns’ etc. Will be modified on the control panel during the training. The training will automatically stopped when the RMS error of all the patterns reaches the target error specified by the user. The training can also be halted any time temporarily by the user.

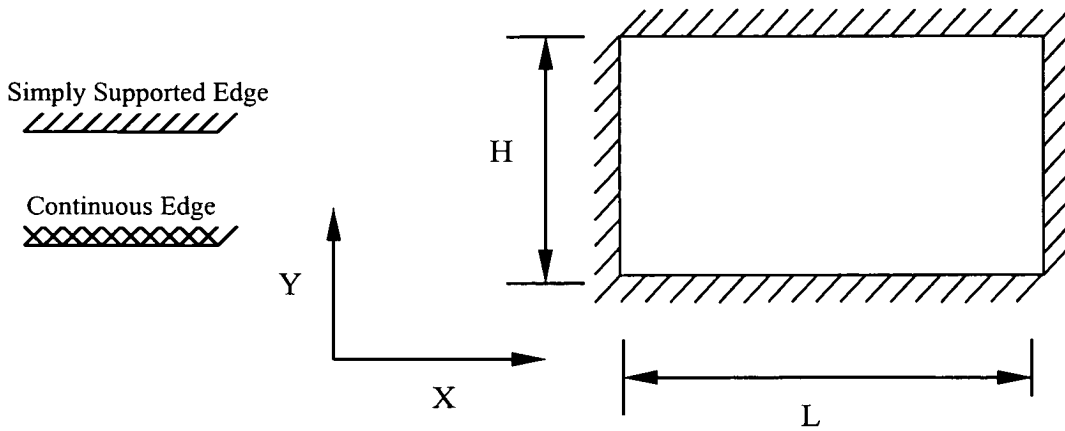
**‘Halt Training’:** This allows the user to stop training any time. This is done to evaluate the performance of the net during training.

**‘Test Training Set’:** This command can be used to see the performance of the net on the patterns that are used for training. The results of this test will be displayed to the user in a small window.

**‘Test Test Set’:** The user can test the performance of the net on unseen problems using this command. This is carried out at regular intervals to evaluate the performance of the net and can be considered as a stopping criterion.

## APPENDIX V

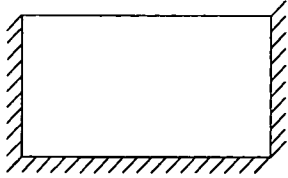
### Moment Coefficients for Design of Laterally Loaded Orthotropic Panels Based on the Finite Element Analysis Incorporating the Bi-axial Failure Criterion



Moment Coefficients ( $\alpha$ ) are Given For Different Boundary Conditions in the Tables

Failure Pressure is given by  $w = \frac{1}{\alpha} \frac{F_x Z}{L^2}$ . These coefficients are calculated by considering the strength in the horizontal direction as given in the code.

	$E_x/E_y$	$L/H$	$F_x/F_y$			
			1.3	2.0	3.0	4.0
0.8		0.5	0.093	0.094	0.102	0.112
		0.75	0.063	0.078	0.094	0.094
		1.0	0.05	0.071	0.071	0.073
		1.5	0.039	0.045	0.045	0.049
		2.0	0.023	0.029	0.033	0.036
1.0		0.5	0.096	0.096	0.099	0.111
		0.75	0.065	0.071	0.098	0.096
		1.0	0.047	0.069	0.074	0.075
		1.5	0.038	0.045	0.046	0.047
		2.0	0.025	0.028	0.029	0.029
1.4		0.5	0.101	0.101	0.101	0.103
		0.75	0.071	0.072	0.082	0.096
		1.0	0.048	0.058	0.079	0.080
		1.5	0.033	0.046	0.049	0.049
		2.0	0.026	0.03	0.03	0.031
1.8		0.5	0.106	0.105	0.105	0.105
		0.75	0.077	0.077	0.080	0.09
		1.0	0.052	0.056	0.075	0.084
		1.5	0.03	0.047	0.053	0.053
		2.0	0.024	0.033	0.033	0.033



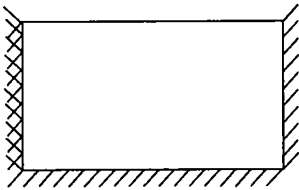
Ex/Ey	L/H	Fx/Fy			
		1.3	2.0	3.0	4.0
0.8	0.5	0.120	0.119	0.119	0.12
	0.75	0.108	0.108	0.108	0.117
	1.0	0.092	0.093	0.102	0.124
	1.5	0.062	0.078	0.090	0.091
	2.0	0.049	0.068	0.071	0.074
1.0	0.5	0.120	0.119	0.118	0.119
	0.75	0.110	0.110	0.11	0.112
	1.0	0.095	0.095	0.098	0.112
	1.5	0.065	0.071	0.093	0.094
	2.0	0.046	0.068	0.075	0.075
1.4	0.5	0.122	0.121	0.120	0.120
	0.75	0.114	0.114	0.113	0.113
	1.0	0.101	0.100	0.101	0.102
	1.5	0.071	0.072	0.081	0.095
	2.0	0.048	0.058	0.076	0.078
1.8	0.5	0.123	0.122	0.121	0.121
	0.75	0.117	0.116	0.115	0.115
	1.0	0.106	0.105	0.104	0.104
	1.5	0.076	0.076	0.080	0.090
	2.0	0.052	0.060	0.075	0.081



Ex/Ey	L/H	Fx/Fy			
		1.3	2.0	3.0	4.0
0.8	0.5	0.200	0.284	0.281	0.289
	0.75	0.163	0.179	0.183	0.186
	1.0	0.111	0.146	0.190	0.189
	1.5	0.065	0.102	0.155	0.191
	2.0	0.038	0.060	0.085	0.098
1.0	0.5	0.187	0.276	0.298	0.301
	0.75	0.148	0.182	0.190	0.183
	1.0	0.114	0.130	0.156	0.171
	1.5	0.063	0.100	0.152	0.185
	2.0	0.038	0.059	0.084	0.098
1.4	0.5	0.192	0.232	0.321	0.323
	0.75	0.130	0.195	0.193	0.197
	1.0	0.105	0.138	0.137	0.155
	1.5	0.061	0.086	0.122	0.127
	2.0	0.037	0.058	0.082	0.087
1.8	0.5	0.210	0.224	0.298	0.347
	0.75	0.120	0.190	0.214	0.209
	1.0	0.097	0.153	0.144	0.147
	1.5	0.060	0.088	0.101	0.120
	2.0	0.037	0.058	0.083	0.089



Ex/Ey	L/H	Fx/Fy			
		1.3	2.0	3.0	4.0
0.8	0.5	0.041	0.040	0.044	0.044
	0.75	0.036	0.037	0.043	0.043
	1.0	0.030	0.039	0.040	0.041
	1.5	0.029	0.033	0.032	0.033
	2.0	0.022	0.022	0.023	0.024
1.0	0.5	0.041	0.041	0.041	0.045
	0.75	0.037	0.037	0.046	0.042
	1.0	0.030	0.034	0.040	0.041
	1.5	0.025	0.033	0.033	0.033
	2.0	0.022	0.023	0.024	0.024
1.4	0.5	0.042	0.041	0.041	0.045
	0.75	0.038	0.038	0.038	0.040
	1.0	0.032	0.033	0.038	0.040
	1.5	0.022	0.033	0.034	0.034
	2.0	0.020	0.025	0.026	0.025
1.8	0.5	0.042	0.042	0.041	0.041
	0.75	0.039	0.039	0.039	0.039
	1.0	0.034	0.034	0.035	0.040
	1.5	0.022	0.028	0.036	0.035
	2.0	0.018	0.027	0.027	0.027



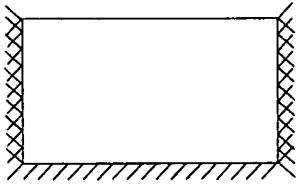
Ex/Ey	L/H	Fx/Fy			
		1.3	2.0	3.0	4.0
0.8	0.5	0.069	0.069	0.068	0.070
	0.75	0.067	0.067	0.067	0.067
	1.0	0.063	0.062	0.064	0.073
	1.5	0.048	0.053	0.065	0.069
	2.0	0.039	0.056	0.055	0.056
1.0	0.5	0.069	0.069	0.069	0.070
	0.75	0.068	0.067	0.067	0.067
	1.0	0.064	0.063	0.064	0.068
	1.5	0.050	0.052	0.062	0.067
	2.0	0.038	0.049	0.057	0.056
1.4	0.5	0.070	0.069	0.069	0.069
	0.75	0.069	0.068	0.068	0.068
	1.0	0.066	0.065	0.065	0.065
	1.5	0.054	0.054	0.056	0.062
	2.0	0.041	0.044	0.058	0.058
1.8	0.5	0.070	0.070	0.069	0.069
	0.75	0.069	0.069	0.069	0.068
	1.0	0.067	0.067	0.066	0.066
	1.5	0.056	0.056	0.057	0.058
	2.0	0.044	0.044	0.050	0.059



Ex/Ey	L/H	Fx/Fy			
		1.3	2.0	3.0	4.0
0.8	0.5	0.120	0.157	0.160	0.161
	0.75	0.115	0.128	0.130	0.132
	1.0	0.099	0.098	0.104	0.106
	1.5	0.062	0.077	0.090	0.098
	2.0	0.038	0.059	0.072	0.080
1.0	0.5	0.121	0.137	0.155	0.164
	0.75	0.101	0.129	0.130	0.132
	1.0	0.093	0.010	0.105	0.107
	1.5	0.060	0.073	0.072	0.084
	2.0	0.037	0.058	0.065	0.080
1.4	0.5	0.128	0.131	0.152	0.166
	0.75	0.087	0.131	0.137	0.144
	1.0	0.080	0.105	0.106	0.109
	1.5	0.057	0.070	0.074	0.080
	2.0	0.036	0.057	0.064	0.073
1.8	0.5	0.135	0.135	0.141	0.163
	0.75	0.087	0.112	0.144	0.144
	1.0	0.072	0.114	0.112	0.115
	1.5	0.054	0.069	0.076	0.077
	2.0	0.036	0.056	0.063	0.071

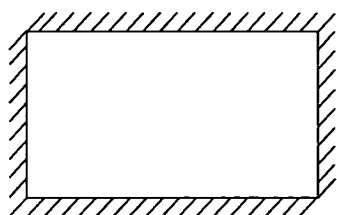


Ex/Ey	L/H	Fx/Fy			
		1.3	2.0	3.0	4.0
0.8	0.5	0.063	0.063	0.065	0.072
	0.75	0.051	0.050	0.067	0.067
	1.0	0.039	0.057	0.058	0.057
	1.5	0.035	0.038	0.049	0.038
	2.0	0.024	0.025	0.027	0.028
1.0	0.5	0.064	0.064	0.064	0.069
	0.75	0.051	0.052	0.062	0.065
	1.0	0.038	0.049	0.058	0.059
	1.5	0.031	0.040	0.040	0.040
	2.0	0.024	0.022	0.027	0.028
1.4	0.5	0.066	0.066	0.065	0.065
	0.75	0.054	0.054	0.056	0.063
	1.0	0.041	0.043	0.058	0.059
	1.5	0.027	0.042	0.043	0.044
	2.0	0.023	0.028	0.029	0.031
1.8	0.5	0.068	0.067	0.067	0.066
	0.75	0.057	0.057	0.057	0.059
	1.0	0.044	0.045	0.050	0.060
	1.5	0.025	0.037	0.046	0.046
	2.0	0.021	0.032	0.031	0.032

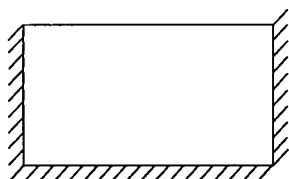


Ex/Ey	L/H	Fx/Fy			
		1.3	2.0	3.0	4.0
0.8	0.5	0.041	0.041	0.045	0.045
	0.75	0.041	0.041	0.043	0.043
	1.0	0.040	0.040	0.042	0.042
	1.5	0.036	0.037	0.041	0.041
	2.0	0.030	0.039	0.039	0.042
1.0	0.5	0.041	0.041	0.041	0.045
	0.75	0.041	0.041	0.041	0.041
	1.0	0.041	0.041	0.040	0.041
	1.5	0.037	0.037	0.038	0.04
	2.0	0.03	0.034	0.039	0.039
1.4	0.5	0.041	0.041	0.041	0.044
	0.75	0.041	0.041	0.041	0.041
	1.0	0.041	0.041	0.041	0.040
	1.5	0.038	0.038	0.038	0.041
	2.0	0.032	0.033	0.037	0.041
1.8	0.5	0.042	0.041	0.041	0.041
	0.75	0.041	0.041	0.041	0.041
	1.0	0.041	0.041	0.041	0.041
	1.5	0.039	0.039	0.039	0.039
	2.0	0.033	0.033	0.035	0.043

Moment coefficients obtained from the finite element analysis are compared with that given in the BS code of practice in the following tables.



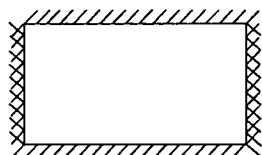
		Fx/Fy			
		L/H	1.3	2.0	3.0
FEM	0.75	0.065	0.071	0.098	
	1.0	0.047	0.069	0.074	
	1.5	0.038	0.045	0.046	
	2.0	0.025	0.028	0.029	
BS	0.75	0.060	0.069	0.077	
	1.0	0.049	0.057	0.065	
	1.5	0.031	0.039	0.047	
	2.0	0.022	0.028	0.036	



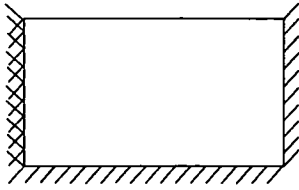
		Fx/Fy			
		L/H	1.3	2.0	3.0
FEM	0.75	0.110	0.110	0.11	
	1.0	0.095	0.095	0.098	
	1.5	0.065	0.071	0.093	
	2.0	0.0465	0.068	0.075	
BS	0.75	0.086	0.092	0.0973	
	1.0	0.076	0.083	0.090	
	1.5	0.056	0.067	0.076	
	2.0	0.050	0.056	0.065	



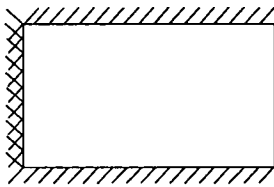
		Fx/Fy			
		L/H	1.3	2.0	3.0
FEM	0.75	0.148	0.182	0.190	
	1.0	0.114	0.130	0.156	
	1.5	0.063	0.100	0.152	
	2.0	0.038	0.059	0.084	
BS	0.75	0.1248	0.167	0.218	
	1.0	0.0855	0.113	0.149	
	1.5	0.047	0.065	0.087	
	2.0	0.029	0.042	0.057	



		Fx/Fy			
		L/H	1.3	2.0	3.0
FEM	0.75	0.037	0.037	0.041	
	1.0	0.030	0.034	0.040	
	1.5	0.025	0.033	0.033	
	2.0	0.022	0.023	0.024	
BS	0.75	0.037	0.041	0.044	
	1.0	0.031	0.036	0.0340	
	1.5	0.022	0.027	0.031	
	2.0	0.016	0.021	0.025	



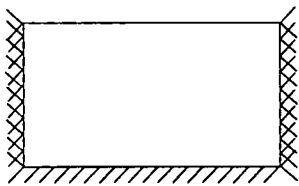
		Fx/Fy			
		L/H	1.3	2.0	3.0
FEM	0.75	0.068	0.0679	0.067	
	1.0	0.064	0.063	0.064	
	1.5	0.0504	0.052	0.062	
	2.0	0.038	0.049	0.057	
BS	0.75	0.063	0.067	0.070	
	1.0	0.057	0.061	0.065	
	1.5	0.046	0.051	0.056	
	2.0	0.038	0.044	0.050	



		Fx/Fy			
		L/H	1.3	2.0	3.0
FEM	0.75	0.101	0.129	0.130	
	1.0	0.093	0.100	0.105	
	1.5	0.060	0.073	0.070	
	2.0	0.037	0.058	0.065	
BS	0.75	0.111	0.116	0.14	
	1.0	0.067	0.085	0.107	
	1.5	0.040	0.052	0.067	
	2.0	0.026	0.035	0.047	



		Fx/Fy			
		L/H	1.3	2.0	3.0
FEM	0.75	0.051	0.052	0.062	
	1.0	0.038	0.049	0.058	
	1.5	0.031	0.040	0.040	
	2.0	0.024	0.022	0.027	
BS	0.75	0.0463	0.053	0.057	
	1.0	0.038	0.044	0.051	
	1.5	0.026	0.032	0.038	
	2.0	0.019	0.024	0.030	

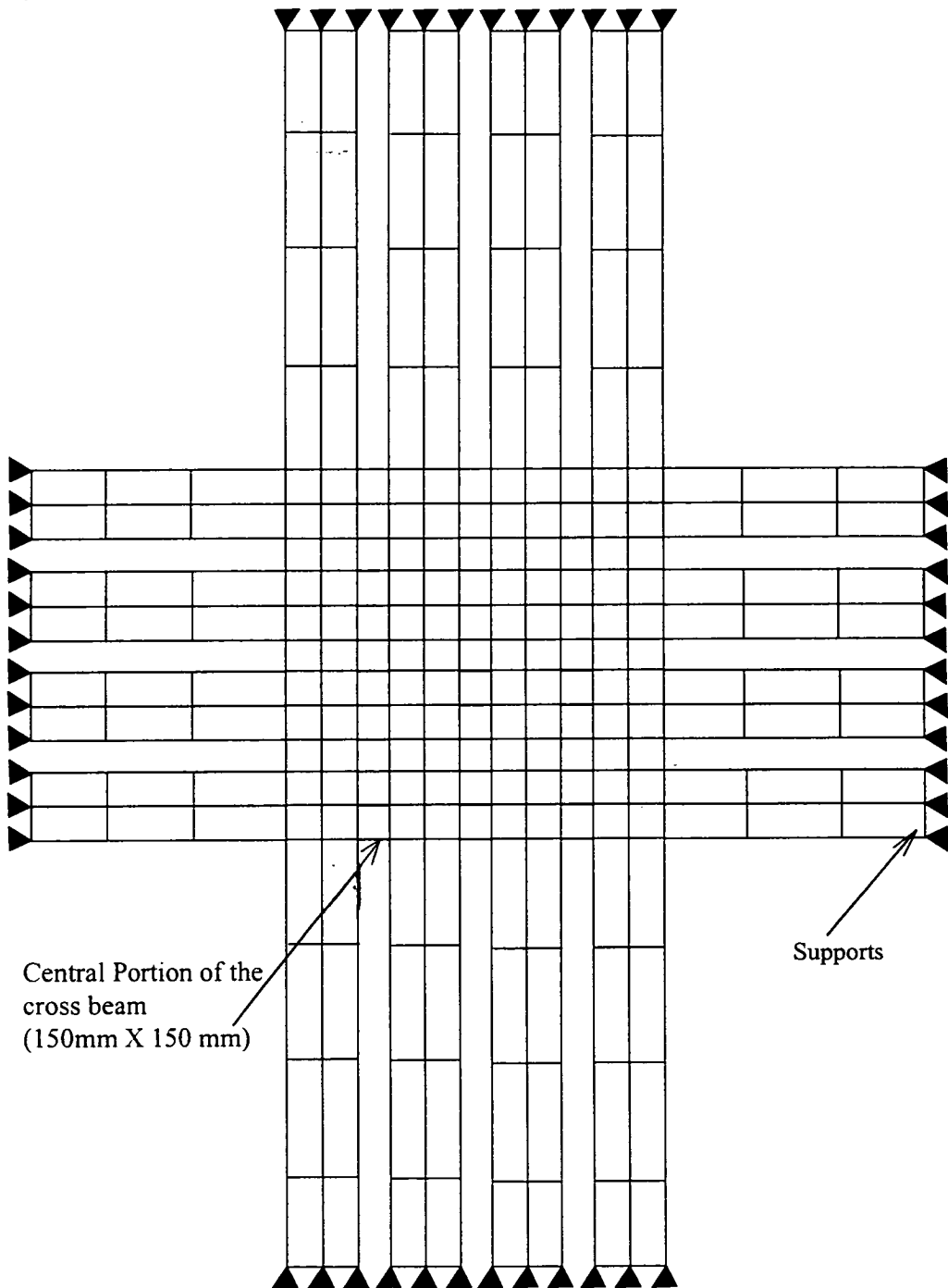


		Fx/Fy			
		L/H	1.3	2.0	3.0
FEM	0.75	0.041	0.041	0.041	
	1.0	0.041	0.041	0.040	
	1.5	0.037	0.037	0.038	
	2.0	0.030	0.034	0.039	
BS	0.75	0.048	0.051	0.0525	
	1.0	0.043	0.047	0.049	
	1.5	0.037	0.040	0.043	
	2.0	0.031	0.035	0.039	



## APPENDIX VI

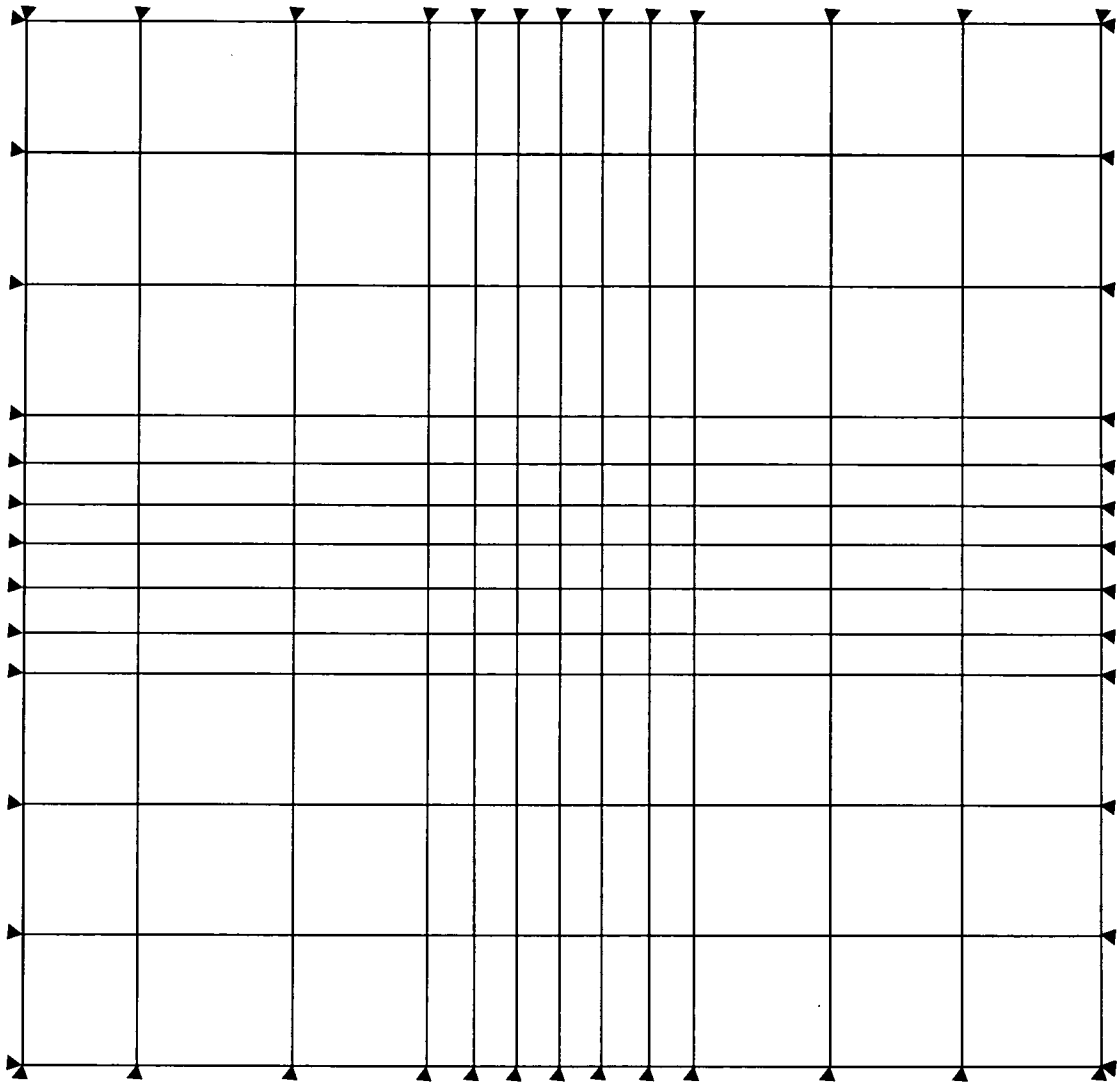
### Finite Element Mesh Used in the Cross Beam Analysis



The central portion of the cross beam is subjected to bi-axial bending and hence is the critical area while analysing the beam. Hence, the finite element mesh is made much finer in this area. The central portion consisted of 11x11 elements and was found to converge in the analysis. However, only fewer number of elements were required in the arms.

## APPENDIX VII

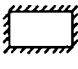
### Typical Finite Element Mesh Used in the Panel Analysis



The finite element mesh used for a four sides supported panel is shown above. As can be seen, the mesh is made finer at the center where the stress concentration occurs under bi-axial bending. In case of panels that are free on one side, the mesh is made finer at the center of the free edge, which forms critical in terms of stress concentration.

## APPENDIX VIII

**The training set used in training the net with the net outputs**

Set1 - 

No	Net inputs				Failure Pressure		
	$\frac{F_x Z}{L^2}$	L/H	Fx/Fy	Ex/Ey	NN $\times 10^{-3}$ (N/mm <sup>2</sup> )	FEM $\times 10^{-3}$ (N/mm <sup>2</sup> )	Ratio $\frac{FEM}{NN}$
1	1434	0.75	2.0	1.0	20.1	19.67	1.02
2	1434	0.75	2.0	1.4	19.85	19.97	0.99
3	1434	0.75	2.0	1.8	18.7	18.82	0.99
4	1434	0.75	2.0	0.8	18.45	18.98	0.97
5	2151	0.75	3.0	1.0	21.6	23.61	0.91
6	2151	0.75	3.0	1.4	26.3	25.58	1.03
7	2151	0.75	3.0	1.8	27.0	26.75	1.01
8	2151	0.75	3.0	0.8	22.78	22.87	1
9	807	1.0	2.0	1.0	11.7	12.62	0.93
10	807	1.0	2.0	1.4	13.9	14.05	0.99
11	807	1.0	2.0	1.8	14.4	14.78	0.97
12	807	1.0	2.0	0.8	11.52	12.06	0.96
13	1210	1.0	3.0	1.0	16.24	15.69	1.04
14	1210	1.0	3.0	1.4	15.02	16.14	0.93
15	1210	1.0	3.0	1.8	16.2	17.55	0.92
16	1210	1.0	3.0	0.8	17.05	15.78	1.08
17	359	1.5	2.0	1.0	8.38	7.75	1.08
18	359	1.5	2.0	1.4	7.52	7.77	0.97
19	359	1.5	2.0	1.8	7.6	8.58	0.89
20	359	1.5	2.0	0.8	8.08	7.89	1.02
21	538	1.5	3.0	1.0	11.8	11.05	1.07
22	538	1.5	3.0	1.4	10.82	10.69	1.01
23	538	1.5	3.0	1.8	10.02	10.41	0.96
24	538	1.5	3.0	0.8	12.16	11.16	1.09
25	202	2.0	2.0	1.0	7.08	6.54	1.08
26	202	2.0	2.0	1.4	6.85	6.55	1.05
27	202	2.0	2.0	1.8	6.12	6.51	0.94
28	202	2.0	2.0	0.8	6.98	6.49	1.08
29	303	2.0	3.0	1.0	10.42	9.37	1.11
30	303	2.0	3.0	1.4	10.18	9.41	1.08
31	303	2.0	3.0	1.8	9.15	9.3	0.98
32	303	2.0	3.0	0.8	9.12	9.29	0.98
33	3227	0.5	2.0	1.0	33.65	33.88	0.99
34	3227	0.5	2.0	1.4	32.0	30.9	1.04
35	3227	0.5	2.0	1.8	30.7	27.8	1.1
36	3227	0.5	2.0	0.8	34.5	34.75	0.99
37	4840	0.5	3.0	1.0	49.1	48.21	1.02
38	4840	0.5	3.0	1.4	48.0	48.65	0.99
39	4840	0.5	3.0	1.8	46.3	45.55	1.02
40	4840	0.5	3.0	0.8	47.3	46.75	1.01
41	637	0.75	2.0	1.0	8.95	8.7	1.03

42	637	0.75	2.0	1.4	8.85	9.0	0.98
43	637	0.75	2.0	1.8	8.3	8.28	1
44	637	0.75	2.0	0.8	8.2	8.28	0.99
45	956	0.75	3.0	1.0	9.95	10.28	0.97
46	956	0.75	3.0	1.4	11.7	11.0	1.06
47	956	0.75	3.0	1.8	12.0	11.81	1.02
48	956	0.75	3.0	0.8	10.28	10.23	1
49	359	1.0	2.0	1.0	5.2	5.34	0.97
50	359	1.0	2.0	1.4	6.2	6.13	1.01
51	359	1.0	2.0	1.8	6.4	6.59	0.97
52	359	1.0	2.0	0.8	4.98	5.16	0.97
53	538	1.0	3.0	1.0	7.25	7.13	1.02
54	538	1.0	3.0	1.4	6.85	6.83	1
55	538	1.0	3.0	1.8	7.2	7.34	0.98
56	538	1.0	3.0	0.8	7.52	7.47	1.01
57	159	1.5	2.0	1.0	3.48	3.44	1.01
58	159	1.5	2.0	1.4	3.28	3.14	1.04
59	159	1.5	2.0	1.8	3.4	3.51	0.97
60	159	1.5	2.0	0.8	3.52	3.69	0.95
61	239	1.5	3.0	1.0	5.18	5.25	0.99
62	239	1.5	3.0	1.4	4.92	4.81	1.02
63	239	1.5	3.0	1.8	4.48	4.29	1.04
64	239	1.5	3.0	0.8	5.25	5.38	0.98
65	90	2.0	2.0	1.0	3.32	3.17	1.05
66	90	2.0	2.0	1.4	3.05	3.11	0.98
67	90	2.0	2.0	1.8	2.75	2.99	0.92
68	90	2.0	2.0	0.8	3.12	3.14	0.99
69	135	2.0	3.0	1.0	4.72	4.38	1.08
70	135	2.0	3.0	1.4	4.62	4.39	1.05
71	135	2.0	3.0	1.8	4.08	4.25	0.96
72	135	2.0	3.0	0.8	4.02	4.3	0.93
73	1434	0.5	2.0	1.0	14.95	15.41	0.97
74	1434	0.5	2.0	1.4	14.2	13.98	1.02
75	1434	0.5	2.0	1.8	13.65	12.29	1.11
76	1434	0.5	2.0	0.8	15.35	15.7	0.98
77	2151	0.5	3.0	1.0	21.8	21.1	1.03
78	2151	0.5	3.0	1.4	21.3	21.6	0.99
79	2151	0.5	3.0	1.8	20.55	20.16	1.02
80	2151	0.5	3.0	0.8	21.05	20.4	1.03
81	2490	0.75	4.0	1.0	25.88	26.04	0.99
82	2490	0.75	4.0	1.4	25.98	26.01	1
83	2490	0.75	4.0	1.8	27.8	27.27	1.02
84	2490	0.75	4.0	0.8	26.43	26.47	1
85	455	1.0	1.3	1.0	9.75	9.02	1.08
86	455	1.0	1.3	1.4	9.5	9.47	1
87	455	1.0	1.3	1.8	8.7	8.91	0.98
88	455	1.0	1.3	0.8	9.1	8.49	1.07
89	1401	1.0	4.0	1.0	18.8	18.6	1.01
90	1401	1.0	4.0	1.4	17.48	17.78	0.98
91	1401	1.0	4.0	1.8	16.62	17.41	0.95
92	1401	1.0	4.0	0.8	19.28	19.04	1.01
93	623	1.5	4.0	1.0	12.72	12.9	0.99
94	623	1.5	4.0	1.4	12.85	12.74	1.01
95	623	1.5	4.0	1.8	11.78	12.32	0.96

96	623	1.5	4.0	0.8	12.95	12.88	1.01
97	114	2.0	1.3	1.0	4.45	4.36	1.02
98	114	2.0	1.3	1.4	4.4	4.34	1.01
99	114	2.0	1.3	1.8	4.65	4.51	1.03
100	114	2.0	1.3	0.8	4.25	4.39	0.97
101	350	2.0	4.0	1.0	12.52	10.66	1.17
102	350	2.0	4.0	1.4	11.38	11.15	1.02
103	350	2.0	4.0	1.8	10.85	11.32	0.96
104	350	2.0	4.0	0.8	10.25	11.29	0.91
105	1821	0.5	1.3	1.0	18.95	19.42	0.98
106	1821	0.5	1.3	1.4	17.9	17.9	1
107	1821	0.5	1.3	1.8	17.2	17.23	1
108	1821	0.5	1.3	0.8	19.65	20.29	0.97
109	5602	0.5	4.0	1.0	50.68	50.93	1
110	5602	0.5	4.0	1.4	54.6	54.06	1.01
111	5602	0.5	4.0	1.8	53.5	55.96	0.96
112	5602	0.5	4.0	0.8	51.18	49.78	1.03
113	1165	0.75	1.3	1.0	17.95	18.11	0.99
114	1165	0.75	1.3	1.4	16.45	17.22	0.96
115	1165	0.75	1.3	1.8	15.2	16.15	0.94
116	1165	0.75	1.3	0.8	18.65	18.17	1.03
117	3585	0.75	4.0	1.0	37.22	37.06	1
118	3585	0.75	4.0	1.4	37.04	37.63	0.98
119	3585	0.75	4.0	1.8	40.0	39.83	1
120	3585	0.75	4.0	0.8	37.78	37.44	1.01
121	656	1.0	1.3	1.0	14.05	13.03	1.08
122	656	1.0	1.3	1.4	13.65	13.62	1
123	656	1.0	1.3	1.8	12.5	13.07	0.96
124	656	1.0	1.3	0.8	13.1	12.36	1.06
125	2017	1.0	4.0	1.0	26.98	26.48	1.02
126	2017	1.0	4.0	1.4	25.02	25.51	0.98
127	2017	1.0	4.0	1.8	23.78	25.39	0.94
128	2017	1.0	4.0	0.8	27.72	27.13	1.02
129	291	1.5	1.3	1.0	7.8	7.26	1.07
130	291	1.5	1.3	1.4	8.9	8.25	1.08
131	291	1.5	1.3	1.8	9.7	9.75	0.99
132	291	1.5	1.3	0.8	7.38	7.09	1.04
133	896	1.5	4.0	1.0	19.05	18.77	1.01
134	896	1.5	4.0	1.4	18.5	18.39	1.01
135	896	1.5	4.0	1.8	17.08	17.83	0.96
136	896	1.5	4.0	0.8	18.35	18.87	0.97
137	164	2.0	1.3	1.0	7.2	5.98	1.2
138	164	2.0	1.3	1.4	6.25	5.96	1.05
139	164	2.0	1.3	1.8	6.7	6.18	1.08
140	164	2.0	1.3	0.8	7.85	5.97	1.31
141	504	2.0	4.0	1.0	16.9	15.48	1.09
142	504	2.0	4.0	1.4	16.75	16.02	1.05
143	504	2.0	4.0	1.8	15.18	16.21	0.94
144	504	2.0	4.0	0.8	12.42	15.07	0.82
145	2622	0.5	1.3	1.0	27.3	27.71	0.99
146	2622	0.5	1.3	1.4	25.8	25.76	1
147	2622	0.5	1.3	1.8	24.75	25.0	0.99
148	2622	0.5	1.3	0.8	28.3	28.86	0.98
149	8067	0.5	4.0	1.0	71.2	73.19	0.97

150	8067	0.5	4.0	1.4	78.65	76.0	1.03
151	8067	0.5	4.0	1.8	77.05	77.3	1
152	8067	0.5	4.0	0.8	71.92	71.86	1
153	518	0.75	1.3	1.0	8.0	8.17	0.98
154	518	0.75	1.3	1.4	7.3	7.47	0.98
155	518	0.75	1.3	1.8	6.75	6.48	1.04
156	518	0.75	1.3	0.8	8.3	8.2	1.01
157	291	1.0	1.3	1.0	6.25	5.83	1.07
158	291	1.0	1.3	1.4	6.05	6.18	0.98
159	291	1.0	1.3	1.8	5.55	5.62	0.99
160	291	1.0	1.3	0.8	5.85	5.41	1.08
161	896	1.0	4.0	1.0	11.95	12.06	0.99
162	896	1.0	4.0	1.4	11.15	11.37	0.98
163	896	1.0	4.0	1.8	10.88	10.83	1
164	896	1.0	4.0	0.8	12.32	12.34	1
165	130	1.5	1.3	1.0	3.45	3.18	1.08
166	130	1.5	1.3	1.4	3.95	3.78	1.04
167	130	1.5	1.3	1.8	4.35	4.91	0.89
168	130	1.5	1.3	0.8	3.32	3.18	1.04
169	73	2.0	1.3	1.0	2.88	3.12	0.92
170	73	2.0	1.3	1.4	2.8	3.05	0.92
171	73	2.0	1.3	1.8	3.0	3.18	0.94
172	73	2.0	1.3	0.8	3.55	3.14	1.13
173	224	2.0	4.0	1.0	7.85	6.91	1.14
174	224	2.0	4.0	1.4	7.35	7.35	1
175	224	2.0	4.0	1.8	6.75	7.51	0.9
176	224	2.0	4.0	0.8	6.76	6.58	1.03
177	1165	0.5	1.3	1.0	12.15	12.52	0.97
178	1165	0.5	1.3	1.4	11.55	11.29	1.02
179	1165	0.5	1.3	1.8	11.0	10.61	1.04
180	1165	0.5	1.3	0.8	12.6	13.17	0.96
181	3585	0.5	4.0	1.0	33.08	32.13	1.03
182	3585	0.5	4.0	1.4	34.95	34.04	1.03
183	3585	0.5	4.0	1.8	34.25	35.61	0.96
184	3585	0.5	4.0	0.8	31.35	31.65	0.99
185	90	2	4.0	1.0	3.12	3.15	0.99
186	90	2	4.0	1.6	2.78	3.63	0.77
187	90	2	4.0	1.3	2.88	3.46	0.83
188	90	2	4.0	0.7	3.12	2.71	1.15
189	347	2	1.3	1.0	12.1	12.19	0.99
190	347	2	1.3	1.6	13.7	12.51	1.1
191	347	2	1.3	1.3	13.22	12.29	1.08
192	347	2	1.3	0.7	11.15	12.06	0.92
193	125	1.5	1.3	1.0	3.08	2.86	1.08
194	125	1.5	4.0	1.6	2.62	2.91	0.9
195	125	1.5	4.0	1.3	2.82	2.98	0.95
196	125	1.5	4.0	0.7	3.15	2.57	1.23
197	906	1.5	4.0	1.0	24.25	24.47	0.99
198	906	1.5	1.3	1.6	29.15	28.98	1.01
199	906	1.5	1.3	1.3	27.0	26.54	1.02
200	906	1.5	1.3	0.7	21.15	23.05	0.92
201	2039	1.0	1.3	1.0	43.65	40.64	1.07
202	2039	1.0	1.3	1.6	40.75	41.87	0.97
203	2039	1.0	1.3	1.3	43.15	41.87	1.03

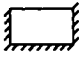
204	2039	1.0	1.3	0.7	38.15	38.15	1
205	316	1.0	4.0	1.0	4.18	4.62	0.9
206	316	1.0	4.0	1.6	3.9	3.72	1.05
207	316	1.0	4.0	1.3	4.0	4.23	0.95
208	316	1.0	4.0	0.7	4.22	4.77	0.88
209	563	0.75	4.0	1.0	5.82	6.02	0.97
210	563	0.75	4.0	1.6	5.95	5.13	1.16
211	563	0.75	4.0	1.3	6.08	5.46	1.11
212	563	0.75	4.0	0.7	6.35	6.55	0.97
213	2543	0.75	1.3	1.0	39.2	38.61	1.02
214	2543	0.75	1.3	1.6	34.45	36.44	0.95
215	2543	0.75	1.3	1.3	36.65	37.63	0.97
216	2543	0.75	1.3	0.7	40.8	38.65	1.06
217	1266	0.5	4.0	1.0	11.88	10.71	1.11
218	1266	0.5	4.0	1.6	12.25	11.15	1.1
219	1266	0.5	4.0	1.3	12.35	10.7	1.15
220	1266	0.5	4.0	0.7	11.25	11.15	1.01
221	5722	0.5	1.3	1.0	59.6	59.88	1
222	5722	0.5	1.3	1.6	55.1	55.78	0.99
223	5722	0.5	1.3	1.3	57.05	57.53	0.99
224	5722	0.5	1.3	0.7	62.95	62.18	1.01
225	1434	0.75	2.0	0.6	15.15	18.14	0.84
226	1434	0.75	2.0	0.9	19.3	19.36	1
227	1434	0.75	2.0	1.2	20.3	20.03	1.01
228	1434	0.75	2.0	1.6	19.3	19.52	0.99
229	2151	0.75	3.0	0.6	22.6	22.44	1.01
230	2151	0.75	3.0	0.9	22.05	23.2	0.95
231	2151	0.75	3.0	1.2	24.5	24.57	1
232	2151	0.75	3.0	1.6	27.05	26.39	1.03
233	807	1.0	2.0	0.6	12.12	11.74	1.03
234	807	1.0	2.0	0.9	10.95	12.32	0.89
235	807	1.0	2.0	1.2	13.0	13.34	0.97
236	807	1.0	2.0	1.6	14.35	14.57	0.98
237	1210	1.0	3.0	0.6	17.65	16.01	1.1
238	1210	1.0	3.0	0.9	16.65	15.71	1.06
239	1210	1.0	3.0	1.2	15.28	15.79	0.97
240	1210	1.0	3.0	1.6	15.1	16.75	0.9
241	359	1.5	2.0	0.6	8.95	8.05	1.11
242	359	1.5	2.0	0.9	8.42	7.81	1.08
243	359	1.5	2.0	1.2	7.42	7.69	0.96
244	359	1.5	2.0	1.6	7.32	8.07	0.91
245	538	1.5	3.0	0.6	10.55	11.23	0.94
246	538	1.5	3.0	0.9	12.05	11.11	1.08
247	538	1.5	3.0	1.2	11.35	10.88	1.04
248	538	1.5	3.0	1.6	10.45	10.52	0.99
249	202	2.0	2.0	0.6	5.45	6.4	0.85
250	202	2.0	2.0	0.9	7.32	6.52	1.12
251	202	2.0	2.0	1.2	7.28	6.56	1.11
252	202	2.0	2.0	1.6	6.48	6.52	0.99
253	303	2.0	3.0	0.6	5.42	9.17	0.59
254	303	2.0	3.0	0.9	10.48	9.33	1.12
255	303	2.0	3.0	1.2	10.05	9.41	1.07
256	303	2.0	3.0	1.6	9.18	9.37	0.98
257	3227	0.5	2.0	0.6	34.25	34.93	0.98

258	3227	0.5	2.0	0.9	34.1	34.39	0.99
259	3227	0.5	2.0	1.2	32.8	32.52	1.01
260	3227	0.5	2.0	1.6	31.3	29.26	1.07
261	4840	0.5	3.0	0.6	40.52	44.85	0.9
262	4840	0.5	3.0	0.9	48.65	47.56	1.02
263	4840	0.5	3.0	1.2	48.75	48.89	1
264	4840	0.5	3.0	1.6	47.1	47.48	0.99
265	637	0.75	2.0	0.6	6.75	7.88	0.86
266	637	0.75	2.0	0.9	8.7	8.5	1.02
267	637	0.75	2.0	1.2	9.0	8.97	1
268	637	0.75	2.0	1.6	8.6	8.74	0.98
269	956	0.75	3.0	0.6	10.35	10.4	1
270	956	0.75	3.0	0.9	10.02	10.23	0.98
271	956	0.75	3.0	1.2	10.9	10.55	1.03
272	956	0.75	3.0	1.6	12.05	11.47	1.05
273	359	1.0	2.0	0.6	5.52	5.2	1.06
274	359	1.0	2.0	0.9	4.85	5.22	0.93
275	359	1.0	2.0	1.2	5.8	5.7	1.02
276	359	1.0	2.0	1.6	6.4	6.46	0.99
277	538	1.0	3.0	0.6	7.65	7.84	0.98
278	538	1.0	3.0	0.9	7.28	7.29	1
279	538	1.0	3.0	1.2	7.02	6.89	1.02
280	538	1.0	3.0	1.6	6.75	6.99	0.97
281	159	1.5	2.0	0.6	3.82	3.94	0.97
282	159	1.5	2.0	0.9	3.52	3.56	0.99
283	159	1.5	2.0	1.2	3.65	3.23	1.13
284	159	1.5	2.0	1.6	3.32	3.22	1.03
285	239	1.5	3.0	0.6	4.55	5.42	0.84
286	239	1.5	3.0	0.9	5.35	5.32	1.01
287	239	1.5	3.0	1.2	5.02	5.06	0.99
288	239	1.5	3.0	1.6	4.48	4.54	0.99
289	90	2.0	2.0	0.6	3.12	3.08	1.01
290	90	2.0	2.0	0.9	3.15	3.16	1
291	90	2.0	2.0	1.2	3.15	3.16	1
292	90	2.0	2.0	1.6	2.88	3.05	0.94
293	135	2.0	3.0	0.6	2.82	4.2	0.67
294	135	2.0	3.0	0.9	4.65	4.35	1.07
295	135	2.0	3.0	1.2	4.78	4.4	1.09
296	135	2.0	3.0	1.6	4.32	4.34	1
297	1434	0.5	2.0	0.6	15.25	15.61	0.98
298	1434	0.5	2.0	0.9	15.15	15.6	0.97
299	1434	0.5	2.0	1.2	14.55	14.8	0.98
300	1434	0.5	2.0	1.6	13.9	13.11	1.06
301	2151	0.5	3.0	0.6	18.68	19.7	0.95
302	2151	0.5	3.0	0.9	21.65	20.77	1.04
303	2151	0.5	3.0	1.2	21.65	21.57	1
304	2151	0.5	3.0	1.6	20.95	21.12	0.99
305	2490	0.75	4.0	0.6	26.75	27.09	0.99
306	2490	0.75	4.0	0.9	26.22	26.23	1
307	2490	0.75	4.0	1.2	25.58	25.87	0.99
308	2490	0.75	4.0	1.6	26.15	26.5	0.99
309	455	1.0	1.3	0.6	7.8	7.94	0.98
310	455	1.0	1.3	0.9	9.5	8.77	1.08
311	455	1.0	1.3	1.2	9.75	9.38	1.04



312	455	1.0	1.3	1.6	9.1	9.3	0.98
313	1401	1.0	4.0	0.6	20.25	19.46	1.04
314	1401	1.0	4.0	0.9	19.08	18.82	1.01
315	1401	1.0	4.0	1.2	18.05	18.16	0.99
316	1401	1.0	4.0	1.6	16.72	17.5	0.96
317	623	1.5	4.0	0.6	10.25	12.78	0.8
318	623	1.5	4.0	0.9	13.28	12.9	1.03
319	623	1.5	4.0	1.2	13.08	12.86	1.02
320	623	1.5	4.0	1.6	12.15	12.56	0.97
321	114	2.0	1.3	0.6	3.75	4.36	0.86
322	114	2.0	1.3	0.9	5.25	4.39	1.2
323	114	2.0	1.3	1.2	4.2	4.36	0.96
324	114	2.0	1.3	1.6	4.5	4.37	1.03
325	350	2.0	4.0	0.6	7.95	9.83	0.81
326	350	2.0	4.0	0.9	11.18	10.49	1.07
327	350	2.0	4.0	1.2	11.65	10.95	1.06
328	350	2.0	4.0	1.6	11.18	11.27	0.99
329	1821	0.5	1.3	0.6	20.45	21.03	0.97
330	1821	0.5	1.3	0.9	19.3	19.86	0.97
331	1821	0.5	1.3	1.2	18.4	18.58	0.99
332	1821	0.5	1.3	1.6	18.15	17.43	1.04
333	5602	0.5	4.0	0.6	48.42	49.2	0.98
334	5602	0.5	4.0	0.9	50.75	50.29	1.01
335	5602	0.5	4.0	1.2	54.25	52.46	1.03
336	5602	0.5	4.0	1.6	54.15	55.34	0.98
337	518	0.75	1.3	0.6	8.1	7.98	1.02
338	518	0.75	1.3	0.9	8.15	8.22	0.99
339	518	0.75	1.3	1.2	7.65	7.9	0.97
340	518	0.75	1.3	1.6	7.0	6.97	1
341	291	1.0	1.3	0.6	5.0	5.0	1
342	291	1.0	1.3	0.9	6.1	5.63	1.08
343	291	1.0	1.3	1.2	6.25	6.12	1.02
344	291	1.0	1.3	1.6	5.85	5.99	0.98
345	896	1.0	4.0	0.6	13.02	12.55	1.04
346	896	1.0	4.0	0.9	12.32	12.21	1.01
347	896	1.0	4.0	1.2	11.65	11.72	0.99
348	896	1.0	4.0	1.6	10.78	11.05	0.98
349	130	1.5	1.3	0.6	3.55	3.32	1.07
350	130	1.5	1.3	0.9	3.35	3.16	1.06
351	130	1.5	1.3	1.2	3.75	3.38	1.11
352	130	1.5	1.3	1.6	4.15	4.34	0.96
353	73	2.0	1.3	0.6	2.62	3.12	0.84
354	73	2.0	1.3	0.9	2.83	3.13	0.9
355	73	2.0	1.3	1.2	3.0	3.08	0.97
356	73	2.0	1.3	1.6	2.9	3.06	0.95
357	224	2.0	4.0	0.6	5.92	6.18	0.96
358	224	2.0	4.0	0.9	8.28	6.76	1.22
359	224	2.0	4.0	1.2	7.48	7.17	1.04
360	224	2.0	4.0	1.6	7.25	7.46	0.97
361	1165	0.5	1.3	0.6	13.1	13.68	0.96
362	1165	0.5	1.3	0.9	12.35	12.86	0.96
363	1165	0.5	1.3	1.2	11.75	11.87	0.99
364	1165	0.5	1.3	1.6	11.2	10.86	1.03
365	3585	0.5	4.0	0.6	31.32	31.58	0.99

366	3585	0.5	4.0	0.9	33.38	31.84	1.05
367	3585	0.5	4.0	1.2	34.75	32.98	1.05
368	3585	0.5	4.0	1.6	34.65	35.03	0.99
369	382	0.75	1.2	0.6	6.25	6.14	1.02
370	382	0.75	1.2	0.9	6.1	6.25	0.98
371	382	0.75	1.2	1.2	5.65	5.85	0.97
372	382	0.75	1.2	1.6	5.2	4.92	1.06
373	1402	0.75	4.4	0.6	14.98	16.31	0.92
374	1402	0.75	4.4	0.9	14.73	15.64	0.94
375	1402	0.75	4.4	1.2	14.78	14.95	0.99
376	1402	0.75	4.4	1.6	14.75	14.27	1.03
377	215	1.0	1.2	0.6	4.05	3.86	1.05
378	215	1.0	1.2	0.9	4.75	4.43	1.07
379	215	1.0	1.2	1.2	4.7	4.79	0.98
380	215	1.0	1.2	1.6	4.35	4.51	0.96
381	789	1.0	4.4	0.6	11.25	10.93	1.03
382	789	1.0	4.4	0.9	10.35	10.86	0.95
383	789	1.0	4.4	1.2	10.18	10.57	0.96
384	789	1.0	4.4	1.6	9.42	9.93	0.95
385	96	1.5	1.2	0.6	2.52	2.57	0.98
386	96	1.5	1.2	0.9	2.7	2.45	1.1
387	96	1.5	1.2	1.2	3.0	2.74	1.09
388	96	1.5	1.2	1.6	3.35	3.72	0.9
389	351	1.5	4.4	0.6	6.52	6.48	1.01
390	351	1.5	4.4	0.9	7.25	6.91	1.05
391	351	1.5	4.4	1.2	6.78	7.19	0.94
392	351	1.5	4.4	1.6	6.65	7.28	0.91
393	54	2.0	1.2	0.6	1.85	2.64	0.7
394	54	2.0	1.2	0.9	2.22	2.64	0.84
395	54	2.0	1.2	1.2	2.28	2.57	0.89
396	54	2.0	1.2	1.6	2.35	2.57	0.91
397	197	2.0	4.4	0.6	3.98	4.55	0.87
398	197	2.0	4.4	0.9	6.38	5.39	1.18
399	197	2.0	4.4	1.2	6.55	6.06	1.08
400	197	2.0	4.4	1.6	6.12	6.67	0.92
401	861	0.5	1.2	0.6	9.7	10.28	0.94
402	861	0.5	1.2	0.9	9.1	9.54	0.95
403	861	0.5	1.2	1.2	8.7	8.69	1
404	861	0.5	1.2	1.6	8.25	7.84	1.05
405	3155	0.5	4.4	0.6	27.35	29.48	0.93
406	3155	0.5	4.4	0.9	29.12	28.68	1.02
407	3155	0.5	4.4	1.2	29.15	28.61	1.02
408	3155	0.5	4.4	1.6	30.3	29.73	1.02

Set2 

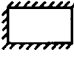
No	Net inputs				Failure Pressure		
	$\frac{F_x Z}{L^2}$	L/H	Fx/Fy	Ex/Ey	NN output	FEM	Ratio
					$\times 10^{-3}$ (N/mm <sup>2</sup> )	$\times 10^{-3}$ (N/mm <sup>2</sup> )	$\frac{\text{FEM}}{\text{NN}}$
1	1434	0.75	2.0	1.0	13	12.8	1.02
2	1434	0.75	2.0	1.4	12.65	12.65	1
3	1434	0.75	2.0	1.8	12.35	13.3	0.93
4	1434	0.75	2.0	0.8	13.3	13.08	1.02
5	2151	0.75	3.0	1.0	19.5	19.3	1.01
6	2151	0.75	3.0	1.4	19.05	19.27	0.99
7	2151	0.75	3.0	1.8	18.65	19.14	0.97
8	2151	0.75	3.0	0.8	19.85	18.95	1.05
9	807	1.0	2.0	1.0	8.45	8.45	1
10	807	1.0	2.0	1.4	8.0	8.26	0.97
11	807	1.0	2.0	1.8	7.7	8.04	0.96
12	807	1.0	2.0	0.8	8.65	7.99	1.08
13	1210	1.0	3.0	1.0	12.3	11.81	1.04
14	1210	1.0	3.0	1.4	12.0	11.75	1.02
15	1210	1.0	3.0	1.8	11.6	11.63	1
16	1210	1.0	3.0	0.8	11.85	11.55	1.03
17	359	1.5	2.0	1.0	5.05	4.82	1.05
18	359	1.5	2.0	1.4	5.0	4.68	1.07
19	359	1.5	2.0	1.8	4.7	4.58	1.03
20	359	1.5	2.0	0.8	4.6	4.58	1
21	538	1.5	3.0	1.0	5.75	6.36	0.9
22	538	1.5	3.0	1.4	6.6	6.26	1.05
23	538	1.5	3.0	1.8	6.75	6.17	1.09
24	538	1.5	3.0	0.8	5.92	6.26	0.95
25	202	2.0	2.0	1.0	2.95	3.53	0.84
26	202	2.0	2.0	1.4	3.5	3.43	1.02
27	202	2.0	2.0	1.8	2.95	3.4	0.87
28	202	2.0	2.0	0.8	3.02	3.4	0.89
29	303	2.0	3.0	1.0	4.05	4.5	0.9
30	303	2.0	3.0	1.4	4.0	4.36	0.92
31	303	2.0	3.0	1.8	4.05	4.24	0.96
32	303	2.0	3.0	0.8	4.18	4.39	0.95
33	3227	0.5	2.0	1.0	26.95	26.86	1
34	3227	0.5	2.0	1.4	26.6	26.62	1
35	3227	0.5	2.0	1.8	26.4	26.32	1
36	3227	0.5	2.0	0.8	27.15	26.15	1.04
37	4840	0.5	3.0	1.0	40.65	41.0	0.99
38	4840	0.5	3.0	1.4	40.2	40.86	0.98
39	4840	0.5	3.0	1.8	39.85	40.5	0.98
40	4840	0.5	3.0	0.8	40.8	40.06	1.02
41	637	0.75	2.0	1.0	5.8	6.05	0.96
42	637	0.75	2.0	1.4	5.6	5.87	0.95
43	637	0.75	2.0	1.8	5.5	5.65	0.97
44	637	0.75	2.0	0.8	5.9	5.57	1.06
45	956	0.75	3.0	1.0	8.7	8.84	0.98
46	956	0.75	3.0	1.4	8.5	8.78	0.97
47	956	0.75	3.0	1.8	8.3	8.6	0.97

48	956	0.75	3.0	0.8	8.85	8.41	1.05
49	359	1.0	2.0	1.0	3.75	3.8	0.99
50	359	1.0	2.0	1.4	3.6	3.66	0.98
51	359	1.0	2.0	1.8	3.45	3.52	0.98
52	359	1.0	2.0	0.8	3.85	3.54	1.09
53	538	1.0	3.0	1.0	5.5	5.39	1.02
54	538	1.0	3.0	1.4	5.35	5.33	1
55	538	1.0	3.0	1.8	5.15	5.22	0.99
56	538	1.0	3.0	0.8	5.3	5.18	1.02
57	159	1.5	2.0	1.0	2.25	2.07	1.09
58	159	1.5	2.0	1.4	2.2	1.98	1.11
59	159	1.5	2.0	1.8	2.1	1.94	1.08
60	159	1.5	2.0	0.8	2.05	2.08	0.99
61	239	1.5	3.0	1.0	2.6	2.73	0.95
62	239	1.5	3.0	1.4	2.95	2.66	1.11
63	239	1.5	3.0	1.8	3.0	2.62	1.15
64	239	1.5	3.0	0.8	2.68	2.76	0.97
65	90	2.0	2.0	1.0	1.3	1.47	0.88
66	90	2.0	2.0	1.4	1.55	1.41	1.1
67	90	2.0	2.0	1.8	1.6	1.44	1.11
68	90	2.0	2.0	0.8	1.35	1.64	0.82
69	135	2.0	3.0	1.0	1.8	1.79	1.01
70	135	2.0	3.0	1.4	1.8	1.69	1.07
71	135	2.0	3.0	1.8	1.8	1.63	1.1
72	135	2.0	3.0	0.8	1.95	1.83	1.07
73	1434	0.5	2.0	1.0	12.15	12.23	0.99
74	1434	0.5	2.0	1.4	11.85	12.01	0.99
75	1434	0.5	2.0	1.8	11.75	11.69	1.01
76	1434	0.5	2.0	0.8	12.1	11.45	1.06
77	2151	0.5	3.0	1.0	18.35	18.36	1
78	2151	0.5	3.0	1.4	17.9	18.32	0.98
79	2151	0.5	3.0	1.8	17.75	18.11	0.98
80	2151	0.5	3.0	0.8	18.15	17.73	1.02
81	2490	0.75	4.0	1.0	22.35	21.43	1.04
82	2490	0.75	4.0	1.4	22.1	21.94	1.01
83	2490	0.75	4.0	1.8	21.65	21.83	0.99
84	2490	0.75	4.0	0.8	21.7	20.93	1.04
85	455	1.0	1.3	1.0	4.75	4.91	0.97
86	455	1.0	1.3	1.4	4.5	4.62	0.97
87	455	1.0	1.3	1.8	4.3	4.44	0.97
88	455	1.0	1.3	0.8	4.95	5.11	0.97
89	1401	1.0	4.0	1.0	12.5	12.73	0.98
90	1401	1.0	4.0	1.4	13.7	13.06	1.05
91	1401	1.0	4.0	1.8	13.4	12.98	1.03
92	1401	1.0	4.0	0.8	11.28	12.4	0.91
93	623	1.5	4.0	1.0	6.52	6.59	0.99
94	623	1.5	4.0	1.4	6.58	6.76	0.97
95	623	1.5	4.0	1.8	6.95	6.8	1.02
96	623	1.5	4.0	0.8	6.85	6.44	1.06
97	114	2.0	1.3	1.0	2.45	2.34	1.05
98	114	2.0	1.3	1.4	2.4	2.28	1.05
99	114	2.0	1.3	1.8	2.2	2.26	0.97
100	114	2.0	1.3	0.8	2.3	2.41	0.95
101	350	2.0	4.0	1.0	4.6	4.55	1.01

102	350	2.0	4.0	1.4	4.5	4.55	0.99
103	350	2.0	4.0	1.8	4.35	4.6	0.95
104	350	2.0	4.0	0.8	4.62	4.53	1.02
105	1821	0.5	1.3	1.0	15.15	15.06	1.01
106	1821	0.5	1.3	1.4	14.9	14.64	1.02
107	1821	0.5	1.3	1.8	14.8	14.32	1.03
108	1821	0.5	1.3	0.8	15.25	15.34	0.99
109	5602	0.5	4.0	1.0	47.2	47.08	1
110	5602	0.5	4.0	1.4	46.75	47.34	0.99
111	5602	0.5	4.0	1.8	46.4	46.89	0.99
112	5602	0.5	4.0	0.8	46.62	46.64	1
113	1165	0.75	1.3	1.0	10.5	10.9	0.96
114	1165	0.75	1.3	1.4	10.2	10.49	0.97
115	1165	0.75	1.3	1.8	9.95	10.19	0.98
116	1165	0.75	1.3	0.8	10.75	11.17	0.96
117	3585	0.75	4.0	1.0	32	31.05	1.03
118	3585	0.75	4.0	1.4	31.8	31.66	1
119	3585	0.75	4.0	1.8	31.2	31.62	0.99
120	3585	0.75	4.0	0.8	29.42	30.47	0.97
121	656	1.0	1.3	1.0	6.9	7.08	0.97
122	656	1.0	1.3	1.4	6.5	6.75	0.96
123	656	1.0	1.3	1.8	6.2	6.52	0.95
124	656	1.0	1.3	0.8	7.1	7.32	0.97
125	2017	1.0	4.0	1.0	18	18.23	0.99
126	2017	1.0	4.0	1.4	19.7	18.7	1.05
127	2017	1.0	4.0	1.8	19.3	18.7	1.03
128	2017	1.0	4.0	0.8	16.12	17.82	0.9
129	291	1.5	1.3	1.0	4.5	4.28	1.05
130	291	1.5	1.3	1.4	4.1	4.08	1
131	291	1.5	1.3	1.8	3.8	3.96	0.96
132	291	1.5	1.3	0.8	4.7	4.43	1.06
133	896	1.5	4.0	1.0	9.45	9.48	1
134	896	1.5	4.0	1.4	9.3	9.68	0.96
135	896	1.5	4.0	1.8	10.0	9.68	1.03
136	896	1.5	4.0	0.8	9.85	9.31	1.06
137	164	2.0	1.3	1.0	3.55	3.33	1.07
138	164	2.0	1.3	1.4	3.4	3.23	1.05
139	164	2.0	1.3	1.8	3.15	3.19	0.99
140	164	2.0	1.3	0.8	3.3	3.41	0.97
141	504	2.0	4.0	1.0	6.75	6.68	1.01
142	504	2.0	4.0	1.4	6.55	6.67	0.98
143	504	2.0	4.0	1.8	6.15	6.69	0.92
144	504	2.0	4.0	0.8	6.62	6.67	0.99
145	2622	0.5	1.3	1.0	21.75	21.52	1.01
146	2622	0.5	1.3	1.4	21.45	21.12	1.02
147	2622	0.5	1.3	1.8	21.35	20.84	1.02
148	2622	0.5	1.3	0.8	21.9	21.81	1
149	8067	0.5	4.0	1.0	67.75	67.47	1
150	8067	0.5	4.0	1.4	67.3	66.92	1.01
151	8067	0.5	4.0	1.8	66.75	65.91	1.01
152	8067	0.5	4.0	0.8	66.92	67.53	0.99
153	518	0.75	1.3	1.0	4.7	4.82	0.98
154	518	0.75	1.3	1.4	4.55	4.51	1.01
155	518	0.75	1.3	1.8	4.45	4.31	1.03

156	518	0.75	1.3	0.8	4.8	5.04	0.95
157	291	1.0	1.3	1.0	3.05	3.1	0.98
158	291	1.0	1.3	1.4	2.9	2.87	1.01
159	291	1.0	1.3	1.8	2.75	2.73	1.01
160	291	1.0	1.3	0.8	3.15	3.28	0.96
161	896	1.0	4.0	1.0	8.0	8.26	0.97
162	896	1.0	4.0	1.4	8.75	8.47	1.03
163	896	1.0	4.0	1.8	8.6	8.34	1.03
164	896	1.0	4.0	0.8	7.32	8.01	0.91
165	130	1.5	1.3	1.0	2.0	1.91	1.05
166	130	1.5	1.3	1.4	1.85	1.78	1.04
167	130	1.5	1.3	1.8	1.7	1.73	0.98
168	130	1.5	1.3	0.8	2.1	2.02	1.04
169	73	2.0	1.3	1.0	1.6	1.54	1.04
170	73	2.0	1.3	1.4	1.55	1.5	1.03
171	73	2.0	1.3	1.8	1.4	1.5	0.93
172	73	2.0	1.3	0.8	1.5	1.59	0.94
173	224	2.0	4.0	1.0	3.02	2.8	1.08
174	224	2.0	4.0	1.4	2.8	2.83	0.99
175	224	2.0	4.0	1.8	2.8	2.89	0.97
176	224	2.0	4.0	0.8	3.22	2.78	1.16
177	1165	0.5	1.3	1.0	9.75	9.66	1.01
178	1165	0.5	1.3	1.4	9.55	9.26	1.03
179	1165	0.5	1.3	1.8	9.5	8.94	1.06
180	1165	0.5	1.3	0.8	9.75	9.93	0.98
181	3585	0.5	4.0	1.0	30.3	29.82	1.02
182	3585	0.5	4.0	1.4	29.95	30.36	0.99
183	3585	0.5	4.0	1.8	29.7	30.12	0.99
184	3585	0.5	4.0	0.8	30.05	29.23	1.03
185	90	2	4.0	1.0	1.28	0.96	1.33
186	90	2	4.0	1.6	1.18	0.99	1.19
187	90	2	4.0	1.3	1.1	1.03	1.07
188	90	2	4.0	0.7	1.2	0.9	1.33
189	347	2	1.3	1.0	7.45	7.02	1.06
190	347	2	1.3	1.6	6.95	6.84	1.02
191	347	2	1.3	1.3	7.35	6.71	1.1
192	347	2	1.3	0.7	6.5	7.27	0.89
193	125	1.5	1.3	1.0	1.4	1.28	1.09
194	125	1.5	4.0	1.6	1.3	1.39	0.94
195	125	1.5	4.0	1.3	1.4	1.44	0.97
196	125	1.5	4.0	0.7	1.4	1.08	1.3
197	906	1.5	4.0	1.0	13.95	13.19	1.06
198	906	1.5	1.3	1.6	12.25	12.81	0.96
199	906	1.5	1.3	1.3	13.05	12.5	1.04
200	906	1.5	1.3	0.7	14.55	13.69	1.06
201	2039	1.0	1.3	1.0	21.3	21.21	1
202	2039	1.0	1.3	1.6	19.65	20.76	0.95
203	2039	1.0	1.3	1.3	20.35	20.42	1
204	2039	1.0	1.3	0.7	22.5	21.82	1.03
205	316	1.0	4.0	1.0	2.85	3.11	0.92
206	316	1.0	4.0	1.6	3.1	3.22	0.96
207	316	1.0	4.0	1.3	3.1	3.17	0.98
208	316	1.0	4.0	0.7	2.95	2.83	1.04
209	563	0.75	4.0	1.0	5.05	5.15	0.98

210	563	0.75	4.0	1.6	4.95	5.24	0.94
211	563	0.75	4.0	1.3	5.05	5.11	0.99
212	563	0.75	4.0	0.7	4.6	4.83	0.95
213	2543	0.75	1.3	1.0	22.95	23.18	0.99
214	2543	0.75	1.3	1.6	21.95	22.79	0.96
215	2543	0.75	1.3	1.3	22.35	22.51	0.99
216	2543	0.75	1.3	0.7	23.75	23.74	1
217	1266	0.5	4.0	1.0	10.65	10.68	1
218	1266	0.5	4.0	1.6	10.55	10.8	0.98
219	1266	0.5	4.0	1.3	10.6	10.59	1
220	1266	0.5	4.0	0.7	10.5	10.22	1.03
221	5722	0.5	1.3	1.0	47.35	47.43	1
222	5722	0.5	1.3	1.6	46.65	46.91	0.99
223	5722	0.5	1.3	1.3	46.95	46.59	1.01
224	5722	0.5	1.3	0.7	48.05	48.22	1

Set3 - 

No	Net inputs				Failure Pressure		
	$\frac{F_x Z}{L^2}$	L/H	Fx/Fy	Ex/Ey	NN output x10 <sup>-3</sup> (N/mm <sup>2</sup> )	FEM x10 <sup>-3</sup> (N/mm <sup>2</sup> )	Ratio $\frac{FEM}{NN}$
1	1434	0.75	2.0	1.0	7.68	7.99	0.96
2	1434	0.75	2.0	1.4	7.45	8.26	0.9
3	1434	0.75	2.0	1.8	7.6	8.44	0.9
4	1434	0.75	2.0	0.8	8.0	7.81	1.02
5	2151	0.75	3.0	1.0	11.2	11.04	1.01
6	2151	0.75	3.0	1.4	11.2	10.59	1.06
7	2151	0.75	3.0	1.8	10.1	10.17	0.99
8	2151	0.75	3.0	0.8	11.6	11.15	1.04
9	807	1.0	2.0	1.0	6.3	5.89	1.07
10	807	1.0	2.0	1.4	5.8	6.22	0.93
11	807	1.0	2.0	1.8	5.65	6.32	0.89
12	807	1.0	2.0	0.8	6.5	5.62	1.16
13	1210	1.0	3.0	1.0	8.15	8.0	1.02
14	1210	1.0	3.0	1.4	8.64	8.48	1.02
15	1210	1.0	3.0	1.8	8.38	8.45	0.99
16	1210	1.0	3.0	0.8	6.93	7.53	0.92
17	359	1.5	2.0	1.0	3.59	3.86	0.93
18	359	1.5	2.0	1.4	4.3	4.44	0.97
19	359	1.5	2.0	1.8	4.05	4.50	0.9
20	359	1.5	2.0	0.8	3.53	3.46	1.02
21	538	1.5	3.0	1.0	3.53	4.07	0.87
22	538	1.5	3.0	1.4	4.12	4.88	0.84
23	538	1.5	3.0	1.8	4.33	5.25	0.82
24	538	1.5	3.0	0.8	3.48	3.56	0.98
25	202	2.0	2.0	1.0	3.41	3.39	1.01
26	202	2.0	2.0	1.4	3.44	3.66	0.94
27	202	2.0	2.0	1.8	3.48	3.52	0.99
28	202	2.0	2.0	0.8	3.39	3.18	1.07
29	303	2.0	3.0	1.0	3.37	3.34	1.01

30	303	2.0	3.0	1.4	3.72	3.84	0.97
31	303	2.0	3.0	1.8	3.43	3.79	0.91
32	303	2.0	3.0	0.8	3.4	2.96	1.15
33	3227	0.5	2.0	1.0	11.7	12.69	0.92
34	3227	0.5	2.0	1.4	13.9	12.96	1.07
35	3227	0.5	2.0	1.8	14.4	13.10	1.1
36	3227	0.5	2.0	0.8	11.4	12.49	0.91
37	4840	0.5	3.0	1.0	16.15	16.76	0.96
38	4840	0.5	3.0	1.4	15.1	16.33	0.92
39	4840	0.5	3.0	1.8	16.2	15.95	1.02
40	4840	0.5	3.0	0.8	17.15	16.96	1.01
41	637	0.75	2.0	1.0	3.4	3.48	0.98
42	637	0.75	2.0	1.4	3.3	3.55	0.93
43	637	0.75	2.0	1.8	3.36	3.60	0.93
44	637	0.75	2.0	0.8	3.5	3.42	1.02
45	956	0.75	3.0	1.0	5.05	5.01	1.01
46	956	0.75	3.0	1.4	4.9	4.67	1.05
47	956	0.75	3.0	1.8	4.4	4.47	0.98
48	956	0.75	3.0	0.8	5.33	5.14	1.04
49	359	1.0	2.0	1.0	2.8	2.46	1.14
50	359	1.0	2.0	1.4	2.6	2.48	1.05
51	359	1.0	2.0	1.8	2.27	2.36	0.96
52	359	1.0	2.0	0.8	2.8	2.37	1.18
53	538	1.0	3.0	1.0	3.5	3.78	0.93
54	538	1.0	3.0	1.4	4.0	3.92	1.02
55	538	1.0	3.0	1.8	3.85	3.76	1.02
56	538	1.0	3.0	0.8	3.1	3.55	0.87
57	159	1.5	2.0	1.0	1.6	1.61	0.99
58	159	1.5	2.0	1.4	2.05	1.87	1.1
59	159	1.5	2.0	1.8	2.0	1.69	1.18
60	159	1.5	2.0	0.8	1.57	1.37	1.15
61	239	1.5	3.0	1.0	1.57	1.78	0.88
62	239	1.5	3.0	1.4	2.12	2.22	0.95
63	239	1.5	3.0	1.8	2.45	2.27	1.08
64	239	1.5	3.0	0.8	1.55	1.45	1.07
65	90	2.0	2.0	1.0	1.52	1.41	1.08
66	90	2.0	2.0	1.4	1.54	1.51	1.02
67	90	2.0	2.0	1.8	1.55	1.24	1.25
68	90	2.0	2.0	0.8	1.51	1.29	1.17
69	135	2.0	3.0	1.0	1.85	1.23	1.5
70	135	2.0	3.0	1.4	1.72	1.48	1.16
71	135	2.0	3.0	1.8	1.66	1.26	1.32
72	135	2.0	3.0	0.8	1.8	0.98	1.84
73	1434	0.5	2.0	1.0	5.2	5.55	0.94
74	1434	0.5	2.0	1.4	6.2	5.54	1.12
75	1434	0.5	2.0	1.8	6.4	5.58	1.15
76	1434	0.5	2.0	0.8	5.05	5.52	0.91
77	2151	0.5	3.0	1.0	7.3	6.88	1.06
78	2151	0.5	3.0	1.4	6.8	6.49	1.05
79	2151	0.5	3.0	1.8	7.25	6.48	1.12
80	2151	0.5	3.0	0.8	7.65	7.16	1.07
81	2490	0.75	4.0	1.0	12.96	13.21	0.98
82	2490	0.75	4.0	1.4	12.72	12.61	1.01
83	2490	0.75	4.0	1.8	11.95	11.90	1



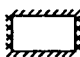
84	2490	0.75	4.0	0.8	13.86	13.28	1.04
85	455	1.0	1.3	1.0	4.0	3.72	1.08
86	455	1.0	1.3	1.4	4.35	4.12	1.06
87	455	1.0	1.3	1.8	4.7	4.44	1.06
88	455	1.0	1.3	0.8	3.8	3.51	1.08
89	1401	1.0	4.0	1.0	8.25	7.90	1.04
90	1401	1.0	4.0	1.4	8.92	8.96	1
91	1401	1.0	4.0	1.8	9.48	9.61	0.99
92	1401	1.0	4.0	0.8	7.02	7.21	0.97
93	623	1.5	4.0	1.0	3.25	3.74	0.87
94	623	1.5	4.0	1.4	4.75	4.34	1.09
95	623	1.5	4.0	1.8	5.32	4.68	1.14
96	623	1.5	4.0	0.8	3.0	3.34	0.9
97	114	2.0	1.3	1.0	3.03	3.28	0.92
98	114	2.0	1.3	1.4	3.06	3.21	0.95
99	114	2.0	1.3	1.8	3.09	2.85	1.08
100	114	2.0	1.3	0.8	3.01	3.27	0.92
101	350	2.0	4.0	1.0	3.74	3.75	1
102	350	2.0	4.0	1.4	4.02	4.16	0.97
103	350	2.0	4.0	1.8	4.02	3.93	1.02
104	350	2.0	4.0	0.8	4.13	3.36	1.23
105	1821	0.5	1.3	1.0	9.75	9.16	1.06
106	1821	0.5	1.3	1.4	9.5	9.56	0.99
107	1821	0.5	1.3	1.8	8.7	9.76	0.89
108	1821	0.5	1.3	0.8	9.1	8.87	1.03
109	5602	0.5	4.0	1.0	18.6	18.97	0.98
110	5602	0.5	4.0	1.4	17.62	17.56	1
111	5602	0.5	4.0	1.8	16.42	16.56	0.99
112	5602	0.5	4.0	0.8	19.12	19.76	0.97
113	1165	0.75	1.3	1.0	7.8	8.14	0.96
114	1165	0.75	1.3	1.4	8.95	8.87	1.01
115	1165	0.75	1.3	1.8	9.7	9.38	1.03
116	1165	0.75	1.3	0.8	7.15	7.71	0.93
117	3585	0.75	4.0	1.0	19.32	18.69	1.03
118	3585	0.75	4.0	1.4	18.12	17.58	1.03
119	3585	0.75	4.0	1.8	16.98	18.29	0.93
120	3585	0.75	4.0	0.8	19.75	18.97	1.04
121	656	1.0	1.3	1.0	5.75	5.63	1.02
122	656	1.0	1.3	1.4	6.25	6.22	1
123	656	1.0	1.3	1.8	6.75	6.71	1.01
124	656	1.0	1.3	0.8	5.62	5.32	1.06
125	2017	1.0	4.0	1.0	11.98	11.49	1.04
126	2017	1.0	4.0	1.4	12.35	12.75	0.97
127	2017	1.0	4.0	1.8	13.88	13.33	1.04
128	2017	1.0	4.0	0.8	9.82	10.61	0.93
129	291	1.5	1.3	1.0	4.59	4.71	0.97
130	291	1.5	1.3	1.4	4.74	4.92	0.96
131	291	1.5	1.3	1.8	4.88	4.64	1.05
132	291	1.5	1.3	0.8	4.51	4.49	1
133	896	1.5	4.0	1.0	4.7	5.18	0.91
134	896	1.5	4.0	1.4	6.3	5.99	1.05
135	896	1.5	4.0	1.8	6.7	6.52	1.03
136	896	1.5	4.0	0.8	5.62	4.66	1.21
137	164	2.0	1.3	1.0	4.35	4.40	0.99

138	164	2.0	1.3	1.4	4.4	4.41	1
139	164	2.0	1.3	1.8	4.45	4.10	1.09
140	164	2.0	1.3	0.8	4.33	4.35	1
141	504	2.0	4.0	1.0	4.18	5.14	0.81
142	504	2.0	4.0	1.4	5.72	5.72	1
143	504	2.0	4.0	1.8	5.55	5.61	0.99
144	504	2.0	4.0	0.8	4.2	4.66	0.9
145	2622	0.5	1.3	1.0	14.05	12.93	1.09
146	2622	0.5	1.3	1.4	13.65	13.54	1.01
147	2622	0.5	1.3	1.8	12.50	13.88	0.9
148	2622	0.5	1.3	0.8	13.1	12.53	1.05
149	8067	0.5	4.0	1.0	26.62	26.35	1.01
150	8067	0.5	4.0	1.4	24.9	24.88	1
151	8067	0.5	4.0	1.8	23.0	23.43	0.98
152	8067	0.5	4.0	0.8	28.05	27.04	1.04
153	518	0.75	1.3	1.0	3.5	3.66	0.96
154	518	0.75	1.3	1.4	4.0	4.08	0.98
155	518	0.75	1.3	1.8	4.35	4.30	1.01
156	518	0.75	1.3	0.8	3.2	3.40	0.94
157	291	1.0	1.3	1.0	2.54	2.17	1.17
158	291	1.0	1.3	1.4	2.78	2.41	1.15
159	291	1.0	1.3	1.8	3.00	2.59	1.16
160	291	1.0	1.3	0.8	2.55	2.05	1.24
161	896	1.0	4.0	1.0	5.42	5.12	1.06
162	896	1.0	4.0	1.4	6.22	5.92	1.05
163	896	1.0	4.0	1.8	6.32	6.50	0.97
164	896	1.0	4.0	0.8	5.45	4.62	1.18
165	130	1.5	1.3	1.0	2.05	2.29	0.9
166	130	1.5	1.3	1.4	2.11	2.25	0.94
167	130	1.5	1.3	1.8	2.17	1.78	1.22
168	130	1.5	1.3	0.8	2.01	2.20	0.91
169	73	2.0	1.3	1.0	1.94	2.39	0.81
170	73	2.0	1.3	1.4	1.96	2.27	0.86
171	73	2.0	1.3	1.8	1.98	1.88	1.05
172	73	2.0	1.3	0.8	1.93	2.40	0.8
173	224	2.0	4.0	1.0	2.85	2.58	1.1
174	224	2.0	4.0	1.4	2.65	2.85	0.93
175	224	2.0	4.0	1.8	2.50	2.53	0.99
176	224	2.0	4.0	0.8	2.5	2.27	1.1
177	1165	0.5	1.3	1.0	6.25	6.14	1.02
178	1165	0.5	1.3	1.4	6.05	6.34	0.95
179	1165	0.5	1.3	1.8	5.55	6.39	0.87
180	1165	0.5	1.3	0.8	5.85	5.96	0.98
181	3585	0.5	4.0	1.0	12.05	12.14	0.99
182	3585	0.5	4.0	1.4	10.95	11.06	0.99
183	3585	0.5	4.0	1.8	10.3	10.63	0.97
184	3585	0.5	4.0	0.8	12.55	12.85	0.98
185	90	2	4.0	1.0	1.15	1.32	0.87
186	90	2	4.0	1.6	1.12	1.32	0.85
187	90	2	4.0	1.3	1.15	1.47	0.78
188	90	2	4.0	0.7	1.10	0.95	1.16
189	347	2	1.3	1.0	9.19	8.75	1.05
190	347	2	1.3	1.6	9.34	9.13	1.02
191	347	2	1.3	1.3	9.27	9.03	1.03

192	347	2	1.3	0.7	9.11	8.40	1.08
193	125	1.5	1.3	1.0	1.1	0.94	1.17
194	125	1.5	4.0	1.6	1.22	1.14	1.07
195	125	1.5	4.0	1.3	1.05	1.11	0.95
196	125	1.5	4.0	0.7	1.1	0.64	1.72
197	906	1.5	4.0	1.0	14.35	14.05	1.02
198	906	1.5	1.3	1.6	15.0	15.79	0.95
199	906	1.5	1.3	1.3	14.7	15.06	0.98
200	906	1.5	1.3	0.7	13.95	12.88	1.08
201	2039	1.0	1.3	1.0	17.8	18.24	0.98
202	2039	1.0	1.3	1.6	20.2	20.07	1.01
203	2039	1.0	1.3	1.3	19.05	19.23	0.99
204	2039	1.0	1.3	0.7	16.4	17.16	0.96
205	316	1.0	4.0	1.0	1.95	2.07	0.94
206	316	1.0	4.0	1.6	2.04	2.70	0.76
207	316	1.0	4.0	1.3	2.22	2.41	0.92
208	316	1.0	4.0	0.7	1.7	1.66	1.02
209	563	0.75	4.0	1.0	3.02	3.32	0.91
210	563	0.75	4.0	1.6	2.75	3.15	0.87
211	563	0.75	4.0	1.3	2.75	3.22	0.85
212	563	0.75	4.0	0.7	2.75	3.31	0.83
213	2543	0.75	1.3	1.0	17.0	17.14	0.99
214	2543	0.75	1.3	1.6	20.45	18.58	1.1
215	2543	0.75	1.3	1.3	18.95	17.95	1.06
216	2543	0.75	1.3	0.7	14.8	16.25	0.91
217	1266	0.5	4.0	1.0	4.2	3.95	1.06
218	1266	0.5	4.0	1.6	4.02	3.41	1.18
219	1266	0.5	4.0	1.3	4.12	3.51	1.17
220	1266	0.5	4.0	0.7	4.4	4.62	0.95
221	5722	0.5	1.3	1.0	30.65	28.89	1.06
222	5722	0.5	1.3	1.6	28.55	29.94	0.95
223	5722	0.5	1.3	1.3	30.3	29.54	1.03
224	5722	0.5	1.3	0.7	26.75	28.05	0.95
225	747	0.75	1.5	1.0	4.35	4.81	0.9
226	747	0.75	1.5	1.4	4.9	5.23	0.94
227	747	0.75	1.5	1.8	5.45	5.49	0.99
228	747	0.75	1.5	0.8	4.32	4.55	0.95
229	1992	0.75	4.0	1.0	10.56	10.61	1
230	1992	0.75	4.0	1.4	10.1	10.21	0.99
231	1992	0.75	4.0	1.8	9.45	9.76	0.97
232	1992	0.75	4.0	0.8	11.03	10.62	1.04
233	420	1.0	1.5	1.0	3.4	3.15	1.08
234	420	1.0	1.5	1.4	3.42	3.41	1
235	420	1.0	1.5	1.8	3.67	3.57	1.03
236	420	1.0	1.5	0.8	3.34	2.99	1.12
237	1120	1.0	4.0	1.0	6.76	6.33	1.07
238	1120	1.0	4.0	1.4	7.32	7.26	1.01
239	1120	1.0	4.0	1.8	7.72	7.89	0.98
240	1120	1.0	4.0	0.8	6.12	5.75	1.06
241	187	1.5	1.5	1.0	2.53	2.70	0.94
242	187	1.5	1.5	1.4	2.61	2.84	0.92
243	187	1.5	1.5	1.8	2.68	2.51	1.07
244	187	1.5	1.5	0.8	2.49	2.51	0.99
245	498	1.5	4.0	1.0	2.72	3.06	0.89

246	498	1.5	4.0	1.4	3.82	3.56	1.07
247	498	1.5	4.0	1.8	4.36	3.81	1.14
248	498	1.5	4.0	0.8	2.58	2.71	0.95
249	105	2.0	1.5	1.0	2.4	2.66	0.9
250	105	2.0	1.5	1.4	2.43	2.65	0.92
251	105	2.0	1.5	1.8	2.45	2.32	1.06
252	105	2.0	1.5	0.8	2.39	2.61	0.92
253	280	2.0	4.0	1.0	2.72	3.10	0.88
254	280	2.0	4.0	1.4	3.35	3.43	0.98
255	280	2.0	4.0	1.8	3.28	3.16	1.04
256	280	2.0	4.0	0.8	2.85	2.76	1.03
257	1681	0.5	1.5	1.0	8.15	7.81	1.04
258	1681	0.5	1.5	1.4	8.5	8.07	1.05
259	1681	0.5	1.5	1.8	7.95	8.21	0.97
260	1681	0.5	1.5	0.8	7.3	7.60	0.96
261	4482	0.5	4.0	1.0	14.95	15.25	0.98
262	4482	0.5	4.0	1.4	14.12	13.99	1.01
263	4482	0.5	4.0	1.8	13.02	13.30	0.98
264	4482	0.5	4.0	0.8	15.78	16.02	0.99
265	2868	0.75	4.0	1.0	15.0	15.15	0.99
266	2868	0.75	4.0	1.4	14.05	14.38	0.98
267	2868	0.75	4.0	1.8	13.32	13.47	0.99
268	2868	0.75	4.0	0.8	14.15	15.29	0.93
269	1613	1.0	4.0	1.0	8.78	9.11	0.96
270	1613	1.0	4.0	1.4	10.62	10.26	1.04
271	1613	1.0	4.0	1.8	11.25	10.91	1.03
272	1613	1.0	4.0	0.8	7.85	8.35	0.94
273	269	1.5	1.5	1.0	3.64	3.83	0.95
274	269	1.5	1.5	1.4	3.76	4.11	0.91
275	269	1.5	1.5	1.8	3.86	3.88	0.99
276	269	1.5	1.5	0.8	3.58	3.58	1
277	151	2.0	1.5	1.0	3.46	3.63	0.95
278	151	2.0	1.5	1.4	3.49	3.68	0.95
279	151	2.0	1.5	1.8	3.53	3.40	1.04
280	151	2.0	1.5	0.8	3.44	3.54	0.97
281	2420	0.5	1.5	1.0	11.7	11.05	1.06
282	2420	0.5	1.5	1.4	12.2	11.50	1.06
283	2420	0.5	1.5	1.8	11.45	11.74	0.98
284	2420	0.5	1.5	0.8	10.5	10.75	0.98
285	6453	0.5	4.0	1.0	21.68	21.65	1
286	6453	0.5	4.0	1.4	19.92	20.17	0.99
287	6453	0.5	4.0	1.8	18.98	18.98	1
288	6453	0.5	4.0	0.8	22.68	22.42	1.01
289	1275	0.75	4.0	1.0	6.65	6.89	0.97
290	1275	0.75	4.0	1.4	6.35	6.70	0.95
291	1275	0.75	4.0	1.8	6.08	6.54	0.93
292	1275	0.75	4.0	0.8	7.28	6.87	1.06
293	120	1.5	1.5	1.0	1.62	1.78	0.91
294	120	1.5	1.5	1.4	1.67	1.83	0.91
295	120	1.5	1.5	1.8	1.72	1.44	1.19
296	120	1.5	1.5	0.8	1.59	1.66	0.96
297	319	1.5	4.0	1.0	1.95	2.06	0.95
298	319	1.5	4.0	1.4	2.68	2.41	1.11
299	319	1.5	4.0	1.8	3.35	2.53	1.32

300	319	1.5	4.0	0.8	1.54	1.79	0.86
301	67	2.0	1.5	1.0	1.56	1.89	0.83
302	67	2.0	1.5	1.4	1.57	1.83	0.86
303	67	2.0	1.5	1.8	1.53	1.47	1.04
304	67	2.0	1.5	0.8	2.1	1.87	1.12
305	179	2.0	4.0	1.0	2.32	2.16	1.07
306	179	2.0	4.0	1.4	2.25	2.38	0.95
307	179	2.0	4.0	1.8	1.65	2.03	0.81
308	179	2.0	4.0	0.8	2.21	1.87	1.18
309	1076	0.5	1.5	1.0	5.19	5.18	1
310	1076	0.5	1.5	1.4	5.41	5.29	1.02
311	1076	0.5	1.5	1.8	5.08	5.29	0.96
312	1076	0.5	1.5	0.8	4.65	5.06	0.92
313	2868	0.5	4.0	1.0	9.55	9.61	0.99
314	2868	0.5	4.0	1.4	9.08	8.70	1.04
315	2868	0.5	4.0	1.8	8.65	8.47	1.02
316	2868	0.5	4.0	0.8	9.68	10.24	0.95

Set4 - 

No	Net inputs				Failure Pressure		
	$\frac{F_x Z}{L^2}$	L/H	F <sub>x</sub> /F <sub>y</sub>	E <sub>x</sub> /E <sub>y</sub>	NN output	FEM	Ratio
					$\times 10^{-3}$ (N/mm <sup>2</sup> )	$\times 10^{-3}$ (N/mm <sup>2</sup> )	$\frac{FEM}{NN}$
1	1434	0.75	2.0	1.0	39.1	38.33	1.02
2	1434	0.75	2.0	1.4	37.95	38.39	0.99
3	1434	0.75	2.0	1.8	37.05	38.11	0.97
4	1434	0.75	2.0	0.8	38.9	38.14	1.02
5	2151	0.75	3.0	1.0	52.34	54.39	0.96
6	2151	0.75	3.0	1.4	56.7	55.36	1.02
7	2151	0.75	3.0	1.8	55.8	56.46	0.99
8	2151	0.75	3.0	0.8	50.1	53.94	0.93
9	807	1.0	2.0	1.0	23.45	23.06	1.02
10	807	1.0	2.0	1.4	24.7	23.44	1.05
11	807	1.0	2.0	1.8	24.0	23.21	1.03
12	807	1.0	2.0	0.8	20.4	22.64	0.9
13	1210	1.0	3.0	1.0	29.9	31.95	0.94
14	1210	1.0	3.0	1.4	31.6	32.54	0.97
15	1210	1.0	3.0	1.8	34.35	32.91	1.04
16	1210	1.0	3.0	0.8	29.85	31.56	0.95
17	359	1.5	2.0	1.0	10.85	11.76	0.92
18	359	1.5	2.0	1.4	10.9	12.22	0.89
19	359	1.5	2.0	1.8	12.75	11.92	1.07
20	359	1.5	2.0	0.8	11.0	11.25	0.98
21	538	1.5	3.0	1.0	16.1	16.05	1
22	538	1.5	3.0	1.4	15.2	16.01	0.95
23	538	1.5	3.0	1.8	15.1	15.41	0.98
24	538	1.5	3.0	0.8	16.65	15.84	1.05
25	202	2.0	2.0	1.0	8.78	8.28	1.06
26	202	2.0	2.0	1.4	7.88	8.93	0.88
27	202	2.0	2.0	1.8	7.68	8.76	0.88

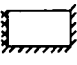
28	202	2.0	2.0	0.8	9.1	7.66	1.19
29	303	2.0	3.0	1.0	12.95	12.27	1.06
30	303	2.0	3.0	1.4	11.85	12.08	0.98
31	303	2.0	3.0	1.8	11.35	11.1	1.02
32	303	2.0	3.0	0.8	13.52	12.05	1.12
33	3227	0.5	2.0	1.0	79.15	78.06	1.01
34	3227	0.5	2.0	1.4	78.25	77.42	1.01
35	3227	0.5	2.0	1.8	77.70	77.32	1
36	3227	0.5	2.0	0.8	79.65	78.51	1.01
37	4840	0.5	3.0	1.0	117.8	114.65	1.03
38	4840	0.5	3.0	1.4	118.25	116.31	1.02
39	4840	0.5	3.0	1.8	117.35	119.06	0.99
40	4840	0.5	3.0	0.8	109.52	114.15	0.96
41	637	0.75	2.0	1.0	17.35	17.02	1.02
42	637	0.75	2.0	1.4	16.85	17.43	0.97
43	637	0.75	2.0	1.8	16.45	17.2	0.96
44	637	0.75	2.0	0.8	17.35	16.57	1.05
45	956	0.75	3.0	1.0	23.73	23.74	1
46	956	0.75	3.0	1.4	25.2	24.52	1.03
47	956	0.75	3.0	1.8	24.8	24.95	0.99
48	956	0.75	3.0	0.8	23.02	23.22	0.99
49	359	1.0	2.0	1.0	10.5	9.91	1.06
50	359	1.0	2.0	1.4	11.0	10.43	1.05
51	359	1.0	2.0	1.8	10.65	10.24	1.04
52	359	1.0	2.0	0.8	9.15	9.39	0.97
53	538	1.0	3.0	1.0	13.25	13.40	0.99
54	538	1.0	3.0	1.4	14.2	13.9	1.02
55	538	1.0	3.0	1.8	15.35	13.94	1.1
56	538	1.0	3.0	0.8	13.52	12.98	1.04
57	159	1.5	2.0	1.0	4.85	4.84	1
58	159	1.5	2.0	1.4	4.9	5.26	0.93
59	159	1.5	2.0	1.8	5.75	4.95	1.16
60	159	1.5	2.0	0.8	4.8	4.34	1.11
61	239	1.5	3.0	1.0	7.12	6.38	1.12
62	239	1.5	3.0	1.4	7.25	6.31	1.15
63	239	1.5	3.0	1.8	6.62	5.64	1.17
64	239	1.5	3.0	0.8	7.35	6.17	1.19
65	90	2.0	2.0	1.0	3.92	3.92	1
66	90	2.0	2.0	1.4	3.72	4.43	0.84
67	90	2.0	2.0	1.8	3.35	4.19	0.8
68	90	2.0	2.0	0.8	4.12	3.38	1.22
69	135	2.0	3.0	1.0	5.78	5.96	0.97
70	135	2.0	3.0	1.4	5.33	5.67	0.94
71	135	2.0	3.0	1.8	5.02	4.62	1.09
72	135	2.0	3.0	0.8	6.02	5.81	1.04
73	1434	0.5	2.0	1.0	35.3	35.11	1.01
74	1434	0.5	2.0	1.4	34.9	35.06	1
75	1434	0.5	2.0	1.8	34.65	34.7	1
76	1434	0.5	2.0	0.8	35.55	34.98	1.02
77	2151	0.5	3.0	1.0	53.15	50.87	1.04
78	2151	0.5	3.0	1.4	52.7	51.86	1.02
79	2151	0.5	3.0	1.8	52.3	52.9	0.99
80	2151	0.5	3.0	0.8	49.62	50.39	0.98
81	2490	0.75	4.0	1.0	59.92	58.3	1.03

82	2490	0.75	4.0	1.4	61.18	60.16	1.02
83	2490	0.75	4.0	1.8	64.35	62.54	1.03
84	2490	0.75	4.0	0.8	57.88	57.54	1.01
85	455	1.0	1.3	1.0	15.05	14.45	1.04
86	455	1.0	1.3	1.4	14.25	14.71	0.97
87	455	1.0	1.3	1.8	13.55	14.14	0.96
88	455	1.0	1.3	0.8	15.2	14.0	1.09
89	1401	1.0	4.0	1.0	34.2	34.59	0.99
90	1401	1.0	4.0	1.4	34.38	35.22	0.98
91	1401	1.0	4.0	1.8	35.3	35.9	0.98
92	1401	1.0	4.0	0.8	34.02	34.27	0.99
93	623	1.5	4.0	1.0	18.58	18.28	1.02
94	623	1.5	4.0	1.4	18.02	17.81	1.01
95	623	1.5	4.0	1.8	17.74	16.88	1.05
96	623	1.5	4.0	0.8	18.9	18.29	1.03
97	114	2.0	1.3	1.0	5.22	5.35	0.98
98	114	2.0	1.3	1.4	5.65	6.66	0.85
99	114	2.0	1.3	1.8	6.35	7.11	0.89
100	114	2.0	1.3	0.8	5.1	4.41	1.16
101	350	2.0	4.0	1.0	14.52	14.66	0.99
102	350	2.0	4.0	1.4	13.95	13.96	1
103	350	2.0	4.0	1.8	12.72	12.43	1.02
104	350	2.0	4.0	0.8	14.92	14.68	1.02
105	1821	0.5	1.3	1.0	44.35	44.38	1
106	1821	0.5	1.3	1.4	43.9	43.31	1.01
107	1821	0.5	1.3	1.8	43.65	42.15	1.04
108	1821	0.5	1.3	0.8	44.7	44.82	1
109	5602	0.5	4.0	1.0	123.75	125.92	0.98
110	5602	0.5	4.0	1.4	124.2	130.21	0.95
111	5602	0.5	4.0	1.8	136.7	135.72	1.01
112	5602	0.5	4.0	0.8	126.92	124.2	1.02
113	1165	0.75	1.3	1.0	31.95	32.49	0.98
114	1165	0.75	1.3	1.4	30.6	30.04	1.02
115	1165	0.75	1.3	1.8	29.9	31.07	0.96
116	1165	0.75	1.3	0.8	32.65	32.49	1
117	3585	0.75	4.0	1.0	85.78	84.76	1.01
118	3585	0.75	4.0	1.4	88.8	87.53	1.01
119	3585	0.75	4.0	1.8	90.8	91.24	1
120	3585	0.75	4.0	0.8	83.5	83.7	1
121	656	1.0	1.3	1.0	21.7	20.6	1.05
122	656	1.0	1.3	1.4	20.55	20.73	0.99
123	656	1.0	1.3	1.8	19.55	20.08	0.97
124	656	1.0	1.3	0.8	21.85	20.22	1.08
125	2017	1.0	4.0	1.0	49.18	50.31	0.98
126	2017	1.0	4.0	1.4	50.22	51.33	0.98
127	2017	1.0	4.0	1.8	50.28	52.74	0.95
128	2017	1.0	4.0	0.8	48.15	49.91	0.96
129	291	1.5	1.3	1.0	11.55	11.46	1.01
130	291	1.5	1.3	1.4	13.25	12.22	1.08
131	291	1.5	1.3	1.8	13.3	12.04	1.1
132	291	1.5	1.3	0.8	10.15	10.73	0.95
133	896	1.5	4.0	1.0	26.97	26.6	1.01
134	896	1.5	4.0	1.4	26.1	26.17	1
135	896	1.5	4.0	1.8	25.64	25.37	1.01

136	896	1.5	4.0	0.8	27.0	26.64	1.01
137	164	2.0	1.3	1.0	7.45	7.36	1.01
138	164	2.0	1.3	1.4	8.15	8.75	0.93
139	164	2.0	1.3	1.8	9.10	9.26	0.98
140	164	2.0	1.3	0.8	6.95	6.37	1.09
141	504	2.0	4.0	1.0	20.94	20.32	1.03
142	504	2.0	4.0	1.4	20.08	19.65	1.02
143	504	2.0	4.0	1.8	18.48	18.16	1.02
144	504	2.0	4.0	0.8	21.48	20.31	1.06
145	2622	0.5	1.3	1.0	63.8	63.54	1
146	2622	0.5	1.3	1.4	63.15	62.01	1.02
147	2622	0.5	1.3	1.8	62.75	60.81	1.03
148	2622	0.5	1.3	0.8	64.3	64.36	1
149	8067	0.5	4.0	1.0	178.8	180.45	0.99
150	8067	0.5	4.0	1.4	180.25	185.6	0.97
151	8067	0.5	4.0	1.8	196.6	191.73	1.03
152	8067	0.5	4.0	0.8	182.55	178.29	1.02
153	518	0.75	1.3	1.0	14.2	14.96	0.95
154	518	0.75	1.3	1.4	13.6	15.0	0.91
155	518	0.75	1.3	1.8	13.25	14.29	0.93
156	518	0.75	1.3	0.8	14.5	14.64	0.99
157	291	1.0	1.3	1.0	9.65	9.55	1.01
158	291	1.0	1.3	1.4	9.15	9.9	0.92
159	291	1.0	1.3	1.8	8.65	9.41	0.92
160	291	1.0	1.3	0.8	9.75	9.04	1.08
161	896	1.0	4.0	1.0	21.78	22.03	0.99
162	896	1.0	4.0	1.4	22.85	22.4	1.02
163	896	1.0	4.0	1.8	22.85	22.58	1.01
164	896	1.0	4.0	0.8	22.42	21.74	1.03
165	130	1.5	1.3	1.0	5.2	5.62	0.93
166	130	1.5	1.3	1.4	5.95	6.36	0.94
167	130	1.5	1.3	1.8	5.9	6.19	0.95
168	130	1.5	1.3	0.8	4.55	4.92	0.92
169	73	2.0	1.3	1.0	3.38	3.72	0.91
170	73	2.0	1.3	1.4	3.65	4.97	0.73
171	73	2.0	1.3	1.8	4.1	5.38	0.76
172	73	2.0	1.3	0.8	3.48	2.82	1.23
173	224	2.0	4.0	1.0	9.28	10.15	0.91
174	224	2.0	4.0	1.4	8.82	9.42	0.94
175	224	2.0	4.0	1.8	8.22	7.88	1.04
176	224	2.0	4.0	0.8	9.55	10.19	0.94
177	1165	0.5	1.3	1.0	28.45	28.89	0.98
178	1165	0.5	1.3	1.4	28.15	28.29	1
179	1165	0.5	1.3	1.8	28.0	27.27	1.03
180	1165	0.5	1.3	0.8	28.7	29.0	0.99
181	3585	0.5	4.0	1.0	79.5	79.84	1
182	3585	0.5	4.0	1.4	81.9	82.77	0.99
183	3585	0.5	4.0	1.8	87.65	86.43	1.01
184	3585	0.5	4.0	0.8	82.05	78.63	1.04
185	90	2	4.0	1.0	3.82	5.49	0.7
186	90	2	4.0	1.6	3.48	4.05	0.86
187	90	2	4.0	1.3	3.78	5.0	0.76
188	90	2	4.0	0.7	3.62	5.5	0.66
189	347	2	1.3	1.0	15.85	15.0	1.06



190	347	2	1.3	1.6	18.1	17.17	1.05
191	347	2	1.3	1.3	16.5	16.35	1.01
192	347	2	1.3	0.7	12.95	13.16	0.98
193	125	1.5	1.3	1.0	4.08	3.75	1.09
194	125	1.5	4.0	1.6	3.75	2.81	1.33
195	125	1.5	4.0	1.3	3.92	3.46	1.13
196	125	1.5	4.0	0.7	4.32	3.65	1.18
197	906	1.5	4.0	1.0	35.3	35.53	0.99
198	906	1.5	1.3	1.6	41.7	36.31	1.15
199	906	1.5	1.3	1.3	40.05	36.2	1.11
200	906	1.5	1.3	0.7	28.85	34.28	0.84
201	2039	1.0	1.3	1.0	67.45	65.32	1.03
202	2039	1.0	1.3	1.6	62.6	63.94	0.98
203	2039	1.0	1.3	1.3	65.1	64.7	1.01
204	2039	1.0	1.3	0.7	65.5	65.69	1
205	316	1.0	4.0	1.0	8.28	8.09	1.02
206	316	1.0	4.0	1.6	7.95	8.17	0.97
207	316	1.0	4.0	1.3	7.72	8.25	0.94
208	316	1.0	4.0	0.7	8.05	7.65	1.05
209	563	0.75	4.0	1.0	13.88	14.2	0.98
210	563	0.75	4.0	1.6	13.8	14.97	0.92
211	563	0.75	4.0	1.3	14.38	14.68	0.98
212	563	0.75	4.0	0.7	13.22	13.53	0.98
213	2543	0.75	1.3	1.0	69.8	71.18	0.98
214	2543	0.75	1.3	1.6	66.25	69.12	0.96
215	2543	0.75	1.3	1.3	67.8	70.11	0.97
216	2543	0.75	1.3	0.7	71.85	72.23	0.99
217	1266	0.5	4.0	1.0	29.52	29.71	0.99
218	1266	0.5	4.0	1.6	31.1	31.62	0.98
219	1266	0.5	4.0	1.3	29.35	30.69	0.96
220	1266	0.5	4.0	0.7	29.58	28.68	1.03
221	5722	0.5	1.3	1.0	138.95	138.65	1
222	5722	0.5	1.3	1.6	136.95	137.84	0.99
223	5722	0.5	1.3	1.3	137.75	137.83	1
224	5722	0.5	1.3	0.7	140.75	140.19	1

Set5 - 

No	Net inputs				Failure Pressure		
	$\frac{F_x Z}{L^2}$	L/H	Fx/Fy	Ex/Ey	NN output $\times 10^{-3}$ (N/mm <sup>2</sup> )	FEM $\times 10^{-3}$ (N/mm <sup>2</sup> )	Ratio $\frac{FEM}{NN}$
1	1434	0.75	2.0	1.0	21.2	21.73	0.98
2	1434	0.75	2.0	1.4	20.9	21.4	0.98
3	1434	0.75	2.0	1.8	20.7	21.08	0.98
4	1434	0.75	2.0	0.8	21.45	21.89	0.98
5	2151	0.75	3.0	1.0	32.0	31.83	1.01
6	2151	0.75	3.0	1.4	31.6	31.73	1
7	2151	0.75	3.0	1.8	31.3	31.56	0.99
8	2151	0.75	3.0	0.8	32.0	31.85	1
9	807	1.0	2.0	1.0	12.7	12.88	0.99

10	807	1.0	2.0	1.4	12.35	12.64	0.98
11	807	1.0	2.0	1.8	12.1	12.43	0.97
12	807	1.0	2.0	0.8	12.9	12.99	0.99
13	1210	1.0	3.0	1.0	18.95	18.78	1.01
14	1210	1.0	3.0	1.4	18.6	18.71	0.99
15	1210	1.0	3.0	1.8	18.25	18.6	0.98
16	1210	1.0	3.0	0.8	18.85	18.8	1
17	359	1.5	2.0	1.0	6.95	6.45	1.08
18	359	1.5	2.0	1.4	6.65	6.3	1.06
19	359	1.5	2.0	1.8	6.35	6.17	1.03
20	359	1.5	2.0	0.8	6.75	6.52	1.04
21	538	1.5	3.0	1.0	8.75	9.09	0.96
22	538	1.5	3.0	1.4	9.65	9.07	1.06
23	538	1.5	3.0	1.8	9.5	9.02	1.05
24	538	1.5	3.0	0.8	8.1	9.08	0.89
25	202	2.0	2.0	1.0	4.15	4.59	0.9
26	202	2.0	2.0	1.4	4.65	4.48	1.04
27	202	2.0	2.0	1.8	4.55	4.39	1.04
28	202	2.0	2.0	0.8	3.55	4.64	0.77
29	303	2.0	3.0	1.0	5.45	5.81	0.94
30	303	2.0	3.0	1.4	5.25	5.82	0.9
31	303	2.0	3.0	1.8	6.05	5.81	1.04
32	303	2.0	3.0	0.8	5.42	5.81	0.93
33	3227	0.5	2.0	1.0	46.7	46.16	1.01
34	3227	0.5	2.0	1.4	46.35	45.67	1.01
35	3227	0.5	2.0	1.8	46.1	45.16	1.02
36	3227	0.5	2.0	0.8	46.95	46.39	1.01
37	4840	0.5	3.0	1.0	70.5	70.45	1
38	4840	0.5	3.0	1.4	70.05	70.44	0.99
39	4840	0.5	3.0	1.8	69.65	70.27	0.99
40	4840	0.5	3.0	0.8	70.7	70.39	1
41	637	0.75	2.0	1.0	9.5	9.55	0.99
42	637	0.75	2.0	1.4	9.35	9.36	1
43	637	0.75	2.0	1.8	9.3	9.2	1.01
44	637	0.75	2.0	0.8	9.6	9.65	0.99
45	956	0.75	3.0	1.0	14.35	14.43	0.99
46	956	0.75	3.0	1.4	14.15	14.39	0.98
47	956	0.75	3.0	1.8	14.0	14.33	0.98
48	956	0.75	3.0	0.8	14.35	14.44	0.99
49	359	1.0	2.0	1.0	5.7	5.46	1.04
50	359	1.0	2.0	1.4	5.5	5.31	1.04
51	359	1.0	2.0	1.8	5.4	5.19	1.04
52	359	1.0	2.0	0.8	5.75	5.53	1.04
53	538	1.0	3.0	1.0	8.45	8.29	1.02
54	538	1.0	3.0	1.4	8.3	8.28	1
55	538	1.0	3.0	1.8	8.15	8.26	0.99
56	538	1.0	3.0	0.8	8.4	8.29	1.01
57	159	1.5	2.0	1.0	3.1	2.79	1.11
58	159	1.5	2.0	1.4	3.0	2.68	1.12
59	159	1.5	2.0	1.8	2.85	2.59	1.1
60	159	1.5	2.0	0.8	3.05	2.84	1.07
61	239	1.5	3.0	1.0	3.9	3.9	1
62	239	1.5	3.0	1.4	4.3	3.91	1.1
63	239	1.5	3.0	1.8	4.25	3.9	1.09

64	239	1.5	3.0	0.8	3.8	3.89	0.98
65	90	2.0	2.0	1.0	1.85	2.38	0.78
66	90	2.0	2.0	1.4	2.0	2.3	0.87
67	90	2.0	2.0	1.8	2.05	2.22	0.92
68	90	2.0	2.0	0.8	1.65	2.42	0.68
69	135	2.0	3.0	1.0	2.4	2.67	0.9
70	135	2.0	3.0	1.4	2.35	2.7	0.87
71	135	2.0	3.0	1.8	2.7	2.71	1
72	135	2.0	3.0	0.8	2.45	2.64	0.93
73	1434	0.5	2.0	1.0	20.9	20.91	1
74	1434	0.5	2.0	1.4	20.75	20.6	1.01
75	1434	0.5	2.0	1.8	20.65	20.3	1.02
76	1434	0.5	2.0	0.8	21.0	21.07	1
77	2151	0.5	3.0	1.0	31.55	31.12	1.01
78	2151	0.5	3.0	1.4	31.35	31.03	1.01
79	2151	0.5	3.0	1.8	31.15	30.88	1.01
80	2151	0.5	3.0	0.8	31.65	31.14	1.02
81	2490	0.75	4.0	1.0	37.1	36.24	1.02
82	2490	0.75	4.0	1.4	36.85	36.56	1.01
83	2490	0.75	4.0	1.8	36.5	36.79	0.99
84	2490	0.75	4.0	0.8	37.35	36.03	1.04
85	455	1.0	1.3	1.0	7.15	7.18	1
86	455	1.0	1.3	1.4	6.9	6.97	0.99
87	455	1.0	1.3	1.8	6.8	6.82	1
88	455	1.0	1.3	0.8	7.3	7.3	1
89	1401	1.0	4.0	1.0	18.85	21.13	0.89
90	1401	1.0	4.0	1.4	21.55	21.34	1.01
91	1401	1.0	4.0	1.8	21.2	21.49	0.99
92	1401	1.0	4.0	0.8	18.4	21.0	0.88
93	623	1.5	4.0	1.0	9.6	9.93	0.97
94	623	1.5	4.0	1.4	9.7	10.09	0.96
95	623	1.5	4.0	1.8	10.65	10.22	1.04
96	623	1.5	4.0	0.8	9.32	9.84	0.95
97	114	2.0	1.3	1.0	3.0	3.23	0.93
98	114	2.0	1.3	1.4	2.8	3.12	0.9
99	114	2.0	1.3	1.8	2.6	3.05	0.85
100	114	2.0	1.3	0.8	2.95	3.3	0.89
101	350	2.0	4.0	1.0	6.2	5.89	1.05
102	350	2.0	4.0	1.4	6.05	6.06	1
103	350	2.0	4.0	1.8	5.95	6.19	0.96
104	350	2.0	4.0	0.8	6.42	5.79	1.11
105	1821	0.5	1.3	1.0	26.25	26.37	1
106	1821	0.5	1.3	1.4	26.1	25.91	1.01
107	1821	0.5	1.3	1.8	25.95	25.52	1.02
108	1821	0.5	1.3	0.8	26.35	26.62	0.99
109	5602	0.5	4.0	1.0	79.5	81.73	0.97
110	5602	0.5	4.0	1.4	81.7	82.44	0.99
111	5602	0.5	4.0	1.8	81.3	82.93	0.98
112	5602	0.5	4.0	0.8	80.35	81.29	0.99
113	1165	0.75	1.3	1.0	17.1	17.87	0.96
114	1165	0.75	1.3	1.4	16.9	17.51	0.97
115	1165	0.75	1.3	1.8	16.75	17.22	0.97
116	1165	0.75	1.3	0.8	17.3	18.06	0.96
117	3585	0.75	4.0	1.0	53.5	52.12	1.03

118	3585	0.75	4.0	1.4	52.9	52.6	1.01
119	3585	0.75	4.0	1.8	52.4	52.93	0.99
120	3585	0.75	4.0	0.8	53.6	51.82	1.03
121	656	1.0	1.3	1.0	10.25	10.59	0.97
122	656	1.0	1.3	1.4	9.95	10.33	0.96
123	656	1.0	1.3	1.8	9.75	10.14	0.96
124	656	1.0	1.3	0.8	10.45	10.73	0.97
125	2017	1.0	4.0	1.0	31.3	29.99	1.04
126	2017	1.0	4.0	1.4	31.0	30.26	1.02
127	2017	1.0	4.0	1.8	30.55	30.44	1
128	2017	1.0	4.0	0.8	25.8	29.82	0.87
129	291	1.5	1.3	1.0	5.8	5.48	1.06
130	291	1.5	1.3	1.4	5.4	5.31	1.02
131	291	1.5	1.3	1.8	5.15	5.19	0.99
132	291	1.5	1.3	0.8	6.0	5.58	1.08
133	896	1.5	4.0	1.0	13.22	14.28	0.93
134	896	1.5	4.0	1.4	14.9	14.46	1.03
135	896	1.5	4.0	1.8	15.35	14.59	1.05
136	896	1.5	4.0	0.8	12.80	14.17	0.9
137	164	2.0	1.3	1.0	4.35	4.25	1.02
138	164	2.0	1.3	1.4	4.05	4.13	0.98
139	164	2.0	1.3	1.8	3.75	4.05	0.93
140	164	2.0	1.3	0.8	4.25	4.33	0.98
141	504	2.0	4.0	1.0	8.95	8.56	1.05
142	504	2.0	4.0	1.4	8.65	8.73	0.99
143	504	2.0	4.0	1.8	8.60	8.87	0.97
144	504	2.0	4.0	0.8	8.95	8.45	1.06
145	2622	0.5	1.3	1.0	37.65	37.48	1
146	2622	0.5	1.3	1.4	37.4	36.91	1.01
147	2622	0.5	1.3	1.8	37.25	36.42	1.02
148	2622	0.5	1.3	0.8	37.85	37.78	1
149	8067	0.5	4.0	1.0	113.92	114.31	1
150	8067	0.5	4.0	1.4	117.3	115.02	1.02
151	8067	0.5	4.0	1.8	116.7	115.51	1.01
152	8067	0.5	4.0	0.8	113.55	113.86	1
153	518	0.75	1.3	1.0	7.65	7.63	1
154	518	0.75	1.3	1.4	7.55	7.42	1.02
155	518	0.75	1.3	1.8	7.50	7.27	1.03
156	518	0.75	1.3	0.8	7.75	7.76	1
157	291	1.0	1.3	1.0	4.6	4.34	1.06
158	291	1.0	1.3	1.4	4.45	4.16	1.07
159	291	1.0	1.3	1.8	4.35	4.05	1.07
160	291	1.0	1.3	0.8	4.65	4.44	1.05
161	896	1.0	4.0	1.0	14.0	13.68	1.02
162	896	1.0	4.0	1.4	13.8	13.85	1
163	896	1.0	4.0	1.8	13.6	14.0	0.97
164	896	1.0	4.0	0.8	13.8	13.58	1.02
165	130	1.5	1.3	1.0	2.6	2.44	1.07
166	130	1.5	1.3	1.4	2.4	2.3	1.04
167	130	1.5	1.3	1.8	2.3	2.22	1.04
168	130	1.5	1.3	0.8	2.7	2.52	1.07
169	73	2.0	1.3	1.0	1.95	2.4	0.81
170	73	2.0	1.3	1.4	1.80	2.29	0.79
171	73	2.0	1.3	1.8	1.70	2.23	0.76

172	73	2.0	1.3	0.8	1.90	2.46	0.77
173	224	2.0	4.0	1.0	4.1	3.68	1.11
174	224	2.0	4.0	1.4	3.95	3.84	1.03
175	224	2.0	4.0	1.8	3.8	3.98	0.95
176	224	2.0	4.0	0.8	4.0	3.59	1.11
177	1165	0.5	1.3	1.0	16.85	16.98	0.99
178	1165	0.5	1.3	1.4	16.75	16.63	1.01
179	1165	0.5	1.3	1.8	16.70	16.36	1.02
180	1165	0.5	1.3	0.8	16.95	17.17	0.99
181	3585	0.5	4.0	1.0	52.15	51.59	1.01
182	3585	0.5	4.0	1.4	52.5	52.06	1.01
183	3585	0.5	4.0	1.8	52.2	52.38	1
184	3585	0.5	4.0	0.8	52.15	51.29	1.02
185	90	2	4.0	1.0	1.7	1.31	1.3
186	90	2	4.0	1.6	1.6	1.54	1.04
187	90	2	4.0	1.3	1.6	1.43	1.12
188	90	2	4.0	0.7	1.6	1.17	1.37
189	347	2	1.3	1.0	9.1	7.97	1.14
190	347	2	1.3	1.6	8.25	7.73	1.07
191	347	2	1.3	1.3	8.7	7.84	1.11
192	347	2	1.3	0.7	8.55	8.11	1.05
193	125	1.5	1.3	1.0	2.05	1.72	1.19
194	125	1.5	4.0	1.6	2.1	1.93	1.09
195	125	1.5	4.0	1.3	2.08	1.83	1.14
196	125	1.5	4.0	0.7	2.12	1.6	1.33
197	906	1.5	4.0	1.0	17.95	16.65	1.08
198	906	1.5	1.3	1.6	16.35	16.2	1.01
199	906	1.5	1.3	1.3	17.05	16.41	1.04
200	906	1.5	1.3	0.7	18.8	16.91	1.11
201	2039	1.0	1.3	1.0	31.8	31.98	0.99
202	2039	1.0	1.3	1.6	30.5	31.24	0.98
203	2039	1.0	1.3	1.3	31.05	31.6	0.98
204	2039	1.0	1.3	0.7	32.8	32.39	1.01
205	316	1.0	4.0	1.0	4.95	4.74	1.04
206	316	1.0	4.0	1.6	4.85	4.97	0.98
207	316	1.0	4.0	1.3	4.90	4.86	1.01
208	316	1.0	4.0	0.7	4.32	4.63	0.93
209	563	0.75	4.0	1.0	8.5	8.53	1
210	563	0.75	4.0	1.6	8.35	8.78	0.95
211	563	0.75	4.0	1.3	8.45	8.66	0.98
212	563	0.75	4.0	0.7	8.08	8.4	0.96
213	2543	0.75	1.3	1.0	37.1	37.75	0.98
214	2543	0.75	1.3	1.6	36.4	36.92	0.99
215	2543	0.75	1.3	1.3	36.7	37.32	0.98
216	2543	0.75	1.3	0.7	37.7	38.19	0.99
217	1266	0.5	4.0	1.0	18.65	18.67	1
218	1266	0.5	4.0	1.6	18.8	18.98	0.99
219	1266	0.5	4.0	1.3	18.9	18.83	1
220	1266	0.5	4.0	0.7	18.50	18.48	1
221	5722	0.5	1.3	1.0	81.15	81.44	1
222	5722	0.5	1.3	1.6	80.3	80.3	1
223	5722	0.5	1.3	1.3	80.7	80.88	1
224	5722	0.5	1.3	0.7	81.9	81.95	1

No	Net inputs				Failure Pressure		
	$\frac{F_x Z}{L^2}$	L/H	F <sub>x</sub> /F <sub>y</sub>	E <sub>x</sub> /E <sub>y</sub>	NN output	FEM	Ratio
					$\times 10^{-3}$ (N/mm <sup>2</sup> )	$\times 10^{-3}$ (N/mm <sup>2</sup> )	$\frac{\text{FEM}}{\text{NN}}$
1	1434	0.75	2.0	1.0	11.12	10.88	1.02
2	1434	0.75	2.0	1.4	10.9	12.03	0.91
3	1434	0.75	2.0	1.8	12.75	13.57	0.94
4	1434	0.75	2.0	0.8	11.18	10.64	1.05
5	2151	0.75	3.0	1.0	16.55	16.01	1.03
6	2151	0.75	3.0	1.4	15.38	15.57	0.99
7	2151	0.75	3.0	1.8	14.42	15.94	0.9
8	2151	0.75	3.0	0.8	16.55	16.34	1.01
9	807	1.0	2.0	1.0	8.08	7.39	1.09
10	807	1.0	2.0	1.4	7.62	7.36	1.04
11	807	1.0	2.0	1.8	7.35	7.9	0.93
12	807	1.0	2.0	0.8	8.15	7.46	1.09
13	1210	1.0	3.0	1.0	11.65	11.57	1.01
14	1210	1.0	3.0	1.4	11.42	11.14	1.03
15	1210	1.0	3.0	1.8	10.72	10.57	1.01
16	1210	1.0	3.0	0.8	11.68	11.63	1
17	359	1.5	2.0	1.0	4.92	5.13	0.96
18	359	1.5	2.0	1.4	5.12	5.17	0.99
19	359	1.5	2.0	1.8	5.0	4.76	1.05
20	359	1.5	2.0	0.8	4.25	4.94	0.86
21	538	1.5	3.0	1.0	7.5	7.0	1.07
22	538	1.5	3.0	1.4	7.14	7.39	0.97
23	538	1.5	3.0	1.8	6.95	7.29	0.95
24	538	1.5	3.0	0.8	5.65	6.65	0.85
25	202	2.0	2.0	1.0	3.45	3.58	0.96
26	202	2.0	2.0	1.4	3.52	3.82	0.92
27	202	2.0	2.0	1.8	3.57	3.7	0.96
28	202	2.0	2.0	0.8	3.42	3.37	1.01
29	303	2.0	3.0	1.0	4.5	4.42	1.02
30	303	2.0	3.0	1.4	4.5	4.69	0.96
31	303	2.0	3.0	1.8	4.8	4.73	1.01
32	303	2.0	3.0	0.8	4.03	4.24	0.95
33	3227	0.5	2.0	1.0	23.5	23.17	1.01
34	3227	0.5	2.0	1.4	24.7	24.15	1.02
35	3227	0.5	2.0	1.8	24.0	23.25	1.03
36	3227	0.5	2.0	0.8	20.45	22.25	0.92
37	4840	0.5	3.0	1.0	31.38	30.84	1.02
38	4840	0.5	3.0	1.4	31.6	32.18	0.98
39	4840	0.5	3.0	1.8	34.35	32.9	1.04
40	4840	0.5	3.0	0.8	30.36	30.44	1
41	637	0.75	2.0	1.0	4.95	4.64	1.07
42	637	0.75	2.0	1.4	4.9	5.12	0.96
43	637	0.75	2.0	1.8	5.7	6.07	0.94
44	637	0.75	2.0	0.8	5.05	4.65	1.09
45	956	0.75	3.0	1.0	7.38	7.62	0.97
46	956	0.75	3.0	1.4	7.02	7.02	1

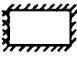
47	956	0.75	3.0	1.8	6.78	6.84	0.99
48	956	0.75	3.0	0.8	7.55	7.92	0.95
49	359	1.0	2.0	1.0	3.62	3.19	1.13
50	359	1.0	2.0	1.4	3.48	2.85	1.22
51	359	1.0	2.0	1.8	3.1	2.88	1.08
52	359	1.0	2.0	0.8	3.68	3.38	1.09
53	538	1.0	3.0	1.0	5.12	5.73	0.89
54	538	1.0	3.0	1.4	5.15	5.21	0.99
55	538	1.0	3.0	1.8	4.85	4.45	1.09
56	538	1.0	3.0	0.8	4.98	5.84	0.85
57	159	1.5	2.0	1.0	2.2	2.38	0.92
58	159	1.5	2.0	1.4	2.28	2.2	1.04
59	159	1.5	2.0	1.8	2.38	1.6	1.49
60	159	1.5	2.0	0.8	2.52	2.31	1.09
61	239	1.5	3.0	1.0	3.34	3.4	0.98
62	239	1.5	3.0	1.4	3.35	3.49	0.96
63	239	1.5	3.0	1.8	3.12	3.13	1
64	239	1.5	3.0	0.8	2.73	3.22	0.85
65	90	2.0	2.0	1.0	1.54	1.58	0.97
66	90	2.0	2.0	1.4	1.57	1.62	0.97
67	90	2.0	2.0	1.8	1.60	1.34	1.19
68	90	2.0	2.0	0.8	1.53	1.47	1.04
69	135	2.0	3.0	1.0	2.15	1.9	1.13
70	135	2.0	3.0	1.4	2.15	1.89	1.14
71	135	2.0	3.0	1.8	2.15	1.66	1.3
72	135	2.0	3.0	0.8	2.04	1.87	1.09
73	1434	0.5	2.0	1.0	10.55	10.15	1.04
74	1434	0.5	2.0	1.4	11.0	11.32	0.97
75	1434	0.5	2.0	1.8	10.65	11.19	0.95
76	1434	0.5	2.0	0.8	9.2	9.52	0.97
77	2151	0.5	3.0	1.0	13.80	13.26	1.04
78	2151	0.5	3.0	1.4	14.25	13.69	1.04
79	2151	0.5	3.0	1.8	15.35	14.78	1.04
80	2151	0.5	3.0	0.8	13.35	13.41	1
81	2490	0.75	4.0	1.0	18.75	18.93	0.99
82	2490	0.75	4.0	1.4	17.28	18.05	0.96
83	2490	0.75	4.0	1.8	17.22	17.1	1.01
84	2490	0.75	4.0	0.8	19.35	19.22	1.01
85	455	1.0	1.3	1.0	4.9	4.46	1.1
86	455	1.0	1.3	1.4	5.65	5.24	1.08
87	455	1.0	1.3	1.8	6.35	6.5	0.98
88	455	1.0	1.3	0.8	4.5	4.29	1.05
89	1401	1.0	4.0	1.0	13.32	12.76	1.04
90	1401	1.0	4.0	1.4	13.22	12.82	1.03
91	1401	1.0	4.0	1.8	12.35	12.35	1
92	1401	1.0	4.0	0.8	13.25	12.53	1.06
93	623	1.5	4.0	1.0	7.58	6.74	1.12
94	623	1.5	4.0	1.4	7.48	7.5	1
95	623	1.5	4.0	1.8	8.15	7.91	1.03
96	623	1.5	4.0	0.8	6.02	6.28	0.96
97	114	2.0	1.3	1.0	3.07	3.4	0.9
98	114	2.0	1.3	1.4	3.13	3.58	0.87
99	114	2.0	1.3	1.8	3.19	3.33	0.96
100	114	2.0	1.3	0.8	3.04	3.19	0.95

101	350	2.0	4.0	1.0	4.4	4.51	0.98
102	350	2.0	4.0	1.4	4.78	4.74	1.01
103	350	2.0	4.0	1.8	4.88	4.88	1
104	350	2.0	4.0	0.8	4.38	4.4	1
105	1821	0.5	1.3	1.0	15.05	15.36	0.98
106	1821	0.5	1.3	1.4	14.25	15.25	0.93
107	1821	0.5	1.3	1.8	13.55	13.44	1.01
108	1821	0.5	1.3	0.8	15.2	14.73	1.03
109	5602	0.5	4.0	1.0	33.78	34.3	0.98
110	5602	0.5	4.0	1.4	33.36	33.88	0.98
111	5602	0.5	4.0	1.8	34.28	34.56	0.99
112	5602	0.5	4.0	0.8	34.18	34.87	0.98
113	1165	0.75	1.3	1.0	11.5	10.92	1.05
114	1165	0.75	1.3	1.4	13.3	12.83	1.04
115	1165	0.75	1.3	1.8	13.3	13.53	0.98
116	1165	0.75	1.3	0.8	10.1	9.99	1.01
117	3585	0.75	4.0	1.0	26.65	26.79	0.99
118	3585	0.75	4.0	1.4	24.85	25.64	0.97
119	3585	0.75	4.0	1.8	24.78	24.66	1
120	3585	0.75	4.0	0.8	26.45	27.26	0.97
121	656	1.0	1.3	1.0	7.0	6.66	1.05
122	656	1.0	1.3	1.4	8.1	7.73	1.05
123	656	1.0	1.3	1.8	9.1	9.33	0.98
124	656	1.0	1.3	0.8	6.45	6.37	1.01
125	2017	1.0	4.0	1.0	18.52	18.16	1.02
126	2017	1.0	4.0	1.4	17.85	18.11	0.99
127	2017	1.0	4.0	1.8	17.45	17.54	0.99
128	2017	1.0	4.0	0.8	19.25	17.96	1.07
129	291	1.5	1.3	1.0	4.85	5.07	0.96
130	291	1.5	1.3	1.4	5.15	5.12	1.01
131	291	1.5	1.3	1.8	5.4	4.94	1.09
132	291	1.5	1.3	0.8	4.7	4.9	0.96
133	896	1.5	4.0	1.0	10.4	9.71	1.07
134	896	1.5	4.0	1.4	10.45	10.73	0.97
135	896	1.5	4.0	1.8	11.06	11.36	0.97
136	896	1.5	4.0	0.8	8.72	9.11	0.96
137	164	2.0	1.3	1.0	4.41	4.46	0.99
138	164	2.0	1.3	1.4	4.50	4.73	0.95
139	164	2.0	1.3	1.8	4.58	4.55	1.01
140	164	2.0	1.3	0.8	4.37	4.19	1.04
141	504	2.0	4.0	1.0	6.56	6.5	1.01
142	504	2.0	4.0	1.4	6.98	6.99	1
143	504	2.0	4.0	1.8	7.08	7.39	0.96
144	504	2.0	4.0	0.8	6.3	6.26	1.01
145	2622	0.5	1.3	1.0	21.7	21.68	1
146	2622	0.5	1.3	1.4	20.55	21.3	0.96
147	2622	0.5	1.3	1.8	19.5	19.34	1.01
148	2622	0.5	1.3	0.8	21.85	21.13	1.03
149	8067	0.5	4.0	1.0	48.92	48.55	1.01
150	8067	0.5	4.0	1.4	48.4	49.24	0.98
151	8067	0.5	4.0	1.8	49.55	50.13	0.99
152	8067	0.5	4.0	0.8	50.2	48.53	1.03
153	518	0.75	1.3	1.0	5.15	4.78	1.08
154	518	0.75	1.3	1.4	5.95	6.08	0.98



155	518	0.75	1.3	1.8	5.95	6.53	0.91
156	518	0.75	1.3	0.8	4.55	4.22	1.08
157	291	1.0	1.3	1.0	3.15	2.69	1.17
158	291	1.0	1.3	1.4	3.65	3.23	1.13
159	291	1.0	1.3	1.8	4.05	4.23	0.96
160	291	1.0	1.3	0.8	3.05	2.61	1.17
161	896	1.0	4.0	1.0	8.35	8.36	1
162	896	1.0	4.0	1.4	8.42	8.42	1
163	896	1.0	4.0	1.8	7.78	8.0	0.97
164	896	1.0	4.0	0.8	8.38	8.14	1.03
165	130	1.5	1.3	1.0	2.16	2.53	0.85
166	130	1.5	1.3	1.4	2.28	2.37	0.96
167	130	1.5	1.3	1.8	2.4	1.98	1.21
168	130	1.5	1.3	0.8	2.09	2.47	0.85
169	73	2.0	1.3	1.0	1.97	2.55	0.77
170	73	2.0	1.3	1.4	2.01	2.66	0.76
171	73	2.0	1.3	1.8	2.05	2.35	0.87
172	73	2.0	1.3	0.8	1.95	2.38	0.82
173	224	2.0	4.0	1.0	2.72	2.92	0.93
174	224	2.0	4.0	1.4	3.08	2.96	1.04
175	224	2.0	4.0	1.8	3.2	2.89	1.11
176	224	2.0	4.0	0.8	2.78	2.9	0.96
177	1165	0.5	1.3	1.0	9.65	10.26	0.94
178	1165	0.5	1.3	1.4	9.15	10.31	0.89
179	1165	0.5	1.3	1.8	8.65	8.67	1
180	1165	0.5	1.3	0.8	9.75	9.64	1.01
181	3585	0.5	4.0	1.0	22.18	22.09	1
182	3585	0.5	4.0	1.4	21.85	21.09	1.04
183	3585	0.5	4.0	1.8	21.9	21.07	1.04
184	3585	0.5	4.0	0.8	22.68	22.75	1
185	90	2	4.0	1.0	1.2	1.27	0.94
186	90	2	4.0	1.6	1.4	1.0	1.4
187	90	2	4.0	1.3	1.3	1.16	1.12
188	90	2	4.0	0.7	1.1	1.38	0.8
189	347	2	1.3	1.0	9.35	8.52	1.1
190	347	2	1.3	1.6	9.6	9.32	1.03
191	347	2	1.3	1.3	9.45	9.06	1.04
192	347	2	1.3	0.7	9.2	7.77	1.18
193	125	1.5	1.3	1.0	1.65	1.54	1.07
194	125	1.5	4.0	1.6	1.62	1.81	0.9
195	125	1.5	4.0	1.3	1.75	1.75	1
196	125	1.5	4.0	0.7	1.30	1.25	1.04
197	906	1.5	4.0	1.0	15.1	15.28	0.99
198	906	1.5	1.3	1.6	16.35	16.62	0.98
199	906	1.5	1.3	1.3	15.7	16.0	0.98
200	906	1.5	1.3	0.7	14.4	14.35	1
201	2039	1.0	1.3	1.0	21.65	22.22	0.97
202	2039	1.0	1.3	1.6	26.45	26.65	0.99
203	2039	1.0	1.3	1.3	24.15	24.27	1
204	2039	1.0	1.3	0.7	19.80	20.78	0.95
205	316	1.0	4.0	1.0	2.95	3.38	0.87
206	316	1.0	4.0	1.6	2.78	3.19	0.87
207	316	1.0	4.0	1.3	2.92	3.4	0.86
208	316	1.0	4.0	0.7	2.88	3.14	0.92

209	563	0.75	4.0	1.0	4.22	4.68	0.9
210	563	0.75	4.0	1.6	4.12	4.03	1.02
211	563	0.75	4.0	1.3	4.18	4.45	0.94
212	563	0.75	4.0	0.7	4.05	4.69	0.86
213	2543	0.75	1.3	1.0	24.85	24.5	1.01
214	2543	0.75	1.3	1.6	29.3	27.43	1.07
215	2543	0.75	1.3	1.3	28.2	26.42	1.07
216	2543	0.75	1.3	0.7	20.25	22.34	0.91
217	1266	0.5	4.0	1.0	8.05	7.86	1.02
218	1266	0.5	4.0	1.6	7.72	6.98	1.11
219	1266	0.5	4.0	1.3	7.72	7.37	1.05
220	1266	0.5	4.0	0.7	8.28	8.27	1
221	5722	0.5	1.3	1.0	47.3	46.26	1.02
222	5722	0.5	1.3	1.6	43.8	44.96	0.97
223	5722	0.5	1.3	1.3	45.6	45.82	1
224	5722	0.5	1.3	0.7	46.2	46.08	1

Set7 - 

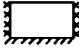
No	Net inputs				Failure Pressure		
	$\frac{F_x Z}{L^2}$	L/H	Fx/Fy	Ex/Ey	NN output x10 <sup>-3</sup> (N/mm <sup>2</sup> )	FEM x10 <sup>-3</sup> (N/mm <sup>2</sup> )	Ratio $\frac{FEM}{NN}$
1	1434	0.75	2.0	1.0	27.55	27.59	1
2	1434	0.75	2.0	1.4	26.55	27.24	0.97
3	1434	0.75	2.0	1.8	25.35	25.69	0.99
4	1434	0.75	2.0	0.8	28.45	26.98	1.05
5	2151	0.75	3.0	1.0	34.5	36.0	0.96
6	2151	0.75	3.0	1.4	38.45	37.82	1.02
7	2151	0.75	3.0	1.8	37.8	37.82	1
8	2151	0.75	3.0	0.8	31.58	34.76	0.91
9	807	1.0	2.0	1.0	16.5	17.19	0.96
10	807	1.0	2.0	1.4	18.6	18.35	1.01
11	807	1.0	2.0	1.8	18.15	17.91	1.01
12	807	1.0	2.0	0.8	14.2	16.28	0.87
13	1210	1.0	3.0	1.0	21.02	21.63	0.97
14	1210	1.0	3.0	1.4	20.8	22.6	0.92
15	1210	1.0	3.0	1.8	24.0	23.81	1.01
16	1210	1.0	3.0	0.8	21.08	21.46	0.98
17	359	1.5	2.0	1.0	9.12	9.24	0.99
18	359	1.5	2.0	1.4	8.4	9.66	0.87
19	359	1.5	2.0	1.8	9.65	10.57	0.91
20	359	1.5	2.0	0.8	9.38	9.17	1.02
21	538	1.5	3.0	1.0	13.48	13.29	1.01
22	538	1.5	3.0	1.4	12.5	12.33	1.01
23	538	1.5	3.0	1.8	11.85	11.6	1.02
24	538	1.5	3.0	0.8	13.88	13.6	1.02
25	202	2.0	2.0	1.0	7.78	7.57	1.03
26	202	2.0	2.0	1.4	7.18	7.49	0.96
27	202	2.0	2.0	1.8	6.52	7.16	0.91
28	202	2.0	2.0	0.8	7.85	7.43	1.06
29	303	2.0	3.0	1.0	11.48	10.82	1.06

30	303	2.0	3.0	1.4	10.62	10.5	1.01
31	303	2.0	3.0	1.8	9.62	9.64	1
32	303	2.0	3.0	0.8	10.55	10.75	0.98
33	3227	0.5	2.0	1.0	50.55	50.48	1
34	3227	0.5	2.0	1.4	48.95	48.47	1.01
35	3227	0.5	2.0	1.8	47.8	46.82	1.02
36	3227	0.5	2.0	0.8	51.35	51.13	1
37	4840	0.5	3.0	1.0	75.4	75.37	1
38	4840	0.5	3.0	1.4	73.85	74.89	0.99
39	4840	0.5	3.0	1.8	72.25	72.44	1
40	4840	0.5	3.0	0.8	74.25	74.18	1
41	637	0.75	2.0	1.0	12.3	12.33	1
42	637	0.75	2.0	1.4	11.85	12.46	0.95
43	637	0.75	2.0	1.8	11.3	11.59	0.97
44	637	0.75	2.0	0.8	12.7	11.72	1.08
45	956	0.75	3.0	1.0	15.5	15.4	1.01
46	956	0.75	3.0	1.4	17.2	16.83	1.02
47	956	0.75	3.0	1.8	16.9	17.52	0.96
48	956	0.75	3.0	0.8	14.13	14.78	0.96
49	359	1.0	2.0	1.0	7.4	7.0	1.06
50	359	1.0	2.0	1.4	8.3	8.09	1.03
51	359	1.0	2.0	1.8	8.05	8.0	1.01
52	359	1.0	2.0	0.8	6.3	6.28	1
53	538	1.0	3.0	1.0	9.4	8.52	1.1
54	538	1.0	3.0	1.4	9.3	8.95	1.04
55	538	1.0	3.0	1.8	10.75	10.08	1.07
56	538	1.0	3.0	0.8	9.42	8.65	1.09
57	159	1.5	2.0	1.0	4.02	3.48	1.16
58	159	1.5	2.0	1.4	3.75	3.74	1
59	159	1.5	2.0	1.8	4.35	4.5	0.97
60	159	1.5	2.0	0.8	4.32	3.46	1.25
61	239	1.5	3.0	1.0	5.95	5.49	1.08
62	239	1.5	3.0	1.4	5.62	4.5	1.25
63	239	1.5	3.0	1.8	5.32	3.71	1.43
64	239	1.5	3.0	0.8	6.22	5.82	1.07
65	90	2.0	2.0	1.0	3.48	3.69	0.94
66	90	2.0	2.0	1.4	3.25	3.58	0.91
67	90	2.0	2.0	1.8	2.98	3.21	0.93
68	90	2.0	2.0	0.8	3.75	3.57	1.05
69	135	2.0	3.0	1.0	4.85	5.19	0.93
70	135	2.0	3.0	1.4	4.78	4.88	0.98
71	135	2.0	3.0	1.8	4.35	4.07	1.07
72	135	2.0	3.0	0.8	4.75	5.14	0.92
73	1434	0.5	2.0	1.0	22.7	23.41	0.97
74	1434	0.5	2.0	1.4	22.05	22.46	0.98
75	1434	0.5	2.0	1.8	21.55	21.43	1.01
76	1434	0.5	2.0	0.8	23.05	23.52	0.98
77	2151	0.5	3.0	1.0	33.9	33.45	1.01
78	2151	0.5	3.0	1.4	33.25	34.0	0.98
79	2151	0.5	3.0	1.8	32.6	33.17	0.98
80	2151	0.5	3.0	0.8	33.3	32.45	1.03
81	2490	0.75	4.0	1.0	38.88	37.72	1.03
82	2490	0.75	4.0	1.4	38.45	39.08	0.98
83	2490	0.75	4.0	1.8	42.5	40.96	1.04

84	2490	0.75	4.0	0.8	37.45	37.38	1
85	455	1.0	1.3	1.0	11.95	11.56	1.03
86	455	1.0	1.3	1.4	11.2	11.51	0.97
87	455	1.0	1.3	1.8	10.4	10.22	1.02
88	455	1.0	1.3	0.8	11.8	10.93	1.08
89	1401	1.0	4.0	1.0	23.65	24.24	0.98
90	1401	1.0	4.0	1.4	23.92	23.30	1.03
91	1401	1.0	4.0	1.8	23.38	23.62	0.99
92	1401	1.0	4.0	0.8	24.6	24.79	0.99
93	623	1.5	4.0	1.0	15.48	15.51	1
94	623	1.5	4.0	1.4	14.28	14.5	0.98
95	623	1.5	4.0	1.8	13.42	13.14	1.02
96	623	1.5	4.0	0.8	16.58	15.77	1.05
97	114	2.0	1.3	1.0	4.4	4.43	0.99
98	114	2.0	1.3	1.4	4.9	4.93	0.99
99	114	2.0	1.3	1.8	5.35	5.67	0.94
100	114	2.0	1.3	0.8	4.52	4.14	1.09
101	350	2.0	4.0	1.0	12.05	11.7	1.03
102	350	2.0	4.0	1.4	11.46	11.57	0.99
103	350	2.0	4.0	1.8	11.08	11.19	0.99
104	350	2.0	4.0	0.8	12.25	11.63	1.05
105	1821	0.5	1.3	1.0	28.45	28.4	1
106	1821	0.5	1.3	1.4	27.55	27.01	1.02
107	1821	0.5	1.3	1.8	26.95	26.22	1.03
108	1821	0.5	1.3	0.8	29.1	29.2	1
109	5602	0.5	4.0	1.0	81.22	82.9	0.98
110	5602	0.5	4.0	1.4	85.95	86.09	1
111	5602	0.5	4.0	1.8	84.45	85.51	0.99
112	5602	0.5	4.0	0.8	80.5	80.23	1
113	1165	0.75	1.3	1.0	23.0	23.72	0.97
114	1165	0.75	1.3	1.4	21.55	22.22	0.97
115	1165	0.75	1.3	1.8	20.45	20.61	0.99
116	1165	0.75	1.3	0.8	23.0	24.02	0.96
117	3585	0.75	4.0	1.0	55.52	54.79	1.01
118	3585	0.75	4.0	1.4	55.6	57.47	0.97
119	3585	0.75	4.0	1.8	61.0	59.58	1.02
120	3585	0.75	4.0	0.8	54.87	53.66	1.02
121	656	1.0	1.3	1.0	17.2	16.61	1.04
122	656	1.0	1.3	1.4	16.15	16.42	0.98
123	656	1.0	1.3	1.8	15.0	14.9	1.01
124	656	1.0	1.3	0.8	16.95	15.96	1.06
125	2017	1.0	4.0	1.0	33.92	34.58	0.98
126	2017	1.0	4.0	1.4	33.68	34.2	0.98
127	2017	1.0	4.0	1.8	33.45	34.97	0.96
128	2017	1.0	4.0	0.8	35.47	34.86	1.02
129	291	1.5	1.3	1.0	9.3	9.04	1.03
130	291	1.5	1.3	1.4	10.85	10.7	1.01
131	291	1.5	1.3	1.8	11.45	11.71	0.98
132	291	1.5	1.3	0.8	8.35	8.35	1
133	896	1.5	4.0	1.0	22.55	22.0	1.03
134	896	1.5	4.0	1.4	20.7	20.98	0.99
135	896	1.5	4.0	1.8	19.18	19.6	0.98
136	896	1.5	4.0	0.8	23.84	22.26	1.07
137	164	2.0	1.3	1.0	6.25	6.21	1.01

138	164	2.0	1.3	1.4	7.0	6.76	1.04
139	164	2.0	1.3	1.8	7.7	7.55	1.02
140	164	2.0	1.3	0.8	6.32	5.9	1.07
141	504	2.0	4.0	1.0	17.25	16.67	1.03
142	504	2.0	4.0	1.4	17.38	16.52	1.05
143	504	2.0	4.0	1.8	15.28	16.08	0.95
144	504	2.0	4.0	0.8	16.85	16.61	1.01
145	2622	0.5	1.3	1.0	40.75	40.46	1.01
146	2622	0.5	1.3	1.4	39.45	38.71	1.02
147	2622	0.5	1.3	1.8	38.6	37.83	1.02
148	2622	0.5	1.3	0.8	41.6	41.55	1
149	8067	0.5	4.0	1.0	117.8	118.69	0.99
150	8067	0.5	4.0	1.4	122.95	121.58	1.01
151	8067	0.5	4.0	1.8	120.9	120.49	1
152	8067	0.5	4.0	0.8	116.3	115.84	1
153	518	0.75	1.3	1.0	10.3	10.68	0.96
154	518	0.75	1.3	1.4	9.65	9.79	0.99
155	518	0.75	1.3	1.8	9.15	8.66	1.06
156	518	0.75	1.3	0.8	10.25	10.74	0.95
157	291	1.0	1.3	1.0	7.65	7.51	1.02
158	291	1.0	1.3	1.4	7.2	7.57	0.95
159	291	1.0	1.3	1.8	6.65	6.46	1.03
160	291	1.0	1.3	0.8	7.55	6.89	1.1
161	896	1.0	4.0	1.0	15.28	15.71	0.97
162	896	1.0	4.0	1.4	15.42	14.47	1.07
163	896	1.0	4.0	1.8	15.05	14.52	1.04
164	896	1.0	4.0	0.8	15.82	16.4	0.96
165	130	1.5	1.3	1.0	4.15	3.97	1.05
166	130	1.5	1.3	1.4	4.85	5.43	0.89
167	130	1.5	1.3	1.8	5.10	6.39	0.8
168	130	1.5	1.3	0.8	3.75	3.38	1.11
169	73	2.0	1.3	1.0	2.8	3.0	0.93
170	73	2.0	1.3	1.4	3.15	3.47	0.91
171	73	2.0	1.3	1.8	3.45	4.15	0.83
172	73	2.0	1.3	0.8	2.9	2.72	1.07
173	224	2.0	4.0	1.0	7.48	7.74	0.97
174	224	2.0	4.0	1.4	7.28	7.64	0.95
175	224	2.0	4.0	1.8	7.15	7.29	0.98
176	224	2.0	4.0	0.8	7.35	7.67	0.96
177	1165	0.5	1.3	1.0	18.3	18.38	1
178	1165	0.5	1.3	1.4	17.8	17.33	1.03
179	1165	0.5	1.3	1.8	17.4	16.66	1.04
180	1165	0.5	1.3	0.8	18.7	18.94	0.99
181	3585	0.5	4.0	1.0	52.3	51.64	1.01
182	3585	0.5	4.0	1.4	55.4	54.21	1.02
183	3585	0.5	4.0	1.8	54.55	54.72	1
184	3585	0.5	4.0	0.8	51.05	50.02	1.02
185	90	2	4.0	1.0	2.98	3.67	0.81
186	90	2	4.0	1.6	2.92	3.46	0.84
187	90	2	4.0	1.3	3.02	3.63	0.83
188	90	2	4.0	0.7	3.28	3.53	0.93
189	347	2	1.3	1.0	13.2	13.05	1.01
190	347	2	1.3	1.6	15.5	14.21	1.09
191	347	2	1.3	1.3	14.4	13.57	1.06

192	347	2	1.3	0.7	11.9	12.45	0.96
193	125	1.5	1.3	1.0	3.28	3.89	0.84
194	125	1.5	4.0	1.6	3.12	2.38	1.31
195	125	1.5	4.0	1.3	3.18	3.25	0.98
196	125	1.5	4.0	0.7	3.45	4.2	0.82
197	906	1.5	4.0	1.0	28.8	29.85	0.96
198	906	1.5	1.3	1.6	34.95	33.14	1.05
199	906	1.5	1.3	1.3	32.6	31.71	1.03
200	906	1.5	1.3	0.7	24.3	28.27	0.86
201	2039	1.0	1.3	1.0	53.45	51.11	1.05
202	2039	1.0	1.3	1.6	48.5	48.49	1
203	2039	1.0	1.3	1.3	51.25	50.46	1.02
204	2039	1.0	1.3	0.7	49.8	49.86	1
205	316	1.0	4.0	1.0	5.62	5.89	0.95
206	316	1.0	4.0	1.6	5.48	4.17	1.31
207	316	1.0	4.0	1.3	3.8	4.77	0.8
208	316	1.0	4.0	0.7	5.68	7.0	0.81
209	563	0.75	4.0	1.0	8.68	8.78	0.99
210	563	0.75	4.0	1.6	9.5	9.16	1.04
211	563	0.75	4.0	1.3	9.75	8.45	1.15
212	563	0.75	4.0	0.7	9.08	9.74	0.93
213	2543	0.75	1.3	1.0	50.05	50.64	0.99
214	2543	0.75	1.3	1.6	45.65	46.66	0.98
215	2543	0.75	1.3	1.3	47.6	48.67	0.98
216	2543	0.75	1.3	0.7	52.5	51.65	1.02
217	1266	0.5	4.0	1.0	19.22	18.64	1.03
218	1266	0.5	4.0	1.6	19.4	21.36	0.91
219	1266	0.5	4.0	1.3	19.7	19.83	0.99
220	1266	0.5	4.0	0.7	18.72	18.22	1.03
221	5722	0.5	1.3	1.0	87.85	87.88	1
222	5722	0.5	1.3	1.6	84.0	84.68	0.99
223	5722	0.5	1.3	1.3	85.65	85.76	1
224	5722	0.5	1.3	0.7	90.85	90.63	1

Set8 - 

No	Net inputs				Failure Pressure		
	$\frac{F_x Z}{L^2}$	L/H	Fx/Fy	Ex/Ey	NN output $\times 10^{-3}$ (N/mm <sup>2</sup> )	FEM $\times 10^{-3}$ (N/mm <sup>2</sup> )	Ratio $\frac{FEM}{NN}$
1	1434	0.75	2.0	1.0	35.3	35.03	1.01
2	1434	0.75	2.0	1.4	35.15	35.21	1
3	1434	0.75	2.0	1.8	35.05	34.84	1.01
4	1434	0.75	2.0	0.8	35.4	35.06	1.01
5	2151	0.75	3.0	1.0	52.35	52.97	0.99
6	2151	0.75	3.0	1.4	53.1	52.63	1.01
7	2151	0.75	3.0	1.8	52.9	52.81	1
8	2151	0.75	3.0	0.8	48.15	52.46	0.92
9	807	1.0	2.0	1.0	19.9	19.63	1.01
10	807	1.0	2.0	1.4	19.7	20.03	0.98
11	807	1.0	2.0	1.8	19.55	19.64	1

12	807	1.0	2.0	0.8	20.05	19.82	1.01
13	1210	1.0	3.0	1.0	30.0	29.68	1.01
14	1210	1.0	3.0	1.4	29.75	29.77	1
15	1210	1.0	3.0	1.8	29.5	29.63	1
16	1210	1.0	3.0	0.8	29.45	29.5	1
17	359	1.5	2.0	1.0	9.75	9.43	1.03
18	359	1.5	2.0	1.4	9.5	9.52	1
19	359	1.5	2.0	1.8	9.25	9.17	1.01
20	359	1.5	2.0	0.8	9.75	9.57	1.02
21	538	1.5	3.0	1.0	13.82	13.49	1.02
22	538	1.5	3.0	1.4	14.15	13.57	1.04
23	538	1.5	3.0	1.8	13.90	13.47	1.03
24	538	1.5	3.0	0.8	13.08	13.34	0.98
25	202	2.0	2.0	1.0	5.95	5.89	1.01
26	202	2.0	2.0	1.4	6.2	5.72	1.08
27	202	2.0	2.0	1.8	6.0	5.86	1.02
28	202	2.0	2.0	0.8	5.2	5.94	0.88
29	303	2.0	3.0	1.0	7.74	8.22	0.94
30	303	2.0	3.0	1.4	8.05	8.03	1
31	303	2.0	3.0	1.8	8.65	8.34	1.04
32	303	2.0	3.0	0.8	7.72	8.1	0.95
33	3227	0.5	2.0	1.0	78.95	78.6	1
34	3227	0.5	2.0	1.4	78.45	77.71	1.01
35	3227	0.5	2.0	1.8	78.05	78.18	1
36	3227	0.5	2.0	0.8	79.3	77.78	1.02
37	4840	0.5	3.0	1.0	117.8	114.52	1.03
38	4840	0.5	3.0	1.4	118.55	114.35	1.04
39	4840	0.5	3.0	1.8	117.9	119.02	0.99
40	4840	0.5	3.0	0.8	108.0	113.18	0.95
41	637	0.75	2.0	1.0	15.7	15.07	1.04
42	637	0.75	2.0	1.4	15.65	15.8	0.99
43	637	0.75	2.0	1.8	15.6	15.25	1.02
44	637	0.75	2.0	0.8	15.75	15.51	1.02
45	956	0.75	3.0	1.0	23.7	23.11	1.03
46	956	0.75	3.0	1.4	23.65	23.87	0.99
47	956	0.75	3.0	1.8	23.55	23.43	1.01
48	956	0.75	3.0	0.8	22.82	22.98	0.99
49	359	1.0	2.0	1.0	8.85	8.48	1.04
50	359	1.0	2.0	1.4	8.75	9.04	0.97
51	359	1.0	2.0	1.8	8.70	8.43	1.03
52	359	1.0	2.0	0.8	8.95	8.89	1.01
53	538	1.0	3.0	1.0	13.35	12.81	1.04
54	538	1.0	3.0	1.4	13.25	13.36	0.99
55	538	1.0	3.0	1.8	13.15	12.81	1.03
56	538	1.0	3.0	0.8	12.92	12.84	1.01
57	159	1.5	2.0	1.0	4.35	4.37	1
58	159	1.5	2.0	1.4	4.25	4.44	0.96
59	159	1.5	2.0	1.8	4.1	3.85	1.06
60	159	1.5	2.0	0.8	4.35	4.62	0.94
61	239	1.5	3.0	1.0	6.25	5.98	1.05
62	239	1.5	3.0	1.4	6.3	6.09	1.03
63	239	1.5	3.0	1.8	6.2	5.6	1.11
64	239	1.5	3.0	0.8	5.88	5.95	0.99
65	90	2.0	2.0	1.0	2.65	2.9	0.91

66	90	2.0	2.0	1.4	2.75	2.68	1.03
67	90	2.0	2.0	1.8	2.70	2.61	1.03
68	90	2.0	2.0	0.8	2.35	3.01	0.78
69	135	2.0	3.0	1.0	3.55	3.82	0.93
70	135	2.0	3.0	1.4	3.6	3.56	1.01
71	135	2.0	3.0	1.8	3.85	3.54	1.09
72	135	2.0	3.0	0.8	3.55	3.76	0.94
73	1434	0.5	2.0	1.0	35.2	34.56	1.02
74	1434	0.5	2.0	1.4	35.0	35.39	0.99
75	1434	0.5	2.0	1.8	34.8	34.98	0.99
76	1434	0.5	2.0	0.8	35.4	34.5	1.03
77	2151	0.5	3.0	1.0	53.15	51.35	1.04
78	2151	0.5	3.0	1.4	52.85	52.37	1.01
79	2151	0.5	3.0	1.8	52.55	52.87	0.99
80	2151	0.5	3.0	0.8	47.3	50.23	0.94
81	2490	0.75	4.0	1.0	46.69	60.75	0.77
82	2490	0.75	4.0	1.4	46.69	60.82	0.77
83	2490	0.75	4.0	1.8	46.69	61.97	0.75
84	2490	0.75	4.0	0.8	46.69	59.7	0.78
85	455	1.0	1.3	1.0	10.51	11.12	0.95
86	455	1.0	1.3	1.4	10.51	11.6	0.91
87	455	1.0	1.3	1.8	10.51	11.03	0.95
88	455	1.0	1.3	0.8	10.51	11.71	0.9
89	1401	1.0	4.0	1.0	28.01	34.73	0.81
90	1401	1.0	4.0	1.4	28.01	34.72	0.81
91	1401	1.0	4.0	1.8	28.01	34.76	0.81
92	1401	1.0	4.0	0.8	28.01	34.26	0.82
93	623	1.5	4.0	1.0	14.15	15.32	0.92
94	623	1.5	4.0	1.4	14.15	15.33	0.92
95	623	1.5	4.0	1.8	14.15	15.33	0.92
96	623	1.5	4.0	0.8	14.15	15.0	0.94
97	114	2.0	1.3	1.0	3.63	3.72	0.98
98	114	2.0	1.3	1.4	3.63	3.55	1.02
99	114	2.0	1.3	1.8	3.63	3.57	1.02
100	114	2.0	1.3	0.8	3.63	3.93	0.92
101	350	2.0	4.0	1.0	8.75	9.06	0.97
102	350	2.0	4.0	1.4	8.75	8.83	0.99
103	350	2.0	4.0	1.8	8.75	9.22	0.95
104	350	2.0	4.0	0.8	8.75	8.82	0.99
105	1821	0.5	1.3	1.0	35.7	44.32	0.81
106	1821	0.5	1.3	1.4	35.7	44.53	0.8
107	1821	0.5	1.3	1.8	35.7	43.97	0.81
108	1821	0.5	1.3	0.8	35.7	44.36	0.8
109	5602	0.5	4.0	1.0	101.85	126.14	0.81
110	5602	0.5	4.0	1.4	101.85	128.24	0.79
111	5602	0.5	4.0	1.8	101.85	136.93	0.74
112	5602	0.5	4.0	0.8	101.85	124.39	0.82
113	1165	0.75	1.3	1.0	28.5	28.31	1.01
114	1165	0.75	1.3	1.4	28.4	28.69	0.99
115	1165	0.75	1.3	1.8	28.3	28.25	1
116	1165	0.75	1.3	0.8	28.55	28.69	1
117	3585	0.75	4.0	1.0	86.72	86.8	1
118	3585	0.75	4.0	1.4	85.92	86.22	1
119	3585	0.75	4.0	1.8	88.6	89.11	0.99



120	3585	0.75	4.0	0.8	80.08	85.92	0.93
121	656	1.0	1.3	1.0	16.05	16.11	1
122	656	1.0	1.3	1.4	15.9	16.55	0.96
123	656	1.0	1.3	1.8	15.8	16.1	0.98
124	656	1.0	1.3	0.8	16.2	16.58	0.98
125	2017	1.0	4.0	1.0	48.4	50.07	0.97
126	2017	1.0	4.0	1.4	49.92	49.46	1.01
127	2017	1.0	4.0	1.8	49.45	50.12	0.99
128	2017	1.0	4.0	0.8	49.43	49.65	1
129	291	1.5	1.3	1.0	7.95	8.05	0.99
130	291	1.5	1.3	1.4	7.65	8.11	0.94
131	291	1.5	1.3	1.8	7.45	7.67	0.97
132	291	1.5	1.3	0.8	8.15	8.41	0.97
133	896	1.5	4.0	1.0	23.27	22.14	1.05
134	896	1.5	4.0	1.4	22.52	22.08	1.02
135	896	1.5	4.0	1.8	23.05	22.52	1.02
136	896	1.5	4.0	0.8	22.25	21.8	1.02
137	164	2.0	1.3	1.0	5.45	5.08	1.07
138	164	2.0	1.3	1.4	5.15	4.93	1.04
139	164	2.0	1.3	1.8	4.90	5.04	0.97
140	164	2.0	1.3	0.8	5.50	5.26	1.05
141	504	2.0	4.0	1.0	12.9	13.05	0.99
142	504	2.0	4.0	1.4	11.92	12.88	0.93
143	504	2.0	4.0	1.8	12.56	13.63	0.92
144	504	2.0	4.0	0.8	12.72	12.77	1
145	2622	0.5	1.3	1.0	63.65	64.11	0.99
146	2622	0.5	1.3	1.4	63.3	63.43	1
147	2622	0.5	1.3	1.8	63.05	63.06	1
148	2622	0.5	1.3	0.8	63.9	63.79	1
149	8067	0.5	4.0	1.0	178.85	179.31	1
150	8067	0.5	4.0	1.4	181.65	183.97	0.99
151	8067	0.5	4.0	1.8	197.55	195.9	1.01
152	8067	0.5	4.0	0.8	179.78	177.78	1.01
153	518	0.75	1.3	1.0	12.7	12.22	1.04
154	518	0.75	1.3	1.4	12.65	12.9	0.98
155	518	0.75	1.3	1.8	12.6	12.34	1.02
156	518	0.75	1.3	0.8	12.7	12.99	0.98
157	291	1.0	1.3	1.0	7.15	7.06	1.01
158	291	1.0	1.3	1.4	7.10	7.57	0.94
159	291	1.0	1.3	1.8	7.05	6.92	1.02
160	291	1.0	1.3	0.8	7.20	7.75	0.93
161	896	1.0	4.0	1.0	22.52	21.99	1.02
162	896	1.0	4.0	1.4	22.4	22.41	1
163	896	1.0	4.0	1.8	22.0	22.07	1
164	896	1.0	4.0	0.8	22.22	21.6	1.03
165	130	1.5	1.3	1.0	3.55	3.94	0.9
166	130	1.5	1.3	1.4	3.40	3.97	0.86
167	130	1.5	1.3	1.8	3.35	3.35	1
168	130	1.5	1.3	0.8	3.65	4.41	0.83
169	73	2.0	1.3	1.0	2.45	2.62	0.94
170	73	2.0	1.3	1.4	2.3	2.43	0.95
171	73	2.0	1.3	1.8	2.2	2.37	0.93
172	73	2.0	1.3	0.8	2.45	2.85	0.86
173	224	2.0	4.0	1.0	5.63	5.82	0.97

174	224	2.0	4.0	1.4	5.48	5.54	0.99
175	224	2.0	4.0	1.8	5.55	5.67	0.98
176	224	2.0	4.0	0.8	4.8	5.61	0.86
177	1165	0.5	1.3	1.0	28.4	27.97	1.02
178	1165	0.5	1.3	1.4	28.25	28.7	0.98
179	1165	0.5	1.3	1.8	28.1	28.16	1
180	1165	0.5	1.3	0.8	28.5	28.48	1
181	3585	0.5	4.0	1.0	79.55	81.5	0.98
182	3585	0.5	4.0	1.4	83.95	83.04	1.01
183	3585	0.5	4.0	1.8	88.05	86.96	1.01
184	3585	0.5	4.0	0.8	80.05	79.43	1.01
185	90	2	4.0	1.0	2.3	2.39	0.96
186	90	2	4.0	1.6	2.35	1.79	1.31
187	90	2	4.0	1.3	2.35	2.27	1.04
188	90	2	4.0	0.7	2.3	2.42	0.95
189	347	2	1.3	1.0	11.5	10.1	1.14
190	347	2	1.3	1.6	10.6	9.99	1.06
191	347	2	1.3	1.3	11.0	10.15	1.08
192	347	2	1.3	0.7	11.35	10.69	1.06
193	125	1.5	1.3	1.0	3.25	2.9	1.12
194	125	1.5	4.0	1.6	3.25	2.63	1.24
195	125	1.5	4.0	1.3	3.15	3.18	0.99
196	125	1.5	4.0	0.7	3.0	3.07	0.98
197	906	1.5	4.0	1.0	24.75	23.88	1.04
198	906	1.5	1.3	1.6	23.45	24.07	0.97
199	906	1.5	1.3	1.3	24.0	24.16	0.99
200	906	1.5	1.3	0.7	25.55	24.4	1.05
201	2039	1.0	1.3	1.0	49.80	50.02	1
202	2039	1.0	1.3	1.6	49.1	49.62	0.99
203	2039	1.0	1.3	1.3	49.4	49.89	0.99
204	2039	1.0	1.3	0.7	50.5	50.33	1
205	316	1.0	4.0	1.0	7.82	7.36	1.06
206	316	1.0	4.0	1.6	7.8	7.8	1
207	316	1.0	4.0	1.3	7.85	8.13	0.97
208	316	1.0	4.0	0.7	7.35	7.76	0.95
209	563	0.75	4.0	1.0	14.05	13.24	1.06
210	563	0.75	4.0	1.6	13.8	14.37	0.96
211	563	0.75	4.0	1.3	13.48	14.41	0.94
212	563	0.75	4.0	0.7	13.22	13.46	0.98
213	2543	0.75	1.3	1.0	62.1	62.18	1
214	2543	0.75	1.3	1.6	61.8	60.69	1.02
215	2543	0.75	1.3	1.3	61.9	61.54	1.01
216	2543	0.75	1.3	0.7	62.35	62.45	1
217	1266	0.5	4.0	1.0	28.88	28.64	1.01
218	1266	0.5	4.0	1.6	31.25	32.23	0.97
219	1266	0.5	4.0	1.3	29.25	30.57	0.96
220	1266	0.5	4.0	0.7	29.25	27.69	1.06
221	5722	0.5	1.3	1.0	138.65	139.91	0.99
222	5722	0.5	1.3	1.6	137.6	138.31	0.99
223	5722	0.5	1.3	1.3	138.05	138.0	1
224	5722	0.5	1.3	0.7	139.5	138.6	1.01

## APPENDIX IX

### Listing of the Source Code for the Neural Network Program

File Type	File Name	Discription
Header Files	Class.h	class definition
	Funct.h	declaration of external functions
	Fdial.h	defining the command Ids
.cpp files	Fdial.cpp	user interface program that communicate between the user and the neural network
	Netarch.cpp	main neural network program
	Act_Func.cpp	various activation functions
	Dotprod.cpp	dotproduct of two matrices
	Maxmin.cpp	maximum and minimum values in a vector
	NetData.cpp	reading and storing a net file
	Randn.cpp	generating random numbers for initial weight coefficients
	Runset.cpp	reading the training and test data during an application development
Others	Fdial.rc	resource codes generated with the user interface
	Fdial.def	project definition file

## HeaderFiles

### Class.h

```
~NetArch();
void Init_Wt(double lolt, double uplt);
void Wt_Copy();
void Read_Wt();
void Learn(int af);
void Test(int af);
void Arng_Layer();
void Normal(double inll,double inul,double outll,double outul);
void Init_data();
void Tng_Rst_Copy();
void Tst_Rst_Copy();
fstream file_wt,file_rst;

const char* wt_out;
const char* tng_rst;
const char* tst_rst;
int nin, nout, nhid, *nhidl, totnode,totwts,b_or_p,*nl,npat, Dyn_or_Stat, Wgt_Stat;
double neterr, *wt_coef,epsav,*y,*epsn,*err,*delw,*del,ALP,MU,*op,*netop ;
double ll,ul, *DelPrev, *x_deriv,*data_set,*invect,*outvect,*results;
double inll,inul,outll,outul, preveps, pergood,Alpha, changes;
double maxin, minin, maxout, minout, *normin, *normout,*nnout,*nop,*nerr;

private:
void ForPass(int i,int af);
void Denorm(double maxout,double outll,double outul);
void netout();
void ErrCal(int i);
void toterr();
void Copy_Dels();
void Modif_Wt();
void DelwCal();
void classif();

};

struct LearnParams
{
double qerror;
double mue;
double alpha;
};

class RunningSet
{
public:

RunningSet(const char* runfile);
~RunningSet();
//int MessageBox(hwndparent,lpsz text, lpsz text,fustyle);
void Read_Data();
void Learn();
```

```

ifstream file_in;
int nin, nout, ntrain, mode;
const char* file;
double *in_data;
};

```

```

struct AppNetInfo {
double TgtErr;
double RMSErr;
double Changes;
int Niter;
double GoodPat;
double MaxWgt;
double MinWgt;
int TotWgts;
int BatchModeRbt;
int PattModeRbt;
double LngRate;
double Momentum;
int LngStaticRbt;
int LngDynRbt;
int Nlayers;
int LayerOne;
int LayerTwo;
int LayerThree;
int LayerFour;
double InpdataMax;
double InpdataMin;
double OutdataMax;
double OutdataMin;
double NInpdataMax;
double NInpdataMin;
double NOutdataMax;
double NOutdataMin;
const char* TngFile;
const char* TstFile;
const char* WgtFile;
};

```

## **Funct.h**

```

// Declaration of all the global functions
// These are separate .cpp files but grouped under the same project.

//extern activity(double *input, double *wt, int n, int m);
extern double dotprod(int n, double *v1, double *v2);
//extern void init_act_func(int af);
extern double func_call(double x, int af);
extern double deriv_func(double out, int af);
extern double randn(double ll, double ul);
extern double maxval(int n, double *vect);
extern double minval(int n, double *vect);
extern void Net_Copy(struct AppNetInfo *NetInfoBuff, const char* netfile);
extern void Net_Read(struct AppNetInfo *NetInfoBuff, const char* netfile);

```

## Fdial.h

```
#define ID_NNET 1000
#define ID_NETOPFILE 1001
#define ID_TNGFILE 1002
#define ID_TSTFILE 1003
#define ID_WGTOPFILE 1004
#define ID_SVNETFILE 1005
#define ID_SVNET_ASFILE 1006
#define ID_SVWGTFILE 1007
#define ID_SVWGT_ASFILE 1008
#define ID_PRINTFILE 1009
#define ID_PRINTSETUP 1010
#define ID_START_TNG 1011
#define ID_HLT_TNG 1012
#define ID_TST_TNG 1013
#define ID_TST_TST 1014
#define ID_PLT_WGTS 1015
#define ID_PLT_TNG 1016
#define ID_PLT_TST 017
#define ID_PLT_ERR 1018
#define ID_PLT_LOUT 1019
#define CM_EXIT(WM_USER + 110)
#define ID_TNG_RSLT_GRP 1020
#define ID_TGT_ERR_TXT 1021
#define ID_TGT_ERR_EDIT 1022
#define ID_RMS_ERR_TXT 1023
#define ID_RMS_ERR_EDIT 1024
#define ID_CHANGES_TXT 1025
#define ID_CHANGES_EDIT 1026
#define ID_NITER_TXT 1027
#define ID_NITER_EDIT 1028
#define ID_GOODPAT_TXT 1029
#define ID_GOODPAT_EDIT 1030
#define ID_INIT_WGTS_GRP 1031
#define ID_MAX_WGT_TXT 1032
#define ID_MIN_WGT_TXT 1033
#define ID_MAX_WGT_EDIT 1034
#define ID_MIN_WGT_EDIT 1035
#define ID_WGT_RGE_TXT 1036
#define ID_RAND_WGTS 1037
#define ID_TNG_MODE_GRP 1038
#define ID_BATCHMODE_RBT 1039
#define ID_PATTERNMODE_RBT 1040
#define ID_LNG_PARA_GRP 1041
#define ID_LNG_RATE_TXT 1042
#define ID_LNG_RATE_EDIT 1043
#define ID_LNG_STATIC_RBT 1044
#define ID_LNG_DYN_RBT 1045
#define ID_MOMENTUM_TXT 1046
#define ID_MOMENTUM_EDIT 1047
#define ID_NET_ARCH_GRP 1048
#define ID_NLAYERS_TXT 1049
///define ID_NLAYERS_SCRL 1050
#define ID_NLAYERS_EDIT 1051
```

```

#define ID_LAYER_SIZE_TXT          1052
#define ID_ACT_FUNC_TXT            1053
//#define ID_LAYER_SIZE_CMB        1054
#define ID_ACT_FUNC_CMB           1055
#define ID_DATA_NORM_GRP          1056
#define ID_DATA_RANGE_TXT         1057
#define ID_DATA_INP_MAX_TXT       1058
#define ID_DATA_INP_MIN_TXT       1059
#define ID_DATA_INP_TXT           1060
#define ID_DATA_INP_MAX_EDIT      1061
#define ID_DATA_INP_MIN_EDIT      1062
#define ID_DATA_OUT_MAX_TXT       1063
#define ID_DATA_OUT_MIN_TXT       1064
#define ID_DATA_OUT_TXT           1065
#define ID_DATA_OUT_MAX_EDIT      1066
#define ID_DATA_OUT_MIN_EDIT      1067
#define ID_DATA_NINP_MAX_TXT      1068
#define ID_DATA_NINP_MIN_TXT      1069
#define ID_DATA_NINP_TXT          1070
#define ID_DATA_NINP_MAX_EDIT     1071
#define ID_DATA_NINP_MIN_EDIT     1072
#define ID_DATA_NOUT_MAX_TXT      1073
#define ID_DATA_NOUT_MIN_TXT      1074
#define ID_DATA_NOUT_TXT          1075
#define ID_DATA_NOUT_MAX_EDIT     1076
#define ID_DATA_NOUT_MIN_EDIT     1077
#define ID_DATA_NRANGE_TXT        1078
#define ID_DATA_NORM              1079
#define ID_OPEN_FILE_TXT          1080
#define ID_OPENF_TNG_SET          1081
#define ID_OPENF_WGT_SET          1082
#define ID_OPENF_TST_SET          1083
#define ID_TNG_FILE_EDIT          1084
#define ID_WGT_FILE_EDIT          1085
#define ID_TST_FILE_EDIT          1086
#define ID_LOAD_ANN_TXT           1087
#define ID_LAYER_ONE_TXT          1088
#define ID_LAYER_TWO_TXT          1089
#define ID_LAYER_THREE_TXT        1090
#define ID_LAYER_FOUR_TXT         1091
#define ID_LAYER_ONE_EDIT         1092
#define ID_LAYER_TWO_EDIT         1093
#define ID_LAYER_THREE_EDIT       1094
#define ID_LAYER_FOUR_EDIT        1095
#define ID_TRANSF_DATA            1096
#define ID_TOT_WGT_EDIT           1097
#define IDC_OP_DISPLY_LST         1200
#define ID_EDITF_TNG_SET          1100
#define ID_EDITF_TST_SET          1101
#define ID_EDITF_WGT_SET          1102
#define IDD_ANN_WINDOW_DLG        1100
#define IDD_OPEN_ANNAPP_DLG       1101
#define IDD_RESULTS_DPLY_DLG      1102

```

## Fdial.CPP

```
#include <stdlib.h>
#include <stdio.h>
#include <string.h>
#include <dos.h>
#include <afxwin.h>
#include <afxdlgs.h>
#include <afx.h>
#include "fdial.h"
#include "c:\anu\chris\main\funct.h"
#include "c:\anu\chris\main\class.h"
#include <iostream.h>
#include <fstream.h>
#include <time.h>
#include <math.h>
#include <malloc.h>
#include <fcntl.h>
#include <sys\types.h>
#include <sys/stat.h>
#include <io.h>

const MaxStringLen = 255;
const int MAX_CHARS = 30;
const int BF_CHECKED = 1;
const int BF_UNCHECKED = 0;

class CFileDialogApp:public CWinApp
{
public:
    virtual BOOL InitInstance();
};

class OpenANNAppDlg:public CDialog
{
public:
    OpenANNAppDlg(CWnd* pParentWnd = NULL): CDialog(OpenANNAppDlg::IDD,
pParentWnd){}
    enum
    {
        IDD = IDD_OPEN_ANNAPP_DLG
    };
};

class LoadANNAppDlg:public CDialog
{
public:
    LoadANNAppDlg(CWnd* pParentWnd = NULL): CDialog(LoadANNAppDlg::IDD,
pParentWnd){}
    enum
    {
        IDD = IDD_ANN_WINDOW_DLG
    };
    double TgtErrBuff;
    double RMSErrBuff;
};
```



```

double ChangesBuff;
int NiterBuff;
double GoodPatBuff;
double MaxWgtBuff;
double MinWgtBuff;
int TotWgtsBuff;
int BatchModeRbtBuff;
int PattModeRbtBuff;
double LngRateBuff;
double MomentumBuff;
int LngStaticRbtBuff;
int LngDynRbtBuff;
int NlayersBuff;
int LayerOneBuff;
int LayerTwoBuff;
int LayerThreeBuff;
int LayerFourBuff;
double InpdataMaxBuff;
double InpdataMinBuff;
double OutdataMaxBuff;
double OutdataMinBuff;
double NInpdataMaxBuff;
double NInpdataMinBuff;
double NOutdataMaxBuff;
double NOutdataMinBuff;
CString TngFileBuff;
CString TstFileBuff;
CString WgtFileBuff;
int DynOrStatLngRate;

NetArch *ANN, *EvalSet;
RunningSet *pattern, *TstSet;
RunningSet *test ;
struct LearnParams lpmtr;
int trmode,n_hids,*hidl,stat, TstStat, act_func, TngFlag,ntr, n_outp,n_inp;
int wgt_stat,net_stat;
double *TgtOp,*NetOp;
CString NetFile;
void CMDisplyTng();
void Transf_Net_Info();
void ReTransf_Net_Info();
void CMTstRstSaveAsFile();
void CMTngRstSaveAsFile();
struct AppNetInfo NetInfoBuff;

void EnableButton(CButton* pBtn)
{
    pBtn->EnableWindow(TRUE);
}
void DisableButton(CButton* pBtn)
{
    pBtn->EnableWindow(FALSE);
}

```

protected:

```
virtual BOOL OnInitDialog();
virtual void DoDataExchange(CDataExchange* pDX);
```

```
public:
```

```
afx_msg void CMOpenNet();
afx_msg void CMTngFile();
afx_msg void CMTstFile();
afx_msg void CMNetOpFile();
afx_msg void CMWgtOpFile();
afx_msg void CMWgtSaveFile();
afx_msg void CMWgtSaveAsFile();
afx_msg void CMNetSaveAsFile();
afx_msg void CMNetSaveFile();
afx_msg void CMRandomize();
afx_msg void CMTransferData();
afx_msg void CMNormalize();
afx_msg void CMStartTng();
afx_msg void CMHalfTng();
afx_msg void CMTestTng();
afx_msg void CMTestTst();
afx_msg void CMEditTngFile();
afx_msg void CMEditTstFile();
afx_msg void CMEditWgtFile();
afx_msg void OnExit()
{
    SendMessage(WM_CLOSE);
}
afx_msg void OnClose();
DECLARE_MESSAGE_MAP()
```

```
};
```

```
class CMainWnd:public CFrameWnd
```

```
{
```

```
public:
```

```
    CMainWnd();
```

```
    ~CMainWnd();
```

```
friend LoadANNAAppDlg;
```

```
protected:
```

```
    CStatic* LoadANNAAppTxt;
```

```
    double pTgtErrBuff;
```

```
    double pRMSErrBuff;
```

```
    double pChangesBuff;
```

```
    int pNiterBuff;
```

```
    double pGoodPatBuff;
```

```
    double pMaxWgtBuff;
```

```
    double pMinWgtBuff;
```

```
    int pTotWgtsBuff;
```

```
    int pBatchModeRbtBuff;
```

```
    int pPattModeRbtBuff;
```

```
    double pLngRateBuff;
```

```
    double pMomentumBuff;
```

```
    int pLngStaticRbtBuff;
```

```
    int pLngDynRbtBuff;
```

```
    int pNlayersBuff;
```

```

int pLayerOneBuff;
int pLayerTwoBuff;
int pLayerThreeBuff;
int pLayerFourBuff;
double pInpdataMaxBuff;
double pInpdataMinBuff;
double pOutdataMaxBuff;
double pOutdataMinBuff;
double pNInpdataMaxBuff;
double pNInpdataMinBuff;
double pNOutdataMaxBuff;
double pNOutdataMinBuff;
CString pTngFileBuff;
CString pTstFileBuff;
CString pWgtFileBuff;

public:

    afx_msg void CMLoadANN();
    DECLARE_MESSAGE_MAP()

};

void LoadANNAppDlg::DoDataExchange(CDataExchange* pDX)
{
    CDialog::DoDataExchange(pDX);
    DDX_Text(pDX,ID_TGT_ERR_EDIT,TgtErrBuff);
    DDX_Text(pDX,ID_RMS_ERR_EDIT, RMSErrBuff);
    DDX_Text(pDX,ID_CHANGES_EDIT,ChangesBuff);
    DDX_Text(pDX,ID_NITER_EDIT,NiterBuff);
    DDX_Text(pDX,ID_GOODPAT_EDIT,GoodPatBuff);
    DDX_Text(pDX,ID_MAX_WGT_EDIT,MaxWgtBuff);
    DDX_Text(pDX,ID_MIN_WGT_EDIT,MinWgtBuff);
    DDX_Text(pDX,ID_TOT_WGT_EDIT,TotWgtsBuff);
    DDX_Text(pDX,ID_CHANGES_EDIT,ChangesBuff);
    DDX_Text(pDX,ID_LNG_RATE_EDIT,LngRateBuff);
    DDX_Text(pDX,ID_MOMENTUM_EDIT,MomentumBuff);
    DDX_Text(pDX,ID_NLAYERS_EDIT,NlayersBuff);
    DDX_Text(pDX,ID_LAYER_ONE_EDIT,LayerOneBuff);
    DDX_Text(pDX,ID_LAYER_TWO_EDIT,LayerTwoBuff);
    DDX_Text(pDX,ID_LAYER_THREE_EDIT,LayerThreeBuff);
    DDX_Text(pDX,ID_LAYER_FOUR_EDIT,LayerFourBuff);
    DDX_Text(pDX,ID_DATA_INP_MAX_EDIT,InpdataMaxBuff);
    DDX_Text(pDX,ID_DATA_INP_MIN_EDIT,InpdataMinBuff);
    DDX_Text(pDX,ID_DATA_OUT_MAX_EDIT,OutdataMaxBuff);
    DDX_Text(pDX,ID_DATA_OUT_MIN_EDIT,OutdataMinBuff);
    DDX_Text(pDX,ID_DATA_NINP_MAX_EDIT,NInpdataMaxBuff);
    DDX_Text(pDX,ID_DATA_NINP_MIN_EDIT,NInpdataMinBuff);
    DDX_Text(pDX,ID_DATA_NOUT_MAX_EDIT,NOutdataMaxBuff);
    DDX_Text(pDX,ID_DATA_NOUT_MIN_EDIT,NOutdataMinBuff);
    DDX_Text(pDX,ID_TNG_FILE_EDIT,TngFileBuff);
    DDX_Text(pDX,ID_TST_FILE_EDIT,TstFileBuff);
    DDX_Text(pDX,ID_WGT_FILE_EDIT,WgtFileBuff);
}

```

```

CMainWnd::CMainWnd()
{

    pTgtErrBuff = 0.01;
    pRMSErrBuff = 0.00;
    pChangesBuff= 0.00;
    pNiterBuff = 0;
    pGoodPatBuff= 0.00;
    pMaxWgtBuff = 1.00;
    pMinWgtBuff = 0.00;
    pTotWgtsBuff = 0;
    pLngRateBuff  = 0.20;
    pMomentumBuff  = 0.70;
    pNlayersBuff   = 3;
    pLayerOneBuff  = 1;
    pLayerTwoBuff  = 2;
    pLayerThreeBuff = 1;
    pLayerFourBuff = 0;
    pInpdataMaxBuff = 0.0;
    pInpdataMinBuff = 0.0;
    pOutdataMaxBuff = 0.0;
    pOutdataMinBuff = 0.0;
    pNInpdataMaxBuff = 1.0;
    pNInpdataMinBuff = 0.0;
    pNOutdataMaxBuff = 1.0;
    pNOutdataMinBuff = 0.0;
    pBatchModeRbtBuff = BF_UNCHECKED;
    pPattModeRbtBuff = BF_CHECKED;
    pLngStaticRbtBuff = BF_UNCHECKED;
    pLngDynRbtBuff = BF_CHECKED;

    OpenANNAppDlg ann(this);
    if (ann.DoModal() == IDOK)
        CMLoadANN();
    else
        OnClose();
};

CMainWnd::~CMainWnd()
{
    DestroyWindow();
}

BOOL LoadANNAppDlg::OnInitDialog()
{
    CMainWnd* pW = (CMainWnd*)(GetParent());
    UpdateData(FALSE);
    //data = (double*)malloc(2000*sizeof(double));
    hidl = (int*)malloc(4*sizeof(int));
    stat = 0;
    TstStat = 0;
    ANN = NULL;
    pattern = NULL;
    EvalSet = NULL;
    TstSet = NULL;
}

```

```

act_func = 1;
TngFlag = 0;
wgt_stat = 0;
net_stat = 0;
CComboBox* ActFuncCmb = (CComboBox*)(GetDlgItem(ID_ACT_FUNC_CMB));
ActFuncCmb->AddString("Sigmoid");
ActFuncCmb->AddString("TanH");
ActFuncCmb->AddString("Linear");
ActFuncCmb->SetCurSel(0);

BatchModeRbtBuff = pW->pBatchModeRbtBuff;
PattModeRbtBuff = pW->pPattModeRbtBuff;
LngStaticRbtBuff = pW->pLngStaticRbtBuff;
LngDynRbtBuff = pW->pLngDynRbtBuff;

CButton* pRBtn = (CButton*)(GetDlgItem(ID_BATCHMODE_RBT));
pRBtn->SetCheck(BatchModeRbtBuff);
pRBtn = (CButton*)(GetDlgItem(ID_PATTERNMODE_RBT));
pRBtn->SetCheck(PattModeRbtBuff);
pRBtn = (CButton*)(GetDlgItem(ID_LNG_STATIC_RBT));
pRBtn->SetCheck(LngStaticRbtBuff);
pRBtn = (CButton*)(GetDlgItem(ID_LNG_DYN_RBT));
pRBtn->SetCheck(LngDynRbtBuff);

return TRUE;
}

```

```

void CMainWnd::CMLoadANN()
{
LoadANNAppDlg Dlg(this);
Dlg.TgtErrBuff = pTgtErrBuff;
Dlg.RMSErrBuff = pRMSErrBuff;
Dlg.ChangesBuff = pChangesBuff;
Dlg.NiterBuff = pNiterBuff;
Dlg.GoodPatBuff = pGoodPatBuff;
Dlg.MaxWgtBuff = pMaxWgtBuff;
Dlg.MinWgtBuff = pMinWgtBuff;
Dlg.TotWgtsBuff = pTotWgtsBuff;
Dlg.LngRateBuff = pLngRateBuff;
Dlg.MomentumBuff = pMomentumBuff;
Dlg.NlayersBuff = pNlayersBuff;
Dlg.LayerOneBuff = pLayerOneBuff;
Dlg.LayerTwoBuff = pLayerTwoBuff;
Dlg.LayerThreeBuff = pLayerThreeBuff;
Dlg.LayerFourBuff = pLayerFourBuff;
Dlg.InpdataMaxBuff = pInpdataMaxBuff;
Dlg.InpdataMinBuff = pInpdataMinBuff;
Dlg.OutdataMaxBuff = pOutdataMaxBuff;
Dlg.OutdataMinBuff = pOutdataMinBuff;
Dlg.NInpdataMaxBuff = pNInpdataMaxBuff;
Dlg.NInpdataMinBuff = pNInpdataMinBuff;
Dlg.NOutdataMaxBuff = pNOutdataMaxBuff;
Dlg.NOutdataMinBuff = pNOutdataMinBuff;
Dlg.TngFileBuff = pTngFileBuff;
Dlg.TstFileBuff = pTstFileBuff;
}

```

```

Dlg.WgtFileBuff = pWgtFileBuff;

Dlg.DoModal();
}

void LoadANNAppDlg::CMTngFile()
{
    CString selectedFile;
    char szFileFilter[] =
        "Training Set Files (*.tng)|*.tng|"
        "All File (*.*)|*.*|"
        "||";

    char szMsgStr[MaxStringLen+1];
    CEdit* transfer = (CEdit*)(GetDlgItem(ID_TNG_FILE_EDIT));
    _find_t selFileInfo;
    unsigned attrib = _A_ARCH | _A_NORMAL;
    CFileDialog FileDialogBox(TRUE, NULL, "*.*", OFN_HIDEREADONLY |
OFN_OVERWRITEPROMPT,
                                                                    szFileFilter, this);

    if (FileDialogBox.DoModal()==IDOK)
    {
        selectedFile = FileDialogBox.GetPathName();
        _dos_findfirst((const char*) selectedFile, attrib, &selFileInfo);
        sprintf(szMsgStr,selectedFile);
        transfer->SetWindowText((const char*)selectedFile);
    }
}

void LoadANNAppDlg::CMTstFile()
{
    CString selectedFile;
    char szFileFilter[] =
        "Test Set Files (*.tst)|*.tst|"
        "All File (*.*)|*.*|"
        "||";

    char szMsgStr[MaxStringLen+1];
    CEdit* transfer = (CEdit*)(GetDlgItem(ID_TST_FILE_EDIT));
    _find_t selFileInfo;
    unsigned attrib = _A_ARCH | _A_NORMAL;
    CFileDialog FileDialogBox(TRUE, NULL, "*.*", OFN_HIDEREADONLY |
OFN_OVERWRITEPROMPT,
                                                                    szFileFilter, this);

    if (FileDialogBox.DoModal()==IDOK)
    {
        selectedFile = FileDialogBox.GetPathName();
        _dos_findfirst((const char*) selectedFile, attrib, &selFileInfo);
        sprintf(szMsgStr,selectedFile);
        transfer->SetWindowText((const char*)selectedFile);
    }
}

void LoadANNAppDlg::CMNetOpFile()
{
    CString selectedFile;
    char szFileFilter[] =

```

```

        "Net Files (*.net)|*.net|"
        "All File (*.*) | *.*|"
        "|";

_find_t selFileInfo;
unsigned attrib = _A_ARCH | _A_NORMAL;
CFileDialog FileDialogBox(TRUE, NULL, "*.*", OFN_HIDEREADONLY |
OFN_OVERWRITEPROMPT,
                                szFileFilter, this);

if (FileDialogBox.DoModal()==IDOK)
{
    selectedFile = FileDialogBox.GetPathName();
    _dos_findfirst((const char*) selectedFile, attrib, &selFileInfo);
    net_stat = 1;
    NetFile = selectedFile;
    Net_Read(&NetInfoBuff,(const char*)NetFile);
    ReTransf_Net_Info();
}
}

void LoadANNAppDlg::CMWgtOpFile()
{
    CString selectedFile;
    char szFileFilter[] =
        "Weight Files (*.wgt)|*.wgt|"
        "All File (*.*) | *.*|"
        "|";

    CEdit* transfer = (CEdit*)(GetDlgItem(ID_WGT_FILE_EDIT));
    _find_t selFileInfo;
    unsigned attrib = _A_ARCH | _A_NORMAL;
    CFileDialog FileDialogBox(TRUE, NULL, "*.*", OFN_HIDEREADONLY |
OFN_OVERWRITEPROMPT,
                                szFileFilter, this);

    if (FileDialogBox.DoModal()==IDOK)
    {
        selectedFile = FileDialogBox.GetPathName();
        _dos_findfirst((const char*) selectedFile, attrib, &selFileInfo);
        transfer->SetWindowText((const char*)selectedFile);
    }
}

void LoadANNAppDlg::CMWgtSaveAsFile()
{
    CString selectedFile;
    char szFileFilter[] =
        "Weight Files (*.wgt)|*.wgt|"
        "All File (*.*) | *.*|"
        "|";

    CEdit* transfer = (CEdit*)(GetDlgItem(ID_WGT_FILE_EDIT));
    _find_t selFileInfo;
    unsigned attrib = _A_ARCH | _A_NORMAL;
    CFileDialog FileDialogBox(FALSE, NULL, "*.*", OFN_HIDEREADONLY |
OFN_OVERWRITEPROMPT,
                                szFileFilter, this);

    if (FileDialogBox.DoModal()==IDOK)
    {

```

```

selectedFile = FileDialogBox.GetPathName();
_dos_findfirst((const char*) selectedFile, attrib, &selFileInfo);
transfer->SetWindowText((const char*)selectedFile);
ANN->wt_out = selectedFile;
ANN->Wt_Copy();
wgt_stat = 1;
}
}

void LoadANNAppDlg::CMWgtSaveFile()
{
if (wgt_stat == 1)
{
ANN->Wt_Copy();
}
else
{
CMWgtSaveAsFile();
}
}

void LoadANNAppDlg::CMNetSaveAsFile()
{
CString selectedFile;
char szFileFilter[] =
                "Weight Files (*.net)|*.net|"
                "All File (*.*) | *.*|"
                "||";

_find_t selFileInfo;
unsigned attrib = _A_ARCH | _A_NORMAL;
CFileDialog FileDialogBox(FALSE, NULL, "*.*", OFN_HIDEREADONLY |
OFN_OVERWRITEPROMPT,
                                szFileFilter, this);

if (FileDialogBox.DoModal()==IDOK)
{
selectedFile = FileDialogBox.GetPathName();
_dos_findfirst((const char*) selectedFile, attrib, &selFileInfo);
net_stat = 1;
NetFile = selectedFile;
Transf_Net_Info();
}
}

void LoadANNAppDlg::CMNetSaveFile()
{
if(net_stat == 1)
{
Transf_Net_Info();
}
else
{
CMNetSaveAsFile();
}
}

```



```

void LoadANNAppDlg::CMTngRstSaveAsFile()
{
    CString selectedFile,pass;
    char szFileFilter[] =
        "Training Results Files (*.rst)|*.rst|"
        "All File (*.*)|*.*|"
        "||";

    _find_t selFileInfo;
    unsigned attrib = _A_ARCH | _A_NORMAL;
    CFileDialog FileDialogBox(FALSE, NULL, "*.*", OFN_HIDEREADONLY |
    OFN_OVERWRITEPROMPT,
        szFileFilter, this);

    if (FileDialogBox.DoModal()==IDOK)
    {
        selectedFile = FileDialogBox.GetPathName();
        _dos_findfirst((const char*) selectedFile, attrib, &selFileInfo);
        ANN->tng_rst = selectedFile;
        ANN->Tng_Rst_Copy();
        pass = "notepad ";
        pass +=selectedFile;
        WinExec(pass,SW_RESTORE);
    }
}

void LoadANNAppDlg::CMTstRstSaveAsFile()
{
    CString selectedFile,pass;
    char szFileFilter[] =
        "Training Results Files (*.rst)|*.rst|"
        "All File (*.*)|*.*|"
        "||";

    _find_t selFileInfo;
    unsigned attrib = _A_ARCH | _A_NORMAL;
    CFileDialog FileDialogBox(FALSE, NULL, "*.*", OFN_HIDEREADONLY |
    OFN_OVERWRITEPROMPT,szFileFilter, this);
    if (FileDialogBox.DoModal()==IDOK)
    {
        selectedFile = FileDialogBox.GetPathName();
        _dos_findfirst((const char*) selectedFile, attrib, &selFileInfo);
        ANN->tst_rst = selectedFile;
        ANN->Tst_Rst_Copy();
        pass = "notepad ";
        pass +=selectedFile;
        WinExec(pass,SW_RESTORE);
    }
}

void LoadANNAppDlg::OnClose()
{
    if (MessageBox("Want to close this application",
        "Query", MB_YESNO | MB_ICONQUESTION) == IDYES)
    {
        DestroyWindow();
    }
}

```

```

void LoadANNAppDlg::Transf_Net_Info()
{
    UpdateData(TRUE);
    NetInfoBuff.TgtErr = TgtErrBuff;
    NetInfoBuff.RMSErr = RMSErrBuff;
    NetInfoBuff.Changes = ChangesBuff;
    NetInfoBuff.Niter = NiterBuff;
    NetInfoBuff.GoodPat = GoodPatBuff;
    NetInfoBuff.MaxWgt = MaxWgtBuff;
    NetInfoBuff.MinWgt = MinWgtBuff;
    NetInfoBuff.TotWgts = TotWgtsBuff;
    NetInfoBuff.BatchModeRbt = BatchModeRbtBuff;
    NetInfoBuff.PattModeRbt = PattModeRbtBuff;
    NetInfoBuff.LngRate = LngRateBuff;
    NetInfoBuff.Momentum = MomentumBuff;
    NetInfoBuff.LngStaticRbt = LngStaticRbtBuff;
    NetInfoBuff.LngDynRbt = LngDynRbtBuff;
    NetInfoBuff.Nlayers = NlayersBuff;
    NetInfoBuff.LayerOne = LayerOneBuff;
    NetInfoBuff.LayerTwo = LayerTwoBuff;
    NetInfoBuff.LayerThree = LayerThreeBuff;
    NetInfoBuff.LayerFour = LayerFourBuff;
    NetInfoBuff.InpdataMax = InpdataMaxBuff;
    NetInfoBuff.InpdataMin = InpdataMinBuff;
    NetInfoBuff.OutdataMax = OutdataMaxBuff;
    NetInfoBuff.OutdataMin = OutdataMinBuff;
    NetInfoBuff.NInpdataMax = NInpdataMaxBuff;
    NetInfoBuff.NInpdataMin = NInpdataMinBuff;
    NetInfoBuff.NOutdataMax = NOutdataMaxBuff;
    NetInfoBuff.NOutdataMin = NOutdataMinBuff;
    NetInfoBuff.TngFile = TngFileBuff;
    NetInfoBuff.TstFile = TstFileBuff;
    NetInfoBuff.WgtFile = WgtFileBuff;

    Net_Copy(&NetInfoBuff,(const char*)NetFile);
}

```

```

void LoadANNAppDlg::ReTransf_Net_Info()
{
    TgtErrBuff = NetInfoBuff.TgtErr;
    RMSErrBuff = NetInfoBuff.RMSErr;
    ChangesBuff = NetInfoBuff.Changes;
    NiterBuff = NetInfoBuff.Niter;
    GoodPatBuff = NetInfoBuff.GoodPat;
    MaxWgtBuff = NetInfoBuff.MaxWgt;
    MinWgtBuff = NetInfoBuff.MinWgt;
    TotWgtsBuff = NetInfoBuff.TotWgts;
    BatchModeRbtBuff = NetInfoBuff.BatchModeRbt;
    PattModeRbtBuff = NetInfoBuff.PattModeRbt;
    LngRateBuff = NetInfoBuff.LngRate;
    MomentumBuff = NetInfoBuff.Momentum;
    LngStaticRbtBuff = NetInfoBuff.LngStaticRbt;
    LngDynRbtBuff = NetInfoBuff.LngDynRbt;
    NlayersBuff = NetInfoBuff.Nlayers;
    LayerOneBuff = NetInfoBuff.LayerOne;
}

```

```

LayerTwoBuff = NetInfoBuff.LayerTwo;
LayerThreeBuff = NetInfoBuff.LayerThree;
LayerFourBuff = NetInfoBuff.LayerFour;
InpdataMaxBuff = NetInfoBuff.InpdataMax;
InpdataMinBuff = NetInfoBuff.InpdataMin;
OutdataMaxBuff = NetInfoBuff.OutdataMax;
OutdataMinBuff = NetInfoBuff.OutdataMin;
NInpdataMaxBuff = NetInfoBuff.NInpdataMax;
NInpdataMinBuff = NetInfoBuff.NInpdataMin;
NOutdataMaxBuff = NetInfoBuff.NOutdataMax;
NOutdataMinBuff = NetInfoBuff.NOutdataMin;
//TngFileBuff = NetInfoBuff.TngFile;
//TstFileBuff = NetInfoBuff.TstFile;
//WgtFileBuff = NetInfoBuff.WgtFile;

UpdateData(FALSE);
}

```

```

void LoadANNAppDlg::CMRandomize()
{
CString Selection;
char s[MaxStringLen];
double pass1,pass2;
CEdit* transfer = (CEdit*)(GetDlgItem(ID_MAX_WGT_EDIT));
transfer->GetWindowText(Selection.GetBuffer(MaxStringLen),MaxStringLen);
pass1 = atof(Selection);
MaxWgtBuff = pass1;
transfer = (CEdit*)(GetDlgItem(ID_MIN_WGT_EDIT));
transfer->GetWindowText(Selection.GetBuffer(MaxStringLen),MaxStringLen);
pass2 = atof(Selection);
MinWgtBuff = pass2;

ANN->Init_Wt(pass1,pass2);
TotWgtsBuff = ANN->totwts;
_itoa(TotWgtsBuff,s,10);
SetDlgItemText(ID_TOT_WGT_EDIT,s);
}

```

```

void LoadANNAppDlg::CMNormalize()
{
double par1,par2,par3,par4;

par1 = NInpdataMinBuff;
par2 = NInpdataMaxBuff;
par3 = NOutdataMinBuff;
par4 = NOutdataMaxBuff;
ANN->Normal(par1,par2,par3,par4);
InpdataMaxBuff = par1;
InpdataMinBuff = par2;
OutdataMaxBuff = par3;
OutdataMinBuff = par4;
UpdateData(FALSE);
}

```

```

void LoadANNAppDlg::CMTransferData()
{
    CString Selection,wgtfile,filename;
    char s[MaxStringLen];
    int cursel;
    UpdateData(TRUE);
    CButton* pRBtm = (CButton*)(GetDlgItem(ID_BATCHMODE_RBT));
    BatchModeRbtBuff = pRBtm->GetCheck();
    pRBtm = (CButton*)(GetDlgItem(ID_PATTERNMODE_RBT));
    PattModeRbtBuff = pRBtm->GetCheck();
    pRBtm = (CButton*)(GetDlgItem(ID_LNG_STATIC_RBT));
    LngStaticRbtBuff = pRBtm->GetCheck();
    pRBtm = (CButton*)(GetDlgItem(ID_LNG_DYN_RBT));
    LngDynRbtBuff = pRBtm->GetCheck();

    if (TngFileBuff == NULL)
    {
        MessageBox("Please Enter Training data file Name","Check", MB_YESNO|MB_ICONHAND);
    }
    else
    {
        filename = TngFileBuff;
        if(stat == 0)
        {
            pattern = new RunningSet((const char*) filename);
        }
        pattern->Read_Data();
        lpmtr.alpha = MomentumBuff;
        lpmtr.mue = LngRateBuff;
        lpmtr.qerror = TgtErrBuff;
        if (PattModeRbtBuff == BF_CHECKED)
            trmode = 1;
        else
            trmode = 2;
        if (LngStaticRbtBuff == BF_CHECKED)
            DynOrStatLngRate = 2;
        else
            DynOrStatLngRate = 1;
        n_inp = pattern->nin;
        n_outp = pattern->nout;
        ntr = pattern->ntrain;
        if (n_inp != LayerOneBuff)
            MessageBox("Number of nodes in the Input Layers in the data file doesn't \
            match the value","Information", MB_OK|MB_ICONINFORMATION);
        n_hids = NlayersBuff-2;
        if (n_hids ==1)
        {
            *(hidl+0) = LayerTwoBuff;
            if (n_outp != LayerThreeBuff)
                MessageBox("Number of Nodes in the Output Layers in the data file doesn't \
                match the value","Information", MB_OK|MB_ICONINFORMATION);
        }
        else if (n_hids ==2)
        {
            *(hidl+0) = LayerTwoBuff;
        }
    }
}

```

```

*(hidl+1) = LayerThreeBuff;
if (n_outp != LayerFourBuff)
{
    MessageBox("Number of Nodes in the Output Layers in the data file doesn't \
    match the value", "Information", MB_OK|MB_ICONINFORMATION);
}
}
if (stat == 0)
{
    if (WgtFileBuff == NULL)
    {
        ANN = new NetArch(n_inp, n_outp, n_hids, hidl, &lpmtr, trmode, ntr, pattern);
    }
    else
    {
        wgtfile = WgtFileBuff;
        wgt_stat = 1;
        ANN = new NetArch(n_inp, n_outp, n_hids, hidl, &lpmtr, trmode, ntr, pattern, (const char*)wgtfile);
    }
}
stat = 1;
srand((unsigned)time(NULL));
ANN->Arng_Layer();
ANN->inul = NInpdataMaxBuff;
ANN->inll = NInpdataMinBuff;
ANN->outul = NOutdataMaxBuff;
ANN->outll = NOutdataMinBuff;
ANN->Dyn_or_Stat = DynOrStatLngRate;
if (wgt_stat == 1)
{
    ANN->Read_Wt();
    sprintf(s, "%g", TotWgtsBuff);
    SetDlgItemText(ID_TOT_WGT_EDIT, s);
}
else
{
    ANN->Init_data();
}
CComboBox* ActFuncCmb = (CComboBox*)(GetDlgItem(ID_ACT_FUNC_CMB));
cursel = ActFuncCmb->GetCurSel();
act_func = cursel+1;
InpdataMaxBuff = ANN->maxin;
InpdataMinBuff = ANN->minin;
OutdataMaxBuff = ANN->maxout;
OutdataMinBuff = ANN->minout;
UpdateData(FALSE);
CButton* StoreBtn = (CButton*)(GetDlgItem(ID_RAND_WGTS));
EnableButton(StoreBtn);
StoreBtn = (CButton*)(GetDlgItem(ID_DATA_NORM));
EnableButton(StoreBtn);
}
}

void LoadANNAppDlg::CMStartTng()
{

```

```

int cyc,flag;
MSG msg;
cyc = 0;
flag = 1;
while (flag==1)
{
    ANN->Learn(act_func);
    RMSErrBuff = ANN->epsav;
    GoodPatBuff = ANN->pergood;
    ChangesBuff = ANN->changes;
    NiterBuff = cyc+1;
    cyc++;
    if (cyc%10 == 0)
    {
        if(GetMessage(&msg, (HWND) NULL, 0,0))
        {
            TranslateMessage(&msg);
            DispatchMessage(&msg);
        }
    }
    UpdateData(FALSE);
    if (ANN->epsav<=TgtErrBuff)
    {
        flag = 0 ;
    }
    if (TngFlag == 1)
    {
        TngFlag = 0;
        flag = 0;
    }
    if ((cyc+1)%10 == 0)
    {
        if (MessageBox("Do you want to continue?", "Information", MB_YESNO |
MB_ICONINFORMATION) == IDNO)
            flag = 0;
    }
}
}

```

```

void LoadANNAppDlg::CMHaltTng()

```

```

{
    char s[MaxStringLen];
    TngFlag = 1;
    MaxWgtBuff = maxval(TotWgtsBuff, ANN->wt_coef);
    MinWgtBuff = minval(TotWgtsBuff, ANN->wt_coef);
    sprintf(s,"%f",MaxWgtBuff);
    SetDlgItemText(ID_MAX_WGT_EDIT,s);
    sprintf(s,"%f",MinWgtBuff);
    SetDlgItemText(ID_MIN_WGT_EDIT,s);
}

```

```

void LoadANNAppDlg::CMTestTng()

```

```

{
    ANN->Test(act_func);
    TgtOp = ANN->outvect;
}

```

```

NetOp = ANN->results;
CMTngRstSaveAsFile();
CMDisplyTng();
free(ANN->results);
}

void LoadANNAppDlg::CMTestTst()
{
    CString filename;
    int n_inp,n_outp,ntr;
    double par1,par2,par3,par4;
    if (TstFileBuff == NULL)
    {
        MessageBox("Please Enter Test data file Name","Check", MB_YESNO|MB_ICONHAND);
    }
    else
    {
        MessageBox(TstFileBuff, "Tst File Information-1", MB_OK | MB_ICONINFORMATION);
        filename = TstFileBuff;
        if(TstStat != 0)
        {
            delete TstSet;
            delete EvalSet;
        }
        TstStat = 1;
        TstSet = new RunningSet((const char*) filename);
        TstSet->Read_Data();
        n_inp = TstSet->nin;
        n_outp = TstSet->nout;
        ntr = TstSet->ntrain;
        if (n_inp != LayerOneBuff)
            MessageBox("Number of nodes in the Input Layers in the data file doesn't \
            match the value","Information", MB_OK|MB_ICONINFORMATION);
        if (n_outp != LayerThreeBuff)
        {
            MessageBox("Number of Nodes in the Output Layers in the data file doesn't \
            match the value","Information", MB_OK|MB_ICONINFORMATION);
        }
        else if (n_outp != LayerFourBuff)
        {
            MessageBox("Number of Nodes in the Output Layers in the data file doesn't \
            match the value","Information", MB_OK|MB_ICONINFORMATION);
        }
        EvalSet = new NetArch(n_inp,n_outp,n_hids,hidl,&lpmtr,trmode,ntr,TstSet); //(const
char*)wgtfile);
        if (MessageBox("Have you set the range of
Normalization?","Check",MB_YESNO|MB_ICONHAND) == IDYES)
        {
            par1 = InpdataMinBuff;
            par2 = InpdataMaxBuff;
            par3 = OutdataMinBuff;
            par4 = OutdataMaxBuff;
            EvalSet->Normal(par1,par2,par3,par4);
            EvalSet->inul = InpdataMaxBuff;
            EvalSet->inll = InpdataMinBuff;
        }
    }
}

```

```

    EvalSet->outul = OutdataMaxBuff;
    EvalSet->outll = OutdataMinBuff;
    EvalSet->Arng_Layer();
    EvalSet->Test(act_func);
}
}
CMTstRstSaveAsFile();
}

class OutputDisplayDlg:public CDialog
{
public:
    OutputDisplayDlg( UINT nIDTemplate, CWnd* pParentWnd);
    double *Outputl;
    int n;

protected:
    virtual BOOL OnInitDialog();
    void OntoScreen();

public:
    afx_msg void OnQuit();
    DECLARE_MESSAGE_MAP();
};

OutputDisplayDlg::OutputDisplayDlg( UINT nIDTemplate, CWnd* pParentWnd)
{
    Create(nIDTemplate,pParentWnd);
}

BOOL OutputDisplayDlg::OnInitDialog()
{
    LoadANNAAppDlg* pD = (LoadANNAAppDlg*)(GetParent());
    Outputl = pD->TgtOp;
    n = pD->ntr;
    CListBox* ListDisplay = (CListBox*) (GetDlgItem(IDC_OP_DISPPLY_LST));
    //sprintf(s,"The Target and NetOutputs");
    ListDisplay->AddString("The target and net outputs");
    OntoScreen();
    return TRUE;
}

void OutputDisplayDlg::OnQuit()
{
    DestroyWindow();
}

void OutputDisplayDlg::OntoScreen()
{
    double temp;
    int i;
    char s[MaxStringLength];
    CListBox* ListDisplay = (CListBox*) (GetDlgItem(IDC_OP_DISPPLY_LST));
    //sprintf(s,"The Target and NetOutputs");
}

```



```

//ListDisplay->AddString("The target and net outputs");
for (i=0;i<n;i++)
{
temp = *(Output1+i);
sprintf(s,"%0.3f",temp);
// ListDisplay->AddString("\n");
ListDisplay->AddString(s);
//updateComboBox(ListDisplay);
}
//ListDisplay->SetCurSel(0);
}

void LoadANNAppDlg::CMDisplyTng()
{
CDialog* DplyDlg;
DplyDlg = new OutputDisplayDlg(IDD_RESULTS_DPLY_DLG,this);
DplyDlg->SendMessage(WM_INITDIALOG);
}

void LoadANNAppDlg::CMEditTngFile()
{
CString filename, pass;
CEdit* transfer = (CEdit*)(GetDlgItem(ID_TNG_FILE_EDIT));
transfer->GetWindowText(filename);
pass = "notepad ";
pass +=filename;
WinExec(pass,SW_RESTORE);
}

void LoadANNAppDlg::CMEditTstFile()
{
CString filename,pass;
CEdit* transfer = (CEdit*)(GetDlgItem(ID_TST_FILE_EDIT));
transfer->GetWindowText(filename);
pass = "notepad";
pass += filename;
WinExec(pass,SW_RESTORE);
}

void LoadANNAppDlg::CMEditWgtFile()
{
CString filename,pass;
CEdit* transfer = (CEdit*)(GetDlgItem(ID_WGT_FILE_EDIT));
transfer->GetWindowText(filename);
pass = "notepad";
pass += filename;
WinExec(pass,SW_RESTORE);
}

BEGIN_MESSAGE_MAP(CMainWnd, CFrameWnd)
ON_BN_CLICKED(IDOK, CMLoadANN)
END_MESSAGE_MAP()

```

```

BEGIN_MESSAGE_MAP(LoadANNAAppDlg, CDialog)
ON_BN_CLICKED(ID_RAND_WGTS,CMRandomize)
ON_BN_CLICKED(ID_TRANSF_DATA,CMTransferData)
ON_BN_CLICKED(ID_OPENF_TNG_SET,CMTngFile)
ON_BN_CLICKED(ID_OPENF_TST_SET,CMTstFile)
ON_BN_CLICKED(ID_OPENF_WGT_SET,CMWgtOpFile)
ON_BN_CLICKED(ID_DATA_NORM,CMNormalize)
ON_BN_CLICKED(ID_EDITF_TNG_SET,CMEditTngFile)
ON_BN_CLICKED(ID_EDITF_TST_SET,CMEditTstFile)
ON_BN_CLICKED(ID_EDITF_WGT_SET,CMEditWgtFile)
ON_COMMAND(ID_TNGFILE, CMTngFile)
ON_COMMAND(ID_TSTFILE, CMTstFile)
ON_COMMAND(ID_NETOPFILE, CMNetOpFile)
ON_COMMAND(ID_WGTOPFILE, CMWgtOpFile)
ON_COMMAND(ID_START_TNG,CMStartTng)
ON_COMMAND(ID_HLT_TNG,CMHalfTng)
ON_COMMAND(ID_TST_TNG,CMTestTng)
ON_COMMAND(ID_TST_TST,CMTestTst)
ON_COMMAND(ID_SVWGT_ASFILE,CMWgtSaveAsFile)
ON_COMMAND(ID_SVWGTFILE,CMWgtSaveFile)
ON_COMMAND(ID_SVNET_ASFILE,CMNetSaveAsFile)
ON_COMMAND(ID_SVNETFILE,CMNetSaveFile)
ON_COMMAND(CM_EXIT, OnExit)
ON_WM_CLOSE()
ON_WM_CREATE()
END_MESSAGE_MAP()

```

```

BEGIN_MESSAGE_MAP(OutputDisplayDlg, CDialog)
ON_BN_CLICKED(IDCANCEL, OnQuit)
END_MESSAGE_MAP()

```

```

BOOL CFileDialogApp::InitInstance()
{
    m_pMainWnd = new CMainWnd();
    m_pMainWnd->ShowWindow(m_nCmdShow);
    m_pMainWnd->UpdateWindow();
    return TRUE;
}

```

```
CFileDialogApp WindowApp;
```

## Netarch.CPP

```
//NN.MAK - PROJECT GROUP
```

```
// This includes the functions in the class NEtArch
// Weight initialisation
```

```

#include <iostream.h>
#include <stdlib.h>
#include <fstream.h>
#include <time.h>
#include <string.h>
#include <math.h>

```

```

#include <malloc.h>
#include "class.h"
#include "funct.h"
#include <process.h>

NetArch::NetArch(int n_inp, int n_outp, int n_hids, int *hidl,
                 struct LearnParams *lpmtr, int trmode, int ntr,
                 class RunningSet *pattern, const char* wgtfile)
{
    int i;

    nin = n_inp;
    nout = n_outp;
    nhid = n_hids;
    neterr = lpmtr->qerror;
    MU = lpmtr->mue;
    ALP = lpmtr->alpha;
    b_or_p = trmode;
    npat = ntr;

    wt_out = wgtfile;
    file_wt.open(wt_out,ios::trunc | ios::in | ios::out);
    if (!file_wt.good())
    {
        // cout << "\n ***** error opening" <<" " <<wt_out<<" " <<"*****";
        exit(0);
        Wgt_Stat = 1;
    }

    totnode = nin+1+nout;
    totwts = 0;

    // Allocate Memory for the weights in all layers
    nhidl = (int*)malloc(nhid*sizeof(int));
    nhidl = hidl;

    for (i=0;i<nhid;i++)
    {
        totnode = totnode + *(nhidl+i)+1;
    }
    if (nhid == 0)
    {
        totwts += (nin+1)*nout;
    }
    else
    {
        totwts += (nin+1)* *(nhidl+0);
        for(i=0;i<(nhid-1);i++)
        {
            totwts += (*(nhidl+i)+1)*(*(nhidl+i+1));
        }
        totwts += (*(nhidl +i)+1)*nout;
    }
}

```

```

wt_coef = (double*)malloc(totwts*sizeof(double));
if(wt_coef == NULL)
{
    //cout << "\n Insufficient Memory to Weight Allocation \n";
    exit(0);
}
y = (double*)malloc(totnode*sizeof(double));
epsn = (double*)malloc(npat*sizeof(double));
err = (double*)malloc(totnode*sizeof(double));
delw = (double*)malloc(totwts*sizeof(double));
del = (double*)malloc(totnode*sizeof(double));
if(y == NULL || epsn == NULL || err == NULL || delw == NULL || del == NULL)
{
    //cout << "\n Insufficient Memory \n";
    exit(0);
}
op = (double*)malloc(nout*sizeof(double));
netop = (double*)malloc(nout*sizeof(double));
DelPrev = (double*)malloc(totwts*sizeof(double));
nl = (int*)malloc((nhid+2)*sizeof(int));
x_deriv = (double*)malloc(totnode*sizeof(double));
if(op == NULL || netop == NULL || DelPrev == NULL || x_deriv == NULL || nl == NULL)
{
    //cout << "\n Insufficient Memory \n";
    exit(0);
}
//data_set = (double*)malloc(ntrain*(nin+nout)*sizeof(double));
invect = (double*)malloc((npat*nin)*sizeof(double));
normin = (double*)malloc((npat*nin)*sizeof(double));
outvect = (double*)malloc((npat*nout)*sizeof(double));
normout = (double*)malloc((npat*nin)*sizeof(double));
mnout = (double*)malloc(nout*sizeof(double));
if (data_set == NULL || invect == NULL || outvect == NULL || mnout == NULL)
{
    //cout << "\n Insufficient memory to read the input file";
    exit(0);
}
nop = (double*)malloc(nout*sizeof(double));
nerr = (double*)malloc(totnode*sizeof(double));
if (nop == NULL || nerr == NULL)
{
    //cout << "\n Insufficient memory";
    exit(0);
}
data_set = pattern->in_data;
}

```

```

NetArch::NetArch(int n_inp, int n_outp, int n_hids, int *hidl,
                struct LearnParams *lpmtr, int trmode, int ntr,
                class RunningSet *pattern)
{
    int i;

    nin = n_inp;
    nout = n_outp;

```

```

nhid = n_hids;
neterr = lpmtr->qerror;
MU = lpmtr->mue;
ALP = lpmtr->alpha;
b_or_p = trmode;
npat = ntr;

totnode = nin+1+nout;
totwts = 0;

// Allocate Memory for the weights in all layers
nhidl = (int*)malloc(nhid*sizeof(int));
nhidl = hidl;

for (i=0;i<nhid;i++)
{
    totnode = totnode + *(nhidl+i)+1;
}
if (nhid == 0)
{
    totwts += (nin+1)*nout;
}
else
{
    totwts += (nin+1)* *(nhidl+0);
    for(i=0;i<(nhid-1);i++)
    {
        totwts += *(nhidl+i)+1)*(*(nhidl+i+1));
    }
    totwts += *(nhidl +i)+1)*nout;
}

wt_coef = (double*)malloc(totwts*sizeof(double));
if(wt_coef == NULL)
{
    //cout <<"\n Insufficient Memory to Weight Allocation \n";
    exit(0);
}
y = (double*)malloc(totnode*sizeof(double));
epsn = (double*)malloc(npat*sizeof(double));
err = (double*)malloc(totnode*sizeof(double));
delw = (double*)malloc(totwts*sizeof(double));
del = (double*)malloc(totnode*sizeof(double));
if(y == NULL || epsn == NULL || err == NULL || delw == NULL || del == NULL)
{
    //cout <<"\n Insufficient Memory \n";
    exit(0);
}
op = (double*)malloc(nout*sizeof(double));
netop = (double*)malloc(nout*sizeof(double));
DelPrev = (double*)malloc(totwts*sizeof(double));
nl = (int*)malloc((nhid+2)*sizeof(int));
x_deriv = (double*)malloc(totnode*sizeof(double));
if(op == NULL || netop == NULL || DelPrev == NULL || x_deriv == NULL || nl == NULL)
{

```

```

//cout << "\n Insufficient Memory \n";
exit(0);
}
//data_set = (double*)malloc(ntrain*(nin+nout)*sizeof(double));
invect = (double*)malloc((npat*nin)*sizeof(double));
normin = (double*)malloc((npat*nin)*sizeof(double));
outvect = (double*)malloc((npat*nout)*sizeof(double));
normout = (double*)malloc((npat*nin)*sizeof(double));
nnout = (double*)malloc(nout*sizeof(double));
if (data_set == NULL || invect == NULL || outvect == NULL || nnout == NULL)
{
//cout << "\n Insufficient memory to read the input file";
exit(0);
}
nop = (double*)malloc(nout*sizeof(double));
nerr = (double*)malloc(totnode*sizeof(double));
if (nop == NULL || nerr == NULL)
{
//cout << "\n Insufficient memory";
exit(0);
}
data_set = pattern->in_data;
}

```

```

NetArch::~NetArch()

```

```

{
free (wt_coef);
free (y);
free (epsn);
free (err);
free (delw);
free (del);
free (op);
free (netop);
free (DelPrev);
free (x_deriv);
free (data_set);
free (invect);
free (outvect);
free (normin);
free (normout);
free (nhidl);
free (nl);
free (nnout);
free (nop);
free (nerr);
//free (wt_out);
file_wt.close();
}

```

```

void NetArch::Init_Wt(double lolt, double uplt)

```

```

{
int i;

ll = lolt;

```

```

ul = uplt;
for(i=0;i<totwts;i++)
{
*(wt_coef+i) = randn(ll,ul);
*(DelPrev+i) = 0;
}
}

```

```

void NetArch::Read_Wt()
{
int i;
char temp[5];
double change;

for (i=0;i<totwts;i++)
{
file_wt >> temp;
change = atof(temp);
*(wt_coef+i) = change;
}
}

```

```

void NetArch::Init_data()
{
int n,j;
classif();
preveps = 10.0;
n = npat*nin;
maxin = maxval(n, invect);
minin = minval(n, invect);
n = npat*nout;
maxout = maxval(n, outvect);
minout = minval(n, outvect);
for (j=0;j<totwts;j++)
{
*(delw+j) = 0;
*(DelPrev+j) = 0;
}
}

```

```

void NetArch::Learn(int af)
{
int i,j,goodpat;
Alpha = ALP;
for (j=0;j<totwts;j++)
{
*(delw+j) = 0;
//*(DelPrev+j) = 0;
}
epsav = 0;
goodpat = 0;
for (i=0;i<npat;i++)
{
for (j=0;j<totnode;j++)
{

```

```

    *(err+j) = 0;
    *(nerr+j) = 0;
    *(del+j) = 0;
}
ForPass(i,af);
netout();
Denorm(maxout,outll,outul);
ErrCal(i);
DelwCal();
if (sqrt(*(epsn+i)/(2*nout)) <=neterr)
{
    goodpat ++;
}
if (b_or_p == 1)
{
    Copy_Dels();
    Modif_Wt();
}
}
if (b_or_p == 2)
{
    Copy_Dels();
    Modif_Wt();
}
}
pergood =goodpat*100/npat;
epsav = sqrt(epsav/npat);
changes = preveps - epsav;
if (epsav<preveps)
{
    if (Dyn_or_Stat == 2)
    {
        MU = MU*1.05;
        Alpha = ALP;
    }
}
else
{
    if (Dyn_or_Stat == 2)
    {
        MU = MU*0.9;
        Alpha = 0;
    }
}
preveps = epsav;
}

void NetArch::Test(int af)
{
    int i,j,temp;
    // double inll,inul,outll,outul;
    results = (double*)malloc((npat*nout)*sizeof(double));
    if (results == NULL )
    {
        exit(0);
    }
}

```



```

epsav = 0;
for (i=0;i<npat;i++)
{
  for (j=0;j<totnode;j++)
  {
    *(err+j) = 0;
    *(nerr+j) = 0;
  }
  ForPass(i,af);
  netout();
  Denorm(maxout,outll,outul);
  for (j=0;j<nout;j++)
  {
    temp = nout*i+j;
    *(results+temp) = *(nnout+j);
  }
}
epsav /= npat;
}

```

```

void NetArch::classif()
{
  int i,j,loc,datloc;

  datloc = 0;
  for (i=0;i<npat;i++)
  {
    for (j=0;j<nin;j++)
    {
      loc = nin*i+j;
      *(invect+loc) = *(data_set+datloc);
      datloc++;
    }
    for (j=0;j<nout;j++)
    {
      loc = nout*i+j;
      *(outvect+loc) = *(data_set+datloc);
      datloc++;
    }
  }
}

```

```

void NetArch::Normal(double inll,double inul,double outll,double outul)
{
  int n,i;

  n = npat*nin;
  for (i=0; i<n;i++)
  {
    *(normin+i) = inll+(*(invect+i)*(inul-inll))/(maxin+1.0);
  }
  n = npat*nout;
  for (i=0; i<n;i++)
  {

```

```

    *(normout+i) = outll+(*(outvect+i)*(outul-outll))/(maxout+1.0);
}
}
void NetArch::ForPass(int i, int af)
{
    int j,loc,temp,locwt,locinp,veclgth,locxy,incrl,ii,jj,kk;
    double *x,*wt_mult,*inp,param;

    x = (double*)malloc(totnode*sizeof(double));
    if(x == NULL)
    {
        cout << "\n Insufficient Memory to Read the Data \n";
    }

    inp = (double*)malloc(25*sizeof(double));
    wt_mult = (double*)malloc(25*sizeof(double));
    if(inp == NULL || wt_mult == NULL)
    {
        cout << "\n Insufficient Memory \n";
    }

    locxy = 0; // Location of X and Y Matrix
    for (j=0;j<nin;j++)
    {
        loc = nin*i+j;
        *(x+j) = *(normin+loc); // The Net input to the first layer = the data itself
        *(y+j) = *(x+j); // The output from the first layer = the data itself
        // As there is no Activation function for the input layer.
        *(x_deriv+j) = 0;
        locxy++;
    }

    *(x+locxy) = -1;
    *(y+locxy) = -1;
    *(x_deriv+locxy) = 0;
    for (j=0;j<nout;j++)
    {
        loc = nout*i+j;
        *(op+j) = *(outvect+loc); // Storing the outputs of all the patterns
        *(nop+j) = *(normout+loc);
    }

    if(nhid==0)
    {
        temp = nout;
    }
    else
    {
        temp = *(nhid+0);
    }

    for (ii=0;ii<temp;ii++)
    {

```

```

for(jj=0;jj<(nin+1);jj++)
{
locwt = (nin+1)*ii+jj;
*(inp+jj) = *(x+jj);
*(wt_mult+jj) = *(wt_coef+locwt);
}
locxy++;
*(x+locxy) = dotprod((nin+1),inp,wt_mult);
param = *(x+locxy);
*(y+locxy) = func_call(param,af);
param = *(y+locxy);
*(x_deriv+locxy) = deriv_func(param, af);
}

if(nhid !=0)
{
locxy++;
*(x+locxy) = -1; // For the Bias Term
*(y+locxy) = -1; // For the Bias Term
*(x_deriv+locxy) = 0;
}

if(nhid>1)
{
incri = nin+1;

for(ii=1;ii<nhid;ii++)
{
temp = *(nhidl+ii);
veclgth = *(nhidl+ii-1)+1;
for(jj=0;jj<temp;jj++)
{
for(kk=0;kk<veclgth;kk++)
{
locinp =incri+kk; // Location of the Input Vector
locwt++; // Location of Weight Coefficient
*(inp+kk) = *(y+locinp);
*(wt_mult+kk) = *(wt_coef+locwt);
}
locxy++;
*(x+locxy) = dotprod(veclgth, inp, wt_mult);
param = *(x+locxy);
*(y+locxy) = func_call(param,af);
param = *(y+locxy);
*(x_deriv+locxy) = deriv_func(param, af);
}

locxy++;
*(x+locxy) = -1;
*(y+locxy) = -1;
*(x_deriv+locxy) = 0;
}
incri = incri+veclgth;
}
if (nhid == 1)

```

```

{
  incre = nin+1;
}
if (nhid != 0)
{
  temp = *(nhid+nhid-1)+1;
  for(ii=0;ii<nout;ii++)
  {
    for(jj=0;jj<temp;jj++)
    {
      locinp = incre + jj;
      locwt++;
      *(inp+jj) = *(y+locinp);
      *(wt_mult+jj) = *(wt_coef+locwt);
    }
    locxy++;
    *(x+locxy) = dotprod(temp, inp, wt_mult);
    param = *(x+locxy);
    *(y+locxy) = func_call(param,af);
    param = *(y+locxy);
    *(x_deriv+locxy) = deriv_func(param, af);
  }
}
free (x);
free (wt_mult);
free (inp);
}

```

```
void NetArch::netout()
```

```

{
  int loc,i;

  loc = totnode-nout;
  for(i=0;i<nout;i++)
  {
    *(netop+i) = *(y+loc);
    loc++;
  }
}

```

```
void NetArch::Denorm(double maxout,double outll, double outul)
```

```

{
  int i;

  for (i=0;i<nout;i++)
  {
    *(nnout+i) = ((* (netop+i)-outll)*(maxout+1))/(outul-outll);
  }
}

```

```
void NetArch::ErrCal(int i)
```

```

{
  int loc,j,locdel,locxy,locerr;

  loc = locdel = locxy = locerr = totnode-nout;

```

```

*(epsn+i) = 0;
for (j=0;j<nout;j++)
{
*(nerr+loc) = fabs(*(nnout+j)-*(op+j));
*(err+loc) = (*(nop+j)-*(netop+j));
*(del+locdel) = *(x_deriv+locxy)*(*(err+locerr));
*(epsn+i) += pow((*(err+loc)),2);
loc++;
locxy++;
locdel++;
locerr++;
}
/*(epsn+i) = *(epsn+i);
epsav += *(epsn+i)/2;
}

```

```

void NetArch::Arng_Layer()

```

```

{
int i, size;

size = nhid+2;

*(nl+0) = nin;
if(nhid != 0)
{
for(i=1;i<(size-1);i++)
{
*(nl+i) = *(nhid+i-1);
}
}
*(nl+size-1) = nout;
}

```

```

void NetArch::DelwCal()

```

```

{
int locdelw,locxy,locwt,temp,locdel,locerr,prevdel,ii,jj,kk;

```

```

locerr = locxy = locdel = totnode-nout;
prevdel = totnode-1;
locwt = locdelw = totwts;

```

```

for(ii=(nhid+1);ii>0;ii--)
{
temp = *(nl+ii-1)+1;
for(jj=0;jj<*(nl+ii);jj++)
{
for (kk=0;kk<temp;kk++)
{
locdelw--;
locwt--;
locxy--;
}
}
}

```

```

locerr--;
if(kk !=0 && ii != 1)
{
*(err+locerr) += *(del+prevdel)*(*(wt_coef+locwt));
}
}
if(kk == temp)
{
locxy += temp;
locerr += temp;
}
prevdel--;
}
for (jj=0;jj<temp;jj++)
{
locdel--;
locxy--;
locerr--;
if (jj == 0 || ii ==1)
{
*(del+locdel) = 0;
}
else
{
*(del+locdel) = *(x_deriv+locxy)*(*(err+locerr));
}
}
}
prevdel--;
}
}

```

```

void NetArch::Modif_Wt()

```

```

{
int ii;

for (ii=0;ii<totwts;ii++)
{
*(wt_coef+ii) = *(wt_coef+ii)+*(delw+ii);
}
}

```

```

void NetArch::Copy_Dels()

```

```

{
int j;

for(j=0;j<totwts;j++)
{
*(delw+j) = -(delw+j)+*(DelPrev+j)*Alpha;
*(DelPrev+j) = *(delw+j);
}
}

```

```

void NetArch::Wt_Copy()

```

```

{

```

```

int i,j,k,loc;

loc = 0;
if(Wgt_Stat != 1)
{
file_wt.open(wt_out,ios::trunc |ios::in | ios::out);
if (!file_wt.good())
{
// cout << "\n ***** error opening" <<" " <<wt_out<<" "<<"*****";
exit(0);
}
}
for (i=0;i<=nhid;i++)
{
k = *(nl+i);
for(j=0;j<=k;j++)
{
file_wt << *(wt_coef+loc)<<"\t";
loc++;
}
file_wt << "\n" ;
}
}

```

```

void NetArch::Tng_Rst_Copy()
{
int i,j,temp;
file_rst.open(tng_rst,ios::trunc|ios::in|ios::out);
if (!file_rst.good())
exit(0);

file_rst <<"The Target and net outputs \n";
for (i=0;i<npat;i++)
{
for (j=0;j<nout;j++)
{
temp = nout*i+j;
file_rst << i << "\t" << *(outvect+temp) << "\t" << *(results+temp);
}
file_rst << "\n";
}
file_rst.close();
}

```

```

void NetArch::Tst_Rst_Copy()
{
int i,j,temp;
file_rst.open(tng_rst,ios::trunc|ios::in|ios::out);
if (!file_rst.good())
exit(0);

file_rst <<"The Target and net outputs \n";
for (i=0;i<npat;i++)
{
for (j=0;j<nout;j++)

```

```

    {
        temp = nout*i+j;
        file_rst << i << "\t" << *(outvect+temp) << "\t" << *(results+temp);
    }
    file_rst << "\n";
}
file_rst.close();
}

```

## Act\_Func.CPP

```

// ACT_FUNC.CPP
//NN.MAK - PROJECT

```

```

// To calculate the Activity function
// either TanH or Sigmoid Function

```

```

#include <iostream.h>
#include <stdlib.h>
#include <math.h>

```

```

double func_call(double x, int af)
{
    double s;

    switch (af)
    {
        case 1:
        {
            s = 1.0/(1.0+exp(-1.2*x));
            return s;
        }
        break;
        case 2:
        {
            s = tanh(x);
            return s;
        }
        break;
        case 3:
        {
            s = x;
            return s;
        }
    }
    return s;
}

```

```

double deriv_func(double out, int af)
{
    double value;

    switch (af)
    {
        case 1:

```



```

{
    value = out*(1.0-out);
    return value;
}
break;
case 2:
{
    value = 1-out*out;
    return value;
}
break;
case 3:
{
    value = 0;
    return value;
}
}
return value;
}

```

## DotProd.CPP

```

// DOTPROD.CPP
//NN.MAK - PROJECT GROUP

// To Calculate the Dot product of two vectors

#include <iostream.h>
#include <stdlib.h>

double dotprod(int n, double *v1, double *v2)
{
    int x,y,i;
    double sum;

    sum =0.0;
    x = n/4;
    y = n%4;

    for(i=0;i<x;i++)
    {
        sum += *(v1+i) * *(v2+i);
        sum += *(v1+i) * *(v2+i+1);
        sum += *(v1+i) * *(v2+i+2);
        sum += *(v1+i) * *(v2+i+3);

        v1 = v1+4;
        v2 = v2+4;
    }

    for(i=0;i<y;i++)
    {
        sum += *v1 * *v2;
        v1++;
    }
}

```

```
    v2++;  
}  
return sum;  
}
```

## MaxMin.CPP

```
/MAXMIN.CPP
```

```
//CALCULATION OF MAXIMUM AND MINIMUM VALUES IN A GIVEN VECTOR
```

```
#include <iostream.h>
```

```
#include <stdlib.h>
```

```
double maxval(int n, double *vect)
```

```
{  
    int i;  
    double max;  
  
    max = *(vect+0);  
    for(i=0;i<n;i++)  
    {  
        if (*(vect+i)>max)  
        {  
            max = *(vect+i);  
        }  
    }  
    return max;  
}
```

```
double minval(int n, double *vect)
```

```
{  
    int i;  
    double min;  
  
    min = *(vect+0);  
    for(i=0;i<n;i++)  
    {  
        if (*(vect+i)<min)  
        {  
            min = *(vect+i);  
        }  
    }  
    return min;  
}
```

## NetData.CPP

```
// Reading and Copying the Net
```

```
#include <string.h>
```

```
#include <stdio.h>
```

```
#include <stdlib.h>
```

```
#include <iostream.h>
```

```
#include <fstream.h>
```

```

#include <afx.h>
#include "c:\anu\chris\main\class.h"

const char* net_out;

fstream file_net;

void Net_Copy(struct AppNetInfo *NetInfoBuff, const char* netfile)
{
    net_out = netfile;

    file_net.open(net_out,ios::trunc|ios::in|ios::out);
    if(!file_net.good())
    {
        exit (0);
    }

    AppNetInfo* NetInfo;
    NetInfo = NetInfoBuff;

    file_net<<NetInfo->TgtErr<<"\t"<<": Target Error"<<"\n";
    file_net<<NetInfo->RMSErr<<"\t"<<": RMS Error"<<"\n";
    file_net<<NetInfo->Changes<<"\t"<<": Changes"<<"\n";
    file_net<<NetInfo->Niter<<"\t"<<": No. of Iterations"<<"\n";
    file_net<<NetInfo->GoodPat<<"\t"<<": Good Patterns"<<"\n";
    file_net<<NetInfo->MaxWgt<<"\t"<<": Max. Connection Weight"<<"\n";
    file_net<<NetInfo->MinWgt<<"\t"<<": Min. Connection Weight"<<"\n";
    file_net<<NetInfo->TotWgts<<"\t"<<": Total Number of Connection Weights"<<"\n";
    file_net<<NetInfo->BatchModeRbt<<"\t"<<": Batch Mode Status"<<"\n";
    file_net<<NetInfo->PattModeRbt<<"\t"<<": Pattern Mode Status"<<"\n";
    file_net<<NetInfo->LngRate<<"\t"<<": Learning Rate"<<"\n";
    file_net<<NetInfo->Momentum<<"\t"<<": Momentum"<<"\n";
    file_net<<NetInfo->LngStaticRbt<<"\t"<<": Learning Rate - Static"<<"\n";
    file_net<<NetInfo->LngDynRbt<<"\t"<<": Learning Rate - Dynamic"<<"\n";
    file_net<<NetInfo->Nlayers<<"\t"<<": No. of Layers"<<"\n";
    file_net<<NetInfo->LayerOne<<"\t"<<": Nodes in Layer 1"<<"\n";
    file_net<<NetInfo->LayerTwo<<"\t"<<": Nodes in Layer 2"<<"\n";
    file_net<<NetInfo->LayerThree<<"\t"<<": Nodes in Layer 3"<<"\n";
    file_net<<NetInfo->LayerFour<<"\t"<<": Nodes in Layer 4"<<"\n";
    file_net<<NetInfo->InpdataMax<<"\t"<<": Input Data - Max. Value"<<"\n";
    file_net<<NetInfo->InpdataMin<<"\t"<<": Input Data - Min. Value"<<"\n";
    file_net<<NetInfo->OutdataMax<<"\t"<<": Output data - Max. Value"<<"\n";
    file_net<<NetInfo->OutdataMin<<"\t"<<": Output Data - Min. Value"<<"\n";
    file_net<<NetInfo->NInpdataMax<<"\t"<<": Normalized Input Data - Max."<<"\n";
    file_net<<NetInfo->NInpdataMin<<"\t"<<": Normalized Input Data - Min."<<"\n";
    file_net<<NetInfo->NOutdataMax<<"\t"<<": Normalized Output Data - Max."<<"\n";
    file_net<<NetInfo->NOutdataMin<<"\t"<<": Normalized Output Data - Min."<<"\n";
    file_net<<NetInfo->TngFile<<"\n";
    file_net<<NetInfo->TstFile<<"\n";
    file_net<<NetInfo->WgtFile<<"\n";
    file_net.close();
}

```

```

void Net_Read(struct AppNetInfo *NetInfoBuff, const char* netfile)
{
    net_out = netfile;

    file_net.open(net_out,ios::in);
    if(!file_net.good())
    {
        exit (0);
    }

    AppNetInfo* NetInfo;
    NetInfo = NetInfoBuff;

    char temp1[40],temp4[3], *temp3;
    const char* temp2;
    double change;
    int convert;
    temp3 = &temp4[0];

    file_net>>temp1;
    change = atof(temp1);
    NetInfo->TgtErr = change;
    file_net>>temp3;
    file_net>>"\n";
    file_net>>temp1;
    change = atof(temp1);
    NetInfo->RMSErr = change;
    file_net>>temp3;
    file_net>>"\n";
    file_net>>temp1;
    convert = atoi(temp1);
    NetInfo->Changes = convert;
    file_net>>temp3;
    file_net>>"\n";
    file_net>>temp1;
    convert = atoi(temp1);
    NetInfo->Niter = convert;
    file_net>>temp3;
    file_net>>"\n";
    file_net>>temp1;
    change = atof(temp1);
    NetInfo->GoodPat = change;
    file_net>>temp3;
    file_net>>"\n";
    file_net>>temp1;
    change = atof(temp1);
    NetInfo->MaxWgt = change;
    file_net>>temp3;
    file_net>>"\n";
    //file_net<<"Max. Connection Weight:"<<"\t"<<NetInfo->MaxWgt<<"\n";
    file_net>>temp1;
    change = atof(temp1);
    NetInfo->MinWgt = change;
    file_net>>temp3;
}

```

```

file_net>>"\n";
//file_net<<"Min. Connection Weight:"<<"\t"<<NetInfo->MinWgt<<"\n";
file_net>>temp1;
convert = atoi(temp1);
NetInfo->TotWgts = convert;
file_net>>temp3;
file_net>>"\n";
file_net>>temp1;
convert = atoi(temp1);
NetInfo->BatchModeRbt = convert;
file_net>>temp3;
file_net>>"\n";
//file_net<<"Batch Mode Status:"<<"\t"<<NetInfo->BatchModeRbt<<"\n";
file_net>>temp1;
convert = atoi(temp1);
NetInfo->PattModeRbt = convert;
file_net>>temp3;
file_net>>"\n";
//file_net<<"Pattern Mode Status:"<<"\t"<<NetInfo->PattModeRbt<<"\n";
file_net>>temp1;
change = atof(temp1);
NetInfo->LngRate = change;
file_net>>temp3;
file_net>>"\n";
//file_net<<"Learning Rate:"<<"\t"<<NetInfo->LngRate<<"\n";
file_net>>temp1;
change = atof(temp1);
NetInfo->Momentum = change;
file_net>>temp3;
file_net>>"\n";
//file_net<<"Momentum:"<<"\t"<<NetInfo->Momentum<<"\n";
file_net>>temp1;
convert = atoi(temp1);
NetInfo->LngStaticRbt = convert;
file_net>>temp3;
file_net>>"\n";
//file_net<<"Learning Rate - Static:"<<"\t"<<NetInfo->LngStaticRbt<<"\n";
file_net>>temp1;
convert = atoi(temp1);
NetInfo->LngDynRbt = convert;
file_net>>temp3;
file_net>>"\n";
//file_net<<"Learning Rate - Dynamic:"<<"\t"<<NetInfo->LngDynRbt<<"\n";
file_net>>temp1;
convert = atoi(temp1);
NetInfo->Nlayers = convert;
file_net>>temp3;
file_net>>"\n";
//file_net<<"No. of Layers:"<<"\t"<<NetInfo->Nlayers<<"\n";
file_net>>temp1;
convert = atoi(temp1);
NetInfo->LayerOne = convert;
file_net>>temp3;
file_net>>"\n";
//file_net<<"Nodes in Layer 1:"<<"\t"<<NetInfo->LayerOne<<"\n";

```

```

file_net>>temp1;
convert = atoi(temp1);
NetInfo->LayerTwo = convert;
file_net>>temp3;
file_net>>"\n";
//file_net<<"Nodes in Layer 2:"<<"\t"<<NetInfo->LayerTwo<<"\n";
file_net>>temp1;
convert = atoi(temp1);
NetInfo->LayerThree = convert;
file_net>>temp3;
file_net>>"\n";
//file_net<<"Nodes in Layer 3:"<<"\t"<<NetInfo->LayerThree<<"\n";
file_net>>temp1;
convert = atoi(temp1);
NetInfo->LayerFour = convert;
file_net>>temp3;
file_net>>"\n";
//file_net<<"Nodes in Layer 4:"<<"\t"<<NetInfo->LayerFour<<"\n";
file_net>>temp1;
change = atof(temp1);
NetInfo->InpdataMax = change;
file_net>>temp3;
file_net>>"\n";
//file_net<<"Input Data - Max. Value:"<<"\t"<<NetInfo->InpdataMax<<"\n";
file_net>>temp1;
change = atof(temp1);
NetInfo->InpdataMin = change;
file_net>>temp3;
file_net>>"\n";
//file_net<<"Input Data - Min. Value:"<<"\t"<<NetInfo->InpdataMin<<"\n";
file_net>>temp1;
change = atof(temp1);
NetInfo->OutdataMax = change;
file_net>>temp3;
file_net>>"\n";
//file_net<<"Output data - Max. Value:"<<"\t"<<NetInfo->OutdataMax<<"\n";
file_net>>temp1;
change = atof(temp1);
NetInfo->OutdataMin = change;
file_net>>temp3;
file_net>>"\n";
//file_net<<"Output Data - Min. Value:"<<"\t"<<NetInfo->OutdataMin<<"\n";
file_net>>temp1;
change = atof(temp1);
NetInfo->NInpdataMax = change;
file_net>>temp3;
file_net>>"\n";
//file_net<<"Normalized Input Data - Max.:"<<"\t"<<NetInfo->NInpdataMax<<"\n";
file_net>>temp1;
change = atof(temp1);
NetInfo->NInpdataMin = change;
file_net>>temp3;
file_net>>"\n";
//file_net<<"Normalized Input Data - Min.:"<<"\t"<<NetInfo->NInpdataMin<<"\n";
file_net>>temp1;

```

```

change = atof(temp1);
NetInfo->NOutdataMax = change;
file_net>>temp3;
file_net>>"\n";
//file_net<<"Normalized Output Data - Max.: "<<"\t"<<NetInfo->NOutdataMax<<"\n";
file_net>>temp1;
change = atof(temp1);
NetInfo->NOutdataMin = change;
file_net>>temp3;
file_net>>"\n";
//file_net<<"Normalized Output Data - Min.: "<<"\t"<<NetInfo->NOutdataMin<<"\n";
file_net>>temp1;
temp2 = &temp1[0];
//strcpy(NetInfo->TngFile,temp2);
//file_net<<"Training Data File Name:"<<"\t"<<NetInfo->TngFile<<"\n";
//file_net>>temp1;
//temp1[0]=temp1[11];
//temp3 = &temp1[0];
//strcpy(NetInfo->TstFile,temp3);
//file_net<<"Test Data File Name:"<<"\t"<<NetInfo->TstFile<<"\n";
//file_net>>temp1;
//temp1[0]=temp1[11];
//temp3 = &temp1[0];
//strcpy(NetInfo->WgtFile,temp3);
//file_net<<"Connection Weight File Name:"<<"\t"<<NetInfo->WgtFile<<"\n";

file_net.close();
}

```

## **Randn.cpp**

```

//RAND.CPP
//NN.MAK - PROJECT GROUP

// Random Number Generation

#include <iostream.h>
#include <stdlib.h>
#include <time.h>

double randn(double ll, double ul)
{
    int k;
    double j,temp;
    j = ll + ((ul-ll)*rand()/(RAND_MAX+1.0));
    temp = j*1000;
    k = (int) temp;
    j = (double)k/1000;
    return(j);
}

```

## **Runset.CPP**

```

//RUN.CPP
//NN.MAK - PROJECT GROUP

```

```
// This Includes the Class for training and testing and Learning the problem
```

```
#include <iostream.h>
#include <stdlib.h>
#include <fstream.h>
#include <string.h>
#include <malloc.h>
#include "class.h"
#include "funct.h"
```

```
RunningSet::RunningSet(const char* runfile) // Constructor
```

```
{
    //file = runfile;
    file = runfile;
    file_in.open((const char*)file,ios::in);
    ntrain = 0;
    if (!file_in.good())
    {
        //MessageBox(NULL,"Error opening the data file", "Error Message", MB_OK |
        MB_ICONINFORMATION);
        //cout << "\n ***** error opening" <<" " << file <<" " <<"*****";
        exit(0);
    }
}
```

```
RunningSet::~RunningSet() // Destructor
```

```
{
    free (in_data);
    //free (file);
    file_in.close();
}
```

```
void RunningSet::Read_Data()
```

```
{
    int insize,i,j,loc;
    char temp[5];
    double change;

    file_in >> ntrain >> nin >> nout ;
    insize = nin + nout;
    in_data = (double*)malloc(ntrain*insize*sizeof(double));
    if (in_data == NULL)
    {
        cout << "\n Insufficient memory to read the input file";
        exit(0);
    }
}
```

```
for (i=0;i<ntrain;i++)
{
```



```

for (j=0;j<insize;j++)
{
file_in >> temp;
change = atof(temp);
loc = i*insize+j;
*(in_data+loc) = change;
}
}
}

```

## Fdial.rc

```

//Microsoft App Studio generated resource script.
//
#include "resource.h"

#define APSTUDIO_READONLY_SYMBOLS
////////////////////////////////////
//
// Generated from the TEXTINCLUDE 2 resource.
//
#define APSTUDIO_HIDDEN_SYMBOLS
#include "windows.h"
#undef APSTUDIO_HIDDEN_SYMBOLS
#include "afxres.h"
#include "fdial.h"

////////////////////////////////////
#undef APSTUDIO_READONLY_SYMBOLS

////////////////////////////////////
//
// Bitmap
//

//MAINMENU BITMAP MOVEABLE PURE "TOOLBAR.BMP"

////////////////////////////////////
//
// Menu
//

MAINMENU MENU DISCARDABLE
BEGIN
POPUP "&File"
BEGIN
MENUITEM "&New Net", ID_NNET
MENUITEM "&Open Net", ID_NETOPFILE
MENUITEM "Open &Training Set", ID_TNGFILE
MENUITEM "Open Te&st Set", ID_TSTFILE
MENUITEM "Open &Weight File", ID_WGTOPFILE
MENUITEM SEPARATOR
MENUITEM "S&ave Net", ID_SVNETFILE
MENUITEM "&Save Net As...", ID_SVNET_ASFILE

```

```

MENUITEM "Save W&eights",      ID_SVWGTFILE
MENUITEM "Save Weigh&ts As..",  ID_SVWGT_ASFILE
MENUITEM SEPARATOR
MENUITEM "&Print",              ID_PRINTFILE
MENUITEM "P&rint Set Up",      ID_PRINTSETUP
END
POPUP "&Training"
BEGIN
  MENUITEM "&Start Training",    ID_START_TNG
  MENUITEM "&Halt Training",     ID_HLT_TNG
  MENUITEM SEPARATOR
  MENUITEM "&Test Training Set",  ID_TST_TNG
  MENUITEM "Test T&est Set",     ID_TST_TST
END
POPUP "&Plot"
BEGIN
  MENUITEM "&Weights",          ID_PLT_WGTS
  POPUP "&Net Outputs"
  BEGIN
    MENUITEM "&Trining Set",     ID_PLT_TNG
    MENUITEM "Te&st Set",        ID_PLT_TST
    MENUITEM "&Error",          ID_PLT_ERR
  END
  MENUITEM "Net &Layout",       ID_PLT_LOUT
END
MENUITEM "E&xit",              CM_EXIT
END

```

```

////////////////////////////////////
//
// Dialog
//

```

```

IDD_OPEN_ANNAPP_DLG DIALOG PRELOAD DISCARDABLE 80, 80, 150, 60
STYLE DS_MODALFRAME | WS_POPUP | WS_CLIPSIBLINGS | WS_CAPTION |
WS_SYSMENU
CAPTION "Load ANN"
FONT 8, "System"
BEGIN
  CTEXT      "Want to load ANN application?",ID_LOAD_ANN_TXT,25,10,
            100,8,NOT WS_GROUP
  DEFPUSHBUTTON "&OK",IDOK,30,30,40,15,WS_GROUP
  PUSHBUTTON   "&Cancel",IDCANCEL,80,30,40,15,WS_GROUP
END

```

```

IDD_ANN_WINDOW_DLG DIALOG PRELOAD DISCARDABLE 10, 10, 330, 240
STYLE DS_MODALFRAME | WS_POPUP | WS_CLIPSIBLINGS | WS_CAPTION |
WS_SYSMENU
CAPTION " Artificial Neural Network Application"
MENU MAINMENU
FONT 8, "System"
BEGIN
  EDITTEXT   ID_TNG_FILE_EDIT,107,180,187,12
  GROUPBOX   "Training Results",ID_TNG_RSLT_GRP,5,5,100,90,WS_GROUP

```

LTEXT "Target Error:",ID\_TGT\_ERR\_TXT,10,15,50,8,NOT WS\_GROUP  
EDITTEXT ID\_TGT\_ERR\_EDIT,70,15,25,12  
LTEXT "RMS Error:",ID\_RMS\_ERR\_TXT,10,30,50,8,NOT WS\_GROUP  
EDITTEXT ID\_RMS\_ERR\_EDIT,70,30,25,12  
LTEXT "Changes:",ID\_CHANGES\_TXT,10,45,50,8,NOT WS\_GROUP  
EDITTEXT ID\_CHANGES\_EDIT,70,45,25,12  
LTEXT "No. of Iterations:",ID\_NITER\_TXT,10,60,58,8,NOT  
WS\_GROUP  
EDITTEXT ID\_NITER\_EDIT,70,60,25,12  
LTEXT "Good Patterns:",ID\_GOODPAT\_TXT,10,75,50,8,NOT WS\_GROUP  
EDITTEXT ID\_GOODPAT\_EDIT,70,75,25,12  
GROUPBOX "Inital Weights",ID\_INIT\_WGTS\_GRP,110,5,100,55,WS\_GROUP  
LTEXT "Max:",ID\_MAX\_WGT\_TXT,155,15,19,8,NOT WS\_GROUP  
EDITTEXT ID\_MAX\_WGT\_EDIT,175,15,25,12  
LTEXT "Min:",ID\_MIN\_WGT\_TXT,155,30,17,8,NOT WS\_GROUP  
EDITTEXT ID\_MIN\_WGT\_EDIT,175,30,25,12  
LTEXT "Range",ID\_WGT\_RGE\_TXT,120,25,30,8,NOT WS\_GROUP  
PUSHBUTTON "&Randomize",ID\_RAND\_WGTS,122,45,50,10,WS\_DISABLED |  
WS\_GROUP  
EDITTEXT ID\_TOT\_WGT\_EDIT,177,46,16,9  
GROUPBOX "Training Mode",ID\_TNG\_MODE\_GRP,110,130,80,40,WS\_GROUP  
CONTROL "Batch Mode",ID\_BATCHMODE\_RBT,"Button",  
BS\_AUTORADIOBUTTON | WS\_TABSTOP,115,140,60,10  
CONTROL "Pattern Mode",ID\_PATTERNMODE\_RBT,"Button",  
BS\_AUTORADIOBUTTON | WS\_TABSTOP,115,155,60,10  
GROUPBOX "Learning Parameters",ID\_LNG\_PARA\_GRP,110,65,100,60,  
WS\_GROUP  
LTEXT "Learning Rate:",ID\_LNG\_RATE\_TXT,125,75,60,8,NOT  
WS\_GROUP  
EDITTEXT ID\_LNG\_RATE\_EDIT,125,90,25,12  
LTEXT "Momentum:",ID\_MOMENTUM\_TXT,115,110,50,8,NOT WS\_GROUP  
EDITTEXT ID\_MOMENTUM\_EDIT,170,110,25,12  
CONTROL "Static",ID\_LNG\_STATIC\_RBT,"Button",BS\_AUTORADIOBUTTON |  
WS\_TABSTOP,155,85,40,10  
CONTROL "Dynamic",ID\_LNG\_DYN\_RBT,"Button",BS\_AUTORADIOBUTTON |  
WS\_TABSTOP,155,98,40,10  
GROUPBOX "NetArchitecture",ID\_NET\_ARCH\_GRP,5,95,100,80,WS\_GROUP  
LTEXT "No. of Layers:",ID\_NLAYERS\_TXT,10,105,50,8,NOT WS\_GROUP  
EDITTEXT ID\_NLAYERS\_EDIT,65,105,10,12  
LTEXT "Layer Size:",ID\_LAYER\_SIZE\_TXT,10,127,41,8,NOT WS\_GROUP  
LTEXT "1",ID\_LAYER\_ONE\_TXT,55,120,10,8,NOT WS\_GROUP  
LTEXT "2",ID\_LAYER\_TWO\_TXT,67,120,10,8,NOT WS\_GROUP  
LTEXT "3",ID\_LAYER\_THREE\_TXT,79,120,10,8,NOT WS\_GROUP  
LTEXT "4",ID\_LAYER\_FOUR\_TXT,91,120,10,8,NOT WS\_GROUP  
EDITTEXT ID\_LAYER\_ONE\_EDIT,55,130,10,12  
EDITTEXT ID\_LAYER\_TWO\_EDIT,67,130,10,12  
EDITTEXT ID\_LAYER\_THREE\_EDIT,79,130,10,12  
EDITTEXT ID\_LAYER\_FOUR\_EDIT,91,130,10,12  
LTEXT "Activation Function:",ID\_ACT\_FUNC\_TXT,10,145,80,8,NOT  
WS\_GROUP  
COMBOBOX ID\_ACT\_FUNC\_CMB,10,155,85,40,CBS\_DROPDOWNLIST |  
WS\_BORDER | WS\_VSCROLL | WS\_TABSTOP  
GROUPBOX "Data Normalization",ID\_DATA\_NORM\_GRP,215,5,110,170,  
WS\_GROUP  
CTEXT "Range of Data",ID\_DATA\_RANGE\_TXT,240,15,60,8,NOT

```

        WS_GROUP
LTEXT      "Max:",ID_DATA_INP_MAX_TXT,255,28,20,8,NOT WS_GROUP
LTEXT      "Min:",ID_DATA_INP_MIN_TXT,255,43,20,8,NOT WS_GROUP
LTEXT      "Input",ID_DATA_INP_TXT,220,34,30,8,NOT WS_GROUP
EDITTEXT   ID_DATA_INP_MAX_EDIT,280,28,25,12
EDITTEXT   ID_DATA_INP_MIN_EDIT,280,43,25,12
LTEXT      "Max:",ID_DATA_OUT_MAX_TXT,255,58,20,8,NOT WS_GROUP
LTEXT      "Min:",ID_DATA_OUT_MIN_TXT,255,73,20,8,NOT WS_GROUP
LTEXT      "Output",ID_DATA_OUT_TXT,220,66,30,8,NOT WS_GROUP
EDITTEXT   ID_DATA_OUT_MAX_EDIT,280,58,25,12
EDITTEXT   ID_DATA_OUT_MIN_EDIT,280,73,25,12
CTEXT      "Normalize to",ID_DATA_NRANGE_TXT,240,88,60,8,NOT
        WS_GROUP
LTEXT      "Max:",ID_DATA_NINP_MAX_TXT,255,100,20,8,NOT WS_GROUP
LTEXT      "Min:",ID_DATA_NINP_MIN_TXT,255,115,20,8,NOT WS_GROUP
LTEXT      "Input",ID_DATA_NINP_TXT,220,108,30,8,NOT WS_GROUP
EDITTEXT   ID_DATA_NINP_MAX_EDIT,280,100,25,12
EDITTEXT   ID_DATA_NINP_MIN_EDIT,280,115,25,12
LTEXT      "Max:",ID_DATA_NOUT_MAX_TXT,255,130,20,8,NOT WS_GROUP
LTEXT      "Min:",ID_DATA_NOUT_MIN_TXT,255,145,20,8,NOT WS_GROUP
LTEXT      "Output",ID_DATA_NOUT_TXT,220,136,30,8,NOT WS_GROUP
EDITTEXT   ID_DATA_NOUT_MAX_EDIT,280,130,25,12
EDITTEXT   ID_DATA_NOUT_MIN_EDIT,280,145,25,12
PUSHBUTTON "&Normalize",ID_DATA_NORM,241,160,60,10,WS_DISABLED |
        WS_GROUP
LTEXT      "Open Files:",ID_OPEN_FILE_TXT,5,195,40,8,NOT WS_GROUP
PUSHBUTTON "&Training Set",ID_OPENF_TNG_SET,50,180,50,10,WS_GROUP
PUSHBUTTON "&Weights File",ID_OPENF_WGT_SET,51,195,49,10
PUSHBUTTON "Test &Set",ID_OPENF_TST_SET,50,210,50,10
EDITTEXT   ID_WGT_FILE_EDIT,107,195,187,12
EDITTEXT   ID_TST_FILE_EDIT,107,210,187,12
PUSHBUTTON "&Transfer Data",ID_TRANSF_DATA,150,225,80,10,WS_GROUP
PUSHBUTTON "&Edit",ID_EDITF_TNG_SET,296,180,32,10
PUSHBUTTON "Edit",ID_EDITF_WGT_SET,296,195,32,10
PUSHBUTTON "Edit",ID_EDITF_TST_SET,296,210,32,10
END

IDD_RESULTS_DPLY_DLG DIALOG DISCARDABLE 50, 30, 200, 200
STYLE WS_POPUP | WS_VISIBLE | WS_CAPTION | WS_SYSMENU
CAPTION "Net Outputs"
FONT 8, "MS Sans Serif"
BEGIN
    DEFPUSHBUTTON "&Save",IDOK,10,133,50,14
    PUSHBUTTON "&Quit",IDCANCEL,123,135,50,14
    EDITTEXT IDC_OP_DISPLAY_LST,4,4,169,120,ES_MULTILINE |
        ES_AUTOVSCROLL | ES_AUTOHSCROLL
END

#ifdef APSTUDIO_INVOKED
////////////////////////////////////
//
// TEXTINCLUDE
//

1 TEXTINCLUDE DISCARDABLE

```

```
BEGIN
"resource.h\0"
END
```

```
2 TEXTINCLUDE DISCARDABLE
BEGIN
"#define APSTUDIO_HIDDEN_SYMBOLS\r\n"
"#include ""windows.h""\r\n"
"#undef APSTUDIO_HIDDEN_SYMBOLS\r\n"
"#include ""afxres.h""\r\n"
"#include ""fdial.h""\r\n"
"\0"
END
```

```
3 TEXTINCLUDE DISCARDABLE
BEGIN
"\r\n"
"\0"
END
```

```
////////////////////////////////////
#endif // APSTUDIO_INVOKED
```

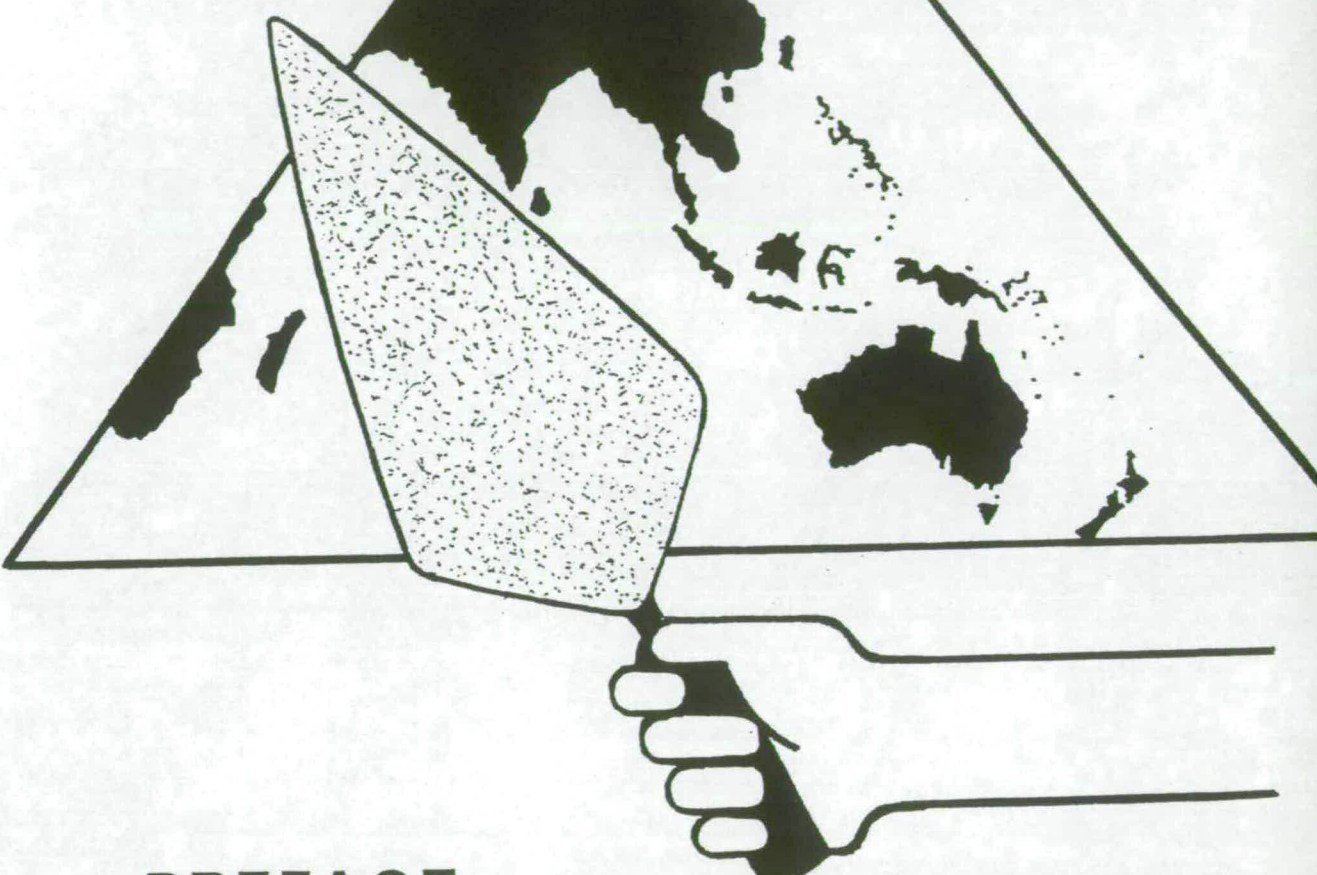
```
#ifndef APSTUDIO_INVOKED
////////////////////////////////////
//
// Generated from the TEXTINCLUDE 3 resource.
//
```

```
////////////////////////////////////
#endif // not APSTUDIO_INVOKED
```

**Fdial.Def**

```
NAME FileDialogs
DESCRIPTION 'An MFC Window Application'
EXETYPE WINDOWS
CODE PRELOAD MOVEABLE DISCARDABLE
DATA PRELOAD MOVEABLE MULTIPLE
HEAPSIZE 2048
```

# 4<sup>TH</sup> AUSTRALASIAN MASONRY CONFERENCE



## PREFACE

The Fourth Australasian Masonry Conference is being held at the University of Technology Sydney on Thursday 23 November and Friday 24 November 1995. Previous Conferences were held at The University of Newcastle (1991), University of Melbourne (1992), and Queensland University of Technology, Brisbane (1994).

These proceedings contain approximately forty (40) papers on a range of practical and theoretical aspects of masonry design and construction with a Keynote Paper related to the seismic rehabilitation of existing masonry buildings.

## ORGANISING COMMITTEE

- Max Granger, Clay Industry Technical Advisory Chamber
- Steve Lawrence, CSIRO
- Adrian Page, The University of Newcastle
- Sia Parsanejad, University of Technology Sydney
- Alan Pearson, Concrete Masonry Association of Australia

## SESSION 6 – STRAND ONE

- “In-Plane Behaviour of Three-Storey Three-Bay RC Frames Infilled With URM Panels: Qualitative Assessment”  
by A. Dukuze, Research Engineer, Atlantic Masonry Research and Advisory Bureau Inc., The University of New Brunswick, and J.L. Dawe, Professor, Department of Civil Engineering, The University of New Brunswick.....208
- “Evaluation of the Compressive Strength of Masonry”  
by F.J. Crisafulli, Postgraduate Student, The University of Canterbury, and Lecturer, The University of Cuyo, Argentina, A.J. Carr, Reader in Civil Engineering, The University of Canterbury, R. Park, Professor in Civil Engineering, The University of Canterbury, and J.L. Restrepo, Post Doctoral Fellow in Civil Engineering, The University of Canterbury.....218
- “Testing of Post-Tensioned Hollow Clay Masonry”  
by K.J. Graham, Engineering Consultant, and A.W. Page, CBPI Professor in Structural Clay Brickwork, Department of Civil Engineering and Surveying, The University of Newcastle .....228
- “A Neural Network Approach for Predicting the Failure Load of Masonry Cladding Panel in Bending”  
by Anu Mathew, Research Student, Department of Civil Engineering, The University of Edinburgh, Bimal Kumar, Lecturer, Department of Civil Engineering, Strathclyde University, B.P. Sinha, Reader, Department of Civil Engineering, The University of Edinburgh, and R. Pedreschi, Senior Lecturer, Department of Architecture, The University of Edinburgh.....240
- “Durability of Mudbrick – Comparison of Three Test Methods”  
by A. Weisz, School of Civil Engineering and Building, Swinburne University of Technology, A. Kobe, School of Civil Engineering and Building, Swinburne University of Technology, K. McManus, School of Civil Engineering and Building, Swinburne University of Technology, and A. Nataamadja, School of Civil Engineering and Building, Swinburne University of Technology .....249

## SESSION 6 – STRAND TWO

- “The Dependence of Sodium Sulfate Salt Cycle Testing on the Crystal Growth Behaviour From Aqueous Solution”  
by L.S. Burgess-Dean, Postgraduate Student, School of Engineering and Technology, Deakin University.....259
- “Measurement of Air Content in Hardened Mortar”  
by P.J. Evans, Associate Professor, School of Architecture Construction and Planning, Curtin University of Technology .....270
- “An Investigation Into the Innovative Use of Volcanic Ash in Disaster Resistant Masonry for Housing in the Philippines”  
by Isolde C. Macatol, Australian Institute of Tropical Architecture, James Cook University of North Queensland.....276
- “A Closer Look at the Structure of Mortars and the Effects of Air Entraining Agent on Bond Strength”  
by H.O. Sugo, Postgraduate Student, Department of Civil Engineering and Surveying, The University of Newcastle, A.W. Page, CBPI Professor in Structural Clay Brickwork, Department of Civil Engineering and Surveying, The University of Newcastle, and S.J. Lawrence, Project Manager – Masonry Structures, CSIRO Division of Building Construction and Engineering .....285
- “Pre-Blended Dry Mortar”  
by C.B. Rigbye, Special Project Manager, Queensland Cement Distributors .....295
- “Influence of Age on the Development of Bond Strength”  
by N. De Vitis, Postgraduate Student, Department of Civil Engineering and Surveying, The University of Newcastle, CBPI Professor in Structural Clay Brickwork, Department of Civil Engineering and Surveying, The University of Newcastle, and S.J. Lawrence, Project Manager – Masonry Structures, CSIRO Division of Building Construction and Engineering.....299

# A NEURAL NETWORK APPROACH FOR PREDICTING THE FAILURE LOAD OF MASONRY CLADDING PANEL IN BENDING

†ANU MATHEW, ††BIMAL KUMAR, ‡SINHA B. P & ††PEDRESCHI R.

† Research Student, Dept. of Civil Engineering, University of Edinburgh, Scotland.  
†† Lecturer, Dept. of Civil Engineering, Strathclyde University, Glasgow, Scotland.  
‡ Reader, Dept. of Civil Engineering, University of Edinburgh, Scotland  
†† Senior Lecturer, Dept. of Architecture, University of Edinburgh, Scotland.

## SUMMARY

A review of the literature on lateral loading of brick masonry shows that no definitive mathematical solution is at present available for the prediction of cracking or failure load for masonry cladding panels subjected to wind loading. The method of design varies from country to country with no justification for the theoretical methods; such as the yield-line or the strip method used at present. Hence there is a lot of controversy about the most appropriate method that can be adopted for the prediction of cracking and failure load of a masonry panel subjected to out-of-plane biaxial bending with no pre compression.

The emergence of Neural Network Systems (NNS) and its successful application in various fields has opened up a promising approach to solve many of the engineering problems, especially in areas where there is a lack of proper theoretical backup. This paper explores the application of NNS for the prediction of failure load of masonry panel. The neural network is trained using a limited number of training sets obtained from the past record of experimental results. Once the neural network is thus trained, it is tested for new sets of input. These inputs may or may not be from the same cases as used in the training set. The NN results are compared then with the experimental results. It is possible that NN application can be used for the prediction of failure load for masonry panel.

## INTRODUCTION

At present, no proper analytical method is available to predict the ultimate pressure of brickwork cladding panels supported on three or four sides. A lot of test data [1],[2],[3],[4] is available for walls subjected to lateral pressure, but lack of information regarding stiffness orthotropy, poisson's ratio, failure criterion and uncertainty of the test's boundary conditions makes it very difficult to use them for the development of a rational method of design. Hence the method of design varies from country to country. The methods, yield line analysis, strip method etc., are shown to give reasonably good results in some of the test cases, though there was no rational justification for the method adopted. This could be due to the fact that the boundary conditions in the tests were not well defined and dead weight stress and rotational restraints were neglected.



A brief description of the currently followed methods in various countries and their limitations is given below.

The British code of practice [5] supports yield line method, which gives an upper bound solution for idealised rigid plastic material and is widely used in the case of under reinforced concrete slabs. The material is assumed to yield along certain pre-defined yield lines according to their geometry and the support conditions. After yielding, the structure is assumed to rotate along these yield lines at constant moment. But in case of brick masonry, which is brittle in its behaviour, this method is always found to overestimate the failure pressure. The British code of practice gives coefficients, which are developed based on the yield line analysis, hence it can no longer be adopted for the design without any risk factor.

The Australian code of practice [6] supports strip method, which gives a lower bound solution for reinforced concrete slabs. This method is mainly used for under reinforced concrete slabs, where variable reinforcements are provided according to the moment field. In the case of unreinforced masonry panel the actual moment capacity of the panel cannot be varied from strip to strip as done in the case of RC slabs. Therefore, the use of this method for design also cannot be justified. Again, this method fails in its application to panels with openings where extra reinforcements are provided to take care of the stress concentrations around the openings for reinforced concrete.

Baker has put forward a failure criterion [7] based on a single joint test, where he applied moments in two directions. Finite element programs were developed [8] to take into account the inherent non-linear behaviour of brick masonry and incorporating the above failure criteria. But as Baker ignored the orthotropic stiffness in the tests carried out for arriving at this failure criterion, it doesn't truly reflect the actual load distribution in a brick panel. [4]

Under such circumstance, it is very desirable and essential to develop a method based on test results that could be universally accepted for the design of masonry panel. The emergence of Neural Network Systems (NNS) and its successful application in various fields including civil engineering [9],[10],[11] has opened up a promising approach to solve many of the engineering problems, especially in areas where there is a lack of proper theoretical backup. Out of the various machine learning methods, NNS turns out to be outstanding due to its ability to support a weak theory and an inadequate data such as the case of masonry panels subjected to lateral loading.

After giving a brief introduction about the artificial neural network, this paper gives the implementation of the net for the prediction of failure pressure of a four sides simply supported masonry panel subjected to biaxial bending. The analysis of four sides simply supported solid panel is adopted as a first step, with an intention to extend it to panels with other support conditions and also for panels with openings.

## **ARTIFICIAL NEURAL NETWORK**

Neural networks are computing systems that simulate the structure and functioning of the biological neural network of the human brain. It is understood that human brain has approximately 100 billion neural cells that are interconnected in a complex manner constituting a large scale network. [12] A typical biological neuron model is shown in figure.

1.[12] When a biological neuron is excited by electrical impulses, it sends out pulses through its axon. The soma (cell body) sums its electrical potential between its dendrites and utilises these to output a voltage spike along its axon. This output voltage is biologically transmitted to a part of the body associated with the particular neuron.

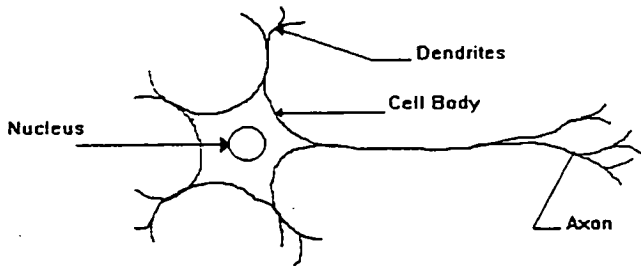


Figure 1. A Biological Neuron

Neural networks are highly simplified version of the human neural systems. There is an input layer to which the data is presented and an output layer which gives the required responses of the network. In a multilayered network, there could be one or intermediate layers, also known as the hidden layers which enables the network to handle complicated mapping more effectively. The units in each layer interacts with all the units in the next layer with a weighted connection, which the net modifies as it learns the problem. The working of the net work can be best explained with a simple processing element as shown in figure 2. [13] Each unit receives a set of input values  $x_1, x_2, x_3, \dots, x_n$ . These inputs are similar to the electrochemical signals received by the neuron in a biological model. In the simplest model, the input signals to the unit are multiplied by the connection weights and the weighted inputs are summed up to form the effective net input to the neuron [14] as given in equation (1).

$$S = \sum_{i=1}^n w_{ij} x_i \quad (1)$$

In a neurobiological system the neuron fires or produces an output signal only if the strength of the incoming signal builds up to a certain level. This is simulated in the ANN by assigning a threshold level for each processing element. The common practice [14] is to introduce an activation function at each processing element to obtain an output signal as shown in equation (2).

$$Y = F(S) \quad (2)$$

Most commonly used activation functions are simple linear function, a threshold function and a non-linear sigmoid [13],[14] as shown in figure 3. The sigmoid function is given as in equation (3).

$$F(S) = \frac{1}{1 + e^{-(S-\theta)}} \quad (3)$$

Where  $\theta$  is the threshold constant that is used to adjust the bias of the activation weight. An artificial neural network is a group of several such interconnected elements called neurons.

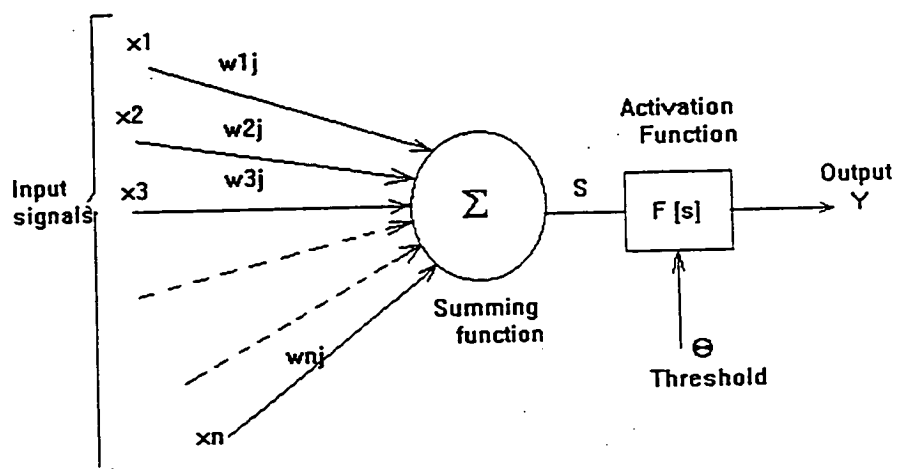


Figure2. Model of a single Neuron

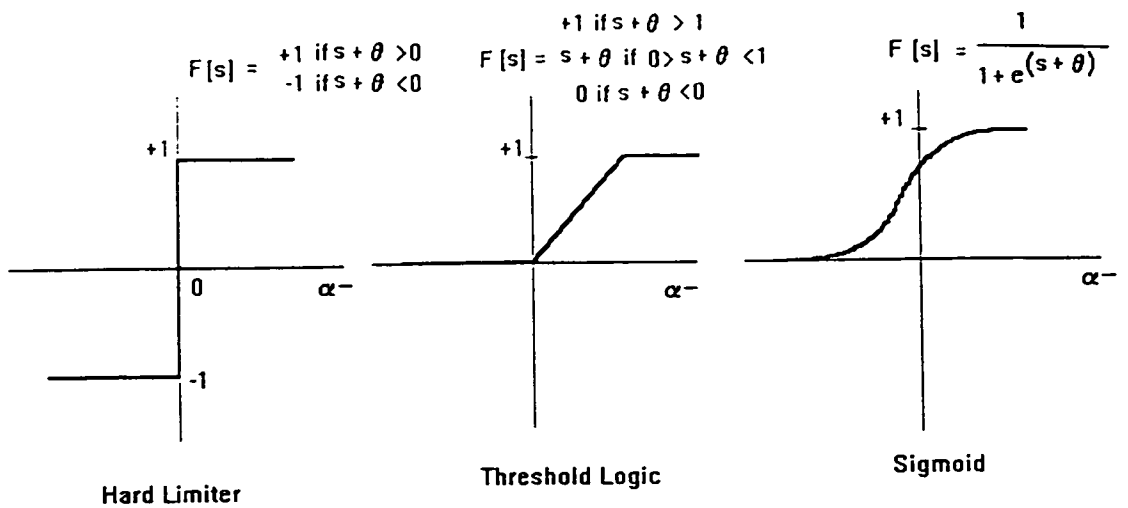


Figure 3. Commonly used Activation Functions

The network training approach used in the present work is that of a supervised learning method where the input and target output patterns are presented to the network. A feed forward multilayered network with back propagation learning algorithm, which uses the gradient descent method to minimise the error function is adopted in this study. More detail on back propagation algorithm is available in Rumelhart & McClelland [15]. A suitable architecture is to be defined for the network to have an effective learning. The number of units in the input layer depends on the parameters involved in characterising the problem and the number of layers in the output layers equals the number of outputs desired. There is no definite method to decide the number of hidden layers and the number of units in each hidden layer. So a trial and error method is adopted to finalise them. The net is trained by initially selecting small random weights and internal thresholds and then presenting all training data repeatedly. The network now learns from the examples presented to it. At the output layer, the network outputs are compared with the desired outputs given in the training pattern. An error term is calculated for each output node as the negative derivative of the error and is propagated backward from the nodes in the output layer to nodes in the lower layers and the connection weights are modified accordingly.

## NEURAL NETWORK FOR ANALYSIS

The first step for the development of an ANN is generating the training set. Due to the practical difficulty in getting the experiments done for panels with different support conditions and material properties, it was decided to use the results published by various other researchers. In this investigation, a four sides simply supported solid panel is trained and tested using the neural net as a first step, which will be extended later on for other support

conditions. The training set is so selected that it reflects all the aspects of the problem at hand. Test results are collected from the work reported by Baker [1], Lawrence [2] Kheir [3] & Sinha[4]. Out of the total data available, two third is used for training the network and the rest is used for evaluating its learning capability.

### ARCHITECTURE OF THE NET

A trial and error approach is adopted to finalise the number of hidden layer and the number of layers in each hidden layer. The finally accepted net architecture is shown in figure 4. Length, height, thickness, scale model used, aspect ratio, Flexural strength of wallette parallel to the bed joints and the strength orthotropic ratio are chosen as the input parameters for predicting the failure load. To minimise the non linearity of the problem the known relationship between the input and the output were given directly to the net and the net is left to resolve the hidden non linearities we don't understand [16]. As the failure load is inversely related to the panel sizes, additional inputs are given as  $1/L^2$  &  $1/H^2$ . As the data includes panels tested in different scale models, in order to reduce the range of input data, the panel dimensions are multiplied with the respective scale. Moment of resistance,  $f_z$  of the panel parallel to the bed joints is given directly by multiplying the flexural strength with the section modulus. Thus the input data consists of length, L in meters, Height, H in meters, Scale model used, M,  $1/M^2$ , Aspect ratio L/H,  $1/L^2$ ,  $1/H^2$ ,  $f_z$  & the orthotropic ratio, R. Nets with varying number of nodes in a single hidden layer were tried and it was found that a net with 5 hidden nodes give the best results when tested with untrained data.

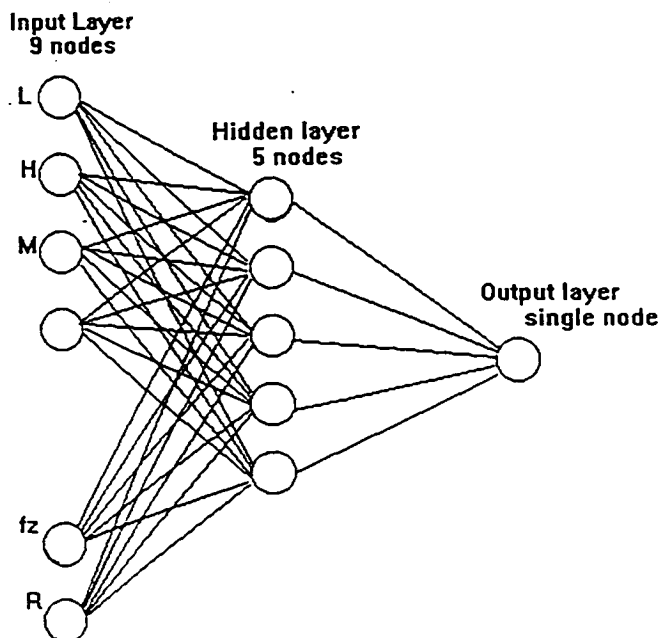


Figure 4. Finalised Architecture of the Net

## TRAINING THE NET

All the input and output data are normalised so that the value of input and output remains in the range of 0 to +1. The back propagation learning algorithm is used to train the net. During training, the network learns by the examples presented to it and forms a generalised internal relationship between the input and the output. Training is carried out by repeatedly presenting the patterns until the average sum of squared errors over all the training patterns are minimised. The weights and thresholds are modified after each cycle of training set and the final weights are saved for further use. Any hidden or incomprehensible non linearities was left for the net to resolve.

## TESTING THE NET

After training the network was evaluated by presenting a set of patterns which are not used for training. There would not be any weight modification during testing. This gave an assessment of the reliability of the net for other problems. The net outputs are compared with the desired outputs. The generalisation capability of the net is evaluated by its performance in this untrained data. The neural net results on trained and untrained samples are given in table 1 & table 2. The results show that neural net was successful in mapping the non-linear relationship between the various input parameters and the output.

Table 1. Training set and the Neural net results

L	H	M	1/M <sup>2</sup>	L/H	1/L <sup>2</sup>	1/H <sup>2</sup>	fz	R	Desired result	NN result	% error
2.4	1.2	6	0.028	2	0.174	0.695	0.00374	2.88	18200	18241	0.22
2.4	2.4	6	0.028	1	0.174	0.174	0.003234	2.34	10500	10522	0.21
1.51	2.26	2	0.25	0.5	0.44	0.196	0.00686	4	20580	20497	0.4
2.4	4.8	6	0.028	0.5	0.174	0.043	0.003366	3.25	7000	6915	1.21
3.75	2.5	1	1	1.5	0.071	0.16	0.00412	2.5	4900	4869	0.63
2.06	2.06	3	0.111	1	0.235	0.235	0.005542	4.21	10980	10989	0.08
4.12	2.06	3	0.111	2	0.059	0.235	0.005525	5.31	5220	5195	0.48
2.06	2.06	3	0.111	1	0.235	0.235	0.004304	3.65	9420	9430	0.11
2.3	2.3	2	0.25	1	0.189	0.189	0.00533	4.11	12200	12280	0.65
2.3	2.3	2	0.25	1	0.189	0.189	0.00533	4.11	12360	12280	0.66
2.4	1.2	6	0.028	2	0.174	0.695	0.003828	3.5	19000	18989	0.06
2.4	2.4	6	0.028	1	0.174	0.174	0.00297	2.9	8400	8410	0.12
2.4	4.8	6	0.028	0.5	0.174	0.043	0.003212	3.07	5600	5607	0.13
4.12	2.06	3	0.111	2	0.059	0.236	0.00595	2.46	6150	6139	0.18
2.5	2.5	1	1	1	0.16	0.16	0.004053	2.38	8600	8587	0.15
6	3	1	1	2	0.028	0.111	0.00392	1.57	3200	3302	3.19

Table 2. Test set and Neural Net Results

L	H	M	1/M <sup>2</sup>	L/H	1/L <sup>2</sup>	1/H <sup>2</sup>	fz	R	Desired result	NN result	% error
2.4	1.2	6	0.028	2	0.174	0.695	0.003212	3.25	18000	15835	12.03
2.4	2.4	6	0.028	1	0.174	0.174	0.00374	3.47	10000	9888	1.12
3.09	2.06	3	0.111	1.5	0.104	0.236	0.0068	4.29	8300	9024	8.73
3.09	2.06	3	0.111	1.5	0.104	0.236	0.0049	3.55	6000	7020	17
6	3	1	1	2	0.028	0.111	0.00466	1.32	3500	3363	3.91
2.28	2.28	2	0.25	1	0.193	0.193	0.0031	2.56	7590	7926	4.43
2.06	2.06	3	0.111	1	0.235	0.235	0.006936	3.47	16350	17291	5.76

## DISCUSSION

It can be seen from table 2 that the neural net predicts failure pressure within 8.75% except in two cases only. In these two cases the maximum error was 12 and 17%. This variation in the results can be attributed to the inconsistency in the testing conditions adopted as the training set consists of tests done by different people in different countries .

Though nine parameters are given as input, the net work caters for the less important parameters by assigning low connection weight to the node containing that parameter. Since the network is trained on results done at different test set ups, it is capable of incorporating any inherent noise and thus takes into account the error due to workmanship also.

## CONCLUSION

The present study demonstrates the feasibility of using neural network for the prediction of failure pressure of masonry panel subjected to biaxial bending. The study will be extended for panels of different support conditions for both solid and panels with openings. Further work will be done to take into account the inconsistency in the test results.

## REFERENCES

1. Baker, L.R., " Brickwork Panels Subjected to face Wind Loads", M.S.Thesis, University of Melbourne, June 1972.
2. Lawrence, S.J., "Behaviour of Brick Masonry Walls Under Lateral Loading", Ph.D.Thesis, University of New South Wales, November 1983.
3. Kheir, A.M.A., "Brickwork Panels Under Lateral Loading", M.S.Thesis, University of Edinburgh, 1975.
4. Sinha, B.P., and Ng, C.L., "Behaviour of Brickwork Panels Under Lateral Pressure", Proceedings of the 10th International Brick Masonry Conference, 1994, pp. 649-658.

5. British Standards Institution. "Code of Practice for Structural Use of Masonry- Part 1: Unreinforced Masonry", BS5628:Part 1, London, 1978, 39 pages.
6. Brickwork in Buildings, CSAA Brickwork Code AS CA47-1969. Standards Association of Australia, Sydney, 1969
7. Baker, L.R., "A Failure Criterion for Brickwork in Bi-Axial Bending", Proceedings of the Vth International Brick Masonry Conference, 1978, pp. 71-78.
8. May, I.M., and Tellett, J., "Non-linear Finite Element Analysis of Reinforced and Unreinforced Brickwork", Proceedings of British Masonry Society 1, 1986, pp. 96-99.
9. Goh, A.T.C., "Back-Propagation Neural Networks for Modelling Complex Systems", Artificial Intelligence in Engineering, Vol.9, 1995, pp.143-151.
10. Hajela, P. and Berke, L., "Neurobiological Computational Models in Structural Analysis and Design", Computers and Structures, Vol. 41, No. 4, 1991, pp. 657-667.
11. Mukherjee, A. and Deshpande, J.M., "Modelling Initial Design Process Using Artificial Neural Networks", Journal of Computing in Civil Engineering, Vol. 9, No. 3, 1995, pp. 194-200.
12. Muller, B., Reinhardt, J., " Neural networks - An Introduction", 1991.
13. Simon Haykin, "Neural Networks - A Comprehensive Foundation", MacMilan publications, 1994.
14. Lippmann, R., P., "An Introduction to Computing with Neural Nets", IEEE ASSP Magazine, Vol. 4, 1987, pp. 4-22.
15. Rumelhart, D.E. and McClelland, J.L., "Parallel Distributed Processing - Explorations in the Micro Structure of Cognition", Vol. 1 and 2, MIT Press, Cambridge, 1986.
16. Crooks, T., "Care and Feeding of Neural Networks", AI Expert, Vol. 7, No. 7, 1992, pp. 36-41.

Notations:-

L- Length of panel in meters  
H- Height of panel in meters  
f- flexural strength(N/mm<sup>2</sup>) in stronger direction  
z- sectional modulus  
R- orthotropy



#### REFERENCES

1. Chen Xingzhi and Liang Jianguo, Shear Strength of Brick Masonry with Reinforced Network in Bed Joints Subject to Combined Action, *Journal of Hunan University*, 1987, (4).
2. Zhou Bingzhang and Xia Jingqian, Experimental Study on Seismic Behaviour of Brick Masonry with Horizontal Reinforcement, *Journal of Building Structures*, 1991, (4).
3. The Design Code of Masonry Structures GBJ3 - 88, Building Industry Publishing House of China, Beijing, 1988.
4. The Common Unified Standard for Building Structures Design GBJ68 - 84, Building Industry Publishing House of China, 1984.



11th INTERNATIONAL BRICK/BLOCK MASONRY CONFERENCE  
TONGJI UNIVERSITY, SHANGHAI, CHINA, 14 - 16 OCTOBER 1997

## STRENGTH AND BEHAVIOUR OF ORTHOTROPIC AND ISOTROPIC PANELS UNDER BIAXIAL BENDING

<sup>1</sup>Anu Mathew, <sup>2</sup>B P Sinha and <sup>3</sup>R F Pedreschi

### 1. ABSTRACT

Cladding panels made of isotropic and orthotropic materials are used in framed buildings. Such panels are subjected to biaxial bending due to wind loading. These panels carry very little or negligible axial load and hence mainly depend on their flexural strength to resist this lateral load. The novel method of testing cross beams has been used to study the fundamental behaviour of such panels under flexure. Test results on orthotropic and isotropic cross beams have been analysed to study the influence of orthotropy on its behaviour under biaxial bending. Tests done on brickwork cross beams showed that, in the case of an orthotropic material, the load was shed from the weaker to the stronger direction, once the maximum strength in that direction is reached. Similar tests were done on mortar cross beams, which is an isotropic material, and no such load shedding was noticed in these cases. The specimens failed as soon as one direction reached its ultimate strength, for all aspect ratios. Failure criteria have been developed for the orthotropic and isotropic material under biaxial bending. It is evident from the experimental results that biaxial flexural strength is higher than the uniaxial strength for both isotropic and orthotropic material. However, the increase in strength in the orthotropic material was noticed only in the weaker direction. The stronger direction didn't show any significant improvement in the strength. The theoretical predictions of the failure loads for the cross beams by a finite element analysis incorporating the above

Keywords: Isotropic; Orthotropic; Biaxial Bending; Failure Criteria.

<sup>1</sup>Anu Mathew, Ph.D Student, Dept. Of Civil Engineering, University of Edinburgh, West Mains Road, Edinburgh, Scotland, UK, EH9 3JN.

<sup>2</sup>B P Sinha, Reader, Dept. Of Civil Engineering, University of Edinburgh, West Mains Road, Edinburgh, Scotland, UK, EH9 3JN.

<sup>3</sup>R F Pedreschi, Senior Lecturer, Dept. Of Architecture, University of Edinburgh, Chambers Street, Edinburgh, Scotland, UK, EH1 1JZ.

criteria are found to be matching well with the experimental results. The experimental results are also compared with other methods of analysis.

## INTRODUCTION

Various types of isotropic and orthotropic panels, such as brickwork or concrete panels, are used as cladding in framed construction. Such panels are subjected to uniaxial or biaxial bending depending on their support conditions and rely mainly on their flexural strength to resist these forces. Walls of the upper floors of multi-storey buildings are also subjected to similar loading conditions. When the panel is supported on two opposite directions, it is under uniaxial bending and the failure load can be calculated using simple theory of bending based on static equilibrium. However, when the panel is supported on three or more sides, it is subjected to biaxial bending and the calculation of the failure load needs detailed understanding of the strength and stiffness orthotropies. It is essential to consider the behaviour of the material under biaxial bending while analysing such panels. Hence, the proper evolution of a failure criterion is imperative before any mathematical solution can be proposed. This paper focuses mainly on the significance of the consideration of the mechanical properties of the material such as strength and stiffness orthotropies on the biaxial behaviour and attempts to develop a failure criteria for orthotropic and isotropic panels under biaxial bending.

The behaviour of brickwork in biaxial bending has been studied by Baker<sup>3</sup> using a single joint element of brickwork by applying moment in both directions. A failure criterion has been developed for the panels under biaxial bending based on the results of his study. However, it has to be pointed out that a single joint fails to take into account the variation in the stiffness of the material in both directions, which plays a significant role in the distribution of the applied load and thus was not able to explain the failure of panels subjected to wind loading.

A novel idea of testing cross beams has been proposed by Sinha<sup>1</sup> to study the fundamental behaviour of a material under biaxial bending. To compare the behaviour of orthotropic and isotropic material, brickwork and cement mortar cross beams have been used. Brickwork beams have different strength and stiffness properties in the two orthogonal directions due to the orientation of the bricks and the presence of bed joints and head joints. The flexural tests done on brick wallettes, where the tension develops in parallel or perpendicular to the bed joints, show that they exhibit definite strength and stiffness properties in these directions. Hence, brickwork cross beams may be considered ideal for the study of orthotropic material under biaxial bending. Cement sand mortar, which is isotropic in strength and stiffness is chosen as the isotropic material to examine its behaviour under biaxial bending.

## 3. CROSS BEAM TESTS

In a cross beam, the applied load at the centre gets distributed in both directions according to the relative stiffness of the material. When the ultimate load is reached in the weaker direction, the specimen may crack, which may be followed by an immediate or delayed failure depending on the orthotropic strength ratio. Thus the cross beam tests enable the study of the behaviour of the material under biaxial bending and takes into account the strength and stiffness orthotropies.

### Construction of Cross Beams

Each cross beam consisted of the central portion for which the material property was to be studied and four arms connected to it as shown in figure 1. The arms were made of high strength mortar ( epoxy resin sand mortar ) to prevent the premature failure of the arms either in bending or in shear. Each arm was made up of four finger like beams of the same thickness as the central part and is connected to the central portion leaving a gap in between as shown in the figure, thus allowing the propagation of cracks. The load was applied at the centre using a hydraulic jack.

In the case of masonry cross beams, the epoxy sand mortar was used for the bricks in the arms<sup>2</sup>. In mortar beams, the arms were completely made of the epoxy sand mortar. The central portion was cast first and the arms were joined later to it using the resin. This allowed the repeated use of the arms, thus saving the material and the cost of construction. Both the mortar and masonry cross beams are as shown in figure 1 a & b.

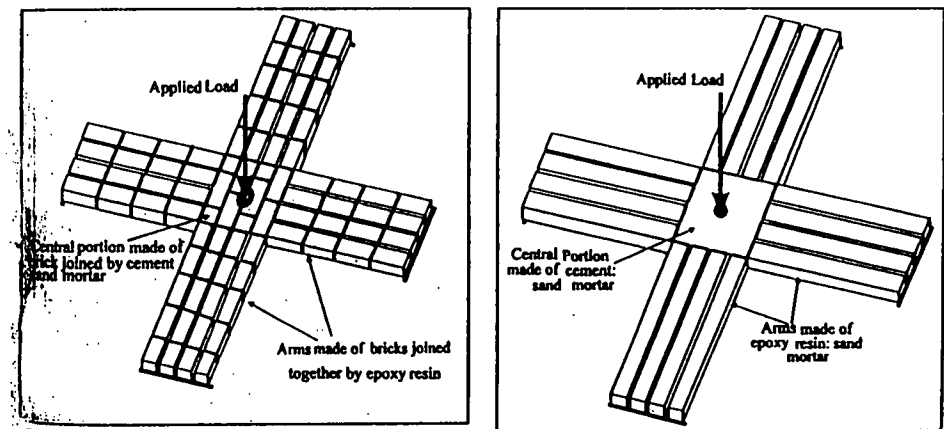


Fig. 1 a) Masonry Cross Beams, b) Mortar Cross Beams.

## 4. TESTS ON CROSS BEAMS

Brick and mortar cross beams of different aspect ratios in the range 1:0.5 to 1:2 were studied. Due to the orthotropic nature of the material, two sets of tests were done for

brickwork for all aspect ratios mentioned above in both directions. The cement mortar cross beams were built using 1:3 cement/sand mortar. Three cross beams were tested for each aspect ratio.

The support reactions and applied load were measured by the load cells connected to a data logger. This was to verify that there was no discrepancy between the applied load and the resultant reactions. The total applied load gets distributed to both directions and can be obtained as the sum of the support reactions in both directions.

The results of the mortar cross beam tests are compared with that of brickwork cross beams to examine the behaviour of both isotropic and orthotropic material under biaxial bending.

Companion specimens were tested along with each batch of cross beams to find out the uniaxial flexural strength of the material. These tests were done on beams of the same thickness as the cross beams by applying two-point loading. In the case of brickwork, two sets of beams were tested to find out the strength in the two orthogonal directions.

## 5. DISCUSSION OF RESULTS

### 5.1 Behaviour of Orthotropic and Isotropic Material

The tests carried out earlier on brickwork<sup>2</sup> are used for comparative purpose. The experimental and theoretical results are given in table 1 & 2. Support reactions of brickwork and mortar beams were compared with Grashoff-Rankine method, where the

Table 1. Experimental and Theoretical failure load of Masonry cross beams<sup>2</sup>

Lx (mm)	Ly (mm)	Expt. Failure load (N)	Lx/Ly	Theoretical Failure load (N)			
				Rankine's Method of (RM) Analysis	Ratio RM Expt	FEM with failure criterion	Ratio FEM Expt
300	585	4974	0.51	4573	0.92	4270	0.95
445	585	3096	0.76	2672	0.86	2887	0.93
585	585	2151	1.0	1975	0.92	1958	0.91
690	585	1925	1.18	1674	0.87	1717	0.89
860	585	1535	1.47	1343	0.88	1424	0.93
1140	585	1293	1.95	1043	0.81	1301	1.01
585	300	2109	1.95	1975	0.94	1976	0.94
585	445	2038	1.31	1975	0.97	1816	0.89
585	690	2050	0.85	1975	0.96	1850	0.90
585	860	2083	0.68	1975	0.95	1986	0.95
585	1140	2266	0.51	1975	0.87	2291	1.01

load is distributed according to the relative stiffness. It can be seen from figure 2, 3 & 4 that the specimens behaved in accordance with the theory.

Table 2, Experimental and Theoretical failure load of Mortar Cross Beams

Lx (mm)	Ly (mm)	Expt. Failure load (N)	Lx/Ly	Theoretical Failure load (N)			
				Rankine's Method of (RM) Analysis	Ratio RM Expt	FEM with proposed failure criterion	Ratio FEM Expt
1200	600	1016	2.0	853	0.84	1029	1.013
1080	600	1036	1.8	888.3	0.858	1070	1.033
720	600	1376	1.2	1197.1	0.87	1290	0.942
600	600	1447	1.0	1511.6	1.045	1398	0.966

In brickwork, most of the specimens cracked when the ultimate load was reached in the weaker direction. It can be seen that the load carried by the weaker direction was then shed to the stronger direction as the specimen was no longer capable of supporting any further load in this direction. The specimens continued to support additional load in the stronger direction until they failed. No such load shedding was observed in mortar cross beams. Once the specimen reached its strength in any one of the directions, it was no longer capable of supporting further loading. The data logger used to measure the applied load and support reactions were consistently monitored for any variation in the

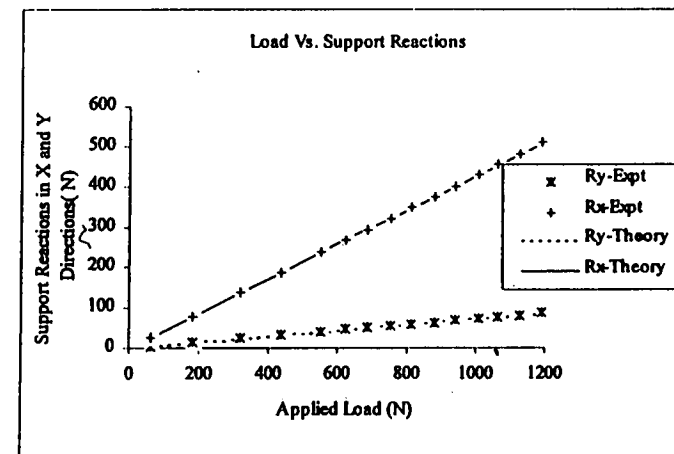


Fig. 2, Support Reactions Vs. Applied Load for Mortar Cross Beams, (Lx = 600mm, Ly = 1080mm)

reading at the time of cracking. With the cracking of the specimen, none of the load cells picked up extra load and the load carried by all the load cells were dropped. This clearly indicate that the phenomenon of load shedding was absent in this type of material.

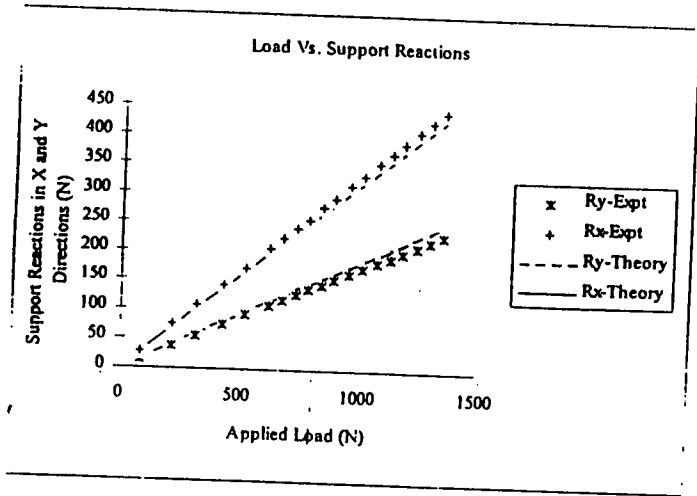


Fig. 3, Support Reactions Vs. Applied Load for Mortar Cross Beams, (Lx = 600mm, Ly = 720mm)

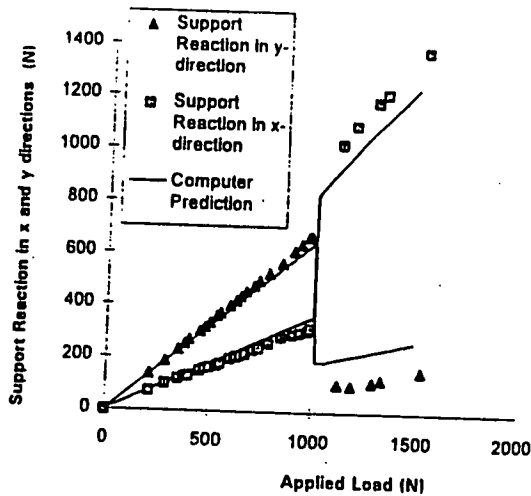


Fig. 4. Support Reactions Vs. Applied load for Masonry Cross Beams

The following types of failures were noticed in brick and mortar cross beams:

1. In the mortar cross beams, failure happened simultaneously in both directions without any prior cracking. Some of the brick cross beams also followed a similar pattern of failure. These specimens failed by a brittle and sudden collapse of the central portion.
2. In the second type, the brickwork cross beams cracked in the weaker direction and the load was shed to the stronger direction. However, these specimens failed immediately because the shed load was sufficient to cause the failure of the beam in the stronger direction.
3. In the third type of failure, after cracking, the specimens continued taking load in the stronger direction as the shed load wasn't large enough to cause the failure. Hence, the cracking and failure in this case was quite distinguishable.

The above three types of failures were characterised due to the different flexural strength in the two orthogonal directions. However, only the first type of failure was observed in the case of isotropic beams.

## 5.2 Failure Criteria

From the experimental results on brickwork cross beams, the biaxial failure criterion has been arrived at which is given by Eqn. (1)<sup>2</sup>.

$$\left(\frac{M_y}{M_{xy}}\right)^2 - 0.75 \frac{M_x}{M_{xx}} \left(\frac{M_y}{M_{xy}}\right)^2 - 0.25 \frac{M_x}{M_{xx}} \frac{M_y}{M_{xy}} + \left(\frac{M_x}{M_{xx}}\right)^2 = 1 \quad (1)$$

Similarly, the failure criterion is developed for an isotropic material from the test results of mortar beams. The best fit curve through the experimental points give the following relationship.

$$\left(\frac{M_y}{M_{xy}}\right)^2 - \frac{M_x}{M_{xx}} \frac{M_y}{M_{xy}} + \left(\frac{M_x}{M_{xx}}\right)^2 = 1.0 \quad (2)$$

The above equation is similar to the Von Mises<sup>4</sup> failure criterion for a ductile material subjected to two dimensional stress system. The failure envelope based on the above Eqn. is shown in Figure 5 and is compared with the Rankine's failure criterion for a brittle material, in which it is assumed that the material fails once the ultimate strength in tension is reached in any one of the directions. It is clear from the figure that the experimental results for the mortar cross beams can't be explained by the Rankine's failure theory. It can be seen that the strength of an isotropic material in biaxial bending is higher than that in a uniaxial bending. The failure criterion for the orthotropic material is also drawn for comparative purposes (Figure 5b). It is evident that although

there is an increase in strength in the weaker direction, no significant improvement of strength is detected in biaxial bending for orthotropic material.

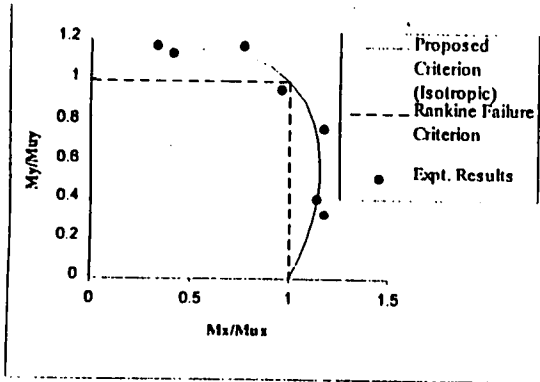


Fig. 5 a) The Proposed Failure Envelope for isotropic material

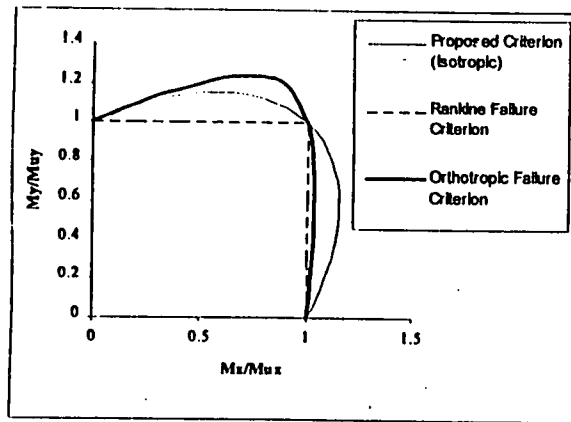


Fig. 5 b) Failure Envelop for Isotropic and Orthotropic cases

A similar observation was made by Kupfer et al.<sup>5</sup> on the behaviour of concrete under biaxial compression/tension, in which they pointed out that the strength of concrete under biaxial compression is larger than under uniaxial compression. However they argued that the biaxial tensile strength is approximately equal to the uniaxial tensile strength. The present observation of the behaviour of mortar beams contradicts their conclusion in regards to the behaviour of the material in tension.

### 5.3 Comparison of the Experimental and Theoretical Results.

The cracking and the failure load of the cross beams were calculated by a finite element program incorporating the above failure criteria and Rankine's maximum stress theory. Comparison of the test results with theoretical predictions are given in Table 1 for brickwork cross beams and is given in table 2 for mortar cross beams. For brickwork cross beams, the Rankine's analysis is carried out based on the strength in the stronger direction, as the specimens continued taking load even after cracking in one direction. As can be seen from tables, the finite element with the failure criteria gave closely matching values with the experimental results in both the cases. The importance of a separate failure criterion for the isotropic and orthotropic material are evident from these test results.

While calculating the failure load using Rankine's maximum stress theory<sup>4</sup>, it is assumed that the specimen, subjected to biaxial bending, fails when the ultimate strength is reached in any one of the directions. But the load shedding behaviour observed in the orthotropic material establishes the load carrying capacity of the specimens even after the failure of the specimen in one direction, where it continues supporting the load in the stronger direction.

### 6. CONCLUSION

The following conclusions can be drawn on the behaviour of orthotropic and isotropic material subjected to biaxial bending by examining the experimental results of brickwork and mortar cross beams:

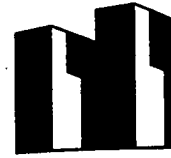
- The applied load gets distributed according to the relative stiffness of the material. In the case of an orthotropic material, the load carried by the weaker direction is shed to the stronger direction, once the ultimate load is reached in the weaker direction. No such load shedding is detected in an isotropic material.
- The flexural strength is increased in biaxial bending than in uniaxial bending for both isotropic and orthotropic material. However, in an orthotropic material, the increase in strength occurs only in the weaker direction. The stronger direction didn't show any significant improvement in strength over the uniaxial strength.
- It is evident from the experimental results that the behaviour of isotropic and orthotropic material are dissimilar and separate failure criteria needs to be used in the analysis. Failure criteria developed in this paper and the earlier work<sup>2</sup> can be used for an isotropic and orthotropic material subjected to biaxial bending.

### NOTATIONS

- Mx - Ultimate Moment in X-direction in Biaxial Bending
- My - Ultimate Moment in Y-direction in Biaxial Bending
- Mux - Uniaxial Strength in X-direction

## REFERENCES

1. Durate, R. B., "A Study of the Lateral Strength of Brickwork Panels with Openings", Ph.D Thesis, University of Edinburgh, 1993.
2. Sinha B P and Ng, C.L., "Failure Criterion and Behaviour of Brickwork in Biaxial Bending", Journal of Materials in Civil Engineering, ASCE, May 1997.
3. Baker, L.R., "A Failure Criterion for Brickwork in Biaxial Bending", Proceedings of the 5th International Brick Masonry Conference, Washington, U.S.A., 1979, pp. 71-78.
4. Megson T H G, "Strength of Materials for Civil Engineers", Thomas Nelson and Sons Ltd.
5. Kupfer H, Hilsdorf H K and Rusch H, "Behaviour of concrete Under Biaxial Stress", ACI Journal, 1969, pp. 656-666.



11th INTERNATIONAL BRICK/BLOCK MASONRY CONFERENCE  
TONGJI UNIVERSITY, SHANGHAI, CHINA, 14 - 16 OCTOBER 1997

## In-plane Stiffness of Three-storey Three-bay RC Frames with Masonry Infills

A. Dukuze \*      J.L. Dawe †

### 1 Abstract

Although infills are present in multistorey, multibay buildings, most experiments conducted to date on infilled frames have dealt with single storey, single bay configurations. In the present study, in-plane behaviour of three-storey, three-bay reinforced concrete (RC) frames with unreinforced masonry panels were investigated. Two one-third scale model specimens were subjected to in-plane inverted triangular loading as suggested in various building codes. Both specimens were similar except that their respective beam-to-column inertia ratios were 1 and 5. Despite extensive damage after being tested in one direction, they were subsequently loaded in reverse direction in order to assess their ability to withstand additional load. At the completion of each test, it was evident that, most of the damage was sustained by the first storey. In-plane behaviour of individual masonry panels was characterized mainly by the development of diagonal compressional struts at an early stage of loading, followed by in-plane expansion of the walls due to shear cracks which initiated and grew under increased lateral load. Although inner columns sustained noticeable cracking, most of the frame damage was concentrated in outer columns which failed in shear because of a combined action of deformed infills and high level of localized shear forces.

### 2 Introduction

Infill structural systems are encountered in various parts of the world including areas subjected to wind forces or/and to earthquakes. Understanding the behaviour of such structures under lateral action has been the goal of many investigators for more than

\*Research Engineer

†Professor and Executive Director Atlantic Masonry Research and Advisory Bureau Inc. University of New Brunswick, Box 4400, Fredericton, NB, Canada, E3B 5A3